ROLES AND REGULATORY MECHANISMS OF MICRORNA IN PLANT DEVELOPMENT, EVOLUTION, AND ADAPTATION

EDITED BY: Lei Li, Xiuren Zhang, Xiaozeng Yang and Turgay Unver

PUBLISHED IN: Frontiers in Plant Science

frontiers Research Topics

frontiers

ISSN 1664-8714
ISBN 978-2-83250-052-1
DOI 10.3389/978-2-83250-052-1

About Frontiers

Frontiers is more than just an open-access publisher of scholarly articles: it is a pioneering approach to the world of academia, radically improving the way scholarly research is managed. The grand vision of Frontiers is a world where all people have an equal opportunity to seek, share and generate knowledge. Frontiers provides immediate and permanent online open access to all its publications, but this alone is not enough to realize our grand goals.

Frontiers Journal Series

The Frontiers Journal Series is a multi-tier and interdisciplinary set of open-access, online journals, promising a paradigm shift from the current review, selection and dissemination processes in academic publishing. All Frontiers journals are driven by researchers for researchers; therefore, they constitute a service to the scholarly community. At the same time, the Frontiers Journal Series operates on a revolutionary invention, the tiered publishing system, initially addressing specific communities of scholars, and gradually climbing up to broader public understanding, thus serving the interests of the lay society, too.

Dedication to Quality

Each Frontiers article is a landmark of the highest quality, thanks to genuinely collaborative interactions between authors and review editors, who include some of the world's best academicians. Research must be certified by peers before entering a stream of knowledge that may eventually reach the public - and shape society; therefore, Frontiers only applies the most rigorous and unbiased reviews.
Frontiers revolutionizes research publishing by freely delivering the most outstanding research, evaluated with no bias from both the academic and social point of view. By applying the most advanced information technologies, Frontiers is catapulting scholarly publishing into a new generation.

What are Frontiers Research Topics?

Frontiers Research Topics are very popular trademarks of the Frontiers Journals Series: they are collections of at least ten articles, all centered on a particular subject. With their unique mix of varied contributions from Original Research to Review Articles, Frontiers Research Topics unify the most influential researchers, the latest key findings and historical advances in a hot research area! Find out more on how to host your own Frontiers Research Topic or contribute to one as an author by contacting the Frontiers Editorial Office: frontiersin.org/about/contact

ROLES AND REGULATORY MECHANISMS OF MICRORNA IN PLANT DEVELOPMENT, EVOLUTION, AND ADAPTATION

Topic Editors:
Lei Li, Peking University, China
Xiuren Zhang, Texas A&M University, United States
Xiaozeng Yang, Beijing Academy of Agricultural and Forestry Sciences, China
Turgay Unver, FicusBio Ankara, Turkey

Citation: Li, L., Zhang, X., Yang, X., Unver, T., eds. (2022). Roles and Regulatory Mechanisms of MicroRNA in Plant Development, Evolution, and Adaptation. Lausanne: Frontiers Media SA. doi: 10.3389/978-2-83250-052-1

Table of Contents

frontiers | Frontiers in Plant Science

TYPE Editorial
PUBLISHED 15 August 2022
DOI 10.3389/fpls.2022.995517

OPEN ACCESS

EDITED BY
Silvia Quaggiotti,
University of Padua, Italy

*CORRESPONDENCE
Xiaozeng Yang
yangxiaozeng@baafs.net.cn;
yangxz@srnaworld.com

SPECIALTY SECTION
This article was submitted to Plant Physiology, a section of the journal Frontiers in Plant Science

RECEIVED 16 July 2022
ACCEPTED 04 August 2022
PUBLISHED 15 August 2022

CITATION
Yang X, Unver T, Zhang X and Li L (2022) Editorial: Roles and regulatory mechanisms of microRNA in plant development, evolution, and adaptation. *Front. Plant Sci.* 13:995517. doi: 10.3389/fpls.2022.995517

Editorial: Roles and regulatory mechanisms of microRNA in plant development, evolution, and adaptation

Xiaozeng Yang[1,2]*, Turgay Unver[3], Xiuren Zhang[4,5] and Lei Li[6]

[1]Institute of Biotechnology, Beijing Academy of Agriculture and Forestry Sciences, Beijing, China, [2]Beijing Key Laboratory of Agricultural Genetic Resources and Biotechnology, Beijing, China, [3]Ficus Biotechnology, Ankara, Turkey, [4]Department of Biochemistry and Biophysics, Texas A&M University, College Station, TX, United States, [5]Department of Biology, Texas A&M University, College Station, TX, United States, [6]State Key Laboratory of Protein and Plant Gene Research, Peking-Tsinghua Center for Life Sciences, School of Life Sciences and School of Advanced Agricultural Sciences, Peking University, Beijing, China

KEYWORDS

microRNA, regulation, plant, morphology, stress, network

Editorial on the Research Topic
Roles and regulatory mechanisms of microRNA in plant development, evolution, and adaptation

MicroRNAs (miRNAs) are a group of endogenous small non-coding RNAs that regulate gene expression. In general, miRNAs can guide their effector partners in the cytoplasm, Argonaute proteins, to silence transcripts with sequence complementarity by mRNA cleavage or translation resting. They can also control gene expression by targeting promoters or enhancers in the nucleus. In plants, miRNAs regulate plant development and response to environmental stresses by controlling expression levels and activities of a variety of downstream genes. Even though a large number of plant miRNAs have been identified and linked to various cellular processes, our understanding of the precise roles and mechanisms of miRNAs in plant development, evolution, and adaptation is still limited. This Research Topic presents new and important findings on three fronts: the roles of miRNAs in plant morphology and environmental stresses, the regulatory network based on multi-omics data, and reviews and applications of two classic methods in miRNA study.

Several classical miRNAs are proven to play an important role in plant morphological development. Ren et al., further confirmed this phenomenon in sweet potato by examining the miRNA circuit between miR319 and its target *TCP*s. Intriguingly, they revealed that the significance of *Ib*miR319-targeted *IbTCP*s in leaf anatomical morphology is accredited to photosynthetic rate caused by the change in leaf submicroscopic structure. Branching is another critical morphologic trait in many plants. Mallet et al., first reviewed and highlighted the regulatory contribution and the action of evolutionarily conserved miRNA factors in different species, and then identified seven miRNAs and their nine corresponding target genes potentially involved in branching in Rosebush.

From the early days of studying miRNAs, scientists have found several miRNAs that were involved in the response to environmental stresses in model plants. Li et al., expanded this line of investigation by examining the mechanism of miRNA-mediated root growth and development in response to nutrient deficiency in peanut (*Arachis hypogaea* L.). Under both nitrogen and potassium deficiency, the dry weight of both shoot and root tissues was significantly reduced. Li et al., identified the down- and up-regulated miRNAs (miR156, miR167, miR393, etc.) that were potentially associated with these changes by screening expression patterns of the miRNA target genes under these stress treatments. Villalba-Bermell et al., performed experiments that mimicked the climate change by inducing combined adverse environmental conditions to scan how the core miRNA network reacts. Under the various combinations of four stresses (cold, salinity, short day, and infection with a fungus), they found that a high proportion of the miRNA families showed a non-additive response to multiple stresses in comparison to that observed under each one of the stresses individually.

A recent hotspot of small RNA (sRNA) studies is to examine their roles in responding to diseases caused by bacteria or fungi. Zhang et al., revealed a novel scenario in which *MIR157d* became the target of *Verticillium dahlia*. They showed that a trans-kingdom fungal sRNA, VdrsR-1, could be secreted into host cells and target miR157d and further modulate plant floral transition by affecting the *miR157d/SPL13A/B* regulatory module, resulting in prolonged host vegetative growth that would benefit fungal propagation. On the other hand, our knowledge on the highly conserved miRNAs is expanding due to more inquiries into the functions of their target genes. Taken miR160 and their target *ARF*s (Auxin response factors) as an example, in addition to the classical role in auxin response, functions of the circuits in many aspects of development such as flowering time, fiber length, germination, tillering, leaf morphology, etc., were also reported in different plants. In addition, they were shown to take part in a series of biotic and abiotic stresses, including responses to stress caused by bacteria, fungi and pest, and induced by heat, cold, and drought (Hao et al.).

As multi-omics has become a powerful tool to uncover gene functions, the high noise often hinders its application, especially in non-model plants. This Research Topic features the reporting of two genome scaled miRNA regulatory networks involving upstream transcription factors and downstream targets constructed in lettuce (*Lactuca sativa*, Deng, Qin et al.) and foxtail millet (*Setaria italic*, Deng, Zhang et al.), respectively. By integrating multiple omics datasets including genome, transcriptome, miRNAome, degradome, and the correlation among them, much noise has been removed from the gene regulatory network centered on miRNAs. Consequently, clearer network motifs such as feed-forward loops were identified, and many regulations were discovered and found to be conserved in other species. Therefore, many previously unknown regulations uncovered by these studies are thought to be legitimate for follow-up studies.

Molecular biological and high-throughput sequencing methods for miRNA research have greatly accelerated the understanding of miRNA functions. For instance, the short tandem target mimic (STTM) approach could capture the endogenous miRNAs as a sponge and reveal the effect of miRNA loss-of-functions. Chen et al., reviewed the development and advance of STTM-based methods in plant research, especially in the model crop rice, and discussed the challenges and potential opportunities of combining STTM and CRISPR technology for crop improvement. Another classical method for high-throughput validation of miRNA targets is Parallel Amplification of RNA Ends sequencing (PARE-Seq). Li and Ren creatively applied this method by using publicly available PARE datasets to systematically explore the miRNA processing modes. Their effort revealed a conserved processing mode existing in four examined plants.

The regulatory roles and mechanisms of miRNAs in plant development, evolution, and adaptation are constantly being discovered and expanded, including new functions of those known and conserved miRNAs, even miRNA themselves have become the target of plant-fungus interaction. At the same time, the methods on miRNA research are also continuously evolving. Expanded use of STTM and PARE-seq are providing strong support for functional studies of miRNAs in non-model plants. It has become very promising that the full mining of multi-omics data centered on miRNAs will greatly improve the existing understanding of miRNA function, evolution, etc., in the future. Functional analysis of miRNAs *via* CRISPR-based genome editing as an emerging technology will also greatly value our knowledge of plant miRNAs. miR-CRISPR approach allows us to concurrently knock out miRNA family loci or selectively knock out individual members. Similar approaches can be applied to the target genes of miRNAs. A sophisticated combination of the strategies will provide clearer pictures of the roles of corresponding plant miRNAs in near future.

Author contributions

XY prepared the first draft of this Editorial. LL, TU, and XZ revised it. All authors approved the Editorial for publication.

Funding

This work was supported by the National Natural Science Foundation of China (32070248) and Beijing Academy of Agriculture and Forestry Sciences (KJCX201907-2, KJCX20200204, JKZX202201, and KJCX20220105).

Conflict of interest

Author TU was employed by Ficus Biotechnology.

The remaining authors declare that the research was conducted in the absence of any commercial or financial relationships that could be construed as a potential conflict of interest.

Publisher's note

frontiers in Plant Science

ORIGINAL RESEARCH
published: 11 June 2021
doi: 10.3389/fpls.2021.695234

Response of Root Growth and Development to Nitrogen and Potassium Deficiency as well as microRNA-Mediated Mechanism in Peanut (*Arachis hypogaea* L.)

Lijie Li[1], Qian Li[1], Kyle E. Davis[2], Caitlin Patterson[2,3], Sando Oo[2,3], Wanying Liu[4], Jia Liu[1], Guo Wang[1], Julia Elise Fontana[2], Thomas Elliott Thornburg[2], Isaac Seth Pratt[2], Fei Li[5], Zhiyong Zhang[1], Yanzhong Zhou[5]*, Xiaoping Pan[2] and Baohong Zhang[2]**

[1]Henan Collaborative Innovation Center of Modern Biological Breeding, Henan Institute of Science and Technology, Xinxiang, China, [2]Department of Biology, East Carolina University, Greenville, NC, United States, [3]Elizabeth City State University, Elizabeth City, NC, United States, [4]College of Life Sciences, Anhui Normal University, Wuhu, China, [5]Peanut Research Institute, Luohe Academy of Agricultural Sciences, Luohe, China

OPEN ACCESS

Edited by:
Turgay Unver, FicusBio, Turkey

Reviewed by:
Fangjun Li, China Agricultural University, China
Yingpeng Han, Northeast Agricultural University, China

***Correspondence:**
Zhiyong Zhang
z_zy123@163.com
Baohong Zhang
zhangb@ecu.edu
Yanzhong Zhou
zyzlhhs@163.com

Specialty section:
This article was submitted to Plant Physiology, a section of the journal Frontiers in Plant Science

Received: *14 April 2021*
Accepted: *17 May 2021*
Published: *11 June 2021*

Citation:
Li L, Li Q, Davis KE, Patterson C, Oo S, Liu W, Liu J, Wang G, Fontana JE, Thornburg TE, Pratt IS, Li F, Zhang Z, Zhou Y, Pan X and Zhang B (2021) Response of Root Growth and Development to Nitrogen and Potassium Deficiency as well as microRNA-Mediated Mechanism in Peanut (Arachis hypogaea L.). Front. Plant Sci. 12:695234. doi: 10.3389/fpls.2021.695234

The mechanism of miRNA-mediated root growth and development in response to nutrient deficiency in peanut (*Arachis hypogaea* L.) is still unclear. In the present study, we found that both nitrogen (N) and potassium (K) deficiency resulted in a significant reduction in plant growth, as indicated by the significantly decreased dry weight of both shoot and root tissues under N or K deficiency. Both N and K deficiency significantly reduced the root length, root surface area, root volume, root vitality, and weakened root respiration, as indicated by the reduced O_2 consuming rate. N deficiency significantly decreased primary root length and lateral root number, which might be associated with the upregulation of miR160, miR167, miR393, and miR396, and the downregulation of AFB3 and GRF. The primary and lateral root responses to K deficiency were opposite to that of the N deficiency condition. The upregulated miR156, miR390, NAC4, ARF2, and AFB3, and the downregulated miR160, miR164, miR393, and SPL10 may have contributed to the growth of primary roots and lateral roots under K deficiency. Overall, roots responded differently to the N or K deficiency stresses in peanuts, potentially due to the miRNA-mediated pathway and mechanism.

Keywords: peanut, nitrogen deficiency, potassium deficiency, microRNA, gene expression

INTRODUCTION

Cultivated peanut (*Arachis hypogaea* L.) is one of the three major legume grain and oilseed crops in China, with a planting area of over 5.0×10^6 ha and annual pod yields of more than 1.6×10^7 t in recent years, which plays a significant role in ensuring nutritional food security in China (Zhang et al., 2020). However, since the soil has been frequently over-exploited in modern agricultural practices, nitrogen (N) and potassium (K) have been the

important limiting factors. Therefore, they were often frequently supplemented in the form of fertilizers (Kuicheski et al., 2015).

There is a large amount of N fertilizer usage all over the world. Still, N fertilizer's recovery rate or efficiency is relatively low in arable land, accounting for only 25–50% of the application amount (Sharma and Bali, 2018; Omara et al., 2019). K deficiency is very common. For example, in China, more than one-third of cultivated soil is in the state of K deficiency (soil available K content is 50–70 mg/kg) or serious K deficiency (soil available K content is less than 50 mg/kg; Wang and Wu, 2009). Therefore, it is of great significance for optimizing nutrient management, particularly the supply of N and K in balance with crop demand and for the genetic improvement of peanut to explore the response mechanism of N deficiency and K deficiency in peanut.

Since N is involved in synthesizing important components such as proteins, nucleic acids, phospholipids, chlorophyll, enzymes, vitamins, alkaloids, and certain growth hormones in plants, it is also called the element of life (Hawkesford et al., 2012; Kant, 2018). The common symptoms of N deficiency include leaf yellowing, cell division slowing down, and enzyme activity decreasing and then leading to plant growth retardation (Salvagiotti et al., 2008). Compared with N, K does not directly participate in synthesizing any chemical substances in plants, but it is the most abundant cation in plants (Salvagiotti et al., 2008). It is widely distributed in various tissues and organs of plants, accounting for about 2–10% of the dry weight of plants (Leigh and Wyn Jones, 1984). K plays a very important role in maintaining cytoplasmic charge balance, regulating enzymatic reaction, promoting protein synthesis, and maintaining cell osmotic pressure and other physiological activities (Leigh and Wyn Jones, 1984). At the same time, K also participates in a series of physiological and biochemical processes, such as stomatal movement, cell signal transduction, cell elongation, and phloem material transport (Sustr et al., 2019). Proper K application is conducive to regulating nutrient transport and distribution in peanuts, promoting nodule formation, improving nodule nitrogen fixation capacity (Wang et al., 2013), regulating carbon and N metabolism, and improving peanut yield, quality, and resistance (Helmy and Ramadan, 2014; Almeida et al., 2015; Chakraborty et al., 2016).

The root is the first plant organ to sense and absorb nutrients, and their morphological response to different growth conditions varies greatly (Gruber et al., 2013). Plant roots show a high degree of plasticity for changes in the availability of nutrient resources, and the degree of this plasticity depends on the plant species in many cases (Sun et al., 2017; Sustr et al., 2019). Apart from the role as a nutrient element, nitrate or ammonium (the main form of N that can be taken by the roots) acting as a signal regulate many physiological processes, including the development of root system architecture (RSA; Sun et al., 2017; Kant, 2018) by regulating cell division and expansion (Luo et al., 2020). The growth and development of RSA depend on K supply that affected root differentiation and elongation (Sustr et al., 2019). Sufficient cytoplasmic K level is required for protein synthesis and enzyme activity in root cells to maintain cytoplasmic pH (Walker et al., 1998) and protein anion charge (Maathuis and Sanders, 1996). In addition, the cells in the elongation region need expansion pressure, which is established by osmotically active substances (including K; Pritchard, 1994; Dolan and Davies, 2004). In the mature zone of roots, root hairs grow through K flux (Guilhem et al., 2003; Zhao et al., 2016). In addition, the RSA and root hair coverage rate in plants changed adaptively, thus improving K uptake under K limitation (Guilhem et al., 2003; Zhao et al., 2016).

Plants have evolved several physiological and molecular adaptive responses to cope with nutrient deficiency stresses (Kuicheski et al., 2015; Nguyen et al., 2015). microRNAs (miRNAs) are short (21–24 nucleotide) RNAs, which can bind to RNA-induced silencing complex (RISC), recognize its target mRNAs, and regulate the expression of the targeted genes through transcriptional cleavage and translation inhibition (Zhang et al., 2006). If miRNA and mRNA are completely complementary, miRNA cleaves the phosphodiester bond between two nucleotides of the target mRNA sequence (generally between the 10th and 11th nucleotides of miRNA), that is to guide the specific cleavage of mRNA; if not, it will cause translation inhibition (Zhang et al., 2006; Sunkar et al., 2012). Studies have shown that miRNAs can regulate the quantity and spatiotemporal accumulation of target mRNAs and thus play a key regulatory role in plant stress response (Sunkar et al., 2012; Zhang, 2015), including in nutrient deficiency stress (Kuicheski et al., 2015; Nguyen et al., 2015).

Studies have shown that nutrient availability would change the expression of miRNAs and their target mRNAs and then affect the growth and development of plants (Kuicheski et al., 2015). Furthermore, different crops respond differently to nutritional deficiencies (Kuicheski et al., 2015; Fontana et al., 2020; Thornburg et al., 2020). However, the mechanism of miRNAs related to root growth and development in response to nutrient deficiency in peanuts is still unclear. In this work, we systematically explored the response of root development and morphology to N deficiency and K deficiency and the potential miRNA-mediated mechanism during these signs of progress. The observation of the expression of the miRNAs and their targeted mRNAs in peanut plants exposed to N deficiency and K deficiency could reveal the mechanisms of the plant suffering from nutrient deficiency stress and help find candidate genes to develop important tools for plant nutrition breeding.

MATERIALS AND METHODS

Plant Growth Conditions, Nutrient Stress Treatments, and Sampling

The peanut (*Arachis hypogaea* L. cv. Yuanza 9,102) seeds of the same size, fully mature, and free of diseases and insect pests were selected, soaked in 10% H_2O_2 solution for 5 min washed with deionized water five to six times. The seeds were wrapped in absorbent paper, soaked in a plastic bucket containing 2 L saturated $CaSO_4$, and placed in the artificial climate chamber (constant temperature 28°C, blue light irradiation) for germination. When the root length of peanut seedlings was about 10 cm (4 days), the seedlings with uniform appearance

were selected and planted in plastic pots containing 5 L of modified Hoagland nutrient solution (pH 6.3 ± 0.1): (1) normal N (NN) nutrient solution; (2) low N (LN) nutrient solution; (3) normal K (NK) nutrient solution; (4) low K (LK) nutrient solution. The nutrient solution group of NN consists of: 2.5 mM $Ca(NO_3)_2$, 2.5 mM KCl, 2 mM NaCl, 1 mM $MgSO_4$, 0.5 mM KH_2PO_4, 0.1 mM EDTA-FeNa, 2×10^{-2} mM H_3BO_3, 1×10^{-3} mM $ZnSO_4$, 1×10^{-3} mM $MnSO_4$ 2×10^{-4} mM·L^{-1} $CuSO_4$, and 5×10^{-6} mM $(NH_4)_6Mo_7O_{24}$. Compared with the nutrient solution group of NN, the 2.5 mM $Ca(NO_3)_2$ was replaced by 0.05 mM $Ca(NO_3)_2$ and 2.45 mM $CaCl_2$ in the nutrient solution group of LN. The nutrient solution group of NK consists of: 2.5 mM $Ca(NO_3)_2$, 2.5 mM KCl, 2 mM NaCl, 1 mM $MgSO_4$, 0.5 mM $NH_4H_2PO_4$, 0.1 mM EDTA-FeNa, 2×10^{-2} mM H_3BO_3, 1×10^{-3} mM $ZnSO_4$, 1×10^{-3} mM $MnSO_4$, 2×10^{-4} mM·L^{-1} $CuSO_4$, and 5×10^{-6} mM $(NH_4)_6Mo_7O_{24}$. Compared with the nutrient solution group of NN, the 0.5 mM KH_2PO_4 was replaced by 0.5 mM $NH_4H_2PO_4$ in the nutrient solution group of NK. Compared with the nutrient solution group of NK, the 2.5 mM KCl was replaced by 0.02 mM KCl and 2.48 mM NaCl in the nutrient solution group of LK. The nutrient solution was changed every 3 days to avoid nutrient depletion. The light source of the growth chamber was a biological sodium lamp. The light/dark period was 14/10 h, and the day and night temperature were 30 ± 2°C/25 ± 2°C. A certain amount of deionized water was added to the culture container every day to supplement the water consumed by transpiration. The air pump was used for ventilation for 24 h. Four and eight days after the nutrient stress treatments, the plants were collected to determine the dry and fresh weight and conduct root morphological analysis; the roots were collected to measure root respiration and root vigor. In addition, the root samples from each treatment were harvested and frozen in liquid nitrogen immediately and then stored at −80°C before RNA extraction.

Plant Growth Determination

Five peanut plants were randomly selected, and the substrate on the surface of the root and dust on the surface of leaves were washed with deionized water. After the surface water was wiped off, the peanut plants were divided into two parts: the aboveground part and the root part, and the fresh weight of each part was weighed. First, the plant height was measured with a ruler. Next, all leaves were scanned by a desktop scanner (EPSON Perfection V700 Photo), and pictures were taken. Then, WinRHIZO was used to analyze the leaf area (cm^2). Finally, the samples were dried at 105°C for 30 min and then to a constant weight at 80°C. Then, the dry weights of aboveground and roots were weighed, respectively.

Root Morphological Analysis

The primary root length was measured with a ruler. Then, counts were taken for the lateral root number. After that, the whole root was scanned with a desktop scanner (EPSON Perfection V700 Photo), and root pictures were taken. Finally, WinRHIZO was used to analyze the length (cm), surface area (cm^2), volume (cm^3), and diameter (mm) of the root samples.

Determination of Root Vitality

Root vitality was determined according to triphenyltetrazolium chloride (TTC) staining method. The roots of five seedlings from each treatment were weighed and cut into a small fragment that was ~1 cm in length. Then the root was soaked in 20 ml of 0.6% TTC solution prepared with 0.1 mol/L phosphate buffer (pH = 7.4). After 24 h, the buffer solution was poured out, and the roots were washed with deionized water three times. Then the roots were soaked in 20 ml 95% ethanol and a water bath at 85°C for 10 min to extract water-insoluble triphenylmethyl hydrazone (TTF). The absorbance of the extract was measured at 485 nm, and the root vitality was expressed as OD g^{-1} FW.

Root Respiration Rate Measurement

The roots of five seedlings from each treatment were weighed and put into the incubator chamber of the Clark Chlorolab2 system. Then, 2 ml saturated $CaSO_4$ solution was added, and the oxygen (O_2) consumption was measured after 10 min. The O_2 consumption rate was calculated and represented by the root respiration rate, expressed as nmol min g^{-1} FW.

RNA Extraction and Gene Expression Analysis

About 200 mg of root samples of peanut seedlings on the 4th and 8th days of N deficiency, K deficiency, and the control treatments were used to extract total RNAs. According to our previous reports, RNA extraction and isolation were performed as outlined in the manufacturer's protocols of the MirVana miRNA Isolation Kit (Candar-Çakir et al., 2016; Fontana et al., 2020; Yu et al., 2020). The quality of the extracted RNAs was firstly tested by Nanodrop ND-1000 (Nanodrop Technologies, Wilmington, DE, United States). One percentage agarose gel electrophoresis was used, and the quality and concentrations of RNAs were detected by micro ultraviolet spectrophotometer. Then the extracted RNA was stored at −80°C for reverse transcription.

According to the procedures of the manufacturer of TianGen miRcute Plus miRNA First Strand cDNA first Synthesis Kit (Beijing, China), the RNA samples were reverse transcribed into cDNAs with miRNA gene-specific primers and pol(T) primers of all protein-coding genes. Then the synthesized cDNA was stored at −20°C used for further analysis.

To investigate the potential mechanism of miRNA-mediated plant response to N deficiency and K deficiency, we targeted miRNAs related to plant root development and/or the dynamic balance of nutrients in other species (Nguyen et al., 2015; Li and Zhang, 2016; Zhang and Unver, 2018; Song et al., 2019). After considering all these criteria, a total of 20 miRNAs were selected for this study. They were miR156, miR160, miR162, miR164, miR165, miR166, miR167, miR169, miR171, miR172, miR319, miR390, miR393, miR395, miR399, miR396, miR778, miR827, miR847, and miR857. The expression of seven targets genes (*NAC4*, *AFB3*, *ARF1*, *ARF2*, *bHLH74*, *SPL10*, and *GRF*) found in the literature was also analyzed. The expression of miRNAs and their target genes were analyzed with the gene-specific forward and reverse primers according to the Tiangen

miRcute Plus miRNA qPCR detection kit (Beijing, China). Each gene and miRNA expression analysis included three biological replicates and three technical replicates. The expression value was standardized with reference gene EF1A. The ΔΔCT method was used to calculate the fold change of the tested miRNAs and their target genes.

Statistical Analysis

The data of each morphological and physiological index was calculated by five biological repeats, and gene expression was obtained by three biological repeats. Statistical software SPSS version 19 was employed for ANOVA and followed by the least significant difference (LSD) test. A value of p less than 0.05 and 0.01 was considered a significant difference and extremely significant difference and marked as * and ** in the graphs.

RESULTS

Effects of N and K Deficiency on the Growth and Development of Peanut Seedlings

As shown in **Figure 1**, the dry weight of shoot and root and leaf areas significantly decreased under both N and K deficiency on the 4th and 8th days. In addition, the plant height was significantly decreased under N and K deficiency on the 8th day. Compared with the seedlings cultured in the normal nutrient solutions, the dry weight of shoot, root, and total plant of the seedlings cultured in N deficiency nutrient solutions on the 8th day decreased by 29.67, 25.73, and 18.60%, respectively, and that of the seedlings cultured in K deficiency nutrient solutions on 8th day decreased by 32.97, 27.15, and 14.29%, respectively. In addition, the leaf area and the plant height of the seedlings cultured in N deficiency nutrient solutions on the 8th day decreased by 51.79 and 48.37%, respectively, and that of the seedlings cultured in K deficiency nutrient solutions on the 8th day decreased by 58.51 and 25.54%, respectively.

Effects of N and K Deficiency on Root Development of Peanut Seedlings

N and K deficiency had significant effects on root development, indicated not only by the root biomass but also the root length, size, and number of branches (**Figure 2**). As shown in **Figure 3**, compared with the seedlings cultured in the normal nutrient solutions, the total root volume and total root surface area as well as the total root length of the seedlings, cultured in N deficiency nutrient solutions on the 8th day, decreased by 50.29, 40.78, and 29.50%, respectively, and that of the seedlings cultured in K deficiency nutrient solutions on 8th day decreased by 19.06, 21.57, and 24.42%, respectively. On the other hand,

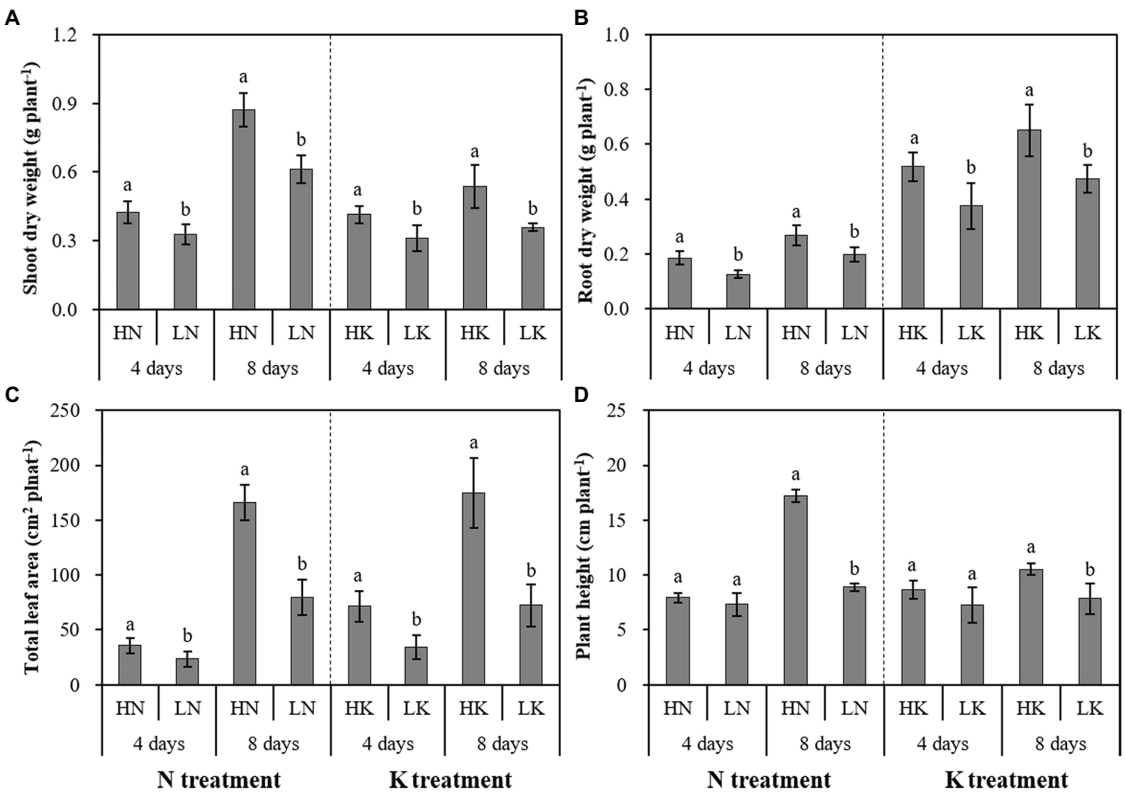

FIGURE 1 | The effect of N deficiency and K deficiency on the shoot dry weight **(A)**, root dry weight **(B)**, total leaf area **(C)**, and plant height **(D)** of peanut seedlings, respectively. The data are the means ± SDs (n = 5). The different letters on the bars indicate significant differences between the different N (or K) treatments and the control treatment on the same day according to the LSD test (p = 0.05). N, nitrogen; K, potassium; and LSD, least significant difference.

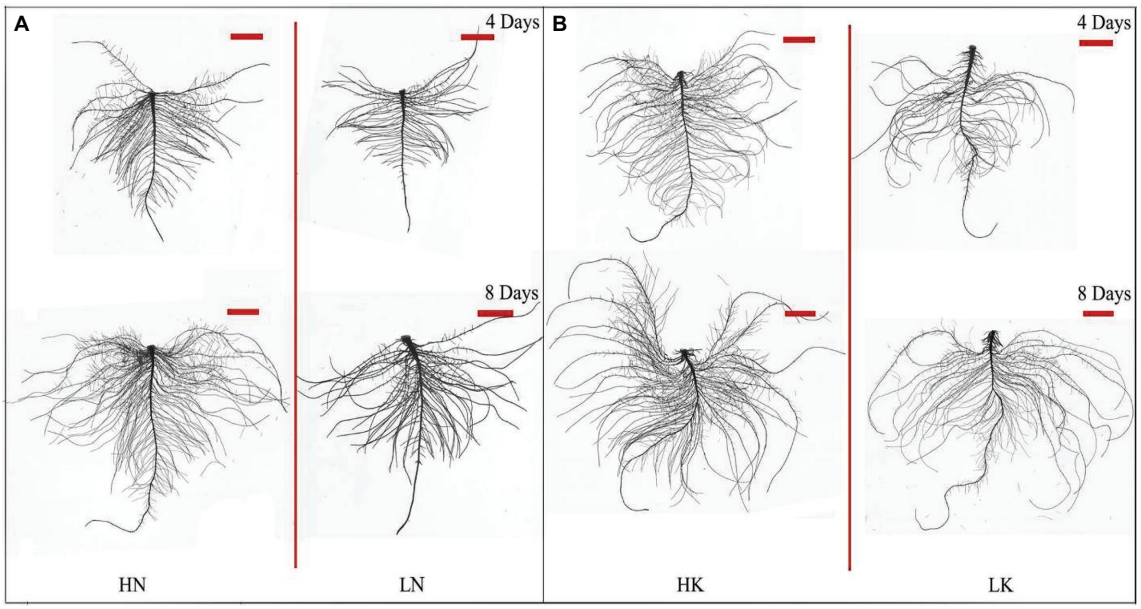

FIGURE 2 | Root morphology difference between high N (HN) group and low N (LN) group **(A)** and the difference between high K (HK) group and low K (LK) group **(B)** after 4 and 8 days of treatments. N, nitrogen and K, potassium. The original size of the target bar is 0.2 cm high and 3.5 cm wide.

compared with the seedlings cultured in the normal nutrient solutions, the average root diameter had no significant change under K deficiency conditions. At the same time, it increased significantly under 8 days of low N treatment.

N and K deficiency effects on the primary root length and lateral root number of peanut seedlings were opposite. N deficiency significantly reduced the primary root length of the seedlings on both the 4th and 8th days of N deficiency treatment. In addition, it decreased the lateral root number of the seedlings on the 8th day of N deficiency treatment. In contrast, K deficiency significantly promoted the growth of the primary root and increased the lateral root number of the seedlings on the 8th day. Compared with the seedlings cultured in the normal nutrient solutions, the primary root length and the lateral root number of the seedlings cultured in N deficiency nutrient solutions on the 8th day decreased by 44.89 and 22.49%, respectively, and that of the seedlings cultured in K deficiency nutrient solutions on 8th day increased by 59.04 and 71.46%, respectively.

N and K Deficiency Affected Root Vigor and Root Respiration in Peanut Seedlings

N and K deficiency significantly impacted the growth and development of roots and significantly affected the health of roots, which was manifested by changes in root vigor and respiration (**Figure 4**). On both the 4th and 8th days of treatment, the root vigor was significantly changed under both N deficiency and K deficiency treatments, and with the extension of the stress time, the root vigor showed a gradual decline trend. Compared with the seedlings cultured in the normal nutrient solutions, the root vigor of the seedlings cultured in N deficiency nutrient solutions and the seedlings cultured in K deficiency nutrient solutions on the 8th day of treatment decreased by 33.84 and 44.64%, respectively. On the 4th day of treatment, there was no significant difference between the root respiration rate of seedlings grown in N deficient nutrient solution and that of seedlings grown in a normal nutrient solution. However, with the extension of stress time, the root respiration kept decreasing. The difference of the root respiration between N deficiency treatment and the controls reached a significant level on the 8th day of treatment. The root respiration of the seedlings cultured in K deficiency nutrient solutions showed a gradual decline trend, and the difference of the root respiration between the seedlings grown in K deficient nutrient solution and the seedlings grown in normal nutrient solution reaches a significant level on both 4th and 8th days of K treatment.

N Deficiency and K Deficiency Changed the Expression of miRNAs and Their Targeted mRNAs

N and K deficiency changed the expression of miRNAs and their targeted mRNAs (**Figure 5**). However, the response of different miRNAs to N deficiency and K deficiency was different. On the 4th day of N deficiency treatment, except miR156, miR162, miR172, miR396, miR778, the expression of other miRNAs was inhibited, and the inhibition of the expression of miR167, miR169, miR395, miR399, and miR857 reached a significant level compared with that in the controls (**Figure 5A**). In contrast, on the 8th day of N deficiency treatment, except miR399, miR778, and miR857, the expression of the other tested miRNAs was induced compared with that in the controls, and the induction of the expression of miR156, miR160, miR165, miR166, miR167, miR169, miR171, miR172, miR319, miR390, miR393, miR396, miR827, and miR847 reached a significant

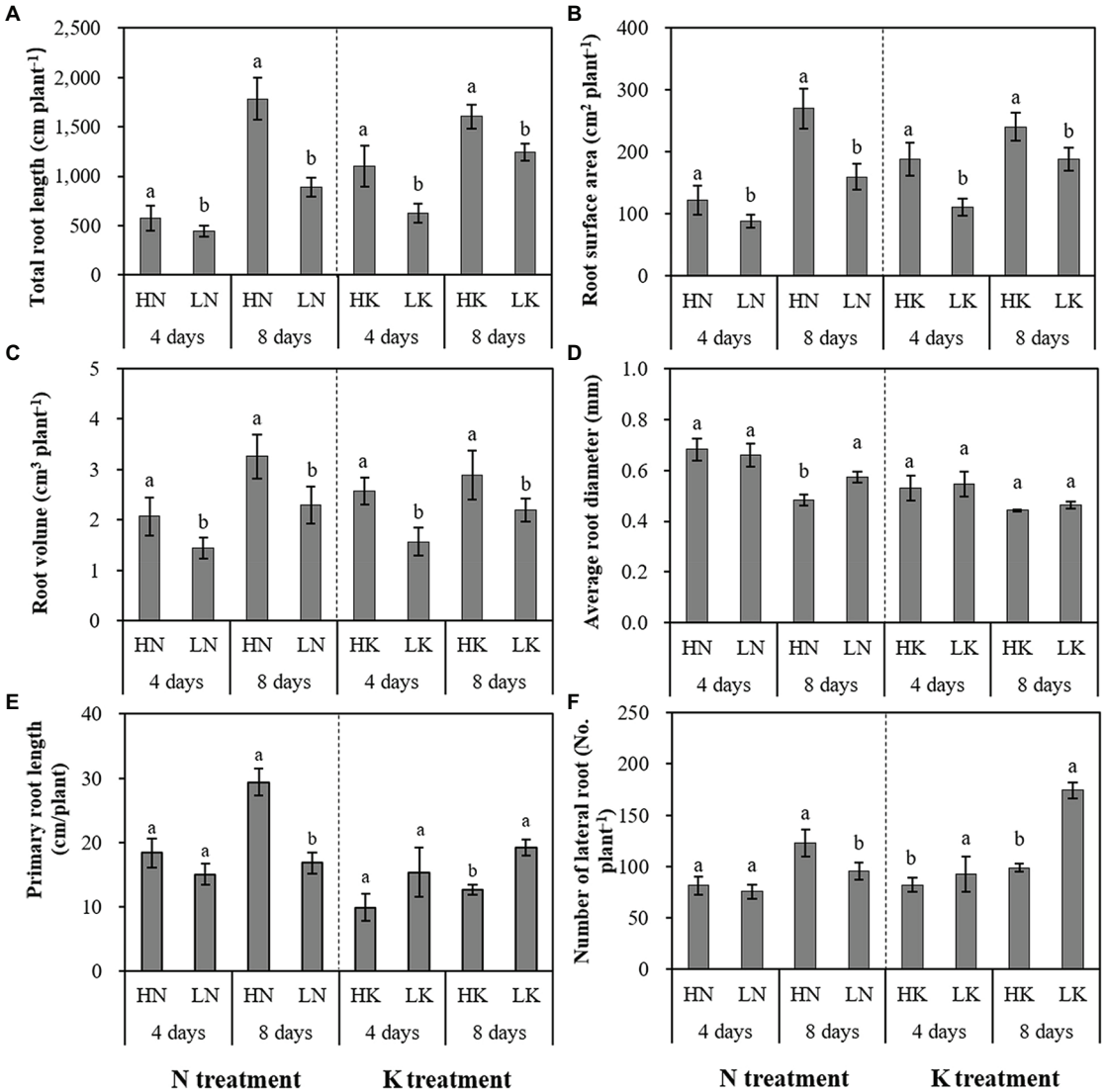

FIGURE 3 | The effect of N deficiency and K deficiency on the total root length **(A)**, root surface area **(B)**, root volume **(C)**, average root diameter **(D)**, primary root length **(E)**, and the number of lateral roots **(F)** of peanut seedlings, respectively. The data are the means ± SDs (n = 5). The different letters on the bars indicate significant differences between the different N (or K) treatments and the control treatment on the same day according to the LSD test (p = 0.05). N, nitrogen; K, potassium; and LSD, least significant difference.

level compared with that in the controls. On the 4th day of K deficiency treatment, all the 20 miRNAs were induced (**Figure 5B**). Among them, miR167 was upregulated the most by 6.32-fold, and the expression of miR156, miR164, miR165, miR166, miR169, miR393, miR396, and miR847 were also upregulated by more than threefold change. On the 8th day of treatment, although the expression of most miRNAs (except for miR160, miR164, miR171, miR393, and miR827) under K deficiency treatments were still higher than that in the control treatment, the value of fold changes was much lower than that determined on 4th day of treatments. On the 8th day of treatments, the expression of miR160, miR164, miR171, and miR393 under K deficiency treatment was significantly lower than that under the controls.

N and K deficiency also changed the expression of protein-coding genes (**Figure 6**). On the 4th day of treatments, the expression of all tested seven miRNA-targeted genes, except NAC4 and ARF2, was inhibited under N deficiency treatment, and the induction of the expression of ARF1 and GRF reached a significant level compared with that in the controls (**Figure 6A**). In contrast, after 8 days of treatments, the total of potential miRNA targets, except the ARF2 and GRF gene, was induced by N deficiency treatment. Compared with the control, among these genes, NAC4 had the highest expression under N deficiency treatment, and the fold change value reached 3.46. On both the 4th and 8th days of K deficiency treatment, all tested seven potential miRNA targets, except AFB3 gene on 4th day of treatments and SPL10 on 8th day of treatments, were

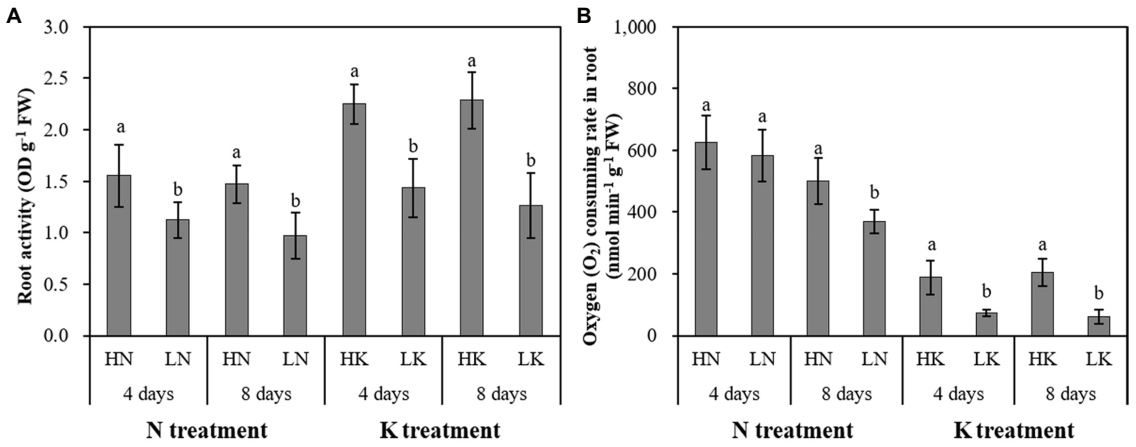

FIGURE 4 | The effect of N deficiency and K deficiency on the root activity **(A)** and oxygen (O_2) consuming rate in the root **(B)** of peanut seedlings, respectively. The data are the means ± SDs (n = 5). The different letters on the bars indicate significant differences between the different N (or K) treatments and the control treatment on the same day according to the LSD test (p = 0.05). N, nitrogen; K, potassium; and LSD, least significant difference.

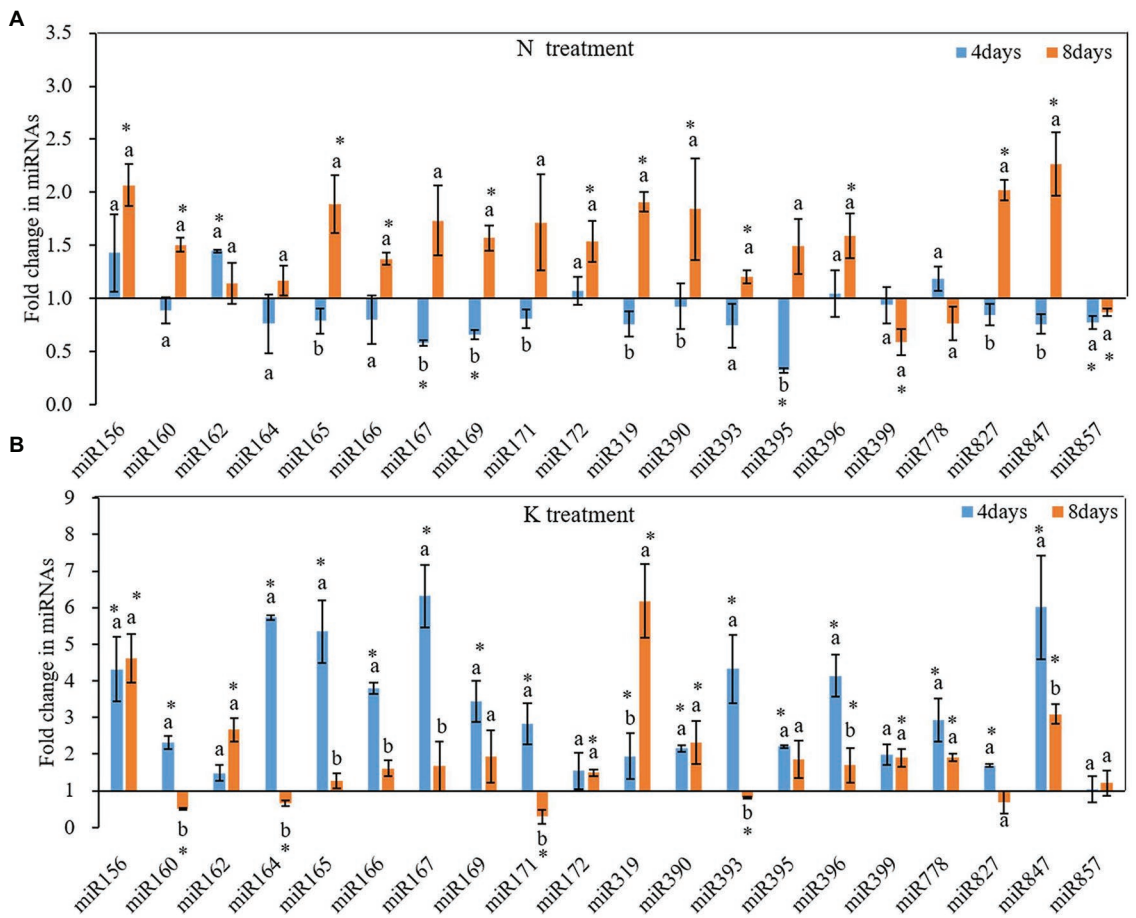

FIGURE 5 | Fold change of microRNAs (miRNA) expression between N deficiency and the controls **(A)** and between K deficiency and the controls **(B)** in the root of peanut seedlings, respectively. Error bars represent SD (n = 3). The different letters on the bars indicate significant differences in the fold change of miRNA target expression between 4 and 8 days of treatment according to the LSD test (p = 0.05). A value of p less than 0.05 was considered as a significant difference between N deficiency and the controls **(A)**, and between K^+ deficiency and the controls **(B)**, which marked as * in the graphs. N, nitrogen; K, potassium; and LSD, least significant difference.

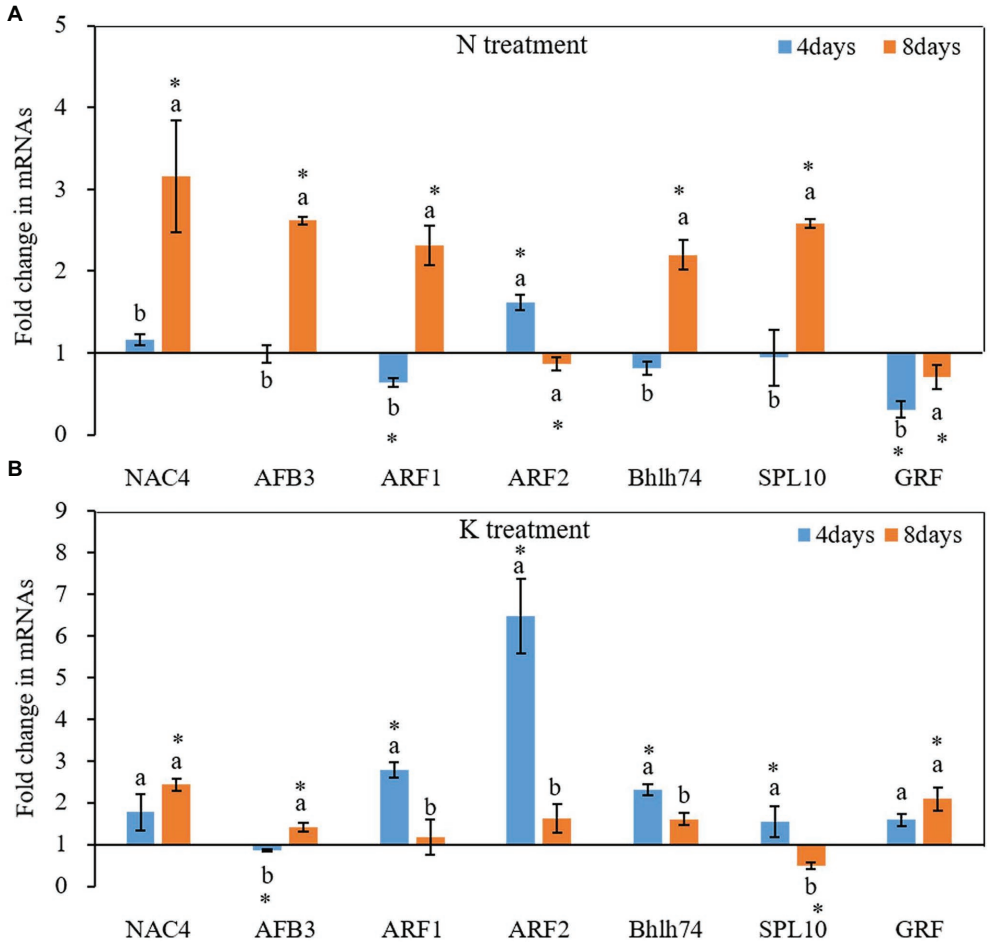

FIGURE 6 | Fold change of miRNA target gene expression between N deficiency and the controls **(A)** and between K deficiency and the controls **(B)** in the root of peanut seedlings, respectively. The different letters on the bars indicate significant differences in the fold change of miRNA target expression between 4 and 8 days of treatment according to the LSD test (p = 0.05). A value of p less than 0.05 was considered as a significant difference between N (or K) deficiency and the controls, which marked as * in the graphs. N, nitrogen; K, potassium; and LSD, least significant difference.

up-expressed in the root of seedlings grown in K deficient nutrient solution than that in normal nutrient solution (**Figure 6B**). ARF2 was the most upregulated among the seven target genes, and the fold changes up to 6.47-fold on the 4th day of K deficiency condition. Although the expression of most potential miRNA targets in the root of seedlings grown in K deficient nutrient solution was still higher than that of the control treatment on the 8th day of treatment, the fold change was much smaller than that determined on the 4th day of treatment. ARF1, ARF2, bHLH74 and SPL10 transcription factor gene expression levels were decreased by 57.75, 75.04, 30.29, and 68.25%, respectively, on the 8th day of treatments compared with that on 4th day of treatments under K deficiency treatments.

The Relationship Between miRNAs and Their Targeted mRNAs Under N and K Deficiency Treatments

miRNA regulates gene expression by shearing target mRNAs or inhibiting protein translation. Therefore, the expression of miRNA is negatively correlated with the expression of its targeted mRNAs. That is, if miRNA is upregulated, the expression of its target gene should be downregulated. The expression pattern of miRNAs and their target mRNA are often complex when secondary reactions and other gene regulatory factors besides miRNAs. In this case, the reverse expression relationship between the miRNAs and their target gene may not be observed. In the present study, we used linear equations to simulate the relationship between the fold change of miRNAs and their targeted mRNAs from the 4th day of treatment to the 8th day of treatment. The results showed that the expression of miRNAs had a negative linear relationship with their targets under both N deficiency and K deficiency treatment. And the reverse relationship could be described by the equation: $y = -4.1416x + 8.9204$ ($R^2 = 0.898$, **Figure 7A**) and the equation: $y = -1.2628x + 1.6193$ ($R^2 = 0.8343$, **Figure 7B**) under N deficiency and K deficiency treatments, respectively. It indicates that the tested miRNAs negatively regulate the expression of their targeted mRNAs.

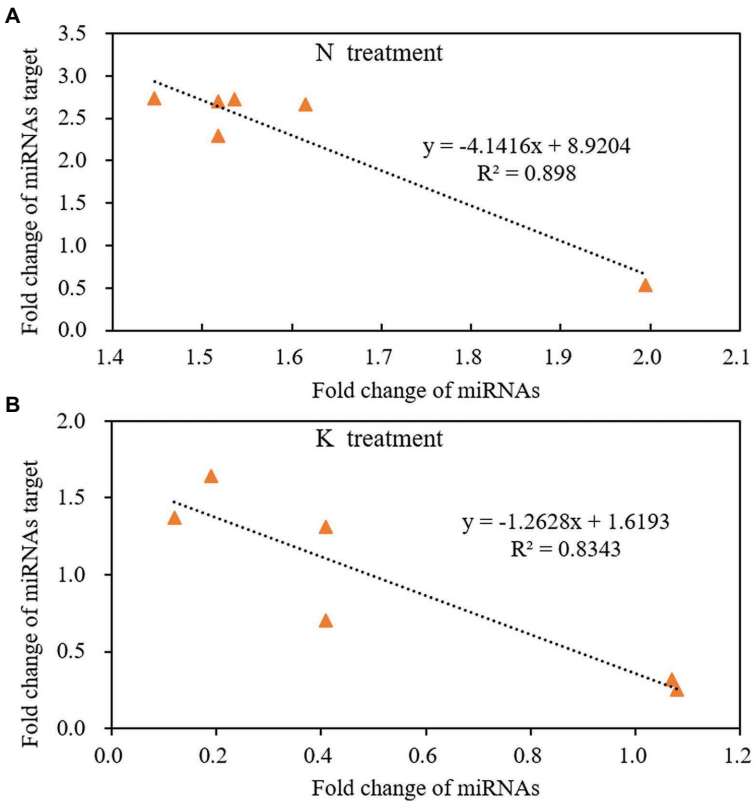

FIGURE 7 | The reverse liner relationship of fold change between miRNAs and their targets under N treatment **(A)** and K treatment **(B)** in the root of peanut seedlings. N, nitrogen and K, potassium.

DISCUSSION

N and K Deficiency Significantly Inhibited the Growth and Development of Peanut Seedlings

Nitrogen is the main component of many important compounds in plants. It participates in plant photosynthesis, a series of biochemical reactions, and plays an important role in biomass accumulation and yield formation in crops (Hawkesford et al., 2012; Kant, 2018). Potassium is the quality element of plants, which participates in osmotic adjustment, photosynthesis, material transport, and other processes, and it can improve the stress resistance of plants (Helmy and Ramadan, 2014; Almeida et al., 2015; Chakraborty et al., 2016). Therefore, the deficiency of these two kinds of macro-elements will lead to the inhibition of plant growth. In this study, the dry weight of shoot and root, leaf area, and plant height of peanut seedlings were significantly reduced under both 0.1 mM NO_3^- and 0.02 mM K^+ treatment. It meant that the 0.1 mM NO_3^- and 0.02 mM K^+ caused the low N stress and low K stress to the peanut seedlings, respectively, and inhibited the growth of peanut seedlings. These N deficiency-induced growth inhibition phenomena were also observed in other plant species, including potatoes (Xie et al., 2018). Studies have also shown that 0.02 mM K^+ can induce aberrant growth and development in cotton (Fontana et al., 2020) and wheat (Thornburg et al., 2020), which probably due to the reduction of chlorophyll content and photosynthetic capacity.

The Peanut Root System Has a Specific Response to N Deficiency and K Deficiency Stresses

Roots are the main organ for plants to absorb nutrients and water. It is also the first organ to sense the changes of rhizosphere environmental conditions and shows strong plasticity to adapt to the external environment changes (Malamy, 2005). Analysis of RSA provides good quantitative readouts that can be used to identify the genes and signaling pathways, enabling plants to sense changes in the root environment and integrate them into adaptive responses (Kellermeier et al., 2014). The traditional view is that each nutrient deficiency will lead to a typical root structure (Kellermeier et al., 2014). This study also found that the peanut root system has a different response to N deficiency and K deficiency conditions. Previous studies have shown that plants intend to develop exploratory roots with more lateral roots (Araya et al., 2014; Kant, 2018). Mohd-Radzman and coworkers demonstrated that a uniform low concentration of nitrate (e.g., ≤1 mM) enhanced the growth of both lateral and primary roots of legumes (Mohd-Radzman et al., 2013). While our result about

the peanut root system has a specific response to low N stress, both the lateral and primary root growth was inhibited under N deficiency conditions. Studies in *Arabidopsis* showed that under mild N deficiency, the average length of the lateral root was significantly promoted, while under severe N deficiency, the total lateral root length decreased, and there was almost no lateral root formation (Mohd-Radzman et al., 2013). Forde (2014) considered that the effect of low N stress or N deficiency on root branches depends on the N nutrition status of plants and the degree of stress on plants. Based on the above results, it can be considered that different crop roots respond differently to N deficiency, and root growth is related to the degree of N deficiency stress.

Previous studies have demonstrated that K deficiency has a negative effect on root elongation and the number of first-order lateral roots (Jung et al., 2009; Kellermeier and Amtmann, 2013), but the response varies among ecotypes, cultivars, species, and even root types (Kellermeier and Amtmann, 2013; Sustr et al., 2019). In this study, low K promotes both lateral and primary root growth while reduced the total root length. Similar results were also observed in wheat (Thornburg et al., 2020), and almost the opposite result was observed in cotton (Fontana et al., 2020). Although the number of lateral roots and the primary root length increased, the root system was inhibited under K deficiency treatment. The inhibition of root growth may be related to K deficiency induced slows down cell volume growth or restricts the transport of assimilation from the phloem to underground organs (Cakmak et al., 1994a,b).

Root vitality can represent the absorption, synthesis, oxidation, and reduction capacity of the root system and is a comprehensive index reflecting the absorption function of roots. 2,3,5-triphenyltetrazolium chloride is often used as a quantitative indicator of cell activity and is a good root metabolic reactive agent (Cakmak et al., 1994a,b). TTC can receive electrons directly from the electron transport link, and its reduction is directly related to mitochondrial respiration rate (Comas et al., 2000; Ruf and Brunner, 2003). Therefore, root vitality is the use of dehydrogenase activity in the respiratory chain to reflect the physiological indicators of root life activities. It is also a reflection of the strength of respiration. In this study, N deficiency and K deficiency significantly decreased the root vitality and the O_2 consuming rate, representing the root respiration rate. Fontana et al. (2020) also found that K deficiency can cause the decline of root vitality and root respiration rate in cotton seedling planted in a low K solution that contained KCl (0.02 mM) for 8 days. The study in wheat showed that low N stress weakens the key enzyme activities of the NADP dehydrogenase system in roots. The decrease of NADPH synthesis affects the respiratory and metabolic activities of roots (Zhou et al., 2018). These results showed that N deficiency and K deficiency blocked root metabolism, decreased absorption capacity, and inhibited root growth, resulting in decreased root vitality.

miRNA Response to N and K Deficiency in Plants

N and K deficiency altered the expression of certain miRNAs and miRNA-mediated genes. There were differences in the miRNA expression patterns between the plants cultivated in N deficiency nutrient solution and those cultivated in K deficiency nutrient solution. Nguyen et al. (2015) observed that under N deficiency stress, the expression of miR156, miR160, and miR171 was induced, and the expression of miR169, miR172, miR319, miR396, and miR399 were reduced in *Arabidopsis* roots, while the expression of these miRNAs in maize roots was opposite. Therefore, it can be seen that the miRNA expression patterns varied with crop varieties and N deficiency. In this study, all 20 tested miRNAs, except for miR160, miR164, miR171, miR393, and miR827, were upregulated after 4 and 8 days of K deficiency treatments (**Figure 5B**). These may be the molecular mechanism of the adaptive response of peanut roots to N and K deficiency.

Previous studies have shown that miRNAs regulate genes encoding AUXIN RESPONSE FACTORS (ARFs) after transcription (Williams et al., 2005; Yuan et al., 2019). ARFs can specifically combine with auxin response elements in the auxin response gene promoter region to activate or inhibit gene expression, thus regulating plant growth and development (Hagen and Guilfoyle, 2002). Conserved miR160 regulates root growth and gravitational properties by negatively regulating three ARFs (ARF10, 16, and 17). In plants, overexpressing mir160c, ARF10, and ARF16 mRNA expression was decreased. The roots were short and attractive, with tumor-like apex related to uncontrolled cell division of apical meristem and failure of small columnar cell differentiation (Wang et al., 2005). The conserved miR167 negatively regulates auxin signaling by targeting ARF6 and ARF8. Under the condition of high nitrate, the expression level of miR167 in the root of *Arabidopsis* was decreased, allowing the accumulation of ARF8 in the pericyclic cell and lateral root cap, thereby stimulating the auxin signal, promoting lateral root formation, but inhibiting root elongation (Gifford et al., 2008). Auxin responsive miR390 is specifically expressed in the basal part of lateral root primordia and the potential vascular parenchymal cells and act as a regulatory factor by triggering the biogenesis of TAS3-derived transacting short-interfering RNAs (tasiRNAs; Marin et al., 2010). These tasiRNAs can repress the expression of ARF2, ARF3, and ARF4, thus promoting the development progression of lateral root (Marin et al., 2010; Du and Scheres, 2017). In this study, miR160, miR167, and miR390 downregulated on the 4th day and upregulated on the 8th day of N deficiency treatment. While ARF upregulated on the 4th day and downregulated on the 8th day of N deficiency treatment. miR160 upregulated on the 4th day and downregulated on the 8th day of K deficiency treatment. miR167 was nearly 6.32- and 1.67-fold upregulated on the 4th and 8th days of K deficiency treatment, respectively. The expression of miR167 on the 8th day was significantly lower than that on the 4th day of K deficiency. In addition, miR390 was upregulated on both the 4th and 8th days of K deficiency, and the ARF2 expression increased on both the 4th and 8th days of K deficiency. Thus, the altered expression of miR160, miR167, and miR390/ARF2 may be related to the inhibition of lateral root under N deficiency and the enhancement of lateral root under K deficiency treatment.

In addition to ARF-mediated auxin signal transduction, miRNAs also regulated auxin perception (Yuan et al., 2019). Studies have demonstrated that conserved miR393 targets genes encoding a small number of F-box-containing auxin receptors in many plants, including TRANSPORT INHIBITOR RESPONSE1 (TIR1) and AUXIN SIGNALING F-BOX (AFBs; Yuan et al., 2019), which are important for the growth of both primary root and lateral root (Vidal et al., 2013). miR393/AFB3 has been considered a nitrate responsive regulatory module that can integrate N and auxin signaling to regulate root growth in plant response to nitrate availability (Vidal et al., 2010, 2013). In this study, miR393 was downregulated on the 4th day and upregulated on the 8th day of N deficiency treatment. The expression of AFB3 was upregulated on the 4th day and further upregulated on the 8th day of N deficiency treatment. The expression pattern of miR393 under K deficiency stress is the opposite of its expression pattern under N deficiency stress. The expression pattern of miR393 was upregulated on the 4th day and downregulated on the 8th day of K deficiency treatment. The expression pattern of AFB3 was the opposite of the expression pattern of miR393 under K deficiency stress. The different changes of miR393/AFB3 under N deficiency and K deficiency conditions may explain the different responses of lateral root number and root length under these two conditions.

miR396 is a conserved miRNA in plants, closely related to plant growth and development (Debernardi et al., 2012; Li and Zhang, 2016). It has been found that miR396 targets the GROWTH REGULATION FACTORS (GRF) gene family and bHLH74, which promote cell proliferation during leaf development (Debernardi et al., 2012). miR396 may regulate root growth by restricting cell proliferation in root apical meristems (Debernardi et al., 2012). In this study, miR396 was significantly upregulated, and its target GRF was significantly downregulated on the 8th day of N deficiency. Thus, the altered expression of miR396/GRF may be related to the inhibition of lateral root under N deficiency treatment. Under K deficiency, miR396 was significantly upregulated on both the 4th and 8th days and compared with the expression on the 4th day, the expression of miR396 on the 8th day was significantly decreased. In contrast, the expression of GRF was significantly upregulated on both the 4th and 8th days of K deficiency. Therefore, the upregulation of GRF could be the reason for the enhancement of root growth in peanut under K deficiency.

Genes of the NAC (NAMATAF-CUC) family are the auxin signal transduction genes responsible for lateral root emergence and have been identified as the target of miR164 (Guo et al., 2005). Plants with low miR164 expression have high NAC1 expression and produced more lateral roots (Guo et al., 2005). In this study, miR164 was downregulated on the 4th day and upregulated on the 8th day of N deficiency. While the expression pattern of miR164 under K deficiency stress is just the opposite of its expression pattern under N deficiency stress. The expression of NAC was upregulated on the 4th day and downregulated on the 8th day of K deficiency. Because NAC transduces auxin signal for lateral root emergence (Guo et al., 2005), the upregulation of NAC under potassium deficiency further indicated that potassium deficiency induced the emergence of lateral roots.

In plants, miR156 targets some SPL (squamosa promoter binding protein-like) genes, which are plant-specific transcription factors in many developmental processes (Gou et al., 2011; Yu et al., 2015). In *Arabidopsis*, 17 members of the *SPL* gene family, 11 of which are regulated by miR156 (Qian et al., 2017). Yu et al. (2015) found that miR156 was differentially expressed in specific cells and tissues of lateral roots and responded to auxin signal transduction pathway by regulating *SPL3*, *SPL9*, and *SPL10* genes, thereby inhibiting the growth of lateral roots, in which SPL10 played a leading role. In the present study, miR156 was nearly 4.3- and 4.6-fold induced on 4th and 8th days of K deficiency treatment. The SPL10 gene was 1.54-fold upregulated on the 4th day and was 0.49-fold downregulated on the 8th day of K deficiency treatment. The upregulated miR156 and the downregulated SPL10 may be the reason for initiating lateral roots under the K deficiency condition. Additionally, the upregulated SPL10 may be the reason for the lower number of lateral roots under the N deficiency condition. Plants overexpressing miR156 produced more lateral roots, while plants with lower miR156 levels had fewer lateral roots (Yu et al., 2015). SPLs can also directly activate miR172 and induce the floral inducer FLOWERING LOCUS (FT) through miR172-mediated AP2 inhibition, promoting plant flowering (Song et al., 2019). Over-expression of miR172 confers early flowering (Wang et al., 2016) and increased nodule numbers in soybean (Wang et al., 2014). A study in *Arabidopsis* suggested that miR172 acts downstream of miR156 and mediated the effect of miR156 on flowering time and the change of vegetative phase (Wu et al., 2009). Further study of the functions of these miRNAs and their regulated gene network will elucidate the molecular mechanism of peanut response to nutrient deficiency, which provides a new strategy for peanut molecular improvement using advanced technology, including the CRISPR/Cas genome editing (Li et al., 2021; Zhang et al., 2021).

CONCLUSION

In this study, both N deficiency and K deficiency caused abnormal growth and development of peanut seedlings. They changed the expression of miRNAs and their target genes related to root development. Under N deficiency condition, the lateral root initiation and emergence inhibition may be related to the upregulation of miR164, miR393, and miR396 and the downregulated AFB3 and GRF (**Figure 8A**). The inhibition of primary root elongation may be associated with the upregulation of miR160 under N deficiency condition. Under the K deficiency condition, the upregulated miR156, miR390, NAC4, ARF2, and AFB3, and the downregulated miR164, miR393, and SPL10 may be involved in the enhancement in the lateral root initiation and emergence (**Figure 8B**). Downregulated miR160 probably contributes to

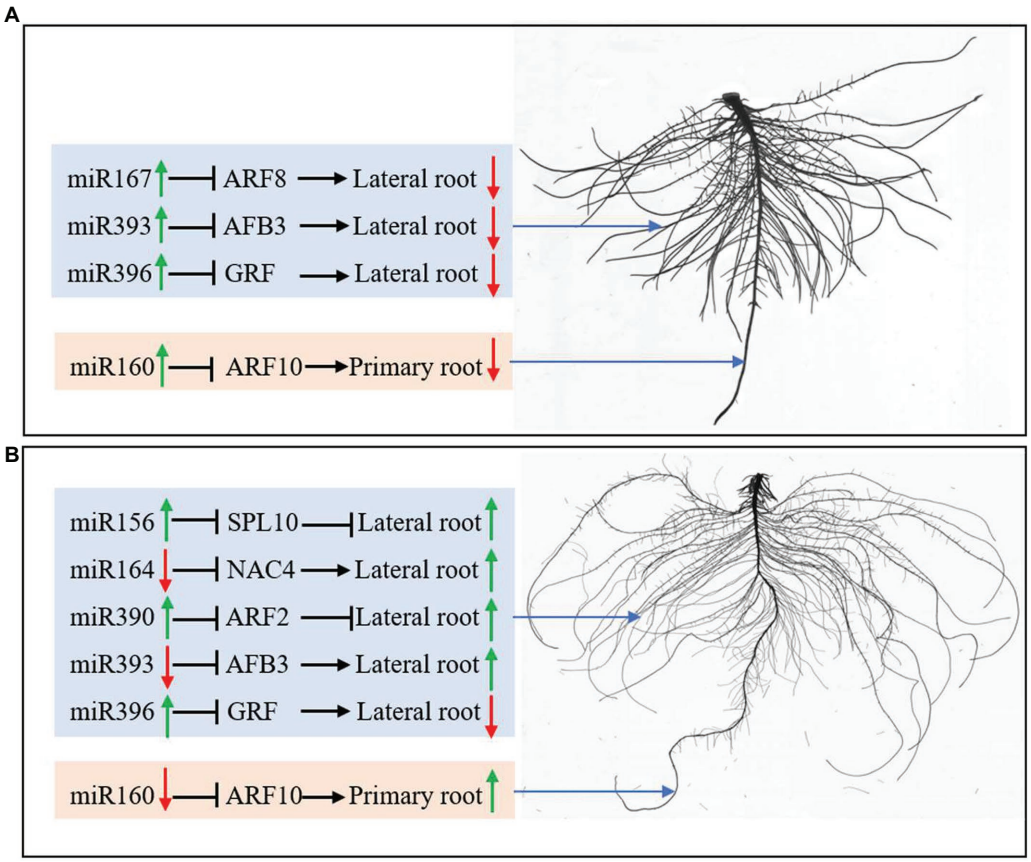

FIGURE 8 | miRNAs regulate root development by controlling protein-coding genes' expression under N deficiency **(A)** and K deficiency **(B)**. The green arrow represents the upregulated expression of miRNAs and the enhanced growth of roots; the red arrow represents the downregulated expression of miRNAs and the inhibited growth of roots. N, nitrogen and K, potassium.

promoting primary root elongation. Overall, the roots of a peanut had different responses to N deficiency and K deficiency stresses, which is potentially due to the miRNAs-mediated pathway and mechanism. In conclusion, the different responses of peanut roots to nitrogen and potassium deficiency stress may be related to miRNA-mediated regulation of root growth and development.

DATA AVAILABILITY STATEMENT

The original contributions presented in the study are included in the article/supplementary material, further inquiries can be directed to the corresponding authors.

AUTHOR CONTRIBUTIONS

LL: data curation, formal analysis, investigation, writing – original draft, and writing – review and editing. QL and WL: data curation and investigation. KD: methodology and investigation. CP: methodology and software. SO: investigation and validation. JL and GW: methodology, data curation, and investigation. JF and TT: investigation. IP: investigation and revision of the manuscript. FL: investigation and software. ZZ: conceptualization, methodology, resources, supervision, funding acquisition, and writing – original draft. YZ: conceptualization, methodology, resources, and supervision. XP: conceptualization, methodology, supervision, and funding acquisition. BZ: conceptualization, methodology, resources, supervision, and funding acquisition. All authors contributed to the article and approved the submitted version.

FUNDING

This work was supported by the Key Science and Technology Special Project of Xinxiang City of China (ZD2020004), the Leading Talent Project in Science and Technology Innovation of Central Plain of China (214200510021), the Program for Innovative Research Team (in Science and Technology) in the University of Henan Province (21IRTSTHN023), and the Key R&D and promotion projects of Henan Province (202102110181 and 212102110070). This project was also supported by the U.S. National Science Foundation (award 1658709 to BZ and XP).

REFERENCES

Almeida, H. J., Pancelli, M. A., Prado, R. M., Cavalcante, V. S., and Cruz, F. J. R. (2015). Effect of potassium on nutritional status and productivity of peanuts in succession with sugarcane. *J. Soil Sci. Plant Nutr.* 15, 1–10. doi: 10.4067/S0718-95162015005000001

Araya, T., Miyamoto, M., Wibowo, J., Suzuki, A., Kojima, S., Tsuchiya, Y. N., et al. (2014). CLE-CLAVATA1 peptide-receptor signaling module regulates the expansion of plant root systems in a nitrogen-dependent manner. *Proc. Natl. Acad. Sci. U. S. A.* 111, 2029–2034. doi: 10.1073/pnas.1319953111

Cakmak, I., Hengeler, C., and Marschner, H. (1994a). Changes in phloem export of sucrose in leaves in response to phosphorus, potassium and magnesium deficiency in bean plants. *J. Exp. Bot.* 45, 1251–1257. doi: 10.1093/jxb/45.9.1251

Cakmak, I., Hengeler, C., and Marschner, H. (1994b). Partitioning of shoot and root dry matter and carbohydrates in bean plants susffering from phosphorus, potassium and magnesium deficiency. *J. Exp. Bot.* 45, 1245–1250. doi: 10.1093/jxb/45.9.1245

Candar-Çakir, B., Arican, E., and Zhang, B. H. (2016). Small RNA and degradome deep sequencing reveals drought- and tissue-specific microRNAs and their important roles in drought-sensitive and -tolerant tomato genotypes. *Plant Biotechnol. J.* 14, 1727–1746. doi: 10.1111/pbi.12533

Chakraborty, K., Bhaduri, D., Meena, H. N., and Kalariya, K. (2016). External potassium (K^+) application improves salinity tolerance by promoting Na^+-exclusion, K^+-accumulation and osmotic adjustment in contrasting peanut cultivars. *Plant Physiol. Biochem.* 103, 143–153. doi: 10.1016/j.plaphy.2016.02.039

Comas, L. H., Eissenstat, D. M., and Lakso, A. N. (2000). Assessing root death and root system dynamics in a study of grape canopy pruning. *New Phytol.* 147, 171–178. doi: 10.1046/j.1469-8137.2000.00679.x

Debernardi, J. M., Rodriguez, R. E., Mecchia, M. A., and Palatnik, J. F. (2012). Functional specialization of the plant miR396 regulatory network through distinct microRNA-target interactions. *PLoS Genet.* 8:e1002419. doi: 10.1371/journal.pgen.1002419

Dolan, L., and Davies, J. (2004). Cell expansion in roots. *Curr. Opin. Plant Biol.* 7, 33–39. doi: 10.1016/j.pbi.2003.11.006

Du, Y., and Scheres, B. (2017). Lateral root formation and the multiple roles of auxin. *J. Exp. Bot.* 69, 155–167. doi: 10.1093/jxb/erx223

Fontana, J. E., Wang, G., Sun, R., Xue, H., and Pan, X. (2020). Impact of potassium deficiency on cotton growth, development and potential microRNA-mediated mechanism. *Plant Physiol. Biochem.* 153, 72–80. doi: 10.1016/j.plaphy.2020.05.006

Forde, B. G. (2014). Nitrogen signalling pathways shaping root system architecture: an update. *Curr. Opin. Plant Biol.* 21, 30–36. doi: 10.1016/j.pbi.2014.06.004

Gifford, M. L., Alexis, D., Gutierrez, R. A., Coruzzi, G. M., and Birnbaum, K. D. (2008). Cell-specific nitrogen responses mediate developmental plasticity. *Proc. Natl. Acad. Sci. U. S. A.* 105, 803–808. doi: 10.1073/pnas.0709559105

Gou, J. Y., Felippes, F. F., Liu, C. J., Weigel, D., and Wang, J. W. (2011). Negative regulation of anthocyanin biosynthesis in *Arabidopsis* by a miR156-targeted SPL transcription factor. *Plant Cell* 23, 1512–1522. doi: 10.1105/tpc.111.084525

Gruber, B. D., Giehl, R. F., Friedel, S., and von Wirén, N. (2013). Plasticity of the *Arabidopsis* root system under nutrient deficiencies. *Plant Physiol.* 163, 161–179. doi: 10.1104/pp.113.218453

Guilhem, D., Caroline, J., Stamatis, R., Polydefkis, H., and Liam, D. (2003). AKT1 and TRH1 are required during root hair elongation in *Arabidopsis*. *J. Exp. Bot.* 54, 781–788. doi: 10.1093/jxb/erg066

Guo, H., Xie, Q., Fei, J., and Chua, N. (2005). MicroRNA directs mRNA cleavage of the transcription factor *NAC1* to downregulate auxin signals for *Arabidopsis* lateral root development. *Plant Cell* 17, 1376–1386. doi: 10.1105/tpc.105.030841

Hagen, G., and Guilfoyle, T. (2002). Auxin-responsive gene expression: genes, promoters and regulatory factors. *Plant Mol. Biol.* 49, 373–385. doi: 10.1023/A:1015207114117

Hawkesford, M., Horst, W., Kichey, T., Lambers, H., Schjoerring, J., Mller, I. S., et al. (2012). "Functions of macronutrients," in *Marschners Mineral Nutrition of Higher Plants*. ed. P. Marschner (Amsterdam, Netherlands: Elsevier), 135–189.

Helmy, A. M., and Ramadan, M. F. (2014). Yield quality parameters and chemical composition of peanut as affected by potassium and gypsum applications under foliar spraying with boron. *Commun. Soil Sci. Plant Anal.* 45, 2397–2412. doi: 10.1080/00103624.2014.929700

Jung, J. Y., Shi, R., and Schachtman, D. P. (2009). Ethylene mediates response and tolerance to potassium deprivation in *Arabidopsis*. *Plant Cell* 21, 607–621. doi: 10.1105/tpc.108.063099

Kant, S. (2018). Understanding nitrate uptake, signaling and remobilisation for improving plant nitrogen use efficiency. *Semin. Cell Dev. Biol.* 74, 89–96. doi: 10.1016/j.semcdb.2017.08.034

Kellermeier, F., and Amtmann, C. A. (2013). Natural variation of *Arabidopsis* root architecture reveals complementing adaptive strategies to potassium starvation. *Plant Physiol.* 161, 1421–1432. doi: 10.1104/pp.112.211144

Kellermeier, F., Armengaud, P., Seditas, T. J., Danku, J., and Salt, D. E. (2014). Analysis of the root system architecture of *Arabidopsis* provides a quantitative readout of crosstalk between nutritional signals. *Plant Cell* 26, 1480–1496. doi: 10.1105/tpc.113.122101

Kuicheski, F. R., Correa, R., Gomes, I., de Lima, J., and Margis, R. (2015). NPK macronutrients and microRNA homeostasis. *Front. Plant Sci.* 6:451. doi: 10.3389/fpls.2015.00451

Leigh, R. A., and Wyn Jones, R. G. (1984). A hypothesis relating critical potassium concentrations for growth and distribution and functions of this ion in the plant cell. *New Phytol.* 97, 1–13. doi: 10.1111/j.1469-8137.1984.tb04103.x

Li, C., Brant, E., Budak, H., and Zhang, B. H. (2021). CRISPR/Cas: a Nobel prize award-winning precise genome editing technology for gene therapy and crop improvement. *J. Zhejiang Univ. Sci. B* 22, 253–284. doi: 10.1631/jzus.B2100009

Li, C., and Zhang, B. H. (2016). MicroRNAs in control of plant development. *J. Cell. Physiol.* 231, 303–313. doi: 10.1002/jcp.25125

Luo, L., Zhang, Y., and Xu, G. (2020). How does nitrogen shape plant architecture? *J. Exp. Bot.* 15, 4415–4427. doi: 10.1093/jxb/eraa187

Maathuis, F. J. M., and Sanders, D. (1996). Mechanisms of potassium absorption by higher plant roots. *Physiol. Plant.* 96, 158–168. doi: 10.1111/j.1399-3054.1996.tb00197.x

Malamy, J. E. (2005). Intrinsic and environmental response pathways that regulate root system architecture. *Plant Cell Environ.* 28, 67–77. doi: 10.1111/j.1365-3040.2005.01306.x

Marin, E., Jouannet, V., Herz, A., Lokerse, A. S., Weijers, D., Vaucheret, H., et al. (2010). miR390, *Arabidopsis TAS3* tasiRNAs, and their *AUXIN RESPONSE FACTOR* targets define an autoregulatory network quantitatively regulating lateral root growth. *Plant Cell* 22, 1104–1117. doi: 10.1105/tpc.109.072553

Mohd-Radzman, N. A., Djordjevic, M. A., and Imin, N. (2013). Nitrogen modulation of legume root architecture signaling pathways involves phytohormones and small regulatory molecules. *Front. Plant Sci.* 4:385. doi: 10.3389/fpls.2013.00385

Nguyen, G., Rothstein, S., Spangenberg, G., and Kant, S. (2015). Role of microRNAs involved in plant response to nitrogen and phosphorous limiting conditions. *Front. Plant Sci.* 6:629. doi: 10.3389/fpls.2015.00629

Omara, P., Aula, L., Oyebiyi, F., and Raun, W. R. (2019). World cereal nitrogen use efficiency trends: review and current knowledge. *Agrosyst. Geosci. Environ.* 2, 1–8. doi: 10.2134/age2018.10.0045

Pritchard, J. (1994). The control of cell expansion in roots. *New Phytol.* 127, 3–26. doi: 10.1111/j.1469-8137.1994.tb04255.x

Qian, M. J., Ni, J. B., Niu, Q. F., Bai, S. L., Bao, L., Li, J. Z., et al. (2017). Response of miR156-SPL module during the red peel coloration of bagging-treated Chinese sand pear (*Pyrus pyrifolia* Nakai). *Front. Physiol.* 8:550. doi: 10.3389/fphys.2017.00550

Ruf, M., and Brunner, I. (2003). Vitality of tree fine roots: reevaluation of the tetrazolium test. *Tree Physiol.* 23, 257–263. doi: 10.1093/treephys/23.4.257

Salvagiotti, F., Cassman, K. G., Specht, J. E., Walters, D. T., Weiss, A., and Dobermann, A. (2008). Nitrogen uptake, fixation and response to fertilizer N in soybeans: a review. *Field Crop Res.* 108, 1–13. doi: 10.1016/j.fcr.2008.03.001

Sharma, L. K., and Bali, S. K. (2018). A review of methods to improve nitrogen use efficiency in agriculture. *Sustainability* 1:51. doi: 10.3390/su10010051

Song, X., Li, Y., Cao, X., and Qi, Y. (2019). MicroRNAs and their regulatory roles in plant—environment interactions. *Annu. Rev. Plant Biol.* 70, 489–525. doi: 10.1146/annurev-arplant-050718-100334

Sun, C., Yu, J., and Hu, D. (2017). Nitrate: a crucial signal during lateral roots development. *Front. Plant Sci.* 8:485. doi: 10.3389/fpls.2017.00485

Sunkar, R., Li, Y. F., and Jagadeeswaran, G. (2012). Functions of microRNAs in plant stress responses. *Trends Plant Sci.* 17, 196–203. doi: 10.1016/j.tplants.2012.01.010

Sustr, M., Soukup, A., and Tylova, E. (2019). Potassium in root growth and development. *Plants* 8:435. doi: 10.3390/plants8100435

Thornburg, T. E., Liu, J., Li, Q., Xue, H., and Pan, X. (2020). Potassium deficiency significantly affected plant growth and development as well as microRNA-mediated mechanism in wheat (*Triticum aestivum* L.). *Front. Plant Sci.* 11:1219. doi: 10.3389/fpls.2020.01219

Vidal, E. A., Araus, V., Lu, C., Parry, G., and Green, P. J. (2010). Nitrate-responsive Mir393/AFB3 regulatory module controls root system architecture in *Arabidopsis thaliana*. *Proc. Natl. Acad. Sci. U. S. A.* 7, 4477–4482. doi: 10.1073/pnas.0909571107

Vidal, E. A., Moyano, T. C., Riveras, E., Contreras-Lopez, O., and Gutierrez, R. A. (2013). Systems approaches map regulatory networks downstream of the auxin receptor AFB3 in the nitrate response of *Arabidopsis thaliana* roots. *Proc. Natl. Acad. Sci. U. S. A.* 110, 12840–12845. doi: 10.1073/pnas.1310937110

Walker, D., Black, C., and Miller, A. (1998). The role of cytosolic potassium and ph in the growth of barley roots. *Plant Physiol.* 118, 957–964. doi: 10.1104/pp.118.3.957

Wang, Y., Kang, Y., Wang, M., and Zhao, C. (2013). Effects of potassium application on the accumulated nitrogen source and yield of peanut. *J. Nucl. Agric. Sci.* 27, 126–131.

Wang, T., Sun, M. Y., Wang, X. S., Li, W. B., and Li, Y. G. (2016). Over-expression of GmGIa-regulated soybean miR172a confers early flowering in transgenic *Arabidopsis thaliana*. *Int. J. Mol. Sci.* 17:645. doi: 10.3390/ijms17050645

Wang, J., Wang, L., Mao, Y., Cai, W., Xue, H., and Chen, X. (2005). Control of root cap formation by microRNA-targeted auxin response factors in *Arabidopsis*. *Plant Cell* 17, 2204–2216. doi: 10.1105/tpc.105.033076

Wang, Y., Wang, L., Zou, Y., Chen, L., Cai, Z., Zhang, S., et al. (2014). Soybean miR172c targets the repressive AP_2 transcription factor NNC1 to activate $ENOD_{40}$ expression and regulate nodule initiation. *Plant Cell* 26, 4782–4801. doi: 10.1105/tpc.114.131607

Wang, Y., and Wu, W. (2009). Molecular genetic mechanism of high efficient potassium uptake in plants. *Chin. Bull. Bot.* 44, 27–36. doi: 10.3969/j.issn.1674-3466.2009.01.003

Williams, L., Carles, C. C., Osmont, K. S., and Fletcher, J. C. (2005). A database analysis method identifies an endogenous transacting short-interfering RNA that targets the *Arabidopsis* ARF2, ARF3, and ARF4 genes. *Proc. Natl. Acad. Sci. U. S. A.* 102, 9703–9708. doi: 10.1073/pnas.0504029102

Wu, G., Park, M. Y., Conway, S. R., Wang, J. W., Weigel, D., and Poethig, R. S. (2009). The sequential action of miR156 and miR172 regulates developmental timing in *Arabidopsis*. *Cell* 138, 750–759. doi: 10.1016/j.cell.2009.06.031

Xie, X., Li, X. Q., Zebarth, B. J., Niu, S., Tang, R., Tai, H. H., et al. (2018). Rapid screening of potato cultivars tolerant to nitrogen deficiency using a hydroponic system. *Am. J. Potato Res.* 95, 157–163. doi: 10.1007/s12230-017-9621-1

Yu, N., Niu, Q., Ng, K., and Chua, N. (2015). The role of miR156/SPLs modules in *Arabidopsis* lateral root development. *Plant J.* 83, 673–685. doi: 10.1111/tpj.12919

Yu, J. J., Su, D., Yang, D., Dong, T., Tang, Z., Li, H., et al. (2020). Chilling and heat stress-induced physiological changes and microRNA-related mechanism in sweetpotato (*Ipomoea batatas* L.). *Front. Plant Sci.* 11:687. doi: 10.3389/fpls.2020.00687

Yuan, W., Suo, J., Shi, B., Zhou, C., Bai, B., Bian, H., et al. (2019). The barley miR393 has multiple roles in regulation of seedling growth, stomatal density, and drought stress tolerance. *Plant Physiol. Biochem.* 142, 303–311. doi: 10.1016/j.plaphy.2019.07.021

Zhang, B. (2015). MicroRNA: a new target for improving plant tolerance to abiotic stress. *J. Exp. Bot.* 66, 1749–1761. doi: 10.1093/jxb/erv013

Zhang, J. L., Geng, Y., Guo, F., Li, X. G., and Wan, S. B. (2020). Research progress on the mechanism of improving peanut yield by single-seed precision sowing. *J. Integr. Agric.* 19, 1919–1927. doi: 10.1016/S2095-3119(19)62763-2

Zhang, B. H., Pan, X. P., Cobb, G. P., and Anderson, T. A. (2006). Plant microRNA: a small regulatory molecule with big impact. *Dev. Biol.* 289, 3–16. doi: 10.1016/j.ydbio.2005.10.036

Zhang, B. H., and Unver, T. (2018). A critical and speculative review on microRNA technology in crop improvement: current challenges and future directions. *Plant Sci.* 274, 193–200. doi: 10.1016/j.plantsci.2018.05.031

Zhang, D., Zhang, Z. Y., Unver, T., and Zhang, B. H. (2021). CRISPR/Cas: a powerful tool for gene function study and crop improvement. *J. Adv. Res.* 29, 207–221. doi: 10.1016/j.jare.2020.10.003

Zhao, S., Zhang, M. L., Ma, T. L., and Wang, Y. (2016). Phosphorylation of ARF2 relieves its repression of transcription of the K^+ transporter gene HAK5 in response to low potassium stress. *Plant Cell* 28, 3005–3019. doi: 10.1105/tpc.16.00684

Zhou, Y., Yang, X., Zhou, S., Wang, Y., Yang, R., Xu, F., et al. (2018). Activities of key enzymes in root NADP-dehydrogenase system and their relationships with root vigor and grain yield formation in wheat. *Sci. Agric. Sin.* 51, 2060–2071. doi: 10.3864/j.issn.0578-1752.2018.11.004

Conflict of Interest: The authors declare that the research was conducted in the absence of any commercial or financial relationships that could be construed as a potential conflict of interest.

frontiers in Plant Science

ORIGINAL RESEARCH
published: 06 August 2021
doi: 10.3389/fpls.2021.686698

Genome-Wide Identification of *TCP* Transcription Factors Family in Sweet Potato Reveals Significant Roles of miR319-Targeted TCPs in Leaf Anatomical Morphology

Lei Ren[1,2†], Haixia Wu[1†], Tingting Zhang[1,2†], Xinyu Ge[1], Tianlong Wang[1], Wuyu Zhou[1], Lei Zhang[1,2], Daifu Ma[3*] and Aimin Wang[1,2*]*

[1] Institute of Integrative Plant Biology, School of Life Sciences, Jiangsu Normal University, Xuzhou, China, [2] Jiangsu Key Laboratory of Phylogenomics & Comparative Genomics, School of Life Sciences, Jiangsu Normal University, Xuzhou, China, [3] Xuzhou Institute of Agricultural Sciences in Jiangsu Xuhuai District, Key Laboratory for Biology and Genetic Breeding of Sweetpotato (Xuzhou), Ministry of Agriculture/Jiangsu Xuzhou Sweetpotato Research Center, Xuzhou, China

OPEN ACCESS

Edited by:
Turgay Unver,
FicusBio, Turkey

Reviewed by:
Anja Schneider,
Ludwig Maximilian University of Munich, Germany
Huseyin Tombuloglu,
Imam Abdulrahman Bin Faisal University, Saudi Arabia

***Correspondence:**
Aimin Wang
aiminwang@jsnu.edu.cn
Daifu Ma
daifuma@163.com
Lei Zhang
leizhang@jsnu.edu.cn

† These authors have contributed equally to this work

Specialty section:
This article was submitted to Plant Physiology, a section of the journal Frontiers in Plant Science

Received: 27 March 2021
Accepted: 21 June 2021
Published: 06 August 2021

Citation:
Ren L, Wu H, Zhang T, Ge X, Wang T, Zhou W, Zhang L, Ma D and Wang A (2021) Genome-Wide Identification of TCP Transcription Factors Family in Sweet Potato Reveals Significant Roles of miR319-Targeted TCPs in Leaf Anatomical Morphology. Front. Plant Sci. 12:686698. doi: 10.3389/fpls.2021.686698

Plant-specific TCP transcription factors play vital roles in the controlling of growth, development, and the stress response processes. Extensive researches have been carried out in numerous species, however, there hasn't been any information available about *TCP* genes in sweet potato (*Ipomoea batatas* L.). In this study, a genome-wide analysis of *TCP* genes was carried out to explore the evolution and function in sweet potato. Altogether, 18 *IbTCPs* were identified and cloned. The expression profiles of the *IbTCPs* differed dramatically in different organs or different stages of leaf development. Furthermore, four CIN-clade *IbTCP* genes contained miR319-binding sites. Blocking *IbmiR319* significantly increased the expression level of *IbTCP11/17* and resulted in a decreased photosynthetic rate due to the change in leaf submicroscopic structure, indicating the significance of IbmiR319-targeted *IbTCPs* in leaf anatomical morphology. A systematic analyzation on the characterization of the *IbTCPs* together with the primary functions in leaf anatomical morphology were conducted to afford a basis for further study of the *IbmiR319/IbTCP* module in association with leaf anatomical morphology in sweet potato.

Keywords: *Ipomoea batatas* L., TCP transcription factors, miR319, chloroplast development, expression analysis

INTRODUCTION

TCP transcription factors (TFs) belong to a small family of plant-specific TFs (Yin et al., 2018) named after its initial members TEOSINTE BRANCHED1 (TB1) in *Zea mays* L. (Doebley et al., 1997), CYCLOIDEA (CYC) in *Antirrhinum majus* L. (Luo et al., 1996), and PROLIFERATING CELL FACTORS 1 and 2 (PCF1 and PCF2) in *Oryza sativa* L. (Kosugi and Ohashi, 1997). TCPs have been ascertained in numerous plant species, such as *Medicago truncatula* Gaertn. (Wang et al., 2018), *Gossypium barbadense* L. (Zheng et al., 2018), *Citrullus lanatus* (Thunb.) Matsum. and Nakai (Shi et al., 2016), *Malus domestica* Borkh. (Xu et al., 2014), *Cucumis sativus* L. (Wei et al., 2014), *Solanum tuberosum* L. (Bao et al., 2019; Wang et al., 2019b), *Solanum lycopersicum* L.

(Parapunova et al., 2014), *Populus euphratica* Oliv. (Ma et al., 2016), *Z. mays* (Chai et al., 2017), and *Panicum virgatum* L. (Zheng et al., 2019). Despite the wide-ranging identification of TCPs, just a few of them have been intensively studied. A non-canonical basic-helix-loop-helix (bHLH) motif was at the N-terminal (about 59 amino acids in length) of all the TCP TFs, commonly referred to as the TCP domain. The TCP domain probably associated with the modulation of DNA binding (Kosugi and Ohashi, 2002) as well as protein–protein interactions (Dhaka et al., 2017). Based on the amino acid residue sequences of the TCP domain, TCPs can be categorized into two classes. For class I, it also referred to as the PCF or TCP-P class, while class II referred to the TCP-C class. The consensus DNA-binding site of class I TCPs is GGNCCCAC, however, which of class II is GTGGNCCC (Kosugi and Ohashi, 2002). Furthermore, class II was categorized into two different subclasses: CIN and CYC/TB1. The R domain rich in arginine with unknown function is present in all members of CYC/TB1 and probably mediating protein interactions through a coiled coil (Lupas et al., 1991; Cubas et al., 1999).

Increasing experimental evidence has showed that *TCPs* play a versatile regulatory role at the different stage of plant growth and development, for instance in leaf morphogenesis (Palatnik et al., 2003), trichome formation (Vadde et al., 2018), flower and fruit development (Nag et al., 2009; Koyama et al., 2011), and hormone biosynthesis, as well as in the response to varies stresses (Danisman, 2016; Zhang et al., 2018; Bao et al., 2019; Liu et al., 2019). Twenty-four *AtTCPs* have been identified in *A. thaliana*. AtTCP18, a member of the CYC/TB1 subgroup, regulated two florigen proteins (FT and TSF) to repress the switching from axillary meristems to premature floral (Niwa et al., 2013). AtTCP21 regulated the transcription of *TOC1* and suppresses the expression of *CCA1* to control the circadian clock (Pruneda-Paz et al., 2009; Giraud et al., 2010). Intriguingly, TCP regulated plant growth and development mainly by regulating the biosynthesis of bioactive substances, especially auxin (Challa et al., 2019), ethylene (Liu et al., 2019), gibberellins (Ferrero et al., 2019), brassinosteroids (Guo et al., 2010), jasmonic acid (Danisman et al., 2012), and flavonoids (Viola et al., 2016; Chahel et al., 2019). AtTCP14/15 directly interacted with *GA20ox1*, a key gene in gibberellin biosynthesis, to control the length of petiole and hypocotyl (Ferrero et al., 2019). In addition, AtTCP15 also directly activates the *SAUR63* gene subfamily to participate in gibberellin-dependent stamen filament elongation (Gastaldi et al., 2020). AtTCP15 also serves as a repressor of anthocyanin accumulation by influencing the expression of anthocyanin biosynthesis genes and upstream transcriptional regulators (Viola et al., 2016).

MicroRNAs (miRNAs) are small single-stranded, non-coding RNAs that are typically 20–24 nucleotides (nt) in length. Usually, miRNAs regulate target gene expression through mRNA cleavage at the post-transcriptional level or translational repression (Bartel, 2009; Taylor et al., 2014; Cui et al., 2017). Since most of the target genes of miRNAs are TFs, which can realize the cascade amplification of signals through transcriptional regulation of their target genes, miRNAs have gradually become a potential target gene for crop improvement due to their function in plant growth, development (Axtell et al., 2007), and stress response (Silvestri et al., 2019; Wang et al., 2019a; Kang et al., 2020). In *Arabidopsis*, eight CIN-like *TCP* genes out of 24 *AtTCPs*, including miRJAW–targeted *AtTCP2*, *AtTCP3*, *AtTCP4*, *AtTCP10,* and *AtTCP24*, as well as miRJAW–resistant *AtTCP5*, *AtTCP13*, and *AtTCP17*, were found to chord with different pathways to regulate leaf development (Palatnik et al., 2003; Koyama et al., 2007). The down-regulated expression of *AtTCP2/4* caused by miR319 target-cleavage resulted in serrated leaves (Palatnik et al., 2003). In switchgrass, miR319 negatively regulated *PvTCPs* to promote ethylene accumulation and enhance salt tolerance (Liu et al., 2019). In cotton, high levels of *GhTCP4*, the target of miR319, repressed a homeobox-containing factor, *GhHOX3* transcriptional activity, to promote the secondary cell wall biosynthetic pathway in fiber cells, resulting in shorter fibers and thicker walls (Cao et al., 2020).

Allohexaploid sweet potato, a major global root and tuber crop, is a significant component as to subsistence agriculture because of its capability to guarantee food security and improving nutrition status regionally (Liu, 2014). However, due to the largeness and complexity of the genome, research on the molecular genetics of sweet potato has lagged behind that of other crops, such as rice and potato. Recently, its whole genome was sequenced (Yang et al., 2017). Additionally, its diploid relative wild species *Ipomoea trifida* (Kunth) G. Don and *Ipomoea triloba* L. have also been sequenced (Wu et al., 2018). These genomic sequences can serve as a reference for the hexaploid sweet potato genome. As we still know little about the *TCPs* family in sweet potato, an analysis concerning *TCP* gene family in sweet potato was performed globally in the present study. Eighteen *IbTCP* genes were ascertained and cloned, and phylogenetic relationships, chromosomal locations, and tissue-specific expression were carried out. Furthermore, we found that the transcription patterns of *IbTCPs* discrepant during leaf development. *IbTCP11* and *IbTCP17* were significantly up-regulated in the mature leaves. Blocking IbmiR319 led to an elongated chloroplast and decreased net photosynthetic rate, which further confirmed the critical roles of IbmiR319-targeted *IbTCPs* in leaf anatomical morphology. As a result, our data offers detailed information of *IbTCPs* category and helps elucidate the function of *IbTCPs* in leaf anatomical morphology in sweet potato.

MATERIALS AND METHODS

Plant Materials

The wild-type (WT) sweet potato (*Ipomoea batatas* L.) cultivar "Xushu 22" (Xu22), developed by the Sweet Potato Research Institute of the China Agriculture Academy of Science, was used for *IbTCP* gene cloning. MIM319, overexpressing an artificial IbmiR319 target mimicry to sequester the normal expression of native IbmiR319, was generated using an *Agrobacterium*-mediated embryogenic calli transformation. Untransformed (WT) and transgenic plants transplanted and planted as described before (Yang et al., 2011). The cuttings of 3–4 cm height plants were transplanted grown into the field at the

experimental station of Jiangsu Normal University (E 117°17.48′, N 34°16.95′, Jiangsu, China) were used for the assessment of the phenotype and agronomic traits. The plants grown in greenhouses were used for RNA extraction, and those grown in the field were used for morphological observations and photosynthesis parameter measurements.

Identification and Evolutionary Analysis

The TCP protein sequences of *Arabidopsis* and rice retrieved from the database PlantTFDB[1] or TAIR[2] were used to perform protein to protein BLASTP searching with the *e*-value of 10^{-5} in the *I. batatas* genome database[3] and its two wild ancestors (*I. trifida* and *I. triloba*) genomics database.[4] All sequences were further validated by the conserved domains database (CDD).[5] We named *IbTCP1* to *IbTCP18* in the light of their allocations in the genome and relative orders on each chromosome. To study the evolutionary relationships of IbTCPs, Clustal X 2.0 was used to align the entire protein sequences of TCPs from sweet potato, *Arabidopsis*, and rice, which were then used to construct an evolutionary tree in MEGA 6.0 as described before (Tamura et al., 2013).

Sequence Analysis of IbTCP Genes

Using the ExPASy proteomics server,[6] the molecular weight (MW) and isoelectric points (pI) of the IbTCPs were predicted.[7] The conserved motifs of the IbTCPs were ascertained with CDD and the ExPASy proteomics server.

Subcellular Localization of *IbTCPs*

The coding sequence (CDS) without the termination codon of the *IbTCP11* and *IbTCP17* were amplified through PCR, and then purified and cloned into pCAMBIA2300-35S-eGFP to obtain subcellular localization vectors 35S: IbTCP11-GFP and 35S:GFP-IbTCP17. The *Agrobacterium tumefaciens* EHA105 strain harboring 35S: IbTCP11-GFP or 35S:GFP-IbTCP17 was infected into leaf of *N. benthamiana*. The IbTCP-GFP fusion proteins were detected as described before (Wang et al., 2018). The sequences of primers were also listed in **Supplementary Table 1**.

Identification of IbmiR319 and Prediction of IbmiR319 Target Genes

The sequence of IbmiR319 was acquired from our microRNA library of sweet potato based on high-throughput sequencing (Xie et al., 2017; Tang et al., 2020). To forecast the target sites of IbmiR319, the CDS of the *IbTCPs* was analyzed using the psRNATarget online tool.[8]

[1]http://planttfdb.gao-lab.org/

[2]https://www.arabidopsis.org/

[3]http://public-genomes-ngs.molgen.mpg.de/SweetPotato/

[4]http://sweetpotato.plantbiology.msu.edu/

[5]https://www.ncbi.nlm.nih.gov/Structure/cdd/wrpsb.cgi

[6]https://prosite.expasy.org/scanprosite/

[7]https://web.expasy.org/compute_pi/

[8]http://plantgrn.noble.org/psRNATarget/home

Plasmid and Agrobacterium-Mediated Sweet Potato Transformation

The miR319 target mimicry vector p35S-MIM319 was constructed as previously described (Franco-Zorrilla et al., 2007). Genetic transformation of sweet potato was implement as previously described by Yang et al. (2011) to obtained the transgenic plant MIM319.

Gene Expression Analysis

qRT-PCR was carried out to check the expression profiles of genes in different tissues, including the shoot buds (Sb), young leaf (YL), mature leaf (ML), stem (S), fibrous roots (FR), pencil roots (PR), and developing storage roots (DR), or leaves at the different developmental stages (L1–L10: the 1st through 10th leaves counted from the stem tip). Total RNAs was extracted from the above samples using TRIzol (Invitrogen) as described before (Meng et al., 2018). The inverse transcription and the *qRT-PCR* were performed as described before (Meng et al., 2018). The *IbActin* gene was used as an internal control. Data from three biological samples were collected, and the mean values were normalized to *IbActin*. NRT (no reverse transcription control) and NTC (no template control) were also implemented for each gene analysis. The $2^{-\Delta\Delta Ct}$ method was used to judge the relative expression level of *IbTCPs* (Livak and Schmittgen, 2001). The sequences for the primers are listed in **Supplementary Table 1**.

Leaf Anatomical Morphology

After 2 months of growth, the third fully-expanded leaf counted from the terminal bud was removed and cross sectioned by hand for optical microscopic examinations and measurement of leaf thickness.

For transmission electron microscopy (TEM) observation, the first fully-expanded fresh leaves were resected and cut into small pieces immediately, fixed with electron microscope fixator (Servicebio, G1102, Wuhan Sevier Biotechnology Co. Ltd.). All the procedure were performed according the described online.[9]

Chlorophyll Content and Photosynthesis Parameter Measurements

The cuttings of WT and MIM319 with four to six expanded leaves transplanted to the field for 4 weeks were used for analysis. The chlorophyll content assay was performed using the third fully-expanded leaves of WT and MIM319 according to the described before (Kuo et al., 2019). The total chlorophyll content was figured out according to the formula in $C_T = 20.29A_{645} - 8.05A_{663}$. C_T: total chlorophyll content. A_{645}, A_{663}: the absorbance of the chlorophyll solution at 645 nm and 663 nm, respectively.

Leaf photosynthesis parameters on the third fully-expanded leaves were scaled using a Li-6400 portable photosynthetic system (Ll-6400, Li-COR) on a sunny day. Ten seedlings per line were scaled.

Chlorophyll fluorescence was measured as described (Kuo et al., 2019). Briefly, after adapting to the dark for 30 min, the

[9]https://www.servicebio.cn/data-detail?id=4305&code=DJSYBG

F_v/F_m values of the third fully-expanded leaves were measured using a Li-6400 system. Ten seedlings per line were measured in total.

RESULTS

Identification and Cloning of the *IbTCP* Gene Family in Sweet Potato

To obtain *TCP* genes in sweet potato, the TCP amino acid sequences of *Arabidopsis* and *O. sativa* were utilized as a reference to BLAST against the hexaploid sweet potato Genome Database, its diploid wild ancestor Sweetpotato Genomics Resource database, and PlantTFDB. After removing the redundant sequences, a total of 18 predicted non-redundant *IbTCP* sequences were identified and further cloned, all of which comprised the conserved TCP domain (**Table 1** and **Figures 1A,B**). Their sequences were listed in **Supplementary Table 2**. The CDS lengths of the *IbTCPs* varied from 396 bp (*IbTCP8*) to 1527 bp (*IbTCP5*). IbTCP8, with 131 amino acid residues (aa), was regarded as the shortest IbTCP, whereas the largest was IbTCP5 with 508 amino acid residues. The MW was in the range of 14.703–52.774 kDa, and the variation of pI is from 5.53 to 9.83 (**Table 1**).

To determine gene allocation pattern on chromosome, investigation of the exact genomic positions of them were carried out. These 18 *IbTCPs* were scattered across 11 chromosomes and two scaffolds of sweet potato (**Table 1** and **Figure 1C**). Among them, the *IbTCPs* on chromosomes 2, 10, and 13 were tightly located on the upper end of the arm, while on chromosome 11, they were located tightly on the lower end of the arm. Chromosome 7 contained the highest number of *IbTCPs*, including *IbTCP7*, *IbTCP8*, *IbTCP9,* and *IbTCP10*. Chromosomes 1 and 14 contained two loci each.

Phylogenetic Analysis and Category of the *IbTCP* Family

A phylogenetic tree was structured aimed to investigating about the categorization and evolutionary relationships of sweet potato TCP proteins. A total of 88 TCP full-length amino acid sequences, including 18 IbTCPs, 31 AtTCPs, 23 ZmTCP, seven OsTCPs, and nine SlTCPs, were assembled to structure a phylogenetic tree using the NJ method with 1000 bootstrap replicates (**Figure 2** and **Supplementary Table 3**). In accordance to the categorization in *Arabidopsis*, the IbTCPs may be divided into two TCP classes as well. Nine IbTCPs comprised Class I, while the other nine pertain to Class II, which could be classified into two subclasses: four members of the CYC/TB1 clade and the five members of the CIN clade (**Figures 1A**, **2**). The results suggested that all the TCPs were evolutionarily conserved.

Conserved Domain Analysis and Recognition Sequence of miR319

To further comprehend the evolutionary relationships of IbTCPs in sweet potato, the domains of the IbTCPs were confirmed using the ScanProsite tool.[10] As expected, all 18 IbTCPs displayed a highly conserved TCP domain that incorporated a bHLH-type motif located near the N-terminal (**Figures 1B**, **3A**). There's a large difference in the components of the loop and helixes I and II between the class I and II. By analyzing the phylogenetic tree and aligning the TCP domains, the IbTCP proteins are anticipated to be categorized into two classes (**Figure 1A**), as has been indicated for all species analyzed up to now. The conserved R domain was only found in IbTCP2, IbTCP7, IbTCP10, IbTCP14, and IbTCP17, all of which are members of Class II (**Figures 1B**, **3B**).

MicroRNA319 (miR319) pertains to one of the most ancient and conserved miRNA families. Previous studies have verified that miR319, targeting TF *TCP* genes, plays important roles in plant growth, morphogenesis, and reproduction (Palatnik et al., 2003; Sun et al., 2017; Cao et al., 2020). The IbmiR319 target sites among the 18 *IbTCPs* were analyzed using psRNATarget online. The putative recognition sites of IbmiR319 were found in *IbTCP1*, *IbTCP11*, *IbTCP16*, and *IbTCP17* (**Figure 3C**). These four *IbTCP* genes all belonged to class II, which corroborates a previous study in *Arabidopsis*. Although mismatches existed at the 3′ end of the IbmiR319 and 5′ end of the targeted *IbTCP*, kernel sequences (3′-GGGAAGUCAGGU-5′) were conserved (**Figure 3C**). These data illustrate that miR319 maintained homologous target interactions in time of the evolution and diversification of plants.

Expression Profiles of *IbTCP* Genes in Different Tissues

To obtain credible information of the growth and developmental functions of *IbTCP* in sweet potato, their organic-specific expression patterns, containing the shoot buds, young leaf, mature leaf, stem, fibrous roots, pencil roots, and developing storage roots, were analyzed by qRT-PCR. As indicated in **Figure 4**, even though all of *IbTCPs* were expressed in all seven tissues tested, there's considerable variation in transcription levels of different genes among different tissues. Generally speaking, the expression levels of *IbTCPs* were relatively low in the belowground organs, whereas constitutively high expression in the aboveground organs examined, especially ten IbTCPs (*IbTCP2*, *IbTCP3*, *IbTCP5*, *IbTCP7, IbTCP8, IbTCP9*, *IbTCP10*, *IbTCP12, IbTCP17,* and *IbTCP19*) showed highly expression levels in the mature leaves. This finding implies that these *IbTCP* genes probably perform different functions during growth and development. Interestingly, the relatively higher expression of all the IbmiR319-targeted CIN subclass *IbTCPs* (*IbTCP1*, *IbTCP11*, *IbTCP16,* and *IbTCP17*) were detected in the shoot bud, young leaf, and mature leaf, while expression levels of the other *IbTCPs* were high mainly in the mature leaf, suggesting that they may play similar or different roles in leaf development.

IbmiR319-Targeted *IbTCPs* Play Vital Roles in Leaf Anatomical Morphology

Leaves, as the major photosynthetic organs of plants, take up a crucial position in plant growth and development. Leaves

[10]https://prosite.expasy.org/prosite.html

TABLE 1 | Characterization of the *IbTCP* family in sweet potato.

Name	CDS	Length (aa)	Type	MW (kDa)	pI	Chromosomes location	TCP domain location	R domain location
IbTCP1	1110	369	CIN	39.748	6.19	chr1: 2912437-2913561	41-99	/
IbTCP2	873	290	CYC/TB1	32.774	9.00	chr1: 13376720-13377604	94-152	193-210
IbTCP3	846	281	CIN	30.752	9.24	chr2: 1303250-1304098	70-128	/
IbTCP4	1236	411	PCF	43.354	7.37	chr3: 5640446-5641595	94-148	/
IbTCP5	1527	508	PCF	52.774	6.93	chr4: 4619412-4620941	130-184	/
IbTCP6	1110	369	PCF	39.187	5.53	chr5: 31785716-31786825	85-139	/
IbTCP7	942	313	CYC/TB1	35.365	6.81	chr7: 2391142-2392071	87-145	184-201
IbTCP8	396	131	PCF	14.703	9.39	chr7: 5690905-5691300	15-69	/
IbTCP9	753	250	PCF	25.885	9.51	chr7: 23186333-23187085	34-88	/
IbTCP10	1284	427	CYC/TB1	47.716	7.61	chr7: 31005038-31006332	82-140	168-185
IbTCP11	1227	408	CIN	44.293	6.27	chr9: 7933602-7938536	41-99	/
IbTCP12	768	255	PCF	26.970	9.83	chr10: 134409-135176	38-92	/
IbTCP13	1260	419	PCF	43.989	7.45	chr11: 40861501-40903635	100-154	/
IbTCP14	1038	345	CYC/TB1	39.199	9.06	chr13: 786394-787434	104-162	208-225
IbTCP15	1458	485	PCF	50.406	5.86	chr14: 3627481-3629689	115-169	/
IbTCP16	1236	411	CIN	44.629	6.31	chr14: 40034341-40035573	41-99	/
IbTCP17	1155	384	CIN	41.319	6.65	scaffold79: 538826-543936	52-110	162-181
IbTCP18	756	252	PCF	26.823	9.56	scaffold13947: 1620-2378	46-100	/

aa: Amino acid; pI: the theoretical isoelectric point of proteins; MW: the theoretical molecular weight of proteins.

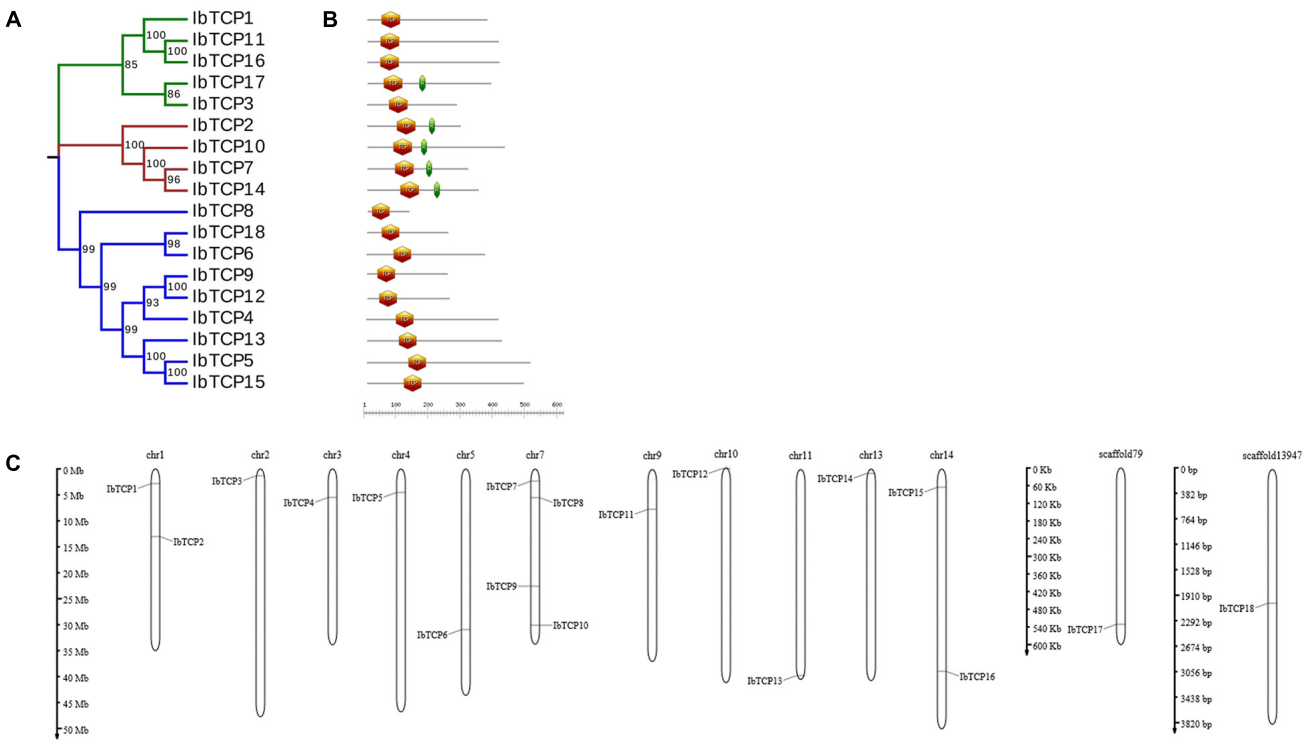

FIGURE 1 | Distribution, phylogenetic tree, and conserved motifs analysis of *IbTCPs* in sweet potato. **(A)** Phylogenetic tree of 18 *IbTCP* genes. The phylogenetic tree was generated using the neighbor-joining method with 1000 bootstrap iterations. Numbers at each node represent the bootstrap values. The blue, green, and red colors indicate the PCF, CIN, and CYC/TB1 clades. **(B)** Conserved motifs analysis. Orange hexagon indicated the TCP domain, and green prism indicated the R domain. The scale refers to the amino acid residues lengths of the TCP proteins. **(C)** Distribution of *IbTCPs* on sweet potato chromosomes or scaffolds. The scale refers to the lengths of the chromosomes or scaffolds in hexaploid sweet potato.

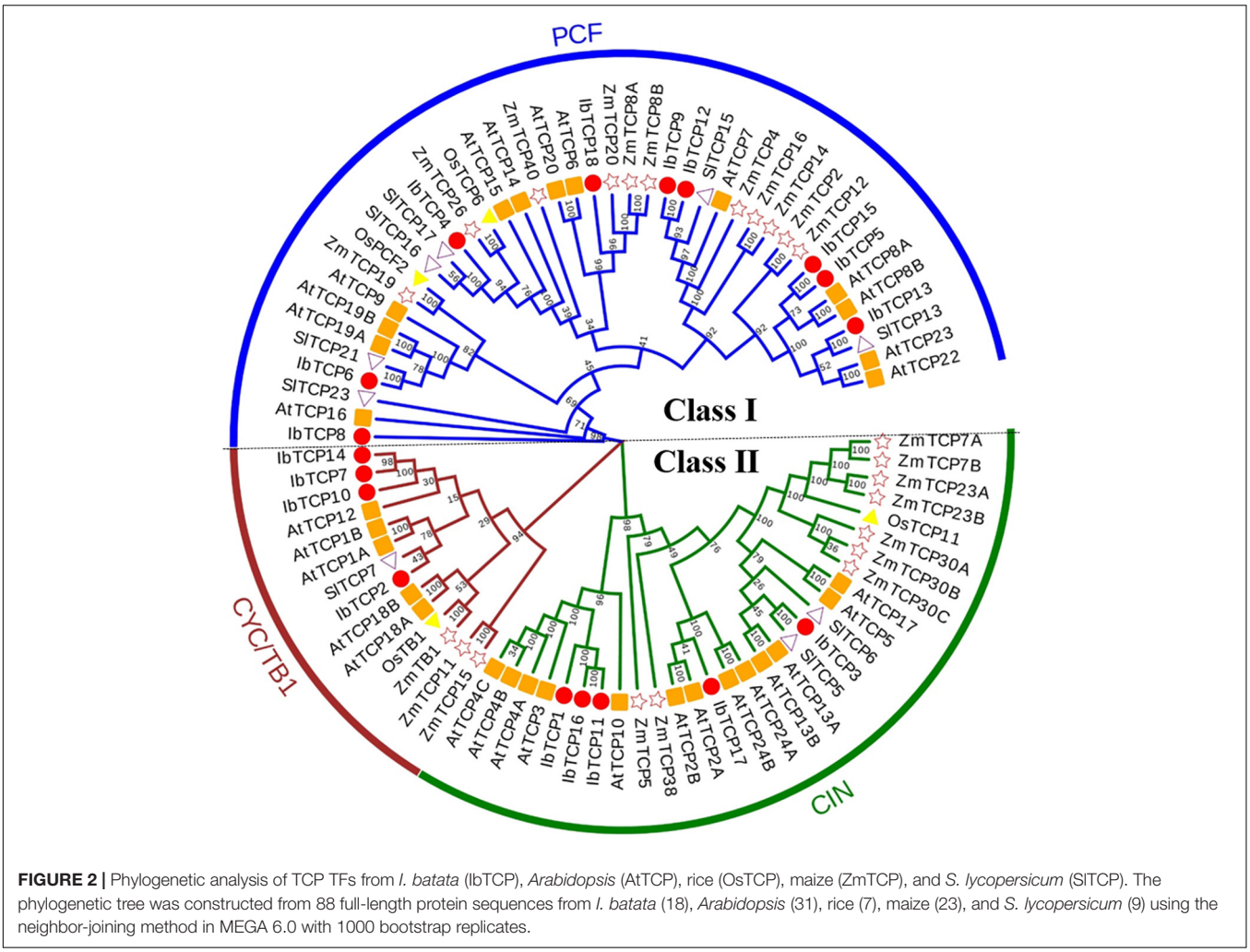

FIGURE 2 | Phylogenetic analysis of TCP TFs from *I. batata* (IbTCP), *Arabidopsis* (AtTCP), rice (OsTCP), maize (ZmTCP), and *S. lycopersicum* (SlTCP). The phylogenetic tree was constructed from 88 full-length protein sequences from *I. batata* (18), *Arabidopsis* (31), rice (7), maize (23), and *S. lycopersicum* (9) using the neighbor-joining method in MEGA 6.0 with 1000 bootstrap replicates.

are also important for tuber crops, since the photosynthetic rate directly affects dry matter accumulation and storage root swelling (Sawada et al., 1999). To understand the function of *IbTCPs* in leaf development, their transcription levels of 18 *IbTCPs* at the different developmental stages of the leaves were investigated (**Figure 5**). The expression levels of most *IbTCPs* exhibited no signification changes at different developmental stages (**Figures 5A,B**). Yet, the transcription levels of IbmiR319-targeted *IbTCPs*, especially *IbTCP11* and *IbTCP17*, presented a significant increase (**Figure 5C**). These data indicate that the IbmiR319-IbTCPs module is likely to associate with leaf development.

For a more thorough evaluation of the duty of the IbmiR319-IbTCPs module, the subcellular localization of the IbmiR319-targeted *IbTCPs* was performed. *IbTCP11* and *IbTCP17* were fused with green fluorescence protein and infiltrated into *N. tabacum* epidermal cells. According to the distribution of green fluorescence signal, these two IbmiR319-target *IbTCPs* were specifically lay within the nuclei, implying that they are functional TFs (**Figure 6**). The IbmiR319 target mimicry vector p35S-MIM319 was then constructed and introduced into WT, and the stable transgenic line MIM319, which blocked IbmiR319, was generated (**Supplementary Figure 1A**). The expression levels of *IbTCP11* and *IbTCP17* were dramatically up-regulated in MIM319 compared with WT (**Supplementary Figure 1B**), indicating that these two *IbTCPs* were the targets of IbmiR319.

The up-regulation of *IbTCP11* and *IbTCP17* caused by blocking IbmiR319 in sweet potato led to dramatic changes in leaf size and leaf shape (**Figures 7A,B**). Quantitative analysis revealed that the width of the third fully-expanded leaves of MIM319 transgenic sweet potato ranged from 14.7 to 18.0 cm, which was dramatically less than that of WT (**Figure 7C**), and the leaf area ranged from 55.50 to 63.25 cm^2, which was also significantly less than that of WT (**Figure 7E**). Conversely, there was no obvious difference in the length of the fully-expanded leaves between MIM319 and WT (**Supplementary Figure 2**). As a result, the ratio of the length to width of MIM319 was greater than that of WT (**Figure 7D**). Taken together, the data indicated that IbmiR319-targeted *IbTCPs* may have conserved functions during leaf development, similar to their functions in *Arabidopsis* and rice (Palatnik et al., 2003; Nag et al., 2009; Yang et al., 2013).

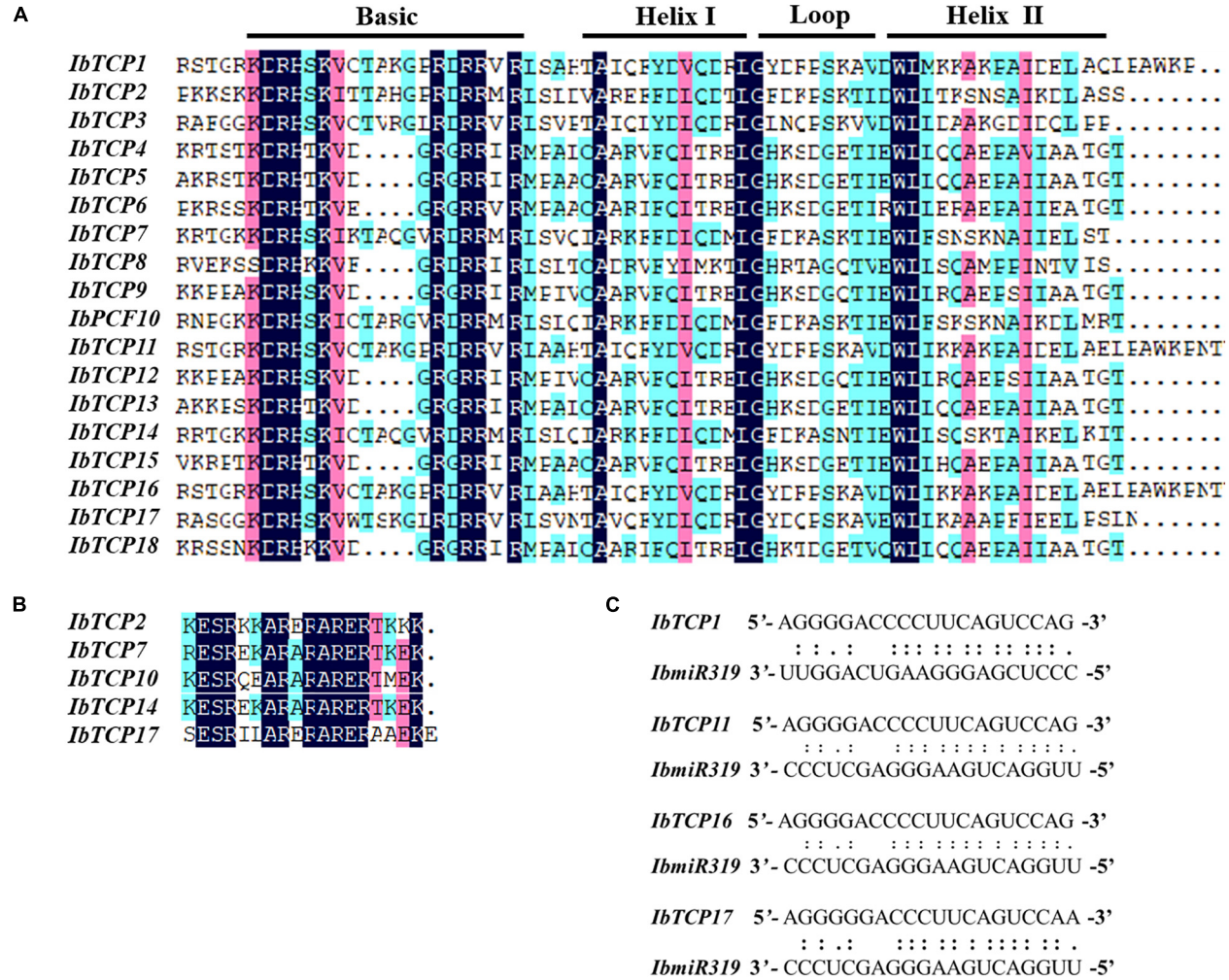

FIGURE 3 | Multiple sequence alignment of IbTCP proteins and the IbmiR319-targeted IbTCPs. **(A)** Alignment of the TCP domain of the 18 TCP proteins in sweet potato. Shaded in different colors indict the conserved amino acids. Conserved domains, including Basic, Helix I, Loop, and Helix II, are shown at the top. **(B)** Alignment of the R-domain of the class II members. Shaded in different colors indict the conserved amino acids. **(C)** Complementarities of IbmiR319 and its target *IbTCP1*, *IbTCP11*, *IbTCP16*, and *IbTCP17* mRNAs.

To elucidate the cellular basis of the morphological changes, microstructure and ultrastructure observations of the leaves were carried out by electron microscopy using hand-sliced paraffin sections. Microscopic analysis of the leaf blade cross-sections revealed fewer mesophyll cells (including the palisade tissue and spongy tissue) and thinner layers of mesophyll cells in MIM319 than in WT (**Figure 7F**). The thickness of MIM319 leaves (0.264 mm on average) was significantly thinner than that of WT (0.464 mm on average) (**Figure 7G**). The chloroplasts were flatter, more elongated, and contained less starch grains compared with WT (**Figure 7H**). In combination, the data indicated that IbmiR319-target *IbTCPs* also play vital roles in leaf anatomical morphology.

Leaf size and structure are important since they impact photosynthetic efficiency (Marcotrigiano, 2010). Thinner leaves with less chlorophyll content are considered to have a detriment for the efficient usage of light energy, and lead to less photosynthetic efficiency (Higuchi et al., 1999). To address whether the changes in leaf anatomical morphology of MIM319 affect photosynthesis, some photosynthetic parameters were quantitatively measured. The total chlorophyll content of the MIM319 transgenic plants was 0.0199 mg g^{-1} FW on average, while that of WT was 0.0331 mg g^{-1} FW. The total chlorophyll contents of MIM319 were dramatically lower than that in WT (**Figure 7I**). Furthermore, the photosynthetic rate of the MIM319 transgenic sweet potato was 22.33 μmol CO_2 m^{-2} s^{-1} on average, which was dramatically lower than 31.24 μmol CO_2 m^{-2} s^{-1} in the WT (**Figure 7J**). Meanwhile, the efficiency of PSII in MIM319 transgenic sweet potato leaves was also examined based on the F_v/F_m values. However, there were no significant differences between MIM319 and WT (**Figure 7K**). Taken together, these data suggested that IbmiR319-targeted *IbTCPs* may play key roles in the anatomical morphology of the leaves to affect photosynthesis.

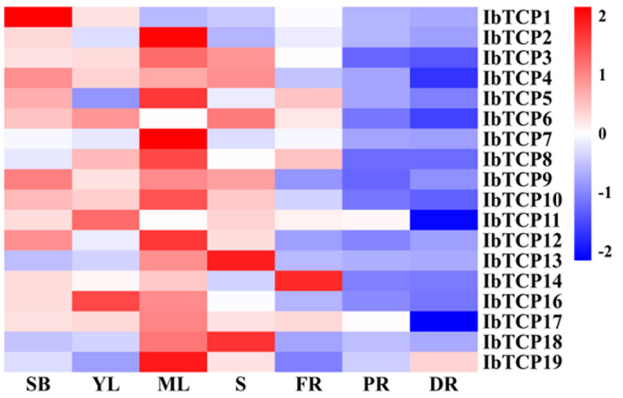

FIGURE 4 | Heatmap representation of the gene expression of 18 *IbTCPs* in various tissues. The tissues used for transcription pattern analysis are listed at the bottom, shoot buds (SB), young leaves (YL), mature leaves (ML), stems (S), fibrous roots (FR), pencil roots (PR), and developing roots (DR). The genes are listed on the right of the expression bars.

DISCUSSION

As plant-specific TFs, TCPs have major functions during growth and development, such as leaf (including single leaf and compound leaf) development, shoot development, flower development (Ori et al., 2007; Broholm et al., 2008; Koyama et al., 2011; Bai et al., 2012), and root development (Hao et al., 2012), and are also involved in phytohormone biosynthesis (Danisman et al., 2012), lignin biosynthesis (Sun et al., 2017; Chahel et al., 2019) and the circadian clock (Giraud et al., 2010; Zhang et al., 2018). Nevertheless, there's scarcely any precise exhaustive information of the TCP TF family in sweet potato which is the seventh largest food crop in terms of production globally and a vital tuber crop. In this study, 18 *IbTCPs* were identified and cloned in sweet potato and were discovered to be distributed on 11 chromosomes and two scaffolds with different densities (**Figure 1C**). Phylogenetic analysis revealed that 18 IbTCPs clustered into two classes according to their evolutionary relationships (**Figures 1A**, **2**). These findings are consistent with previous classifications of TCPs from *Arabidopsis*, *Z. mays*, and *S. lycopersicum* (Kim et al., 2014; Parapunova et al., 2014; Chai et al., 2017). Conserved motif analysis showed that TCP domain with a bHLH-type motif existed in both class I and class II of IbTCPs, while the R domain only existed in class II (**Table 1** and **Figures 1B**, **3A,B**). Collectively, this evidence supports the classification and conservation of the sweet potato TCP TF family.

It is well-known that class II TCPs precisely regulate the transition from division to expansion (Tsukaya, 2010; Qi et al., 2017). For the leaf lamina, the timing of the transition is a significant determinant of the final size, shape, flatness, and complexity. Class II CYC/TB1 clade TCPs basically participate in the developmental regulation of axillary meristems, which results in the growth of either lateral branches or flowers. This clade included AtTCP2/3/4/5/10 and IbTCP11/17 (**Figure 2**). We therefore examined the expression patterns of *IbTCPs* to investigate whether they have essential functions in the growth and development of these organs or tissues. The expression in different tissues and different organs varied widely among *IbTCP* genes and different development stages of the leaf for individual *TCP* genes (**Figures 4**, **5**). This states the functional divergence of *IbTCPs* at different stages of developmental processes, especially leaf development in sweet potato. In our study, all 18 *IbTCPs* showed relatively weak expression in the belowground organs, but high expression in the aboveground organs, with even *IbTCP11* and *IbTCP17* showing higher expression in the mature leaves (**Figure 5C**). *AtTCP3* and *AtTCP4*, orthologs of *IbTCP11*, act as decisive modulators of *de novo* shoot organogenesis (Woorim et al., 2020). A previous study demonstrated that the overexpression of *AtTCP4* led to in miniature cotyledons and shoot apical-meristem termination (Efroni et al., 2008), and the ectopic expression of *AtTCP3* caused the failure of shoot-meristem formation (Koyama et al., 2007). Double, triple, or even quadruple knockouts for the miR319-regulated *TCP* genes, *AtTCP2*, *AtTCP3*, *AtTCP4*, and *AtTCP10*, demonstrate leaf crinkling to varying degrees, yet single knockouts present only slight effects on leaf morphology (Schommer et al., 2008; Bresso et al., 2018). *AtTCP5* represses the initiation and outgrowth of leaf serrations by directly promoting the expression of *KNAT3* and indirectly activating the transcription of SAW1 (Yu et al., 2020). Together, these data reveal the tissue expression diversity of *TCPs* in various plants. Compared with other plants, the great number of highly-expressed *IbTCPs* in the aboveground organs indicates their important function in sweet potato development, especially leaf development.

Previous study recorded that TCPs are fundamental regulators of plant growth and development, especially leaf development and senescence (Schippers, 2015). The leaf is the pivotal organ of photosynthesis, and its size and anatomical morphology directly affect photosynthetic efficiency (Marcotrigiano, 2010; Pan et al., 2018). Many genes and pathways can regulate leaf morphogenesis so as to generate organs of a wide variety of sizes and shapes (Rodriguez et al., 2014). Meanwhile, more and more experimental data show that miRNAs regulate the TFs which involved in plant development. The MiR164 family includes post-transcriptionally regulated *CUC1*, *CUC2*, and other *NAC* TFs. The overexpression of the miR164 family in *Arabidopsis* compromised organ separation, causing fusion between cotyledons and leaves, and also between the inflorescence stem and cauline leaves (Laufs et al., 2004; Mallory et al., 2004; Nikovics et al., 2006). MiR165/166 precisely regulated the expression pattern of polarity genes during leaf development in maize (Juarez et al., 2004). Increased miR408 expression leads to enhanced photosynthesis by elevating the abundance of plastocyanin to improve irradiation utilization efficiency in *Arabidopsis*, tobacco, and rice (Pan et al., 2018). This study indicates that blocking miR319 in sweet potato increases *TCP* gene expression to limit photosynthetic performance through thinner and flatter chloroplasts, a lower chlorophyll content, and the development of thinner and smaller leaves.

Our findings provide evidence for the connection between structure and function in the *IbTCPs* as well as lay a basis for

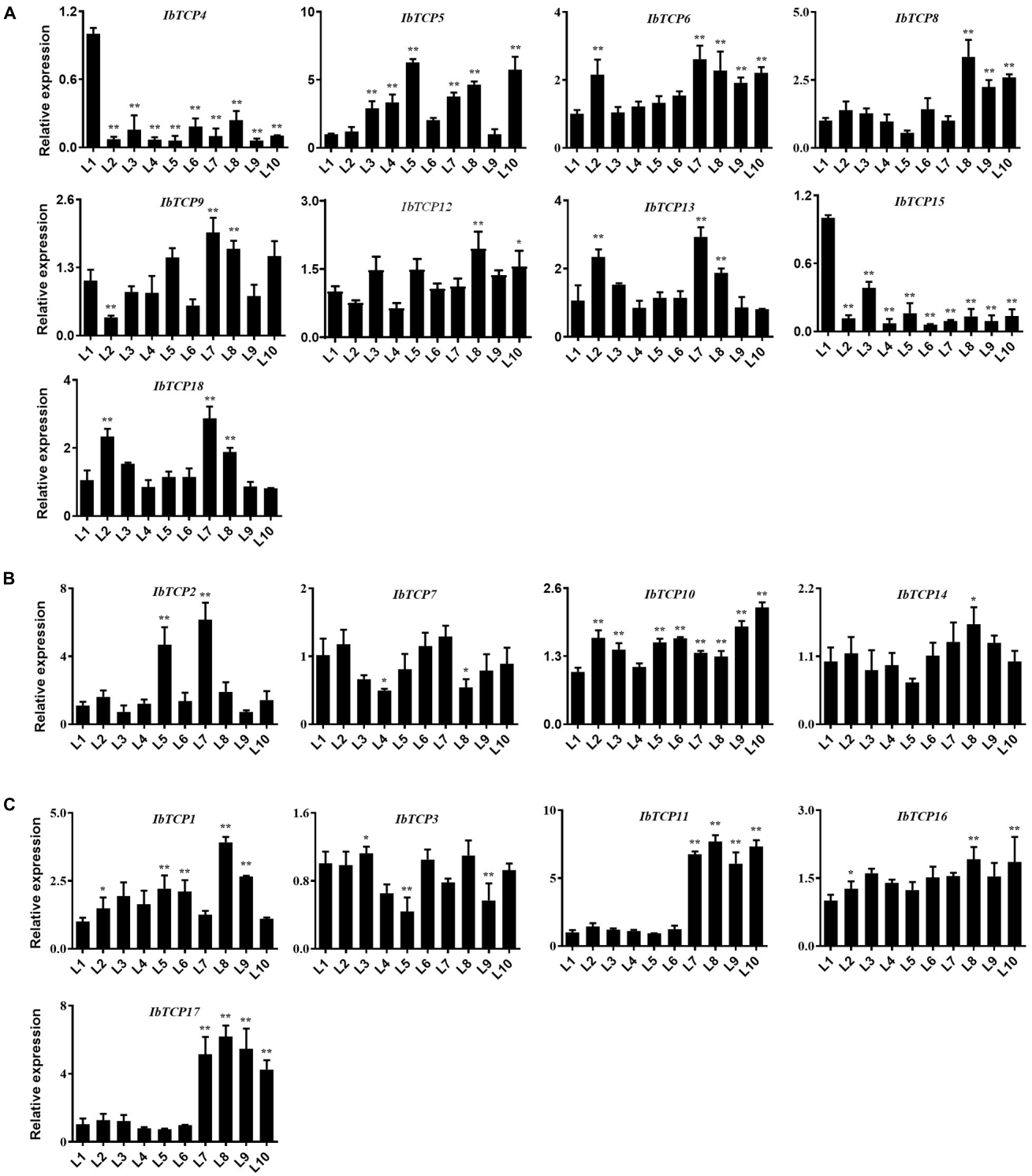

FIGURE 5 | Expression pattern analysis of *IbTCPs* in varying leaf developmental periods. The qRT-PCR transcript analysis of *IbTCPs* of Class I **(A)**, Class II CIN clade **(B)**, and CYC/TB1 clade **(C)** in the 1st, 2nd, 3rd, to 10th leaf (L1–L10). The expression profiles were normalized using *IbActin*. Values are the mean and SD of three replicates. The asterisks indicate statistical significance to L1 (Student's *t*-test; $^{*}P < 0.05$, $^{**}P < 0.01$).

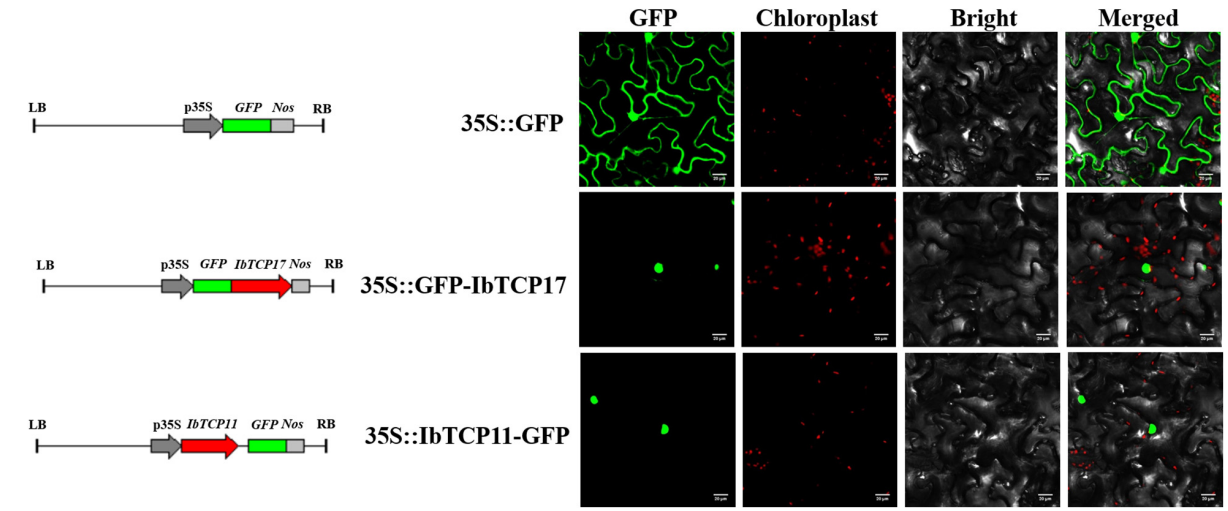

FIGURE 6 | Subcellular localization of two GFP-fused sweet potato TCP proteins. The two IbTCP-GFP fusion proteins (IbTCP11-GFP and IbTCP17-GFP) were transiently expressed in tobacco leaves and observed by confocal microscopy 72 h later. GFP driven by the 35S promoter was used as a control. The left, middle-left, middle-right, and right panels stand for photoes taken in dark, chloroplast, bright, and merged views, respectively. Bars are 20 μm.

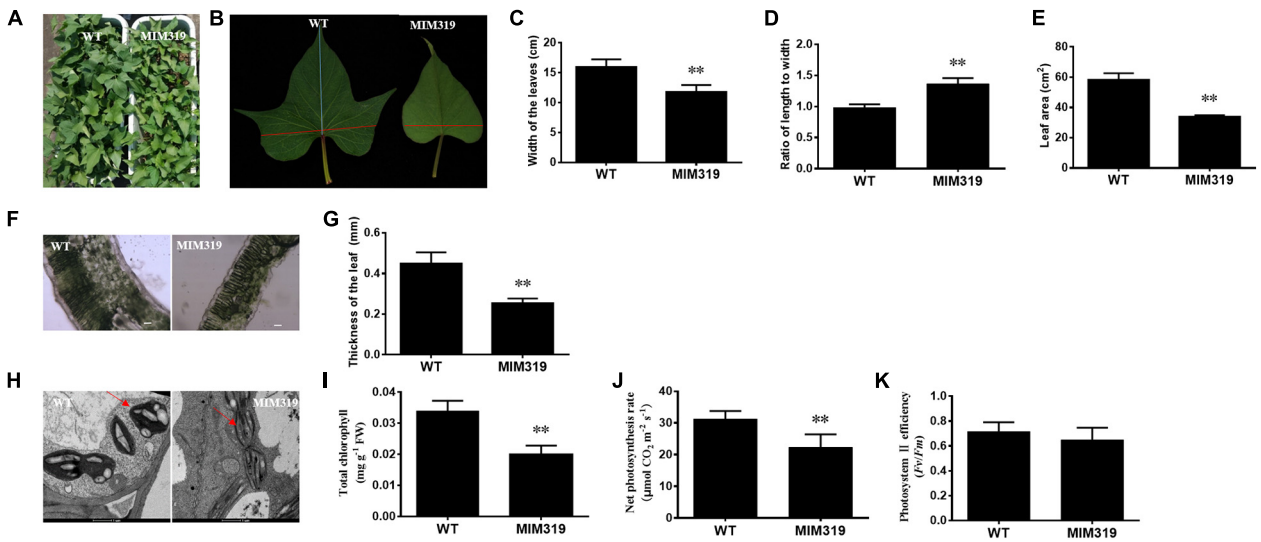

FIGURE 7 | The phenotypes and anatomical morphology of MIM319 and WT sweet potato leaf. **(A)** Phenotype of the whole plant of WT and MIM319. **(B)** Phenotype of the third fully-expanded leaf of WT and MIM319. **(C–E)** The width, ratio of length to width, and area of the third fully-expanded leaf of WT and MIM319. **(F)** The microstructure of the hand-sliced third-fully expanded leaves of WT and MIM319 observed using an optical microscope. Bars are 50 μm. **(G)** The thickness of the third fully-expanded leaf of WT and MIM319. **(H)** The TEM image of the third fully-expanded leaf of WT and MIM319. The red arrows indicate the chloroplast. Bars indicate 1 μm in length. **(I–K)** The total chlorophyll, net photosynthesis rate, and photosystem II efficiency of WT and MIM319. The error bars and asterisks indicate the SD and statistical significance of 10 biological replicates (Student's *t*-test; $^{**}P < 0.01$), respectively.

further illustrating the functions of *IbTCPs* and their relationship with miR319 in sweet potato.

DATA AVAILABILITY STATEMENT

The original contributions presented in the study are included in the article/**Supplementary Materials**, further inquiries can be directed to the corresponding authors.

AUTHOR CONTRIBUTIONS

LR, LZ, DM, and AW designed the research. LR, HW, and TZ implemented most of the research and analysis. XG, WZ, and TW implemented *IbTCPs* identification, cloning, and bioinformatics analysis. LZ contributed analytical tools. LR, LZ, and AW wrote the manuscript. LZ and DM modified the manuscript. All authors contributed to the article and approved the submitted version.

FUNDING

This work was supported by the National Key R&D Program of China (2018YFD1000705 and 2018YFD1000700), the China Agriculture Research System of MOF and MARA (Grant No. CARS-10-B03), the Natural Science Foundation of the Jiangsu Higher Education Institutions of China (Grant No. 18KJB180005), the Project of Xuzhou Science and Technology Key R&D Program (Grant No. KC18143), the Research Support Program for Teachers' Doctoral Degree of Jiangsu Normal University (Grant No. 18XLRS014), the Priority Academic Program Development of Jiangsu Higher Education Institutions (PAPD), the Undergraduate Innovation and Entrepreneurship Training Program of Jiangsu (Grant No. 201910320114Y), and the Research Innovation Program for College Graduates of Jiangsu Normal University (Grant No. 2020XKT497).

ACKNOWLEDGMENTS

We thank LetPub (www.letpub.com) for its linguistic assistance during the preparation of this manuscript.

SUPPLEMENTARY MATERIAL

The Supplementary Material for this article can be found online at: https://www.frontiersin.org/articles/10.3389/fpls.2021.686698/full#supplementary-material

Supplementary Figure 1 | The expression of IbmiR319 **(A)** and its target genes IbTCP11, 17 **(B)** in MIM319.

Supplementary Figure 2 | The length of leaf in MIM319.

REFERENCES

Axtell, M. J., Snyder, J. A., and Bartell, D. P. (2007). Common functions for diverse small RNAs of land plants. *Plant Cell.* 19, 1750–1769. doi: 10.1105/tpc.107.051706

Bai, F., Reinheimer, R., Durantini, D., Kellogg, E. A., and Schmidt, R. J. (2012). TCP transcription factor, BRANCH ANGLE DEFECTIVE 1 (BAD1), is required for normal tassel branch angle formation in maize. *Proc. Natl. Acad. Sci. U. S. A.* 109, 12225–12230. doi: 10.1073/pnas.1202439109

Bao, S., Zhang, Z., Lian, Q., Sun, Q., and Zhang, R. (2019). Evolution and expression of genes encoding TCP transcription factors in Solanum tuberosum reveal the involvement of StTCP23 in plant defence. *BMC Genet.* 20:91. doi: 10.1186/s12863-019-0793-1

Bartel, D. P. (2009). MicroRNAs: target Recognition and Regulatory Functions. *Cell* 136, 215–233. doi: 10.1016/j.cell.2009.01.002

Bresso, E. G., Chorostecki, U., Rodriguez, R. E., Palatnik, J. F., and Schommer, C. (2018). Spatial Control of Gene Expression by miR319-Regulated TCP Transcription Factors in Leaf Development. *Plant Physiol.* 176, 1694–1708. doi: 10.1104/pp.17.00823

Broholm, S. K., Tahtiharju, S., Laitinen, R. A. E., Albert, V. A., Teeri, T. H., and Elomaa, P. (2008). A TCP domain transcription factor controls flower type specification along the radial axis of the Gerbera (Asteraceae) inflorescence. *Proc. Natl. Acad. Sci. U. S. A.* 105, 9117–9122. doi: 10.1073/pnas.0801359105

Cao, J.-F., Zhao, B., Huang, C.-C., Chen, Z.-W., Zhao, T., Liu, H.-R., et al. (2020). The miR319-Targeted GhTCP4 Promotes the Transition from Cell Elongation to Wall Thickening in Cotton Fiber. *Mol. Plant* 13, 1063–1077. doi: 10.1016/j.molp.2020.05.006

Chahel, A. A., Zeng, S., Yousaf, Z., Liao, Y., Yang, Z., Wei., X., et al. (2019). Plant-specific transcription factor LrTCP4 enhances secondary metabolite biosynthesis in Lycium ruthenicum hairy roots. *Plant Cell Tissue Org. Cult.* 136, 323–337. doi: 10.1007/s11240-018-1518-2

Chai, W., Jiang, P., Huang, G., Jiang, H., and Li, X. (2017). Identification and expression profiling analysis of TCP family genes involved in growth and development in maize. *Physiol. Mol. Biol. Plants* 23, 779–791. doi: 10.1007/s12298-017-0476-1

Challa, K. R., Rath, M., and Nath, U. (2019). The CIN-TCP transcription factors promote commitment to differentiation in Arabidopsis leaf pavement cells via both auxin-dependent and independent pathways. *PLoS Genet.* 15:e1007988. doi: 10.1371/journal.pgen.1007988

Cubas, P., Lauter, N., Doebley, J., and Coen, E. (1999). The TCP domain: a motif found in proteins regulating plant growth and development. *Plant J.* 18, 215–222. doi: 10.1046/j.1365-313x.1999.00444.x

Cui, J., You., C., and Chen, X. (2017). The evolution of microRNAs in plants. *Curr. Opin. Plant Biol.* 35, 61–67. doi: 10.1016/j.pbi.2016.11.006

Danisman, S. (2016). TCP Transcription Factors at the Interface between Environmental Challenges and the Plant's Growth Responses. *Front. Plant Sci.* 7:1930. doi: 10.3389/fpls.2016.01930

Danisman, S., van der Wal, F., Dhondt, S., Waites, R., de Folter, S., Bimbo, A., et al. (2012). Arabidopsis Class I and Class II TCP Transcription Factors Regulate Jasmonic Acid Metabolism and Leaf Development Antagonistically. *Plant Physiol.* 159, 1511–1523. doi: 10.1104/pp.112.200303

Dhaka, N., Bhardwaj, V., Sharma, M. K., and Sharma, R. (2017). Evolving Tale of TCPs: new Paradigms and Old Lacunae. *Front. Plant Sci.* 8:479. doi: 10.3389/fpls.2017.00479

Doebley, J., Stec, A., and Hubbard, L. (1997). The evolution of apical dominance in maize. *Nature* 386, 485–488. doi: 10.1038/386485a0

Efroni, I., Blum, E., Goldshmidt, A., and Eshed, Y. (2008). A protracted and dynamic maturation schedule underlies Arabidopsis leaf development. *Plant Cell* 20, 2293–2306. doi: 10.1105/tpc.107.057521

Ferrero, L. V., Viola, I. L., Ariel, F. D., and Gonzalez, D. H. (2019). Class I TCP Transcription Factors Target the Gibberellin Biosynthesis Gene GA20ox1 and the Growth-Promoting Genes HBI1 and PRE6 during Thermomorphogenic Growth in Arabidopsis. *Plant Cell Physiol.* 60, 1633–1645. doi: 10.1093/pcp/pcz137

Franco-Zorrilla, J. M., Valli, A., Todesco, M., Mateos, I., Puga, M. I., Rubio-Somoza, I., et al. (2007). Target mimicry provides a new mechanism for regulation of microRNA activity. *Nat. Genet.* 39, 1033–1037. doi: 10.1038/ng2079

Gastaldi, V., Lucero, L. E., Ferrero, L. V., Ariel, F. D., and Gonzalez, D. H. (2020). Class-I TCP Transcription Factors Activate the SAUR63 Gene Subfamily in Gibberellin-Dependent Stamen Filament Elongation(1)(OPEN). *Plant Physiol.* 182, 2096–2110. doi: 10.1104/pp.19.01501

Giraud, E., Ng, S., Carrie, C., Duncan, O., Low, J., Lee, C. P., et al. (2010). TCP Transcription Factors Link the Regulation of Genes Encoding Mitochondrial Proteins with the Circadian Clock in Arabidopsis thaliana. *Plant Cell* 22, 3921–3934. doi: 10.1105/tpc.110.074518

Guo, Z., Fujioka, S., Blancaflor, E. B., Miao, S., Gou, X., and Li, J. (2010). TCP1 Modulates Brassinosteroid Biosynthesis by Regulating the Expression of the Key Biosynthetic Gene DWARF4 in Arabidopsis thaliana. *Plant Cell* 22, 1161–1173. doi: 10.1105/tpc.109.069203

Hao, J., Tu, L., Hu, H., Tan, J., Deng, F., Tang, W., et al. (2012). GbTCP, a cotton TCP transcription factor, confers fibre elongation and root hair development by a complex regulating system. *J. Exp. Bot.* 63, 6267–6281. doi: 10.1093/jxb/ers278

Higuchi, H., Sakuratani, T., and Utsunomiya, N. (1999). Photosynthesis, leaf morphology, and shoot growth as affected by temperatures in cherimoya (Annona cherimola Mill.) trees. *Sci. Horticult.* 80, 91–104. doi: 10.1016/s0304-4238(98)00221-0

Juarez, M. T., Kui, J. S., Thomas, J., Heller, B. A., and Timmermans, M. C. P. (2004). microRNA-mediated repression of rolled leaf1 specifies maize leaf polarity. *Nature* 428, 84–88. doi: 10.1038/nature02363

Kang, T., Yu, C.-Y., Liu, Y., Song, W.-M., Bao, Y., Guo, X.-T., et al. (2020). Subtly Manipulated Expression of ZmmiR156 in Tobacco Improves Drought and Salt Tolerance Without Changing the Architecture of Transgenic Plants. *Front. Plant Sci.* 10:1664. doi: 10.3389/fpls.2019.01664

Kim, H. E., Choi, Y. G., Lee, A. R., Seo, Y. J., Kwon, M. Y., and Lee, J. H. (2014). Temperature dependent hydrogen exchange study of DNA duplexes containing binding sites for Arabidopsis TCP transcription factors. *J. Korean Magn. Reson. Soc.* 18, 52–57. doi: 10.6564/jkmrs.2014.18.2.052

Kosugi, S., and Ohashi, Y. (1997). PCF1 and PCF2 specifically bind to cis elements in the rice proliferating cell nuclear antigen gene. *Plant Cell* 9, 1607–1619. doi: 10.2307/3870447

Kosugi, S., and Ohashi, Y. (2002). , DNA binding and dimerization specificity and potential targets for the TCP protein family. *Plant J.* 30, 337–348. doi: 10.1046/j.1365-313x.2002.01294.x

Koyama, T., Furutani, M., Tasaka., M., and Ohme-Takagi, M. (2007). TCP transcription factors control the morphology of shoot lateral organs via negative regulation of the expression of boundary-specific genes in Arabidopsis. *Plant Cell* 19, 473–484. doi: 10.1105/tpc.106.044792

Koyama, T., Ohme-Takagi, M., and Sato, F. (2011). Generation of serrated and wavy petals by inhibition of the activity of TCP transcription factors in Arabidopsis thaliana. *Plant Signal. Behav.* 6, 697–699. doi: 10.4161/psb.6.5.14979

Kuo, Y. W., Lin, J. S., Li, Y. C., Jhu, M. Y., King, Y. C., and Jeng, S. T. (2019). MicroR408 regulates defense response upon wounding in sweet potato. *J. Exp. Bot.* 70, 469–483. doi: 10.1093/jxb/ery381

Laufs, P., Peaucelle, A., Morin, H., and Traas, J. (2004). MicroRNA regulation of the CUC genes is required for boundary size control in Arabidopsis meristems. *Development* 131, 4311–4322. doi: 10.1242/dev.01320

Liu, Q. (2014). *Encyclopedia of Agriculture and Food Systems*. Netherlands: Elsevier.

Liu, Y., Li, D., Yan, J., Wang, K., Luo, H., and Zhang, W. (2019). MiR319-mediated ethylene biosynthesis, signalling and salt stress response in switchgrass. *Plant Biotechnol. J.* 17, 2370–2383. doi: 10.1111/pbi.13154

Livak, K. J., and Schmittgen, T. D. (2001). Analysis of relative gene expression data using real-time quantitative PCR and the 2(T)(-Delta Delta C) method. *Methods* 25, 402–408. doi: 10.1006/meth.2001.1262

Luo, D., Carpenter, R., Vincent, C., Copsey, L., and Coen, E. (1996). Origin of floral asymmetry in Antirrhinum. *Nature* 383, 794–799. doi: 10.1038/383794a0

Lupas, A., Dyke., M. Van, and Stock, J. (1991). Predicting coiled coils from protein sequences. *Science* 252, 1162–1164. doi: 10.1126/science.252.5009.1162

Ma, X., Ma, J., Fan, D., Li, C., Jiang, Y., and Luo, K. (2016). Genome-wide Identification of TCP Family Transcription Factors from Populus euphratica and Their Involvement in Leaf Shape Regulation. *Sci. Rep.* 6:32795.

Mallory, A. C., Dugas, D. V., Barte, D. P., and Bartel, lB (2004). MicroRNA regulation of NAC-domain targets is required for proper formation and separation of adjacent embryonic, vegetative, and floral organs. *Curr. Biol.* 14, 1035–1046. doi: 10.1016/j.cub.2004.06.022

Marcotrigiano, M. (2010). A role for leaf epidermis in the control of leaf size and the rate and extent of mesophyll cell division. *Am. J. Bot.* 97, 224–233. doi: 10.3732/ajb.0900102

Meng, X., Li, G., Yu, J., Cai, J., Dong, T., Sun, J., et al. (2018). Isolation, Expression Analysis, and Function Evaluation of 12 Novel Stress-Responsive Genes of NAC Transcription Factors in Sweetpotato. *Crop Sci.* 58, 1328–1341. doi: 10.2135/cropsci2017.12.0738

Nag, A., King, S., and Jack, T. (2009). miR319a targeting of TCP4 is critical for petal growth and development in Arabidopsis. *Proc. Natl. Acad. Sci. U. S. A.* 106, 22534–22539. doi: 10.1073/pnas.0908718106

Nikovics, K., Blein, T., Peaucelle, A., Ishida, T., Morin, H., Aida, M., et al. (2006). The balance between the MIR164A and CUC2 genes controls leaf margin serration in Arabidopsis. *Plant Cell* 18, 2929–2945. doi: 10.1105/tpc.106.045617

Niwa, M., Daimon, Y., Kurotani, K.-I., Higo, A., Pruneda-Paz, J. L., Breton, G., et al. (2013). BRANCHED1 Interacts with FLOWERING LOCUS T to Repress the Floral Transition of the Axillary Meristems in Arabidopsis. *Plant Cell* 25, 1228–1242. doi: 10.1105/tpc.112.109090

Ori, N., Cohen, A. R., Etzioni, A., Brand, A., Yanai, O., Shleizer, S., et al. (2007). Regulation of LANCEOLATE by miR319 is required for compound-leaf development in tomato. *Nature Genet.* 39, 787–791. doi: 10.1038/ng2036

Palatnik, J. F., Allen, E., Wu, X., Schommer, C., Schwab, R., Carrington, J. C., et al. (2003). Control of leaf morphogenesis by microRNAs. *Nature* 425, 257–263. doi: 10.1038/nature01958

Pan, J. W., Huang, D. H., Guo, Z. L., Kuang, Z., Zhang, H., Xie, X. Y., et al. (2018). Overexpression of microRNA408 enhances photosynthesis, growth, and seed yield in diverse plants. *J. Integr. Plant Biol.* 60, 323–340. doi: 10.1111/jipb.12634

Parapunova, V., Busscher, M., Busscher-Lange, J., Lammers, M., Karlova, R., Bovy, A. G., et al. (2014). Identification, cloning and characterization of the tomato TCP transcription factor family. *BMC Plant Biol.* 14:157. doi: 10.1186/1471-2229-14-157

Pruneda-Paz, J. L., Breton, G., Para, A., and Kay, S. A. (2009). A Functional Genomics Approach Reveals CHE as a Component of the Arabidopsis Circadian Clock. *Science* 323, 1481–1485. doi: 10.1126/science.1167206

Qi, J., Wu, B., Feng, S., Lü, S., Guan, C., Zhang, X., et al. (2017). Mechanical regulation of organ asymmetry in leaves. *Nat. Plants* 3, 724–733. doi: 10.1038/s41477-017-0008-6

Rodriguez, R. E., Debernardi, J. M., and Palatnik, J. F. (2014). Morphogenesis of simple leaves: regulation of leaf size and shape. *Wiley Interdiscip. Rev. Dev. Biol.* 3, 41–57. doi: 10.1002/wdev.115

Sawada, S., Sakai, N., and Sano, T. (1999). Feed-Forward Effects on the Photosynthetic Source-Sink Balance in Single-Rooted Leaves of Sweet Potato. *Plant Prod. Sci.* 2, 87–91. doi: 10.1626/pps.2.87

Schippers, J. H. M. (2015). Transcriptional networks in leaf senescence. *Curr. Opin. Plant Biol.* 27, 77–83. doi: 10.1016/j.pbi.2015.06.018

Schommer, C., Palatnik, J. F., Aggarwal, P., Chételat, A., Cubas, P., Farmer, E. E., et al. (2008). Control of jasmonate biosynthesis and senescence by miR319 targets. *PLoS Biol.* 6:e230. doi: 10.1371/journal.pbio.0060230

Shi, P., Guy, K. M., Wu, W., Fang, B., Yang, J., Zhang, M., et al. (2016). Genome-wide identification and expression analysis of the ClTCP transcription factors in Citrullus lanatus. *BMC Plant Biol.* 16:85. doi: 10.1186/s12870-016-0765-9

Silvestri, A., Fiorilli, V., Miozzi, L., Accotto, G. P., Turina, M., and Lanfranco, L. (2019). In silico analysis of fungal small RNA accumulation reveals putative plant mRNA targets in the symbiosis between an arbuscular mycorrhizal fungus and its host plant. *BMC Genom.* 20:169. doi: 10.1186/s12864-019-5561-0

Sun, X., Wang, C., Xiang, N., Li, X., Yang, S., Du, J., et al. (2017). Activation of secondary cell wall biosynthesis by miR319-targeted TCP4 transcription factor. *Plant Biotechnol. J.* 15, 1284–1294. doi: 10.1111/pbi.12715

Tamura, K., Stecher, G., Peterson, D., Filipski, A., and Kumar, S. (2013). MEGA6: molecular Evolutionary Genetics Analysis version 6.0. *Mol. Biol. Evol.* 30, 2725–2729. doi: 10.1093/molbev/mst197

Tang, C., Han, R., Zhou, Z., Yang, Y., Zhu, M., Xu, T., et al. (2020). Identification of candidate miRNAs related in storage root development of sweet potato by high throughput sequencing. *J. Plant Physiol.* 251, 153224–153224. doi: 10.1016/j.jplph.2020.153224

Taylor, R. S., Tarver, J. E., Hiscock, S. J., and Donoghue, P. C. J. (2014). Evolutionary history of plant microRNAs. *Trends Plant Sci.* 19, 175–182. doi: 10.1016/j.tplants.2013.11.008

Tsukaya, H. (2010). The Mechanism of Cell Cycle Arrest Front Progression Explained by a KLUH/CYP78A5-dependent Mobile Growth Factor in Developing Leaves of Arabidopsis thaliana. *Plant Cell Physiol.* 51, 1046–1054. doi: 10.1093/pcp/pcq051

Vadde, B. V. L., Challa, K. R., and Nath, U. (2018). The TCP4 transcription factor regulates trichome cell differentiation by directly activating GLABROUS INFLORESCENCE STEMS in Arabidopsis thaliana. *Plant J.* 93, 259–269. doi: 10.1111/tpj.13772

Viola, I. L., Camoirano, A., and Gonzalez, D. H. (2016). Redox-Dependent Modulation of Anthocyanin Biosynthesis by the TCP Transcription Factor TCP15 during Exposure to High Light Intensity Conditions in Arabidopsis. *Plant Physiol.* 170, 74–85. doi: 10.1104/pp.15.01016

Wang, H., Wang, H., Liu, R., Xu, Y., Lu, Z., and Zhou, C. (2018). Genome-Wide Identification of TCP Family Transcription Factors in Medicago truncatula Reveals Significant Roles of miR319-Targeted TCPs in Nodule Development. *Front. Plant Sci.* 9:774. doi: 10.3389/fpls.2018.00774

Wang, W., Liu, D., Chen, D., Cheng, Y., Zhang, X., Song, L., et al. (2019a). MicroRNA414c affects salt tolerance of cotton by regulating reactive oxygen species metabolism under salinity stress. *RNA Biol.* 16, 362–375. doi: 10.1080/15476286.2019.1574163

Wang, Y., Zhang, N., Li, T., Yang, J., Zhu, X., Fang, C., et al. (2019b). Genome-wide identification and expression analysis of StTCP transcription factors of potato (Solarium tuberosum L.). *Comput. Biol. Chem.* 78, 53–63. doi: 10.1016/j.compbiolchem.2018.11.009

Wei, Y., Gu, Z., Chu, W., Ye, L., and Yang, G. (2014). Identification and Structure Analysis of TCP Transcription Factors in Cucumber. *Mol. Plant Breed.* 12, 287–295.

Woorim, Y., Myung-Hwan, C., Bos, N., and Yoo-Sun, lN (2020). De Novo Shoot Regeneration Controlled by HEN1 and TCP3/4 in Arabidopsis. *Plant Cell Physiol.* 9:9.

Wu, S., Lau, K. H., Cao, Q. H., Hamilton, J. P., Sun, H. H., Zhou, C. X., et al. (2018). Genome sequences of two diploid wild relatives of cultivated sweetpotato reveal targets for genetic improvement. *Nat. Commun.* 9:12.

Xie, Z., Wang, A., Li, H., Yu, J., Jiang, J., Tang, Z., et al. (2017). High throughput deep sequencing reveals the important roles of microRNAs during sweetpotato storage at chilling temperature. *Sci. Rep.* 7:16578.

Xu, R., Sun, P., Jia, F., Lu, L., Li, Y., Zhang, S., et al. (2014). Genomewide analysis of TCP transcription factor gene family in Malus domestica. *J. Genet.* 93, 733–746. doi: 10.1007/s12041-014-0446-0

Yang, C., Li, D., Mao, D., Liu, X., Ji, C., Li, X., et al. (2013). Overexpression of microRNA319 impacts leaf morphogenesis and leads to enhanced cold tolerance in rice (Oryza sativa L.). *Plant Cell Environ.* 36, 2207–2218. doi: 10.1111/pce.12130

Yang, J., Bi, H.-P., Fan, W.-J., Zhang, M., Wang, H.-X., and Zhang, P. (2011). Efficient embryogenic suspension culturing and rapid transformation of a range of elite genotypes of sweet potato (Ipomoea batatas L. Lam.). *Plant Sci.* 181, 701–711. doi: 10.1016/j.plantsci.2011.01.005

Yang, J., Moeinzadeh, M. H., Kuhl, H., Helmuth, J., Xiao, P., Haas, S., et al. (2017). Haplotype-resolved sweet potato genome traces back its hexaploidization history. *Nat. Plants* 3, 696–703. doi: 10.1038/s41477-017-0002-z

Yin, Z., Li, Y., Zhu, W., Fu, X., Han, X., Wang, J., et al. (2018). Identification, Characterization, and Expression Patterns of TCP Genes and microRNA319 in Cotton. *Int. J. Mol. Sci.* 19:3655. doi: 10.3390/ijms19113655

Yu, H., Zhang, L., Wang, W., Tian, P., Wang, W., Wang, K., et al. (2020). TCP5 controls leaf margin development by regulating the KNOX and BEL-like transcription factors in Arabidopsis. *J. Exp. Bot.* 72, 1809–1821. doi: 10.1093/jxb/eraa569

Zhang, N., Wang, Z., Bao, Z., Yang, L., Wu, D., Shu, X., et al. (2018). MOS1 functions closely with TCP transcription factors to modulate immunity and cell cycle in Arabidopsis. *Plant J.* 93, 66–78. doi: 10.1111/tpj.13757

Zheng, A., Sun, F., Cheng, T., Wang, Y., Xie, K., Zhang, C., et al. (2019). Genome-wide identification of members of the TCP gene family in switchgrass (Panicum virgatum L.) and analysis of their expression. *Gene* 702, 89–98. doi: 10.1016/j.gene.2019.03.059

Zheng, K., Ni, Z., Qu, Y., Cai, Y., Yang, Z., Sun, G., et al. (2018). Genome-wide identification and expression analyses of TCP transcription factor genes in Gossypium barbadense. *Sci. Rep.* 8:14526.

Conflict of Interest: The authors declare that the research was conducted in the absence of any commercial or financial relationships that could be construed as a potential conflict of interest.

Publisher's Note: All claims expressed in this article are solely those of the authors and do not necessarily represent those of their affiliated organizations, or those of the publisher, the editors and the reviewers. Any product that may be evaluated in this article, or claim that may be made by its manufacturer, is not guaranteed or endorsed by the publisher.

frontiers in Plant Science

ORIGINAL RESEARCH
published: 27 August 2021
doi: 10.3389/fpls.2021.741415

DNA Methylation and RNA-Sequencing Analysis Show Epigenetic Function During Grain Filling in Foxtail Millet (*Setaria italica* L.)

Tao Wang[1,2†], Quanwei Lu[1†], Hui Song[3], Nan Hu[1], Yangyang Wei[1], Pengtao Li[1], Yuling Liu[1], Zilin Zhao[1], Jinrong Liu[3], Baohong Zhang[4] and Renhai Peng[1]**

[1] College of Biology and Food Engineering, Anyang Institute of Technology, Anyang, China, [2] Innovation and Practice Base for Postdoctors, Anyang Institute of Technology, Anyang, China, [3] Anyang Academy of Agriculture Sciences, Anyang, China, [4] Department of Biology, East Carolina University, Greenville, NC, United States

OPEN ACCESS

Edited by:
Turgay Unver,
FicusBio, Turkey

Reviewed by:
Lin Zhao,
Northeast Agricultural University, China
Youlu Yuan,
Cotton Research Institute (CAAS), China

***Correspondence:**
Renhai Peng
aydxprh@163.com
Baohong Zhang
zhangb@ecu.edu

[†] These authors have contributed equally to this work

Specialty section:
This article was submitted to Plant Physiology, a section of the journal Frontiers in Plant Science

Received: 14 July 2021
Accepted: 06 August 2021
Published: 27 August 2021

Citation:
Wang T, Lu Q, Song H, Hu N, Wei Y, Li P, Liu Y, Zhao Z, Liu J, Zhang B and Peng R (2021) DNA Methylation and RNA-Sequencing Analysis Show Epigenetic Function During Grain Filling in Foxtail Millet (Setaria italica L.). Front. Plant Sci. 12:741415. doi: 10.3389/fpls.2021.741415

Grain filling is a crucial process for crop yield and quality. Certain studies already gained insight into the molecular mechanism of grain filling. However, it is unclear whether epigenetic modifications are associated with grain filling in foxtail millet. Global DNA methylation and transcriptome analysis were conducted in foxtail millet spikelets during different stages to interpret the epigenetic effects of the grain filling process. The study employed the whole-genome bisulfite deep sequencing and advanced bioinformatics to sequence and identify all DNA methylation during foxtail millet grain filling; the DNA methylation-mediated gene expression profiles and their involved gene network and biological pathway were systematically studied. One context of DNA methylation, namely, CHH methylation, was accounted for the largest percentage, and it was gradually increased during grain filling. Among all developmental stages, the methylation levels were lowest at T2, followed by T4, which mainly occurred in CHG. The distribution of differentially methylated regions (DMR) was varied in the different genetic regions for three contexts. In addition, gene expression was negatively associated with DNA methylation. Evaluation of the interconnection of the DNA methylome and transcriptome identified some stage-specific differentially expressed genes associated with the DMR at different stages compared with the T1 developmental stage, indicating the potential function of epigenetics on the expression regulation of genes related to the specific pathway at different stages of grain development. The results demonstrated that the dynamic change of DNA methylation plays a crucial function in gene regulation, revealing the potential function of epigenetics in grain development in foxtail millet.

Keywords: DNA methylation, grain filling, gene expression, foxtail millet, crop

INTRODUCTION

Gene expression is not only controlled by DNA sequences but also by epigenetic marks in eukaryotes. DNA methylation as one of the important epigenetic modifications has been demonstrated as closely related to gene expression in biological processes, such as transcriptional activity, developmental regulation, and environmental responses (Maunakea et al., 2010; Huang et al., 2019; Xing et al., 2020; Zhu et al., 2020). In eukaryotes, the methylation at the 5′ position of cytosine (5 mC) is the main type of DNA methylation, which could be found to occur in the CG, CHG contexts (symmetrical), or in CHH contexts (asymmetrical) in various regions of a genome (Huang et al., 2019). Many emerging studies proved that methylated DNA is widely involved in plant growth regulation. The level of DNA methylation decreased gradually during the development of tomato and strawberry fruits, and the application of methyltransferase inhibitor promoted premature ripening of tomato and strawberry fruits (Zhong et al., 2013; Cheng et al., 2018). Changes in DNA methylation were also observed during pepper ripening (Xiao et al., 2020). In contrast, the orange fruit showed obvious DNA hypermethylation as ripening (Huang et al., 2019). However, the function and dynamic change of methylated DNA have not been reported during grain filling in foxtail millet.

Grain filling could affect grain quality and yield in many crops as it is the most important developmental phase (Saini and Westgate, 1999). The grain filling process is complicated and can be regulated by endogenous metabolism and the external environment. Sucrose and starch metabolism are closely related to grain filling (Kato et al., 2007). Increasing expression of SuSase genes enhance the breakdown of sucrose in spikelets and promoted the transport of sucrose to grains (Ranwala and Miller, 1998). Grain filling could be improved through promoting starch synthesis done by *GIF2*, which also encodes an ADP-glucose pyrophosphorylase large subunit. Inhibition of *GIF2* had a negative effect on grain filling rate and yield (Wei et al., 2017). The grain size in rice was regulated by *GSA1* through encoding a UDP-glucosyltransferase (Dong et al., 2020). Plant hormones could also affect spikelet development and participate in regulating grain filling. Grain development could be prolonged through auxin and cytokinin done by DEP1/qPE9-1, which also promotes starch accumulation (Zhang et al., 2019). Abscisic acid (ABA) biosynthesis also promoted endosperm cell division and grain-filling (Yang et al., 2006; Wang et al., 2015). Polyamines (PAs) which regulated various metabolic processes in plants could also regulate grain filling (Chen et al., 2013; Liu et al., 2016). High-throughput sequencing technology makes it possible to identify genes associated with grain filling. Gene expression dynamics during grain development have been studied through transcriptome sequencing in different plant species (Wang et al., 2019, 2020b; Wen et al., 2019). The previous study found that genes, related to polyamine metabolism, sucrose-starch conversion, and hormone metabolism, were specifically expressed during grain development which indicates that they may play specific roles at different stages of grain filling in foxtail millet (Wang et al., 2020).

Foxtail millet is an ancient crop originating in China which is a C_4 cereal with many elite traits, including high tolerance to drought stresses (Lata et al., 2013). Additionally, the suitable genome size, low repetitive DNA, and short life cycle of foxtail millet make it an ideal model plant for studying C_4 photosynthesis and abiotic stress tolerance (Muthamilarasan and Prasad, 2015; Peng and Zhang, 2021). However, the study on molecular mechanisms of important growth and development processes in foxtail millet is limited compared with rice, maize, and wheat. Especially, the epigenetic modification and the potential function of DNA methylation are limited during grain filling in foxtail millet.

The objective of this study is to explore the potential connection between epigenetic modification and transcription changes during grain development. To achieve this, the study employed the whole-genome bisulfite sequencing (BS) approach to probe the epigenetic changes associated with grain filling at five different development stages in foxtail millet. These results are helpful for us to understand the effect of epigenetics in grain filling in foxtail millet and potentially other C_4 cereals.

MATERIALS AND METHODS

Plant Materials, Whole-Genome BS Library Construction, and Sequencing

The seeds of foxtail millet variety "Yu Gu 18" were planted and grown in the experimental station of Anyang Institute of Technology (Anyang, Henan, China). The same-aged panicle with the same size was harvested from T1–T5 developmental stages (T1: 7 days after anthesis, T2: 14 days after anthesis, T3: 21 days after anthesis, T4: 28 days after anthesis, and T5: 35 days after anthesis). The experimental field, agronomical practices situation, and sampling process are described in the previous study (Wang et al., 2020).

In isolating genomic DNA, DNeasy Blood and Tissue Kit (Qiagen, Dusseldorf, Germany) was used. Fifteen high-quality BS libraries were constructed and then sequenced with the Illumina Hiseq X Ten platform by Shanghai OE Biotech (Shanghai, China). Briefly, DNA was first fragmented to an approximate size of 250 bp. Then, dA was added to the 3′ end by blunt-end cloning and methylated adaptor ligation. The EZ DNA Methylation-Gold kit (ZYMO, Tustin, CA, United States) was used to bisulfite-convert the ligated DNA. Different DNA fragment lengths were excised from a 2% agarose gel and purified and amplified by PCR.

BS-Seq Data Analysis

All sequence data were deposited into the NCBI database (Accession number: PRJNA699635). Clean data were obtained by filtering the low-quality sequences and mapped to the foxtail millet genome (Bennetzen et al., 2012) using the mapping program, Bismark (Krueger and Andrews, 2011).

Differentially methylated regions (DMRs) were identified by MethylKit (Akalin et al., 2012), which used a sliding window approach. The window was 1,000 bp, and the step length was 100 bp. The logistic regression was applied to detect significant

DMRs and the screened criteria as methylation difference of ≥10% and $p \leq 0.05$. After DMRs were identified, differentially methylated genes (DMGs) located in DMRs were characterized.

For the identification of differentially methylated promoter (DMP), 2 kb upstream of the transcription start site (TSS) was used as the gene promoter region, and the methylation level in this region was counted. The methylation level of the promoter region between different samples was compared. To analyze DMP between groups, a *t*-test was used. The differences in methylation levels of all genes among all groups were analyzed. DMP regions were screened according to methylation differences of ≥10% and $p \leq 0.05$.

RNA Extraction, Library Construction, and Sequencing

The total RNA of kernels from spikelets was extracted using a mirVana miRNA Isolation Kit (Ambion, Inc., Austin, TX, United States) with three biological replicates. Afterward, high-quality libraries were sequenced on the Illumina HiSeq 2500 platform (Illumina, San Diego, CA, United States) with 125 paired-end sequencings. The data analysis was performed according to previously described methods (Wang et al., 2020).

Integration of DNA Methylation and Gene Expression Analysis

For integration with DNA methylation, RNA-seq data were used representing the same stages of grain filling in foxtail millet from the previous study.

The Pearson correlation analysis of RNA-seq data and DNA methylation levels in each sample was completed as previously described (Jin et al., 2014).

Gene Function Analysis and Enrichment

Differentially expressed genes associated with DMR were subjected to Kyoto Encyclopedia of Genes and Genomes (KEGG) analysis[1] (Kanehisa et al., 2008) to map them to the specific pathways they were involved in using the Blast_v2.2.26 software.

RESULTS

BS of Foxtail Millet at Different Stages During Grain Filling

Deoxyribonucleic acid libraries for five different stages were constructed for sequencing to get the characteristics and change of DNA methylation during grain development. A total of 2.16 billion raw reads were obtained, and the mapping rate was 76.6–83.5%. Moreover, conversion rates of each library were >99.56% (**Supplementary Table 1**). Sequencing depth was >30-fold coverage per DNA strand (**Supplementary Table 2**). Furthermore, the proportion of the 5 mC methylation for three contexts in each chromosome was shown in **Supplementary Figure 1**. The genome-wide pattern of methylated DNA was similar across chromosomes at different stages (**Figure 1A** and **Supplementary Figure 2**). The methylation level of different chromosomal positions showed significant differences, and the lowest CHH methylation was found across the genome (**Figure 1B** and **Supplementary Figure 3**).

DNA Methylation Dynamics During Grain Filling in Foxtail Millet

The context CHH methylation was accounted for the largest percentage during the whole grain filling stage followed by

[1]http://www.genome.jp/kegg/pathway.html

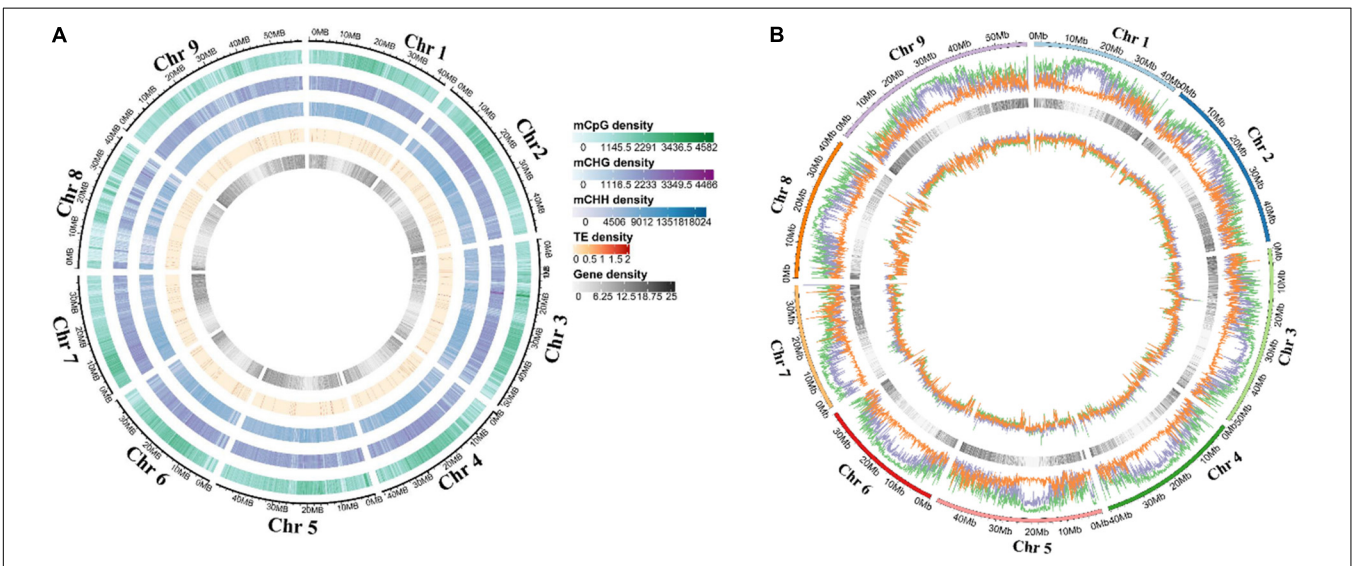

FIGURE 1 | Distribution of DNA methylation in each foxtail millet chromosome. **(A)** Circos plots of foxtail millet chromosomes. Track order: density plot of 5 mC in CG, CHG, and CHH contexts; density of TEs; gene density of each chromosome at the T1. **(B)** Density plot of 5 mC in CG (green), CHG (purple), and CHH (orange) contexts in the gene bodies on each chromosome at the T1.

CG and CHG methylation. Furthermore, CHH methylation remained elevated during grain filling (38–46%), but CG and CHG methylation showed the opposite trend (33–29 and 29–25%, respectively) (**Figure 2A**). The mean methylation levels were lowest at T2, followed by T4, which mainly occurred in the CHG context (**Figure 2B**). Moreover, methylation level in the promoter, gene-body, and downstream regions of genes also reached the bottom at T2, and then at T4 (**Figure 2C**). Besides, methylation patterns of TEs were compared among different stages. No significant differences were found in the 2 kb upstream region among five developmental stages. Interestingly, the CG methylation level of the TE-body region was less at T2 than that at other stages (**Figure 2C**). The CHH methylation level of the TE-body and 2-kb downstream region was methylated the least at T1 (**Figure 2C**). Circos plots of DNA methylation at later stages compared with T1 uncovered the distinctions in the three contexts at different genomic regions (**Figure 3** and **Supplementary Figure 4**).

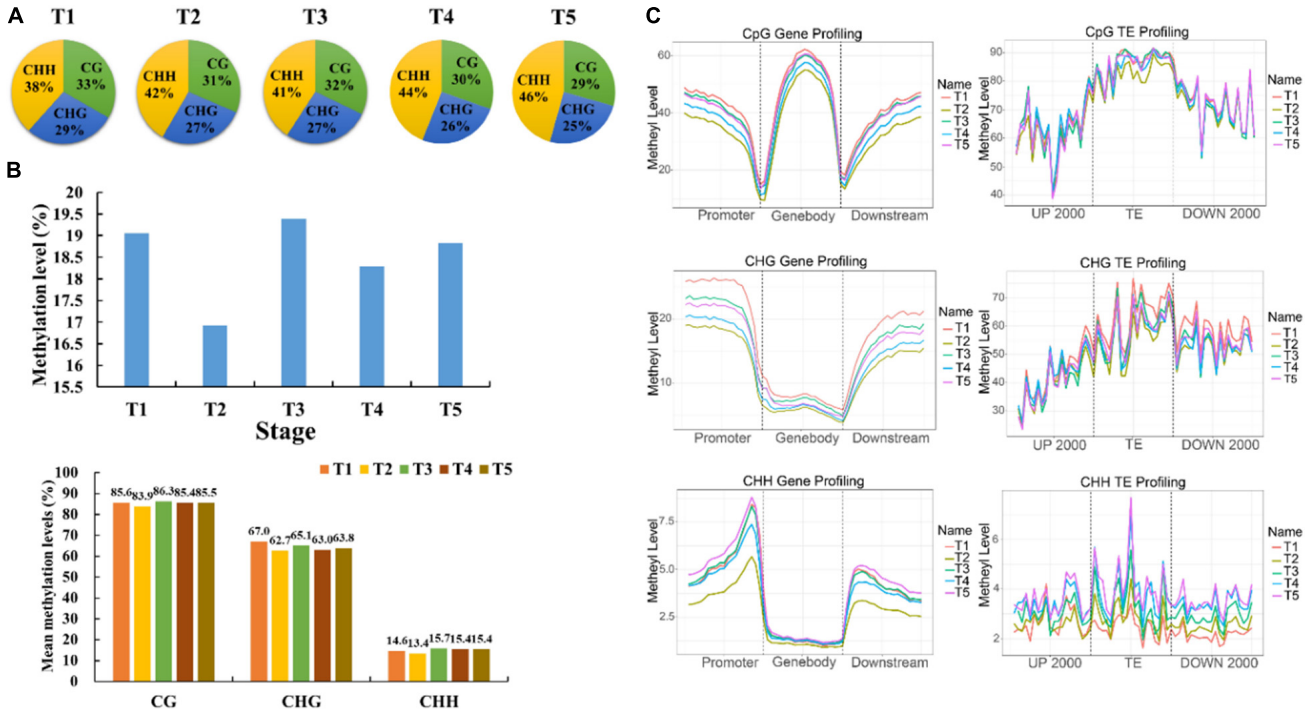

FIGURE 2 | Characteristics of DNA methylation in foxtail millet. **(A)** Relative proportions of mCs in three sequence contexts (CG, CHG, and CHH) in foxtail millet. **(B)** mC, mCG, mCHG, and mCHH methylation levels from 7 to 35 DAA. **(C)** Methylation levels (%) of CG, CHG, and CHH among gene/TE bodies and their 2-kb upstream and downstream regions at different stages.

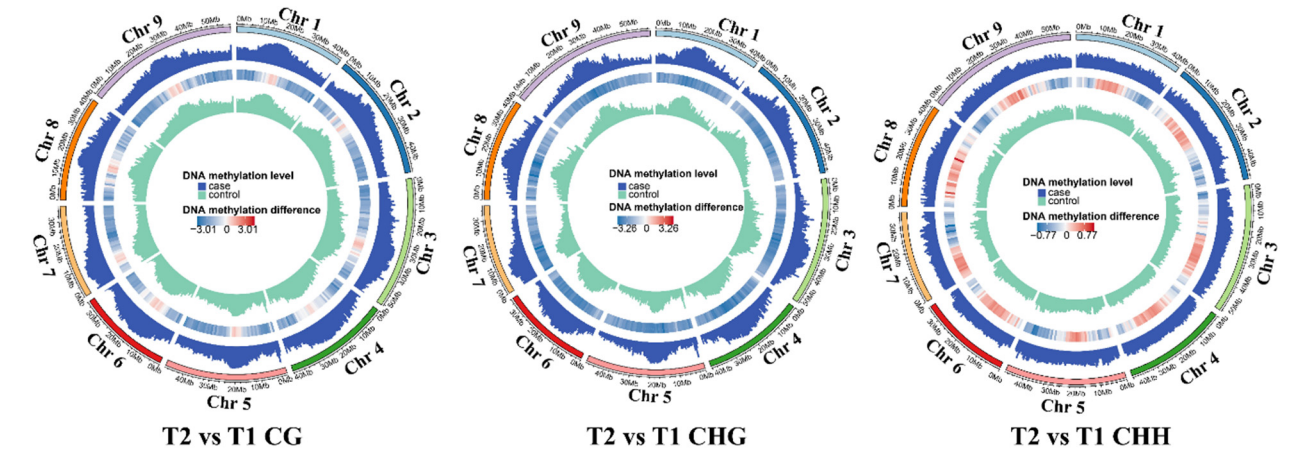

FIGURE 3 | Comparative analysis of DNA methylation levels in different genomic regions.

Identification, Distribution, and Functional Annotation of DMRs and DMPs During Grain Filling in Foxtail Millet

The differentially methylated region was analyzed for understanding the methylation differences at later stages compared with T1. The number of hyper-DMRs identified at later stages relative to T1 was gradually increased from T2 to T3, then decreased from T3 to T4, and increased again from T4 to T5. The hypo-DMRs showed an opposite trend. Furthermore, the number of CG DMRs was far more than other types of DMRs (**Supplementary Figure 5**). In CG and CHG context, the exon and intergenic regions had the most DMRs, respectively. In the CHH context, the promoter regions had the most hypo-DMRs, while hyper-DMRs were mostly distributed in the intergenic (T2 and T4), exon (T3), and promoter (T5) (**Supplementary Figure 6**). The numbers of genes with DMRs in gene-body regions (DMR_genes) and promoter regions (DMP_genes) among the different comparisons were shown in Venn analysis. For example, a total of 7,460, 2,186, and 907 DMR genes were identified for CG, CHG, and CHH contexts in the T2 vs. T1, and the number of DMP genes was 1,234, 1,234, and 183 (**Figure 4A**). Additionally, the methylation levels of the DMRs were decreased at later stages, but T3 and T5 showed higher CHH methylation levels than those in the T1 stage (**Figure 4B**).

DNA Methylation Is Regulated by DNA Methyltransferase and Demethylase

A total of 11 methyltransferases, including 3 chromomethylases (CMT), 4 domain-rearranged methyltransferases (DRM), 3 methyltransferase 1 (MET1), and 1 DNA methyltransferase-2 (DNMT2), were identified (**Supplementary Table 3**). Among the 11 methyltransferase genes, *CMT3*, *DRM3*, *MET1-1*, and *MET1-3* are barely expressed (FPKM < 1) at all five stages

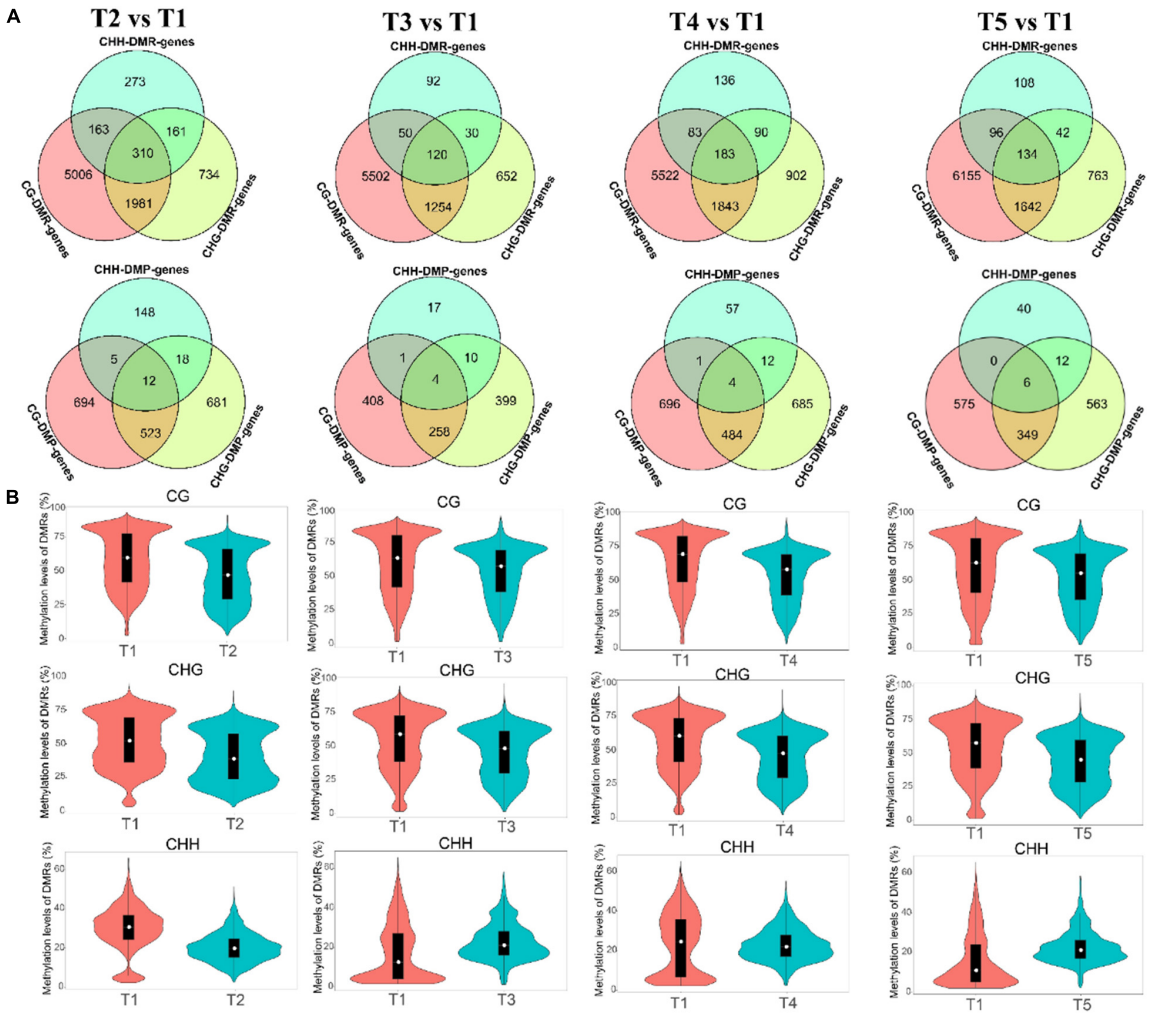

FIGURE 4 | Differentially methylated regions (DMRs) and DNA methylation levels at the T2 vs. T1, T3 vs. T1, T4 vs. T1, and T5 vs. T1 comparisons. **(A)** Venn analysis of genes with DMRs in the CG, CHG, and CHH contexts of gene-body regions (DMR genes) and promoter regions [differentially methylated promoter (DMP) genes] among the different comparisons. **(B)** DMR methylation levels in the CG, CHG, and CHH contexts of different comparisons.

(**Supplementary Table 3**). The foxtail millet genome harbors 7 DNA demethylase homologs, including 2 DEMETER (DME), 1 DEMETER-like2 (DML2), DEMETER-like3 (DML3), and 3 Repressor of Silencing1 (ROS1). *DML2* and *ROS1-3* are barely expressed (FPKM < 1) at each developmental stage (**Supplementary Table 3**).

A correlation analysis was performed to analyze the relationship among DNA methylation levels, DNA methyltransferase, and demethylase (**Supplementary Table 4**). The expression level of *SiCMT2* and *SiDRM4* were highly positively correlated with methylation levels of C, CG, and CHG, but showed a highly negative correlation with CHH. The expression level of *SiDRM2* was highly positively correlated with methylation levels of CG but showed a highly negative correlation with C, CHG, and CHH. The expression level of *SiMET1-2* was highly positively correlated with methylation levels of C and CHH.

The deoxyribonucleic acid demethylase gene *SiDME1* showed a highly positive correlation between expression and methylation level of C and CG. The expression level of *SiDME2* was highly positively correlated with methylation levels of C and CHG but showed a highly negative correlation with methylation levels of CHH. The expression levels of *SiDML3* and *SiROS1-1* were highly positively correlated with the methylation levels of CHH and C.

Regulation of Transcriptional Dynamics by DNA Methylation

Based on the FPKM, all genes were classified into four groups (**Figure 5**). Genes in the none-group were highest CG methylated in all genetic regions (**Figure 5**). The levels of none-expression genes of CHG methylation were highest in gene-body and upstream. By contrast, genes in the none-group were the lowest CHH methylated in all genetic regions. As expected, high expression genes had the lowest CG and CHG methylation and the highest levels of CHH methylation in gene-body. In low and moderate groups, no significant correlation was found between gene expression and methylation status of CG and CHH in most genetic regions. By contrast, genes with higher expression levels presented lower CHG methylation levels in gene-body (**Figure 5**).

Methylated genes were also grouped by the promoter and gene-body methylation levels (**Figure 6**). The methylation level in the gene-body region was positively correlated with the gene expression level, except the high methylated genes (fifth group), which had the lower expression levels (**Figure 6A**). However, the methylation level in the promoter region of most genes had no significant effect on gene expression, except the genes in the first group that also showed a lower expression level (**Figure 6B**).

Analysis of DEGs Associated With DNA Methylation at T2 Stage Compared With T1

To verify the effect of altered DNA methylation on DEGs, we focused on the overlapped genes of DMGs and DEGs for different comparisons. The correlation between DEGs and methylation was calculated by Pearson correlation analysis based on the expression level of DEGs and methylation level of DMR. We identified the DEGs associated with DMR in line with Pearson correlation $\geq$ 0.90 (positive correlation) or $\leq$–0.90 (negative correlation). There were 77, 49, and 14 DEGs associated with CG, CHG, and CHH DMR for T2 vs. T1, respectively (**Figure 7B**). DEGs associated with CG DMR were significantly enriched in photosynthesis-antenna proteins, metabolic pathways, and cysteine and methionine metabolism, respectively (**Figure 7A**). Representative CG DMRs in the promoter of *LHCB5* (which encoded chlorophyll a-b binding protein CP26) were methylated less at T2 than at T1 and expressed at significantly lower levels at T2 than at T1.

The enriched categories of DEGs associated with CHG DMR included amino sugar and nucleotide sugar metabolism, biosynthesis of secondary metabolites, and phenylalanine metabolism (**Figure 7A**). Representative DMRs were methylated less at T2 than that at T1, such as *APS1* (which encoded glucose-1-phosphate adenylyltransferase small subunit) and *VTC1* (which encoded mannose-1-phosphate guanylyltransferase 1) in the CHG context in the promoter, whereas an opposite trend was observed in the expression level (**Figure 7C**).

Differentially expressed genes associated with CHH DMR were enriched in fructose and mannose metabolism, inositol phosphate metabolism, and protein export. In addition, representative CHH DMRs of *VTC1* were methylated less at T2 than at T1, also expressed at significantly higher levels at T2 than at T1.

Analysis of DEGs Associated With DNA Methylation at T3 Stage Compared With T1

For T3 vs. T1, 245, 137, and 24 DEGs associated with CG, CHG, and CHH DMR were identified, respectively (**Supplementary Figure 7B**). KEGG enrichment of DEGs associated with CG DMR showed that the four most significantly altered pathways were metabolic pathways, glyoxylate, and dicarboxylate metabolism, inositol phosphate metabolism, and starch and sucrose metabolism, respectively (**Supplementary Figure 7A**). Representative CG DMRs in promoter or gene-body of four DEGs associated with starch and sucrose metabolism, *SS4* (which encoded soluble starch synthase), *PHO* (which encoded alpha-1,4 glucan phosphorylase L isozyme), *DPE1* (which encoded 4-alpha-glucanotransferase), and *BGLU31* (which encoded beta-glucosidase 31) were methylated less at T3 than at T1 but expressed at significantly higher levels at T3 than at T1. In contrast, the expression level of *FRK6* (which encoded fructokinase-6) was positively correlated with its methylation (**Supplementary Figure 7C**).

Differentially expressed genes associated with CHG DMR were enriched in seleno compound metabolism, other glycan degradation, and biosynthesis of secondary metabolites, respectively (**Supplementary Figure 7A**). Representative CHG DMRs in the promoter of *MS1* (which encoded Cobalamin-independent methionine synthase 1) were methylated less at T3 than that at T1, and also expressed at significantly lower levels at T3 than at T1.

Differentially expressed genes associated with CHH DMR were enriched in porphyrin and chlorophyll metabolism, MAPK signaling pathway, and plant hormone signal transduction

(**Supplementary Figure 7A**). The methylation of CHH DMR in gene-body of *CHLH* (which encoded magnesium-chelatase subunit) showed a negative correlation with its expression level.

Analysis of DEGs Associated With DNA Methylation at T4 Stage Compared With T1

For T4 vs. T1, 150, 134, and 34 DEGs associated with CG, CHG, and CHH DMR were identified respectively (**Supplementary Figure 8B**). KEGG pathway analysis of DEGs associated with CG DMR indicated that the three most significantly changed pathways were pyrimidine metabolism, oxidative phosphorylation, and purine metabolism (**Supplementary Figure 8A**). Representative CG DMRs in gene-body of four DEGs associated with pyrimidine metabolism, *POLA* (DNA polymerase I A), *pyrH* (uridylate kinase), *RNR1* (ribonucleoside-diphosphate reductase large subunit), and *PBY1* (5′-nucleotidase SurE) were methylated less at T4 than at T1, and the majority of them were expressed at

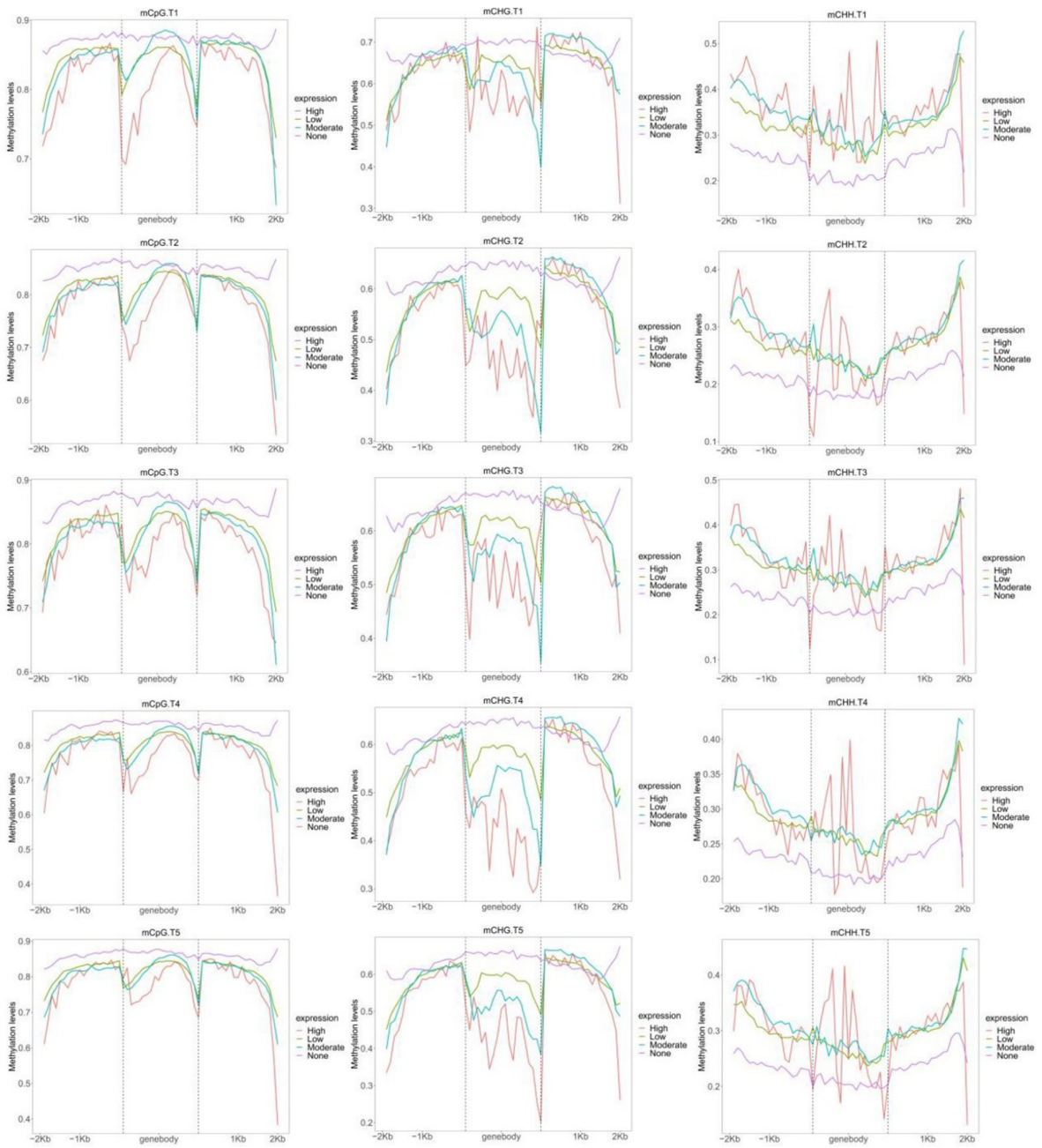

FIGURE 5 | Distribution of CG, CHG, and CHH methylation levels within gene bodies based on four different expression levels: none, high, moderate, and low.

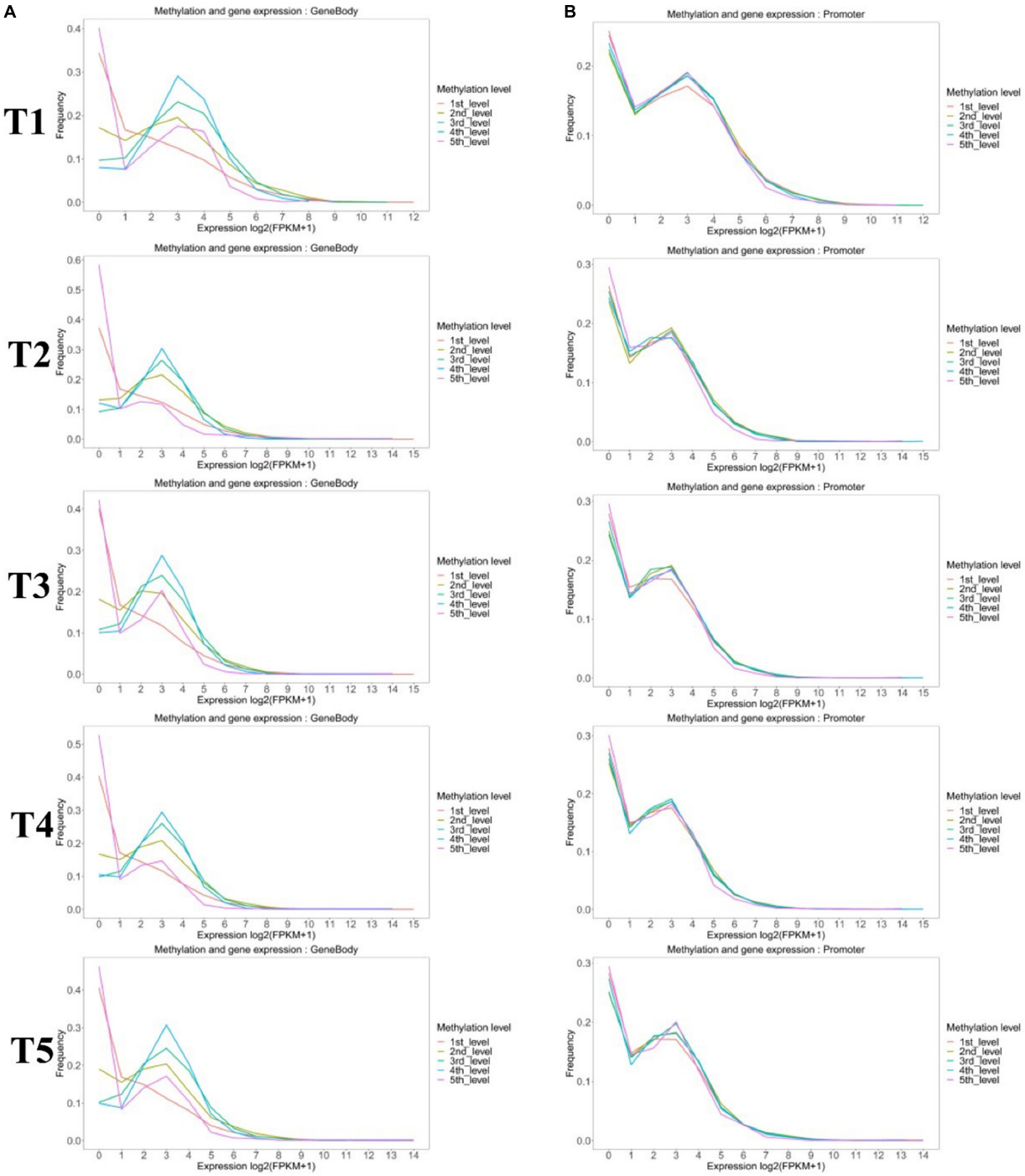

FIGURE 6 | Comparison of the expression profiles of methylated and unmethylated genes. Methylated genes were further divided into quintiles based on **(A)** gene-body and **(B)** promoter methylation levels as follows: first: methylation level < 20%; second: 20% <methylation level <40%; third: 40% <methylation level <60%; fourth: 60% <methylation level <80%; and fifth: methylation level > 80%.

significantly lower levels at T4 than at T1 except for *POLA* (**Supplementary Figure 8C**).

Kyoto Encyclopedia of Genes and Genomes pathway analysis demonstrated that the DEGs associated with CHG DMR were primarily related to photosynthesis, beta-alanine metabolism and ascorbate, and aldarate metabolism (**Supplementary Figure 8A**). Representative CHG DMRs in promoter and gene-body of *FDX5* (which encoded ferredoxin) and *FDC1* (which encoded ferredoxin-2) were methylated less at T4 than at T1 and were expressed at significantly lower levels at T4 than at T1.

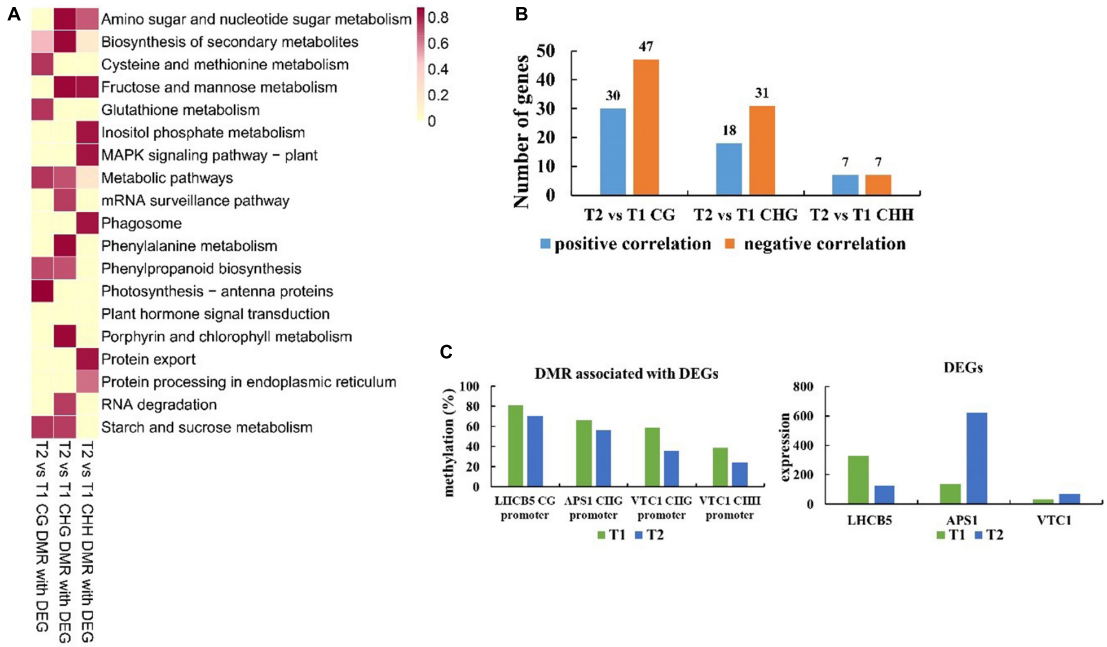

FIGURE 7 | Function, methylation, and expression analysis of differentially expressed genes (DEGs) associated with CG, CHG, and CHH DMR for T2 vs. T1. **(A)** Kyoto Encyclopedia of Genes and Genomes (KEGG) analysis of DEGs associated with CG, CHG, and CHH DMR for T2 vs. T1. Enriched KEGG pathways are shown *via* heatmap. The scale represents $-\log_{10}{}^{p\text{-value}}$ of enriched KEGG pathways. **(B)** The numbers of DEGs present a positive or negative correlation between methylation and expression levels. **(C)** Methylation and expression levels of specific genes between T2 and T1.

Differentially expressed genes associated with CHH DMR were enriched in the biosynthesis of unsaturated fatty acids, alpha-linolenic acid metabolism, and pentose phosphate pathway (**Supplementary Figure 8A**). The methylation of CHH DMR in the promoter of *ACX4* (which encoded acyl-coenzyme A oxidase 4) showed a positive correlation with its expression level.

Analysis of DEGs Associated With DNA Methylation at T5 Stage Compared With T1

There were 249, 147, and 28 DEGs associated with CG, CHG, and CHH DMR identified at T5 compared with T1, respectively (**Supplementary Figure 9B**). The top three KEGG pathways of DEGs associated with CG DMR were nitrogen metabolism, base excision repair, and anthocyanin biosynthesis (**Supplementary Figure 9A**). Representative CG DMRs in promoter or gene-body of DEGs associated with nitrogen metabolism, *ACA7* (alpha carbonic anhydrase 7) and *GLN2* (glutamine synthetase) were methylated and expressed less at T5 than that at T1, but the expression level of *NRT2.4* (high-affinity nitrate transporter 2.4) was negatively correlated with its methylation.

The functional enrichment of DEGs associated with CHG DMR primarily included arginine and proline metabolism, phenylalanine, tyrosine, and tryptophan biosynthesis, and tropane, piperidine, and pyridine alkaloid biosynthesis (**Supplementary Figure 9A**). Representative CHG DMRs in the promoter of *PAO1* (which encoded polyamine oxidase 5) and *ASP5* (which encoded aspartate aminotransferase) were methylated less at T5 than that at T1 and expressed at significantly lower levels at T5 than at T1.

Differentially expressed genes associated with CHH DMR were enriched in the pentose phosphate pathway, fructose, and mannose metabolism, and MAPK signaling pathway (**Supplementary Figure 9A**). The methylation levels of CHH DMR in gene-body and promoter of *PFP-ALPHA* (which encoded pyrophosphate–fructose 6-phosphate 1-phosphotransferase subunit alpha) and *G6PDH* (glucose-6-phosphate 1-dehydrogenase) were higher at T5 than at T1 but expressed at significantly lower levels at T5 than at T1.

DISCUSSION

Deoxyribonucleic acid methylation mediates plant development and phase transition. In apple, DNA methylation influenced apple flower bud formation (Xing et al., 2019). During the juvenile-to-adult phase transition, there was a significant correlation between DNA methylation and gene expression in *Malus hupehensis* (Xing et al., 2020). The genomic DNA methylation level was gradually increased during the ripening stage of sweet orange (Huang et al., 2019). DNA methylation dynamic played a pivotal role during seed development in chickpeas (Rajkumar et al., 2020). Nonetheless, the potential effect of epigenetic regulation on grain filling remains unknown despite the works done regarding its grain development and filling. Integrated herein is the epigenome and transcriptome

analysis to gain new insights into DNA methylation in foxtail millet.

The contexts mCG were dominated followed by mCHG and mCHH in *Arabidopsis thaliana* and *mulberry* (Lister et al., 2008; Li et al., 2020). However, mCHH accounted for the highest proportion of total mC in the study, followed by the CG and CHG context. These findings are consistent with studies in apple trees, *M. hupehensis*, and cotton (Xu et al., 2018; Xing et al., 2019, 2020; Zhang et al., 2020). It is worth noting that CHH methylation remained elevated during grain filling (38–46%) and CG and CHG methylation showed the opposite trend (33–29 and 29–25%, respectively). Additionally, the fractional methylation levels in foxtail millet were similar with other plants, such as rice, *Beta vulgaris*, soybean, and poplar, with the highest levels in the CG context, followed by the CHG and CHH contexts (Li et al., 2008; Niederhuth et al., 2016). Previous studies have shown that DNA was methylated differently at different genetic regions, which also could affect gene expression (Ibarra et al., 2012; Liu et al., 2015). More methylated DNAs were found upstream of a gene in certain plants (Xing et al., 2019, 2020). However, in the present study, the CG methylation of gene-body was significantly higher than that in other regions, which was consistent with earlier reports in strawberry, orange, and peach (Cheng et al., 2018; Huang et al., 2019; Zhu et al., 2020).

Deoxyribonucleic acid methylation levels could be affected by the interaction, either coordination or antagonism, between DNA methyltransferase and demethylase. The regulation patterns varied from different plants between DNA methyltransferase and demethylase. During the fruit development, the expression of demethylase and DNA methylation level showed an opposite trend in orange and tomato (Huang et al., 2019; Wang et al., 2020a). The expression of DNA methyltransferase and demethylase could only affect methylation levels in specific contexts in some plants. For instance, only the methylation levels of C and CHH could be positively regulated by the expression level of *PpDRM1* in peach (Zhu et al., 2020). Sometimes, antagonism between DNA methyltransferase and demethylase affects the dynamic DNA methylation changes. For instance, drought induces DNA methylation levels in rice, but gene expression of methyltransferase and demethylase were both increased (Wang et al., 2020a). In this study, it is shown that the expression of some DNA methyltransferases and demethylase could enhance DNA methylation in specific contexts, and inhibit the methylation levels in others. Thus, the antagonism and synergy of DNA methyltransferases and demethylase could affect the dynamic change of methylation in specific contexts during grain filling in foxtail millet.

Deoxyribonucleic acid methylation-mediated gene regulation varied among different genetic regions. Global methylation and transcriptional analyses found that gene-body methylation could repress gene expression. DNA methylation in promoters may increase gene expression during flower bud formation in apples (Xing et al., 2019). In contrast, methylation analysis found that genes with unmethylated promoters presented a higher expression level and gene-body methylation may increase gene expression level under water deficit stress in apples (Xu et al., 2018). In cotton, genes with promoter DNA methylation had a low expression level, whereas the expression level of genes with gene-body methylation was higher than those without gene-body methylation (Zhang et al., 2020). Genes herein with hypermethylation in gene-body also showed a higher gene expression except for the highest methylated gene (fifth level). No distinct correlation was found between gene expression and methylated level in the promoters of most genes.

The specific role of methylated DNA in foxtail millet is largely unknown. To understand whether methylated DNA participated in transcription dynamic changes and the regulation of grain development, DEGs associated with DMR at T2, T3, T4, and T5 compared with T1 were identified. Previous studies demonstrated that the photosynthetic capacity and grain chlorophyll contents were closely related to grain filling rate in rice (Chen et al., 2020). In this study, DEGs involved in photosynthesis-antenna proteins, porphyrin and chlorophyll metabolism, and photosynthesis were identified as associated with CG, CHH, and CHG DMR, such as *LHCB5*, *CHLH*, and *FDX5*. Genes related to carbohydrate metabolism, nucleic acid, and protein metabolism were enriched for ontologies during grain development (Yu et al., 2016; Yang et al., 2017; Brinton and Uauy, 2019). As expected, DNA methylation altered the expression level of DEGs related to carbohydrate metabolisms, such as *APS1*, *VTC1*, and *MS1*, which were responsible for amino sugar and nucleotide sugar metabolism, fructose and mannose metabolism, and other glycan degradation, respectively. In addition, DEGs involved in cysteine and methionine metabolism and arginine and proline metabolism were also associated with DMR. It is well known that starch and sucrose metabolism were important factors for grain filling (Wang et al., 2015). In the current study, four DEGs associated with starch and sucrose metabolism, which are *SS4*, *PHO*, *DPE1*, and *BGLU31*, presented a negative correlation between methylation and their expression, but *FRK6* showed a positive correlation between its methylation and its expression level at T3 compared with T1. The results of this study demonstrated that the dynamic change of DNA methylation plays a crucial function in gene regulation, revealing the potential function of epigenetics in grain development in foxtail millet. This can be further studied using the currently more advanced genome editing technology, such as CRISPR/Cas, which studies gene function not only genetically but also epigenetically (Li et al., 2021; Zhang et al., 2021).

CONCLUSION

In conclusion, we showed global DNA methylation dynamics and its regulatory function in gene expression in foxtail millet. Gene expression was negatively associated with CG and CHG DNA methylation, while that in the CHH context was positively associated with methylation in gene-body regions. The evaluation of the interconnection of the DNA methylome and transcriptome identified some stage-specific DEGs associated with grain filling, indicating that the expression of certain genes, involved in specific pathways, could be regulated by DNA methylation modification during grain development. We found, herein, that DNA methylation of different genetic regions has an important

influence on the transcriptome changes, suggesting an epigenetic regulatory mechanism in the grain filling process in foxtail millet.

DATA AVAILABILITY STATEMENT

The datasets presented in this study can be found in online repositories. The names of the repository/repositories and accession number(s) can be found below: NCBI database with BioProject accession: PRJNA699635; BioSample: SAMN17804127 (https://www.ncbi.nlm.nih.gov/bioproject/PRJNA699635).

AUTHOR CONTRIBUTIONS

TW and RP conceived and designed the experiments. TW, QL, and HS performed the experiments. NH, PL, YW, YL, ZZ, and JL contributed reagents, materials, and analysis tools. TW, BZ, and RP wrote and revised the manuscript. All authors contributed to the article and approved the submitted version.

FUNDING

This research was funded by the National Key R&D Program of China (Nos. 2019YFD1000700 and 2019YFD1000702), Science and Technology Project of Henan Province (212102110239), Central Plains Science and Technology Innovation Leader Project (No. 214200510029), and Initial Fund for Innovation and Practice Base for Postdoctors of Anyang Institute of Technology (No. BHJ2020001).

SUPPLEMENTARY MATERIAL

The Supplementary Material for this article can be found online at: https://www.frontiersin.org/articles/10.3389/fpls.2021.741415/full#supplementary-material

REFERENCES

Akalin, A., Kormaksson, M., Li, S., Garrett-Bakelman, F., Figueroa, M., Melnick, A., et al. (2012). MethylKit: a comprehensive R package for the analysis of genome-wide DNA methylation profiles. *Genome Biol.* 13:87. doi: 10.1186/gb-2012-13-10-r87

Bennetzen, J. L., Schmutz, J., Wang, H., Percified, R., Hawkins, H., Pontaroli, A. C., et al. (2012). Reference genome sequence of the model plant Setaria. *Nat. Biotechnol.* 30, 555–561.

Brinton, J., and Uauy, C. (2019). A reductionist approach to dissecting grain weight and yield in wheat. *J. Integr. Plant Biol.* 61, 337–358. doi: 10.1111/jipb.12741

Chen, J., Cao, F., Li, H., Shan, S., Tao, Z., Lei, T., et al. (2020). Genotypic variation in the grain photosynthetic contribution to grain filling in rice. *J. Plant Physiol.* 253:153269. doi: 10.1016/j.jplph.2020.153269

Chen, T., Xu, Y., Wang, J., Wang, Z., Yang, J., and Zhang, J. (2013). Polyamines and ethylene interact in rice grains in response to soil drying during grain filling. *J. Exp. Bot.* 64, 2523–2538. doi: 10.1093/jxb/ert115

Cheng, J., Niu, Q., Zhang, B., Chen, K., Yang, R., Zhu, J. K., et al. (2018). Downregulation of RdDM during strawberry fruit ripening. *Genome Biol.* 19:212.

Dong, N. Q., Sun, Y., Guo, T., Shi, C. L., Zhang, Y. M., Kan, Y., et al. (2020). UDP-glucosyltransferase regulates grain size and abiotic stress tolerance associated with metabolic flux redirection in rice. *Nat. Commun.* 11:2629.

Huang, H., Li, R., Niu, Q., Tang, K., Zhang, B., Zhang, H., et al. (2019). Global increase in DNA methylation during orange fruit development and ripening. *Proc. Natl. Acad. Sci. U. S. A.* 116, 1430–1436. doi: 10.1073/pnas.1815441116

Ibarra, C. A., Feng, X., Schoft, V. K., Hsieh, T. F., Uzawa, R., Rodrigues, J. A., et al. (2012). Active DNA demethylation in plant companion cells reinforces transposon methylation in gametes. *Science* 337, 1360–1364. doi: 10.1126/science.1224839

Jin, L., Jiang, Z., Xia, Y., Lou, P., Chen, L., Wang, H., et al. (2014). Genome-wide DNA methylation changes in skeletal muscle between young and middle-aged pigs. *BMC Genomics* 15:653. doi: 10.1186/1471-2164-15-653

Kanehisa, M., Araki, M., Goto, S., Hattori, M., Hirakawa, M., Itoh, M., et al. (2008). KEGG for linking genomes to life and the environment. *Nucleic Acids Res.* 36, D480–D484.

Kato, T., Shinmura, D., and Taniguchi, A. (2007). Activities of Enzymes for Sucrose-Starch Conversion in Developing Endosperm of Rice and Their Association with Grain Filling in Extra-Heavy Panicle Types. *Plant Product. Sci.* 10, 442–450. doi: 10.1626/pps.10.442

Krueger, F., and Andrews, S. R. (2011). Bismark: a flexible aligner and methylation caller for Bisulfite-Seq applications. *Bioinformatics* 27, 1571–1572. doi: 10.1093/bioinformatics/btr167

Lata, C., Gupta, S., and Prasad, M. (2013). Foxtail millet: a model crop for genetic and genomic studies in bioenergy grasses. *Crit. Rev. Biotechnol.* 33, 328–343. doi: 10.3109/07388551.2012.716809

Li, C., Brant, E., Budak, H., Zhang, B., et al. (2021). CRISPR/Cas: a Nobel Prize award-winning precise genome editing technology for gene therapy and crop improvement. *J. Zhejiang Univ. Sci. B* 22, 253–284. doi: 10.1631/jzus.b2100009

Li, R., Hu, F., Li, B., Zhang, Y., Chen, M., Fan, T., et al. (2020). Whole genome bisulfite sequencing methylome analysis of mulberry (Morus alba) reveals epigenome modifications in response to drought stress. *Sci. Rep.* 10:8013.

Li, X., Wang, X., He, K., Ma, Y., Su, N., He, H., et al. (2008). High-resolution mapping of epigenetic modifications of the rice genome uncovers interplay between DNA methylation, histone methylation, and gene expression. *Plant Cell* 20, 259–276. doi: 10.1105/tpc.107.056879

Lister, R., O'Malley, R. C., Tonti-Filippini, J., Gregory, B. D., Berry, C. C., Millar, A. H., et al. (2008). Highly integrated single-base resolution maps of the epigenome in Arabidopsis. *Cell* 133, 523–536. doi: 10.1016/j.cell.2008.03.029

Liu, R., How-Kit, A., Stammitti, L., Teyssier, E., Rolin, D., Mortain-Bertrand, A., et al. (2015). A DEMETER-like DNA demethylase governs tomato fruit ripening. *Proc. Natl. Acad. Sci. U. S. A.* 112, 10804–10809. doi: 10.1073/pnas.1503362112

Liu, Y., Liang, H., Lv, X., Liu, D., Wen, X., and Liao, Y. (2016). Effect of polyamines on the grain filling of wheat under drought stress. *Plant Physiol. Biochem.* 100, 113–129. doi: 10.1016/j.plaphy.2016.01.003

Maunakea, A. K., Nagarajan, R. P., Bilenky, M., Ballinger, T. J., D'Souza, D., Fouse, S. D., et al. (2010). Conserved role of intragenic DNA methylation in regulating alternative promoters. *Nature* 466, 253–257. doi: 10.1038/nature09165

Muthamilarasan, M., and Prasad, M. (2015). Advances in Setaria genomics for genetic improvement of cereals and bioenergy grasses. *Theor. Appl. Genet.* 128, 1–14. doi: 10.1007/s00122-014-2399-3

Niederhuth, C. E., Bewick, A. J., Ji, L., Alabady, M. S., Kim, K. D., Li, Q., et al. (2016). Widespread natural variation of DNA methylation within angiosperms. *Genome Biol.* 17:194.

Peng, R., and Zhang, B. (2021). Foxtail Millet: a New Model for C4 Plants. *Trends Plant Sci.* 26, 199–201. doi: 10.1016/j.tplants.2020.12.003

Rajkumar, M. S., Gupta, K., Khemka, N. K., Garg, R., and Jain, M. (2020). DNA methylation reprogramming during seed development and its functional relevance in seed size/weight determination in chickpea. *Commun. Biol.* 3:340.

Ranwala, A. P., and Miller, W. B. (1998). Sucrose-cleaving enzymes and carbohydrate pools in Lilium longiflorum floral organs. *Physiol. Plant.* 103, 541–550. doi: 10.1034/j.1399-3054.1998.1030413.x

Saini, H. S., and Westgate, M. E. (1999). Reproductive development in grain crops during drought. *Adv. Agron.* 68, 59–96. doi: 10.1016/s0065-2113(08)60843-3

Wang, G., Li, H., Meng, S., Yang, J., Ye, N., and Zhang, J. (2020a). Analysis of Global Methylome and Gene Expression during Carbon Reserve Mobilization in Stems under Soil Drying. *Plant Physiol.* 183, 1809–1824. doi: 10.1104/pp.20.00141

Wang, G., Li, H., Wang, K., Yang, J., Duan, M., Zhang, J., et al. (2020b). Regulation of gene expression involved in the remobilization of rice straw carbon reserves results from moderate soil drying during grain filling. *Plant J.* 101, 604–618. doi: 10.1111/tpj.14565

Wang, G. Q., Li, H. X., Feng, L., Chen, M. X., Meng, S., Ye, N. H., et al. (2019). Transcriptomic analysis of grain filling in rice inferior grains under moderate soil drying. *J. Exp. Bot.* 70, 1597–1611. doi: 10.1093/jxb/erz010

Wang, T., Song, H., Li, P., Wei, Y., Hu, N., Chen, Z., et al. (2020). Transcriptome Analysis Provides Insights into Grain Filling in Foxtail Millet (*Setaria italica* L.). *Int. J. Mol. Sci.* 21:5031. doi: 10.3390/ijms21145031

Wang, Z., Xu, Y., Chen, T., Zhang, H., Yang, J., and Zhang, J. (2015). Abscisic acid and the key enzymes and genes in sucrose-to-starch conversion in rice spikelets in response to soil drying during grain filling. *Planta* 241, 1091–1107. doi: 10.1007/s00425-015-2245-0

Wei, X., Jiao, G., Lin, H., Sheng, Z., Shao, G., Xie, L., et al. (2017). GRAIN INCOMPLETE FILLING 2 regulates grain filling and starch synthesis during rice caryopsis development. *J. Integr. Plant Biol.* 59, 134–153. doi: 10.1111/jipb.12510

Wen, D., Li, Y., He, L., and Zhang, C. (2019). Transcriptome analysis reveals the mechanism by which spraying diethyl aminoethyl hexanoate after anthesis regulates wheat grain filling. *BMC Plant Biol.* 19:327. doi: 10.1186/s12870-019-1925-5

Xiao, K., Chen, J., He, Q., Wang, Y., Shen, H., and Sun, L. (2020). DNA methylation is involved in the regulation of pepper fruit ripening and interacts with phytohormones. *J. Exp. Bot.* 71, 1928–1942. doi: 10.1093/jxb/eraa003

Xing, L., Li, Y., Qi, S., Zhang, C., Ma, W., Zuo, X., et al. (2019). Comparative RNA-Sequencing and DNA Methylation Analyses of Apple (Malus domestica Borkh.) Buds with Diverse Flowering Capabilities Reveal Novel Insights into the Regulatory Mechanisms of Flower Bud Formation. *Plant Cell Physiol.* 60, 1702–1721. doi: 10.1093/pcp/pcz080

Xing, L., Qi, S., Zhou, H., Zhang, W., Zhang, C., Ma, W., et al. (2020). Epigenomic Regulatory Mechanism in Vegetative Phase Transition of *Malus hupehensis*. *J. Agric. Food Chem.* 68, 4812–4829. doi: 10.1021/acs.jafc.0c00478

Xu, J., Zhou, S., Gong, X., Song, Y., Nocker, S. V., Ma, F., et al. (2018). Single-base methylome analysis reveals dynamic epigenomic differences associated with water deficit in apple. *Plant Biotechnol. J.* 16, 672–687. doi: 10.1111/pbi.12820

Yang, J., Zhang, J., Wang, Z., Liu, K., and Wang, P. (2006). Post-anthesis development of inferior and superior spikelets in rice in relation to abscisic acid and ethylene. *J. Exp. Bot.* 57, 149–160. doi: 10.1093/jxb/erj018

Yang, M., Gao, X., Dong, J., Gandhi, N., Cai, H., von Wettstein, D. H., et al. (2017). Pattern of Protein Expression in Developing Wheat Grains Identified through Proteomic Analysis. *Front. Plant Sci.* 8:962. doi: 10.3389/fpls.2017.00962

Yu, Y., Zhu, D., Ma, C., Cao, H., Wang, Y., Xu, Y., et al. (2016). Transcriptome analysis reveals key differentially expressed genes involved in wheat grain development. *Crop J.* 4, 92–106. doi: 10.1016/j.cj.2016.01.006

Zhang, D., Zhanf, M., Zhou, Y., Shen, J., Chen, H., et al. (2019). The Rice G Protein gamma Subunit DEP1/qPE9-1 Positively Regulates Grain-Filling Process by Increasing Auxin and Cytokinin Content in Rice Grains. *Rice (N Y)* 12:91.

Zhang, D., Zhang, Z., Unver, T., and Zhang, B. (2021). CRISPR/Cas: a powerful tool for gene function study and crop improvement. *J. Adv. Res.* 29, 207–221. doi: 10.1016/j.jare.2020.10.003

Zhang, M., Zhang, X., Guo, L., Qi, T., Liu, G., Feng, J., et al. (2020). Single-base resolution methylome of cotton cytoplasmic male sterility system reveals epigenomic changes in response to high-temperature stress during anther development. *J. Exp. Bot.* 71, 951–969.

Zhong, S., Fei, Z., Chen, Y., Zheng, Y., Huang, M., Vrebalov, J., et al. (2013). Single-base resolution methylomes of tomato fruit development reveal epigenome modifications associated with ripening. *Nat. Biotechnol.* 31, 154–159. doi: 10.1038/nbt.2462

Zhu, Y. C., Zhang, B., Allan, A. C., Lin-Wang, K., Zhao, Y., Wang, K., et al. (2020). DNA demethylation is involved in the regulation of temperature-dependent anthocyanin accumulation in peach. *Plant J.* 102, 965–976. doi: 10.1111/tpj.14680

Conflict of Interest: The authors declare that the research was conducted in the absence of any commercial or financial relationships that could be construed as a potential conflict of interest.

Publisher's Note: All claims expressed in this article are solely those of the authors and do not necessarily represent those of their affiliated organizations, or those of the publisher, the editors and the reviewers. Any product that may be evaluated in this article, or claim that may be made by its manufacturer, is not guaranteed or endorsed by the publisher.

frontiers in Plant Science

REVIEW
published: 20 September 2021
doi: 10.3389/fpls.2021.744357

MicroRNA Techniques: Valuable Tools for Agronomic Trait Analyses and Breeding in Rice

Jiwei Chen[1,2], Sachin Teotia[3], Ting Lan[1,2] and Guiliang Tang[4]**

[1]Guangdong Provincial Key Laboratory for Plant Epigenetics, Longhua Bioindustry and Innovation Research Institute, College of Life Sciences and Oceanography, Shenzhen University, Shenzhen, China, [2]Key Laboratory of Optoelectronic Devices and Systems of Ministry of Education and Guangdong Province, College of Optoelectronic Engineering, Shenzhen University, Shenzhen, China, [3]Department of Biotechnology, Sharda University, Greater Noida, India, [4]Department of Biological Sciences, Life Science and Technology Institute, Michigan Technological University, Houghton, MI, United States*

MicroRNAs (miRNAs) are a class of small noncoding RNAs that regulate gene expression at the post-transcriptional level. Extensive studies have revealed that miRNAs have critical functions in plant growth, development, and stress responses and may provide valuable genetic resources for plant breeding research. We herein reviewed the development, mechanisms, and characteristics of miRNA techniques while highlighting widely used approaches, namely, the short tandem target mimic (STTM) approach. We described STTM-based advances in plant science, especially in the model crop rice, and introduced the CRISPR-based transgene-free crop breeding. Finally, we discussed the challenges and unique opportunities related to combining STTM and CRISPR technology for crop improvement and agriculture.

Keywords: microRNA, short tandem target mimic, agronomic traits, crop breeding, CRISPR/Cas9

OPEN ACCESS

Edited by:
Xiaozeng Yang,
Beijing Academy of Agricultural and Forestry Sciences, China

Reviewed by:
Wen-Xue Li,
Chinese Academy of Agricultural Sciences (CAAS), China
Guodong Ren,
Fudan University, China

****Correspondence:***
Ting Lan
lantingchn@foxmail.com
Guiliang Tang
gtang1@mtu.edu

Specialty section:
This article was submitted to Plant Physiology, a section of the journal Frontiers in Plant Science

Received: *20 July 2021*
Accepted: *16 August 2021*
Published: *20 September 2021*

Citation:
Chen J, Teotia S, Lan T and Tang G (2021) MicroRNA Techniques: Valuable Tools for Agronomic Trait Analyses and Breeding in Rice. Front. Plant Sci. 12:744357. doi: 10.3389/fpls.2021.744357

INTRODUCTION

MicroRNAs (miRNAs) are a class of short noncoding RNAs (20–24 nt) that mediate gene expression by complementarily binding to their targeted transcripts for mRNA cleavage or protein translation inhibition (Sanei and Chen, 2015). Mature miRNAs are generated from precursor stem-loop structures (pre-miRNAs), which are the intermediates processed from primary miRNA transcripts (pri-miRNAs) transcribed by RNA polymerase II from *MIR* genes (Yu et al., 2019). Substantial evidence has shown that miRNAs play crucial roles in diverse biological processes, including plant development and biotic and abiotic stress responses. A growing number of yield-related agronomic traits have also been found to be associated with miRNAs (Zheng and Qu, 2015; Peng et al., 2019), which makes miRNAs promising targets for crop improvement.

Since the first set of plant miRNAs was identified in *Arabidopsis* in 2002 (Llave et al., 2002; Park et al., 2002; Reinhart et al., 2002), an increasing number of miRNAs have been discovered and annotated due to high-throughput sequencing. However, the biological functions of most miRNAs have not been thoroughly explored. To decipher the function of miRNAs, multiple molecular-based approaches have been applied, such as the overexpression of *MIR* genes (Aukerman and Sakai, 2003), anti-microRNA oligonucleotides (AMOs; Hutvágner et al., 2004), RNA interference (RNAi; Vaistij et al., 2010), artificial miRNA (amiRNA; Eamens et al., 2011), endogenous and artificial target mimicry (Ebert et al., 2007; Franco-Zorrilla et al., 2007;

Yan et al., 2012), transcription activator-like effector nucleases (TALEN; Hu et al., 2013), and clustered regularly interspaced short palindromic repeats/CRISPR-associated nuclease 9 (CRISPR/Cas9; Jacobs et al., 2015; **Figure 1**). Functional analyses of miRNAs have been achieved through overexpression for gain-of-function or knockdown/knockout for loss-of-function. Among these techniques, RNAi, amiRNA, TALEN, and CRISPR/Cas9, which were initially applied for the functional analysis of protein-encoding genes, have proven to be useful for the subsequent regulation of miRNAs (Fire et al., 1998; Schwab et al., 2006; Morbitzer et al., 2010; Shan et al., 2013). AMOs and sponges (SPs) were initially developed to inhibit miRNA action in animal systems and subsequently adopted in plants (Xian et al., 2014; He et al., 2016). MiRNA decoys/mimics such as target mimic (TMs) and short tandem target mimics (STTMs) were developed based on the discovery of miRNA sequestration by endogenous target mimics in plants (Franco-Zorrilla et al., 2007; Todesco et al., 2010; Yan et al., 2012).

These techniques have greatly expanded our abilities in plant miRNA research; more importantly, these methods are constantly being improved for broader applications in research and plant breeding. Thus, there is a strong need for a comprehensive understanding of the key features of each technique and effective controls on these methods for various research purposes. Here, we reviewed the major approaches used for determining the function of miRNAs, with a focus on the STTM technique and its applications in the functional characterization of miRNAs involved in various rice agronomic traits, and illustrated transgene-free breeding practices based on transgenic outcomes *via* CRISPR/Cas9. We also discussed the challenges and potential future trends of STTM applications in the functional analysis of miRNAs and in crop breeding.

TECHNIQUES FOR DETERMINING miRNA FUNCTIONS IN PLANTS

Gain-of-Function Analysis Techniques

There are several approaches to functionally characterize miRNAs based on gain-of-function strategies (**Figure 2A**). Both precursor miRNAs (pre-miRNAs; Boualem et al., 2008) and the full-length cDNA of *MIR* genes (Yang et al., 2013) can be used for miRNA overexpression. In addition, a vector system containing two-hit artificial miRNA in *Arabidopsis* miR168a backbone can also successfully overexpress endogenous miRNAs. In this approach, endogenous miRNAs are introduced by the insertion of complementary endogenous miRNA* with mismatches at positions corresponding to site 1 and site 12 of the miRNA strand (Ji et al., 2011). A strong constitutive 35S promoter is widely used to achieve gain-of-function effects, but conclusions derived from this strategy should be evaluated cautiously due to the misrepresentative expression level and pattern of miRNAs *in vivo*. In addition, given the involvement of miRNAs in diverse and complex regulatory networks, different transgenesis strategies should be adopted by exploiting specific promoters, such as tissue-specific, stress-induced, or developmental stage-specific promoters that correspond to specific research goals and can avoid pleiotropic effects (Peng et al., 2018).

Loss-of-Function Analysis Techniques

Techniques Targeting the Genome Sequences of miRNAs

In recent years, several gene-editing tools, such as zinc-finger nucleases (ZFNs), TALENs, and CRISPR/Cas systems, have been developed based on different sequence-specific engineered endonucleases (SSNs), and some of them have been adopted for functional analysis of miRNAs in plants (**Figure 2B**). ZFNs and TALENs recognize target sequences by protein motifs, which requires researchers to assemble specific proteins for each target and limits their widespread adoption (Gaj et al., 2013). In contrast, the CRISPR/Cas system recognizes genomic target sites by base complementary pairing between the single-guide RNA (sgRNA) and the target DNA, which greatly simplifies its application (Xie and Yang, 2013). Many miRNAs have been characterized by TALENs in animals, but only one study has made TALEN constructs for miRNA gene editing that resulted in heritable mutations in plants (Bi et al., 2020). The CRISPR/Cas9 system was successfully used to conduct protein-coding

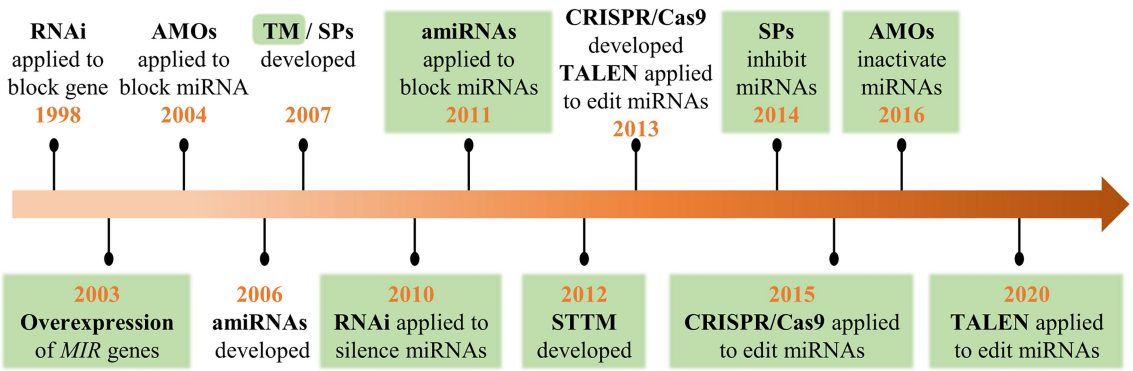

FIGURE 1 | A historical timeline of the crucial technological developments in the functional analysis of genes and microRNAs (miRNAs). Green areas highlight the first application for plant miRNAs.

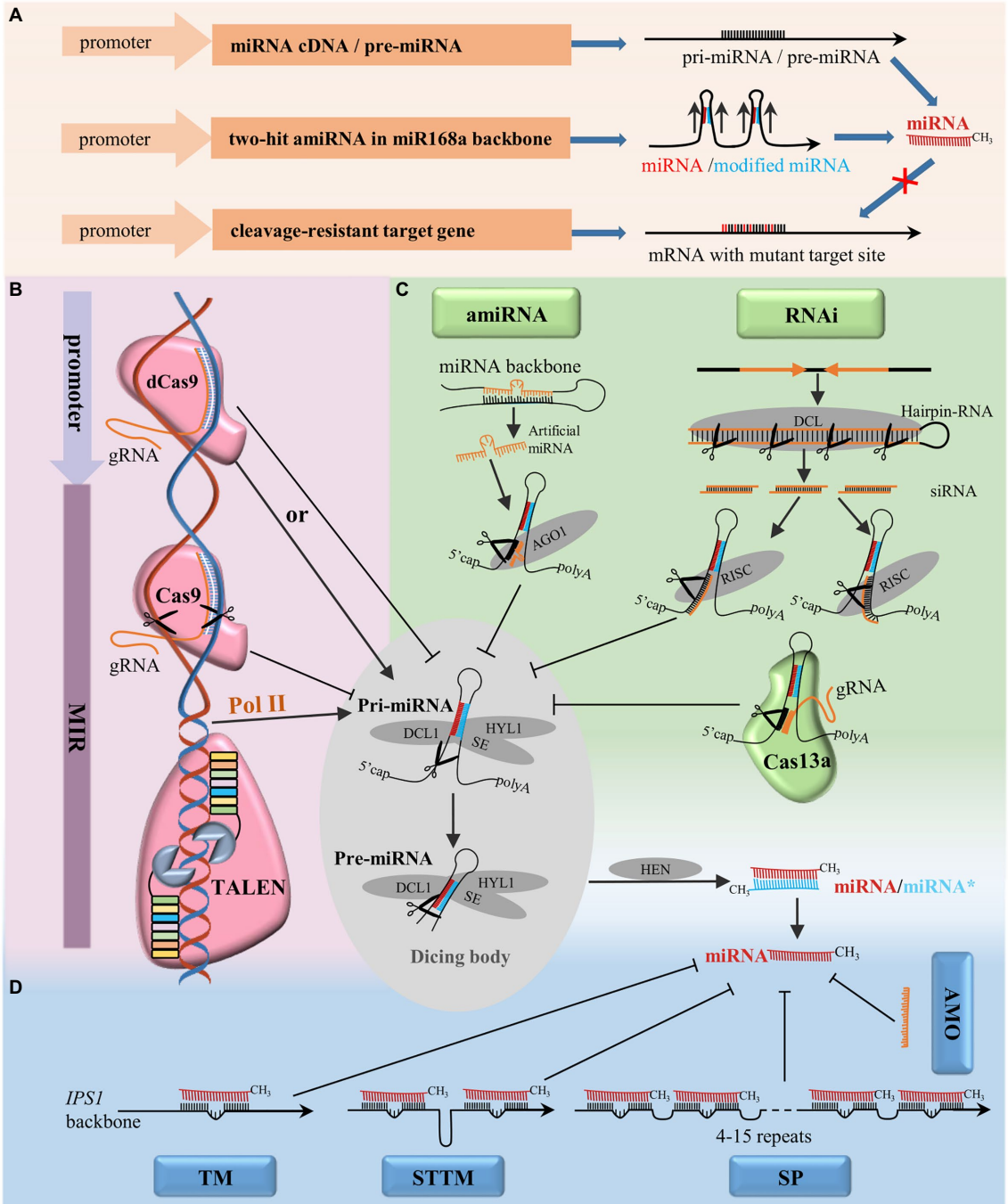

FIGURE 2 | Techniques for the functional analysis of miRNAs in plants. **(A)** Transgenesis strategies to identify the functions of miRNAs *via* gain-of-function, overexpression of miRNAs by pre-miRNA, cDNA of miRNA or amiRNA, overexpression of miRNA cleavage-resistant target genes to mimic the effect of downregulating the expression of miRNA. **(B)** Techniques targeting miRNA genes: CRISPR-associated nuclease 9 (CRISPR/Cas9) system and TALEN for miRNA gene editing, CRISPR/dCas9 system for transcriptional regulation by targeting the promoter region. **(C)** Techniques targeting pri-/pre-miRNA: RNAi, amiRNA, and the CRISPR/Cas13a system. **(D)** Techniques targeting mature miRNA: AMO, TM, short tandem target mimic (STTM), and SP. AGO1, ARGONAUTE1; DCL1, DICER-LIKE1; HEN1, HUA ENHANCER1; HYL1, HYPONASTIC LEAVES1; RISC: RNA-induced silencing complex; SE, SERRATE.

gene editing in *Arabidopsis* (Li et al., 2013), *Nicotiana benthamiana* (Nekrasov et al., 2013), and rice (Shan et al., 2013) soon after its establishment. Recently, many miRNAs have been successfully knocked out in various plant species by the introduction of indels at *MIR* genes *via* CRISPR/Cas9 nonhomologous end joining (NHEJ; Damodharan et al., 2018; Hou et al., 2019; Miao et al., 2019). In addition, the full-length deletion and knock-in of *MIR* genes can also be achieved by CRISPR/Cas9

editing *via* homology-directed repair (HDR; Zhao et al., 2016). Moreover, the CRISPR/Cas9 system can be used to modulate gene expression through the transcriptional activation or repression of target genes by fusing a deactivated Cas9 nuclease (dCas9) with transcriptional regulators such as transcriptional activators (Li et al., 2017) and repressors (Tang et al., 2017). Although the CRISPR/Cas9 system is an efficient tool to modify the sequence of miRNA genes and generate miRNA null mutant plants, the short length of *MIR* genes limits the design of gRNA targets that target *MIR* genes. In addition, multiple miRNA family members in the genome may limit the application of CRISPR/Cas9 in knocking out the whole *MIR* gene family simultaneously.

Techniques Targeting Pri-/Pre-miRNAs

Various techniques that are commonly applied to silence protein-coding genes by targeting the transcripts have been adopted for functional analyses of miRNAs (**Figure 2C**). RNAi, widely used for the knockdown of coding genes, is also able to suppress the accumulation of miRNAs. MiR163 and miR171a were successfully blocked by RNAi constructs designed to target both the primary miRNA transcripts and their promoters (Vaistij et al., 2010). Through RNAi, a diverse set of siRNAs are produced that might potentially trigger off-target effects. To avoid off-target effects, an amiRNA strategy was developed to specifically silence targets by expressing amiRNA with miRNA precursors as backbones (Carbonell et al., 2016). By replacing the original miRNA/miRNA* with amiRNA/amiRNA* designed to target a specific mRNA, genes of interest can be successfully blocked (Warthmann et al., 2008). It has been reported that all family members can be silenced by an amiRNA designed to target the mature sequence of a miRNA, in contrast, only the individual member can be silenced by an amiRNA designed to target the nonconserved stem-loop region of the precursor transcript, which benefits the functional validation of individual *MIR* loci in the genome (Eamens et al., 2011). To silence targets of interest effectively and specifically, the selection of both amiRNA and pre-amiRNA sequences should be accurate and suitable, this is the main challenging task associated with the utilization of amiRNA (Carbonell et al., 2016; Peng et al., 2018).

Furthermore, with class II type VI-A endoribonuclease, CRISPR/Cas13a can target and cleave single-stranded RNA guided by gRNA, which can also be used to target pri-/pre-miRNA transcripts of *MIR* genes (Aman et al., 2018). However, the CRISPR/Cas13a system has not yet been tested for miRNA silencing in plants.

Techniques Targeting Mature miRNAs

Mature miRNAs can be decoyed by exogenous synthetic AMOs and endogenous target mimics (**Figure 2D**). AMOs are chemically modified antisense oligonucleotides designed to pair with and block mature microRNAs by sequence complementarity, this approach was initially used in animals to suppress miRNA activity (Hutvágner et al., 2004; Meister et al., 2004). In the recent years, it has been reported that AMO can induce the efficient inhibition of miRNAs by sucrose-mediated delivery in rice protoplasts and intact leaves (He et al., 2016). AMOs function in a sequence-specific manner against targeted miRNAs and transiently induce miRNA blockages, which enables a quick assessment for the characterization of miRNAs in plants. A study by Franco-Zorrilla et al. (2007) demonstrated that endogenous target mimics could block the interaction between miRNAs and their targets, thereby silencing miRNA function. In *Arabidopsis*, *INDUCED BY PHOSPHATE STARVATION 1* (*IPS1*), an endogenous long noncoding RNA, was found to have a miR399-binding site with a central "bulge" formed by three nucleotides (CUA) that could effectively trap miR399 and abolish miR399-guided cleavage (Franco-Zorrilla et al., 2007). In plants, miRNAs were decoyed by replacing the endogenous miR399 target site of *IPS1* with artificial TMs of interest (Todesco et al., 2010; Sun et al., 2020). In animal cells, four copies of the miRNA-binding sites with two central mismatches at the cleavage site linked by 4-nt spacers were used to inhibit miRNA action in SP systems (Ebert et al., 2007). In recent years, SPs have been successfully applied to block miRNAs in plants (Reichel et al., 2015; Tong et al., 2017; Beltramino et al., 2018). More miRNA-binding sites (up to 15) are used in a sponge to increase its efficacy in inhibiting miRNA action in plants. Nevertheless, it is difficult to construct a long SP with multiple tandem repeats, which may limit the application of SPs. STTM was initially developed based on the principle of TMs and SPs. STTM is a modified artificial RNA structure containing two miRNA-binding sites linked by an RNA spacer of 48–88 nt. Like those of TMs, miRNA-binding sites of STTMs have mismatches at the miRNA cleavage sites, which help STTMs sequester miRNAs without being cleaved by them. The spacer between the two miRNA-binding sites forms a mild "stem," which serves as an optimal structure important for both preventing Dicer attack and stabilizing the expressed STTM in cells (Yan et al., 2012). STTMs can block or destroy specific endogenous small RNA functions in plants and effectively knock down the expression of miRNAs of an entire family (Yan et al., 2012). MiRNA degradation triggered by STTM is partly dependent on SDN-mediated miRNA degradation, but the mechanism is not fully understood (Yan et al., 2012; Teotia et al., 2016). In addition, the F-box protein HAWAIIAN SKIRT (HWS) plays a critical role in miRNA degradation triggered by TM/STTM system, which may result from its function in the clearance of non-optimal RISC induced by mimicry target (Lang et al., 2018; Mei et al., 2019). Perturbing the function of miRNAs as miRNA decoys, it has been reported that the silencing efficacy of TMs, SPs, and STTMs varies among different miRNA families. STTMs have been verified to be effective in perturbing activities of highly abundant miRNAs (e.g., miR165/166), TM more effectively targets low-abundance miRNAs (e.g., miR159), and SPs function as an alternative for miRNAs that cannot be effectively blocked by either TM or STTM (Reichel et al., 2015). Thus, multiple decoy strategies are recommended in order to generate the desired outcome.

Techniques Mimicking the Loss of Function of miRNAs

Another approach to mimicking the loss-of-function state of a miRNA is upregulating the targets of miRNAs by overexpressing the cleavage-resistant target genes (Li and Millar, 2013; **Figure 2A**). Since overexpressed original targets can still be cleaved by miRNAs, cleavage-resistant targets are generated by modifying the miRNA cleavage site by creating synonymous mutations. Many transgenic plants overexpressing cleavage-resistant targets have been created, such as *Arabidopsis* expressing miR156-resistant *AtSPL3* (*rSPL3*; Kim et al., 2012) and the miR172-resistant form of *AtTOE3* (Jung et al., 2014), tomato expressing miR164-resistant *SlNAM2* (Hendelman et al., 2013), and rice expressing miR319-resistant *OsTCP21* (*rTCP21*; Zhang et al., 2016a) and miR166-resistant *OsHB4* (Zhang et al., 2018b). This approach could be an additional way to investigate the functions of the corresponding miRNAs.

STTM TECHNIQUES IN PLANT RESEARCH

A gain-of-function system that constitutively overexpresses a miRNA may alter its localization and dose. Therefore, the non-authentic phenotypes may not reflect the normal function of the miRNA. Thus, various loss-of-function strategies have been extensively exploited as alternative and effective approaches to evaluate the roles of many miRNAs. Of these approaches, miRNA decoy techniques such as TM and STTM, and the genome-editing system CRISPR/Cas9 are applied much more widely than others (**Figure 3**). As the first miRNA decoy technique created for plants, the TM approach has been applied in many studies, and the functions of many miRNAs have been successfully uncovered (Todesco et al., 2010). In recent years, STTM and CRISPR/Cas9 techniques have been developed rapidly and have become the two most widely adopted approaches in functional analysis of miRNAs in plants.

The STTM technique is widely accepted in miRNA functional studies in plants because it can be applied in a variety of ways. First, the STTM structure has two miRNA-binding sites, and it can efficiently silence some highly abundant miRNAs (e.g., miR156/157, miR165/166, and miR398) and generate visible phenotypes (Yan et al., 2012; Reichel et al., 2015; Zhang et al., 2017). Second, STTMs can be used to study the interactions between two miRNAs by inserting two different miRNAs in the same STTM construct (Peng et al., 2018). Moreover, it has been reported that STTMs can silence multiple distinct miRNAs simultaneously with an increased number of tandem miRNA-binding sites (Fei et al., 2015). Finally, the STTM approach can be adopted as an important complement to CRISPR/Cas9 in certain situations, such as the knockout of miRNAs resulting in drastic or lethal developmental defects (Teotia et al., 2016) or the locations of miRNAs overlapping with other genes in the chromosome.

The STTM approach can be applied in a constitutive (Tang et al., 2012), inducible (Peng et al., 2018) or tissue-specific (Zhao et al., 2019) manner driven by the corresponding promoter. This makes it possible to study miRNA functions spatiotemporally and to precisely modify the crop traits of interest. Since its development, the STTM approach has been extensively adopted for the functional analysis of numerous miRNAs in multiple species, including rice (Xia et al., 2015; Zhang et al., 2017; Zhao et al., 2019), tomato (Damodharan et al., 2016; Jiang et al., 2018; Yang et al., 2020), soybean (Wang et al., 2014; Nizampatnam et al., 2015), cotton (Wang et al., 2017; Liu et al., 2019), maize (Zhang et al., 2019), wheat (Guo et al., 2018), and tobacco (Diao et al., 2019; **Figure 3**). Rice is the most important staple crop worldwide, and several of its agriculturally important traits are controlled by miRNAs (Tang and Chu, 2017; Peng et al., 2019). Given the extensive application of STTMs in rice, we reviewed STTM-based functional studies of miRNAs in rice and focused specially on agronomic traits.

APPLICATION OF THE STTM TECHNIQUE FOR RICE FUNCTIONAL GENOMICS AND BREEDING

Higher yield and enhanced stress resistance are important breeding goals of crop breeders. Yield is a sophisticated agronomic trait in rice that is generally determined by four decisive factors: the number of tillers per plant, number of grains per panicle, grain size/weight, and the ratio of filled grains (Sakamoto and Matsuoka, 2008; Xing and Zhang, 2010). In addition, tiller angle and plant height are important agronomic traits that determine the ideal architecture and the leaf size, shape, and inclination determine the leaf architecture, all of which eventually affect the grain yield (Zuo and Li, 2014). Extensive studies have supported the vital roles of miRNAs in regulating diverse important agronomic traits and stress responses in crops (Zheng and Qu, 2015; Tang and Chu, 2017; Peng et al., 2019). To date, dozens of miRNA families have obtained STTM transgenic lines in rice, and several of them show obvious phenotypic alterations associated with yield-related agronomic traits and stress responses (**Figure 4**; **Table 1**). Hereafter, we provide an overview of the application of STTM in rice classified by different agronomic traits.

Tiller Number Related miRNA Confirmed by the STTM Approach

The tiller number per plant is one of the factors that contribute to rice yield, and several miRNA-target modules have been reported to play roles in regulating the tiller number per plant (Peng et al., 2019). It is well characterized that miR156 functions in rice tiller formation by cleaving its target *OsSPL14* in the vegetative stage (Jiao et al., 2010; Miura et al., 2010). Transgenic lines overexpressing miR156 showed increased tiller numbers per plant (Xie et al., 2006; Hayashi-Tsugane et al., 2015; Liu et al., 2015). The knockdown of miR156 by the STTM approach revealed additional roles in the control of shoot and root development at the seedling stage (Zhang et al., 2017).

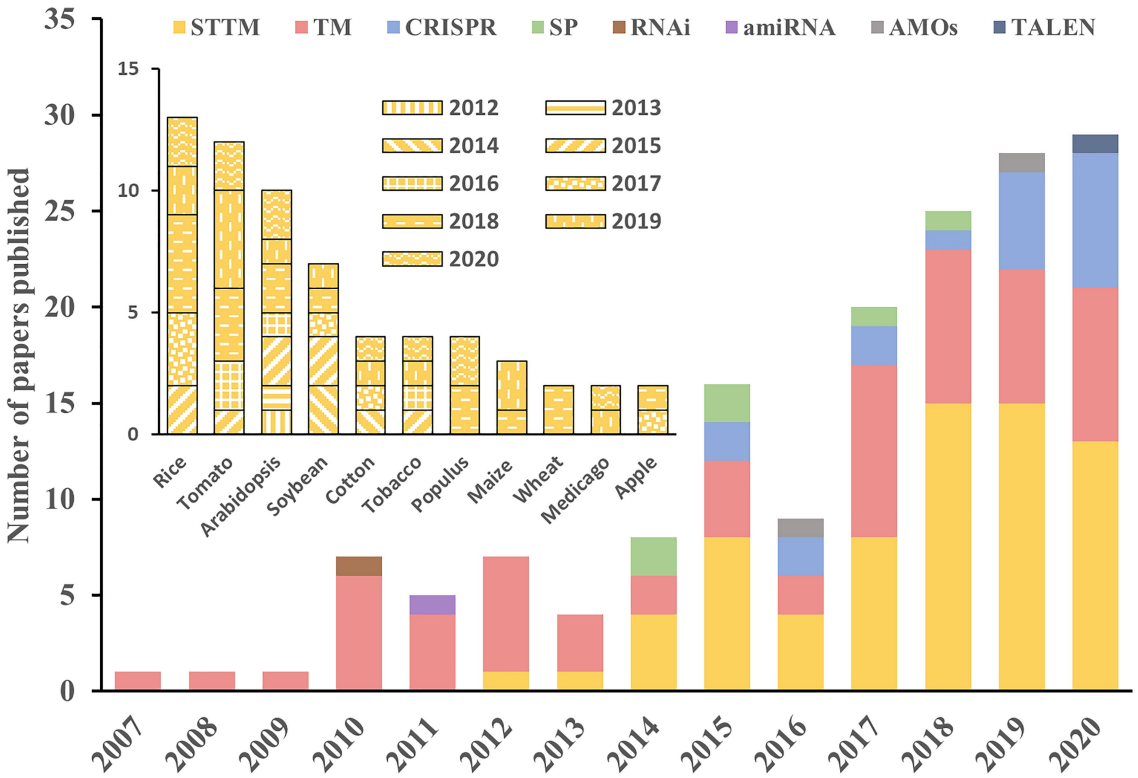

FIGURE 3 | Applications of different approaches in the literature. The histograms show the number of manuscripts published per year using the different approaches for miRNA study in plants (outer) and the application of STTM in different species (inner). The information used in this figure was retrieved through April 30, 2021, from PubMed.

Grain Number-Related miRNAs Confirmed by the STTM Approach

The grain numbers per panicle are determined by the panicle architecture: branches, panicle axis, and spikelets. It was reported that *Arabidopsis* miR398 plays role in various stresses by targeting Cu/Zn-superoxide dismutases (*CSD1* and *CSD2*; Zhu et al., 2011), and no obvious developmental or architectural phenotypes have been revealed. In rice, silencing miR398 by the STTM approach led to reduced grain numbers per panicle because of shorter and smaller panicles (Zhang et al., 2017), suggesting its significant function in panicle growth.

Grain Weight-Related miRNAs Confirmed by the STTM Approach

Grain weight is determined by grain length, width, and thickness, the grain-filling rate and grain-filling period. STTM156 plants had slightly increased grain length and 1,000-grain weight. STTM159 lines in rice showed smaller grains and lower grain weight through its target *OsGAMYBL2* (Zhang et al., 2017; Zhao et al., 2017). In addition, OsmiR159d STTM lines specifically blocking the functions of miR159d also had smaller grains (Gao et al., 2018). STTM166 lines showed decreased rice grain weight with decreased grain width but increased grain length (Zhang et al., 2018b). STTM167 transgenic *Arabidopsis* often shows incompletely filled seeds. Rice STTM167 driven by the Gt13a endosperm-specific promoter showed a substantial increase in the grain weight, indicating that miR167 regulates seed development oppositely in monocot and dicot plants (Peng et al., 2018). Blocking miR398 by the STTM approach also results in significantly decreased grain length and width, causing a 40% decrease in 1,000-grain weight (Zhang et al., 2017). STTM1432 plants showed a substantial increase (46.69%) in grain weight due to an improved grain filling rate, which was photocopied by overexpression of miR1432-resistant *OsACOT* (Zhao et al., 2019). STTM5144-3p plants produce grains with increased 1,000-grain weight, which was also the result of the overexpression of its target *OsPDIL1;1* (Xia et al., 2017).

Seed Setting Rate-Related miRNAs Confirmed by the STTM Approach

Seed-setting rate relies strongly on seed setting after successful double fertilization and starch accumulation. Knockdown of miR172 by the STTM approach resulted in a significantly decreased seed-setting rate (Zhang et al., 2017). The lower seed-setting rate of STTM172 plants was presumably resulted from the enclosed panicle since normal fertile pollens were produced. In addition, the STTM160 and STTM1428 lines were reported to show dramatically decreased seed-setting rates

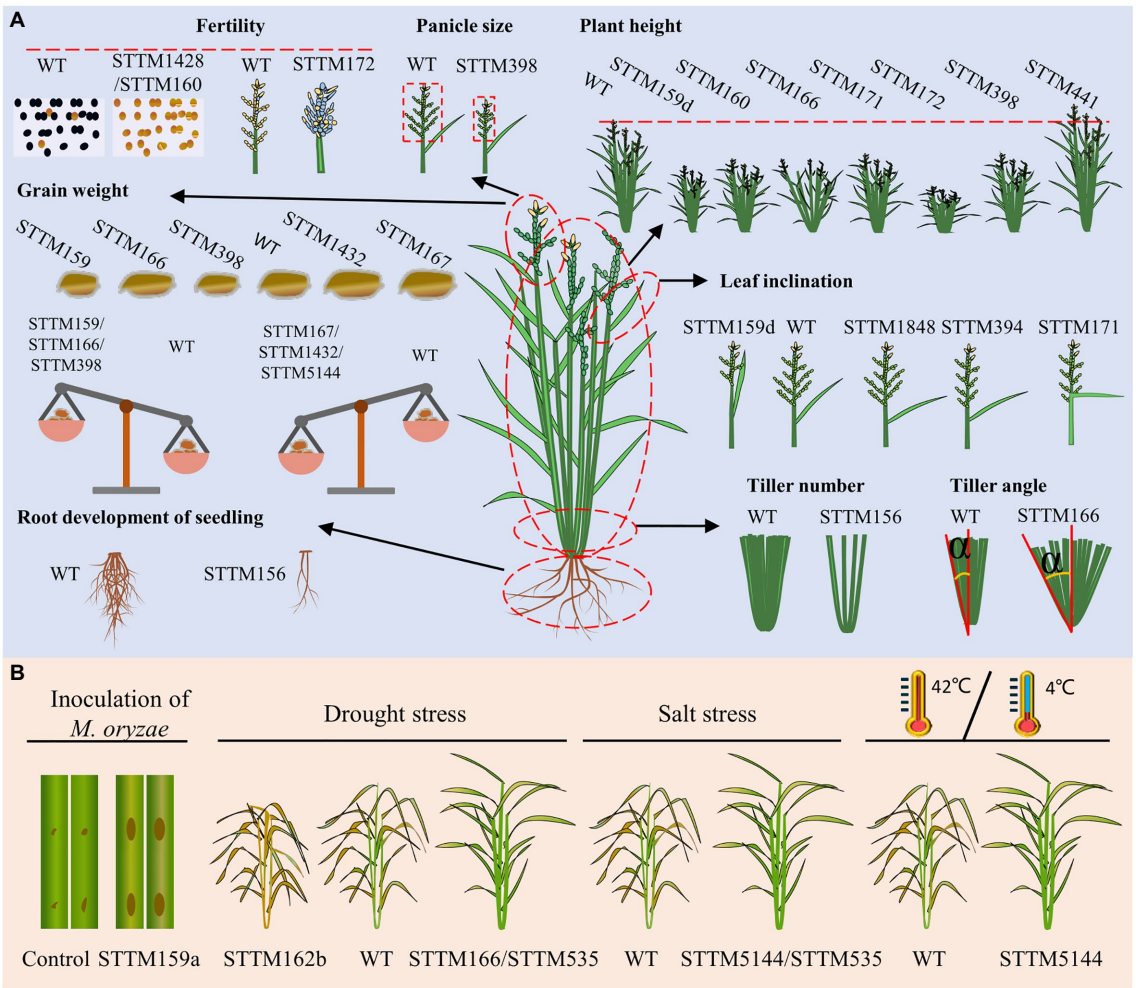

FIGURE 4 | Experimentally verified phenotypes of rice STTM lines: agronomic trait-related **(A)** and stress response-related **(B)**. **(A)** Variations in agronomic traits, including the fertility, panicle size, plant height, grain weight, leaf inclination, tiller number, tiller angle, and root development, of seedlings are diagrammatized. Fertility: fertile (black dots), sterile (yellow dots), filled seeds (yellow grains), empty seeds (blue grains). Grain weight: smaller grains (left side of WT), larger grains (right side of WT), each part of the balance represents the 1,000-grain weight. Leaf inclination: smaller leaf angle (left side of WT), increased leaf angle (right side of WT). **(B)** Diagrams from left to right represent biotic stress from blast disease caused by *Magnaporthe oryzae* and abiotic stress, including drought stress, salt stress, high temperature (42°C), and low temperature (4°C). Brown dots on the leaves indicate disease lesions, deep yellow plants indicate dead tissues and green plants indicate surviving tissues.

because of complete male sterility in rice (Zhang et al., 2017). Overall, the roles of miRNAs in the regulation of fertility and panicle morphology contribute to the seed-setting rate.

Plant Architecture-Related miRNAs Confirmed by the STTM Approach

In addition to the tiller number, the tiller angle, leaf inclination, and plant height are important agronomic traits that contribute to ideal plant architecture and grain production (Sakamoto and Matsuoka, 2008; Zuo and Li, 2014; Mantilla-Perez and Salas Fernandez, 2017). STTM166 lines showed an increased tiller angle, but the underlying regulatory mechanism of this is not yet clear (Zhang et al., 2017). MiR1848-*OsCYP51G3* module determines leaf inclination by affecting BR biosynthesis. STTM1848- and *OsCYP51G3*-overexpressing transgenic lines showed a larger leaf inclination (Xia et al., 2015). An auxin-responsive module, miR394-*OsLC4*, functions in determining rice leaf inclination through auxin homeostasis. STTM394 lines showed greatly enhanced leaf inclination and altered auxin responses (Qu et al., 2019). STTM159 lines showed reduced stature and stem diameter (Zhang et al., 2017; Zhao et al., 2017). The silencing of miR160 by STTM in rice reduced plant height, similar to the results in *Arabidopsis*, indicating its conserved function in plant height between monocots and dicots (Zhang et al., 2017). STTM166 lines exhibited reduced plant height resulting from decreased length of internodes by targeting *OsHB4*, a member of HD-Zip III gene family (Teotia et al., 2017; Zhang et al., 2017). In addition, miR166b was reported to regulate cell wall biosynthesis by targeting *OsHox32*. The knockdown of miR166b by STTM resulted in droopy leaves and brittle culms due to reduced cell wall thickness with decreased accumulation of lignin and cellulose

TABLE 1 | Summary of functionally validated miRNAs by STTM in rice.

Agronomic traits		STTM-miRNA lines	Promoter used	Reference
Fertility	Sterile pollen	miR160, miR1428	35S	Zhang et al., 2017
	Decreased seed setting rate	miR172		
Grain weight	Decreased grain weight	miR156, miR159, miR165/166, miR398	35S	Zhang et al., 2017; Zhao et al., 2017; Gao et al., 2018; Zhang et al., 2018b
	Increased grain weight	miR167, miR1432	Gt13a	Peng et al., 2018; Zhao et al., 2019
		miR5144-3p	Ubi-1	
Panicle	Shorter panicle	miR159, miR171, miR398	35S	Zhang et al., 2017; Zhao et al., 2017
	Semi-enclosed panicle	miR159, miR171	35S	Zhang et al., 2017; Gao et al., 2018
Plant height	Decreased plant height	miR159, miR165/166, miR171, miR172, miR398	35S	Zhang et al., 2017; Zhao et al., 2017; Gao et al., 2018; Zhang et al., 2018b; Chen et al., 2021a
	Increased plant height	miR441	35S	Zhang et al., 2017
Leaf inclination	Decreased leaf inclination	miR159	35S	Gao et al., 2018
	Enhanced leaf inclination	miR171, miR394	35S	Xia et al., 2015; Zhang et al., 2017; Qu et al., 2019
		miR1848	Ubi-1	
Tiller number	Fewer tillers	miR156	35S	Zhang et al., 2017
Tiller angle	Wider tiller angle	miR165/166	35S	
Root	Shorter roots with reduced root number	miR156	35S	
Abiotic stress	Enhanced susceptibility to *M. oryzae*	miR159	35S	Chen et al., 2021b
Drought stress	Reduced tolerance	miR162b	Ubi-1	Tian et al., 2015
	Enhanced tolerance	miR166	35S	Zhang et al., 2018b
		miR535	Ubi-1	Yue et al., 2020
Salt stress	Enhanced tolerance	miR5144-3p, miR535	Ubi-1	Xia et al., 2017; Yue et al., 2020
High/low temperature	Enhanced tolerance	miR5144-3p	Ubi-1	Xia et al., 2017

(Chen et al., 2021a). Knockdown of miR171 by STTM resulted in semi-dwarf plants, semi-enclosed panicles, and droopy flag leaves (Zhang et al., 2017). STTM172 lines showed unexpected phenotypes in rice, dwarf plants resulted from shorter culms compared with wild-type plants (Zhang et al., 2017). MiR441 was identified to increase plant height after knockdown by STTM in rice, but the underlying mechanism is not clear yet (Zhang et al., 2017).

Stress Response-Related miRNAs Confirmed by the STTM Approach

In addition to their involvement in agronomic traits observed under natural paddy field conditions, several STTM-miRNA transgenic lines showed altered responses to biotic and abiotic stresses (**Figure 4B**; **Table 1**). MiR159a is a positive regulator of resistance to *Magnaporthe oryzae* (*M. oryzae*) by targeting *OsGAMYB*, *OsGAMYBL*, and *OsZF*. STTM159a lines showed enhanced susceptibility (Chen et al., 2021b). MiR162b, miR166, and miR535 were confirmed to participate in the response to drought stress. STTM162b lines showed a greatly decreased survival rate compared to WT, and miR162b was identified as a positive regulator of drought resistance by targeting *OsTRE1* (Tian et al., 2015). MiR166 modulates the morphology of leaves and the size of xylem vessels by targeting *OsHB4*. STTM166 lines showed enhanced drought resistance resulting from decreased transpiration rates and hydraulic conductivity due to reduced stomatal conductance and xylem vessel diameter, respectively (Zhang et al., 2018b). STTM535 lines showed enhanced resistance to drought and salinity, and *OsSPL19* is presumed to be the main functional target of miR535 in response to drought and salinity (Yue et al., 2020). MiR5144-*OsPDIL1;1* module modulates the formation of protein disulfide bonds, which affects the correct folding of proteins and is important for protein function in the stress response. STTM5144- or *OsPDIL1;1*-overexpressing lines showed enhanced resistance to various abiotic stresses including $HgCl_2$, salinity, high temperature, and low temperature, due to the increased content of protein–disulfide bonds (Xia et al., 2017). To date, only a small portion of STTM lines have been evaluated under stress conditions. All these STTM transgenic lines generate a resource pool that contributes to mining novel targets for agronomic improvement by assessing their responses to biotic and abiotic stresses.

APPLICATIONS OF THE CRISPR/Cas9 SYSTEM IN TRANSGENE-FREE CROP BREEDING

Although many agronomically improved STTM transgenic lines have been generated, these achievements have not yet been commercialized. Currently, the commercial development of

genetically modified organisms (GMOs) is considered a threat to human health and the environment and is thus under stringent governmental regulations (Prado et al., 2014). Transgene-free edited crops created *via* CRISPR/Cas9 receive the regulatory waivers in many countries (Chen and Gao, 2020). Transgene-free edited crops can be generated through conventional and transient expression methods. In conventional transformation methods, transgene-free edited progenies can be obtained by eliminating CRISPR transgenes *via* genetic segregation through selfing or crossing (Gao, 2021). In the transient expression methods, transgene-free genome editing can be generated through the transient expression of CRISPR/Cas9 DNA, RNA, or RNP (ribonucleoprotein) delivered into plant cells (Woo et al., 2015; Zhang et al., 2016b; Liang et al., 2017). Recently, transgene-free gene-edited non-browning white button mushrooms (Waltz, 2016) and high-GABA tomato (EUROFRUIT, 2021) have been commercialized outside of GMO regulations. Furthermore, due to the precise genome modifications, time savings, and transgene-free nature of these crops (Zhu et al., 2020), some practices for translating the outcomes of transgenic into transgene-free breeding by CRISPR/Cas9 in crops have been developed.

Great progress has been made by using a transgene-free edited system on protein-coding genes. A series of transgene-free edited crops with increased yield (Li et al., 2016), improved quality with low amylose content (Zhang et al., 2018a), high amylose content (Sun et al., 2017; Tuncel et al., 2019; Li et al., 2021), higher grain fragrance (Usman et al., 2020), enriched γ-aminobutyric acid (Akama et al., 2020), and enhanced biotic stress resistance (Zhou et al., 2020) have been generated. Currently, several studies are also trying to convert the accumulating knowledge of miRNA functions into a transgene-free edited system. In rice, the overexpression of *OsmiR535* resulted in reduced tolerance to drought and salinity, while the knockdown of *OsmiR535* by STTM conferred enhanced tolerance to drought and salinity (Yue et al., 2020). A transgene-free, drought-tolerant *osmir535* mutant was generated by CRISPR/Cas9 mediated knockout, which provides a successful example for abiotic stress-resistant breeding (Yue et al., 2020). In soybean (*Glycine max* L.), gma-miR398c functions negatively in drought tolerance by targeting multiple peroxisome-related genes, *GmCSDs* and *GmCCS* (Zhou et al., 2020). *Arabidopsis* and soybean overexpressing gma-miR398c both showed decreased drought tolerance, while the *gma-miR398c* mutant generated by CRISPR/Cas9 showed increased drought resistance. Gma-miR398c was demonstrated to be a valuable locus for crop improvement by creating drought resistance-enhanced soybean *via* CRISPR/Cas9 (Zhou et al., 2020). In tomato, one of the most important horticultural crops, late blight caused by *Phytophthora infestans* (*P. infestans*) is a great threat to production (Fry et al., 2015). MiR482 was identified as a negative regulator of the resistance to *P. infestans* by targeting *NBS–LRR* disease-resistance genes in tomato (Jiang et al., 2018; Canto-Pastor et al., 2019). The overexpression of miR482b caused more severe disease symptoms in plants infected by *P. infestans*, while the silencing of miR482b by STTM resulted in enhanced resistance to *P. infestans* in tomato (Jiang et al., 2018). Based on these transgenic outcomes, *mir482b* and *mir482b/c* were generated by CRISPR/Cas9, and both showed enhanced resistance to *P. infestans*. In addition, *mir482b/c* was more resistant to *P. infestans* than *mir482b* in tomato, demonstrating that miR482 is an important target for cultivating pathogen-resistant tomatoes *via* CRISPR/Cas9 (Hong et al., 2020). The ever-expanding genetic resources created by these miRNA techniques provide us with a promising prospect for crop improvement and breeding.

CONCLUSION AND PERSPECTIVES

Multiple tools have been developed for the functional analysis of miRNAs, thus contributing to the crop improvement and future agriculture. Given the advantages and drawbacks of each approach, it is important to design proper strategies for each specific study and the miRNAs of interest. STTM is one of the most widely adopted miRNA techniques, and a large collection of STTM lines have been generated in crops, especially in rice. STTM and related miRNA techniques help to reveal the complex molecular mechanisms involved in the regulation of agronomic traits, and also provide potential breeding materials for crop improvement and breeding. These transgenic achievements, together with the CRISPR/Cas gene-editing system and many other breeding techniques, will allow the generation of transgene-free plants and greatly facilitate precision crop breeding.

To date, as the majority of functional studies focus on conserved miRNAs, our knowledge about species and tissue specific miRNAs is extremely limited, which offers a broad space for the application of STTM and other approaches. Further identification and validation of these miRNAs will lead to a great leap for the application of miRNAs in crop improvement. Due to the multiple roles of miRNAs in plant developmental processes, STTM lines of these miRNAs driven by the 35S promoter show pleiotropic effects that alter more than one trait (**Table 1**). Tissue-specific or inducible promoters may be an appropriate alternative to facilitate STTM as a useful tool to study the functions of miRNAs in specific tissues and increase yield without penalty on other agronomic traits. Not all STTM rice lines showed apparently altered morphologies (Zhang et al., 2017), and other approaches mentioned previously are advocated to be adopted for the desired loss-of-function outcome. Multiple genetics-based approaches are imperative and may work complementarily in fully mining and using vital miRNAs associated with superior agronomic traits. MiRNAs are important regulators in biotic and abiotic stress responses. Fine-tuning the accumulation of stress-related miRNAs by STTM techniques may provide valuable resources for the assessment of varying stress responses. Additionally, due to public safety concerns over transgenic crops, the commercialization of improved crops bred by STTM-based techniques is restricted. Some successful breeding practices on translation of transgenic outcomes into transgene-free outcomes *via* CRISPR/Cas9 in

rice have been adopted. Useful targets for crop improvement confirmed by STTM have huge potential for application in breeding through non-transgenic translation, which may accelerate the creation of new varieties and strengthen food security.

AUTHOR CONTRIBUTIONS

GT supervised the project. JC and TL wrote this paper. ST edited and gave suggestions for the manuscript. All authors contributed to manuscript revision, read, and approved the submitted version.

FUNDING

This work was supported by funding from the Guangdong Innovation Research Team Fund (grant no. 2014ZT05S078), the National Natural Science Foundation of China (grant no. 32070852) and the open fund of the Guangdong Key Laboratory of Plant Epigenetics.

REFERENCES

Akama, K., Akter, N., Endo, H., Kanesaki, M., Endo, M., and Toki, S. (2020). An in vivo targeted deletion of the calmodulin-binding domain from rice glutamate decarboxylase 3 (OsGAD3) increases γ-aminobutyric acid content in grains. *Rice* 13:20. doi: 10.1186/s12284-020-00380-w

Aman, R., Ali, Z., Butt, H., Mahas, A., Aljedaani, F., Khan, M. Z., et al. (2018). RNA virus interference via CRISPR/Cas13a system in plants. *Genome Biol.* 19:1. doi: 10.1186/s13059-017-1381-1

Aukerman, M. J., and Sakai, H. (2003). Regulation of flowering time and floral organ identity by a MicroRNA and its APETALA2-like target genes. *Plant Cell* 15, 2730–2741. doi: 10.1105/tpc.016238

Beltramino, M., Ercoli, M., Debernardi, J. M., Goldy, C., Rojas, A. M. L., Nota, F., et al. (2018). Robust increase of leaf size by *Arabidopsis thaliana* GRF3-like transcription factors under different growth conditions. *Sci. Rep.* 8:13447. doi: 10.1038/s41598-018-29859-9

Bi, H., Fei, Q., Li, R., Liu, B., Xia, R., Char, S. N., et al. (2020). Disruption of miRNA sequences by TALENs and CRISPR/Cas9 induces varied lengths of miRNA production. *Plant Biotechnol. J.* 18, 1526–1536. doi: 10.1111/pbi.13315

Boualem, A., Laporte, P., Jovanovic, M., Laffont, C., Plet, J., Combier, J. P., et al. (2008). MicroRNA166 controls root and nodule development in *Medicago truncatula*. *Plant J.* 54, 876–887. doi: 10.1111/j.1365-313X.2008.03448.x

Canto-Pastor, A., Santos, B. A. M. C., Valli, A. A., Summers, W., Schornack, S., and Baulcombe, D. C. (2019). Enhanced resistance to bacterial and oomycete pathogens by short tandem target mimic RNAs in tomato. *Proc. Natl. Acad. Sci. U. S. A.* 116, 2755–2760. doi: 10.1073/pnas.1814380116

Carbonell, A., Fahlgren, N., Mitchell, S., Cox, K. L. Jr., Reilly, K. C., Mockler, T. C., et al. (2016). Highly specific gene silencing in a monocot species by artificial microRNAs derived from chimeric miRNA precursors. *Plant J.* 82, 1061–1075. doi: 10.1111/tpj.12835

Chen, H., Fang, R., Deng, R., and Li, J. (2021a). The OsmiRNA166b-OsHox32 pair regulates mechanical strength of rice plants by modulating cell wall biosynthesis. *Plant Biotechnol. J.* 19, 1468–1480. doi: 10.1111/pbi.13565

Chen, K., and Gao, C. (2020). Genome-edited crops: how to move them from laboratory to market. *Front. Agric. Sci. Eng.* 7, 181–187. doi: 10.15302/J-FASE-2020332

Chen, J., Zhao, Z., Li, Y., Li, T., Zhu, Y., Yang, X., et al. (2021b). Fine-tuning roles of Osa-miR159a in rice immunity against magnaporthe oryzae and development. *Rice* 14:26. doi: 10.1186/s12284-021-00469-w

Damodharan, S., Corem, S., Gupta, S. K., and Arazi, T. (2018). Tuning of SlARF10A dosage by sly-miR160a is critical for auxin-mediated compound leaf and flower development. *Plant J.* 96, 855–868. doi: 10.1111/tpj.14073

Damodharan, S., Zhao, D., and Arazi, T. (2016). A common miRNA160-based mechanism regulates ovary patterning, floral organ abscission and lamina outgrowth in tomato. *Plant J.* 86, 458–471. doi: 10.1111/tpj.13127

Diao, P., Zhang, Q., Sun, H., Ma, W., Cao, A., Yu, R., et al. (2019). miR403a and SA are involved in NbAGO2 mediated antiviral defenses against TMV infection in *Nicotiana benthamiana*. *Gene* 10:526. doi: 10.3390/genes10070526

Eamens, A. L., Agius, C., Smith, N. A., Waterhouse, P. M., and Wang, M.-B. (2011). Efficient silencing of endogenous microRNAs using artificial microRNAs in *Arabidopsis thaliana*. *Mol. Plant* 4, 157–170. doi: 10.1093/mp/ssq061

Ebert, M., Neilson, J., and Sharp, P. (2007). MicroRNA sponges: competitive inhibitors of small RNAs in mammalian cells. *Nat. Methods* 4, 721–726. doi: 10.1038/nmeth1079

EUROFRUIT (2021). *Sanatech Seed Launches World's First GE Tomato*. Available at: http://www.fruitnet.com/eurofruit/article/184662/sanatech-seed-launches-worlds-first-ge-tomato (Accessed March 16, 2021).

Fei, Q., Li, P., Teng, C., and Meyers, B. C. (2015). Secondary siRNAs from Medicago NB-LRRs modulated via miRNA–target interactions and their abundances. *Plant J.* 83, 451–465. doi: 10.1111/tpj.12900

Fire, A., Xu, S., Montgomery, M. K., Kostas, S. A., Driver, S. E., and Mello, C. C. (1998). Potent and specific genetic interference by double-stranded RNA in *Caenorhabditis elegans*. *Nature* 391, 806–811. doi: 10.1038/35888

Franco-Zorrilla, J., Valli, A., Todesco, M., Mateos, I., Puga, M., Rubio-Somoza, I., et al. (2007). Target mimicry provides a new mechanism for regulation of microRNA activity. *Nat. Genet.* 39, 1033–1037. doi: 10.1038/ng2079

Fry, W. E., Birch, P. R., Judelson, H. S., Grünwald, N. J., Danies, G., Everts, K. L., et al. (2015). Five reasons to consider phytophthora infestans a reemerging pathogen. *Phytopathology* 105, 966–981. doi: 10.1094/PHYTO-01-15-0005-FI

Gaj, T., Gersbach, C. A., Fau-Barbas, C. F., and Barbas, C. F. (2013). ZFN, TALEN, and CRISPR/Cas-based methods for genome engineering. *Trends Biotechnol.* 31, 397–405. doi: 10.1016/j.tibtech.2013.04.004

Gao, C. (2021). Genome engineering for crop improvement and future agriculture. *Cell* 184, 1621–1635. doi: 10.1016/j.cell.2021.01.005

Gao, J., Chen, H., Yang, H., He, Y., Tian, Z., and Li, J. (2018). A brassinosteroid responsive miRNA-target module regulates gibberellin biosynthesis and plant development. *New Phytol.* 220, 488–501. doi: 10.1111/nph.15331

Guo, G., Liu, X., Sun, F., Cao, J., Huo, N., Wuda, B., et al. (2018). Wheat miR9678 affects seed germination by generating phased siRNAs and modulating abscisic acid/gibberellin signaling. *Plant Cell* 30, 796–814. doi: 10.1105/tpc.17.00842

Hayashi-Tsugane, M., Maekawa, M., and Tsugane, K. (2015). A gain-of-function bushy dwarf tiller 1 mutation in rice microRNA gene miR156d caused by insertion of the DNA transposon nDart1. *Sci. Rep.* 5:14357. doi: 10.1038/srep14357

He, L., Xie, M., Huang, J., Zhang, T., Shi, S., and Tang, T. (2016). Efficient and specific inhibition of plant microRNA function by anti-microRNA oligonucleotides (AMOs) in vitro and in vivo. *Plant Cell Rep.* 35, 933–945. doi: 10.1007/s00299-016-1933-y

Hendelman, A., Stav, R., Zemach, H., and Arazi, T. (2013). The tomato NAC transcription factor SlNAM2 is involved in flower-boundary morphogenesis. *J. Exp. Bot.* 64, 5497–5507. doi: 10.1093/jxb/ert324

Hong, Y., Meng, J., He, X., Zhang, Y., Liu, Y., Zhang, C., et al. (2020). Editing miR482b and miR482c simultaneously by CRISPR/Cas9 enhanced tomato resistance to Phytophthora infestans. *Phytopathology*. doi: 10.1094/PHYTO-08-20-0360-R [Epub ahead of print]

Hou, N., Cao, Y., Li, F., Yuan, W., Bian, H., Wang, J., et al. (2019). Epigenetic regulation of miR396 expression by SWR1-C and the effect of miR396 on leaf growth and developmental phase transition in *Arabidopsis*. *J. Exp. Bot.* 70, 5217–5229. doi: 10.1093/jxb/erz285

Hu, R., Wallace, J., Dahlem, T. J., Grunwald, D. J., and O'Connell, R. M. (2013). Targeting human microRNA genes using engineered Tal-effector nucleases (TALENs). *PLoS One* 8:e63074. doi: 10.1371/journal.pone.0063074

Hutvágner, G., Simard, M. J., Mello, C. C., and Zamore, P. D. (2004). Sequence-specific inhibition of small RNA function. *PLoS Biol.* 2:E98. doi: 10.1371/journal.pbio.0020098

Jacobs, T. B., LaFayette, P. R., Schmitz, R. J., and Parrott, W. A. (2015). Targeted genome modifications in soybean with CRISPR/Cas9. *BMC Biotechnol.* 15:16. doi: 10.1186/s12896-015-0131-2

Ji, L., Liu, X., Yan, J., Wang, W., Yumul, R., Kim, Y., et al. (2011). ARGONAUTE10 and ARGONAUTE1 regulate the termination of floral stem cells through two microRNAs in *Arabidopsis*. *PLoS Genet.* 7:e1001358. doi: 10.1371/journal.pgen.1001358

Jiang, N., Meng, J., Cui, J., Sun, G., and Luan, Y. (2018). Function identification of miR482b, a negative regulator during tomato resistance to *Phytophthora infestans*. *Hortic. Res.* 5:9. doi: 10.1038/s41438-018-0017-2

Jiao, Y., Wang, Y., Xue, D., Wang, J., Yan, M., Liu, G., et al. (2010). Regulation of OsSPL14 by OsmiR156 defines ideal plant architecture in rice. *Nat. Genet.* 42, 541–544. doi: 10.1038/ng.591

Jung, J., Lee, S., Yun, J., Lee, M., and Park, C. (2014). The miR172 target TOE3 represses AGAMOUS expression during *Arabidopsis* floral patterning. *Plant Sci.* 215-216, 29–38. doi: 10.1016/j.plantsci.2013.10.010

Kim, J. J., Lee, J. H., Kim, W., Jung, H. S., Huijser, P., and Ahn, J. H. (2012). The microRNA156-SQUAMOSA PROMOTER BINDING PROTEIN-LIKE3 module regulates ambient temperature-responsive flowering via FLOWERING LOCUS T in *Arabidopsis*. *Plant Physiol.* 159, 461–478. doi: 10.1104/pp.111.192369

Lang, P. L. M., Christie, M. D., Dogan, E. S., Schwab, R., Hagmann, J., van de Weyer, A.-L., et al. (2018). A role for the F-box protein HAWAIIAN SKIRT in plant microRNA function. *Plant Physiol.* 176, 730–741. doi: 10.1104/pp.17.01313

Li, J., Jiao, G., Sun, Y., Chen, J., Zhong, Y., Yan, L., et al. (2021). Modification of starch composition, structure and properties through editing of TaSBEIIa in both winter and spring wheat varieties by CRISPR/Cas9. *Plant Biotechnol. J.* 19, 937–951. doi: 10.1111/pbi.13519

Li, M., Li, X., Zhou, Z., Wu, P., Fang, M., Pan, X., et al. (2016). Reassessment of the four yield-related genes Gn1a, DEP1, GS3, and IPA1 in rice using a CRISPR/Cas9 system. *Front. Plant Sci.* 7:377. doi: 10.3389/fpls.2016.00377

Li, J., and Millar, A. A. (2013). Expression of a microRNA-resistant target transgene misrepresents the functional significance of the endogenous microRNA: target gene relationship. *Mol. Plant* 6, 577–580. doi: 10.1093/mp/sss136

Li, J.-F., Norville, J. E., Aach, J., McCormack, M., Zhang, D., Bush, J., et al. (2013). Multiplex and homologous recombination-mediated genome editing in *Arabidopsis* and *Nicotiana benthamiana* using guide RNA and Cas9. *Nat. Biotechnol.* 31, 688–691. doi: 10.1038/nbt.2654

Li, Z., Zhang, D., Xiong, X., Yan, B., Xie, W., Sheen, J., et al. (2017). A potent Cas9-derived gene activator for plant and mammalian cells. *Nat. Plants* 3, 930–936. doi: 10.1038/s41477-017-0046-0

Liang, Z., Chen, K., Li, T., Zhang, Y., Wang, Y., Zhao, Q., et al. (2017). Efficient DNA-free genome editing of bread wheat using CRISPR/Cas9 ribonucleoprotein complexes. *Nat. Commun.* 8:14261. doi: 10.1038/ncomms14261

Liu, G., Liu, J., Pei, W., Li, X., Wang, N., Ma, J., et al. (2019). Analysis of the MIR160 gene family and the role of MIR160a_A05 in regulating fiber length in cotton. *Planta* 250, 2147–2158. doi: 10.1007/s00425-019-03271-7

Liu, Q., Shen, G., Peng, K., Huang, Z., Tong, J., Kabir, M. H., et al. (2015). The alteration in the architecture of a T-DNA insertion rice mutant osmtd1 is caused by up-regulation of MicroRNA156f. *J. Integr. Plant Biol.* 57, 819–829. doi: 10.1111/jipb.12340

Llave, C., Kasschau, K. D., Rector, M. A., and Carrington, J. C. (2002). Endogenous and silencing-associated small RNAs in plants. *Plant Cell* 14, 1605–1619. doi: 10.1105/tpc.003210

Mantilla-Perez, M. B., and Salas Fernandez, M. G. (2017). Differential manipulation of leaf angle throughout the canopy: current status and prospects. *J. Exp. Bot.* 68, 5699–5717. doi: 10.1093/jxb/erx378

Mei, J., Jiang, N., and Ren, G. (2019). The F-box protein HAWAIIAN SKIRT is required for mimicry target-induced microRNA degradation in *Arabidopsis*. *J. Integr. Plant Biol.* 61, 1121–1127. doi: 10.1111/jipb.12761

Meister, G. M. L., Dorsett, Y., and Tuschl, T. (2004). Sequence-specific inhibition of microRNA- and siRNA-induced RNA silencing. *RNA* 10, 544–550. doi: 10.1261/rna.5235104

Miao, C., Wang, Z., Zhang, L., Yao, J., Hua, K., Liu, X., et al. (2019). The grain yield modulator miR156 regulates seed dormancy through the gibberellin pathway in rice. *Nat. Commun.* 10:3822. doi: 10.1038/s41467-019-11830-5

Miura, K., Ikeda, M., Matsubara, A., Song, X.-J., Ito, M., Asano, K., et al. (2010). OsSPL14 promotes panicle branching and higher grain productivity in rice. *Nat. Genet.* 42, 545–549. doi: 10.1038/ng.592

Morbitzer, R., Römer, P., Boch, J., and Lahaye, T. (2010). Regulation of selected genome loci using de novo-engineered transcription activator-like effector (TALE)-type transcription factors. *Proc. Natl. Acad. Sci. U. S. A.* 107, 21617–21722. doi: 10.1073/pnas.1013133107

Nekrasov, V., Staskawicz, B., Weigel, D., Jones, J. D. G., and Kamoun, S. (2013). Targeted mutagenesis in the model plant *Nicotiana benthamiana* using Cas9 RNA-guided endonuclease. *Nat. Biotechnol.* 31, 691–693. doi: 10.1038/nbt.2655

Nizampatnam, N. R., Schreier, S. J., Damodaran, S., Adhikari, S., and Subramanian, S. (2015). MicroRNA160 dictates stage-specific auxin and cytokinin sensitivities and directs soybean nodule development. *Plant J.* 84, 140–153. doi: 10.1111/tpj.12965

Park, W., Li, J., Song, R., Messing, J., and Chen, X. (2002). CARPEL FACTORY, a Dicer homolog, and HEN1, a novel protein, act in microRNA metabolism in *Arabidopsis thaliana*. *Curr. Biol.* 12, 1484–1495. doi: 10.1016/s0960-9822(02)01017-5

Peng, T., Qiao, M., Liu, H., Teotia, S., Zhang, Z., Zhao, Y., et al. (2018). A resource for inactivation of microRNAs using short tandem target mimic technology in model and crop plants. *Mol. Plant* 11, 1400–1417. doi: 10.1016/j.molp.2018.09.003

Peng, T., Teotia, S., Tang, G. A.-O., and Zhao, Q. (2019). MicroRNAs meet with quantitative trait loci: small powerful players in regulating quantitative yield traits in rice. *WIREs RNA* 10:1556. doi: 10.1002/wrna.1556

Prado, J. R., Segers, G., Voelker, T., Carson, D., Dobert, R., Phillips, J., et al. (2014). Genetically engineered crops: from idea to product. *Annu. Rev. Plant Biol.* 65, 769–790. doi: 10.1146/annurev-arplant-050213-040039

Qu, L., Lin, L.-B., and Xue, H.-W. (2019). Rice miR394 suppresses LEAF inclination through targeting an F-box gene, LEAF INCLINATION 4. *J. Integr. Plant Biol.* 61, 406–416. doi: 10.1111/jipb.12713

Reichel, M., Li, Y., Li, J., and Millar, A. A. (2015). Inhibiting plant microRNA activity: molecular SPONGEs, target MIMICs and STTMs all display variable efficacies against target microRNAs. *Plant Biotechnol. J.* 13, 915–926. doi: 10.1111/pbi.12327

Reinhart, B. J., Weinstein, E. G., Rhoades, M. W., Bartel, B., and Bartel, D. P. (2002). MicroRNAs in plants. *Genes Dev.* 16, 1616–1626. doi: 10.1101/gad.1004402

Sakamoto, T., and Matsuoka, M. (2008). Identifying and exploiting grain yield genes in rice. *Curr. Opin. Plant Biol.* 11, 209–214. doi: 10.1016/j.pbi.2008.01.009

Sanei, M., and Chen, X. (2015). Mechanisms of microRNA turnover. *Curr. Opin. Plant Biol.* 27, 199–206. doi: 10.1016/j.pbi.2015.07.008

Schwab, R., Ossowski, S., Riester, M., Warthmann, N., and Weigel, D. (2006). Highly specific gene silencing by artificial microRNAs in *Arabidopsis*. *Plant Cell* 18, 1121–1123. doi: 10.1105/tpc.105.039834

Shan, Q., Wang, Y., Li, J., Zhang, Y., Chen, K., Liang, Z., et al. (2013). Targeted genome modification of crop plants using a CRISPR-Cas system. *Nat. Biotechnol.* 31, 686–688. doi: 10.1038/nbt.2650

Sun, Y., Jiao, G., Liu, Z., Zhang, X., Li, J., Guo, X., et al. (2017). Generation of high-amylose rice through CRISPR/Cas9-mediated targeted mutagenesis of starch branching enzymes. *Front. Plant Sci.* 8:298. doi: 10.3389/fpls.2017.00298

Sun, W., Xu, X. H., Li, Y., Xie, L., He, Y., Li, W., et al. (2020). OsmiR530 acts downstream of OsPIL15 to regulate grain yield in rice. *New Phytol.* 226, 823–837. doi: 10.1111/nph.16399

Tang, J., and Chu, C. (2017). MicroRNAs in crop improvement: fine-tuners for complex traits. *Nat. Plants* 3:17077. doi: 10.1038/nplants.2017.77

Tang, X., Lowder, L. G., Zhang, T., Malzahn, A. A., Zheng, X., Voytas, D. F., et al. (2017). A CRISPR-Cpf1 system for efficient genome editing and transcriptional repression in plants. *Nat. Plants* 3:17103. doi: 10.1038/s41477-017-0001-0

Tang, G., Yan, J., Gu, Y., Qiao, M., Fan, R., Mao, Y., et al. (2012). Construction of short tandem target mimic (STTM) to block the functions of plant and animal microRNAs. *Methods* 58, 118–125. doi: 10.1016/j.ymeth.2012.10.006

Teotia, S., Singh, D., Tang, X., and Tang, G. (2016). Essential RNA-based technologies and their applications in plant functional genomics. *Trends Biotechnol.* 34, 106–123. doi: 10.1016/j.tibtech.2015.12.001

Teotia, S., Zhang, D., and Tang, G. (2017). Knockdown of rice microRNA166 by short tandem target mimic (STTM). *Methods Mol. Biol.* 1654, 337–349. doi: 10.1007/978-1-4939-7231-9_25

Tian, C., Zuo, Z., and Qiu, J. L. (2015). Identification and characterization of ABA-responsive microRNAs in rice. *J. Genet. Genom.* 42, 393–402. doi: 10.1016/j.jgg.2015.04.008

Todesco, M., Rubio-Somoza, I., Paz-Ares, J., and Weigel, D. (2010). A collection of target mimics for comprehensive analysis of microRNA function in

Arabidopsis thaliana. *PLoS Genet.* 6:e1001031. doi: 10.1371/journal.pgen.1001031

Tong, A., Yuan, Q., Wang, S., Peng, J., Lu, Y., Zheng, H., et al. (2017). Altered accumulation of Osa-miR171b contributes to rice stripe virus infection by regulating disease symptoms. *J. Exp. Bot.* 68, 4357–4367. doi: 10.1093/jxb/erx230

Tuncel, A., Corbin, K. R., Ahn-Jarvis, J., Harris, S., Hawkins, E., Smedley, M. A., et al. (2019). Cas9-mediated mutagenesis of potato starch-branching enzymes generates a range of tuber starch phenotypes. *Plant Biotechnol. J.* 17, 2259–2271. doi: 10.1111/pbi.13137

Usman, B., Nawaz, G., Zhao, N., Liu, Y., and Li, R. (2020). Generation of high yielding and fragrant rice (*Oryza sativa* L.) lines by CRISPR/Cas9 targeted mutagenesis of three homoeologs of cytochrome P450 gene family and OsBADH2 and transcriptome and proteome profiling of revealed changes triggered by mutations. *Plan. Theory* 9:788. doi: 10.3390/plants9060788

Vaistij, F. E., Elias, L., George, G. L., and Jones, L. (2010). Suppression of microRNA accumulation via RNA interference in *Arabidopsis thaliana*. *Plant Mol. Biol.* 73, 391–397. doi: 10.1007/s11103-010-9625-4

Waltz, E. (2016). Gene-edited CRISPR mushroom escapes US regulation. *Nature* 532:293. doi: 10.1038/nature.2016.19754

Wang, C., He, X., Wang, X., Zhang, S., and Guo, X. (2017). Ghr-miR5272a-mediated regulation of GhMKK6 gene transcription contributes to the immune response in cotton. *J. Exp. Bot.* 68, 5895–5906. doi: 10.1093/jxb/erx373

Wang, Y., Wang, L., Zou, Y., Chen, L., Cai, Z., Zhang, S., et al. (2014). Soybean miR172c targets the repressive AP2 transcription factor NNC1 to activate ENOD40 expression and regulate nodule initiation. *Plant Cell* 26, 4782–4801. doi: 10.1105/tpc.114.131607

Warthmann, N., Chen, H., Ossowski, S., Weigel, D., and Hervé, P. (2008). Highly specific gene silencing by artificial miRNAs in rice. *PLoS One* 3:e1829. doi: 10.1371/journal.pone.0001829

Woo, J. W., Kim, J., Kwon, S. I., Corvalán, C., Cho, S. W., Kim, H., et al. (2015). DNA-free genome editing in plants with preassembled CRISPR-Cas9 ribonucleoproteins. *Nat. Biotechnol.* 33, 1162–1164. doi: 10.1038/nbt.3389

Xia, K., Ou, X., Tang, H., Wang, R., Wu, P., Jia, Y., et al. (2015). Rice microRNA Osa-miR1848 targets the obtusifoliol 14α-demethylase gene OsCYP51G3 and mediates the biosynthesis of phytosterols and brassinosteroids during development and in response to stress. *New Phytol.* 208, 790–802. doi: 10.1111/nph.13513

Xia, K., Zeng, X., Jiao, Z., Li, M., Xu, W., Nong, Q., et al. (2017). Formation of protein disulfide bonds catalyzed by OsPDIL1;1 is mediated by microRNA5144-3p in rice. *Plant Cell Physiol.* 59, 331–342. doi: 10.1093/pcp/pcx189

Xian, Z., Huang, W., Yang, Y., Tang, N., Zhang, C., Ren, M., et al. (2014). miR168 influences phase transition, leaf epinasty, and fruit development via SlAGO1s in tomato. *J. Exp. Bot.* 65, 6655–6666. doi: 10.1093/jxb/eru387

Xie, K., Wu, C., and Xiong, L. (2006). Genomic organization, differential expression, and interaction of SQUAMOSA promoter-binding-like transcription factors and microRNA156 in rice. *Plant Physiol.* 142, 280–293. doi: 10.1104/pp.106.084475

Xie, K., and Yang, Y. (2013). RNA-guided genome editing in plants using a CRISPR-Cas system. *Mol. Plant* 6, 1975–1983. doi: 10.1093/mp/sst119

Xing, Y., and Zhang, Q. (2010). Genetic and molecular bases of rice yield. *Annu. Rev. Plant Biol.* 61, 421–442. doi: 10.1146/annurev-arplant-042809-112209

Yan, J., Gu, Y., Jia, X., Kang, W., Pan, S., Tang, X., et al. (2012). Effective small RNA destruction by the expression of a short tandem target mimic in *Arabidopsis*. *Plant Cell* 24, 415–427. doi: 10.1105/tpc.111.094144

Yang, C., Li, D., Mao, D., Liu, X. U. E., Ji, C., Li, X., et al. (2013). Overexpression of microRNA319 impacts leaf morphogenesis and leads to enhanced cold tolerance in rice (*Oryza sativa* L.). *Plant Cell Environ.* 36, 2207–2218. doi: 10.1111/pce.12130

Yang, T., Wang, Y., Liu, H., Zhang, W., Chai, M., Tang, G., et al. (2020). MicroRNA1917-CTR1-LIKE PROTEIN KINASE 4 impacts fruit development via tuning ethylene synthesis and response. *Plant Sci.* 291:110334. doi: 10.1016/j.plantsci.2019.110334

Yu, Y., Zhang, Y., Chen, X., and Chen, Y. (2019). Plant noncoding RNAs: hidden players in development and stress responses. *Annu. Rev. Cell Dev. Biol.* 35, 407–431. doi: 10.1146/annurev-cellbio-100818-125218

Yue, E., Cao, H., and Liu, B. (2020). OsmiR535, a potential genetic editing target for drought and salinity stress tolerance in *Oryza sativa*. *Plan. Theory* 9:1337. doi: 10.3390/plants9101337

Zhang, C., Ding, Z., Wu, K., Yang, L., Li, Y., Yang, Z., et al. (2016a). Suppression of jasmonic acid-mediated defense by viral-inducible microRNA319 facilitates virus infection in rice. *Mol. Plant* 9, 1302–1314. doi: 10.1016/j.molp.2016.06.014

Zhang, Y., Liang, Z., Zong, Y., Wang, Y., Liu, J., Chen, K., et al. (2016b). Efficient and transgene-free genome editing in wheat through transient expression of CRISPR/Cas9 DNA or RNA. *Nat. Commun.* 7:12617. doi: 10.1038/ncomms12617

Zhang, Z., Teotia, S., Tang, J., and Tang, G. (2019). Perspectives on microRNAs and phased small interfering RNAs in maize (*Zea mays* L.): functions and big impact on agronomic traits enhancement. *Plan. Theory* 8:170. doi: 10.3390/plants8060170

Zhang, J., Zhang, H., Botella, J. R., and Zhu, J.-K. (2018a). Generation of new glutinous rice by CRISPR/Cas9-targeted mutagenesis of the waxy gene in elite rice varieties. *J. Integr. Plant Biol.* 60, 369–375. doi: 10.1111/jipb.12620

Zhang, J., Zhang, H., Srivastava, A. K., Pan, Y., Bai, J., Fang, J., et al. (2018b). Knockdown of rice microRNA166 confers drought resistance by causing leaf rolling and altering stem xylem development. *Plant Physiol.* 176, 2082–2094. doi: 10.1104/pp.17.01432

Zhang, H., Zhang, J., Yan, J., Gou, F., Mao, Y., Tang, G., et al. (2017). Short tandem target mimic rice lines uncover functions of miRNAs in regulating important agronomic traits. *Proc. Natl. Acad. Sci. U. S. A.* 114, 5277–5282. doi: 10.1073/pnas.1703752114

Zhao, Y.-F., Peng, T., Sun, H.-Z., Teotia, S., Wen, H.-L., Du, Y.-X., et al. (2019). miR1432-OsACOT (acyl-CoA thioesterase) module determines grain yield via enhancing grain filling rate in rice. *Plant Biotechnol. J.* 17, 712–723. doi: 10.1111/pbi.13009

Zhao, Y., Wen, H., Teotia, S., Du, Y., Zhang, J., Li, J., et al. (2017). Suppression of microRNA159 impacts multiple agronomic traits in rice (*Oryza sativa* L.). *BMC Plant Biol.* 17:215. doi: 10.1186/s12870-017-1171-7

Zhao, Y., Zhang, C., Liu, W., Gao, W., Liu, C., Song, G., et al. (2016). An alternative strategy for targeted gene replacement in plants using a dual-sgRNA/Cas9 design. *Sci. Rep.* 6:23890. doi: 10.1038/srep23890

Zheng, L.-L., and Qu, L.-H. (2015). Application of microRNA gene resources in the improvement of agronomic traits in rice. *Plant Biotechnol. J.* 13, 329–336. doi: 10.1111/pbi.12321

Zhou, Y., Liu, W., Li, X., Sun, D., Xu, K., Feng, C., et al. (2020). Integration of sRNA, degradome, transcriptome analysis and functional investigation reveals gma-miR398c negatively regulates drought tolerance via GmCSDs and GmCCS in transgenic Arabidopsis and soybean. *BMC Plant Biol.* 20:190. doi: 10.1186/s12870-020-02370-y

Zhu, C., Ding, Y., and Liu, H. (2011). MiR398 and plant stress responses. *Physiol. Plant.* 143, 1–9. doi: 10.1111/j.1399-3054.2011.01477.x

Zhu, H., Li, C., and Gao, C. (2020). Applications of CRISPR–Cas in agriculture and plant biotechnology. *Nat. Rev. Mol. Cell Biol.* 21, 661–677. doi: 10.1038/s41580-020-00288-9

Zuo, J., and Li, J. (2014). Molecular dissection of complex agronomic traits of rice: a team effort by Chinese scientists in recent years. *Natl. Sci. Rev.* 1, 253–276. doi: 10.1093/nsr/nwt004

Conflict of Interest: The authors declare that the research was conducted in the absence of any commercial or financial relationships that could be construed as a potential conflict of interest.

Publisher's Note: All claims expressed in this article are solely those of the authors and do not necessarily represent those of their affiliated organizations, or those of the publisher, the editors and the reviewers. Any product that may be evaluated in this article, or claim that may be made by its manufacturer, is not guaranteed or endorsed by the publisher.

frontiers in Plant Science

ORIGINAL RESEARCH
published: 25 November 2021
doi: 10.3389/fpls.2021.769093

Combined Stress Conditions in Melon Induce Non-additive Effects in the Core miRNA Regulatory Network

*Pascual Villalba-Bermell[1], Joan Marquez-Molins[1], María-Carmen Marques[1], Andrea G. Hernandez-Azurdia[1], Julia Corell-Sierra[1], Belén Picó[2], Antonio J. Monforte[3], Santiago F. Elena[1,4] and Gustavo G. Gomez[1]**

[1] Instituto de Biología Integrativa de Sistemas (I[2]SysBio), Consejo Superior de Investigaciones Científicas (CSIC), Universitat de València (UV), Valencia, Spain, [2] Instituto de Conservacióny Mejora de la Agrodiversidad Valenciana (COMAV), Universitat Politècnica de València (UPV), Valencia, Spain, [3] Instituto de Biología Molecular y Celular de Plantas (IBMCP), Consejo Superior de Investigaciones Científicas (CSIC), Universitat Politècnica de València (UPV), Valencia, Spain, [4] The Santa Fe Institute, Santa Fe, NM, United States

Climate change has been associated with a higher incidence of combined adverse environmental conditions that can promote a significant decrease in crop productivity. However, knowledge on how a combination of stresses might affect plant development is still scarce. MicroRNAs (miRNAs) have been proposed as potential targets for improving crop productivity. Here, we have combined deep-sequencing, computational characterization of responsive miRNAs and validation of their regulatory role in a comprehensive analysis of response of melon to several combinations of four stresses (cold, salinity, short day, and infection with a fungus). Twenty-two miRNA families responding to double and/or triple stresses were identified. The regulatory role of the differentially expressed miRNAs was validated by quantitative measurements of the expression of the corresponding target genes. A high proportion (ca. 60%) of these families (mainly highly conserved miRNAs targeting transcription factors) showed a non-additive response to multiple stresses in comparison with that observed under each one of the stresses individually. Among those miRNAs showing non-additive response to stress combinations, most interactions were negative, suggesting the existence of functional convergence in the miRNA-mediated response to combined stresses. Taken together, our results provide compelling pieces of evidence that the response to combined stresses cannot be easily predicted from the study individual stresses.

Keywords: crop production and climate change, miRNAs and stress response in *Cucumis melo*, RNA regulatory networks, RNA-seq and systems biology, biotic and abiotic stress

OPEN ACCESS

Edited by:
Xiuren Zhang,
Texas A&M University, United States

Reviewed by:
Xinwei Guo,
Chinese Academy of Medical Sciences and Peking Union Medical College, China
Zofia Szweykowska-Kulinska,
Adam Mickiewicz University, Poland

****Correspondence:***
Gustavo G. Gomez
gustavo.gomez@csic.es

Specialty section:
This article was submitted to Plant Physiology, a section of the journal Frontiers in Plant Science

Received: *01 September 2021*
Accepted: *14 October 2021*
Published: *25 November 2021*

Citation:
Villalba-Bermell P, Marquez-Molins J, Marques M-C, Hernandez-Azurdia AG, Corell-Sierra J, Picó B, Monforte AJ, Elena SF and Gomez GG (2021) Combined Stress Conditions in Melon Induce Non-additive Effects in the Core miRNA Regulatory Network. Front. Plant Sci. 12:769093. doi: 10.3389/fpls.2021.769093

INTRODUCTION

During their life cycle, plants are exposed to a wide array of adverse environmental conditions that, in general, limit their normal development and productivity. These complex interactions result in several stress situations that disturb the homeostasis of the cell, negatively affecting plant growth. Consequently, stress-induced damages in productivity are the primary cause of extensive agricultural losses worldwide (Priya et al., 2019). Reduction in crop yield due to environmental variations has increased steadily over the last decades. In addition, several production models project a reduction in the yields of major agricultural crops in the future, mostly due to climatic changes (Rosenzweig et al., 2014).

Climate change, entailing shifts in temperature, precipitation, and atmospheric composition, among other factors, represents a moving target for plant developmental adaptation. In parallel, environmental modifications can favor the development of new plant pest and/or pathogens or increase the incidence levels of already existing ones. As a consequence of this complex environmental scenario, it is expected that combined abiotic and biotic stresses can affect plants at the level of molecular functions, developmental processes, morphological traits, and physiology, resulting in a significant decrease in crop production and quality (Gray and Brady, 2016; Morales-Castilla et al., 2020).

Multiples studies focused on plant responses to individual stresses have been carried out over the last years. However, less attention has been paid to the effect that combinations of adverse environmental conditions might exert on plant development (Bai et al., 2018). In order to improve crop yield and to meet the growing challenges stemming from rapid population growth, extensive efforts are needed to understand the mechanisms underlying plant responses to simultaneous exposure to multiple stresses (Zhang and Sonnewald, 2017). Previous works have pointed out that studying stress conditions separately would not allow inferring the expected plant response to multiple stresses. Using *Arabidopsis thaliana* as an experimental model, it was shown that the response to a combination of drought and heat was unique and could not be directly extrapolated from the plant response to each stress applied individually (Rizhsky et al., 2004; Suzuki et al., 2005; Rossel et al., 2007). Similar findings were also reported for a combination of heat and high light intensity in sunflower (Hewezi et al., 2008), and heat and salinity in wheat (Keleş and Öncel, 2002). Consequently, plant response to combined adverse environmental conditions should be handled as a new state of stress that requires a novel conceptual viewpoint (Mittler and Blumwald, 2010).

In general, plants respond to stress conditions through complex reprogramming of their transcriptional activities, aiming to reduce the impact of stress on their physiological and cell homeostasis. Environmental variations have selected diverse responses among plant lineages, landraces, and wild crops relatives. Studies on natural variations can provide novel insights into evolutionary processes modulating stress response (Meyers et al., 2008; Haak et al., 2017). Elucidation of how endogenous regulators and the environment interact during plant development is a long-standing grand challenge in modern biology as well as in crop breeding (Lovell et al., 2015).

MicroRNAs play a versatile role as regulators of gene expression. Plant genes-encoding miRNAs are transcribed by RNA polymerase II as primary transcripts harboring a fold back structure that is processed by DICER-LIKE 1 (DCL1) in a duplex (21 or 22 nt in length), which once 2′-*O*-methylated by HEN1 is loaded into an AGO complex (Bartel, 2004; Bologna and Voinnet, 2014; Reis et al., 2015; Achkar et al., 2016). miRNAs regulate gene expression by means of sequences complementarity with both RNA and DNA targets (Song et al., 2019). Their functions include modulation of a vast array of plant biological processes related to grown and development (Bologna and Voinnet, 2014), including the recovering of the plant-cell homeostasis during exposure to adverse environmental condition (Song et al., 2019; Xu et al., 2019). In addition, it has been recently described that the biogenesis and turnover of certain miRNAs are also susceptible to be controlled by external stimulus (Bustamante et al., 2018; Manavella et al., 2019). Indeed, it has been proposed that miRNAs are ideal targets to be manipulated to improve crop productivity (Tang and Chu, 2017; Xu et al., 2019). However, most of the described stress-responsive miRNAs come from rice and tomato, as very few miRNAs have been investigated in detail in other crops. Henceforth, additional efforts are needed to decipher the role of miRNA-mediated responses to adverse environmental conditions in other economically relevant crops (Tang and Chu, 2017).

Although increasing pieces of evidence support the role of miRNAs as key modulators of plant response to both biotic (Sun et al., 2017; Xie et al., 2017; Brant and Budak, 2018) and abiotic stress conditions (Cervera-Seco et al., 2019; Wang et al., 2020; Cheng et al., 2021; Zhao et al., 2021), research focusing on elucidating the regulatory role of the miRNAs during exposure to combined adverse environmental conditions is still scarce (Xu et al., 2019), and only a few studies considering the effects of a unique combination of stresses have been addressed in soybean (Ning et al., 2019), *A. thaliana* (Gupta et al., 2020), wheat (Liu et al., 2020), and tomato (Zhou et al., 2020).

Melon (*Cucumis melo*) is one of the cucurbit crops with more economic impact. Melon has high adaptability to warm and dry climates, so it can be a target crop to cope with the climate change threats. Previous genetic studies in cucurbits have been focused mainly on fruit quality and disease resistance (Gonzalo and Monforte, 2017). However, the study of the response to combined stress conditions has not been thoroughly addressed in cucurbits. Consequently, there is a lack of consensus protocols, target traits, and, therefore, identification of tolerant genotypes to develop efficiently resilient cultivars.

Here, we used deep-sequencing, computational approaches and specific miRNA-targets quantification to present a comprehensive functional analysis of miRNA expression profiles in response to one triple (cold, salinity, and short day) and five double (cold and drought, cold and salinity, cold and short day, drought and salinity, and drought and infection with the fungus *Monosporascus cannonballus*) combinations of stress conditions in melon (*Cucumis melo*), a crop extensively cultivated in semiarid regions worldwide. The analyzed stress conditions were coincident, in part, with those employed recently to infer the miRNA-mediated regulatory network of response to individual stresses in melon (Sanz-Carbonell et al., 2019, 2020). The parallelism between both simultaneous experimental approaches made possible to unambiguously analyze the effects that the combined adverse environmental conditions have on the accumulation of the stress-responsive miRNAs.

MATERIALS AND METHODS

Plant Material, Growth Conditions, and Stress Treatments

Melon seeds of cv. Piel de Sapo were germinated in Petri dishes at 37°C/48 h in darkness, followed by 24 h/25°C

(16/8 light/darkness). Melon seedlings were sown in pots and maintained for 10 days under controlled conditions (28°C/16-h light and 20°C/8-h darkness). At day 11, plants were exposed to six stress-combined treatments (detailed in **Supplementary Table 1**). We selected abiotic conditions well established as crucial for plant development (cold, salinity, and short day) and *Monosporascus cannonballus* (a soil-borne fungal pathogen capable of causing root rot and wilting in melon (Pollack and Uecker, 1974) as biotic inducers of stress. At 11 days post-treatment, the first leaf under the apical end per plant was collected in liquid nitrogen and maintained at –80°C until processing. Each analyzed sample corresponds to a pool of three treated plants. Three biological replicates were performed per treatment. Leaves recovered from non-treated plants were considered as controls. This stress assay was performed simultaneously with the recent work describing the response to single stress conditions in melon (Sanz-Carbonell et al., 2019).

RNA Extraction and Small RNA Purification and Sequencing

Total RNA was extracted from leaves (∼0.1 g) recovered from treated and control melon as previously described (Sanz-Carbonell et al., 2019, 2020). The low-molecular weight RNA (<200 nt) fraction was enriched from total RNA using TOTAL-miRNA (miRNA isolation Kit, REAL) according to the manufacturer's instructions. Production and sequencing of the libraries were carried out by Novogene[1]. Eighteen cDNA libraries were obtained by following Illumina's recommendations and sequenced in HiSeq 2000 (Illumina) equipment. Adaptors and low-quality reads were trimmed by using the cutadapt software (Martin, 2011). For the sake of comparing the results generated in here with those obtained for single stresses, data previously obtained from melon plants exposed to identical single stress conditions for 11 days (Sanz-Carbonell et al., 2019) were also included in the study. Melon miRNA sequences used in this study have been submitted to the genomic repository SRA of the NCBI and are available in the BioProject (PRJNA741881).

RT-qPCR Assays

To analyze the expression of target genes and miRNA precursors, total RNA (1.5 μg) was subjected to DNase treatment (EN0525, Thermo Scientific™), followed by reverse transcription using RevertAid First Strand cDNA Synthesis Kit (Thermo Scientific™) according to the manufacturer's instructions for use with oligo-dT. cDNAs were amplified by conventional end-point RT-PCR using specific primers to assess for sequence specificity. Then, real-time PCR was performed as described previously (Bustamante et al., 2018). All analyses were done in triplicate on a QuantStudio qPCR instrument (Thermo Scientific™) using a standard protocol. The efficiency of PCR amplification was derived from a standard curve generated by four 10-fold serial dilution points of cDNA obtained from a mix of all the samples. Relative RNA expression was quantified by the comparative $\Delta\Delta C_T$ method (Livak and Schmittgen, 2001) and normalized to the geometric mean of Profilin (NM_001297545.1) expression. The statistical significance of the observed differences was evaluated by the paired *t*-test. Primers used for miRNA-targets amplification and profiling were described previously (Sanz-Carbonell et al., 2019). Primers used to analyze miRNA precursors are detailed in **Supplementary Table 9**.

Bioinformatic Analysis of miRNA Sequences

To study the correlation exhibited by the miRNA expression profiles among the different stresses and their biological replicates, principal component analysis (PCA) was used. PCA was performed using the prcomp function with scaling in the stats R package v. 4.0.4 (R Core Team, 2013). Mann–Whitney–Wilcoxon tests were performed to assess for significant differences in the data clusters for Euclidean distances calculated between groups and among groups with the wilcox.test function in the stats R package.

Differential expression of melon small RNAs (sRNAs) was estimated using three R packages NOISeq (Tarazona et al., 2015), DESeq2 (Love et al., 2014) and edgeR (Robinson and Oshlack, 2010) for pairwise differential expression analysis of expression data. Differentially expressed sRNAs were filtered out using three criteria: (i) $\log_2$-fold change $|\log_2 FC| \geq 1.25$, (ii) adjusted $p \leq 0.05$ (DESeq2 and edgeR), probability ≥ 0.95 (NOISeq), and (iii) RPMs ≥ 5 for at least three libraries in control samples or at least two libraries in any stress. sRNAs identified as responding to stress by the three methods were aligned against miRNA sequences in miRBase (release 22) (Kozomara et al., 2019). To generate robust knowledge suitable to be transferred to diverse plant species, only sequences fully homologous to previously described mature melon miRNAs and known *Viridiplantae* miRNAs with well-established regulatory roles were kept.

Afterward, these sequences were re-annotated by aligning them against miRNA precursors of melon deposited in miRBase and were considered as known stress-responsive miRNAs. Unaligned sequences were realigned allowing for one mismatch against the melon genome to identify potential precursors. These sequences were also identified as known stress-responsive miRNAs; the rest were discarded. The entire pipeline is shown in **Supplementary Figure 1**.

To determine the general sense of the expression for each miRNA family, we employed the median value of expression estimated by box-plot analysis of all family-related sequences under each stress condition, considering the $\log_2 FC$ values obtained by edgeR. The most frequent sequence in each miRNA family and stress was used to generate heatmaps with an R interface to a morpheus.js heatmap widget[2].

Analysis of the Stress Combination Effect

The expression of reactive miRNAs in response to combined stress conditions can be enfolded in at least one of the three following categories: (i) additive if the observed response to combined stresses is just the sum of the magnitude responses

[1]https://en.novogene.com

[2]https://github.com/cmap/morpheus.R

observed for each individual stress, i.e., this represents the null hypothesis of independent actions, (ii) negative if the observed response is smaller than the expected additive response, and (iii) positive if the observed value is greater than the expected additive response. In this framework, if a given miRNA shows an additive response upon exposure to two stresses, it can be assumed that both stresses trigger independent miRNA-mediated responses. In contrast, a miRNA showing a significantly negative or positive deviation from the null hypothesis shall be taken as indicative of a specific response to the combined stresses beyond the simple additive case. To quantitatively test the null hypothesis of additive effects on miRNA-mediated response to stress combinations, we defined an *stress combination effect* (*SCE*) index that refers to the miRNA response value to combined stresses in comparison to what should be expected from individual stress conditions as $SCE = (C + S_{ij}) - (S_i + S_j)$, where C refers to the means of the normalized reads recovered in control, S_{ij} to the reads observed in plants exposed to combined stresses i and j and S_i and S_j to the reads arising from each individual stress (**Supplementary Tables 6A,B**). Under the null hypothesis of purely additive effects of stresses i and j on miRNA expression, the observed expression under both stresses will be equal to the sum of expression observed for each individual stress and hence $SCE = 0$. Positive ($SCE > 0$) or negative ($SCE < 0$) deviations from this null hypothesis will result from an over- or under-expression of the miRNA when stresses i and j are combined, respectively. For the triple stress condition (S_{ijk}) and additional value (S_k)—referred to the means of normalized reads in the additional stress condition k—should be added to the second terms of the equation. As written above, for the action of two combined stresses i and j, it is straightforward to show mathematically that *SCE* is equivalent to the coefficient of the interaction term between stresses i and j in a two-way ANOVA model. The statistical significance of the *SCE* was calculated on the basis of a standard normal distribution and the adjusted p-value by the false discovery rate (FDR) approach. Only the miRNAs with a p-value equal or smaller than its respective FDR q-value were considered as reliable indicators of effects of stress combinations onto miRNA accumulation (**Supplementary Table 6A**). Reads exhibiting zero means values in any of the analyzed combinations were filtered out. The data associated with the miRNA expression under single stress conditions were extracted from a previous work, analyzing the differential expression of melon miRNAs in response to seven biotic and abiotic single stress conditions (Sanz-Carbonell et al., 2019). The statistical significance of *SCE* was calculated on the basis of a standard normal distribution. Then, the 22 stress-responsive miRNA-families were organized in a binary table of presence and absence (**Supplementary Table 8**), in which the values one and zero represent, respectively, whether or not a miRNA family has at least a member exhibiting a significant non-additive (positive or negative) effect in response to a combined stress condition. The hclust function in stats R package (v. 4.0.4) was used to compute hierarchical clustering (HC), specifying Ward linkage (ward.D) as an agglomeration method and using the simple matching coefficient metric to calculate the distance matrix. The statistical significance of the HC was estimated with a Mann–Whitney–Wilcoxon test.

RESULTS

Stress Combinations and sRNAs Dataset

High-throughput sequencing of sRNAs was performed, starting from 22 (three replicates for each stress condition plus four non-treated controls) sRNA libraries constructed with RNA extracted from leaves of melon plants 11 days after exposure to six (five double and one triple) combined stress conditions: (i) cold and drought (C-D), (ii) cold and salinity (C-Sal), (iii) cold and short day (C-SD), (iv) drought and salinity (D-Sal), (v) drought and *M. cannonballus* infection (D-Mon), and (vi) cold, salinity, and short day (C-Sal-SD) (**Supplementary Table 1**). As has been pointed in section "Materials and Methods," this assay was performed in parallel and simultaneously with our previous work, analyzing the response to single stressors in melon (Sanz-Carbonell et al., 2019). Regarding the stress conditions analyzed, we selected abiotic conditions well established as crucial for melon plant development (cold, drought, salinity, and short day) and infection with *M. cannonballus*, a soil-borne fungal pathogen, causing root rot and wilting in melon (Pollack and Uecker, 1974). Only sequences with size ranging between 20 and 25 nt in length and non-matching to rRNA, tRNA, snoRNA, and snRNA sequences deposited in the Rfam data base[3] were further included in this study. A total of 80,620,994 reads (representing 36,836,230 unique sequences) were recovered. The distribution of reads by stress condition is detailed in **Supplementary Table 2**.

Associations between sRNA expression profiles (considering the different treatments and their biological replicates) were evaluated using PCA. The percentages of variance explained by the first three PCs were 20.4, 17.1, and 13.8%, respectively (adding up to 51.3% of the total observed variance). The PCA plot in **Figure 1A** shows that biological replicates clustered together (attesting for the reproducibility of our assays) and treatments clearly separated in the PC space with high significance ($p = 5.886 \times 10^{-15}$). The sRNAs exhibited a distribution of read lengths strongly enriched for 24-nt long (45.7%), followed by similar accumulations of 21- (13.5%), 22- (12.6%), and 23 (13.5%)-nt long molecules. As expected, reads of 20 and 25 nt represented the less-abundant categories (5.9 and 8.5%, respectively) (**Figure 1B**). These differences in accumulation of different sRNA lengths were statistically significant (two-way non-parametric ANOVA, **Supplementary Table 3A** $p < 10^{-5}$). The effect was entirely due to the large enrichment in 24-nt-long sRNAs (Dunn's *post hoc* pairwise tests, **Supplementary Table 3A**: $p \leq 0.0134$ in all pairwise comparisons) and consistent with what has been previously described in melon (Sattar et al., 2012; Herranz et al., 2015; Sanz-Carbonell et al., 2019, 2020) and other members of the *Cucurbitaceae* family (Jagadeeswaran et al., 2012). Non-significant differences were found between stress conditions regarding the observed distribution of sRNAs sizes (**Supplementary Table 3A**: $p = 0.857$), nor the interaction between both factors (**Supplementary Table 3A**: $p = 0.750$). The effect of the stress conditions on sRNAs accumulation was evaluated by pairwise comparisons between control and treated samples. As described above, only sequences that match the

[3]http://rfam.xfam.org

conditions $|\log_2 FC| \geq 1.25$ and $p < 0.05$ were considered as significantly differentially expressed and retained for subsequent analysis (**Supplementary Figure 2**). A total of 35,906 unique reads fulfilled these conditions. The combinations that included cold as one of the stressors showed the most drastic alteration in sRNAs accumulation (21,592 reactive sRNAs in C-D, 20,760 in C-Sal, 23,506 in C-SD, and 21,263 in C-Sal-SD). In contrast, only 1,595 and 3,988 differentially expressed sRNAs were identified in plants treated with the combination D-Mon and D-S, respectively (**Supplementary Figure 2**). These results support the notion that exposition to low temperature (in any combination) is the most stressful environmental condition, resulting in the strongest alteration of the sRNA metabolism in melon (**Figure 1C**).

Combined Stresses Induce a General Decrease of miRNA Expression

To identify melon miRNAs reactive to combined stress conditions, differentially expressed sRNAs were aligned against miRNA sequences (both mature and precursors) recovered from miRBase[4]. Only sRNAs ranging 20–22 nt and fully homologous to database sequences were considered. Two sequences homologous to mature *miR6478* but lacking a known transcript in melon with a canonical hairpin were excluded for subsequent analysis (**Supplementary Figure 1**). After filtering, 100 unique sequences belonging to 22 known miRNA families were identified as responsive to the combined stress conditions studied (**Supplementary Table 3**). In general, all family-related sequences showed a comparable trend of accumulation in response to the stress conditions analyzed (**Figure 2A**). A sequence variant of *miR398b* (downregulated in C-D treatment but showing a minority accumulation rate with respect to predominant family-related sequences) and the non-canonical miRNAs derived of the alternative processing of *miR319* (*miR319nc*) (Bustamante et al., 2018) and *miR159* (*miR159nc*) (Bologna et al., 2009) precursors (upregulated in cold-containing combinations and without regulatory activity described yet) showed a discordant response with the family-wise trend. In these two circumstances, the response trend of the more representative family members was considered for ulterior analysis.

The general response to stress conditions was the downregulation of miRNAs (**Figure 2B**). Sequences included in miRNA families *miR157, miR159, miR167, miR168, miR319,* and *miR396* showed significantly decreased accumulation in all the stress conditions analyzed. Diminished accumulation in response to stress was also observed for *miR156, miR160* (except under C-Sal-SD), *miR164, miR166, miR169* (except for D-Sal), *miR171, miR172* (except for D-Sal and D-Mon), *miR393* (except for D-Mon), *miR394*, and *miR1515*. Finally, *miR165* was downregulated in three stress conditions involving cold (C-SD, C-D, and C-Sal). Regarding miRNAs upregulated in response to stress, the *miR398* and *miR408* family-related members (except for the reads related to *miR398b* described above) showed increased accumulation in all stress conditions, whereas *miR159* was significantly overexpressed in response to C-SD and C-D, and *miR397* family was so in plants exposed to C-Sal, C-Sal-SD, and D-Mon. Sequences related to *miR156*, *miR166*, and *miR395* were specifically upregulated under D-Sal stress.

The analysis of the miRNA expression focused on each particular stress combination evidenced that cold was the most adverse environmental condition with major impact on miRNA expression in melon. A total of 20 miRNA families were reactive to C-SD and C-D and 19 to C-Sal (**Figure 2B** and **Supplementary Table 4**). While 18 miRNAs families showed differential expression under the combination of three stresses. A weaker response was associated with treatments with D-Sal (14 reactive miRNA families) and D-Mon (13 miRNAs with altered expression). Considering both stress condition and miRNA expression trend, except *miR156* and *miR166* (upregulated in D-Sal and downregulated in the other stress conditions), all miRNAs exhibit a homogenous response to the six combinations of adverse environmental conditions analyzed. The estimation of the relative accumulation of representative miRNA-precursors by RT-qPCR evidenced that only *miR398* and *miR408* showed consistence between the expression of MIR genes and the abundance of mature miRNAs in the totality of the stress conditions studied here (**Supplementary Figure 3**). For *miR396*, consistence was observed only in cold-containing stress combinations. In contrast, analyzed members of *miR156, miR157, miR167*, and *miR168* families exhibit, in general, antagonist accumulation when the accumulation of precursors and mature miRNAs was compared.

It has been recently proposed that certain melon miRNAs are predominantly reactive to diverse biotic and abiotic stress conditions, while other specifically respond to certain stressor and/or expositions time (Sanz-Carbonell et al., 2020). Based on this particular behavior, miRNAs belonging to both different groups were identified as stress-responsive miRNAs with *broad* and *narrow* response range, respectively, while a third group that exhibits a moderated reactivity in response to stress was identified as *intermediates*. According to our data, 10 miRNA families showed the higher response rate to combined stress, with significant differential expression (either up or down) in the six analyzed conditions (**Supplementary Table 4**). Eight of these miRNA families (*miR156, miR157, miR166, miR167, miR319, miR396, miR398*, and *miR408*) were mostly coincident with melon miRNAs families classified in the broad response category (*generalists*), while *miR159* and *miR168* were previously categorized as intermediates. In contrast, miRNAs with a lower response rate to double and triple stresses (responsive in three or less conditions) pervasively pertained to miRNAs families previously reported as showing *specific* response to stress conditions in melon.

To test the functional role of the miRNAs reactive to combined stresses, we analyzed the correlation between miRNA levels and transcripts accumulation in 16 representative miRNA-target modules (**Supplementary Table 5**) previously established and validated to occur in melon plants (Bustamante et al., 2018; Sanz-Carbonell et al., 2019, 2020). We focused on the miRNAs reactive to at least three different stress conditions (*miR156, miR159, miR160, miR164, miR166, miR167, miR169, miR171, miR172, miR319, miR393, miR396, miR397, miR398*, and *miR408*). As

[4]http://www.mirbase.org/

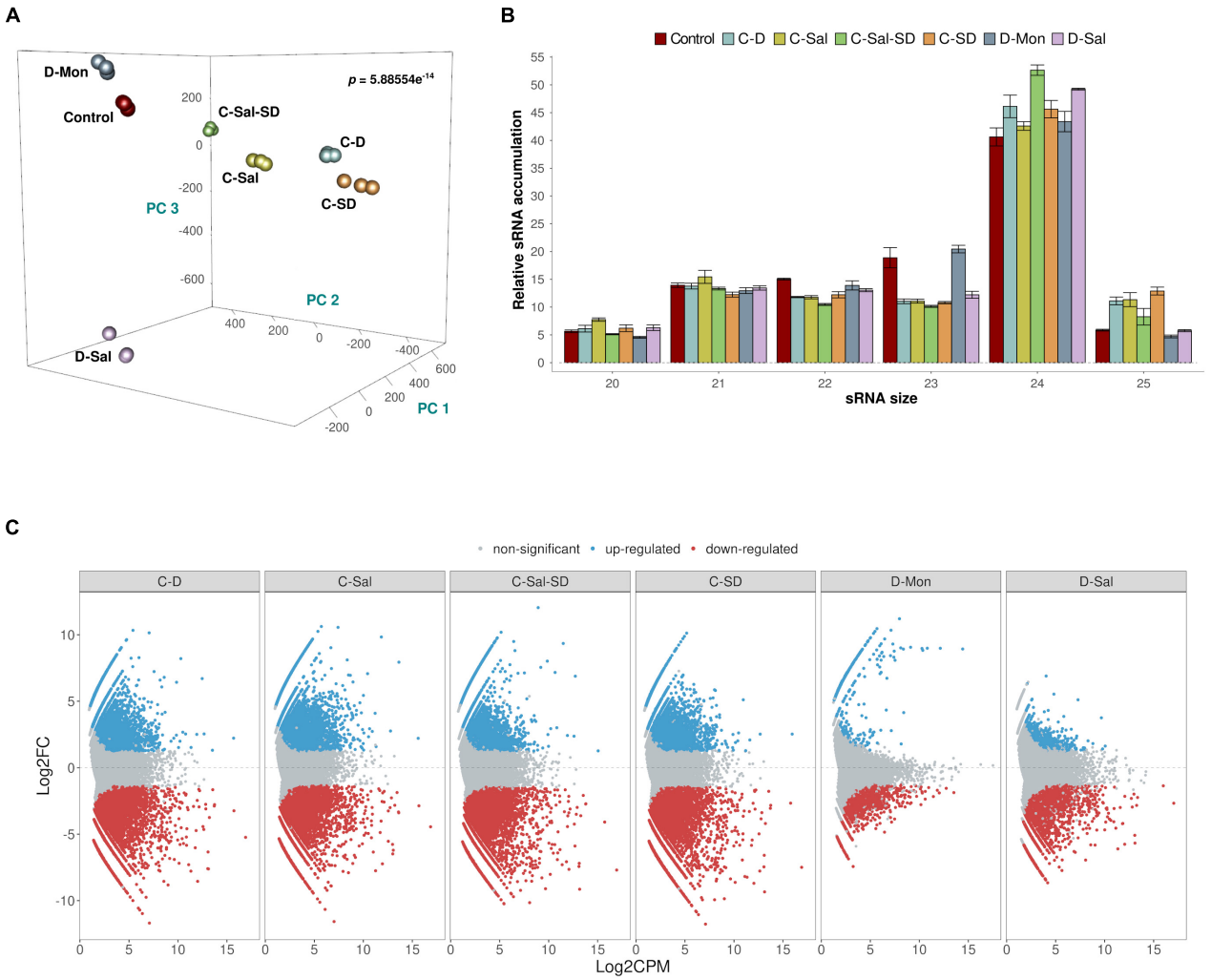

FIGURE 1 | Analysis of the sRNA populations. **(A)** PCA based on sRNAs accumulation in three biological replicates of melon plants exposed to the six stress-combined treatments and controls. The statistical significance ($p = 5.886 \times 10^{-14}$) was estimated by Mann–Whitney–Wilcoxon test, considering the inter- and intragroup Euclidean distances. **(B)** A diagram showing the relative accumulation (and distribution of the total clean reads of melon sRNAs ranging between 20 and 25 nt obtained from the analyzed sequenced libraries. The control and the different analyzed treatments are represented with colors. The shown values represent the sum of all repetitions. Bars indicate the standard error. **(C)** Graphic representation of the expression values (estimated by edgeR) of sRNA sequences recovered from melon exposed to different stress conditions. The dots indicate the expression value of each sRNA. Red and blue dots indicate significant values for differential expression with $|\log_2 FC| \geq 1.25$, respectively. Gray dots indicate sRNAs with non-significant differential expression.

expected, a significant negative correlation ($r = -0.514$, 83 df, $p < 0.001$) was obtained when the expression values of stress-responsive miRNAs were compared with the accumulation (estimated by RT-qPCR) of their target transcripts (**Figure 2C**).

The miRNA-Mediated Response to Stress Combinations Cannot Be Predicted From the Response to Single Stresses

To determine the dynamic of the miRNA-mediated response to multiple stress conditions, we compared the accumulation levels of stress-responsive miRNAs in plants subjected to the individual stress conditions with those of plants exposed to combined stresses. To do so, we computed *SCE* as defined in section "Materials and Methods." Except for the combination C-Sal-SD, the additive effect was predominant in number of unique miRNA sequences in the analyzed stress combinations (65.26% of the unique reads) (**Figure 3A**). However, considering the entire miRNAs population (total reads), a comparable abundance of additive (50.07%) and non-additive (49.93%) instances was observed in response to combined stresses. Interestingly, when evaluating only by the miRNA family, 57.58% had at least a member showing a significant (negative or positive) *SCE* value (**Figure 3A** and **Supplementary Table 7**).

Regarding significant non-additive interactions, the stress combination predominantly exerted a negative effect in four (C-Sal, D-Sal, D-Mon, and C-Sal-SD) of the six analyzed treatments

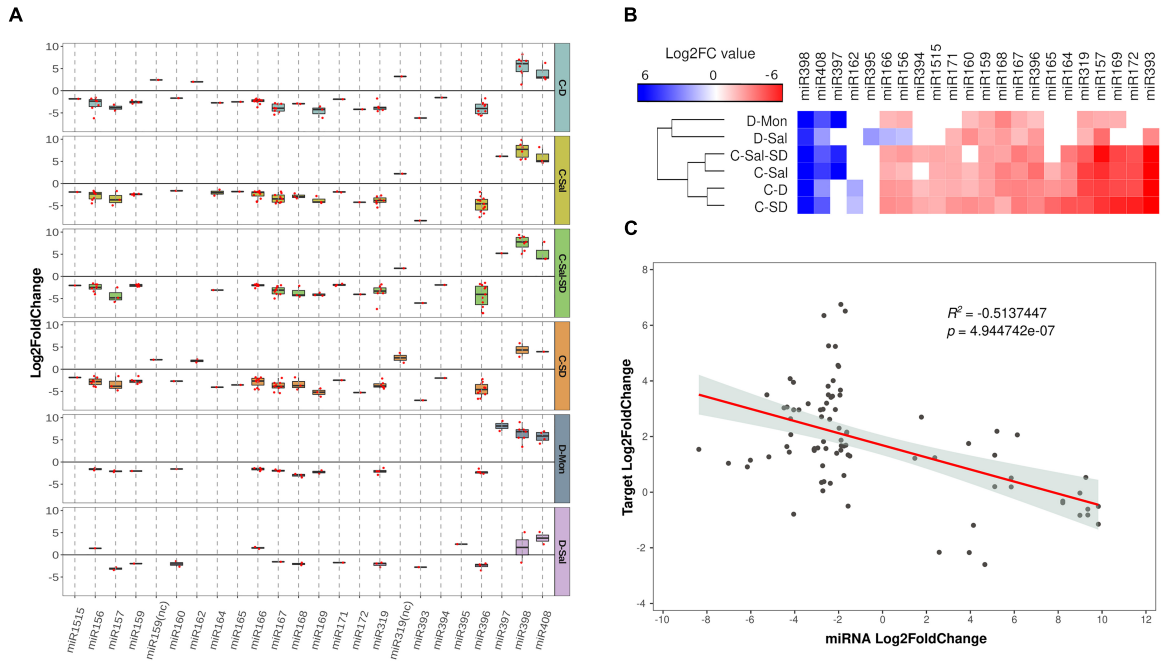

FIGURE 2 | General description of stress-responsive miRNA families. **(A)** Boxplot analysis showing the general expression value observed for each miRNA family member. To determine the general sense of the expression for each miRNA family, we employed the median value of expression (represented by internal box line) estimated by boxplot analysis of all family-related sequences. The differential expression values represented in the figure correspond to the log_2FC obtained using edgeR. **(B)** Heatmap of 22 miRNAs differentially expressed in melon in response to combined stress. The differential expression values represented correspond to the median of the log_2FC values obtained using edgeR for each miRNA family. **(C)** A scatter plot showing the significant negative correlation (estimated by Pearson correlation coefficient) between the expression levels of 16 selected stress-responsive miRNAs with differential accumulation determined by sequencing and the accumulation of their targets in the corresponding stress conditions, estimated by RT-qPCR.

(**Figure 3B**). By contrast, in C-D and C-SD, *SCE* > 0 values were the most common case. Analyzing each stress combination individually, C-SD was the condition in which miRNAs show the smallest fraction of specific response to combined stresses (14.46% of unique reads, 7.77% of total reads and 40.91% of the miRNA families). In contrast, a higher differential interaction (76.47% for negative and 2.94% for positive) was observed in response to the triple combinations C-Sal-SD (61.45% of unique reads, 92.05% of total reads, and 77.27% of the miRNA families) (**Figure 3B**). A more general view of the additive and non-additive effects of the combined stresses onto the global population of miRNA-related reads in each analyzed stress condition is shown in the **Figure 3C**.

Considering the response trend of miRNA family members, we observed that, in general, reads showed a coordinated interaction (*SCE* positive or negative) in response to the combination of stresses (**Figure 4A**). Consequently, a negative response was also pervasive under a global miRNA-family viewpoint. Exceptions were observed for the families *miR157* in C-SD and *miR159* in D-Sal, which contained members showing both positive and negative *SCE* values under the indicated stress combination. However, it is worth nothing that the miRNA sequences with a non-coincident trend are minority relative to the other family members (**Supplementary Table 6A**). Therefore, in these two specific cases, the response trend of the predominant reads was considered as representative of the family behavior for ulterior analysis (**Figure 4B**). The highest number (17) of miRNA families showing significant *SCE* values was observed in plants exposed to the triple combinations of stresses, followed by C-Sal and D-Mon (14) and D-Sal (13). In contrast, only nine miRNA families were identified as significantly interactive in response to C-D and C-SD, respectively.

Different miRNA Families Act Distinctively in Response to Combined Stresses

To get further insights into the response of each miRNA family to combined stress conditions, we analyzed the rate of differential response to double and triple stresses. The 22 stress-responsive miRNA families were organized into a table of presence and absence (**Supplementary Table 8**) in which the values one and zero represent, respectively, whether or not a miRNA shows a significant response value (with either positive or negative effect) under a combined stress condition. Members of *miR156, miR157, miR319, miR396*, and *miR398* families showed significant positive or negative *SCE* in the six stress conditions analyzed here, while *miR159, miR166, miR167*, and *miR408* members accumulate differentially in five stresses combinations. Sequences belonging to *miR164, miR165, miR171*, and *miR393* (with positive or negative *SCE* in four conditions), *miR168* and *miR169* (in three), *miR172, miR395*, and *miR1515*

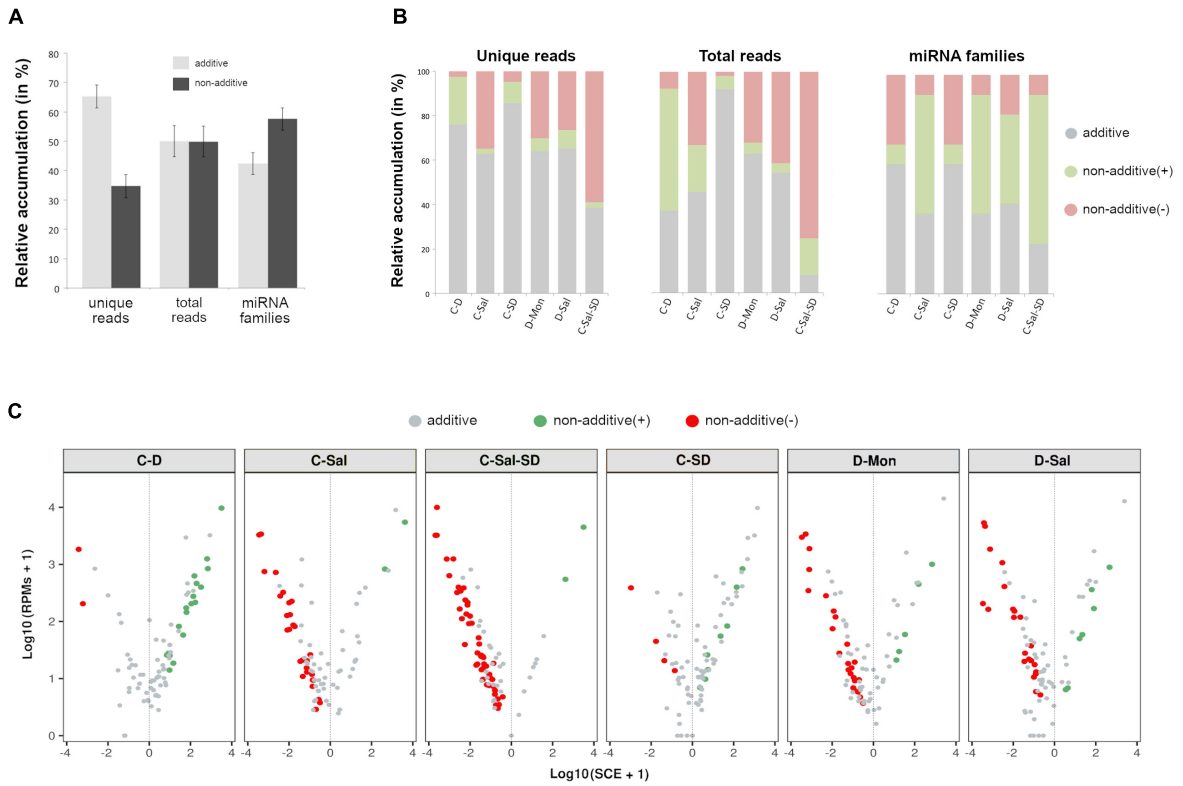

FIGURE 3 | Effects of the stresses combination on the accumulation rate of stress-responsive miRNAs. **(A)** Graphic representation of the mean percentage for the six analyzed treatments of miRNA-related reads that exhibit additive (gray) or non-additive (black) response to combined stress conditions in comparison to single stresses, considering unique reads (left columns), total reads (central columns), and miRNA families (right). Bars represent the standard error between means. **(B)** The detail of the global response rate in each stress condition, considering the two (positive or negative) types of possible non-additive response to combined stresses. **(C)** A volcano plot showing significant positive (green dots) and negative (red dots) *SCE* values obtained for each miRNA-related read in response to each combined stress condition. miRNAs with non-significant deviations from the additive null model are in gray. More detailed information is provided in the **Supplementary Table 6B**.

(in two), and *miR162* (negative effect under C-Sal-SD) showed the lowest differential accumulation in response to the combined stress. Responsive miRNAs included in the *miR160, miR394*, and *miR397* families lacked significant interactions in any of the six analyzed stress conditions.

Correlation between miRNA responses (considering miRNA behavior and the different combined treatments) was estimated by multi-cluster analysis (MCA). MCA evidenced that the response values to combined stresses can be organized into three significantly different groups (**Figure 5A**). The group, including *miR156, miR157, miR166, miR319, miR396, miR398*, and *miR408*, contained the miRNA families that exclusively show significant non-additive response values ($SCE \neq 0$ values) to combined stress conditions. In contrast, families (*miR160, miR162, miR168, miR172, miR394, miR397, miR395*, and *miR1515*) with predominantly independent responses were clustered in the second group. Families of miRNAs in which the proportion of significant ($SCE \neq 0$ values) and non-significant (additive *SCE* values) response was comparable (*miR159, miR164, miR165, miR167, miR169, miR171*, and *miR393*) were also clustered together.

Interestingly, all the miRNAs clustered in the group showing significant non-additive expression in response to combined stresses correspond to melon miRNA families already identified as reactive to a broad range of stress (generalists) (Sanz-Carbonell et al., 2020), while miRNAs characterized by a narrow response range (specialists) are the most frequent class (five out of eight) in the group, showing mainly an additive response to double and triple stresses (**Figure 5A** – lower part). Finally, miRNAs identified previously as intermediates are mainly (four out of seven) included in the group where significant and non-significant responses to the combination of stressor were observed at comparable frequencies. The specialist miRNAs exhibit exclusively $SCE < 0$ response to double and triple stresses, whereas miRNAs identified as generalists showed an even distribution of significant non-additive responses (20 positive and 25 negative *SCE* values). Intermediate miRNAs, although showed a few miRNAs (five) with positive effects, were predominantly (16 miRNA families) characterized by a negative response to the combination of stresses. The relationship between miRNA trend response and stress condition was generally dependent of the specific stress/miRNA interaction, although the *miR398* and *miR408* families showed a coordinated response in

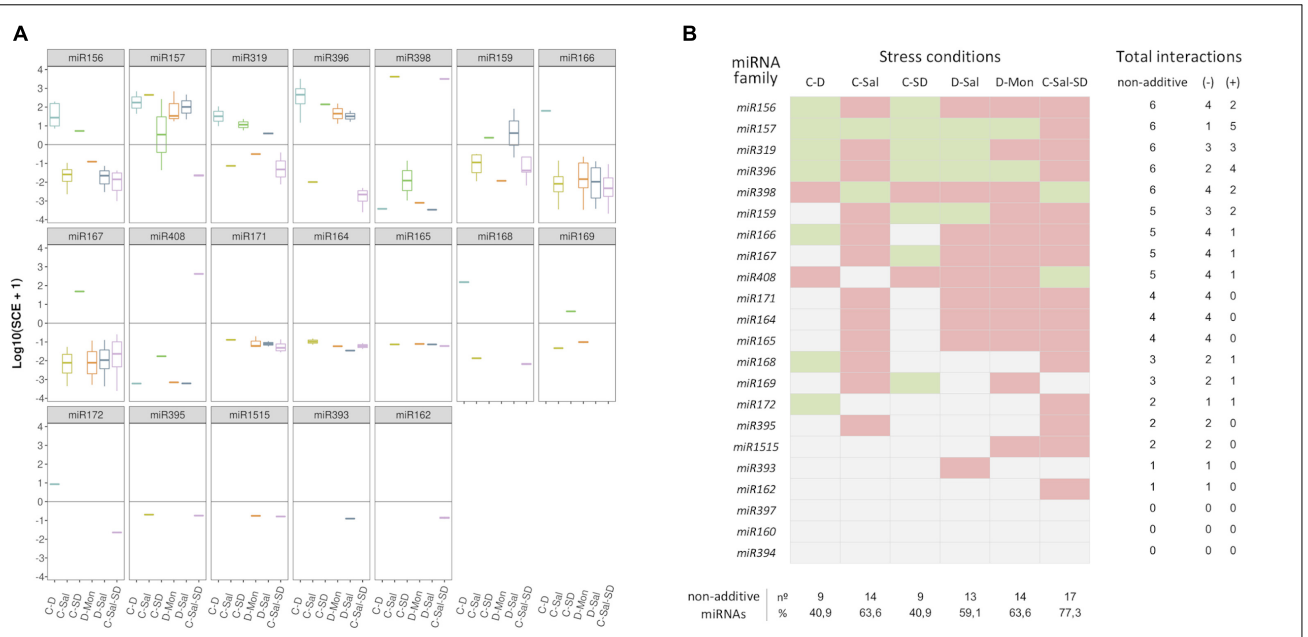

FIGURE 4 | Members of each miRNA family respond in a coordinated manner to combined stresses. **(A)** Boxplot analysis showing the *SCE* values for family-miRNA-related members in each combined stress condition. To determine the general sense of the effect induced by combined stresses for each miRNA family, we employed the median of the *SCE* values obtained for the totality of the family members (represented by the internal box line). **(B)** Graphic representation of the global non-additive positive (green) or negative (red) effects associated with combined stresses estimated for each miRNA family in the six stress conditions analyzed here. The number of combined stresses that induce positive and/or negative non-additive responses in each miRNA family is detailed in the right columns. The proportion of miRNA families with non-additive effects in response to each combined stresses is detailed below.

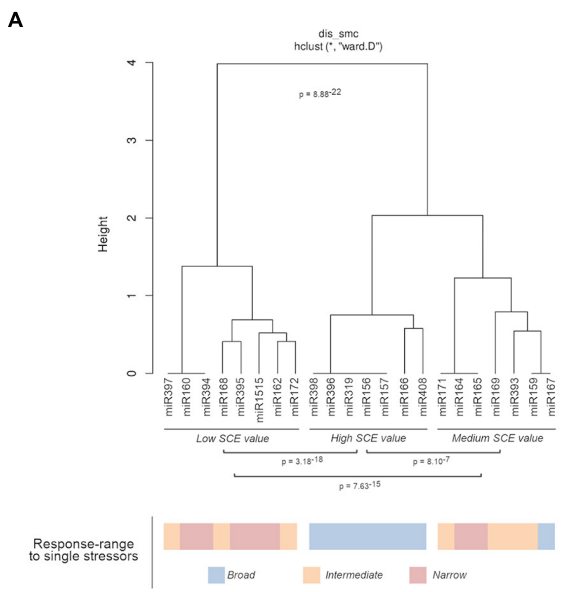

B

miRNA family	Combinations with non-additive response	Target	ID	GO Functions
miR157	6	Squamosa promoter-binding-like protein	SPL	Transcription regulation Development
miR319	6	Teosinte Branched1 Cycloidea Proliferating Cell Factor 2	TCP2	
miR156	6	Squamosa promoter-binding-like protein	SPL	
miR396	6	Growth-regulating factor 9	GRF9	
miR398	6	Superoxide dismutase (Cu-Zn)	SOD	Cooper metabolism
miR408	5	Basic blue protein-like 2	BBP2	
miR166	5	Homeobox-leucine zipper protein ATHB-14-like	ATHB14	Transcription regulation Development
miR167	5	Auxine response factor 7	ARF7	
miR159	5	BES1/BZR1 homolog protein 4	BEH	
miR171	4	Scarecrow-like protein 6	SCL6	
miR164	4	NAC domain-containing protein 100-like	NAC	
miR165	4	Homeobox-leucine zipper protein ATHB-14-like	ATHB14	
miR169	3	Nuclear transcription factor Y subunit A1-like	NFY	
miR168	3	Argonaute 1	AGO1	RNA Silencing
miR395	2	ATP sulfurylase 1	APS1	Metals metabolism
miR172	2	AP2-like ethylene-responsive TF	AP2	Transcription regulation Development
miR1515	2	Glioxilate/succinic semialdehyde reductase-2	GLYR2	Oxidation-reduction process
miR393	1	Auxin signaling F-BOX 2-like	AFB2	Stress Response
miR162	1	Chlorophyllase 2	CLH2	Photosynthesis metabolism
miR160	0	Auxine response factor 17	ARF17	Transcription regulation Development
miR397	0	Heat shock 70kDa protein	HSP70	Stress response
miR394	0	EG45-like domain containing protein	EG45	

FIGURE 5 | Biological functions of miRNAs with non-additive response to combined stresses. **(A)** Dendrogram showing the clustering of miRNAs families with at least a member with significant non-additive response to combined stresses in three main groups according to their *SCE* values in the analyzed stress conditions. The global statistical significance of the identified clusters ($p = 8.88 \times 10^{-22}$) was estimated by Mann–Whitney–Wilcoxon test, considering the inter- and intragroup Euclidean distances. The lower panel shows the response range determined for each miRNA family in response to single stresses with both biotic and abiotic sources (using a color scale). **(B)** Description and detailed information of the targets for miRNAs with significant non-additive response to combined stresses identified in melon plants. The GO terms were estimated in a base to information of homologous transcripts in *A. thaliana*.

all the analyzed conditions, with the exception of C-Sal. However, a positive response (*SCE* = 654.96, p = 0.04) was observed for *miR408* in this condition, although was considered as non-significant based on the FDR criterion (**Supplementary Table 6**). This specifically coordinated activity of the *miR398/miR408* tandem was particularly evident in response to C-SD and C-Sal-SD in which their response was the opposite to the general trend observed for the remaining miRNA families.

Regarding miRNA-regulated targets, it was evident that miRNAs involved in the regulation of transcription factors (TF) associated with plant development exhibit the higher rate of differential response to combined stress (**Figure 5B**). In contrast, miRNA families expected to modulate the expression of transcripts related (according to GO terms) to a more diverse range of biological functions (RNA silencing, metals metabolism, photosynthesis, response to stress, etc.) showed predominantly a non-significant response to stresses combination.

DISCUSSION

Much effort has been dedicated to elucidating the mechanisms underlying stress response in crops. Although great progress has been made in the last years, including the identification of both protein-coding and non-coding transcripts responsive to different stresses, most studies focused on deciphering the plant regulatory pathways were triggered in response to single stress conditions. Alas, no much effort has been devoted to understand the plant responses to multiple stresses acting simultaneously, a situation that is most common in the wild (Pandey et al., 2017).

Here, we have addressed this question by measuring the miRNA-mediated responses to combined stresses in melon plants exposed to five different double and one triple stressful conditions. Our strategy comprises two principal steps: first to identify the miRNA families responding to double and triple stress conditions; second, we compared the expression level of such responding miRNAs with the values obtained in melon plants exposed to the respective single stresses. This comparative analysis has allowed us to determine how the stress combinations affect the differential expression of miRNAs, disentangling stress-specific responses to general responses. This information enabled the inference of the global structure of the miRNA-mediated differential response to combined stress conditions in melon.

The computational analysis identified 22 miRNA families with significant differential expression in response to the analyzed stresses. Regarding their functional role, these reactive families mainly target melon homologous to well-described TFs [e.g., *SPOROCYTELESS, BES1/BZR1 HOMOLOG 4*, *AUXINE RESPONSE FACTORS (ARF)*, *ARABIDOPSIS THALIANA HOMEOBOX PROTEIN 14*, *TEOSINTE BRANCHED 1/CYCLOIDEA/PROLOFERATING CELL FACTOR*, *APETALA 2*, *GENERAL REGULATORY FACTOR (GR)*, and *NUCLER FACTOR Y*] This is in agreement with previous observations in other species (*A. thaliana*, rice, maize, sorghum, sunflower, etc.) in which it has been reported that, in general, miRNAs reactive to stress target predominantly TFs (Samad et al., 2017). This reinforces the emerging notion that the role played by miRNAs during the stress response is evolutionary conserved in plants (Rubio-Somoza and Weigel, 2011; Megraw et al., 2016; Sanz-Carbonell et al., 2020) and emphasizes the potential of miRNAs as targets for improving stress tolerance in crops (Tang and Chu, 2017; Chaudhary et al., 2021). The totality of these stress-responsive miRNA families was coincident with the previously described as reactive in single biotic and abiotic stress conditions in melon (Sanz-Carbonell et al., 2019, 2020). The observation that double and triple stresses do not induce the differential accumulation of any miRNA family reactive, specifically to combined stress, suggests that (at least under the conditions analyzed here), the miRNA families involved in the response to stress comprise the general structure that modulates the recovery of the plant-cell homeostasis under both single and combined adverse environmental conditions.

Considering the response rate to each stress combination, we observed a more consistent activity in certain miRNA families. Our results evidenced that melon miRNAs (*miR156, miR157, miR166, miR167, miR319, miR396, miR398*, and *miR408*) previously characterized by exhibit differential accumulation in response to a wide range of biotic and abiotic stress conditions in melon, maize, and soybean (dubbed as generalists) were differentially expressed in the six analyzed conditions, evidencing a high-response range, independently of the stresses combination. Interestingly, miRNAs families reactive to four or less conditions (*miR162, miR164, miR165, miR172, miR394, miR397, miR395*, and *miR1515*) predominantly corresponded to miRNAs characterized by exhibiting differential response to specific stresses (specialists). It has been recently suggested that generalists stress-responsive miRNAs might be involved in the modulation of the central steps in the recovery of the cell homeostasis during the exposition to adverse environmental conditions, while specialists families responding to specific stress conditions and/or exposition times had been hypothesized to be involved in the regulation of metabolic processes associated with each particular stressor (Sanz-Carbonell et al., 2019, 2020). Assuming this responsive behavior, it is expected that generalist miRNAs were the predominant class reactive to double and triple stresses. Sequences related to generalist miRNA families are characterized by mainly modulating master regulators or central hubs, predominantly TFs related with plant development (Sanz-Carbonell et al., 2020). It is well established that alteration in the expression of TF genes normally results in remarkable changes in the global gene expression during plant growth and development (Li et al., 2015). Furthermore, it has been proposed that such TFs might, for example, by co-regulatory feedback and feed-forward loops miRNA/TF, act as amplifiers of the plant response to stress (Rubio-Somoza and Weigel, 2011; Megraw et al., 2016; Samad et al., 2017). The generalist class is comprised by miRNAs previously described as reactive to different biotic and/or abiotic stress conditions in diverse plant species. Several studies support that the module *miR156*-SPLs besides exhibiting a broad response range to low temperatures in diverse plant species (Zhou and Tang, 2019) also improve tolerance to salinity, heat, and drought in *Medicago sativa* (Arshad et al., 2017a,b; Matthews et al., 2019). Moreover, the

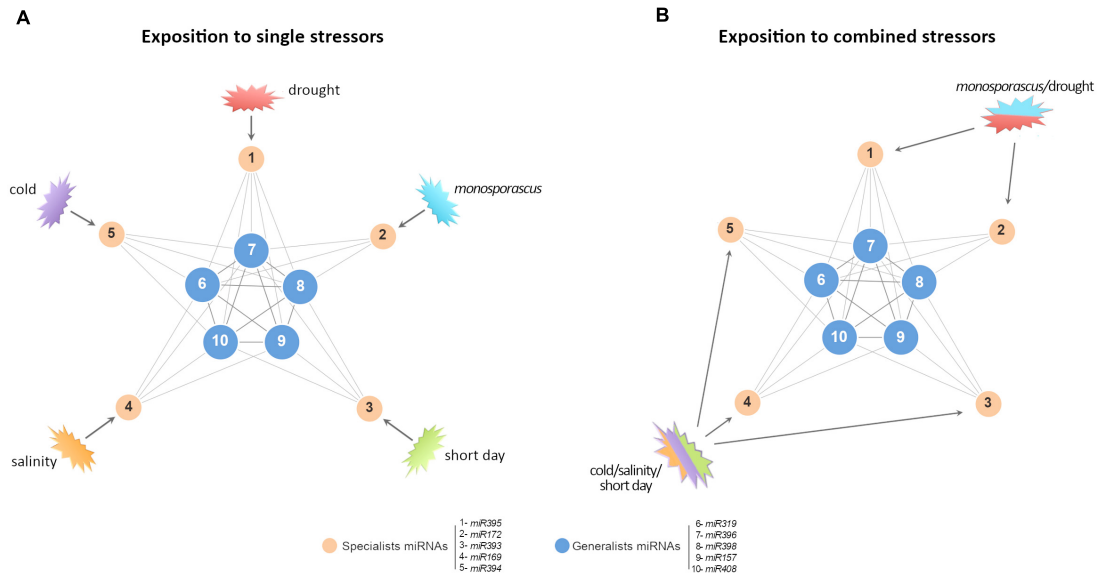

FIGURE 6 | A proposed model to explain predominant non-additive response in certain miRNAs families. **(A)** Simplified graphic representation of the proposed miRNA-mediated network of response to stress in melon (Sanz-Carbonell et al., 2019, 2020). Blue nodes represent highly connected miRNAs with a broad response range to biotic and/or abiotic stress conditions (*generalists*). Orange nodes represent miRNAs reactive to specific stress conditions (*specialists*). Numbers indicate representative miRNAs for each functional group. **(B)** When the network is exposed to double (for example, *Monosporascus*/drought) or triple (cold/salinity/short day) stress conditions, it is expected that the stresses combinations should not affect specialist miRNAs (poorly connected between them), and, consequently, they exhibit additive *SCE* values (comparable to the resultant of the sum of both individual responses). In contrast, generalist miRNAs (highly interconnected) respond to stresses combination in a differential (non-additive) manner, related to each stress combination.

interaction between *miR396* and GRF is involved in the modulation of the response to diverse biotic (*Phytophthora nicotianae*) and abiotic (drought, salt, alkali, UV-B radiation, and osmotic unbalance) stress conditions (Gao et al., 2010; Kim et al., 2012; Casadevall et al., 2013; Chen et al., 2015). Cotton plants overexpressing *miR157* suppressed the auxin signal and showed enhanced sensitivity to heat (Ding et al., 2017). Recent studies have evidenced a critical function for *miR166* in tolerance to abiotic stresses in maize (Li et al., 2020) and Cd^{++}-induced toxicity in rice (Ding et al., 2018). By means of transgenic approaches, it was established that *miR167* acts as a transcriptional regulator in response to bacterial infection (Jodder et al., 2017) and temperature-induced stress in tomato plants (Jodder et al., 2018). Multiple pieces of evidence obtained by both sRNA sequencing and transgenic approaches support the role of the members of the *miR319* family, an ancient miRNA conserved across plant species ranging from mosses to higher plants, as a key modulator of the plant-environment interrelation (at biotic and abiotic levels) in monocotyledonous and dicotyledonous species (Bustamante et al., 2018; Liu et al., 2019; Shi et al., 2019; Wu et al., 2020; Fang et al., 2021; nee Joshi et al., 2021). Finally, regarding *miR398* and *miR408* families, it has been recently proposed that these conserved miRNAs involved in the maintenance of the cooper homeostasis in plants might be also involved in the systemic signaling of the response to biotic and abiotic stresses (Burkhead et al., 2009; Sanz-Carbonell et al., 2020).

Except for *miR398* and *miR408*, we did not observe a positive relationship between the accumulation rate of certain mature miRNAs (by RNA-seq) with the estimated precursors (by RT-qPCR). This result is in coincidence with the demonstration of a frequent inconsistency between the expression of MIR genes and the abundance of mature miRNAs in plants exposed to stress conditions (Barciszewska-Pacak et al., 2015; Bustamante et al., 2018; Choi et al., 2020), which suggest the existence of an additional regulatory layer downstream transcriptional activity to control miRNA accumulation (Szweykowska-Kulinska and Jarmolowski, 2018; Manavella et al., 2019; Grabowska et al., 2020). It has been demonstrated that *CHROMATIN REMODELING FACTOR 2* (*CHR2*) acts as an ATP-dependent RNA helicase that remodels the structure of the miRNA precursors and inhibits their processing in *A. thaliana* (Wang et al., 2018). Since low temperature impacts helicases activity (Guan et al., 2013; Liu et al., 2016) and pri-RNA structures (Bustamante et al., 2018), the possibility that the significant reduction in mature miRNA accumulation observed in plants exposed to cold might be a consequence of posttranscriptional alterations of miRNA precursors that cannot be ruled out. Further studies focused on deep analysis of the transcriptional activity of MIR genes will be needed for understanding the involvement of posttranscriptional events in the regulation of the mature miRNA level in plants in response to stress.

Upon determining the melon miRNAs responsive to combined stress conditions, we attempted to analyze whether the expression of these stress-responsive miRNAs was different

in comparison with that observed under each one of the stresses individually. Our conceptual premise assumes that miRNAs that did not show a significant differential (positive or negative) response to combined stresses exhibit an independent behavior to the combination of the stress conditions. The obtained results demonstrated that, in a considerable proportion of the analyzed miRNA-stress combinations (59.85%), the stress-responsive miRNAs families exhibit a differential response to the action of combined stresses. This evidences that, although the miRNAs involved in the regulation of the response to a particular stress combination are coincident with such described under individual stresses, the regulatory effects exerted on their targets are considerably different when the plant is exposed to a combination of adverse environmental conditions.

Considering in detail the differentially reactive miRNAs, we observed that generalist miRNAs showed the higher rate of differential accumulation (compared with the observed response to single stresses) in response to combined adverse environmental conditions, thus supporting that the biosynthesis and/or processing of such miRNA families is particularly (and differentially) susceptible to the combined exposition to two or three stress conditions. In contrast, the data obtained when miRNAs identified previously as specialists were analyzed that evidenced that the expression of this class de miRNA families is predominantly independent of the effects of the combined stresses and corresponds principally to the expression levels observed in response to each stressor individually. This functional behavior of responsive miRNAs to combined stresses is compatible with the architecture of the miRNA-mediated regulatory network of response to adverse environmental stimuli described recently in melon (Sanz-Carbonell et al., 2019, 2020). Structurally, this network is characterized by exhibiting a central core of highly connected miRNAs (generalist) and another peripheral layer comprised of miRNA families with lower connectivity (*specialists*) (**Figure 6A**). According to this structure, it is expected that the expression of generalist miRNAs (highly interconnected and reactive to a broad range of stress conditions) might be differentially affected (either positively or negatively) by the incidence of two or more distinct stresses (**Figure 6B**). In contrast, specialist miRNA families (with low connectivity and reactive to particular stress conditions) remain functionally independent to the effects of additional non-related stresses and respond mainly to the exposition to combined stress conditions in an additive (non-differential) manner (**Figure 6A**). The observation that the architecture of the miRNA-mediated regulatory network of response to stress in melon is able to predict the predominant reactivity rate of the miRNA response to combined stresses provides additional robustness to this inferred regulatory structure involved in the miRNA-mediated modulation of plant-environment interactions. Furthermore, the fact that structurally comparable miRNA networks of response to stress have been also proposed in rice and soybean plants exposed to diverse biotic and abiotic stress conditions (Sanz-Carbonell et al., 2020), allows to speculate about the possibility that the response pattern to combined stresses observed in melon may well be extended to another crops. In general, the transcripts of well-established TFs were the targets modulated by miRNAs with significant non-additive effects in response to combined stresses, reinforcing the key role assumed for the circuits miRNA-TF in the regulation of the stress response in plants (Rubio-Somoza and Weigel, 2011).

Regarding the trend of the global differential miRNA-mediated response to combined stresses, negative values were the most abundant. Response values lower than the expected for stress-independent effects might be initially assumed as an indicative of functional convergence in the miRNA-mediated response to combined stresses. It has been recently suggested that specific developmental events may be usually modulated by diverse miRNAs in rice (Tang and Chu, 2017). In this proposed model, miRNAs functionally converged *via* direct or indirect interaction between their targets. It is well established that osa-*miR393* regulates the auxin receptors *OsTIR1* and *OsAFB2*, both involved in the ubiquitin-mediated degradation of specific substrates during auxin signaling (Bian et al., 2012; Li et al., 2016). Furthermore, osa-*miR160* and osa-*miR167* modulate the expression of at least three *ARF* transcripts (*OsARF8*, *OsARF16*, and *OsARF18*) (Yang et al., 2006; Li et al., 2014; Huang et al., 2016). Interestingly, cmel-*miR393* and cmel-*miR167* exhibit a predominant negative differential response to the combined stresses analyzed here. Furthermore, it is expected that, according to the role of genetic redundancy in robustness (Fares, 2015), the role played by a determined cellular component (a stress-responsive miRNA in this case) may be guaranteed by another with total or partial functional overlap.

Altogether, our results support that the miRNA-mediated response to combined stress exhibits a predominant non-additive effect (indicative of that stress-responsive miRNAs might act in an interdependent and coordinated manner) mainly characterized by $SCE < 0$ values (assumed as indicators of functional convergence). Additionally, this response is a global phenomenon indistinctly triggered by diverse combination of abiotic and biotic stressors. Under a functional viewpoint, this evidence may suggest the existence of a common stress-responsive *core* (composed by non-additive miRNAs with $SCE < 0$ values) involved (by modulating pivotal TFs) in the recovering of the plant-cell homeostasis under distinct environmental pressures. On the other hand, non-additive miRNAs might be part of a more specific regulatory response to each particular stress condition. This viewing is consistent with an anticipated notion that plants may use the miRNA-mediated regulation as a pivotal mechanism to mediate the response to both simple and combined stresses (Zhang, 2015; Samad et al., 2017; Zhu et al., 2019; Zhou et al., 2020).

Finally, the confirmation that the previously described as generalist miRNAs are also the predominant components of the global miRNA-mediated response to combined stress conditions highlights the possibility that this class de miRNAs may emerge as a valuable breeding target for improving, in the near future, crop tolerance to the multiple adverse environmental conditions associated with climate change.

DATA AVAILABILITY STATEMENT

The datasets presented in this study can be found in online repositories. The names of the repository/repositories and accession number(s) can be found below: https://www.ncbi.nlm.nih.gov/, PRJNA741881.

AUTHOR CONTRIBUTIONS

PV-B performed and designed computational analysis, prepared figures, and discussed the results. JM-M analyzed the results, prepared figures, and contributed to wrote the manuscript. M-CM conceived and performed RT-qPCR analyses and discussed the results. AH-A performed RT-qPCR analysis. JC-S performed computational analysis. BP provided the *Monosporascus* isolate and contributed to the design of the stress treatments. AM provided melon seeds and contributed to the design of the stress treatments. SE conceived and performed the estimation of the *SCE* values and revised the manuscript. GG conceived and designed the experiments, analyzed the results, and drafted the manuscript. All the authors read and approved the final manuscript.

FUNDING

This work was supported by grants PID2019-104126RB-I00 (GG), PIE2019-103998GB-I00 (SE), and AGL2017-85563-C2-1-R (BP) funded by MCIN/Spain's Agencia Estatal de Investigación (AEI) and "ERDF A way of making Europe" and by PROMETEO projects 2019/012 (SE) and 2017/078 and 2021/072 (BP) (to promote excellence groups) by the Conselleria d'Educació, Investigació, Cultura i Esports (Generalitat Valenciana).

ACKNOWLEDGMENTS

JM-M (ACIF-2017-114) and AH-A (ACIF-2021-202) are recipients of a predoctoral contract from the Generalitat Valenciana.

SUPPLEMENTARY MATERIAL

The Supplementary Material for this article can be found online at: https://www.frontiersin.org/articles/10.3389/fpls.2021.769093/full#supplementary-material

REFERENCES

Achkar, N. P., Cambiagno, D. A., and Manavella, P. A. (2016). miRNA biogenesis: a dynamic pathway. *Trends Plant Sci.* 21, 1034–1044. doi: 10.1016/j.tplants.2016.09.003

Arshad, M., Feyissa, B. A., Amyot, L., Aung, B., and Hannoufa, A. (2017a). MicroRNA156 improves drought stress tolerance in alfalfa (*Medicago sativa*) by silencing SPL13. *Plant Sci.* 258, 122–136. doi: 10.1016/j.plantsci.2017.01.018

Arshad, M., Gruber, M. Y., Wall, K., and Hannoufa, A. (2017b). An insight into microRNA156 role in salinity stress responses of Alfalfa. *Front. Plant Sci.* 8:356. doi: 10.3389/fpls.2017.00356

Bai, Y., Kissoudis, C., Yan, Z., Visser, R. G. F., and van der Linden, G. (2018). Plant behaviour under combined stress: tomato responses to combined salinity and pathogen stress. *Plant J.* 93, 781–793. doi: 10.1111/tpj.13800

Barciszewska-Pacak, M., Milanowska, K., Knop, K., Bielewicz, D., Nuc, P., Plewka, P., et al. (2015). *Arabidopsis* microRNA expression regulation in a wide range of abiotic stress responses. *Front. Plant Sci.* 6:410. doi: 10.3389/fpls.2015.00410

Bartel, D. P. (2004). MicroRNAs: genomics, biogenesis, mechanism, and function. *Cell* 116, 281–297. doi: 10.1016/S0092-8674(04)00045-5

Bian, H., Xie, Y., Guo, F., Han, N., Ma, S., Zeng, Z., et al. (2012). Distinctive expression patterns and roles of the miRNA393/TIR1 homolog module in regulating flag leaf inclination and primary and crown root growth in rice (*Oryza sativa*). *New Phytol.* 196, 149–161. doi: 10.1111/j.1469-8137.2012.04248.x

Bologna, N. G., and Voinnet, O. (2014). The diversity, biogenesis, and activities of endogenous silencing small RNAs in *Arabidopsis*. *Annu. Rev. Plant Biol.* 65, 473–503. doi: 10.1146/annurev-arplant-050213-035728

Bologna, N. G., Mateos, J. L., Bresso, E. G., and Palatnik, J. F. (2009). A loop-to-base processing mechanism underlies the biogenesis of plant microRNAs miR319 and miR159. *EMBO J.* 28, 3646–3656. doi: 10.1038/emboj.2009.292

Brant, E. J., and Budak, H. (2018). Plant small non-coding RNAs and their roles in biotic stresses. *Front. Plant Sci.* 9:1038. doi: 10.3389/fpls.2018.01038

Burkhead, J. L., Gogolin Reynolds, K. A., Abdel-Ghany, S. E., Cohu, C. M., and Pilon, M. (2009). Copper homeostasis. *New Phytol.* 182, 799–816. doi: 10.1111/j.1469-8137.2009.02846.x

Bustamante, A., Marques, M. C., Sanz-Carbonell, A., Mulet, J. M., and Gomez, G. (2018). Alternative processing of its precursor is related to miR319 decreasing in melon plants exposed to cold. *Sci. Rep.* 8:15538. doi: 10.1038/s41598-018-34012-7

Casadevall, R., Rodriguez, R. E., Debernardi, J. M., Palatnik, J. F., and Casati, P. (2013). Repression of growth regulating factors by the MicroRNA396 inhibits cell proliferation by UV-B radiation in *Arabidopsis* leaves. *Plant Cell* 25, 3570–3583. doi: 10.1105/tpc.113.117473

Cervera-Seco, L., Marques, M. A. C., Sanz-Carbonell, A., Marquez-Molins, J., Carbonell, A., Darós, J. A., et al. (2019). Identification and characterization of stress-responsive TAS3-Derived TasiRNAs in melon. *Plant Cell Physiol.* 60, 2382–2393. doi: 10.1093/pcp/pcz131

Chaudhary, S., Grover, A., and Sharma, P. C. (2021). MicroRNAs: potential targets for developing stress-tolerant crops. *Life* 11:289. doi: 10.3390/life11040289

Chen, L., Luan, Y., and Zhai, J. (2015). Sp-miR396a-5p acts as a stress-responsive genes regulator by conferring tolerance to abiotic stresses and susceptibility to *Phytophthora nicotianae* infection in transgenic tobacco. *Plant Cell Rep.* 34, 2013–2025. doi: 10.1007/s00299-015-1847-0

Cheng, X., He, Q., Tang, S., Wang, H., Zhang, X., Lv, M., et al. (2021). The miR172/IDS1 signaling module confers salt tolerance through maintaining ROS homeostasis in cereal crops. *New Phytol.* 230, 1017–1033. doi: 10.1111/nph.17211

Choi, S. W., Ryu, M. Y., Viczián, A., Jung, H. J., Kim, G. M., Arce, A. L., et al. (2020). Light triggers the miRNA-Biogenetic inconsistency for de-etiolated seedling survivability in *Arabidopsis thaliana*. *Mol. Plant* 13, 431–445. doi: 10.1016/j.molp.2019.10.011

Ding, Y., Gong, S., Wang, Y., Wang, F., Bao, H., Sun, J., et al. (2018). MicroRNA166 modulates cadmium tolerance and accumulation in rice. *Plant Physiol.* 177, 1691–1703. doi: 10.1104/pp.18.00485

Ding, Y., Ma, Y., Liu, N., Xu, J., Hu, Q., Li, Y., et al. (2017). microRNAs involved in auxin signalling modulate male sterility under high-temperature stress in cotton (*Gossypium hirsutum*). *Plant J.* 91, 977–994. doi: 10.1111/tpj.13620

Fang, Y., Zheng, Y., Lu, W., Li, J., Duan, Y., Zhang, S., et al. (2021). Roles of miR319-regulated TCPs in plant development and response to abiotic stress. *Crop J.* 9, 17–28. doi: 10.1016/j.cj.2020.07.007

Fares, M. A. (2015). The origins of mutational robustness. *Trends Genet.* 31, 373–381. doi: 10.1016/j.tig.2015.04.008

Gao, P., Bai, X., Yang, L., Lv, D., Li, Y., Cai, H., et al. (2010). Over-expression of osa-MIR396c decreases salt and alkali stress tolerance. *Planta* 231, 991–1001. doi: 10.1007/s00425-010-1104-2

Gonzalo, M., and Monforte, A. (2017). Genetic mapping of complex traits. *Genomics Essent. Methods* 269–290. doi: 10.1002/9780470711675.ch4

Grabowska, A., Bhat, S. S., Smoczynska, A., Bielewicz, D., Jarmolowski, A., and Kulinska, Z. S. (2020). "Regulation of plant microRNA biogenesis," in *Plant microRNAs. Concepts and Strategies in Plant Sciences*, eds C. Miguel, T. Dalmay, and I. Chaves (Cham: Springer), 3–24. doi: 10.1007/978-3-030-35772-6_1

Gray, S. B., and Brady, S. M. (2016). Plant developmental responses to climate change. *Dev. Biol.* 419, 64–77. doi: 10.1016/j.ydbio.2016.07.023

Guan, Q., Wu, J., Zhang, Y., Jiang, C., Liu, R., Chai, C., et al. (2013). A DEAD box RNA helicase is critical for pre-mRNA splicing, cold-responsive gene regulation, and cold tolerance in *Arabidopsis*. *Plant Cell* 25, 342–356. doi: 10.1105/tpc.112.108340

Gupta, A., Patil, M., Qamar, A., and Senthil-Kumar, M. (2020). ath-miR164c influences plant responses to the combined stress of drought and bacterial infection by regulating proline metabolism. *Environ. Exp. Bot.* 172:103998. doi: 10.1016/j.envexpbot.2020.103998

Haak, D. C., Fukao, T., Grene, R., Hua, Z., Ivanov, R., Perrella, G., et al. (2017). Multilevel regulation of abiotic stress responses in plants. *Front. Plant Sci.* 8:1564. doi: 10.3389/fpls.2017.01564

Herranz, M. C., Navarro, J. A., Sommen, E., and Pallas, V. (2015). Comparative analysis among the small RNA populations of source, sink and conductive tissues in two different plant-virus pathosystems. *BMC Genomics* 16:117. doi: 10.1186/s12864-015-1327-5

Hewezi, T., Léger, M., and Gentzbittel, L. (2008). A comprehensive analysis of the combined effects of high light and high temperature stresses on gene expression in sunflower. *Ann. Bot.* 102, 127–140. doi: 10.1093/aob/mcn071

Huang, J., Li, Z., and Zhao, D. (2016). Deregulation of the OsmiR160 target gene OsARF18 causes growth and developmental defects with an alteration of Auxin signaling in rice. *Sci. Rep.* 6:29938. doi: 10.1038/srep29938

Jagadeeswaran, G., Nimmakayala, P., Zheng, Y., Gowdu, K., Reddy, U. K., and Sunkar, R. (2012). Characterization of the small RNA component of leaves and fruits from four different cucurbit species. *BMC Genomics* 13:329. doi: 10.1186/1471-2164-13-329

Jodder, J., Basak, S., Das, R., and Kundu, P. (2017). Coherent regulation of miR167a biogenesis and expression of auxin signaling pathway genes during bacterial stress in tomato. *Physiol. Mol. Plant Pathol.* 100, 97–105. doi: 10.1016/j.pmpp.2017.08.001

Jodder, J., Das, R., Sarkar, D., Bhattacharjee, P., and Kundu, P. (2018). Distinct transcriptional and processing regulations control miR167a level in tomato during stress. *RNA Biol.* 15, 130–143. doi: 10.1080/15476286.2017.1391438

Keleş, Y., and Öncel, I. (2002). Response of antioxidative defence system to temperature and water stress combinations in wheat seedlings. *Plant Sci.* 163, 783–790. doi: 10.1016/S0168-9452(02)00213-3

Kim, J.-S., Mizoi, J., Kidokoro, S., Maruyama, K., Nakajima, J., Nakashima, K., et al. (2012). Arabidopsis growth-regulating factor7 functions as a transcriptional repressor of abscisic acid- and osmotic stress-responsive genes, including DREB2A. *Plant Cell* 24, 3393–3405. doi: 10.1105/tpc.112.100933

Kozomara, A., Birgaoanu, M., and Griffiths-Jones, S. (2019). miRBase: from microRNA sequences to function. *Nucleic Acids Res.* 47, D155–D162. doi: 10.1093/nar/gky1141

Li, J., Han, S., Ding, X., He, T., Dai, J., Yang, S., et al. (2015). Comparative transcriptome analysis between the cytoplasmic male sterile line NJCMS1A and its maintainer NJCMS1B in soybean (*Glycine max* (L.) Merr.). *PLoS One* 10:e0126771. doi: 10.1371/journal.pone.0126771

Li, N., Yang, T., Guo, Z., Wang, Q., Chai, M., Wu, M., et al. (2020). Maize microRNA166 inactivation confers plant development and abiotic stress resistance. *Int. J. Mol. Sci.* 21:9506. doi: 10.3390/ijms21249506

Li, X., Xia, K., Liang, Z., Chen, K., Gao, C., and Zhang, M. (2016). MicroRNA393 is involved in nitrogen-promoted rice tillering through regulation of auxin signal transduction in axillary buds. *Sci. Rep.* 6:32158. doi: 10.1038/srep32158

Li, Y., Lu, Y.-G., Shi, Y., Wu, L., Xu, Y.-J., Huang, F., et al. (2014). Multiple rice MicroRNAs are involved in immunity against the blast fungus *Magnaporthe oryzae*. *Plant Physiol.* 164, 1077–1092. doi: 10.1104/pp.113.230052

Liu, H., Able, A. J., and Able, J. A. (2020). Integrated analysis of small RNA, transcriptome, and degradome sequencing reveals the water-deficit and heat stress response network in durum wheat. *Int. J. Mol. Sci.* 21:6017. doi: 10.3390/ijms21176017

Liu, Y., Li, D., Yan, J., Wang, K., Luo, H., and Zhang, W. (2019). MiR319 mediated salt tolerance by ethylene. *Plant Biotechnol. J.* 17, 2370–2383. doi: 10.1111/pbi.13154

Liu, Y., Tabata, D., and Imai, R. (2016). A cold-inducible DEAD-Box RNA helicase from *Arabidopsis thaliana* regulates plant growth and development under low temperature. *PLoS One* 11:e0154040. doi: 10.1371/journal.pone.0154040

Livak, K. J., and Schmittgen, T. D. (2001). Analysis of relative gene expression data using real-time quantitative PCR and the $2-\Delta\Delta CT$ method. *Methods* 25, 402–408. doi: 10.1006/meth.2001.1262

Love, M. I., Huber, W., and Anders, S. (2014). Moderated estimation of fold change and dispersion for RNA-seq data with DESeq2. *Genome Biol.* 15:550. doi: 10.1186/s13059-014-0550-8

Lovell, J. T., Mullen, J. L., Lowry, D. B., Awole, K., Richards, J. H., Sen, S., et al. (2015). Exploiting differential gene expression and epistasis to discover candidate genes for drought-associated QTLs in *Arabidopsis thaliana*. *Plant Cell* 27, 969–983. doi: 10.1105/tpc.15.00122

Manavella, P. A., Yang, S. W., and Palatnik, J. (2019). Keep calm and carry on: miRNA biogenesis under stress. *Plant J.* 99, 832–843. doi: 10.1111/tpj.14369

Martin, M. (2011). Cutadapt removes adapter sequences from high-throughput sequencing reads. *EMBnet. J.* 17, 10–12. doi: 10.14806/ej.17.1.200

Matthews, C., Arshad, M., and Hannoufa, A. (2019). Alfalfa response to heat stress is modulated by microRNA156. *Physiol. Plant.* 165, 830–842. doi: 10.1111/ppl.12787

Megraw, M., Cumbie, J. S., Ivanchenko, M. G., and Filichkin, S. A. (2016). Small genetic circuits and MicroRNAs: big players in polymerase II transcriptional control in plants. *Plant Cell* 28, 286–303. doi: 10.1105/tpc.15.00852

Meyers, B. C., Axtell, M. J., Bartel, B., Bartel, D. P., Baulcombe, D., Bowman, J. L., et al. (2008). Criteria for annotation of plant MicroRNAs. *Plant Cell* 20, 3186–3190. doi: 10.1105/tpc.108.064311

Mittler, R., and Blumwald, E. (2010). Genetic engineering for modern agriculture: challenges and perspectives. *Annu. Rev. Plant Biol.* 61, 443–462. doi: 10.1146/annurev-arplant-042809-112116

Morales-Castilla, I., García de Cortázar-Atauri, I., Cook, B. I., Lacombe, T., Parker, A., van Leeuwen, C., et al. (2020). Diversity buffers winegrowing regions from climate change losses. *Proc. Natl. Acad. Sci. U.S.A.* 117, 2864–2869. doi: 10.1073/pnas.1906731117

nee Joshi, G. A., Chauhan, C., and Das, S. (2021). Sequence and functional analysis of MIR319 promoter homologs from *Brassica juncea* reveals regulatory diversification and altered expression under stress. *Mol. Genet. Genomics* 296, 731–749. doi: 10.1007/s00438-021-01778-x

Ning, L.-H., Du, W., Song, H.-N., Shao, H.-B., Qi, W.-C., Sheteiwy, M. S. A., et al. (2019). Identification of responsive miRNAs involved in combination stresses of phosphate starvation and salt stress in soybean root. *Environ. Exp. Bot.* 167:103823. doi: 10.1016/j.envexpbot.2019.103823

Pandey, P., Irulappan, V., Bagavathiannan, M. V., and Senthil-Kumar, M. (2017). Impact of combined abiotic and biotic stresses on plant growth and avenues for crop improvement by exploiting physio-morphological traits. *Front. Plant Sci.* 8:537. doi: 10.3389/fpls.2017.00537

Pollack, F. G., and Uecker, F. A. (1974). *Monosporascus cannonballus* an unusual ascomycete in cantaloupe roots. *Mycologia* 66, 346–349. doi: 10.2307/3758370

Priya, M., Dhanker, O. P., Siddique, K. H. M., HanumanthaRao, B., Nair, R. M., Pandey, S., et al. (2019). Drought and heat stress-related proteins: an update about their functional relevance in imparting stress tolerance in agricultural crops. *Theor. Appl. Genet.* 132, 1607–1638. doi: 10.1007/s00122-019-03331-2

R Core Team (2013). *R: A Language and Environment for Statistical Computing*. Vienna: R Foundation for Statistical Computing. Available online at: http://www.R-project.org/

Reis, R. S., Eamens, A. L., and Waterhouse, P. M. (2015). Missing pieces in the puzzle of plant MicroRNAs. *Trends Plant Sci.* 20, 721–728. doi: 10.1016/j.tplants.2015.08.003

Rizhsky, L., Liang, H., Shuman, J., Shulaev, V., Davletova, S., and Mittler, R. (2004). When defense pathways collide. The response of *Arabidopsis* to a combination of drought and heat stress. *Plant Physiol.* 134, 1683–1696. doi: 10.1104/pp.103.033431

Robinson, M. D., and Oshlack, A. (2010). A scaling normalization method for differential expression analysis of RNA-seq data. *Genome Biol.* 11:R25. doi: 10.1186/gb-2010-11-3-r25

Rosenzweig, C., Elliott, J., Deryng, D., Ruane, A. C., Müller, C., Arneth, A., et al. (2014). Assessing agricultural risks of climate change in the 21st century in a global gridded crop model intercomparison. *Proc. Natl. Acad. Sci. U.S.A.* 111, 3268–3273. doi: 10.1073/pnas.1222463110

Rossel, J. B., Wilson, P. B., Hussain, D., Woo, N. S., Gordon, M. J., Mewett, O. P., et al. (2007). Systemic and intracellular responses to photooxidative stress in *Arabidopsis*. *Plant Cell* 19, 4091–4110. doi: 10.1105/tpc.106.045898

Rubio-Somoza, I., and Weigel, D. (2011). MicroRNA networks and developmental plasticity in plants. *Trends Plant Sci.* 16, 258–264. doi: 10.1016/j.tplants.2011.03.001

Samad, A. F. A., Sajad, M., Nazaruddin, N., Fauzi, I. A., Murad, A. M. A., Zainal, Z., et al. (2017). MicroRNA and transcription factor: key players in plant regulatory network. *Front. Plant Sci.* 8:565. doi: 10.3389/fpls.2017.00565

Sanz-Carbonell, A., Marques, M. C., Bustamante, A., Fares, M. A., Rodrigo, G., and Gomez, G. (2019). Inferring the regulatory network of the miRNA-mediated response to biotic and abiotic stress in melon. *BMC Plant Biol.* 19:78. doi: 10.1186/s12870-019-1679-0

Sanz-Carbonell, A., Marques, M. C., Martinez, G., and Gomez, G. (2020). Dynamic architecture and regulatory implications of the miRNA network underlying the response to stress in melon. *RNA Biol.* 17, 292–308. doi: 10.1080/15476286.2019.1697487

Sattar, S., Song, Y., Anstead, J. A., Sunkar, R., and Thompson, G. A. (2012). Cucumis melo MicroRNA expression profile during aphid herbivory in a resistant and susceptible interaction. *Mol. Plant Microbe Interact.* 25, 839–848. doi: 10.1094/MPMI-09-11-0252

Shi, X. P., Jiang, F. L., Wen, J. Q., Cui, S. Y., Zhou, Y. Z., and Wu, Z. (2019). MicroRNA319 family members play an important role in *Solanum habrochaites* and S. *lycopersicum* responses to chilling and heat stresses. *Biol. Plant.* 63, 200–209. doi: 10.32615/bp.2019.023

Song, X., Li, Y., Cao, X., and Qi, Y. (2019). MicroRNAs and their regulatory roles in plant–environment interactions. *Annu. Rev. Plant Biol.* 70, 489–525. doi: 10.1146/annurev-arplant-050718-100334

Sun, Y., Niu, X., and Fan, M. (2017). Genome-wide identification of cucumber green mottle mosaic virus-responsive microRNAs in watermelon. *Arch. Virol.* 162, 2591–2602. doi: 10.1007/s00705-017-3401-6

Suzuki, N., Rizhsky, L., Liang, H., Shuman, J., Shulaev, V., and Mittler, R. (2005). Enhanced tolerance to environmental stress in transgenic plants expressing the transcriptional coactivator multiprotein bridging factor 1c. *Plant Physiol.* 139, 1313–1322. doi: 10.1104/pp.105.070110

Szweykowska-Kulinska, Z., and Jarmolowski, A. (2018). Post-transcriptional regulation of MicroRNA accumulation and function: new insights from plants. *Mol. Plant* 11, 1006–1007. doi: 10.1016/j.molp.2018.06.010

Tang, J., and Chu, C. (2017). MicroRNAs in crop improvement: fine-tuners for complex traits. *Nat. Plants* 3:17077. doi: 10.1038/nplants.2017.77

Tarazona, S., Furió-Tarí, P., Turrà, D., Di Pietro, A., Nueda, M. J., Ferrer, A., et al. (2015). Data quality aware analysis of differential expression in RNA-seq with NOISeq R/Bioc package. *Nucleic Acids Res.* 43:e140. doi: 10.1093/nar/gkv711

Wang, Y., Feng, C., Zhai, Z., Peng, X., Wang, Y., Sun, Y., et al. (2020). The Apple microR171i-SCARECROW-LIKE PROTEINS26.1 module enhances drought stress tolerance by integrating ascorbic acid metabolism. *Plant Physiol.* 184, 194–211. doi: 10.1104/pp.20.00476

Wang, Z., Ma, Z., Castillo-González, C., Sun, D., Li, Y., Yu, B., et al. (2018). SWI2/SNF2 ATPase CHR2 remodels pri-miRNAs via Serrate to impede miRNA production. *Nature* 557, 516–521. doi: 10.1038/s41586-018-0135-x

Wu, F., Qi, J., Meng, X., and Jin, W. (2020). miR319c acts as a positive regulator of tomato against Botrytis cinerea infection by targeting TCP29. *Plant Sci.* 300:110610. doi: 10.1016/j.plantsci.2020.110610

Xie, S., Jiang, H., Xu, Z., Xu, Q., and Cheng, B. (2017). Small RNA profiling reveals important roles for miRNAs in *Arabidopsis* response to *Bacillus velezensis* FZB42. *Gene* 629, 9–15. doi: 10.1016/j.gene.2017.07.064

Xu, J., Hou, Q. M., Khare, T., Verma, S. K., and Kumar, V. (2019). Exploring miRNAs for developing climate-resilient crops: a perspective review. *Sci. Total Environ.* 653, 91–104. doi: 10.1016/j.scitotenv.2018.10.340

Yang, J. H., Han, S. J., Yoon, E. K., and Lee, W. S. (2006). 'Evidence of an auxin signal pathway, microRNA167-ARF8-GH3, and its response to exogenous auxin in cultured rice cells.'. *Nucleic Acids Res.* 34, 1892–1899. doi: 10.1093/nar/gkl118

Zhang, B. (2015). MicroRNA: a new target for improving plant tolerance to abiotic stress. *J. Exp. Bot.* 66, 1749–1761. doi: 10.1093/jxb/erv013

Zhang, H., and Sonnewald, U. (2017). Differences and commonalities of plant responses to single and combined stresses. *Plant J.* 90, 839–855. doi: 10.1111/tpj.13557

Zhao, Y., Xie, J., Wang, S., Xu, W., Chen, S., Song, X., et al. (2021). Synonymous mutation of miR396a target sites in Growth Regulating Factor 15 (GRF15) enhances photosynthetic efficiency and heat tolerance in poplar. *J. Exp. Bot.* 72, 4502–4519. doi: 10.1093/jxb/erab120

Zhou, M., and Tang, W. (2019). MicroRNA156 amplifies transcription factor-associated cold stress tolerance in plant cells. *Mol. Genet. Genomics* 294, 379–393. doi: 10.1007/s00438-018-1516-4

Zhou, R., Yu, X., Ottosen, C.-O., Zhang, T., Wu, Z., and Zhao, T. (2020). Unique miRNAs and their targets in tomato leaf responding to combined drought and heat stress. *BMC Plant Biol.* 20:107. doi: 10.1186/s12870-020-2313-x

Zhu, Y.-X., Jia, J.-H., Yang, L., Xia, Y.-C., Zhang, H.-L., Jia, J.-B., et al. (2019). Identification of cucumber circular RNAs responsive to salt stress. *BMC Plant Biol.* 19:164. doi: 10.1186/s12870-019-1712-3

Conflict of Interest: The authors declare that the research was conducted in the absence of any commercial or financial relationships that could be construed as a potential conflict of interest.

Publisher's Note: All claims expressed in this article are solely those of the authors and do not necessarily represent those of their affiliated organizations, or those of the publisher, the editors and the reviewers. Any product that may be evaluated in this article, or claim that may be made by its manufacturer, is not guaranteed or endorsed by the publisher.

frontiers in Plant Science

ORIGINAL RESEARCH
published: 07 December 2021
doi: 10.3389/fpls.2021.793549

Systematic Characterization of MicroRNA Processing Modes in Plants With Parallel Amplification of RNA Ends

*Ning Li and Guodong Ren**

State Key Laboratory of Genetic Engineering and Ministry of Education Key Laboratory for Biodiversity Science and Ecological Engineering, School of Life Sciences, Institute of Plant Biology, Fudan University, Shanghai, China

In plants, the RNase III-type enzyme Dicer-like 1 (DCL1) processes most microRNAs (miRNAs) from their primary transcripts called pri-miRNAs. Four distinct processing modes (i.e., short base to loop, sequential base to loop, short loop to base, and sequential loop to base) have been characterized in Arabidopsis, mainly by the Specific Parallel Amplification of RNA Ends (SPARE) approach. However, SPARE is a targeted cloning method which requires optimization of cloning efficiency and specificity for each target. PARE (Parallel Amplification of RNA Ends) is an untargeted method *per se* and is widely used to identify miRNA mediated target slicing events. A major concern with PARE in characterizing miRNA processing modes is the potential contamination of mature miRNAs. Here, we provide a method to estimate miRNA contamination levels and showed that most publicly available PARE libraries have negligible miRNA contamination. Both the numbers and processing modes detected by PARE were similar to those identified by SPARE in Arabidopsis. PARE also determined the processing modes of 36 Arabidopsis miRNAs that were unexplored by SPARE, suggesting that it can complement the SPARE approach. Using publicly available PARE datasets, we identified the processing modes of 36, 91, 90, and 54 miRNAs in maize, rice, soybean, and tomato, respectively, and demonstrated that the processing mode was conserved overall within each miRNA family. Through its power of tracking miRNA processing remnants, PARE also facilitated miRNA characterization and annotation.

Keywords: microRNA, plants, degradome, parallel analysis of RNA ends (PARE), DCL1

OPEN ACCESS

Edited by:
Xiaozeng Yang,
Beijing Academy of Agricultural and Forestry Sciences, China

Reviewed by:
Andrzej Miroslaw Pacak,
Adam Mickiewicz University, Poland
Jose Luis Reyes,
National Autonomous University of Mexico, Mexico

***Correspondence:**
Guodong Ren
gdren@fudan.edu.cn

Specialty section:
This article was submitted to Plant Physiology, a section of the journal Frontiers in Plant Science

Received: *12 October 2021*
Accepted: *19 November 2021*
Published: *07 December 2021*

Citation:
Li N and Ren G (2021) Systematic Characterization of MicroRNA Processing Modes in Plants With Parallel Amplification of RNA Ends. Front. Plant Sci. 12:793549. doi: 10.3389/fpls.2021.793549

INTRODUCTION

MiRNAs are a class of endogenous small non-coding RNAs that direct post-transcriptional gene silencing through bases complementary with their target genes. Most miRNAs are transcribed by DNA-dependent RNA polymerase II (Pol II); they are folded into imperfect stem-loop structures, and undergo processing by the RNase III enzyme-containing microprocessor (Song et al., 2019; Wang et al., 2019). Precise releasing of miRNA/miRNA* duplexes from their precursor RNAs is vital for miRNA biogenesis with minimal off targets. Understanding the molecular features of miRNA processing is beneficial for designing artificial miRNAs with enhanced efficiency.

In animals, pri-miRNAs exhibit rigid secondary structures that consist of a ∼35-bp stem, a terminal loop, and long single-stranded RNAs (ssRNAs) flanking the fold-back region (Han et al., 2006). Pri-miRNAs are diced by Drosha at the lower stem ∼11-bp away from the ssRNA-dsRNA junction, releasing pre-miRNAs with 2 nucleotides (nt) overhangs (Han et al., 2006; Kwon et al., 2016). After export to the cytoplasm, a second cut is performed by Dicer at ∼22-bp upstream of the Drosha cut site, yielding mature miRNA-5p/miRNA-3p (miR-5p/miR-3p) duplexes (Grishok et al., 2001; Ketting et al., 2001; Treiber et al., 2019). In plants, however, pri-miRNAs are more heterogeneous in size, with fold-back lengths varying from 60 to over 500 nt (Reinhart et al., 2002; Zhang et al., 2006; Cuperus et al., 2011). Consequently, four different processing modes have been described: (a) short base to loop; (b) short loop to base; (c) sequential base to loop; and (d) sequential loop to base (Bologna and Voinnet, 2014). In the canonical short base-to-loop mode, an internal bulge at 15–17 bp below the miR-5p/miR-3p region guides the first cut at the loop-distal miRNA site (Cuperus et al., 2010; Mateos et al., 2010; Bologna et al., 2013; Moro et al., 2018). Whereas in the loop-to-base mode, a terminal loop or bulge at 15–17 bp above the miR-5p/miR-3p region directs DCL1 processing from the loop-proximal cleavage site (Bologna et al., 2009, 2013; Axtell et al., 2011; Moro et al., 2018). In both cases, the 15–17 bp lower or upper stem tends to be conserved with paired status at different taxonomic levels (Chorostecki et al., 2017). Longer stems may cause additional cuts, which are termed sequential base-to-loop or loop-to-base processing modes, according to their processing direction.

Specific Parallel Amplification of RNA Ends (SPARE) is a modified 5′ RACE (rapid amplification of cDNA ends) with pri-miRNA specific primers for targeted cloning of 3′ DCL processing remnants. It provides a high-throughput solution for the identification of miRNA processing modes (Bologna et al., 2013). Although the method provides high precision and sensitivity, it only clones DCL processing remnants with predesigned primers. Parallel Amplification of RNA Ends [PARE; also referred to as degradome sequencing and GMUCT (genome-wide mapping of uncapped transcripts)] is a well-established method that captures 5′ termini of uncapped and polyadenylated RNA fragments. It has been widely used to track miRNA mediated target slicing events and to estimate RNA degradation levels (Addo-Quaye et al., 2008; German et al., 2008; Gregory et al., 2008). In principle, PARE could also detect 3′ dicing products and infer miRNA processing modes in an untargeted manner. In fact, it has been employed to discover the conserved loop-first processing of miR319 precursors in plants (Addo-Quaye et al., 2009). Concern over mature miRNAs contamination limits its use in probing miRNA processing (Lu et al., 2009). However, there have been no rigorously tests to determine whether PARE tags matching mature miRNA sequences are a result of contamination or not.

Using SPARE results in Arabidopsis as a benchmark, we here provided a solution for the estimation of mature miRNA contamination of PARE data. We found that most PARE tags matching mature miRNA sequences were likely not miRNA contaminations. Overall, PARE had comparable accuracy and sensitivity to SPARE and could be used as a complementary method. Using publicly available PARE data, we systematically identified miRNA processing modes in four crop species and found that miRNAs within the same family tended to share the same processing modes across species. We also showed that PARE could provide independent supporting evidence during miRNA annotation when combined with known miRNA prediction/annotation tools, which are largely relied on small RNA sequencing (sRNA-seq) data.

MATERIALS AND METHODS

Data Sources

PARE and sRNA-seq datasets from *Arabidopsis thaliana*, *Zea mays*, *Oryza sativa*, *Glycine max*, and *Solanum lycopersicum* were downloaded from the Sequence Read Archive (SRA) database (Leinonen et al., 2011). The accession numbers are listed in **Supplementary Table 1**. The SPARE datasets of *Arabidopsis thaliana* used in this study are stored under the accession numbers SRP021538 and SRP137005.

The miRNA annotation information for Arabidopsis, maize, and rice were retrieved from miRbase v.22 (Kozomara and Griffiths-Jones, 2011). The miRNA annotation information for soybean and tomato were obtained from the Plant small RNA genes website (Lunardon et al., 2020). The genome sequences of different species were retrieved from TAIR (TAIR10) (Lamesch et al., 2012), Ensembl Plants (B73_RefGen_v4, IRGSP-1.0, SL2.50) (Bolser et al., 2016), and the Plant small RNA genes (Glycine_max_V1-0) (Lunardon et al., 2020).

Parallel Amplification of RNA Ends, Specific Parallel Amplification of RNA Ends, and sRNA-Seq Analysis

Fastq-dump was used to convert SRA format to fastq format (Leinonen et al., 2011). FastQC[1] and fastp (Chen et al., 2018) were used for quality evaluation and adapter trimming, respectively. Reads with 20 nt (PARE), 18–51 nt (SPARE) and 17–26 nt (sRNA) were kept for further analysis. ShortStack (Axtell, 2013) was used to assign multiple-mapped PARE and sRNA-seq reads to the genome. Bowtie (Langmead, 2010) was used to map SPARE reads to the genome.

miR-3p Information

For miR-3p with poor or no annotation, after loading merged sRNA-seq alignment bam files (**Supplementary Table 1**) with Integrative Genomics Viewer (IGV)-sRNA genome browser, we folded the precursor using the built-in RNAfold program and determined the miR-5p/miR-3p positions according to the most abundant reads on one side (usually the miR-5p in this case) and deduced the other side by the 2 nt 3′ overhang rule.

[1]https://www.bioinformatics.babraham.ac.uk/projects/fastqc/

miRNA Processing Modes Characterization

Only precursors with 10 reads in at least one sample, or five reads in at least two samples within a ±50 nt window surrounding miR-3p were kept. Deduction of miRNA processing modes from patterns of PARE signatures is depicted in **Figure 1A** and is determined manually.

RESULTS

Deducing miRNA Processing Modes From Parallel Amplification of RNA Ends Patterns Around miR-3p

In PARE, polyadenylated RNAs are isolated, and an RNA adaptor containing an *Mme*I enzyme recognition site is ligated to the 5′ end of uncapped RNA fragments. *Mme*I cuts reverse transcribed DNA ∼20 nt downstream of its recognition site. The cleaved 20-nt tags are cloned and sequenced to track the 5′ end of uncapped RNAs (German et al., 2008). In principle, for miRNA processed from loop to base, two (short loop to base) or more (sequential loop to base) 3′ remnants of DCL cleavage products will be cloned. Meanwhile, for miRNA processed from base to loop, only one 3′ remnant of the DCL processing products downstream of the first cleavage site carries the poly(A) tail, and consequently will be cloned. **Figure 1A** shows schematic PARE patterns for different processing modes.

To test whether PARE is suitable for the characterization of miRNA processing modes, we collected 24 Arabidopsis PARE datasets from public databases (**Supplementary Table 1**). After removing adapters, the 20-nt of degradome tags were kept for further analysis. ShortStack software was employed to allocate multi-mapping reads based on the number of unique mapped reads on different loci (Johnson et al., 2016).

We selected four miRNAs with different processing modes pre-determined by SPARE and checked whether they displayed expected PARE patterns. For the short loop-to-base processed miR162a, we detected a major PARE peak at miR162a-3p and a minor peak afterward (**Figure 1B**). For the sequentially loop-to-base processed miR319a, two additional PARE peaks upstream of miR319a-3p were found (**Figure 1C**). For the short base-to-loop processed miR168a, one major peak right after miR168a-3p was observed (**Figure 1D**), and finally, for the sequentially base-to-loop processed miR169b, a distinct peak 21 nt downstream of miR169b-3p was detected (**Figure 1E**). These data indicate the robustness of PARE in miRNA processing mechanism recognition.

Quality Control for miRNAs Contamination

Because only 20-nt degradome tags were retrieved after *Mme*I digestion, one major concern regarding the use of PARE in characterizing miRNA processing modes was the contamination of mature miRNAs (Lu et al., 2009). As such, a quality control step for each PARE dataset was crucial to avoid misidentification. As described above, base-to-loop processed miRNAs should have no miR-3p tags if there is no contamination; this could therefore be used to estimate the miRNAs contamination levels of PARE data. 16 wild-type (Wt) PARE libraries (Three of them from a same experiment were combined due to low sequencing depth) were analyzed for possible miRNA contamination. Remarkably, for miRNAs with known short base-to-loop processing modes, distinct PARE tags were observed right after miR-3ps, with almost no miR-3ps detected in most analyzed libraries (**Figure 2A**). In sharp contrast, for miRNAs with known short loop-to-base processing modes, significantly higher miR-3p tags than downstream tags were detected (**Figure 2B**). This strongly suggested that in most PARE libraries the contamination of mature miRNAs was low and had negligible impact on miRNA processing modes determination. Twelve out of 14 libraries passed the quality control step with a stringent *p*-value cut-off (0.005).

Parallel Amplification of RNA Ends as a Promising Tool in Systematic Characterization of miRNA Processing Modes

We next determined the miRNA processing modes in Arabidopsis based on PARE patterns and compared them with SPARE results. We not only validated most of the results (71/107, 66%) by SPARE, but, more importantly, we determined the processing modes of 36 additional miRNAs (**Supplementary Table 2** and **Figures 3A,B**). In particular, PARE showed comparable first-cut accuracy as SPARE (**Figure 3C**; Moro et al., 2018), indicating the robustness of PARE in the characterization of miRNA processing modes. The processing modes of 49 miRNAs from the two unpassed libraries were identified, and surprisingly all were concordant with those from passed libraries (**Supplementary Figure 1**).

Notably, six miRNAs (miR158a, miR390a, miR390b, miR391, miR396a, and miR396b) displayed inconsistent processing modes between PARE and SPARE (**Figure 3A**). For miR391, the conclusion by PARE may have been inaccurate as only a few degradome tags were obtained (**Supplementary Figure 2**). For the remaining five miRNAs, SPARE annotated them as short base-to-loop, but all PARE data treated them as short loop-to-base. We thus reanalyzed the SPARE signals around these miRNAs. For miR158a, miR390b, miR396a, and miR396b, robust signals were only detected in the *fiery1* (*fry1*) mutant but not in the Wt (**Figures 4A,B** and **Supplementary Figures 3B,C**). For miR390a, robust and consistent signals were detected in both *fry1* and Wt (**Supplementary Figure 3A**). *fry1* has been frequently used in PARE and SPARE experiments because the *FRY1* mutation attenuates RNA degradation from 5′ to 3′ by XRNs, thereby accumulating more miRNA targets cleavage remnants and miRNA processing intermediates (Gy et al., 2007). A comparison between Wt and *fry1* revealed additional inconsistent patterns, including miR400 and miR408 (**Figures 4C,D**). More strikingly, in another amino acid substitution allele of FRY1, *sal1/alx8* (Wilson et al., 2009), the processing of more miRNAs changed from short base-to-loop to short/sequential loop-to-base, including miR166b,

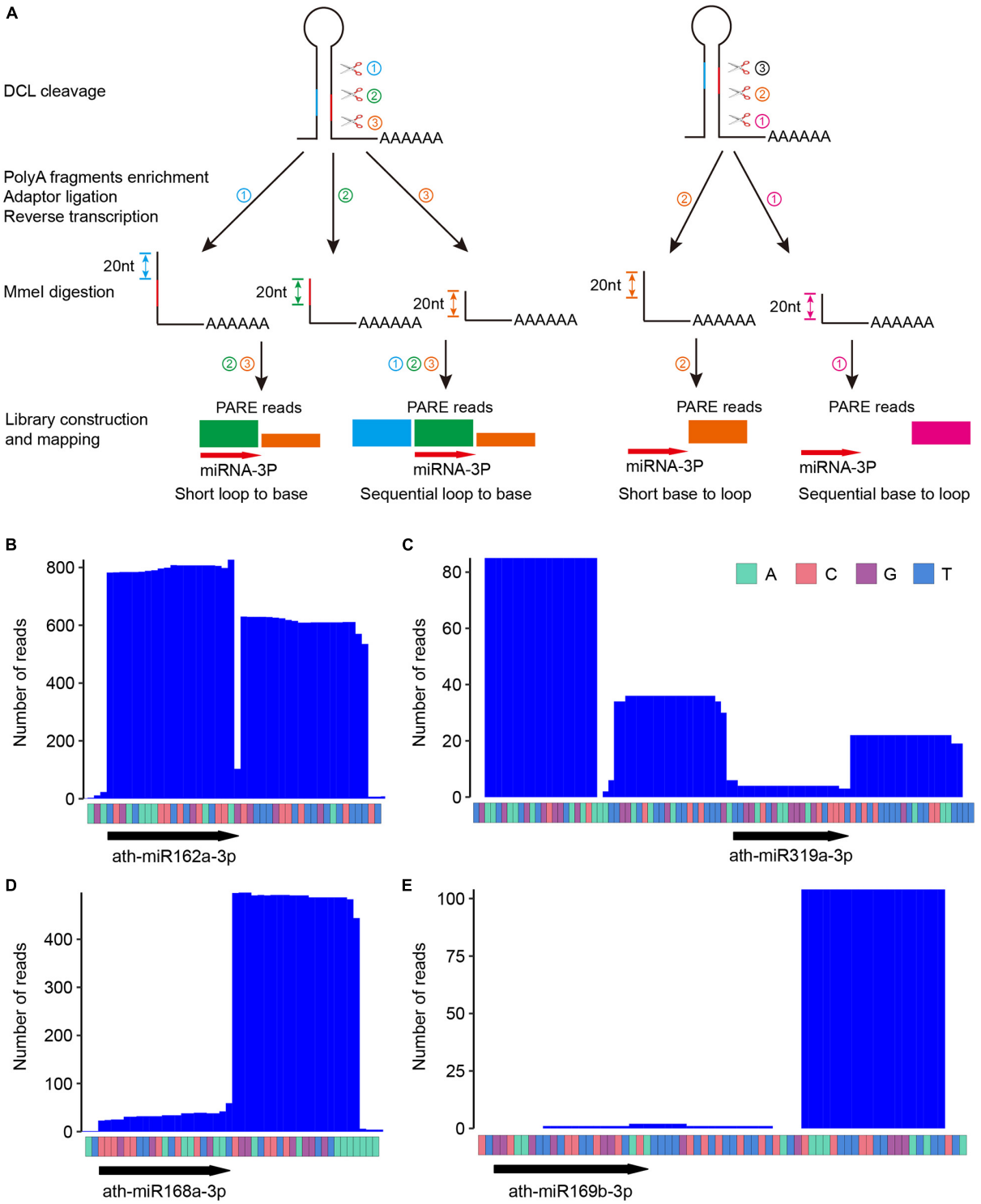

FIGURE 1 | Parallel Amplification of RNA Ends (PARE) patterns reflect different miRNA processing modes. **(A)** Schematic diagram of PARE library construction and typical PARE patterns for different miRNA processing modes. ①②③ depicts the order of cleavage. Note that for short loop-to-base processing, only two cuts (i.e., ②③) are executed, and for sequential processing, additional cuts (i.e., more than three cuts) may occur but are not shown here. Different colors of PARE signals reflects their sources of cleavage remnants. Bottom arrow highlights the position of miR-3p. **(B–E)** Degradome profiles of four selected miRNAs with known processing modes. ath-miR162a **(B)**, short loop to base; ath-miR319a **(C)**, sequential loop to base; ath-miR168a **(D)**, short base to loop; ath-miR169b **(E)**, sequential base to loop. Raw counts from four representative datasets with high abundance at respective analyzed miRNA locus (miR162a, SRR1171803; miR319a, SRR7652709; miR168a, SRR1171802, ath-miR169b, SRR7652709) were used for plotting the figures.

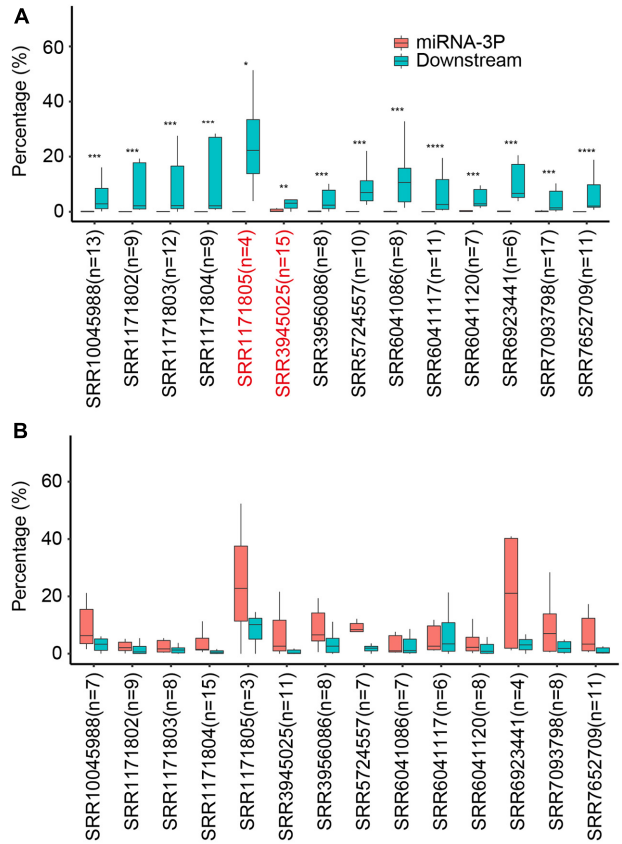

FIGURE 2 | Quality control of miRNA contamination of Arabidopsis Wt Parallel Amplification of RNA Ends (PARE) libraries. **(A,B)** Relative abundance of miR-3p and downstream PARE reads from known short base-to-loop processed miRNAs **(A)** or short loop-to-base processed miRNAs **(B)** pre-determined by Specific Parallel Amplification of RNA Ends (SPARE). Percentage was calculated as reads of miR-3p tags or downstream tags vs. total reads from miR-3p and downstream tags of miRNAs with respective processing modes. For each PARE library, only miRNAs with a percentage of miR-3p or downstream tags >0.5%, and a sum number >10 were kept. The number of analyzed miRNAs in each library are indicated in brackets. $^{*}p < 0.05$; $^{**}p < 0.01$; $^{***}p < 0.005$, $^{****}p < 0.001$ (Wilcoxon test). SRR6923441, SRR6923442, and SRR6923443 were merged under the entry of SRR6923441, owing to low sequencing depth.

miR167d, miR168a, miR403, miR841a, miR841b, and miR850 (**Figures 4E–G** and **Supplementary Figures 3D–G**), implying that the SAL1/FRY1 mutation may influence the characterization of miRNA processing and should be used carefully.

Identification of miRNA Processing Modes in Four Crops

Though SPARE results from crops are lacking, evolutionary conservation analysis reveals that miRNAs within a same family tend to share conserved processing modes across angiosperms (Chorostecki et al., 2017). We retrieved 6, 16 (Four of them from a same experiment were combined due to low sequencing depth), 14, and 13 PARE datasets of *Zea mays*, *Oryza sativa*, *Glycine max* and *Solanum lycopersicum* from public databases (**Supplementary Table 1**). MiRNAs whose counterparts in Arabidopsis are processed in short base-to-loop were used to evaluate the miRNA contamination levels in each library (**Supplementary Figure 4**). After filtering with a *p*-value cut-off of 0.05, two, nine, four, and seven libraries from *Zea mays*, *Oryza sativa*, *Glycine max* and *Solanum lycopersicum*, respectively, were kept for further analysis. For miRNAs lacking miR-3p annotation, sRNA-seq data (**Supplementary Table 1**) and RNA folding structures were used to infer their positions based on the 2-nt overhang rule of the miR-5p/miR-3p duplexes (**Supplementary Table 3**). Following the procedures described above, we obtained the degradome profiles around miR-3ps. We determined the processing modes of 36, 91, 90, and 54 miRNAs in *Zea mays*, *Oryza sativa*, *Glycine max*, and *Solanum lycopersicum*, respectively (**Supplementary Table 2**). The relatively fewer numbers in crops compared with Arabidopsis are likely owing to poor annotation of miRNAs and low or even no expression because of the limited amount of sequencing data. Consistent with previous notions (Chorostecki et al., 2017), an inspection of processing modes identified in at least three species revealed that 14 miRNA families (i.e., miR159, miR162, miR164, miR167, miR168, miR169, miR172, miR319, miR393, miR394, miR398, miR399, miR408, and miR2118) shared conserved processing modes (**Figure 5**). Members of the miR171 family in Arabidopsis utilize different processing modes (Bologna et al., 2013). Here, we also detected different processing modes in five miRNA families (i.e., miR156, miR160, miR166, miR396, and miR827) at different degrees (**Figure 5**). These analyses suggest that although members in the same miRNA family tend to share the same processing mode, differential processing modes may occur at intraspecific or interspecific levels.

Parallel Amplification of RNA Ends Assists miRNA Annotation

Accurate detection of miRNA processing remnants suggests that PARE is a useful tool for assisting miRNA annotation and/or prediction. We re-examined the annotation of miRBase and corrected 43 records (**Supplementary Table 4**). For instances, the Arabidopsis miR169 family has 14 members with miR169a being the most abundant (Bologna et al., 2013). According to the annotation from miRBase, the length of ath-miR169a-3p is 20-nt with the sequence being GGCAAGUUGUCCUUGGCUAC. The 3′ end of the ath-miR169a-3p reads from sRNA-seq data is ragged. In sharp contrast, we detected a sharp degradome signal starting 1 nt downstream of the end of the miRBase annotation (**Figure 6A**), revealing that the correct ath-miR169a-3p sequence should be 21-nt in size (i.e., GGCAAGUUGUCCUUGGCUACA). Gma-miR408c belongs to the conserved miR408 family and is processed in a short loop-to-base direction. The miRBase annotation shows that the sequence of gma-miR408c-3p is AUGCACUGCCUCUUCCCUGGC. We detected a major degradome peak that began 1 nt downstream of the above annotation (**Figure 6B**), suggesting that the majority of Gma-miR408c-3p started 1 nt after the annotated start site (i.e., UGCACUGCCUCUUCCCUGGCU). In both cases, the corrected version but not the miRBase annotation meets

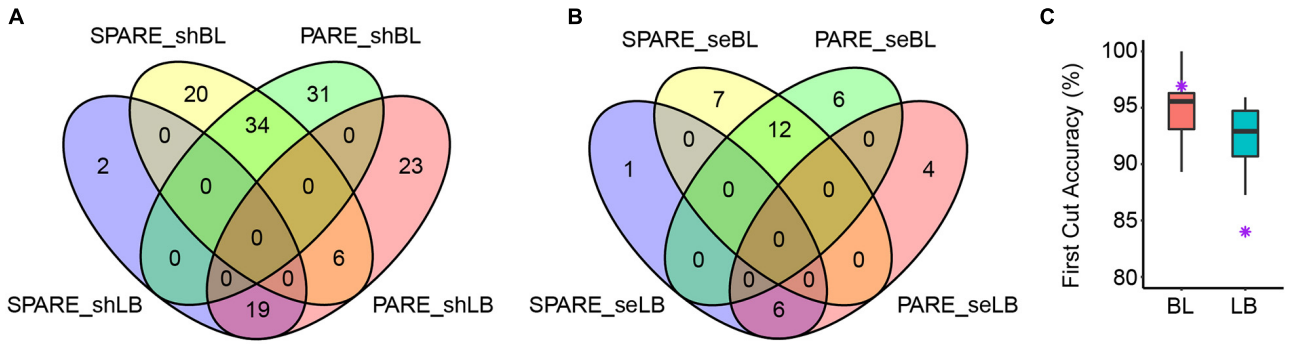

FIGURE 3 | Comparison of Parallel Amplification of RNA Ends (PARE) and Specific Parallel Amplification of RNA Ends (SPARE) results in Arabidopsis. **(A)** Venn diagram showing the number of short base-to-loop and short loop-to-base processed miRNAs as determined by PARE and SPARE. **(B)** Venn diagram showing the number of sequential base-to-loop and sequential loop-to-base processed miRNAs as determined by PARE and SPARE. shBL, short base to loop; shLB, short loop to base; seBL, sequential base to loop; seLB, sequential loop to base. **(C)** First cut accuracy of PARE in miRNA processing. Purple star, first-cut accuracy of SPARE (SRR6930534). LB, loop to base; BL, base to loop. Calculation of first cut accuracy was performed according to Moro et al. (2018).

the 2-nt overhang rule (**Supplementary Figure 5**). We also predicted the targets of different versions of ath-miR169a-3p and gma-miR408c-3p with TarHunter and determined their cleavage site using PARE datasets (Ma et al., 2017) (**Supplementary Figure 6** and **Supplementary Table 5**). For ath-miR169a-3p, one same potential target was retrieved, which showed a weak target plot (T-plot) signal. This could be due to the fact that ath-miR169a-3p is the passenger strand of the miR169a/* duplex. For gma-miR408c-3p, multiple conserved copper-related targets were identified with strong T-plots signals for both versions (Ma et al., 2015). An additional target (EBP1) was retrieved only for the corrected version (**Supplementary Figure 6** and **Supplementary Table 5**). Importantly, all the cleavage sites were located at positions complementary to the 10th and the 11th nucleotides of the corrected gma-miR408c-3p, which is canonical for miRNA-guided slicing (Kasschau et al., 2003).

Taken together, our study suggested that PARE was effective for comprehensively analyzing miRNA processing modes and assisting miRNA annotation in an untargeted manner with satisfactory accuracy.

DISCUSSION

Having more variable hairpin sizes and fold-back structures than their animal counterparts, plants evolve more complicated miRNA processing modes. Hitherto, systematic investigation of miRNA processing modes has only been conducted in the model plant Arabidopsis using SPARE. Though the same miRNA families across different species tend to share conserved processing modes, exceptions are frequently observed, and as such, experimental approaches for the characterization of miRNA processing modes are indispensable.

Although effective, SPARE is a targeted approach that only captures selected DCL processing remnants and is time-consuming. By contrast, PARE is an untargeted approach that captures 5′ end uncapped and 3′ end polyadenylated RNAs. More importantly, PARE is commercialized and has been widely used to determine the miRNA targets in various plant species and many PARE datasets are publicly available. In principle, PARE is capable of tracking miRNA processing intermediates and has been used to determine the processing modes of miR319 and miR159 (Addo-Quaye et al., 2009; Li et al., 2011). Yet, concerns of potential miRNA contamination impede its application in the systematic characterization of miRNA processing modes (Lu et al., 2009). Here, we provide a solution for evaluating miRNA contamination and demonstrate that PARE can be used to dissect miRNA processing modes globally. As an untargeted approach, PARE can identify miRNA processing modes in an unbiased manner. On the other hand, PARE has less sensitivity and requires higher sequencing depth. Moreover, some PARE libraries may have higher miRNA contamination that influence the prediction (**Figure 2** and **Supplementary Figure 4**). Thus, a quality control step for miRNA contamination is crucial for accuracy. Alternatively, replacing *Mme*I with *Eco*P15I, which produces 27-nt tags will effectively overcome this defect (Addo-Quaye et al., 2009; Li et al., 2019). Overall, SPARE and PARE can complement each other in dissecting miRNA processing modes in plants.

During our analysis, we also frequently detected obvious degradome signals at the beginning of the miR-5p or internal of miRNAs (**Supplementary Figure 7**). This could be owing to partial or misprocessing by DCL1, or slicing by ARGONAUTE 1 (AGO1) (Bologna et al., 2013). Other possible causes include: (i) 5′ processing remnants are re-polyadenylated and captured during library construction (Chekanova et al., 2007); (ii) the 5′ end of 3′ processing remnants are trimmed *in vivo* or during library construction *in vitro*; and (iii), multiple overlapped miRNAs/siRNAs exist in the same primary transcript that generates complex processing remnants (Reinhart et al., 2002; Allen et al., 2004; German et al., 2008).

FRY1/SAL1 encodes a phosphatase with dual activities, including converting 3′-phosphoadenosine 5′-phosphosulfate (PAPS) into adenosyl phosphosulfate (APS) and dephosphorylates 3′-phosphoadenosine 5′-phosphate (PAP)

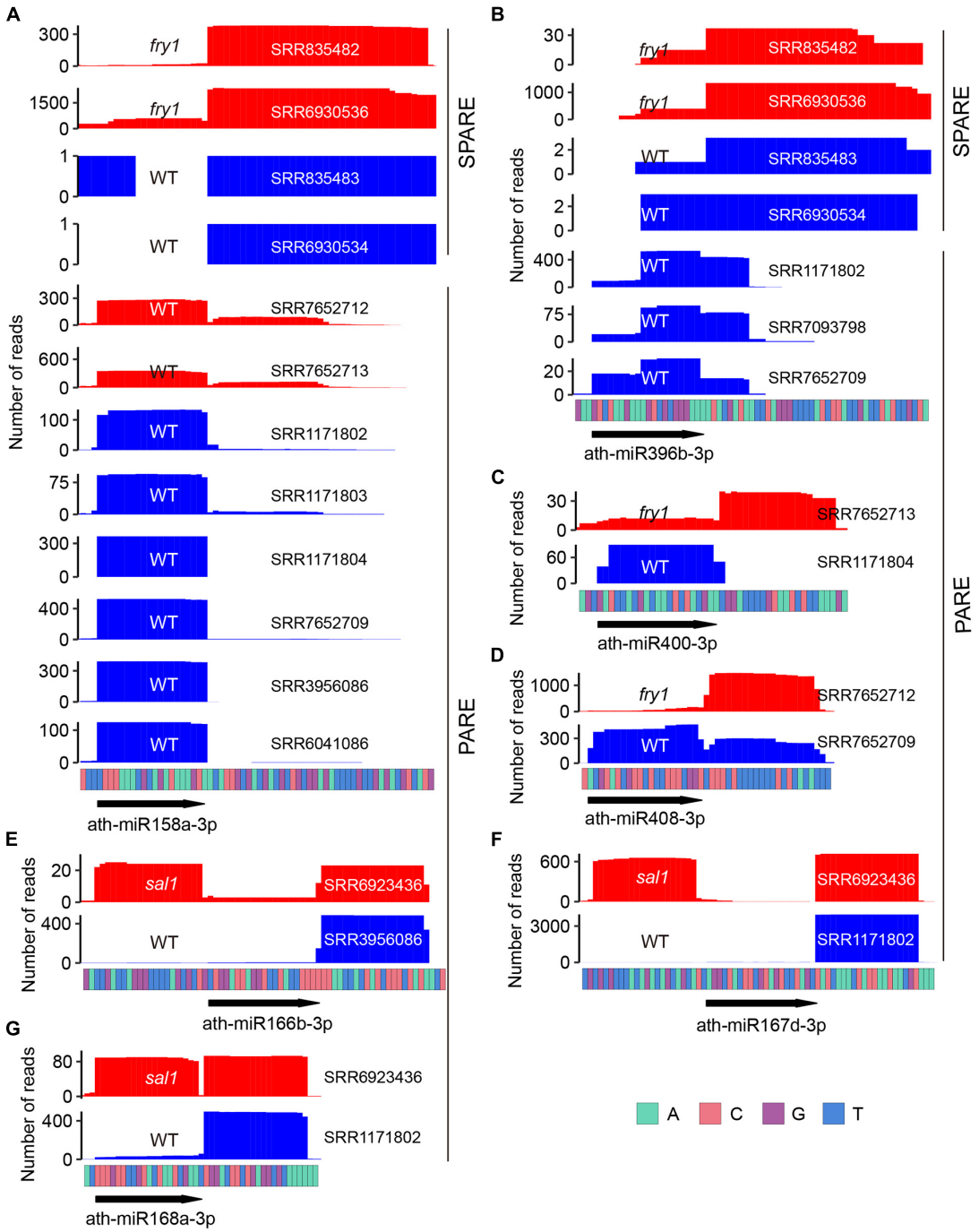

FIGURE 4 | *fry1/sal1* impacts miRNA processing. **(A)** Specific Parallel Amplification of RNA Ends (SPARE) and Parallel Amplification of RNA Ends (PARE) profiles of ath-miR158a-3p in *fry1* (red) and Wt (blue). **(B)** SPARE and PARE profiles of ath-miR396b-3p in *fry1* (red) and Wt (blue). **(C,D)** PARE profiles show that the processing modes of ath-miR400 **(C)** and ath-miR408 **(D)** changed from short loop-to-base to short base-to-loop in *fry1*. **(E–G)** PARE profiles show that the processing modes of ath-miR166b **(E)**, ath-miR167d **(F)**, and ath-miR168a **(G)** changed from short base-to-loop to short/sequential loop-base in *sal1*.

to adenosine 5′-phosphate (AMP) (Quintero et al., 1996; Gil-Mascarell et al., 1999). *FRY1* plays important roles in multiple biological processes including post-transcriptional gene silencing (PTGS) (Gy et al., 2007) and RNA quality control (You et al., 2019). In the *fry1* mutant, the accumulation of toxic PAP in *fry1* impaired the activity of 5′ to 3′ exoribonucleases (XRNs). Consequently, *MIRNA*-derived loop and 3′ products become over-accumulated owing to the inhibition activities of XRN2 and XRN3 (Gy et al., 2007). It has been reported that 90% of degradome tags of loop-to-base processed

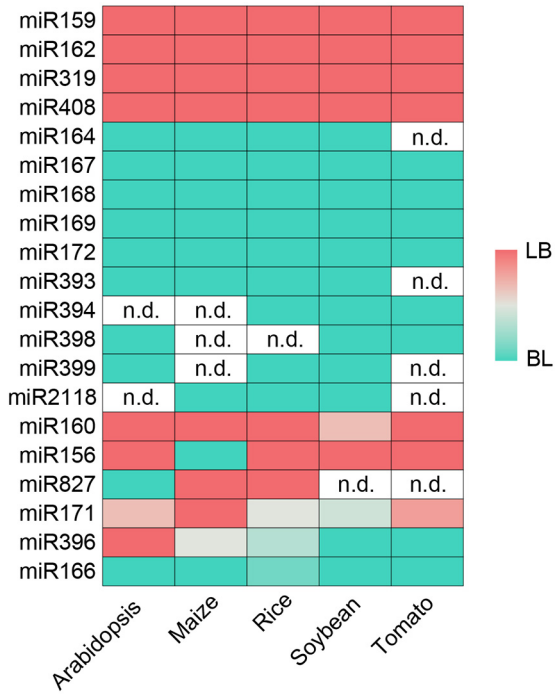

FIGURE 5 | Conservation of miRNA processing modes determined by Parallel Amplification of RNA Ends (PARE). LB, short/sequential loop to base; BL, short/sequential base to loop. The intensity of color reflects the degree of intraspecific conservation. White (n.d.): not determined.

miRNAs in *fry1* correspond to the position of the second cleavage site (Moro et al., 2018), indicating that *FRY1* may influence miRNA processing. Strikingly, opposite processing modes were frequently detected between Wt and *fry1*/*sal1* (**Figure 4** and **Supplementary Figure 3**). Moreover, dramatic elevated partial cleavage was observed only in *fry1*/*sal1* (**Supplementary Figure 8**). Thus, *fry1* should be used only cautiously in the identification of processing mode. We analyzed the *fry1* small RNA sequencing data and found that misprocessed miRNA ratios were slightly elevated in *fry1-6* and *fry1-8* (**Supplementary Figure 9**), suggesting that FRY1 may also affect DCL1 processing. Nuclear exosome components HUA ENHANCER 2 (HEN2) and SUPPRESSOR OF PAS2 1 (SOP1) act on miRNA precursor degradation with selective impacts on loop-to-base miRNA processing when HYPONASTIC LEAVES 1 (HYL1) is impaired (Gao et al., 2020). It will be interesting to investigate the relationship between 5′ to 3′ and 3′ to 5′ degradation pathways on miRNA processing.

In plants, exhaustive efforts have been paid to miRNA prediction and annotation with a huge number of sRNA-seq datasets and different prediction tools. Although miRNA isoforms are frequently reported, the heterogenous ends of sRNA reads from sRNA-seq data can lead to misannotation, which may cause mistaken inferences about their AGO sorting and/or target identification (Mi et al., 2008; Zhang et al., 2014; **Supplementary Figure 6**). As an independent method, we showed that PARE can assist with accurate miRNA annotation (**Supplementary Table 4** and **Figure 6**). Moreover, owing to the complexity of small RNA compositions in plants, false positives lead to many questionable miRNA annotations, which have now become a major concern to the community (Axtell and Meyers, 2018). To solve this issue, the Axtell group developed ShortStack, which has high precision and near-zero false positives; however, it shows limited sensitivity and high false negatives. By analyzing 28 Arabidopsis sRNA-seq libraries, only 143 out of 325 entries in miRBase were designated as *bona fide*

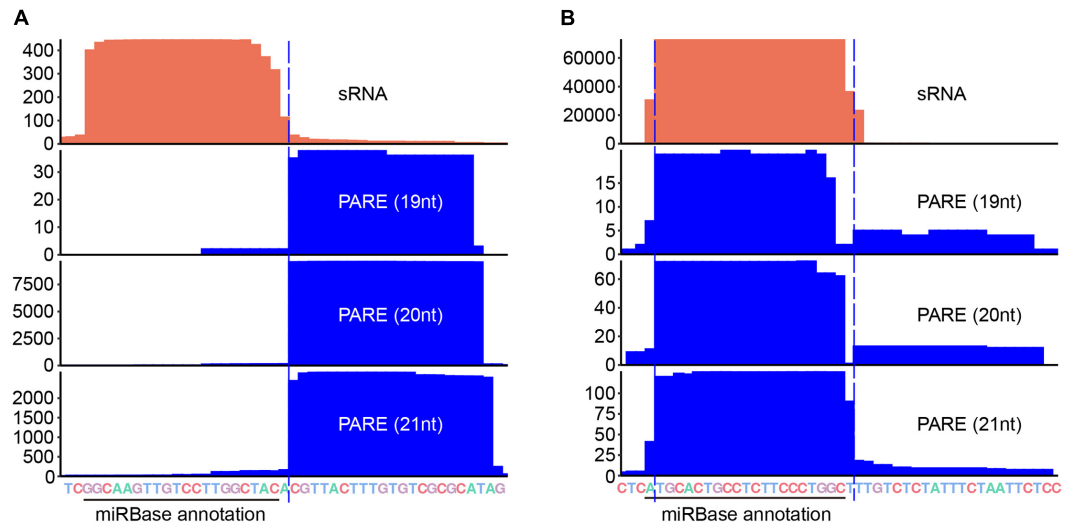

FIGURE 6 | Parallel Amplification of RNA Ends (PARE) corrects miR-3p annotations. Coverage of sRNA (orange) and PARE (blue) read alignments around ath-miR169a-3p **(A)** and gma-miR408c-3p **(B)**. Black solid line, miRBase annotated miR-3p border; blue dashed line, PARE corrected miR-3p border. Merged sRNA datasets (**Supplementary Table 1**) were used for sRNA analysis and datasets under the accession numbers SRR1171802 (for ath-miR169a-3p) and SRR1451679 (for gma-miR408c-3p) were used for PARE analysis.

miRNAs by ShortStack (Lunardon et al., 2020). Unpassed entries were largely due to imprecise processing, unpaired bases, bulges limitation and undetected miRNA*. We suggest that PARE may also be used to help with miRNA characterization by tracking processing remnants. Our preliminary analysis revealed that 113 entries had robust PARE support, including 30 miRNAs that were not designated as miRNAs by ShortStack (**Supplementary Figure 10**). We believe that integration of degradome signatures into miRNA prediction tools will improve both accuracy and sensitivity.

In conclusion, we provided a solution for the estimation of miRNA contamination and demonstrated the capacity of PARE in characterizing miRNA processing and miRNA annotation.

DATA AVAILABILITY STATEMENT

The original contributions presented in the study are included in the article/**Supplementary Material**, further inquiries can be directed to the corresponding author.

AUTHOR CONTRIBUTIONS

GR and NL conceived the idea and wrote the manuscript. NL conducted the analysis. Both authors contributed to the article and approved the submitted version.

FUNDING

This work was supported by grants from the National Natural Science Foundation of China (31970275) and the "Shuguang Program" sponsored by Shanghai Education Development Foundation and Shanghai Municipal Education Commission (20SG02).

SUPPLEMENTARY MATERIAL

The Supplementary Material for this article can be found online at: https://www.frontiersin.org/articles/10.3389/fpls.2021.793549/full#supplementary-material

REFERENCES

Addo-Quaye, C., Eshoo, T. W., Bartel, D. P., and Axtell, M. J. (2008). Endogenous siRNA and miRNA targets identified by sequencing of the Arabidopsis degradome. *Curr. Biol.* 18, 758–762. doi: 10.1016/j.cub.2008.04.042

Addo-Quaye, C., Snyder, J. A., Park, Y. B., Li, Y. F., Sunkar, R., and Axtell, M. J. (2009). Sliced microRNA targets and precise loop-first processing of MIR319 hairpins revealed by analysis of the Physcomitrella patens degradome. *RNA* 15, 2112–2121. doi: 10.1261/rna.1774909

Allen, E., Xie, Z., Gustafson, A. M., Sung, G. H., Spatafora, J. W., and Carrington, J. C. (2004). Evolution of microRNA genes by inverted duplication of target gene sequences in Arabidopsis thaliana. *Nat. Genet.* 36, 1282–1290. doi: 10.1038/ng1478

Axtell, M. J. (2013). ShortStack: comprehensive annotation and quantification of small RNA genes. *RNA* 19, 740–751. doi: 10.1261/rna.035279.112

Axtell, M. J., and Meyers, B. C. (2018). Revisiting criteria for Plant MicroRNA annotation in the era of big data. *Plant Cell* 30, 272–284.

Axtell, M. J., Westholm, J. O., and Lai, E. C. (2011). Vive la difference: biogenesis and evolution of microRNAs in plants and animals. *Genome Biol.* 12:221. doi: 10.1186/gb-2011-12-4-221

Bologna, N. G., Mateos, J. L., Bresso, E. G., and Palatnik, J. F. (2009). A loop-to-base processing mechanism underlies the biogenesis of plant microRNAs miR319 and miR159. *EMBO J.* 28, 3646–3656. doi: 10.1038/emboj.2009.292

Bologna, N. G., Schapire, A. L., Zhai, J., Chorostecki, U., Boisbouvier, J., Meyers, B. C., et al. (2013). Multiple RNA recognition patterns during microRNA biogenesis in plants. *Genome Res.* 23, 1675–1689. doi: 10.1101/gr.153387.112

Bologna, N. G., and Voinnet, O. (2014). The diversity, biogenesis, and activities of endogenous silencing small RNAs in Arabidopsis. *Annu. Rev. Plant Biol.* 65, 473–503. doi: 10.1146/annurev-arplant-050213-035728

Bolser, D., Staines, D. M., Pritchard, E., and Kersey, P. (2016). Ensembl plants: integrating tools for visualizing, mining, and analyzing plant genomics data. *Methods Mol. Biol.* 1374, 115–140. doi: 10.1007/978-1-4939-3167-5_6

Chekanova, J. A., Gregory, B. D., Reverdatto, S. V., Chen, H., Kumar, R., Hooker, T., et al. (2007). Genome-wide high-resolution mapping of exosome substrates reveals hidden features in the Arabidopsis transcriptome. *Cell* 131, 1340–1353. doi: 10.1016/j.cell.2007.10.056

Chen, S., Zhou, Y., Chen, Y., and Gu, J. (2018). fastp: an ultra-fast all-in-one FASTQ preprocessor. *Bioinformatics* 34, i884–i890. doi: 10.1093/bioinformatics/bty560

Chorostecki, U., Moro, B., Rojas, A. M. L., Debernardi, J. M., Schapire, A. L., Notredame, C., et al. (2017). Evolutionary footprints reveal insights into plant MicroRNA biogenesis. *Plant Cell* 29, 1248–1261. doi: 10.1105/tpc.17.00272

Cuperus, J. T., Fahlgren, N., and Carrington, J. C. (2011). Evolution and functional diversification of MIRNA genes. *Plant Cell* 23, 431–442. doi: 10.1105/tpc.110.082784

Cuperus, J. T., Montgomery, T. A., Fahlgren, N., Burke, R. T., Townsend, T., Sullivan, C. M., et al. (2010). Identification of MIR390a precursor processing-defective mutants in Arabidopsis by direct genome sequencing. *Proc. Natl. Acad. Sci. U.S.A.* 107, 466–471. doi: 10.1073/pnas.0913203107

Gao, S., Wang, J., Jiang, N., Zhang, S., Wang, Y., Zhang, J., et al. (2020). Hyponastic Leaves 1 protects pri-miRNAs from nuclear exosome attack. *Proc. Natl. Acad. Sci. U.S.A.* 117, 17429–17437. doi: 10.1073/pnas.2007203117

German, M. A., Pillay, M., Jeong, D. H., Hetawal, A., Luo, S., Janardhanan, P., et al. (2008). Global identification of microRNA-target RNA pairs by parallel analysis of RNA ends. *Nat. Biotechnol.* 26, 941–946. doi: 10.1038/nbt1417

Gil-Mascarell, R., Lopez-Coronado, J. M., Belles, J. M., Serrano, R., and Rodriguez, P. L. (1999). The Arabidopsis HAL2-like gene family includes a novel sodium-sensitive phosphatase. *Plant J.* 17, 373–383. doi: 10.1046/j.1365-313x.1999.00385.x

Gregory, B. D., O'Malley, R. C., Lister, R., Urich, M. A., Tonti-Filippini, J., Chen, H., et al. (2008). A link between RNA metabolism and silencing affecting Arabidopsis development. *Dev. Cell* 14, 854–866. doi: 10.1016/j.devcel.2008.04.005

Grishok, A., Pasquinelli, A. E., Conte, D., Li, N., Parrish, S., Ha, I., et al. (2001). Genes and mechanisms related to RNA interference regulate expression of the small temporal RNAs that control C. elegans developmental timing. *Cell* 106, 23–34. doi: 10.1016/s0092-8674(01)00431-7

Gy, I., Gasciolli, V., Lauressergues, D., Morel, J. B., Gombert, J., Proux, F., et al. (2007). Arabidopsis FIERY1, XRN2, and XRN3 are endogenous RNA silencing suppressors. *Plant Cell* 19, 3451–3461. doi: 10.1105/tpc.107.055319

Han, J., Lee, Y., Yeom, K. H., Nam, J. W., Heo, I., Rhee, J. K., et al. (2006). Molecular basis for the recognition of primary microRNAs by the Drosha-DGCR8 complex. *Cell* 125, 887–901. doi: 10.1016/j.cell.2006.03.043

Johnson, N. R., Yeoh, J. M., Coruh, C., and Axtell, M. J. (2016). Improved Placement of Multi-mapping Small RNAs. *G3 (Bethesda)* 6, 2103–2111. doi: 10.1534/g3.116.030452

Kasschau, K. D., Xie, Z. X., Allen, E., Llave, C., Chapman, E. J., Krizan, K. A., et al. (2003). P1/HC-Pro, a viral suppressor of RNA silencing, interferes with Arabidopsis development and miRNA function. *Dev. Cell* 4, 205–217. doi: 10.1016/S1534-5807(03)00025-X

Ketting, R. F., Fischer, S. E., Bernstein, E., Sijen, T., Hannon, G. J., and Plasterk, R. H. (2001). Dicer functions in RNA interference and in synthesis of small RNA involved in developmental timing in C. elegans. *Genes Dev.* 15, 2654–2659. doi: 10.1101/gad.927801

Kozomara, A., and Griffiths-Jones, S. (2011). miRBase: integrating microRNA annotation and deep-sequencing data. *Nucleic Acids Res.* 39, D152–D157. doi: 10.1093/nar/gkq1027

Kwon, S. C., Nguyen, T. A., Choi, Y. G., Jo, M. H., Hohng, S., Kim, V. N., et al. (2016). Structure of human DROSHA. *Cell* 164, 81–90. doi: 10.1016/j.cell.2015.12.019

Lamesch, P., Berardini, T. Z., Li, D., Swarbreck, D., Wilks, C., Sasidharan, R., et al. (2012). The Arabidopsis Information Resource (TAIR): improved gene annotation and new tools. *Nucleic Acids Res.* 40, D1202–D1210. doi: 10.1093/nar/gkr1090

Langmead, B. (2010). Aligning short sequencing reads with Bowtie. *Curr. Protoc. Bioinform.* Chapter 11, Unit 11.7. doi: 10.1002/0471250953.bi1107s32

Leinonen, R., Sugawara, H., Shumway, M., International Nucleotide Sequence Database Collaboration (2011). The sequence read archive. *Nucleic Acids Res.* 39, D19–D21. doi: 10.1093/nar/gkq1019

Li, Y., Li, C., Ding, G., and Jin, Y. (2011). Evolution of MIR159/319 microRNA genes and their post-transcriptional regulatory link to siRNA pathways. *BMC Evol. Biol.* 11:122. doi: 10.1186/1471-2148-11-122

Li, Y. F., Zhao, M., Wang, M., Guo, J., Wang, L., Ji, J., et al. (2019). An improved method of constructing degradome library suitable for sequencing using Illumina platform. *Plant Methods* 15:134. doi: 10.1186/s13007-019-0524-7

Lu, S. F., Sun, Y. H., and Chiang, V. L. (2009). Adenylation of plant miRNAs. *Nucleic Acids Res.* 37, 1878–1885. doi: 10.1093/nar/gkp031

Lunardon, A., Johnson, N. R., Hagerott, E., Phifer, T., Polydore, S., Coruh, C., et al. (2020). Integrated annotations and analyses of small RNA-producing loci from 47 diverse plants. *Genome Res.* 30, 497–513. doi: 10.1101/gr.256750.119

Ma, C., Burd, S., and Lers, A. (2015). miR408 is involved in abiotic stress responses in Arabidopsis. *Plant J.* 84, 169–187. doi: 10.1111/tpj.12999

Ma, X., Liu, C., Gu, L., Mo, B., Cao, X., and Chen, X. (2017). TarHunter, a tool for predicting conserved microRNA targets and target mimics in plants. *Bioinformatics* 34, 1574–1576. doi: 10.1093/bioinformatics/btx797

Mateos, J. L., Bologna, N. G., Chorostecki, U., and Palatnik, J. F. (2010). Identification of microRNA processing determinants by random mutagenesis of Arabidopsis MIR172a precursor. *Curr. Biol.* 20, 49–54. doi: 10.1016/j.cub.2009.10.072

Mi, S., Cai, T., Hu, Y., Chen, Y., Hodges, E., Ni, F., et al. (2008). Sorting of small RNAs into Arabidopsis argonaute complexes is directed by the 5′ terminal nucleotide. *Cell* 133, 116–127. doi: 10.1016/j.cell.2008.02.034

Moro, B., Chorostecki, U., Arikit, S., Suarez, I. P., Hobartner, C., Rasia, R. M., et al. (2018). Efficiency and precision of microRNA biogenesis modes in plants. *Nucleic Acids Res.* 46, 10709–10723. doi: 10.1093/nar/gky853

Quintero, F. J., Garciadeblas, B., and Rodriguez-Navarro, A. (1996). The SAL1 gene of Arabidopsis, encoding an enzyme with 3′(2′),5′-bisphosphate nucleotidase and inositol polyphosphate 1-phosphatase activities, increases salt tolerance in yeast. *Plant Cell* 8, 529–537. doi: 10.1105/tpc.8.3.529

Reinhart, B. J., Weinstein, E. G., Rhoades, M. W., Bartel, B., and Bartel, D. P. (2002). MicroRNAs in plants. *Genes Dev.* 16, 1616–1626. doi: 10.1101/gad.1004402

Song, X., Li, Y., Cao, X., and Qi, Y. (2019). MicroRNAs and Their regulatory roles in plant-environment interactions. *Annu. Rev. Plant Biol.* 70, 489–525. doi: 10.1146/annurev-arplant-050718-100334

Treiber, T., Treiber, N., and Meister, G. (2019). Regulation of microRNA biogenesis and its crosstalk with other cellular pathways. *Nat. Rev. Mol. Cell Biol.* 20, 5–20. doi: 10.1038/s41580-018-0059-1

Wang, J. L., Mei, J., and Ren, G. D. (2019). Plant microRNAs: biogenesis, homeostasis, and degradation. *Front. Plant Sci.* 10:360. doi: 10.3389/Fpls.2019.00360

Wilson, P. B., Estavillo, G. M., Field, K. J., Pornsiriwong, W., Carroll, A. J., Howell, K. A., et al. (2009). The nucleotidase/phosphatase SAL1 is a negative regulator of drought tolerance in Arabidopsis. *Plant J.* 58, 299–317. doi: 10.1111/j.1365-313X.2008.03780.x

You, C., He, W., Hang, R., Zhang, C., Cao, X., Guo, H., et al. (2019). FIERY1 promotes microRNA accumulation by suppressing rRNA-derived small interfering RNAs in Arabidopsis. *Nat. Commun.* 10:4424. doi: 10.1038/s41467-019-12379-z

Zhang, B. H., Pan, X. P., Cannon, C. H., Cobb, G. P., and Anderson, T. A. (2006). Conservation and divergence of plant microRNA genes. *Plant J.* 46, 243–259. doi: 10.1111/j.1365-313X.2006.02697.X

Zhang, X., Niu, D., Carbonell, A., Wang, A., Lee, A., Tun, V., et al. (2014). ARGONAUTE PIWI domain and microRNA duplex structure regulate small RNA sorting in Arabidopsis. *Nat. Commun.* 5:5468. doi: 10.1038/ncomms6468

Conflict of Interest: The authors declare that the research was conducted in the absence of any commercial or financial relationships that could be construed as a potential conflict of interest.

Publisher's Note: All claims expressed in this article are solely those of the authors and do not necessarily represent those of their affiliated organizations, or those of the publisher, the editors and the reviewers. Any product that may be evaluated in this article, or claim that may be made by its manufacturer, is not guaranteed or endorsed by the publisher.

frontiers in Plant Science

ORIGINAL RESEARCH
published: 24 December 2021
doi: 10.3389/fpls.2021.781836

Comprehensive Annotation and Functional Exploration of MicroRNAs in Lettuce

Yang Deng[1,2†], Yajuan Qin[1,2†], Pan Yang[1,3,4†], Jianjun Du[1,5†], Zheng Kuang[1,4], Yongxin Zhao[1,2], Ying Wang[4], Dayong Li[1,6], Jianhua Wei[1,2], Xinyu Guo[1,5], Lei Li[4]* and Xiaozeng Yang[1,2]**

[1] Beijing Academy of Agriculture and Forestry Sciences, Beijing, China, [2] Beijing Key Laboratory of Agricultural Genetic Resources and Biotechnology, Beijing Agro-Biotechnology Research Center, Beijing, China, [3] College of Life Sciences, Fujian Agriculture and Forestry University, Fuzhou, China, [4] State Key Laboratory of Protein and Plant Gene Research, Peking-Tsinghua Center for Life Sciences, School of Advanced Agricultural Sciences and School of Life Sciences, Peking University, Beijing, China, [5] Beijing Key Lab of Digital Plant, Beijing Research Center for Information Technology in Agriculture, Beijing, China, [6] Beijing Key Laboratory of Vegetable Germplasm Improvement, Beijing Vegetable Research Center, Beijing, China

MicroRNA (miRNA) is an important endogenous post-transcriptional regulator, while lettuce (*Lactuca sativa*) is a leafy vegetable of global economic significance. However, there are few studies on miRNAs in lettuce, and research on miRNA regulatory network in lettuce is absent. In this study, through deep sequencing of small RNAs in different tissues, together with a reference genome, 157 high-confidence miRNA loci in lettuce were comprehensively identified, and their expression patterns were determined. Using a combination of computational prediction and high-throughput experimental verification, a set of reliable lettuce miRNA targets were obtained. Furthermore, through RNA-Seq, the expression profiles of these targets and a comprehensive view of the negative regulatory relationship between miRNAs and their targets was acquired based on a correlation analysis. To further understand miRNA functions, a miRNA regulatory network was constructed, with miRNAs at the core and combining transcription factors and miRNA target genes. This regulatory network, mainly composed of feed forward loop motifs, greatly increases understanding of the potential functions of miRNAs, and many unknown potential regulatory links were discovered. Finally, considering its specific expression pattern, *Lsa-MIR408* as a hub gene was employed to illustrate the function of the regulatory network, and genetic experiments revealed its ability to increase the fresh weight and achene size of lettuce. In short, this work lays a solid foundation for the study of miRNA functions and regulatory networks in lettuce.

Keywords: lettuce, microRNA (miRNA), sRNA-Seq, expression correlation, regulatory network, miR408

OPEN ACCESS

Edited by:
Lei Wang,
Institute of Botany, Chinese Academy of Sciences (CAS), China

Reviewed by:
Jianbo Xie,
Beijing Forestry University, China
Yun Ju Kim,
Institute for Basic Science (IBS), South Korea

***Correspondence:**
Xinyu Guo
guoxy@nercita.org.cn
Lei Li
lei.li@pku.edu.cn
Xiaozeng Yang
yangxiaozeng@baafs.net.cn;
yangxz@srnaworld.com

† These authors have contributed equally to this work and share first authorship

Specialty section:
This article was submitted to Plant Physiology, a section of the journal Frontiers in Plant Science

Received: *23 September 2021*
Accepted: *28 October 2021*
Published: *24 December 2021*

Citation:
Deng Y, Qin Y, Yang P, Du J, Kuang Z, Zhao Y, Wang Y, Li D, Wei J, Guo X, Li L and Yang X (2021) Comprehensive Annotation and Functional Exploration of MicroRNAs in Lettuce. Front. Plant Sci. 12:781836. doi: 10.3389/fpls.2021.781836

INTRODUCTION

Lettuce (*Lactuca sativa*), of the Asteraceae family, is a leafy vegetable with important economic value. According to the Food and Agriculture Organization[1], the global production of lettuce, together with chicory, exceeded 29 million tons in 2019, ranking third of all leafy vegetables. In the United States alone, lettuce production in 2019 exceeded 3.6 million tons, with a market value of over 1.5 billion USD. The worldwide popularity of lettuce is due to its diverse cultivars, taste, and high nutritional value, being rich in vitamins, folates, and minerals (Tamura et al., 2018). With the availability of a reference genome (Reyes-Chin-Wo et al., 2017) and numerous transcriptomes (Zhang L. et al., 2017), lettuce has become a model for studying Asteraceae and related plants. Lettuce has numerous cultivars, including butterhead, crisphead, looseleaf, romaine, stem, and many mixed types, which are highly varied in morphology, and provide good material for studying the morphological development of plants (Seki et al., 2020; Yu et al., 2020). The same is true for lettuce in terms of leaf colors (Su et al., 2020), metabolites (Zhang et al., 2020), heat responses (Chen et al., 2017, 2018), viral resistance (Inderbitzin et al., 2019), etc. Lettuce is also an important example of crop domestication and for adaptation research (Zhang L. et al., 2017; Wei et al., 2021). Recently, lettuce has been used as a novel platform for biopharmaceutical production due to its numerous advantages, including low processing cost, consistent and scalable production, and the excellent biosafety profile of transgenic plants (Daniell et al., 2019; Zhang et al., 2019).

MicroRNA (miRNA) is an important post-transcriptional regulatory factor, which has received considerable research interest (Fromm et al., 2020). In plants, major mature miRNAs only have 20–24 nucleotides (nts), which can find target mRNAs through nearly perfect sequence complementation, leading to degradation or translation block (Voinnet, 2009). MiRNA genes share many common features with protein-coding genes such as defined promoters and transcription start sites as well as the exon-intron gene structure (Voinnet, 2009). In general, RNA polymerase II (Pol II) is responsible for transcriptional activation of miRNA genes in plants (Lee et al., 2004). The initially transcribed miRNA, called pri-miRNA, has a stem-loop structure (Bartel, 2009). In plants, pri-miRNA is first cut into pre-miRNA by Dicer-like, and then further processed into a duplex composed of mature miRNA and miRNA*. Only the mature miRNA guides the miRNA-induced silencing complex to regulate its mRNA targets, and other parts are degraded (Bartel, 2009; Voinnet, 2009). Studies have found that plant miRNAs have very diverse functions in development, responses to environmental challenges, etc. (Chandra et al., 2017). For example, miR156 can regulate the transition from juvenile to adult developmental stages (Wang et al., 2009; Wu et al., 2009), miR319/159 is related to leaf morphology and reproduction (Yang et al., 2013; Cheng et al., 2020), and miR399 is associated with the phosphate-starvation response (Fujii et al., 2005). It has recently been discovered that miRNAs in plants can also be used as carriers for information exchange between different species (Shahid et al., 2018; Tsikou et al., 2018).

In the last decade, high-throughput sequencing has become the most powerful method to identify miRNAs. The combination of small RNA sequencing (sRNA-Seq) and subsequent bioinformatic analysis has uncovered a large number of new miRNAs (Guo et al., 2020). The method of miRNA target gene exploration is constantly improving, which further improved the prediction accuracy of miRNA targets as well (Zhao et al., 2021). The high-throughput target gene verification method, parallel analysis of RNA ends sequencing [PARE-Seq (German et al., 2009)] or degradome sequencing enables identification of miRNA target genes on a genomic scale. In addition, combined with RNA-Seq data, the correlation of expression patterns between miRNAs and potential targets provides not only a reference for target gene prediction, but also the potential for the discovery of new regulatory miRNA-target pairs. Motif scanning, together with methods such as Chromatin Immunoprecipitation Sequencing (Johnson et al., 2007) or DNA Affinity Purification Sequencing (Bartlett et al., 2017), has been widely employed as a high-throughput means to detect the regulation between transcriptional factors (TFs) and their targets, which could be used to discover the upstream regulation from TFs to miRNAs. With all these technical advantages, a whole genome scaled picture of miRNA-based regulatory networks in a specific species can be achieved. For example, a multiple layer regulation network was recently constructed in Arabidopsis (Gao et al., 2021). However, despite being an important economic crop, case studies of miRNAs in lettuce are scarce (Huo et al., 2016), and the systematic identification and annotation of miRNAs and their regulatory networks are absent.

In this study, by sequencing sRNAs in four different tissues and using a pipeline centered by miRDeep-P2 (Kuang et al., 2019), 157 high-confidence miRNAs were identified in lettuce. The detailed characteristics of these miRNAs were annotated, including sequences, structure, conservation, clusters, selection after duplication, and expression patterns in different tissues. The targets of these miRNAs were predicted by three different methods, and Gene Ontology [GO (Mi et al., 2019)] and Kyoto Encyclopedia of Genes and Genomes [KEGG (Ogata et al., 1999)] enrichment analyses indicated that these target genes are widely involved in signal transduction, protein binding, and various enzyme activities, partially reflecting the diversification of miRNA functions and the role of a specific group of miRNA targets, TFs. Furthermore, a correlation analysis on miRNA and target expression patterns was performed, and the negative regulatory relationship between miRNAs and target genes is highlighted, although this correlation is affected by numerous factors. In addition, a regulatory network involving miRNAs, TFs, and targets, was constructed, and the connection between different feed forward loops (FFLs) helped in defining a number of new regulatory links. Finally, based on its specific expression pattern and potential function, miR408 was used as an example to verify this exploration of miRNAs and miRNA regulatory network. Genetic experiments not only confirmed the solidity of the data, but also found that *Lsa-MIR408* can promote the vegetative growth of lettuce and increase achene size. This

[1]http://www.fao.org/

work systematically identified and annotated miRNAs in lettuce, and conducted preliminary explorations of the functions of these miRNAs by means of target genes, expression correlation, regulatory networks, etc., and lays a solid foundation for further research on lettuce miRNAs.

MATERIALS AND METHODS

Plant Materials

Lettuce (*Lactuca sativa L.*) achenes were purchased from the vegetable institute of Beijing Academy of Agriculture and Forestry Sciences, Beijing. Achenes were first sown on a wet filter paper in a petri dish and moved directly to the soil in plastic pots after germination. The seedlings were cultured in a greenhouse (16 h/8 h day/night cycle, light intensity 200 μmol m^{-2} s^{-1}, relative humidity 30–50%). The root, stem, and leaf were collected from 4-week-old plants. The flowers were collected at full bloomed capitula (19-week-old plants). After collection, the samples of each tissue were quickly frozen in liquid nitrogen and stored at −80°C for the extraction of total RNA, respectively.

Small RNA and mRNA Libraries Construction and Sequencing

The RNA from roots, stems, leaves, and flowers of lettuce was, respectively, isolated using the OminiPlant RNA Kit (Cwbio, China), following the manufacturer's protocol. The integrity and quality of RNAs were validated by an Agilent 2100 Bioanalyzer. Small RNA cDNA libraries were prepared using the Small RNA Sample Prep Kit (Illumina, United States), and mRNA cDNA libraries were prepared using the TruSeq Stranded RNA LT Kit (Illumina, United States), based on the manufacturer's protocols. Briefly, sRNAs were isolated from 20 μg of total RNA by 15% polyacrylamide gel electrophoresis and ligated two adaptors, including a 5′-RNA and a 3′-RNA adaptor. Then, the samples were converted and amplified to cDNA by RT-PCR (mRNA cDNA library preparation is similar). Lastly, the validated cDNA libraries were sequenced by Illumina Hiseq2500. Small RNA and mRNA cDNA libraries included two biological replicates, and 16 libraries were produced.

Identification of Conserved, Asteraceae-Specific, and Lettuce-Specific MicroRNAs

After sRNA library sequencing, clean reads were obtained by filtering low-quality sequences, including junk reads, adaptor sequences, polyA tags and reads <18 bp and >30 bp. The extracted clean reads (19–25 nt in length) were used for miRNA prediction. Reads matching plant non-coding RNAs, including tRNA, rRNA snRNA, and snoRNA sequences in the Rfam database (version 13.0; Kalvari et al., 2018), with no more than one mismatch were further filtered. Next, the remaining sequences were mapped to the lettuce genome (Reyes-Chin-Wo et al., 2017), and candidate miRNAs were detected via miRDeep-P2 software (version 1.1.4; Kuang et al., 2019). The adjacent sequences of mapped sRNAs were extracted as candidate miRNA precursor sequences (details in the miRDeep-P2 manual). The secondary structures of all candidates were predicted by RNAfold (version 2.1.2; Tav et al., 2016). The newly updated plant miRNA criteria (Axtell and Meyers, 2018) were employed to identify miRNAs.

To annotate the conservation of miRNAs in lettuce, all the predicted mature miRNA sequences with ± 1 nt adjacent nucleotide were aligned with all plant miRNAs in PmiREN1.0 (Guo et al., 2020), with no more than two mismatches, using Bowtie (version 1.2.2; Langmead, 2010) software. Those with no matched miRNAs in PmiREN1.0 were assigned as lettuce-specific miRNAs, while those which only hit miRNAs in other Asteraceae species were considered Asteraceae-specific miRNAs, and others were annotated as conserved.

Synteny Analysis of Identified MicroRNAs

The synteny analysis of miRNAs was carried out using JCVI (MCscanX python version 1.1.18; Wang et al., 2012). Firstly, the transformed Browser Extensible Data (BED) file and protein sequences were set as input files, and the collinearity blocks across the whole lettuce genome were obtained. Subsequently, the genomic locations of all miRNAs were reflected to these collinearity blocks via BEDTools (version 2.26.0; Quinlan and Hall, 2010; subfunction: intersect), and members from the same miRNA family that followed similar gene orders in these collinearity blocks were considered as syntenic miRNAs. The result plot was generated with Circos (version 0.69.9; Krzywinski et al., 2009).

Targets Prediction of Identified MicroRNAs

Two plant miRNA target prediction toolkits, psRNATarget (Dai et al., 2018) and RNAhybrid (Kruger and Rehmsmeier, 2006), were used to predict miRNA targets. The identified lettuce miRNA sequences and mRNA transcript sequences were uploaded to psRNATarget webserver[2] and the latest default parameters (2017 release) were used. Targets with an *E*-value ≤ 3.0 were kept as possible miRNA targets. Meanwhile, RNAhybrid (version 2.1.2) was used to predict energetically plausible miRNA-mRNA duplexes with plant-specific constraints where "−*d*" parameter was set as "8,12." A strict cut-off value for minimum free energy/minimum duplex energy of 0.75 was used (Alves et al., 2009).

Degradome-seq (PARE-seq) data downloaded from GEO datasets (SRP078275) were also used to predict miRNA targets. CleaveLand4.0 (Addo-Quaye et al., 2009) software was used to identify putative miRNA cleavage sites with default settings. The reads were aligned to lettuce transcript sequences to generated density files. The predicted miRNA mature sequences were aligned to transcript sequences to identify potential miRNA target sites. The density distribution of reads and miRNA-mRNA alignment were used together to classify miRNA target candidates. All potential miRNA targets were assigned into one

[2]https://www.zhaolab.org/psRNATarget/

of five categories, and to reduce false positives, only results from categories 0, 1, and 2 were retained.

MicroRNA and mRNA Expression Analysis

For miRNA expression, expression of mature and star miRNAs was normalized by RPM. For each sRNA-seq dataset, reads mapped to pri-miRNAs (no mismatches allowed) and localized in genomic positions of mature miRNAs (no more than 2-nt shift allowed) were considered to correspond to mature miRNAs. The total numbers of these reads were counted to calculate the RPM for the mature miRNAs.

For mRNA expression, all raw mRNA reads were checked by Fastqc (version 0.11.9; Brown et al., 2017) and low-quality reads and adapters were removed by Cutadapt (version 3.2; Kechin et al., 2017). Clean reads were aligned to the lettuce genome using HISTAT2 (version 2.1.0; Kim et al., 2019). StringTie (version 2.1.5; Pertea et al., 2015) was used to assemble the transcript and quantify each mRNA-seq dataset. The expression values of transcripts were normalized by fragments per kilobase per million fragments (FPKM) and the results of StringTie were extracted.

Correlation Analysis Between the Expression of MicroRNAs and Predicted Targets

The Pearson correlation coefficient between the expression matrix of miRNAs and targets was calculated using the R function "cor.test()." Firstly, according to the biological replicates of four tissues, the raw expression matrix of miRNAs and targets were averaged and transposed by the R function "*t*()" to obtain a matrix with miRNAs and targets as factors. Then, the "for loop" of R language, was used to calculate the correlation coefficient between each miRNA and target, and a Student's *t*-test was used to test significance. The results were displayed by the R package (Pheatmap), where blue bars showed positive correlation, red bars showed negative correlation, and a *P*-value of <0.05 is presented as "*" (**Figure 3A**).

Network Construction

For the miRNA network, TFs of lettuce were annotated by searching all mRNA transcripts of lettuce against TF datasets from PlantTFDB[3] (Jin et al., 2017), and the default filtered result was kept. Upstream 2000 nts were extracted as putative promoter sequences for each pre-miRNAs and miRNA target transcripts, and then submitted into PlantRegMap webserver[4] (Tian et al., 2020) to scan TF binding sites. FFL motifs were selected by an in-house perl script based on these interactions between TFs-miRNAs, miRNAs-targets and TF-miRNA targets. Then, a genome-wide miRNA network was constructed in terms of all FFL motifs and Cytoscape (version 3.7.1; Shannon et al., 2003) was employed to display the network structure (**Figure 5B**).

[3]http://planttfdb.gao-lab.org/prediction.php

[4]http://plantregmap.gao-lab.org/

Construction of Plant Expression Vector and Lettuce Transformation

To construct the miR408 overexpression vector, genomic DNA of lettuce containing pre-miR408 was PCR amplified using the primers MIR408-F/R (**Supplementary Table 22**). This fragment was then cloned into pBI121 vector after *Xba*I and *Sac*I double digestion, to create the MIR408-overexpressing vector 35S:MIR408. The vector containing the overexpression cassette for MIR408 was then introduced into the *Agrobacterium tumefaciens* strain EHA105 by the freeze-thaw method. Cotyledon explants of lettuce plants were transformed with Agrobacterium EHA105 containing the 35S:MIR408 construct, following the reported protocol.

Quantitative RT-PCR

Total RNA from lettuce was reverse transcribed using the Maxima First Strand cDNA Synthesis Kit (Thermofisher, United States). The resultant cDNA was analyzed by SYBR premix Ex Taq (ABMgood, United States) with the CFX96 Touch System (Bio-Rad, United States). The PCR protocol was 95°C for 30 s, 40 cycles of 95°C for 1 min, and 60°C for 10 s. 18S ribosomal RNA was used as the internal control gene. Total small RNA was extracted by the miRcute miRNA Isolation Kit (TianGen, China), following the manufacturer's instructions. Reverse miRNA transcription was conducted using the miRcute Plus miRNA First-Strand cDNA SynthesisKit (TianGen, China). The resultant cDNA was analyzed using the miRcute miRNA qPCR Detection Kit, SYBR Green (TianGen, China), with the CFX96 Touch System (Bio-Rad, United States). PCR was performed under the following conditions: 95°C for 15 min, 34 cycles of 94°C for 30 s, and 60°C for 34 s. U6 snRNA was used as the reference gene. PCR reactions were carried out with three biological replicates and each biological replicate was performed with four technical repeats. The results were calculated using the $2^{-\Delta\Delta Ct}$ method. All primers used for qRT-PCR analysis are listed in **Supplementary Table 22**.

RESULTS

Comprehensive Identification and Annotation of MicroRNAs in Lettuce

To comprehensively identify miRNAs in lettuce, sRNA libraries from different tissues, including leaf, stem, root and flower, were prepared in duplicate (details in section "Materials and Methods") and observed with well consistency (**Supplementary Figure 1A**). These eight libraries produced 240 million raw reads and 235 million clean reads (**Supplementary Table 1**). Length distribution of these sRNA libraries showed two peaks at 21 and 24 nt in both clean and unique sRNAs, potentially reflecting the abundance of miRNAs and small interference RNAs (siRNAs), respectively (**Figures 1A,B** and **Supplementary Tables 2**, **3**). The large decrease at 21 nt from clean to unique read distributions further supports this speculation (**Figures 1A,B**) because, in general, miRNAs prefer to accumulate many identical reads, while siRNAs possess much greater

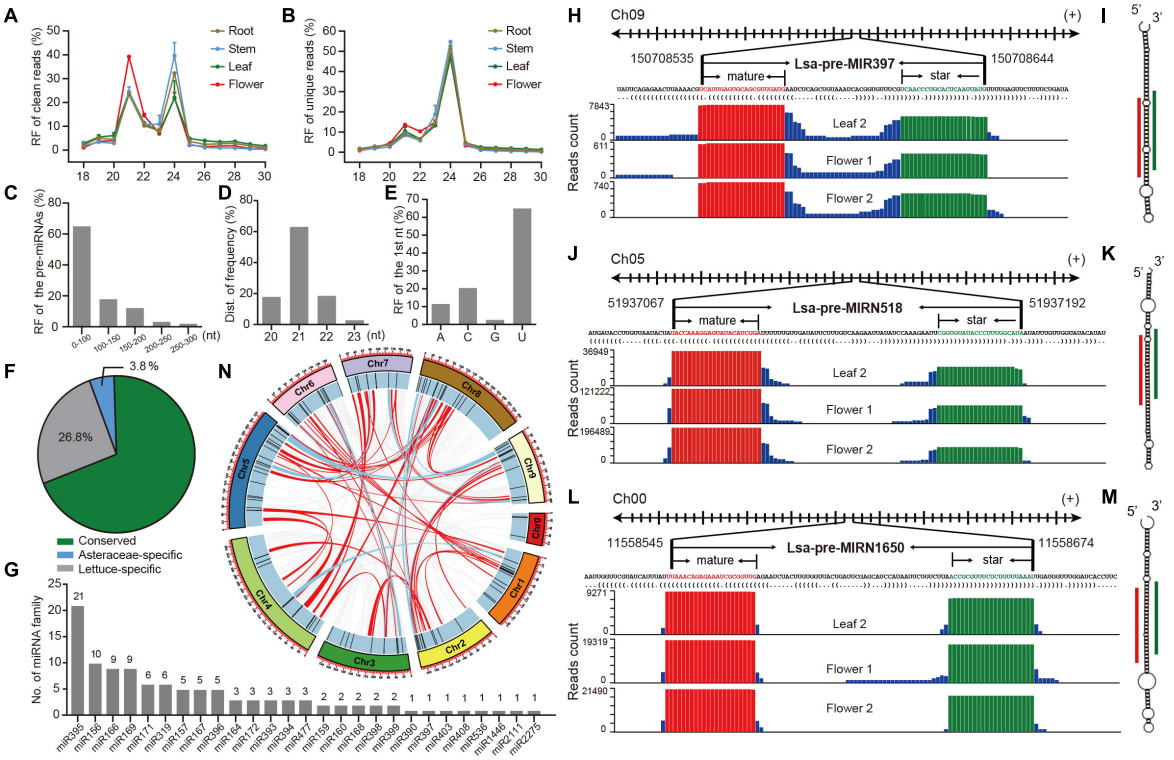

FIGURE 1 | Identification and annotation of miRNAs in lettuce. **(A,B)** Relative frequency (RF) in length of clean and unique reads, respectively, from sRNA libraries in different tissues. **(C)** RF of pre-miRNAs in length. **(D)** RF of mature miRNAs in length. **(E)** RF of the first nucleotide (nt) of mature miRNAs. **(F)** The proportion of conserved, Asteraceae-specific and lettuce-specific miRNAs. **(G)** Member numbers of conserved miRNA families. **(H,J,L)** Examples of conserved, Asteraceae-specific, and lettuce-specific miRNA candidates, miR397, miRN518, and miRN1650, respectively. For each miRNA, presented information includes pri-miRNA excerpt, pre-miRNA, secondary structure in dot-bracket notation, and read abundance along the precursor. Letters with red and green colors indicate mature and star miRNAs, respectively, while the histogram shows the copy number of small reads from sRNA libraries. **(I,K,M)** Respective secondary structures of pre-miR397, pre-miRN518, and pre-miRN1650, predicted by RNAfold. Red lines indicate positions of mature miRNAs, while green lines show positions of miRNA stars. **(N)** Synteny analysis of lettuce miRNAs across all pseudo-chromosomes. Red lines indicate miRNAs are located in synteny blocks while light blue lines indicate there are paired miRNAs in synteny blocks.

sequence diversity (Carthew and Sontheimer, 2009; Axtell and Meyers, 2018). Compared to other tissues, abundance at the 21-nt peak is higher than that at 24-nt in the flower (**Figure 1A**), suggesting higher miRNA activities in flower tissue.

MiRDeep-P2 (Kuang et al., 2019) was employed to identify miRNAs when only 19–25 nt reads were selected as inputs. Filtered with strict plant miRNA criteria (Axtell and Meyers, 2018), 157 miRNA loci, belonging to 67 families, were annotated (**Supplementary Table 4**). Several features of the miRNA loci were scanned, and most of their precursors, accounting for 80%, were less than 150 nts (**Figure 1C**), and the length of mature miRNAs were predominantly 21 nts (**Figure 1D**), while the first nucleic acid of mature miRNAs is frequently U (**Figure 1E**). All of these observations meet plant miRNA characteristics, as indicated by previous research (Axtell and Meyers, 2018), suggesting that the identification and annotation is reliable. A conservation search against all miRNA entries in PmiREN1.0 (Guo et al., 2020), found that 109, including 27 families, are conserved since their counterparts could be found in other non-Asteraceae species, while only six are considered Asteraceae-specific, because counterparts were only detected in Asteraceae species. Forty-two items were annotated as lettuce specific, considering no conserved ones were detected (**Supplementary Table 4** and **Figure 1F**). Among the conserved families, miR395 has the most abundant members, while the other 18 families have multiple members (**Figure 1G**). The annotation for each miRNA includes all relevant information, including genomic location, sequences (**Supplementary Table 4**), secondary structure, and reads signature along precursors. **Figures 1H–M**, show conserved, Asteraceae-specific and lettuce-specific examples, respectively. Standard stem-loop structure and reads signature, such as the accumulation at mature and star miRNAs, strongly support them being highly confident candidates.

The miRNA clusters were further scanned, and nine clusters were obtained when a cluster region length not exceeding 10 kb was defined (**Supplementary Table 5**). There were four miR395 clusters, containing 13 miR395 members (61.2% of 21 miR395s), indicating why miR395 is the most abundant miRNA family, and its family expansion may be due to segmental duplication after a tandem duplication, considering all four clusters are located at the same chromosome (**Supplementary Table 5** and

Figure 1G). Since there exists a whole genome triplication (WGT) event during the evolution of the lettuce genome (Reyes-Chin-Wo et al., 2017), the WGT impact on miRNA selection was further investigated. Interestingly, even though there are clearly numerous synteny blocks (**Supplementary Tables 6**, **7**), only six were kept in two-paired synteny blocks after the WGT event (**Supplementary Table 7**); most duplicated miRNA members were lost during the genome evolution (**Figure 1N**).

Expression Patterns of Lettuce MicroRNAs in Different Tissues

The replicated tissue samples enabled a systematic examination of the expression patterns of lettuce miRNAs. Normalized by reads per million (RPM), the complete expression profile of 157 miRNAs was obtained (**Figure 2A**, **Supplementary Table 8**, and **Supplementary Figure 1B**). In general, conserved miRNAs had higher average expression (**Figure 2B**). MiRNAs varied in their expression patterns, and some were consistently highly expressed in different tissues, while some varied significantly between different tissues (**Figure 2A**). When the low ($<$10 RPM) and high expression ($>$500 RPM) was defined, approximately 16 miRNAs were consistently highly expressed in different tissues, such as house-keeping genes, which account for 10% of all miRNAs (**Figures 2C,D**), while 31 miRNAs were highly expressed in a specific tissue (**Figures 2C,E**). Over half of the miRNAs were expressed at an ordinary level, and approximately 14% were had constantly low expression (**Figure 2C**). To further explore the expression pattern of miRNAs in different tissues, a *k*-means cluster analysis was performed. When $k = 16$, the expression patterns of all miRNAs could be separated well (**Figure 2F**, **Supplementary Figure 2**, and **Supplementary Table 8**).

Differently expressed miRNAs were compared among the sampled tissues. In general, 35 to 64 miRNAs were up or down-regulated between a pair of tissues (**Figures 2G,H**, **Supplementary Figure 3A**, and **Supplementary Table 9**), but less than 10 of them were differently expressed in multiple tissues (**Figure 2I**). Analysis of a specific miRNA or miRNA family identified that, as in other species, miR166 is the house-keeping miRNA, highly expressed in all examined tissues (**Figure 2D**). As expected, considering their roles in the transition between juvenile and adult, miR156 was highly expressed in juvenile leaf tissue, while miR172 was highly expressed in flower tissue (Wang et al., 2009; Wu et al., 2009; **Figure 2E**). However, Lsa-miR156i, an miR156 member, was highly expressed in flower tissue (**Figure 2E**). Meanwhile, a number of lettuce-specific miRNAs were consistently highly expressed in all tissues, including Lsa-miRN1709, Lsa-miRN1652a/b, and Lsa-miRN1664 (**Figure 2D**), and some of them, including Lsa-miRN1, Lsa-miRN40, Lsa-miRN69 (**Figure 2E**), were highly expressed in a specific tissue. This was less common, as species-specific miRNAs, in general, had low expression (Yang et al., 2021).

Integrative Target Identification of Lettuce MicroRNAs

To elucidate the function of miRNAs in lettuce, a combination of computational methods and high-throughput experiments were employed to explore potential miRNA targets. Two computational tools, psRNATarget and RNAhybrid with strict selection criteria (details in Materials and Methods), were first used to predict miRNA targets, with 157 miRNAs and all annotated transcripts of lettuce as inputs. The CleaveLand4.0 (Addo-Quaye et al., 2009) with PARE-Seq data was employed to further detect miRNA targets, where only categories 0–2 were kept for high confidence. As shown in **Figure 3A**, the "union" includes 157 miRNAs and 3,629 transcripts, comprised of 6,540 miRNA-target regulatory pairs when the result from these three methods was united, while the "intersection" possesses 152 miRNAs and 658 transcripts if only the intersected result was kept by at least two methods (**Supplementary Table 10** and **Supplementary Data 1**).

Among the regulatory pairs between these miRNAs and target genes, almost all conserved regulatory relationships that have been studied or reported in model plants, such as Arabidopsis, rice, and maize, were detected, indicating that the predictions are reliable (**Supplementary Table 10**). A number of new regulatory relationships were also discovered. For example, the target genes of conserved miR172 and miR396 can be TFs, ERF and WRKY, respectively, and these predictions are well supported by the PARE-Seq data (**Supplementary Data 1**). In addition, the regulatory relationships between many miRNAs specific to Asteraceae or lettuce and their target genes were discovered. For example, TFs, Dof, and ERF, could potentially be regulated by Lsa-miRN1655 and Lsa-miRN69, which is strongly supported by the evidence (**Supplementary Table 10** and **Supplementary Data 1**). **Figure 3B** shows six examples: miR157a and miR156j are representatives of conserved miRNAs, miRN518 is Asteraceae-specific, while miRN28 is lettuce-specific. All of the regulatory pairs are well supported by PARE-Seq results.

To understand the overall situation of miRNA target genes at the genome-wide level, GO and KEGG enrichment analyses were performed on all miRNA target genes. In GO, biological process (BP) analysis showed the largest enrichment groups were protein binding, protein kinase activity, protein phosphorylation, and signal transduction (**Figure 3C** and **Supplementary Table 11**). In the cellular component analysis, the largest enriched group was nucleus, indicating that a large part of the gene regulated by miRNAs functions in the nucleus. In molecular function analysis, the most abundant genes were related to cellular process, ATP and ADP binding, and various enzyme activities. KEGG enrichment analysis identified signaling pathway or transduction as the main enriched pathways (**Figure 3D** and **Supplementary Table 12**). These are all closely related to miRNAs as regulatory factors and its a large class of target genes, TFs, such as the transmission and transduction of various signals, and functions in the nucleus. The TFs that miRNAs can regulate were investigated further, and 41/23 families with different constrictions were identified (**Figure 3E**).

Expression Correlation Between MicroRNA-Target Regulatory Pairs

Identifying expression patterns of miRNAs and targets in different tissues provides strong evidence for determining

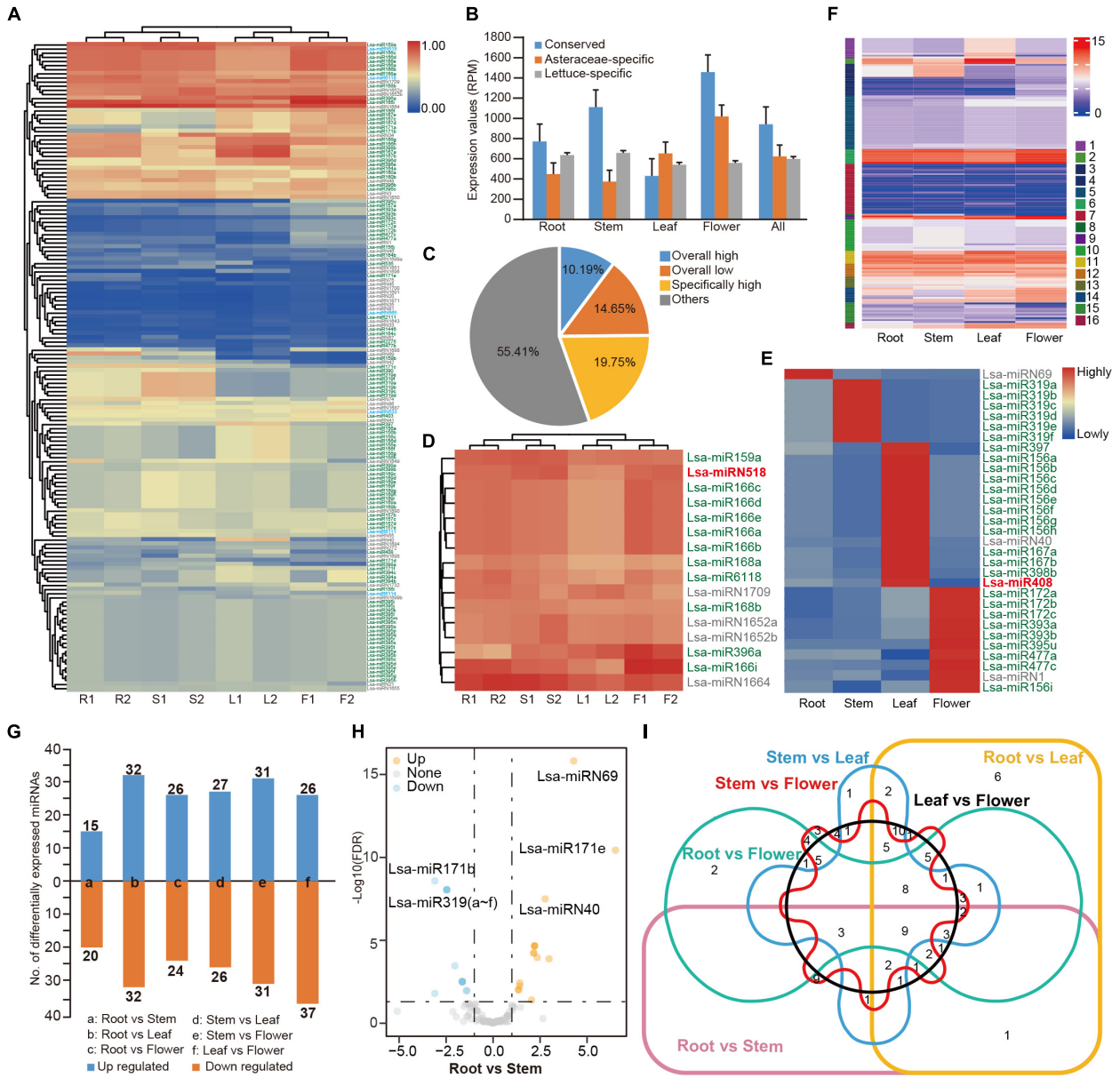

FIGURE 2 | Expression profile of miRNAs in lettuce. **(A)** Heat map of expression profile of 157 miRNAs in four tissues. miRNA IDs with green, blue, and gray colors represent conserved, Asteraceae-specific, and lettuce-specific miRNAs, respectively. R1 and R2 indicate two samples from root tissue while S, L, and F represent samples from stem, leaf and flower, respectively. **(B)** Average expression values of three types of miRNAs. Values were normalized by reads per million (RPM). **(C)** The percentage of miRNAs based on expression pattern. Overall high, low, and specifically high, indicate miRNAs with high or low expression in all tissues, or with high expression in specific tissues, respectively. **(D)** Highly expressed miRNAs (house-keeping miRNAs) in all tissues. **(E)** Tissue-specific highly expressed miRNAs. **(F)** Expression pattern categories by k-means cluster analysis (k = 16). **(G)** Differentially expressed miRNAs in a paired-tissue comparison. **(H)** Volcano plot displaying differentially expressed miRNAs between root and stem. **(I)** Venn diagram showing the differentially expressed miRNAs in six paired-tissue comparisons.

whether there is a real regulatory relationship between them. High-throughput sequencing enables the identification of expression patterns between miRNAs and target genes in batches. To further confirm the regulation between miRNAs and target genes, the mRNAs were sequenced from four tissues, as before. Principal component analysis showed consistency between mRNA and miRNA samples, indicating the reliability of these data (**Supplementary Figures 1**, **4**). The expression patterns of all potential miRNA targets were obtained from these four tissues. To understand these miRNA-target regulatory pairs, a matrix analysis of the expression patterns of all miRNAs and their targets was pioneered (**Figure 4A** and **Supplementary Table 13**). Considering one miRNA can regulate multiple targets, the same target can inversely accept regulations from different miRNAs, and differential spatiotemporal expression exists between miRNAs and targets; thereby a complex matrix

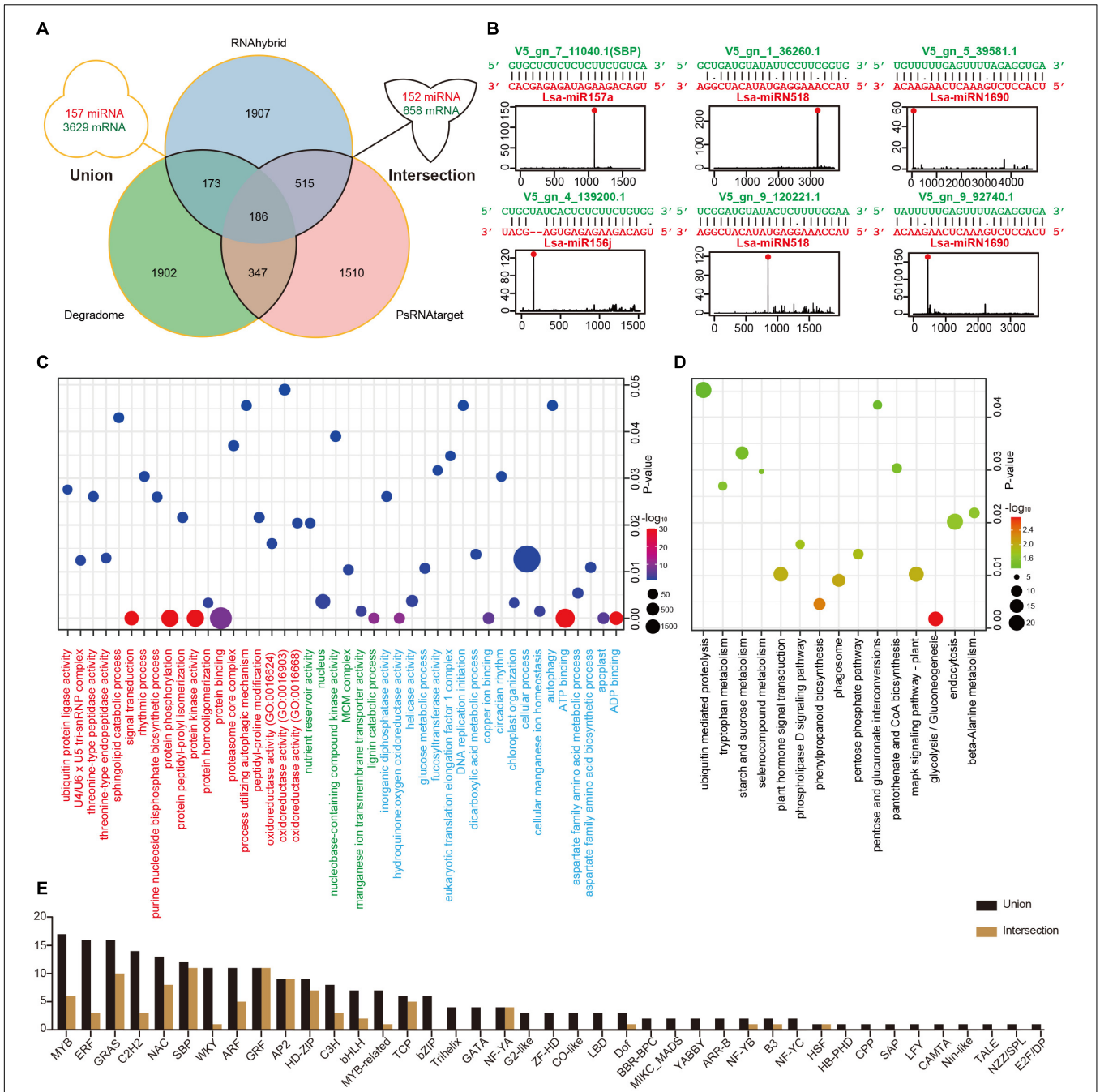

FIGURE 3 | Target identification of miRNAs in lettuce. **(A)** Potential miRNA targets identified via three methods. The "intersection" indicates targets detected by at least two methods, while the "union" shows all targets predicted by any of the three methods. **(B)** Examples of high confidence miRNA-target pairs. Six pairs represent conserved (Lsa-miR156j, Lsa-miR157a, and their targets), Asteraceae-specific (two circuses of Lsa-miRN518), and lettuce-specific (two circuses of Lsa-miRN1690) examples, respectively. **(C)** Gene Ontology (GO) enrichment analysis of miRNA targets. Terms under red, green, and blue present the enrichment analyses in three ontologies, biological process (BP), cellular component (CC), and molecular function (MF), respectively. **(D)** Kyoto Encyclopedia of Genes and Genomes (KEGG) enrichment analysis of miRNA targets. **(E)** List of transcriptional factor families regulated by miRNAs. The "intersection" and "union" are the same as described in **(A)**.

was formed (**Figure 4A**). Interestingly, although these miRNAs and their targets potentially only have a negative regulatory relationship in a specific tissue, the entire matrix showed good support for the negative regulation of miRNAs and target genes (**Figures 4A,B**). Data analysis based on "intersection" datasets showed that >46% of the miRNA-target pairs support a strict negative regulatory relationship ($R < = 0.9$, $P < 0.05$, **Figure 4C**).

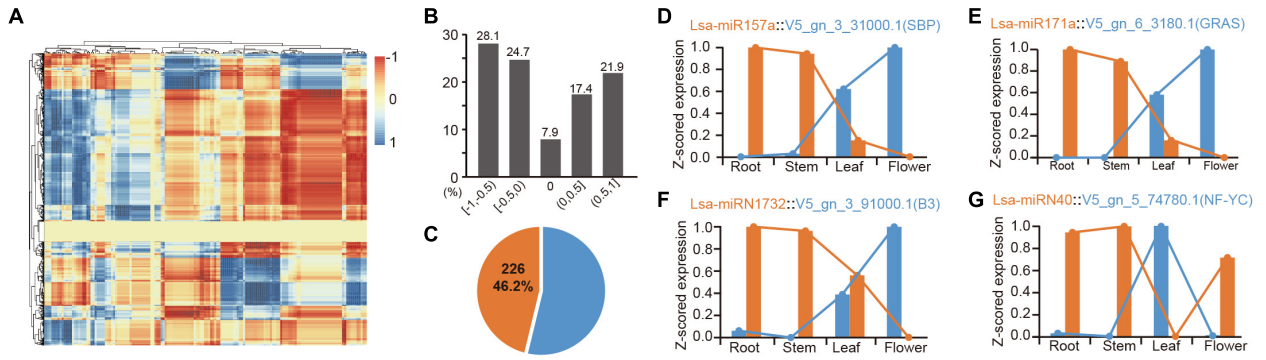

FIGURE 4 | Expression correlation of miRNAs and their targets. **(A)** The heatmap of expression correlation of all miRNAs and their targets. Each dot indicates a value of expression correlation of a miRNA, and one of its specific target. Color range shows the variation from totally positive (1) to full negative (−1) correlation. **(B)** Distribution of miRNA-target expression correlation in divided sections. The five respective sections from −1 to 1, are $-1 \leq R < -0.5$ ([−1, −0.5]), $-0.5 \leq R < 0$ ([−0.5, 0]), $R = 0$ [0], $0 < R \leq 0.5$ ([0, 0.5]), and $0.5 < R \leq 1$ ([0.5, 1]), where R indicates the correlation values between miRNA and target expression. **(C)** Percentage of high confidence negative correlation: over 46% of these correlations are high confidence ($R < -0.9$, $P < 0.05$). **(D,E)** Two representative examples of negative correlation of conserved miRNAs. **(F,G)** Two representative examples of negative correlation of lettuce-specific miRNAs.

There are numerous classic cases, such as the expression pattern of miR156 and miR172 in these tissues, which are well supported for their role in developmental transition (Wang et al., 2009; Wu et al., 2009; **Supplementary Table 13**). MiR157a is a good example, where Lsa-miR157a and its target V5_gn_3_31000.1, a gene harboring SBP (Squamosa-promoter binding protein) domain, have a reverse expression pattern in the four tissues (**Figure 4D**). Lsa-miR171a is another representative conserved miRNA, whose target, V5_gn_6_3180.1, a GRAS transcriptional factor, has opposite expression patterns (**Figure 4E**). A number of novel regulatory relationships were also revealed, including the relationship between the Asteraceae- and lettuce-specific miRNAs (**Supplementary Table 13**). **Figures 4F,G** lists the two representative lettuce-specific examples that have a strong negative correlation.

Regulatory Network Exploration of Lettuce MicroRNAs

The regulatory elements of miRNAs and target genes do not exist independently, and further constitute a regulatory network. Taking into account the particularity of TFs, that is, they are important miRNA targets that can, in return, regulate miRNA expression, a regulatory network was explored, with TFs, miRNAs, and targets as basic elements. First, miRNA targets from 23 TF families were collected (**Figure 3E**), then the promoter sequences of miRNAs and target genes were extracted, and by a search of known binding motifs of these 23 TFs, a preliminary regulatory relationship of TFs on miRNA and miRNA target genes was constructed. At the same time, using the predicted regulatory relationship between miRNAs and targets, the regulatory relationship between miRNA and target genes was determined (**Figure 5A**). In detail, 1,051 interactions were found between TFs and miRNAs, named TMIs, and 73,133 interactions identified between TFs and miRNA targets, so called TTIs. Together with the 6,540 interactions predicted between miRNAs and targets (MTIs), 46,083 cascades binding TMIs and MTIs were achieved, and 43,554 FFL motifs were constructed (**Figure 5A**). Based on these FFLs and the links crossing them, a complex regulatory network with TFs, miRNAs, and targets was constructed (**Figure 5B**).

The regulatory network was constructed to further understand the regulation between miRNAs, as the core, and a combination of TFs and target genes. In this network, any element centered on a specific miRNA can independently become a module. For example, miR408 accepts regulations from four TFs, and a dozen targets could be regulated by both miR408 and these four TFs (**Figure 5C**). As described previously, Lsa-miRN518 is an Asteraceae-specific miRNA (**Figure 2D**), and its 30 targets can also be regulated by several TFs (**Figure 5D**). **Figure 5E** shows a lettuce-specific miRNA, Lsa-miRN46, which has a relatively simple FFL module. When the function of each gene was added into these modules, their functions could be further determined. Using **Figure 5F** as an example where all non-TFs and non-miRNA nodes were filtered out, the regulatory network uncovered numerous new links between miRNAs and TFs. In this two particles of the large network, regulations between MYB to miR156, miR156 to SBP, and miR396 to GRF and WRKY, and miR166 to HD-ZIP, have been well established by previous studies (Wu et al., 2009; Zhu et al., 2011; Liebsch and Palatnik, 2020). However, this data supports that more TFs could regulate miR156, and the targets of miR156 could further regulate the modules of miR399 and miRN565. Moreover, more modules are involved in the regulation network of miR396 and miR166, forming a seven-layer network system. Based on the known functions of these miRNAs and TFs, these two network particles, could potentially be involved in development, circadian clock, flowering, response to insect damage and environmental challenges, etc.

Functional Study of Lsa-MIR408

The above expression pattern analysis indicated that Lsa-miR408 is highly expressed in leaf, while Lsa-miR408 as a hub gene is in

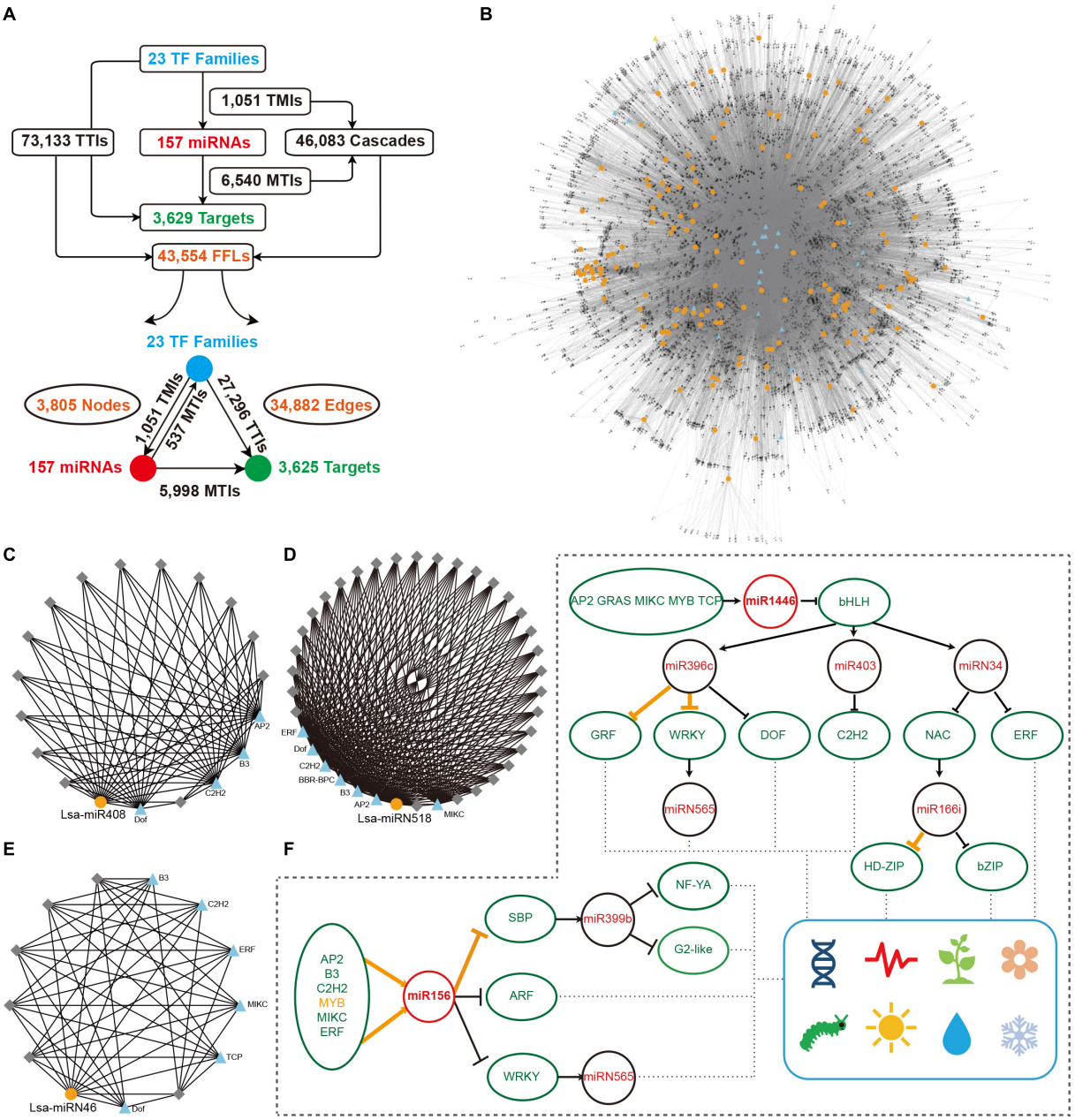

FIGURE 5 | Construction of miRNA regulatory network. **(A)** Overall interactions and feed forward loops (FFLs) in an miRNA regulatory network. **(B)** Entire regulatory network based on all FFLs. Blue triangles and gray diamonds represent transcriptional factors (TFs) and targets, respectively, while yellow dots indicate miRNAs. **(C–E)** Examples of a local FFL network hubbed by three miRNAs: Lsa-miR408, Lsa-miRN518; and Lsa-miRN46. Blue triangles and yellow dots represent TFs and miRNAs, respectively, while gray diamonds indicate targets that could be regulated by these TFs and miRNAs. **(F)** A particle of miRNA and TF regulatory network. Orange lines show the regulations have been validated in other species, while black lines indicate new regulatory relationships expanded by this regulatory network. These expanded networks might be related to development, circadian clock, flowering, responses to insect and environmental challenges, etc. TMI: TF and miRNA interaction; MTI: miRNA and target interaction; and TTI: TF and target interaction.

the miRNA regulatory network (**Figure 5E** and **Supplementary Table 20**). In addition, previous (Zhao et al., 2016; Zhang J. P. et al., 2017; Pan et al., 2018) research shows that miR408 is highly conserved in the plant kingdom, and has multiple roles in different life activities, especially in promoting growth which is critical to leafy vegetables. Thus, to further verify the function of the miRNA regulatory network, miR408 was chosen as an example, and a series of experiments were carried out. **Supplementary Table 4** shows that only one miR408 locus was identified, namely Lsa-MIR408, which has a standard stem-loop and a comparable secondary structure to model species, such as Arabidopsis thaliana (**Supplementary Figure 6A**).

Target gene prediction, together with the PARE-Seq experiment, identified that the top three targets of Lsa-miR408 are copper related genes: basic blue protein (LsaBBP), blue copper protein (LsaBCP), and copper-transporting ATPase PAA2 (LsaPAA2; **Figures 6A–C**, **Supplementary Figure 6B**, and **Supplementary Table 21**). Furthermore, two of the top three targets of Ath-miR408 are shared with Arabidopsis (**Supplementary Figures 6C–E**), suggesting that *Lsa-MIR408* might have similar functions as its companion in Arabidopsis. To further explore its function, an Lsa-miR408 overexpression construct was conducted and introduced into lettuce by *A. tumefaciens*-mediated plant transformation (see section "Materials and Methods"). Compared with wild type plants (WTs), eight independent transgenic lines showed higher accumulation of mature miR408, and were designated as OE/408OE (**Figure 6D**). Based on the expression level of miR408, three transgenic lines, OE-2, OE-5, and OE-6, were used in subsequent experiments. To test whether the higher expression level of miR408 is functional, the expression level of three target genes was examined. Quantitative reverse transcription PCR showed that expression of three targets was significantly suppressed in the three independent transgenic lines (**Figure 6E**), indicating that constitutive expression of miR408 is functional.

Compared to WTs, 408OE plants showed increased growth vigor, exhibiting larger leaves and longer petiole at the seedling stage (**Figures 6F–J**). The petiole of left side blade of 15-day seedlings was used as representatives to quantitatively detect differences in petiole length. Petiole length of 408OE plants increased by 20% (**Figures 6G,H**). At the harvest stage, transgenic plants showed a significant improvement in vegetative development and size (**Figure 6I**). Thus, 50-day 408OE plants were weighed, and were significantly heavier (a 15% increase) than the respective control (**Figure 6J**). Achenes in the transgenic line were also significantly larger than those of WTs (**Figures 6K,L**), and the achenes of 408OE plants were 20% longer than the controls (**Figure 6L**). All of these phenotypic changes are comparable to these in Arabidopsis (Jiang et al., 2021) and rice (Zhang J. P. et al., 2017), suggesting the similar molecular mechanism of miR408 exists in lettuce.

DISCUSSION

The systematic identification and annotation of miRNAs is the first step in studying their functions in a specific species. In this study, based on the lettuce reference genome (Reyes-Chin-Wo et al., 2017), miRNAs in lettuce were systematically annotated by sRNA sequencing and the plant miRNA identification pipeline (Kuang et al., 2019) developed by our laboratory. For the 157 high confidence miRNAs, detailed basic information is provided, such as sequences, locations, structures, miRNA clusters, etc., as well as an analysis of the overall characteristics of these miRNAs, such as the length distribution of precursors, the base preference of the first nt of mature miRNA, conservation between species, and the first attempt to scan their selection after the WGT event. Furthermore, the expression pattern of these miRNAs in four selected tissues was established through sRNA sequencing. The combination of these analyses provides a strong foundation for understanding and mining miRNA functions in lettuce.

The function of a miRNA is mainly reflected in its targets, and accurate prediction of miRNA targets is critical for exploring miRNA functions. Through the psRNATarget (Dai et al., 2018) and RNAhybrid (Kruger and Rehmsmeier, 2006) pipelines, and high-throughput experimental verification, PARE-Seq, all potential target genes of miRNAs in lettuce were systematically identified. GO and KEGG analyses identified the diversity of these miRNA target genes, and also explained the significance of miRNA functions, being involved in almost all biological activities (Mi et al., 2019). According to the analysis of TFs, many conservative regulations were also detected in lettuce, such as miR156-SPB, miR172-AP2, etc., confirming reliability of these data. In addition, the expression patterns between miRNAs and their targets in different tissues were correlated: although the expression correlation among them is highly complicated, a general negative expression correlation was observed between miRNAs and their target genes.

In the past few years, plant miRNA research has continued to expand, and new functions of well-studied miRNAs are being continuously discovered. For example, miR156 research has moved beyond its role in development transition, and new functions in seed dormancy have been discovered (Miao et al., 2019), while the miR168-AOG1 module has a newly discovered role in plant immunity (Wang H. et al., 2021). At the same time, the study of the miRNA regulation network is becoming increasingly popular because it can promote the discovery of new miRNA functions or regulatory mechanisms. To this end, the miRNA regulatory network in lettuce was constructed, which centered on miRNAs and combined upstream TFs and downstream target genes. Since TFs are also an important class of miRNA target genes, the FFL motifs composed of miRNAs, miRNA targets, and TFs are powerful way to understand the miRNA regulatory network. The regulatory network constructed in this study, not only verified the conserved regulatory relationships found in other species, but discovered numerous novel regulatory modules and potential new connections between different modules. For example, a particle of this network displayed in **Figure 5F** could be involved in many biological activities, as the regulatory network centered on miR156, miR396, and miR166 has been expanded.

To further confirm the function of this regulation network, miR408 was selected as an example, given its role in promoting vegetative growth in model species (Zhao et al., 2016; Zhang J. P. et al., 2017; Pan et al., 2018). As one of the most commercially important leafy vegetables, accelerating vegetative growth and increasing the fresh weight are of great significance to the lettuce industry. Thus, via genetic experiments, the function of miR408 was verified. Compared with WT lettuce, the fresh weight of the over-expressed *Lsa-MIR408* lines was significantly increased. More interestingly, the plants overexpressing *Lsa-MIR408* can bear larger achenes, which has important potential for lettuce breeding and industrial application. Lettuce achenes in general are very small; therefore, increasing achene size is beneficial to mechanized achene screening and planting, as well as potentially increasing the yield of oil-rich achene

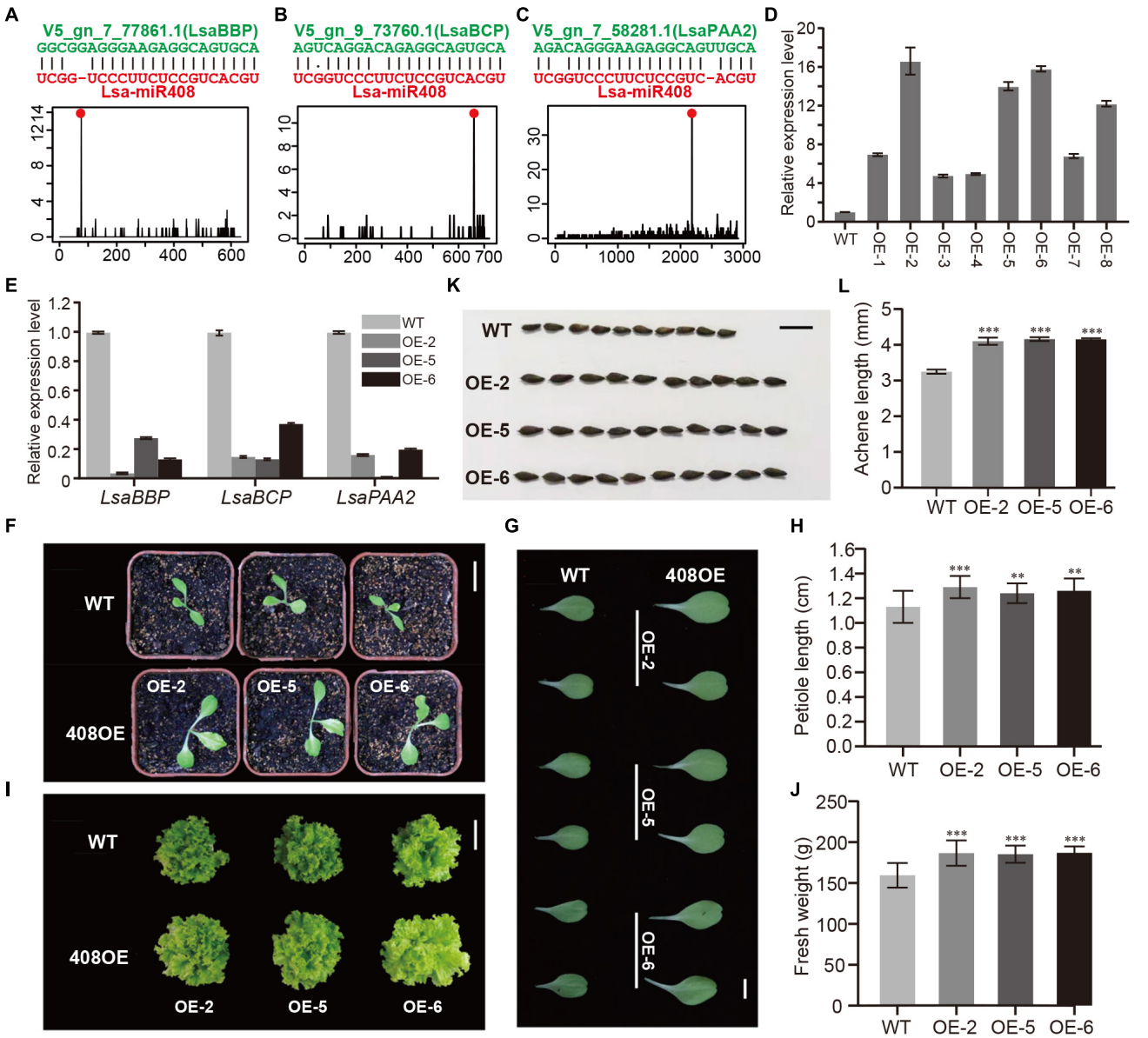

FIGURE 6 | Functional study of Lsa-miR408. **(A–C)** Sequence alignments and degradome profiles of three target genes of Lsa-miR408. The top of each panel shows miRNA-target alignment, while the bottom diagram represents the reads count of degradome data across the target transcript, where the red dot indicates miRNA cleavage site. **(D)** Relative expression levels of miR408 in transgenic lines and wild-type (WT) plants through qRT-PCR analysis. **(E)** Relative expression levels of three target transcripts in three transgenic lines and WT plants by qRT-PCR analysis. **(F)** 12-day seedlings of WT and three transgenic lines, bar = 5 cm. **(G)** Comparison of 12-day cotyledons between WT and three transgenic lines, bar = 1 cm. **(H)** Quantitative measurement of petiole length of 12-day WT and 408OE plants, bar = 1 cm. **(I)** Size comparison of 50-day WT and 408OE plants (top view), bar = 15 cm. **(J)** Quantitative measurement of fresh weight of 50-day WT and miR408-OE plants. **(K)** Comparison of achene morphology and achene size between WT and 408OE plants, bar = 50 mm. **(L)** Quantitative measurement of achene length of WT and 408OE lines. Among these panels, OE/408OE indicates the transgenic lines in which *Lsa-MIR408* was overexpressed. Error bars represent standard deviations (SDs), the number of plants and achenes for quantitative measurement are 20 and 30, respectively, $P < 0.01$ (**), and $P < 0.001$ (***) by Student's *t*-test.

lettuce, as described in watermelon (Wang Y. et al., 2021). The example of miR408 demonstrates the significance of constructing the miRNA regulatory network for understanding miRNA functions.

In brief, as an important economic crop and a representative Asteraceae species, research on the variation in morphology, color selection, and domesticated trait evolution of lettuce is very limited. Here, miRNAs in lettuce were systematically identified and annotated, and a comprehensive miRNA regulatory network was constructed. This research lays the foundation and provides resources for studying the functions of miRNAs in lettuce, and also provides new ideas for lettuce research and breeding.

DATA AVAILABILITY STATEMENT

The sequencing data for this study can be found in the NCBI Sequence Read Archive (SRA) under accession number PRJNA748591. All annotated miRNA loci were deposited into PmiREN database (https://www.pmiren.com/).

AUTHOR CONTRIBUTIONS

XY, LL, and XG initiated and designed the research. YD, ZK, and JD analyzed the data. YQ, PY, YZ, and YW performed the experiments. XY, YD, and PY wrote the manuscript. XY, LL, DL, and JW revised the manuscript. All authors contributed to the article and approved the submitted version.

FUNDING

This work was supported by the National Natural Science Foundation of China (NSFC; 32070248 to XY), the Beijing Academy of Agriculture and Forestry Sciences (BAAFS; KJCX20200204 to XY, KJCX201907-2 to JW, KJCX201917 to XG, and QNJJ202019 to YZ), and Peking University Qidong Innovation Project (PUDIP to LL).

SUPPLEMENTARY MATERIAL

The Supplementary Material for this article can be found online at: https://www.frontiersin.org/articles/10.3389/fpls.2021.781836/full#supplementary-material

Supplementary Table 1 | Reads summary in sRNA libraries.

Supplementary Table 2 | Length distribution of clean reads in sRNA libraries.

Supplementary Table 3 | Length distribution of unique reads in sRNA libraries.

Supplementary Table 4 | Summary of 157 miRNAs in lettuce.

Supplementary Table 5 | List of miRNA clusters within 10 kb.

Supplementary Table 6 | List of single miRNAs in synteny blocks.

Supplementary Table 7 | List of paired miRNAs in synteny blocks.

Supplementary Table 8 | Expression profile of 157 miRNAs in lettuce.

Supplementary Table 9 | Differentially expressed miRNAs among tissues.

Supplementary Table 10 | Detailed annotation information and expression profile of 6,540 miRNA-target pairs.

Supplementary Table 11 | The result of gene ontology (GO) enrichment analysis of 3,629 candidate targets.

Supplementary Table 12 | The result of Kyoto Encyclopedia of Genes and Genomes (KEGG) enrichment analysis of 3,629 candidate targets.

Supplementary Table 13 | Correlation analysis of expression profile between 157 miRNAs and 3,629 targets.

Supplementary Table 14 | Detailed information of 46,083 Cascade motifs based on "union" datasets.

Supplementary Table 15 | Detailed information of 8,859 Cascade motifs based on "intersection" datasets.

Supplementary Table 16 | Detailed information of 43,554 FFLs based on "union" datasets.

Supplementary Table 17 | Detailed information of 8,424 FFLs based on "intersection" datasets.

Supplementary Table 18 | Regulatory network statistics of 157 miRNAs as hub nodes based on "union" datasets.

Supplementary Table 19 | Regulatory network statistics of 152 miRNAs as hub nodes based on "intersection" datasets.

Supplementary Table 20 | The information between Lsa-miR408 and its target.

Supplementary Table 21 | The result of gene ontology (GO) enrichment analysis of Lsa-miR408 targets.

Supplementary Table 22 | Primers used in this study.

Supplementary Data 1 | Results of categories 0–2 from PARE-Seq analysis (including three subfiles:1_1, 1_2, 1_3).

REFERENCES

Addo-Quaye, C., Miller, W., and Axtell, M. J. (2009). CleaveLand: a pipeline for using degradome data to find cleaved small RNA targets. *Bioinformatics* 25, 130–131. doi: 10.1093/bioinformatics/btn604

Alves, L. Jr., Niemeier, S., Hauenschild, A., Rehmsmeier, M., and Merkle, T. (2009). Comprehensive prediction of novel microRNA targets in *Arabidopsis thaliana*. *Nucleic Acids Res.* 37, 4010–4021. doi: 10.1093/nar/gkp272

Axtell, M. J., and Meyers, B. C. (2018). Revisiting criteria for plant MicroRNA annotation in the era of big data. *Plant Cell* 30, 272–284. doi: 10.1105/tpc.17.00851

Bartel, D. P. (2009). MicroRNAs: target recognition and regulatory functions. *Cell* 136, 215–233. doi: 10.1016/j.cell.2009.01.002

Bartlett, A., O'Malley, R. C., Huang, S. C., Galli, M., Nery, J. R., Gallavotti, A., et al. (2017). Mapping genome-wide transcription-factor binding sites using DAP-seq. *Nat. Protoc.* 12, 1659–1672. doi: 10.1038/nprot.2017.055

Brown, J., Pirrung, M., and McCue, L. A. (2017). FQC Dashboard: integrates FastQC results into a web-based, interactive, and extensible FASTQ quality control tool. *Bioinformatics* 33, 3137–3139. doi: 10.1093/bioinformatics/btx373

Carthew, R. W., and Sontheimer, E. J. (2009). Origins and Mechanisms of miRNAs and siRNAs. *Cell* 136, 642–655. doi: 10.1016/j.cell.2009.01.035

Chandra, S., Vimal, D., Sharma, D., Rai, V., Gupta, S. C., and Chowdhuri, D. K. (2017). Role of miRNAs in development and disease: lessons learnt from small organisms. *Life Sci.* 185, 8–14. doi: 10.1016/j.lfs.2017.07.017

Chen, Z., Han, Y., Ning, K., Ding, Y., Zhao, W., Yan, S., et al. (2017). Inflorescence development and the role of LsFT in regulating bolting in lettuce (*Lactuca sativa* L.). *Front. Plant Sci.* 8:2248. doi: 10.3389/fpls.2017.02248

Chen, Z., Zhao, W., Ge, D., Han, Y., Ning, K., Luo, C., et al. (2018). LCM-seq reveals the crucial role of LsSOC1 in heat-promoted bolting of lettuce (*Lactuca sativa* L.). *Plant J* 95, 516–528. doi: 10.1111/tpj.13968

Cheng, Z., Hou, D., Ge, W., Li, X., Xie, L., Zheng, H., et al. (2020). Integrated mRNA, MicroRNA transcriptome and degradome analyses provide insights into stamen development in Moso Bamboo. *Plant Cell Physiol.* 61, 76–87. doi: 10.1093/pcp/pcz179

Dai, X., Zhuang, Z., and Zhao, P. X. (2018). psRNATarget: a plant small RNA target analysis server (2017 release). *Nucleic Acids Res.* 46, W49–W54. doi: 10.1093/nar/gky316

Daniell, H., Kulis, M., and Herzog, R. W. (2019). Plant cell-made protein antigens for induction of Oral tolerance. *Biotechnol. Adv.* 37:107413. doi: 10.1016/j.biotechadv.2019.06.012

Fromm, B., Keller, A., Yang, X., Friedlander, M. R., Peterson, K. J., and Griffiths-Jones, S. (2020). Quo vadis microRNAs? *Trends Genet* 36, 461–463. doi: 10.1016/j.tig.2020.03.007

Fujii, H., Chiou, T. J., Lin, S. I., Aung, K., and Zhu, J. K. (2005). A miRNA involved in phosphate-starvation response in Arabidopsis. *Curr. Biol.* 15, 2038–2043. doi: 10.1016/j.cub.2005.10.016

Gao, Z., Li, J., Li, L., Yang, Y., Li, J., Fu, C., et al. (2021). Structural and Functional Analyses of Hub MicroRNAs in an integrated gene regulatory network of Arabidopsis. *Genomics Proteomics Bioinformatics.* [Epub ahead of print]. doi: 10.1016/j.gpb.2020.02.004

German, M. A., Luo, S., Schroth, G., Meyers, B. C., and Green, P. J. (2009). Construction of Parallel Analysis of RNA Ends (PARE) libraries for the study of cleaved miRNA targets and the RNA degradome. *Nat. Protoc.* 4, 356–362. doi: 10.1038/nprot.2009.8

Guo, Z., Kuang, Z., Wang, Y., Zhao, Y., Tao, Y., Cheng, C., et al. (2020). PmiREN: a comprehensive encyclopedia of plant miRNAs. *Nucleic Acids Res.* 48, D1114–D1121. doi: 10.1093/nar/gkz894

Huo, H., Wei, S., and Bradford, K. J. (2016). DELAY OF GERMINATION1 (DOG1) regulates both seed dormancy and flowering time through microRNA pathways. *Proc. Natl. Acad. Sci. U.S.A.* 113, E2199–E2206. doi: 10.1073/pnas.1600558113

Inderbitzin, P., Christopoulou, M., Lavelle, D., Reyes-Chin-Wo, S., Michelmore, R. W., Subbarao, K. V., et al. (2019). The LsVe1L allele provides a molecular marker for resistance to *Verticillium dahliae* race 1 in lettuce. *BMC Plant Biol.* 19:305. doi: 10.1186/s12870-019-1905-9

Jiang, A., Guo, Z., Pan, J., Yang, Y., Zhuang, Y., Zuo, D., et al. (2021). The PIF1-miR408-PLANTACYANIN repression cascade regulates light-dependent seed germination. *Plant Cell* 33, 1506–1529. doi: 10.1093/plcell/koab060

Jin, J., Tian, F., Yang, D. C., Meng, Y. Q., Kong, L., Luo, J., et al. (2017). PlantTFDB 4.0: toward a central hub for transcription factors and regulatory interactions in plants. *Nucleic Acids Res.* 45, D1040–D1045. doi: 10.1093/nar/gkw982

Johnson, D. S., Mortazavi, A., Myers, R. M., and Wold, B. (2007). Genome-wide mapping of *in vivo* Protein-DNA Interactions. *Science* 316, 1497–1502. doi: 10.1126/science.1141319

Kalvari, I., Argasinska, J., Quinones-Olvera, N., Nawrocki, E. P., Rivas, E., Eddy, S. R., et al. (2018). Rfam 13.0: shifting to a genome-centric resource for non-coding RNA families. *Nucleic Acids Res.* 46, D335–D342. doi: 10.1093/nar/gkx1038

Kechin, A., Boyarskikh, U., Kel, A., and Filipenko, M. (2017). cutPrimers: a new tool for accurate cutting of primers from reads of targeted next generation sequencing. *J. Comput. Biol.* 24, 1138–1143. doi: 10.1089/cmb.2017.0096

Kim, D., Paggi, J. M., Park, C., Bennett, C., and Salzberg, S. L. (2019). Graph-based genome alignment and genotyping with HISAT2 and HISAT-genotype. *Nat. Biotechnol.* 37, 907–915. doi: 10.1038/s41587-019-0201-4

Kruger, J., and Rehmsmeier, M. (2006). RNAhybrid: microRNA target prediction easy, fast and flexible. *Nucleic Acids Res.* 34, W451–W454. doi: 10.1093/nar/gkl243

Krzywinski, M., Schein, J., Birol, I., Connors, J., Gascoyne, R., Horsman, D., et al. (2009). Circos: an information aesthetic for comparative genomics. *Genome Res.* 19, 1639–1645. doi: 10.1101/gr.092759.109

Kuang, Z., Wang, Y., Li, L., and Yang, X. (2019). miRDeep-P2: accurate and fast analysis of the microRNA transcriptome in plants. *Bioinformatics* 35, 2521–2522. doi: 10.1093/bioinformatics/bty972

Langmead, B. (2010). Aligning short sequencing reads with Bowtie. *Curr Protoc. Bioinformatics* Chapter 11:Unit 11.7. doi: 10.1002/0471250953.bi1107s32

Lee, Y., Kim, M., Han, J., Yeom, K. H., Lee, S., Baek, S. H., et al. (2004). MicroRNA genes are transcribed by RNA polymerase II. *EMBO J.* 23, 4051–4060. doi: 10.1038/sj.emboj.7600385

Liebsch, D., and Palatnik, J. F. (2020). MicroRNA miR396, GRF transcription factors and GIF co-regulators: a conserved plant growth regulatory module with potential for breeding and biotechnology. *Curr. Opin. Plant Biol.* 53, 31–42. doi: 10.1016/j.pbi.2019.09.008

Mi, H., Muruganujan, A., Ebert, D., Huang, X., and Thomas, P. D. (2019). PANTHER version 14: more genomes, a new PANTHER GO-slim and improvements in enrichment analysis tools. *Nucleic Acids Res.* 47, D419–D426. doi: 10.1093/nar/gky1038

Miao, C., Wang, Z., Zhang, L., Yao, J., Hua, K., Liu, X., et al. (2019). The grain yield modulator miR156 regulates seed dormancy through the gibberellin pathway in rice. *Nat. Commun.* 10:3822. doi: 10.1038/s41467-019-11830-5

Ogata, H., Goto, S., Sato, K., Fujibuchi, W., Bono, H., and Kanehisa, M. (1999). KEGG: kyoto encyclopedia of genes and genomes. *Nucleic Acids Res.* 27, 29–34. doi: 10.1093/nar/27.1.29

Pan, J., Huang, D., Guo, Z., Kuang, Z., Zhang, H., Xie, X., et al. (2018). Overexpression of microRNA408 enhances photosynthesis, growth, and seed yield in diverse plants. *J. Integr. Plant Biol.* 60, 323–340. doi: 10.1111/jipb.12634

Pertea, M., Pertea, G. M., Antonescu, C. M., Chang, T. C., Mendell, J. T., and Salzberg, S. L. (2015). StringTie enables improved reconstruction of a transcriptome from RNA-seq reads. *Nat. Biotechnol.* 33, 290–295. doi: 10.1038/nbt.3122

Quinlan, A. R., and Hall, I. M. (2010). BEDTools: a flexible suite of utilities for comparing genomic features. *Bioinformatics* 26, 841–842. doi: 10.1093/bioinformatics/btq033

Reyes-Chin-Wo, S., Wang, Z., Yang, X., Kozik, A., Arikit, S., Song, C., et al. (2017). Genome assembly with in vitro proximity ligation data and whole-genome triplication in lettuce. *Nat. Commun.* 8:14953. doi: 10.1038/ncomms14953

Seki, K., Komatsu, K., Tanaka, K., Hiraga, M., Kajiya-Kanegae, H., Matsumura, H., et al. (2020). A CIN-like TCP transcription factor (*LsTCP4*) having retrotransposon insertion associates with a shift from Salinas type to Empire type in crisphead lettuce (*Lactuca sativa* L.). *Hortic. Res.* 7:15. doi: 10.1038/s41438-020-0241-4

Shahid, S., Kim, G., Johnson, N. R., Wafula, E., Wang, F., Coruh, C., et al. (2018). MicroRNAs from the parasitic plant Cuscuta campestris target host messenger RNAs. *Nature* 553, 82–85. doi: 10.1038/nature25027

Shannon, P., Markiel, A., Ozier, O., Baliga, N. S., Wang, J. T., Ramage, D., et al. (2003). Cytoscape: a software environment for integrated models of biomolecular interaction networks. *Genome Res.* 13, 2498–2504. doi: 10.1101/gr.1239303

Su, W., Tao, R., Liu, W., Yu, C., Yue, Z., He, S., et al. (2020). Characterization of four polymorphic genes controlling red leaf colour in lettuce that have undergone disruptive selection since domestication. *Plant Biotechnol. J.* 18, 479–490. doi: 10.1111/pbi.13213

Tamura, Y., Mori, T., Nakabayashi, R., Kobayashi, M., Saito, K., Okazaki, S., et al. (2018). Metabolomic evaluation of the quality of leaf lettuce grown in practical plant factory to capture metabolite signature. *Front. Plant Sci.* 9:665. doi: 10.3389/fpls.2018.00665

Tav, C., Tempel, S., Poligny, L., and Tahi, F. (2016). miRNAFold: a web server for fast miRNA precursor prediction in genomes. *Nucleic Acids Res.* 44, W181–W184. doi: 10.1093/nar/gkw459

Tian, F., Yang, D. C., Meng, Y. Q., Jin, J., and Gao, G. (2020). PlantRegMap: charting functional regulatory maps in plants. *Nucleic Acids Res.* 48, D1104–D1113. doi: 10.1093/nar/gkz1020

Tsikou, D., Yan, Z., Holt, D. B., Abel, N. B., Reid, D. E., Madsen, L. H., et al. (2018). Systemic control of legume susceptibility to rhizobial infection by a mobile microRNA. *Science* 362, 233–236. doi: 10.1126/science.aat6907

Voinnet, O. (2009). Origin, biogenesis, and activity of plant microRNAs. *Cell* 136, 669–687. doi: 10.1016/j.cell.2009.01.046

Wang, H., Li, Y., Chern, M., Zhu, Y., Zhang, L. L., Lu, J. H., et al. (2021). Suppression of rice miR168 improves yield, flowering time and immunity. *Nat. Plants* 7, 129–136. doi: 10.1038/s41477-021-00852-x

Wang, J. W., Czech, B., and Weigel, D. (2009). miR156-regulated SPL transcription factors define an endogenous flowering pathway in Arabidopsis thaliana. *Cell* 138, 738–749. doi: 10.1016/j.cell.2009.06.014

Wang, Y., Tang, H., Debarry, J. D., Tan, X., Li, J., Wang, X., et al. (2012). MCScanX: a toolkit for detection and evolutionary analysis of gene synteny and collinearity. *Nucleic Acids Res.* 40:e49. doi: 10.1093/nar/gkr1293

Wang, Y., Wang, J., Guo, S., Tian, S., Zhang, J., Ren, Y., et al. (2021). CRISPR/Cas9-mediated mutagenesis of ClBG1 decreased seed size and promoted seed germination in watermelon. *Hortic. Res.* 8:70. doi: 10.1038/s41438-021-00506-1

Wei, T., van Treuren, R., Liu, X., Zhang, Z., Chen, J., Liu, Y., et al. (2021). Whole-genome resequencing of 445 Lactuca accessions reveals the domestication history of cultivated lettuce. *Nat. Genet.* 53, 752–760. doi: 10.1038/s41588-021-00831-0

Wu, G., Park, M. Y., Conway, S. R., Wang, J. W., Weigel, D., and Poethig, R. S. (2009). The sequential action of miR156 and miR172 regulates developmental timing in Arabidopsis. *Cell* 138, 750–759. doi: 10.1016/j.cell.2009.06.031

Yang, C., Li, D., Mao, D., Liu, X., Ji, C., Li, X., et al. (2013). Overexpression of microRNA319 impacts leaf morphogenesis and leads to enhanced cold tolerance in rice (*Oryza sativa* L.). *Plant Cell Environ.* 36, 2207–2218. doi: 10.1111/pce.12130

Yang, X., Fishilevich, E., German, M. A., Gandra, P., Narva, K. E. J. G. P., and Bioinformatics. (2021). Elucidation of the microRNA transcriptome in western corn rootworm reveals its dynamic and evolutionary complexity. *Genomics Proteomics Bioinformatics*. [Epub ahead of print]. doi: 10.1016/j.gpb.2019.03.008

Yu, C., Yan, C., Liu, Y., Liu, Y., Jia, Y., Lavelle, D., et al. (2020). Upregulation of a KN1 homolog by transposon insertion promotes leafy head development in lettuce. *Proc. Natl. Acad. Sci. U.S.A.* 117, 33668–33678. doi: 10.1073/pnas.2019698117

Zhang, J. P., Yu, Y., Feng, Y. Z., Zhou, Y. F., Zhang, F., Yang, Y. W., et al. (2017). MiR408 regulates grain yield and photosynthesis via a phytocyanin protein. *Plant Physiol.* 175, 1175–1185. doi: 10.1104/pp.17.01169

Zhang, L., Su, W., Tao, R., Zhang, W., Chen, J., Wu, P., et al. (2017). RNA sequencing provides insights into the evolution of lettuce and the regulation of flavonoid biosynthesis. *Nat. Commun.* 8:2264. doi: 10.1038/s41467-017-02445-9

Zhang, S., Sang, X., Hou, D., Chen, J., Gu, H., Zhang, Y., et al. (2019). Plant-derived RNAi therapeutics: a strategic inhibitor of HBsAg. *Biomaterials* 210, 83–93. doi: 10.1016/j.biomaterials.2019.04.033

Zhang, W., Alseekh, S., Zhu, X., Zhang, Q., Fernie, A. R., Kuang, H., et al. (2020). Dissection of the domestication-shaped genetic architecture of lettuce primary metabolism. *Plant J.* 104, 613–630. doi: 10.1111/tpj.14950

Zhao, X. Y., Hong, P., Wu, J. Y., Chen, X. B., Ye, X. G., Pan, Y. Y., et al. (2016). The tae-miR408-Mediated Control of TaTOC1 genes transcription is required for the regulation of heading time in wheat. *Plant Physiol.* 170, 1578–1594. doi: 10.1104/pp.15.01216

Zhao, Y., Kuang, Z., Wang, Y., Li, L., and Yang, X. (2021). MicroRNA annotation in plants: current status and challenges. *Brief. Bioinform.* 22:bbab075. doi: 10.1093/bib/bbab075

Zhu, H., Hu, F., Wang, R., Zhou, X., Sze, S. H., Liou, L. W., et al. (2011). Arabidopsis Argonaute10 specifically sequesters miR166/165 to regulate shoot apical meristem development. *Cell* 145, 242–256. doi: 10.1016/j.cell.2011.03.024

Conflict of Interest: The authors declare that the research was conducted in the absence of any commercial or financial relationships that could be construed as a potential conflict of interest.

Publisher's Note: All claims expressed in this article are solely those of the authors and do not necessarily represent those of their affiliated organizations, or those of the publisher, the editors and the reviewers. Any product that may be evaluated in this article, or claim that may be made by its manufacturer, is not guaranteed or endorsed by the publisher.

frontiers in Plant Science

HYPOTHESIS AND THEORY
published: 31 January 2022
doi: 10.3389/fpls.2021.770363

Photocontrol of Axillary Bud Outgrowth by MicroRNAs: Current State-of-the-Art and Novel Perspectives Gained From the Rosebush Model

*Julie Mallet[1], Patrick Laufs[2], Nathalie Leduc[1] and José Le Gourrierec[1]**

[1] University of Angers, Institut Agro, INRAE, IRHS, SFR QUASAV, Angers, France, [2] Université Paris-Saclay, INRAE, AgroParisTech, Institut Jean-Pierre Bourgin (IJPB), Versailles, France

OPEN ACCESS

Edited by:
Turgay Unver, FicusBio, Turkey

Reviewed by:
Marcelo Carnier Dornelas, State University of Campinas, Brazil
Lili Zhuang, Nanjing Agricultural University, China
Munevver Dogramaci, Edward T. Schafer Agricultural Research Center, United States Department of Agriculture, Agricultural Research Service (USDA-ARS), United States

***Correspondence:**
José Le Gourrierec
jose.gentilhomme@univ-angers.fr

Specialty section:
This article was submitted to Plant Physiology, a section of the journal Frontiers in Plant Science

Received: *03 September 2021*
Accepted: *13 December 2021*
Published: *31 January 2022*

Citation:
Mallet J, Laufs P, Leduc N and Le Gourrierec J (2022) Photocontrol of Axillary Bud Outgrowth by MicroRNAs: Current State-of-the-Art and Novel Perspectives Gained From the Rosebush Model. Front. Plant Sci. 12:770363. doi: 10.3389/fpls.2021.770363

Shoot branching is highly dependent on environmental factors. While many species show some light dependence for branching, the rosebush shows a strict requirement for light to allow branching, making this species an excellent model to further understand how light impinges on branching. Here, in the first part, we provide a review of the current understanding of how light may modulate the complex regulatory network of endogenous factors like hormones (SL, IAA, CK, GA, and ABA), nutrients (sugar and nitrogen), and ROS to control branching. We review the regulatory contribution of microRNAs (miRNAs) to branching in different species, highlighting the action of such evolutionarily conserved factors. We underline some possible pathways by which light may modulate miRNA-dependent regulation of branching. In the second part, we exploit the strict light dependence of rosebush for branching to identify putative miRNAs that could contribute to the photocontrol of branching. For this, we first performed a profiling of the miRNAs expressed in early light-induced rosebush buds and next tested whether they were predicted to target recognized regulators of branching. Thus, we identified seven miRNAs (miR156, miR159, miR164, miR166, miR399, miR477, and miR8175) that could target nine genes (*CKX1/6*, *EXPA3*, *MAX4*, *CYCD3;1*, *SUSY*, *6PFK*, *APX1*, and *RBOHB1*). Because these genes are affecting branching through different hormonal or metabolic pathways and because expression of some of these genes is photoregulated, our bioinformatic analysis suggests that miRNAs may trigger a rearrangement of the regulatory network to modulate branching in response to light environment.

Keywords: branching, light control, lateral meristem, post-transcriptional regulation, small RNAs, rose

INTRODUCTION

Important agronomic traits such as yield, visual and sanitary qualities, harvest index and even organoleptic quality are determined by plant architecture in general and shoot branching in particular (Boumaza et al., 2010; Garbez et al., 2015; Zhu and Wagner, 2020). A lot of research efforts are therefore produced to decipher mechanisms that control branching (Rameau et al., 2015;

Roman et al., 2016; Le Moigne et al., 2018; Schneider et al., 2019; Wang M. et al., 2020; Barbier et al., 2021).

Branching relies on the ability of an axillary bud, a structure containing a miniature shoot comprising a meristem, short internodes and immature leaves, to break dormancy and to grow through cell proliferation and expansion into a new branch. Dormancy is complex and includes endo-, para-, and eco-dormancies that can in part overlap (Lang et al., 1987; Cline, 1997). While endodormancy is controlled by mechanisms endogenous to the bud, paradormancy is due to the control of other organs on a given bud, as it is the case in apical dominance. Apical dominance can be lifted by stem beheading (Dun et al., 2006) or by exogenous application of chemical products (Ophir et al., 2009; Suttle, 2009; Walton et al., 2009). Ecodormancy relies on environmental control over a bud. Bud ability to grow out is therefore controlled both by internal factors [i.e., genetic background, hormones, metabolites, reactive oxygen species (ROS)] (Girault et al., 2010; Mason et al., 2014; Barbier et al., 2015; Li-Marchetti et al., 2015; Porcher et al., 2021) and also external ones. Among them, nutrients and water availability (Demotes-Mainard et al., 2013), temperature (Djennane et al., 2014), and light (Djennane et al., 2014; Roman et al., 2016; Porcher et al., 2021) are major determinants. Responses to abiotic factors are indeed critical for the plant to adapt its own development to resource availability, seasons and environmental stresses and to compete with other plants.

Light signal is particularly informative for the plant since it varies in intensity, quality, direction, and duration (Leduc et al., 2014). The shade avoidance syndrome triggered by decreased photosynthetic radiations and R/FR (Red/Far Red) ratio leads for example to axillary bud outgrowth inhibition. Dependence on light for axillary bud growth is varying from one species to another. Some species are able to show axillary bud growth in darkness where in the rosebush, light is particularly essential for this. Indeed, in this species axillary bud outgrowth and organogenesis are totally inhibited and no axillary branches are produced in the absence of light (Girault et al., 2008). Beside rosebush's primary importance among ornamentals, this response has also made it an excellent model for exploring light control of axillary bud outgrowth in plants (Demotes-Mainard et al., 2016; Huché-Thélier et al., 2016).

At the molecular level, most knowledge on axillary bud outgrowth and its photocontrol has been gained at the transcriptional level in the rosebush (Girault et al., 2010; Djennane et al., 2014; Roman et al., 2016; Schneider et al., 2019; Porcher et al., 2020, 2021). Yet, as for other developmental processes, post-transcriptional regulations are likely important and need to be further explored. Some studies have revealed post-transcriptional regulation in axillary bud outgrowth control with post-transcriptional regulation of Rosa *BRANCHED1* (*RhBRC1*) in interaction with sugars and regulation of its 3′UTR region with the potential role of *PUMILIO RNA-BINDING PROTEIN FAMILY 4* (*RhPUF4*) (Wang et al., 2019b).

MicroRNA (miRNA) regulation is a major component of post-transcriptional regulation of all biological processes in eukaryotes. First discovered in *Caenorhabditis elegans* (Wightman et al., 1993), miRNAs are small (20–21 nucleotides) single stranded non-coding RNAs. In *Arabidopsis thaliana*, 728 mature miRNAs have been identified (Kozomara et al., 2019). MiRNAs modulate the expression of their target genes through binding to their mRNA, causing either transcript cleavage or translation inhibition (Voinnet, 2009). Some miRNAs and their targets show a high conservation within plants while non-conserved ones can be found only in a group of plants, a species or even be specific to a landrace (Rajagopalan et al., 2006; Fahlgren et al., 2007). Conserved miRNAs target preferentially genes coding for transcription factors that play important roles in developmental control, while non-conserved target genes code for much more diverse functions (Zhang and Zhang, 2012).

Some knowledge has been gained on the roles of miRNAs in meristem initiation (see reviews by Zhang et al., 2006; Wang et al., 2011; Wu, 2013; Li and Zhang, 2016; Liu et al., 2018) as well as on leaf organogenesis (Pulido and Laufs, 2010; Maugarny-Calès and Laufs, 2018; Yang et al., 2018), two processes that contribute to axillary bud initiation and development (Sussex and Kerk, 2001). However, little is known about the roles of miRNAs during axillary bud outgrowth *per se*. Here, we provide a survey of the current knowledge on this subject, first sketching how the main mechanisms regulating axillary bud outgrowth may be connected to light control. Next, we provide a comprehensive view of axillary bud outgrowth regulation by miRNAs and, exploring the wider literature, we provide hypotheses on how light controls miRNAs activity and may contribute to the photocontrol of axillary bud outgrowth. In a second part, based on our expertise in rosebush and using *in silico* analysis based on the miRNA profiling we performed, we further explored the rose genome to identify and discuss novel miRNAs-gene target couples that may play a potential role in the regulation of axillary bud outgrowth and in its photocontrol in rosebush. Thus, we provide novel hypotheses on the miRNA-mediated regulation of bud growth photocontrol on which future research may stand.

AXILLARY BUD OUTGROWTH AND ITS LIGHT CONTROL: CURRENT KNOWLEDGE ON MAIN ACTORS

Several reviews have recently described in depth the current knowledge on the processes controlling axillary bud outgrowth in plants and their control by light (Leduc et al., 2014; Schneider et al., 2019; Wang M. et al., 2020; Kotov et al., 2021). As a pre-requisite to discuss their possible regulation by miRNAs, we provide here a brief overview of the main actors involved in the photocontrol of axillary bud outgrowth with a particular focus on rosebush. Main actors and their interactions are presented in **Figure 1**.

Main Actors and Their Roles in the Control of Axillary Bud Outgrowth

Axillary bud outgrowth is controlled by a complex interplay between several main actors such as hormones, nutrients in particular sugars and ROS (**Figure 1**).

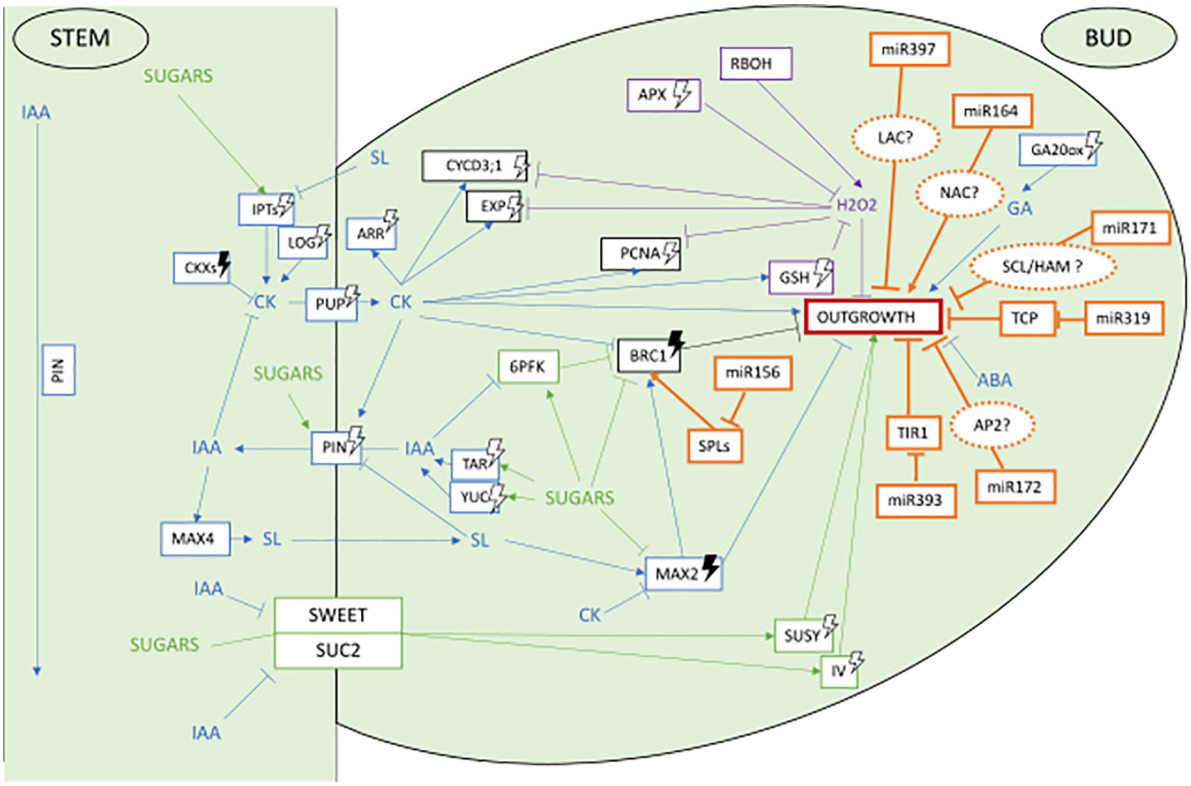

FIGURE 1 | Network of main actors controlling axillary bud outgrowth in the rosebush Rosa 'Radrazz'* and the potential targets of miRNAs based on literature in other plant species** Potential gene targets of these miRNAs in the control of bud outgrowth are represented in dotted orange circles. miRNAs involved in control of bud outgrowth according to the literature are represented in orange. Blue represents hormonal pathway, green sugars pathway, purple ROS pathway. Arrows head means induction, straight lines mean repression, white lightning bolt means induction by light, darked lightning bolts means induction by darkness. *Girault et al. (2008), Girault et al. (2010), Henry et al. (2011), Choubane et al. (2012), Rabot et al. (2012), Rabot et al. (2014), Djennane et al. (2014), Barbier et al. (2015), Roman et al. (2016), Roman et al. (2017), Porcher et al. (2020), Porcher et al. (2021), Wang M. et al. (2021). **Jiao et al. (2010), Miura et al. (2010), Wang et al. (2010), Wei et al. (2012), Xia et al. (2012), Curaba et al. (2013), Zhou et al. (2013), Zhang et al. (2013), Aung et al. (2015), Wang L. et al. (2015), Wang Y. et al. (2015), Huang et al. (2017), Kravchik et al. (2019), Sun et al. (2019), Cui et al. (2020), Lian et al. (2021), Wang R. et al. (2021), Zhan et al. (2021).

Concerning hormones, strong interactions between auxin (IAA), cytokinins (CK), and strigolactones (SL) form a core regulatory hormonal network instrumental for the release of apical dominance and induction of axillary bud outgrowth (Domagalska and Leyser, 2011; Barbier et al., 2019, **Figure 1**, blue lines). A first proposed mechanism suggests IAA inhibits axillary bud outgrowth indirectly through repression of CK synthesis and promotion of SL synthesis and signaling, both hormones being able to enter axillary buds and to act directly on axillary buds (Beveridge et al., 2000; Brewer et al., 2009; Ferguson and Beveridge, 2009). The balance of their opposing effects (CK promoting and SL repressing bud growth) would determine the fate (paradormancy vs. outgrowth) of the axillary bud. Through a second suggested mechanism, the basipetal flux of IAA produced by the apical meristem would also cause inhibition of axillary bud outgrowth by acting on the polarized distribution of the IAA efflux transporters PIN-FORMED (PIN) proteins in the axillary bud and by preventing it to export its own auxin (Bennett et al., 2006; Prusinkiewicz et al., 2009). In addition, a repressive role of ABA on axillary bud outgrowth was demonstrated in several species such as tomato, bean, arabidopsis, and rosebush (Tucker, 1976; Knox and Wareing, 1984; Gocal et al., 1991; Le Bris et al., 1999; Chatfield et al., 2000; Corot et al., 2017). In rosebush, a continued *de novo* synthesis of ABA contributes to maintaining bud endodormancy through control of cell cycle arrest in G2 phase (Le Bris et al., 1999). Application of ABA on the stem of rosebush and of other species also inhibits outgrowth of non-endodormant axillary buds nearby (Chatfield et al., 2000; Cline and Oh, 2006; Corot et al., 2017) while beheading of the main shoot causes a decrease in ABA contents in axillary buds along with their outgrowth (Knox and Wareing, 1984; Gocal et al., 1991). Last, gibberellins (GA) are hormones that control meristem cell differentiation in leaf primordia and internode elongation, both processes taking place during axillary bud outgrowth (Koornneef and van der Veen, 1980; Dodsworth, 2009). In rosebush, GA synthesis under the control of *RoGA20-oxidase* (*RoGA20ox*) and *RoGA3ox* and reduction of GA catabolism through down-regulation of *RoGA2ox* were shown to contribute to axillary bud outgrowth (Choubane et al., 2012).

As providers of energy, osmolytes and cell wall material, sugars are other key players in axillary bud outgrowth control

(Bonicel et al., 1987; Marquat et al., 1999; Le Hir et al., 2006, **Figure 1**, green lines). In the rosebush, pea and sorgho, defoliation, decapitation or *in vitro* experiments showed axillary bud outgrowth is dependent on sucrose availability (Girault et al., 2010; Henry et al., 2011; Kebrom et al., 2012; Rabot et al., 2012; Mason et al., 2014). In rosebush *Rosa* 'Radrazz', *SUCROSE TRANSPORTER 2* (*RhSUC2*) and *RhSWEET10* control sucrose transport to the bud (Henry et al., 2011; Roman et al., 2016) where *RhSUSY* and *VACUOLAR INVERTASE 1* (*RhVI1*) catabolize sucrose into fructose and glucose for growth (Girault et al., 2010; Rabot et al., 2014). Promoting effects of non-metabolizable sucrose analogs on axillary bud outgrowth in rosebush suggests that sucrose may also play a signaling role during axillary bud outgrowth (Rabot et al., 2012; Barbier et al., 2015). Sucrose interacts with the hormonal control of axillary bud outgrowth (Barbier et al., 2015). Using detached rosebush buds *in vitro*, Barbier et al. (2015) showed that sucrose upregulates auxin synthesis [*TRYPTOPHAN AMINOTRANSFERASE RELATED 1* (*RhTAR1*), *YUCCA 1* (*RhYUC1*)] and auxin efflux [*PIN-FORMED 1* (*RhPIN1*), *SERINE/THREONINE PROTEIN PHOSPHATASE 2A* (*RhPP2A*), *PINOID* (*RhPID*)] genes in buds and represses strigolactones *MORE AXILLARY BRANCHES 2* (*RwMAX2*) signaling gene. Promoting effect of sucrose onto axillary bud outgrowth also relies on repression of a main negative regulator of axillary bud outgrowth *BRANCHED1* (*BRC1*) (Aguilar-Martínez et al., 2007; Finlayson et al., 2010; Dun et al., 2012; Brewer, 2015; Wang et al., 2019a) by sucrose (Barbier et al., 2015; Wang M. et al., 2021).

Evidence is also repetitively brought showing that the oxidative metabolism contributes to the control of axillary bud outgrowth (**Figure 1**, purple lines). In grape, for example, application of sodium azide or hydrogen cyanamide or heat shock on endodormant buds represses *CATALASE* (*CAT*) scavenging activity, causing accumulation of hydrogen peroxide (H_2O_2) that promotes bud outgrowth (Or et al., 2002; Ophir et al., 2009; Pérez et al., 2009; Vergara et al., 2012; Sudawan et al., 2016; Meitha et al., 2018). In non-endodormant buds, H_2O_2 appears to play an opposite role. Hence, in tomato, *rboh* mutants in which the capacity to produce apoplastic H_2O_2 is altered, a highly branched phenotype is observed suggesting that H_2O_2 contributes to axillary bud outgrowth inhibition (Sagi et al., 2004; Chen et al., 2016). In non-endodormant rosebush axillary buds subjected to apical dominance, a high content of H_2O_2 is present and contributes to bud arrest. Upon stem decapitation, activation of ROS scavenging activity is observed that causes a rapid decrease in H_2O_2 content along with axillary bud outgrowth (Porcher et al., 2020). In rosebush buds, scavenging activity is mainly due to the ascorbate–glutathione cycle (AsA–GSH). Transcription of glutathione biosynthesis genes *RhGSH1* as *RhGSH2* as well as of ascorbate peroxidase *RhAPX1* and glutathione reductase *RhGR1* are indeed actively transcribed in axillary buds after plant beheading and during axillary bud outgrowth while catalase *RhCAT* is not. These up-regulations are followed by increased corresponding enzymatic activities (Porcher et al., 2020).

Suppression of bud dormancies allows axillary bud outgrowth characterized by resumption of DNA replication and cell cycle (Shimizu and Mori, 1998; González-Grandío et al., 2013). Increased transcriptional activity of *PROLIFERATING CELL NUCLEAR ANTIGEN* (*PCNA*), *CELL DIVISION CYCLE 2* (*CDC2*), *CYCLIN B* (*CYCB*, Devitt and Stafstrom, 1995), and *CYCLIN D3* (*CYCD3*) takes for example rapidly place in pea (Shimizu and Mori, 1998), apple trees (Li et al., 2018) and in *Rosa* buds (Roman et al., 2016; Porcher et al., 2020) upon dormancy break. Cell division along with cell wall expansion contribute to growth of organ primordia and lead to protrusion of young leaves out of buds scales. In rosebush, up-regulation of *EXPANSINS RhEXPA1, 2,* and *3* take place in axillary buds within a few hours after stem decapitation and is promoted by CK (Roman et al., 2016, 2017).

Light Regulation of Main Actors of Axillary Bud Outgrowth

Spectral quality and light intensity both impact axillary bud outgrowth in a range of herbaceous and perennial species (Leduc et al., 2014; Demotes-Mainard et al., 2016; Huché-Thélier et al., 2016). Unlike other species such as Arabidopsis, tomato, and poplar (Girault et al., 2008), axillary buds of rosebush have an absolute need for light to grow out (Girault et al., 2008). Total inhibition of axillary bud outgrowth under darkness and promotion by light offers a great opportunity to examine the light control of bud outgrowth in this species and to deepen our knowledge of this ecodormancy in plants (Leduc et al., 2014; Demotes-Mainard et al., 2016; Huché-Thélier et al., 2016; Bertheloot et al., 2020).

In the rosebush, red (R) and blue (B) lights promote axillary bud outgrowth while far-red (FR) light is inhibitory (Girault et al., 2008). These responses are consistent with the shade avoidance syndrome of plants. In rosebush, monochromatic blue or red light alone is also able to trigger and sustain all processes involved in axillary bud outgrowth, suggesting cross links and redundancy in the transduction pathways of R and B lights (Abidi et al., 2013). The acrotonic outgrowth pattern observed in rosebush can also be deeply modified by localized dark treatment along the rosebush stem (Djennane et al., 2014) or temporary exposure to low light prior to full light exposure (Demotes-Mainard et al., 2013), indicating fine spatial regulation of axillary bud outgrowth patterns along the stem by light.

Transcriptional control of light over hormones, sugars, ROS, cell division and growth was demonstrated in the rosebush using contrasted lighting conditions (darkness vs. white light, monochromatic vs. white light) and exogenous hormonal and sugar treatments. From these studies, demonstration was made that CK are initial targets of the light control pathway (Roman et al., 2016). More precisely, bud exposure to light triggers a rapid and strong upregulation of genes involved in CK synthesis [*ISOPENTENYLTRANSFERASE* (*RhIPT3*, *RhIPT5*)], activation [*LONELY GUY 8* (*RhLOG8*)], and transport [*PURINE PERMEASE 5* (*RhPUP5*)] and to the repression of CK catabolism gene *CYTOKININ OXIDASE/DEHYDROGENASE 1* (*RhCKX1*). This leads to CK accumulation in nodes and buds which then causes an up-regulation of IAA biosynthesis and transport (*RhYUC1*, *RhPIN1*), sugar (*RhSUSY*, *RhVI*, *RhSUC2*, and *RhSWEET10*) synthesis and transport genes, and repression

of axillary bud outgrowth inhibitory genes (*RhBRC1* and SL signaling *RwMAX2*). CK upregulation during light control of rosebush axillary bud outgrowth also acts through ROS scavenging (Porcher et al., 2021). In particular, the AsA-GSH pathway is activated by light and CK, causing a decrease in H_2O_2 content in bud (Porcher et al., 2021). These light regulations finally lead to axillary bud outgrowth through activation of cell cycle *RhPCNA*, and cell expansion *RhEXPA* genes (Roman et al., 2016, 2017). Additionally, in response to reduced light intensity, Corot et al. (2017) showed that inhibition of axillary bud outgrowth in the rosebush is associated with reduced levels of CK and increased levels of ABA. Exogenous delivery of CK and ABA to the stem confirmed their antagonistic action in the control of axillary bud outgrowth by light intensity (Corot et al., 2017). Light regulation of GA also contributes to the photocontrol of axillary bud outgrowth in the rosebush through upregulation of the expressions of biosynthesis genes *GA20ox* and *GA3ox* and repression of catabolic gene *GA2ox* (Choubane et al., 2012).

In dark, conversely, repression of axillary bud outgrowth results from up-regulation of repressor genes such as *RhBRC1* and SL signaling *RwMAX2* as well as repression of ROS scavenging AsA-GSH pathway (Djennane et al., 2014; Roman et al., 2016; Porcher et al., 2021). Repression of sucrose transport and catabolism under darkness leads to a switch toward sorbitol metabolism, seemingly as a survival mechanism. Strong upregulation of *NAD-DEPENDANT SORBITOL DEHYDROGENASE* (*RhNAD-SDH*) transcriptional activity is indeed observed upon exposure of buds to darkness (Girault et al., 2010).

EXTENDING OUR KNOWLEDGE OF CONSERVED MiRNAS AND THEIR REGULATION OF AXILLARY BUD OUTGROWTH TO ROSEBUSH

Beside the regulatory pathways discussed above, the role of miRNAs in bud outgrowth control was more recently discovered. Numerous miRNAs showing high degree of similarity in their sequence were found in the genomes of many plant species and thus defined as conserved miRNAs (Weber, 2004; Zhang et al., 2006). Some of these were identified as key players in axillary bud outgrowth. Yet, the role of these miRNAs has been explored only in a few model species such as Arabidopsis, maize, and rice, the two latter concentrating on a grass specific branching process, called tillering. Here, we provide an up-to-date summary of roles of conserved miRNAs in branching and provide new data of the putative role of these conserved miRNAs in rosebush. Branching phenotypes of miRNAs and target gene-resistant mutants are summarized in **Table 1**.

The study of tillering in rice (*Oryza sativa*) has been instrumental in uncovering the role of miRNAs in bud outgrowth. To-date, miR156 is one of the best characterized miRNA families. MiR156 plays a major role in regulating shoot branching by targeting a subset of the *SQUAMOSA PROTEIN-LIKE* (*SPLs*) genes. SPL transcription factors are found in all green plants and are involved in many developmental regulatory processes such as phase transition and flowering, plastochron control, leaf development, fruit ripening and response to stresses (Wang and Wang, 2015). *SPL* genes are ordered into nine clades, of which six are regulated by miR156 (Preston and Hileman, 2013). In rice, increased expression level of *OsSPL14* resulting from a mutation in its miR156 binding site leads to reduced branching from vegetative buds (Jiao et al., 2010; Miura et al., 2010). Interestingly, this mutation has opposite effects on branching during the reproductive phase, as it leads to increased inflorescence (panicle) branching and altogether forms the molecular basis of a quantitative locus known as *WEALTHY FARMER'S PANICLE* or *IDEAL PLANT ARCHITECTURE 1 (IPA1)* that improves rice productivity. On the contrary, high miR156 levels increase tiller formation in the dominant *Corngrass1* maize mutant (Chuck et al., 2007). An increased branching resulting from miR156 overexpression was also reported in other species including Arabidopsis (Wei et al., 2012; Tian et al., 2014), alfalfa (Aung et al., 2015), lotus (Wang Y. et al., 2015), soya (Sun et al., 2019), and tomato. In this last species, the increased branching phenotype can be reverted by expression of a miR156-resistant *SPL13* gene (Cui et al., 2020). Modulation of miR156/SPL interaction affects branching through both initiation and outgrowth of the axillary buds (Wang L. et al., 2015). At least three pathways have been associated with such increased branching. First, *UNBRANCHED3*, the maize ortholog of *OsSPL14*, directly targets and represses the expression of cytokinin biosynthesis and signaling genes while promoting expression of cytokinin degradation genes, thus resulting in lower cytokinin levels and signaling (Du et al., 2017). Second, *OsSPL7*, another target of miR156 in rice, represses the expression of *OsGH3.8* which codes for an enzyme conjugating auxin to aspartate (Dai Z. et al., 2018). Hence, miR156 may affect auxin/cytokinin balance that is important for both formation and growth of the axillary meristems. Last, *OsSPL14* directly promotes the expression of *OsTB1*, the rice homolog of bud outgrowth repressor *AtBRC1* (Lu et al., 2013). In this last case, miR156 repression of *OsSPL14* would reduce *AtBRC1* inhibitory effect on bud outgrowth.

The study of tillering in rice has revealed additional miRNAs that contribute to the regulation of branching in this species (Yue et al., 2017). MiR529 that partially overlaps with miR156 also targets a subset of *SPL* genes. MiR529 is found in monocots but was specifically lost in some dicots (Morea et al., 2016). Recently, Yan et al. (2021) showed that modulation of miR529 activity increases rice tillering in a similar way as miR156.

Increased tillering was also observed in rice lines overexpressing miR393. This miRNA targets genes coding for auxin receptors [*TRANSPORT INHIBITOR RESPONSE 1* (*OsTIR1*) and *AUXIN SIGNALING F-BOX 2* (*OsAFB2*)]. Accordingly, rice lines overexpressing miR393 show a reduced response to auxin and lower expression of the *OsTB1* gene, which may account for increased axillary bud growth (Li et al., 2016).

Modified auxin signaling is also observed in rice plants expressing a miR160-resistant version of the *AUXIN RESPONSE FACTOR* (*OsARF18)* that develop less tillers (Huang et al., 2016).

TABLE 1 | Main conserved miRNA families and their associated targets causing shoot branching modulation.

miRNA families	Known target	Species	Plants	References
156	SPL	Rice, Lotus, Medicago, Soya, Arabidopsis	MiR-OE: Increased branching	Wei et al., 2012; Aung et al., 2015; Wang L. et al., 2015; Wang Y. et al., 2015; Sun et al., 2019
		Tomato	TG-LF: Increased branching	Cui et al., 2020
		Rice	TG-MR: reduced branching	Jiao et al., 2010; Miura et al., 2010
164	NAC	Arabidopsis, Cotton	MiR-OE: Increased branching TG-MR: Reduced branching	Zhan et al., 2021
171	GRAS/SCL/HAM	Arabidopsis, Barley	MiR-OE: Reduced branching	Wang et al., 2010; Curaba et al., 2013
		Tomato	MiR-LF: Increased branching	Schulze et al., 2010; Wang et al., 2010; Kravchik et al., 2019
		Arabidopsis	TG-LF: Reduced shoot branching	Huang et al., 2017
		Tomato	TG-OE: Increased branching	Wang et al., 2010
		Arabidopsis	TG-MR: Increased branching	
172	AP2	Arabidopsis	MiR-LF: Increased branching	Lian et al., 2021
319	TCP	Bentgrass	MiR-OE: Decreased branching	Zhou et al., 2013
		Rice	MiR-LF: Increased branching	Wang R. et al., 2021
393	TIR1/AFB	Rice	MiR-OE: Increased branching	Xia et al., 2012
397	LAC	Rice	MiR-OE: Decreased branching	Zhang et al., 2013
444	MADS	Rice	MiR-OE: Reduced branching TG-OE: Increased branching TG-MR: Increased branching	Guo et al., 2013
529	SPL	Rice	MiR-OE: Increased tillering MiR-LF: Reduced branching	Yan et al., 2021

MiR-OE, miRNA overexpression phenotype; MiR-LF, miRNA loss-of-function or knock-down phenotype; TG-MR: target resistant phenotype; TG-LF, target loss-of-function or knock-down phenotype; TG-OE, target overexpression phenotype.

While overexpression of miR156, miR529 or miR393 increases rice tillering, overexpression of the monocot-specific miR444 has an opposite effect (Guo et al., 2013). miR444 targets *OsMADS57* which is expressed in developing buds where *OsMADS57* represses expression of *D14* gene coding for the SL receptor. Hence, miR444 overexpression may lead to increased SL response and thus inhibition of bud outgrowth.

Finally, overexpression of miR397 that targets rice *OsLAC*, a laccase polymerizing monolignols into lignin (Berthet et al., 2011; Zhao et al., 2013) also leads to a slight reduction in rice tiller number (Zhang et al., 2013).

Study in *Arabidopsis thaliana* also revealed the potential role of three other miRNAs in the control of branching. For example, miR171 was shown to target genes coding for the GRAS transcription factors *SCARECROW-LIKE SCL6-II*, *SCL6-III*, and *SCL6-IV* [also named *LOST MERISTEMS1-3* (*LOM*) or *HAIRY MERISTEM* (*HAM*)] (Schulze et al., 2010; Wang et al., 2010). These proteins are required for proper meristem function, including axillary meristem formation, and act by promoting the specification of the stem cells in the apical region of the meristem (Zhou et al., 2018; Han et al., 2020). Arabidopsis lines overexpressing miR171 show a massive reduction in the number of secondary branches, which is reverted by the expression of a miR171-resistant version of any of the 3 *HAM* genes (Wang et al., 2010). In tomato also, reduced miR171 activity or overexpression of the tomato *HAM* gene *SlGRAS24* leads to increased branching suggesting that miR171 represses *HAM* gene expression to limit branching in these species (Huang et al., 2017; Kravchik et al., 2019). *SlGRAS24* modulates auxin and gibberellin signaling, but whether it affects the formation of the axillary meristem, or its outgrowth is not known yet (Huang et al., 2017). The function of miR171 in shoot branching inhibition appears to be conserved in monocots, as overexpression of this miRNA reduces branching in barley (Curaba et al., 2013).

In Arabidopsis, miR164 targets a subset of the NAC genes, including *CUP-SHAPED COTYLEDON* (*CUC*) genes that are important for a wide range of meristem-related developmental processes. Recent studies performed in cotton and in the heterologous Arabidopsis system suggest that repression of *CUC2* by miR164 is important for branch outgrowth (Zhan et al., 2021). Specifically, *CUC2* interaction with *BRC1* may modulate ABA levels to control bud growth (Zhan et al., 2021).

An antagonistic role of miR172 and of miR156 in the regulation of Arabidopsis branching was also demonstrated (Wang et al., 2009). The quintuple mutant of the five *MIR172* genes indeed shows an increased branching as does a line overexpressing *MIR156b* (Wei et al., 2012; Lian et al., 2021). *MiR172a* and *d* are the *MIR172* genes playing a major role in the repression of branching in Arabidopsis (Lian et al., 2021).

Research in other less studied plant species has also brought additional knowledge on the role of other miRNAs in branching. For instance, in bentgrass (*Agrostis stolonifera*), overexpression of miR319 leads to a slight decrease in tillering (Zhou et al., 2013). MiR319 targets a subset of the *TEOSINTE*

BRANCHED1/CYCLOIDEA/PCF (*TCP*) transcription factor family which are involved among others in the transition from cell proliferation to differentiation during plant development (Palatnik et al., 2003). In line with these data, recent work in rice shows that inactivation of miR319 correlates with increased expression of *OsTCP21* and increased number and length of tiller buds (Wang R. et al., 2021). In *Camellia sinensis*, the expression of *MIR319c* is significantly reduced during bud outgrowth while that of its target *TCP2* is significantly upregulated (Liu et al., 2019).

Altogether, it appears that several conserved miRNAs contribute to branching control. While in some cases, their effect could be precisely attributed to meristem initiation or to their later outgrowth (Wang L. et al., 2015), this has not been systematically analyzed (Huang et al., 2017; Lian et al., 2021). In addition, as some of these miRNA/target couples are involved in many processes, the effect on branching could be sometimes indirect. This may be the case for example for miR156 that affects the duration of the vegetative phase and therefore the number of nodes bearing axillary meristems.

As described in part 1, a lot of information has been gained on axillary bud outgrowth regulatory pathways and its photocontrol through study of the rosebush *Rosa* 'Radrazz'. However, the role of miRNAs in rosebush axillary bud outgrowth has not yet been explored. As a first step toward this, we analyzed whether the conserved miRNAs described in **Table 1** were also expressed in rosebush axillary buds and if they could interact with the same known targets. To answer these questions and since no annotation of the mature miRNA sequences is available on the reference *Rosa* genome (*Rosa chinensis*, Hibrand Saint-Oyant et al., 2018; Raymond et al., 2018), we performed a high throughput profiling of the miRNA components of *Rosa* 'Radrazz' axillary buds. To induce axillary bud outgrowth, stems were beheaded to release apical dominance and were grown in light. We collected buds samples right after beheading and 6 h after beheading. This time point was chosen as it was late enough after beheading to allow key molecular mechanisms of the outgrowth process and of the light control to take place (Barbier et al., 2015; Roman et al., 2016; Porcher et al., 2020, 2021; Method detailed in **Supplementary Method I**) and early enough to minimize feed-back loop regulations of miRNAs that could be activated following resumption of axillary meristem outgrowth. From the sequenced small RNAs, prediction and annotation of the *Rosa* mature miRNAs sequences were achieved using *Arabidopsis thaliana* miRNAs database[1] (**Supplementary Data 1**). Annotated *Rosa* miRNAs sequences were next aligned against orthologs of the known target genes described in literature (**Table 1**) and found in *Rosa chinensis* genome using target prediction web server's psRNAtarget (Dai X. et al., 2018).[2] Together this allowed us to take a snapshot of miRNAs present in buds upon suppression of apical dominance and during an early phase of bud growth and then predict their targets in *Rosa* (**Table 2**).

[1]http://www.mirbase.org/index.shtml

[2]https://www.zhaolab.org/psRNATarget/

Our bioinformatic analysis shows that out of the 9 miRNAs families previously described as involved in the control of bud outgrowth (as mentioned above), 7 were found in *Rosa* (**Table 2**). The two missing families, miR444 and mi529, are also missing in other dicots. This result reinforces the hypothesis that miR529 was lost in eudicots during evolution and that miR444 is only present in monocots (Sunkar et al., 2005; Ortiz-Morea et al., 2013). Each *Rosa* miRNA family is represented by several members (i.e., 14 in miR156 family; 7 in miR164 family). Similar numbers of members were found in Arabidopsis except for miR171, 172, and 319 families in which a much lower number of members were identified in *Arabidopsis* (6, 9, and 3 members, respectively) in comparison to *Rosa*. This may suggest differences in the tuning of the regulations controlled by these miRNA families between *Rosa* and *Arabidopsis*.

Binding ability of *Rosa* miRNAs to known targets was predicted by searching sequences complementary to the miRNAs in the putative targets. Same target gene families were found in the *Rosa* genome as described for other species (**Table 1**). These findings suggest that regulations involving these miRNA families and their associated targets may also be conserved in *Rosa* axillary buds.

Bioinformatic analysis allowed identification of several members of each target gene family in *Rosa* (**Table 2**). Further experimental investigations are needed for confirmation of their interaction.

Results are summed up in orange in **Figure 1** showing the network of main actors controlling axillary bud outgrowth in the rosebush Rosa 'Radrazz' and the potential roles of miRNAs based on literature in other plant species and the miRNA/target pairs we identified here.

CROSSTALK BETWEEN LIGHT SIGNALING PATHWAY AND MiRNAS ENCODING GENE EXPRESSION

Light is a major environmental cue that controls bud outgrowth in many plant species and light regulation of axillary bud outgrowth at transcriptional level has been well documented in rosebush (Girault et al., 2008; Rabot et al., 2014; Roman et al., 2016; Porcher et al., 2020). Yet, little is known to-date on the involvement of miRNAs in light-mediated axillary bud outgrowth mechanisms. Therefore, we summarize here the present knowledge on light effects on the miRNA pathway in general, affecting for instance the stability or functionality of the core proteins involved in the maturation of miRNAs (Sánchez-Retuerta et al., 2018; Park et al., 2021). In addition to such a general effect on the whole miRNA pathway, light also affects the expression of some *MiRNA* genes specifically. Red (R) and Blue (B) light signal transduction engages photoreceptors, including phytochromes (PHY) and cryptochromes (CRY) and their downstream effectors as *ELONGATED HYPOCOTYL 5* (*HY5*) and *PHYTOCHROME INTERACTING FACTORS* (*PIF4*). *PHYB* plays a main role in the photocontrol of bud outgrowth (Kebrom and Mullet, 2016). Recently, Holalu et al. (2020) reported that PIF4 and PIF5 contribute to the suppression of

TABLE 2 | Conserved miRNAs expressed in *Rosa* 'Radrazz' buds and their predicted gene targets.

Conserved miRNA families	Total number of miRNA family members identified in *Rosa* 'Radrazz' buds and names of those presenting binding ability to known target identified in other plants species	Target genes identified in *Rosa chinensis* genome with an expectation ≤3.5.	*Rosa chinensis* homologs accession number (Hibrand Saint-Oyant et al., 2018)	*Arabidopsis thaliana* orthologs accession number (TAIR 10 release)
156	14	*SPL2*	RC4G0346800	AT5G43270
	miR156c/miR156f/ miR156c_1/miR156k_ 1/ miR156a/miR156a-5p/ miR156j_1/miR156k_2/ miR156_2/miR156g_1	*SPL3*	RC5G0081600	AT2G33810
		SPL6A	RC4G0415800	AT1G69170
		SPL6B	RC7G0063500	AT1G69170
		SPL6C	RC7G0063900	AT1G69170
		SPL9	RC3G0139500	AT2G42200
		SPL10	RC1G0282700	AT1G27370
		SPL13A	RC7G0120000	AT5G50570
		SPL16A	RC2G0684700	no SPL16 in
		SPL16B	RC4G0344900	Arabidopsis
164	7	*NAC1*	RC5G0238100	AT1G56010
	miR164a_2/miR164a_4/miR164b/164e-5p/ miR164f_1	*NAC100_1*	RC7G0049200	AT5G61430
		NAC100_2	RC7G0049800	AT5G61430
		NAC100_3	RC2G0616000	AT5G61430
		CUC2	RC0G0187100	AT5G53950
171	19	*SCL6*	RC1G0287300	AT4G00150
	miR171b/miR171b-3p/miR171b-3p_3/miR171f-3p/miR171a-3p/miR171a-3p_1/miR171a_3/ miR171b_2/miR171b_ 3/miR171_2/miR171c_3/ miR171d_1/miR171f_3	*SCL6*	RC7G0240100	AT4G00150
172	17	*RAP*	RC1G0423500	AT2G28550
	miR172a_4/miR172i/miR172a_2/miR172a_3/ miR172c-3p/miR172d_2/miR172e-3p_1/ miR172a_1/miR172b/miR172e-3p/miR172g-3p/ miR172f	*2.7/TOE 1*	RC5G0530900	AT2G28550
		RAP	RC2G0197000	AT4G36920
		2.7/TOE 1	RC3G0243000	AT5G67180
		AP2		
		TOE3		
319	11	*TCP2*	RC5G0134300	AT4G18390
	miR319_1/miR319a_1/miR319a-3p/ miR319c_1/miR319f_1/ miR319g/miR319a/ miR319b_1/miR319c_2	*TCP4*	RC5G0279600	AT3G15030
393	8	*AFB2*	RC2G0688700	AT3G26810
	miR393a_1/miR393a_3/miR393-5p/miR393a/ miR393a-5p/miR393b-5p/miR393h	*TIR1*	RC6G0421400	AT3G62980
397	3	*LAC2*	RC5G0566900	AT2G29130
	miR397-5p_1/miR397a_6/miR397a_3	*LAC3*	RC5G0617100	AT2G30210
		LAC4A	RC3G0283200	AT2G38080
		LAC4B	RC5G0590200	AT2G38080
		LAC7A	RC3G0278900	AT3G09220
		LAC7B	RC5G0655700	AT3G09220
		LAC11A	RC6G0173800	AT5G03260
		LAC11B	RC6G0174100	AT5G03260
		LAC11C	RC6G0176400	AT5G03260
		LAC11D	RC6G0176600	AT5G03260
		LAC11E	RC6G0177800	AT5G03260
		LAC11F	RC6G0181300	AT5G03260
		LAC17A	RC3G0261900	AT5G60020
		LAC17B	RC3G0262200	AT5G60020
		LAC17C	RC5G0533800	AT5G60020

Conserved Rosa 'Radrazz' mature miRNAs were identified from small RNA high throughput sequencing of axillary buds upon beheading and 6 h after beheading under light conditions. Target prediction was achieved using the web server's psRNAtarget (Dai X. et al., 2018; https://www.zhaolab.org/psRNATarget/) by using an expectation ≤3.5 to avoid false positive results. For target genes, corresponding accession numbers of Rosa chinensis homologs and Arabidopsis thaliana orthologs are indicated.

branching resulting from *phyB* loss-of-function and a low R/FR ratio. This phenotype is correlated to *BRC1* expression induction by PIF4/PIF5 and to abscisic acid (ABA) accumulation in axillary buds. Interestingly, several reports indicated that modulation of miRNA expression may contribute to the PHY-mediated light response, raising the hypothesis that this may contribute to branching modulation. For instance, analysis of miRNAs and their PHYB-mediated targets in rice leaves identified a total of 135 miRNAs differentially expressed between the WT and *phyB* mutant (Sun et al., 2015). This finding suggests that these miRNAs are directly or indirectly controlled by PHYB and participate in PHYB-mediated light signaling. In the same line, HY5 and PIFs transcription factors were reported to directly control the expression of several miRNA genes (Zhang et al., 2011; Xie et al., 2017). More recently, in Arabidopsis, PIF4 was reported to promote expression of genes encoding miR156/157, miR160, miR165/166, miR167, miR170/171, and miR394 and to reduce the expression of the genes encoding miR172 and miR319 by binding to the promoters of these miRNA genes (Sun et al., 2018). Compared to wild type, corresponding miRNA mutants had altered hypocotyl phenotypes, supporting a role for specific miRNAs in photomorphogenesis (Sun et al., 2018). In the extremophile plant *Eutrema salsugineum* under long-term action of R, Pashkovskiy et al. (2021) reported an increase in the expression of *PHYA*, *PHYB*, and *PHYC* as well as of *PIF4* and *PIF5* together with that of miR395, miR408 and miR165. In addition, they also observed a decrease in *HY5*, *miR171*, *miR157*, and *miR827* expressions. These data suggest that the quantity of these miRNAs in *E. salsugineum* is light-regulated in a PHY and PIF-mediated manner. Also, in *Solanum tuberosum* leaves, R light can induce miR398, 399, 408, 482, 8036, and 8049 expressions (Qiao et al., 2017). Among miRNAs whose expression is regulated by light, some (miRNA156, 171, 172, and 319) are involved in branching control (**Table 1**). These observations thus indicate that light *via* a PHY-dependent pathway may control bud outgrowth through modifying the expression of several miRNAs.

A key event in bud outgrowth is the initiation and expansion of leaves. While no experimental data report direct interaction between light signaling and miRNAs biogenesis in the control of leaf organogenesis during bud outgrowth, some works demonstrate that light regulates leaf expansion (Romanowski et al., 2021), and this partly occurs through miRNAs regulation (Pashkovskiy et al., 2016). Hence, Pashkovskiy et al. (2016) reported that blue light causes a significant increase in *miR167* expression which decreases the level of auxin-dependent *ARF6* transcripts in *Arabidopsis* leaves, thereby allowing leaf expansion. ARF transcription factors play an important role in the auxin-mediated gene transcription pathway by interacting with Aux/IAAs proteins, a key pathway involved in bud outgrowth (Vanneste and Friml, 2009; Dierck et al., 2016). In the same line, blue light (B) specifically down-regulates miR156 and miR157 and upregulates their target genes *SPL9* and *SPL15* during *Brassica rapa* subsp. Rapa seedling development (Zhou et al., 2016). These results, combined to increase shoot branching phenotype caused by *miR156* overexpression in *Brassica napus* (Wei et al., 2010), support the hypothesis of a crosstalk between light signaling and miRNAs regulation and suggest miR156/SPL couple acts as regulatory hub of bud outgrowth in response to light. More recently, Dong et al. (2020), found 20 miRNAs differentially expressed in tomato leaves after blue light treatment. Among them, *sly-miR9472-3p* expression is up-regulated by blue light treatment and is negatively correlated to the expression of its target gene *IPT5*, a cytokinin biosynthesis gene which plays a crucial role in promoting axillary bud outgrowth (Barbier et al., 2015; Roman et al., 2016). All these data suggest that miRNAs may well be involved in the light control of leaf expansion during bud outgrowth.

BIOINFORMATIC ANALYSIS OF PUTATIVE NEW MiRNAs IN THE CONTROL AND PHOTOCONTROL OF BUD OUTGROWTH IN *ROSA*

As described above, rosebush is a pertinent model to understand how light controls axillary bud outgrowth. Since little has been described on the role of miRNAs in the photocontrol of axillary bud outgrowth, we took advantage of the rose model to further examine whether components of the axillary bud outgrowth regulatory network (**Figure 1**) may be targets of post-transcriptional regulation *via* miRNAs.

To address this question, full length sequences of genes from this network were identified on *Rosa chinensis* genomes (Hibrand Saint-Oyant et al., 2018; Raymond et al., 2018) and confronted against the mature miRNAs sequences we identified in *Rosa* axillary bud from small RNA-seq using target prediction web server's psRNAtarget (Dai X. et al., 2018; see text footnote 2) (**Supplementary Table 1**).

Our bioinformatic analysis reveals that 9 out of the sixty-five genes related to axillary bud outgrowth and its photocontrol in *Rosa* are predicted to be targeted by 7 miRNA families. These families are conserved in plants. Out of these 7 miRNAs, only miR156 and miR164 have already been described as involved in control of bud outgrowth (**Table 1**). On the contrary, five miRNAs (miR159, miR166, miR399, miR477, and miR8175) were not yet identified for a possible role in the control of bud outgrowth but were characterized for other functions. This could be either because their contribution to axillary bud outgrowth could be masked by the action of other more prominent miRNAs or, alternatively, because the strict light dependence of rosebush axillary bud outgrowth involves novel regulatory circuits that are less conserved in other species, and thus less characterized. MiR159 has been reported in growth transition, programmed cell death, and seed germination (Reyes and Chua, 2007; Alonso-Peral et al., 2010; Guo et al., 2017). MiR166 is implicated in different developmental processes such as regulation of shoot meristem development (Zhang and Zhang, 2012), root growth and development (Boualem et al., 2008; Singh et al., 2014) and seed maturation (Tang et al., 2012). MiR399 has been studied for its role in phosphate homeostasis and starvation (Baek et al., 2013; Tian et al., 2018). For the two last, miR477 and miR8175, to date little data is available concerning their biological function. MiR477 is implicated in plant immunity in *Camellia sinensis*

and in *Gossypium hirsutum* (Hu et al., 2020; Wang S. et al., 2020), while miR8175 has been studied in *Arabidopsis thaliana* roots, and found to be upregulated by high-light intensity (Anna et al., 2019).

Among the nine genes identified as predicted targets, three genes participate in hormone signaling including two genes involved in the cytokinin pathway (*RhCKX1*, *RhCKX6*) both targeted by *miR159a_1* and one in the strigolactones pathway (*RwMAX4*) targeted by six miR166 members. These genes are involved in the repression of bud outgrowth in *Rosa*. Interestingly, none of the genes involved in auxin and gibberellin pathways are found as potential targets of post-transcriptional regulation *via* miRNAs. Concerning sugar control, two genes (*RhSUSY1*, *Rh6PFK*) are targeted by two different miRNAs: *miR8175* and *miR166e-5p*, respectively. Besides hormonal and sugar control, two genes involved in ROS metabolism are potential targets of miRNAs. The first one, *RhAPX1*, encoding antioxidant enzyme is targeted by three miR164 isoforms (miR164a_4, 164b, and 164e-5p), the other one (*RhRBOHB1*) encoding a NADPH oxidase is targeted by *miR399e_5*. Finally, two genes involved in the cell division (*RhCYCD3*;2) and expansion (*RhEXPA3*) are identified as potential targets of miR477e and miR156j_1, respectively. The validation of the interaction between these 7 miRNAs and the predicted rosebush targets awaits experimental confirmation. It is however noteworthy that, in agreement with our findings, miR159 was previously shown as targeting CKX with negative correlation of their expression in response to pathogens in poplar (Zhao et al., 2012). Furthermore, suppressing miR159 leads to a decreased expression of the CK synthesis gene, *OsIPT*, of CK signaling genes *OsRR* and of the CK degradation genes *OsCKX* in rice (Zhao et al., 2017). Taken together, these data suggest that miR159 may play a role in cytokinin metabolism and signaling and support our prediction of miR159 targeting two *CKX* in rosebush during bud outgrowth.

Our study reveals that even though few genes of the regulatory network of axillary bud outgrowth appear under miRNA regulation, most of the pathways identified in *Rosa* are potential targets of miRNA regulation (**Figure 2**). This suggests that miRNAs act on multiple pathways of the complex network regulating bud outgrowth in rosebush. Interestingly, six of the nine identified genes targeted by miRNAs have a light regulated expression (**Supplementary Table 1**). This brings up the hypothesis that their respective associated miRNAs might potentially act in the light transduction pathway (**Figure 2**).

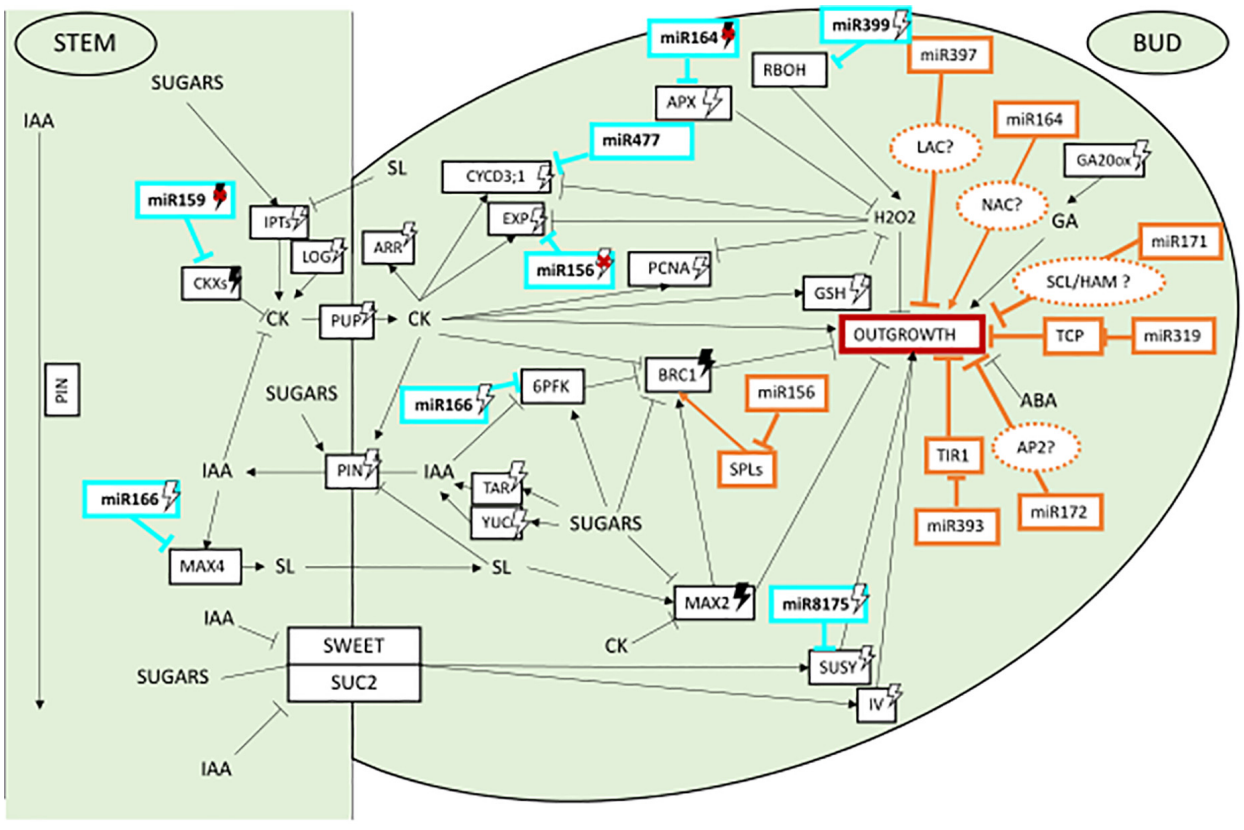

FIGURE 2 | Potential role of miRNAs in the control of axillary bud outgrowth and their light regulation in plants. In bright blue miRNAs identified in the present study as putative novel regulators in control of bud outgrowth. Black arrows heads mean induction, straight lines mean repression, white lightning bolt means induction by light, darked lightning bolt means induction by darkness, red cross means repression of the miRNA.

Further studies addressing the light regulation of these miRNAs in rosebush will be required to progress in the understanding of their role during axillary bud outgrowth.

The other two miRNAs identified here, miR156 and miR164 were already described to play a role in regulating shoot branching (as mentioned above). While miR156j_1 *Rosa* isoform and the 3 miR164 *Rosa* isoforms are predicted to bind to their conserved targets *SPL* and *NAC* (Laufs et al., 2004; Wang and Wang, 2015; Blein and Laufs, 2016; Xu et al., 2016), new targets were also identified by our analysis: *EXPA3* and *APX1*, respectively, both genes being light-regulated during bud outgrowth in *Rosa* (**Supplementary Table 1**). The Arabidopsis orthologs of these Rosa targets (*AtEXP15* and *AtAPX1*) lack a binding site for the miRNA (data not shown). Therefore, it is attractive to speculate that the addition of these new targets may have appeared by evolution of their sequence to create a novel miRNA binding site. The resulting bifurcated pathway downstream the miRNA, with one conserved branch (*SPL* or *NAC*) and one branch more species-specific (*EXPA3* or *APX1*) could provide robustness to the effect of the miRNA on bud outgrowth.

CONCLUSION AND FUTURE PERSPECTIVES

Multiple regulators have been described as acting in concert to fine tune, in an intricate network, axillary bud outgrowth as well as its photoregulation. While this network is mostly built on integrating knowledge gained at the transcriptional level, little is known to date about how post-transcriptional regulation fits into this network. Here, we provide new information by integrating post-transcriptional regulation of the photocontrol bud growth into this network. Based on the literature published mainly on Arabidopsis, rice and maize combined with our bioinformatic analysis on *Rosa* we explored specifically the potential role of miRNAs in the control of bud growth and how they may manage to interact with this network. Thus, we identified through bioinformatic analysis some conserved miRNAs families and their associated target genes as good candidates to play a potential role in the control of axillary bud outgrowth in the rosebush. Interestingly, these miRNAs have the ability to target key molecular players in all major pathways regulating bud outgrowth (including hormones, sugars, and ROS) with a far broader spectrum compared to previously reported studies. Additionally, according to literature, several of those such as miR156, miR164, miR166, and miR8175 are under light regulation which leads us to suggest that they may participate in the light-mediated mechanisms of axillary bud outgrowth. Whether or not these novel miRNA-gene target couples physically interact and demonstrate a biological relevance in the regulation of bud outgrowth and its photocontrol is still to be addressed. To this end, we need to move toward functional analysis and use of mutants.

Involvement of post-transcriptional factors in bud outgrowth control is not limited to miRNAs. Indeed, some studies have brought to light the possible role of small interfering RNAs (siRNAs) in this process (Ortiz-Morea et al., 2013; Kamthan et al., 2015). In this purpose, future research should be conducted to identify precisely which small RNAs are involved using deep sequencing and understand how they interact with miRNAs in the control of axillary bud outgrowth.

The understanding of the mechanisms behind miRNA control of bud outgrowth could be a great opportunity for improving agriculturally important traits such as plant architecture (Boumaza et al., 2010; Leduc et al., 2014; Huché-Thélier et al., 2016). Notably, it was shown recently that plant 5′ of primary miRNA contains a short open reading-frame (ORF) that encodes a peptide called micro-peptide (miPEPs). These miPEPs can raise the mature miRNA level by enhancing the transcription of their associated primary miRNA in a specific manner (Lauressergues et al., 2015). For that miPEPs could be used as powerful tools to lead to agronomic traits improvement under miRNA control (Couzigou et al., 2015).

DATA AVAILABILITY STATEMENT

The original contributions presented in the study are included in the article/**Supplementary Material**, further inquiries can be directed to the corresponding author/s.

AUTHOR CONTRIBUTIONS

JM, PL, NL, and JLG designed the experiments and wrote the manuscript. JM performed the experiments and bio informatic analysis. PL, NL, and JLG supervised the work. All authors read and approved the final manuscript.

FUNDING

This work was supported by University of Angers and Pays de la Loire Region, project ROSAPEPS funded by RFI-Objectif Vegetal. The IJPB benefits from the support of Saclay Plant Sciences-SPS (ANR-17-EUR-0007). JM was the recipient of a Ph.D. scholarship from the Ministére de l'Enseignement Supérieur et de la Recherche.

ACKNOWLEDGMENTS

We are grateful to Nathalie Brouard and Anita Lebrec for their help in bud sampling. We are most grateful to the ImorPhen core facility (Angers, France) for its technical support.

SUPPLEMENTARY MATERIAL

The Supplementary Material for this article can be found online at: https://www.frontiersin.org/articles/10.3389/fpls.2021.770363/full#supplementary-material

REFERENCES

Abidi, F., Girault, T., Douillet, O., Guillemain, G., Sintes, G., Laffaire, M., et al. (2013). Blue light effects on rose photosynthesis and photomorphogenesis: blue light and rose development. *Plant Biol.* 15, 67–74. doi: 10.1111/j.1438-8677.2012.00603.x

Aguilar-Martínez, J. A., Poza-Carrión, C., and Cubas, P. (2007). *Arabidopsis* BRANCHED1 Acts as an Integrator of Branching Signals within Axillary Buds. *Plant Cell* 19, 458–472. doi: 10.1105/tpc.106.048934

Alonso-Peral, M. M., Li, J., Li, Y., Allen, R. S., Schnippenkoetter, W., Ohms, S., et al. (2010). The MicroRNA159-Regulated *GAMYB-like* Genes Inhibit Growth and Promote Programmed Cell Death in *Arabidopsis*. *Plant Physiol.* 154, 757–771. doi: 10.1104/pp.110.160630

Anna, B.-B., Grzegorz, B., Marek, K., Piotr, G., and Marcin, F. (2019). Exposure to High-Intensity Light Systemically Induces Micro-Transcriptomic Changes in *Arabidopsis thaliana* Roots. *Int. J. Mol. Sci.* 20:5131. doi: 10.3390/ijms20205131

Aung, B., Gruber, M. Y., Amyot, L., Omari, K., Bertrand, A., and Hannoufa, A. (2015). MicroRNA156 as a promising tool for alfalfa improvement. *Plant Biotechnol. J.* 13, 779–790. doi: 10.1111/pbi.12308

Baek, D., Kim, M. C., Chun, H. J., Kang, S., Park, H. C., Shin, G., et al. (2013). Regulation of *miR399f* Transcription by AtMYB2 Affects Phosphate Starvation Responses in *Arabidopsis*. *Plant Physiol.* 161, 362–373. doi: 10.1104/pp.112.205922

Barbier, F. F., Cao, D., Fichtner, F., Weiste, C., Perez-Garcia, M., Caradeuc, M., et al. (2021). HEXOKINASE1 signalling promotes shoot branching and interacts with cytokinin and strigolactone pathways. *New Phytol.* 231, 1088–1104. doi: 10.1111/nph.17427

Barbier, F. F., Dun, E. A., Kerr, S. C., Chabikwa, T. G., and Beveridge, C. A. (2019). An Update on the Signals Controlling Shoot Branching. *Trends Plant Sci.* 24, 220–236. doi: 10.1016/j.tplants.2018.12.001

Barbier, F., Péron, T., Lecerf, M., Perez-Garcia, M.-D., Barrière, Q., Rolčík, J., et al. (2015). Sucrose is an early modulator of the key hormonal mechanisms controlling bud outgrowth in *Rosa hybrida*. *J. Exp. Bot.* 66, 2569–2582. doi: 10.1093/jxb/erv047

Bennett, T., Sieberer, T., Willett, B., Booker, J., Luschnig, C., and Leyser, O. (2006). The *Arabidopsis* MAX Pathway Controls Shoot Branching by Regulating Auxin Transport. *Curr. Biol.* 16, 553–563. doi: 10.1016/j.cub.2006.01.058

Bertheloot, J., Barbier, F., Boudon, F., Perez-Garcia, M. D., Péron, T., Citerne, S., et al. (2020). Sugar availability suppresses the auxin-induced strigolactone pathway to promote bud outgrowth. *New Phytol.* 225, 866–879. doi: 10.1111/nph.16201

Berthet, S., Demont-Caulet, N., Pollet, B., Bidzinski, P., Cézard, L., Le Bris, P., et al. (2011). Disruption of *LACCASE4* and *17* Results in Tissue-Specific Alterations to Lignification of *Arabidopsis thaliana* Stems. *Plant Cell* 23, 1124–1137. doi: 10.1105/tpc.110.082792

Beveridge, C. A., Symons, G. M., and Turnbull, C. G. N. (2000). Auxin Inhibition of Decapitation-Induced Branching Is Dependent on Graft-Transmissible Signals Regulated by Genes *Rms1* and *Rms2*. *Plant Physiol.* 123, 689–698. doi: 10.1104/pp.123.2.689

Blein, T., and Laufs, P. (2016). "MicroRNAs (miRNAs) and Plant Development," in *eLS*, (Chichester, UK: John Wiley & Sons, Ltd), eds John Wiley & Sons, Ltd. 1–11. doi: 10.1002/9780470015902.a0020106.pub2

Bonicel, A., Haddad, G., and Gagnaire, J. (1987). Seasonal variations of starch and major soluble sugars in the different organs of young poplars. *Plant Physiol. Biochem.* 25, 451–459.

Boualem, A., Laporte, P., Jovanovic, M., Laffont, C., Plet, J., Combier, J.-P., et al. (2008). MicroRNA166 controls root and nodule development in *Medicago truncatula*. *Plant J.* 54, 876–887. doi: 10.1111/j.1365-313X.2008.03448.x

Boumaza, R., Huché-Thélier, L., Demotes-Mainard, S., Coz, E. L., Leduc, N., Pelleschi-Travier, S., et al. (2010). Sensory profiles and preference analysis in ornamental horticulture: the case of the rosebush. *Food Qual. Prefer.* 21, 987–997. doi: 10.1016/j.foodqual.2010.05.003

Brewer, P. B. (2015). - Plant Architecture The Long and the Short of Branching in Potato. *Curr. Biol.* 25, R724–R725.

Brewer, P. B., Dun, E. A., Ferguson, B. J., Rameau, C., and Beveridge, C. A. (2009). Strigolactone Acts Downstream of Auxin to Regulate. bud outgrowth in pea and *Arabidopsis*. *Plant Physiol.* 150, 482–493.

Chatfield, S. P., Stirnberg, P., Forde, B. G., and Leyser, O. (2000). The hormonal regulation of axillary bud growth in *Arabidopsis*. *Plant J.* 24, 159–169. doi: 10.1046/j.1365-313x.2000.00862.x

Chen, X., Xia, X., Guo, X., Zhou, Y., Shi, K., Zhou, J., et al. (2016). Apoplastic H_2O_2 plays a critical role in axillary bud outgrowth by altering auxin and cytokinin homeostasis in tomato plants. *New Phytol.* 211, 1266–1278. doi: 10.1111/nph.14015

Choubane, D., Rabot, A., Mortreau, E., Legourrierec, J., Péron, T., Foucher, F., et al. (2012). Photocontrol of bud burst involves gibberellin biosynthesis in Rosa sp. *J. Plant Physiol.* 169, 1271–1280. doi: 10.1016/j.jplph.2012.04.014

Chuck, G., Cigan, A. M., Saeteurn, K., and Hake, S. (2007). The heterochronic maize mutant Corngrass1 results from overexpression of a tandem microRNA. *Nat. Genet.* 39, 544–549. doi: 10.1038/ng2001

Cline, M. G. (1997). Concepts and terminology of apical dominance. *Am. J. Bot.* 84, 1064–1069. doi: 10.2307/2446149

Cline, M. G., and Oh, C. (2006). A Reappraisal of the Role of Abscisic Acid and its Interaction with Auxin in Apical Dominance. *Ann. Bot.* 98, 891–897. doi: 10.1093/aob/mcl173

Corot, A., Roman, H., Douillet, O., Autret, H., Perez-Garcia, M.-D., Citerne, S., et al. (2017). Cytokinins and Abscisic Acid Act Antagonistically in the Regulation of the Bud Outgrowth Pattern by Light Intensity. *Front. Plant Sci.* 8:1724. doi: 10.3389/fpls.2017.01724

Couzigou, J.-M., Lauressergues, D., Bécard, G., and Combier, J.-P. (2015). miRNA-encoded peptides (miPEPs): a new tool to analyze the roles of miRNAs in plant biology. *RNA Biol.* 12, 1178–1180. doi: 10.1080/15476286.2015.1094601

Cui, L., Zheng, F., Wang, J., Zhang, C., Xiao, F., Ye, J., et al. (2020). miR156a-targeted SBP-Box transcription factor SlSPL13 regulates inflorescence morphogenesis by directly activating *SFT* in tomato. *Plant Biotechnol. J.* 18, 1670–1682. doi: 10.1111/pbi.13331

Curaba, J., Talbot, M., Li, Z., and Helliwell, C. (2013). Over-expression of microRNA171 affects phase transitions and floral meristem determinancy in barley. *BMC Plant Biol.* 13:6. doi: 10.1186/1471-2229-13-6

Dai, X., Zhuang, Z., and Zhao, P. X. (2018). psRNATarget: a plant small RNA target analysis server (2017 release). *Nucleic Acids Res.* 46, W49–W54. doi: 10.1093/nar/gky316

Dai, Z., Wang, J., Yang, X., Lu, H., Miao, X., and Shi, Z. (2018). Modulation of plant architecture by the miR156f–OsSPL7–OsGH3.8 pathway in rice. *J. Exp. Bot.* 69, 5117–5130. doi: 10.1093/jxb/ery273

Demotes-Mainard, S., Huché-Thélier, L., Morel, P., Boumaza, R., Guérin, V., and Sakr, S. (2013). Temporary water restriction or light intensity limitation promotes branching in rose bush. *Sci. Hortic.* 150, 432–440. doi: 10.1016/j.scienta.2012.12.005

Demotes-Mainard, S., Péron, T., Corot, A., Bertheloot, J., Le Gourrierec, J., Pelleschi-Travier, S., et al. (2016). Plant responses to red and far-red lights, applications in horticulture. *Environ. Exp. Bot.* 121, 4–21. doi: 10.1016/j.envexpbot.2015.05.010

Devitt, M. L., and Stafstrom, J. P. (1995). Cell cycle regulation during growth-dormancy cycles in pea axillary buds. *Plant Mol. Biol.* 29, 255–265. doi: 10.1007/BF00043650

Dierck, R., De Keyser, E., De Riek, J., Dhooghe, E., Van Huylenbroeck, J., Prinsen, E., et al. (2016). Change in Auxin and Cytokinin Levels Coincides with Altered Expression of Branching Genes during Axillary Bud Outgrowth in Chrysanthemum. *PLoS One* 11:e0161732. doi: 10.1371/journal.pone.0161732

Djennane, S., Hibrand-Saint Oyant, L., Kawamura, K., Lalanne, D., Laffaire, M., Thouroude, T., et al. (2014). Impacts of light and temperature on shoot branching gradient and expression of strigolactone synthesis and signalling genes in rose: light and temperature effects on rose branching. *Plant Cell Environ.* 37, 742–757. doi: 10.1111/pce.12191

Dodsworth, S. (2009). A diverse and intricate signalling network regulates stem cell fate in the shoot apical meristem. *Dev. Biol.* 336, 1–9. doi: 10.1016/j.ydbio.2009.09.031

Domagalska, M. A., and Leyser, O. (2011). Signal integration in the control of shoot branching. *Nat. Rev. Mol. Cell Biol.* 12, 211–221. doi: 10.1038/nrm3088

Dong, F., Wang, C., Dong, Y., Hao, S., Wang, L., Sun, X., et al. (2020). Differential expression of microRNAs in tomato leaves treated with different light qualities. *BMC Genomics* 21:37. doi: 10.1186/s12864-019-6440-4

Du, Y., Liu, L., Li, M., Fang, S., Shen, X., Chu, J., et al. (2017). UNBRANCHED3 regulates branching by modulating cytokinin biosynthesis and signaling in maize and rice. *New Phytol.* 214, 721–733. doi: 10.1111/nph.14391

Dun, E. A., de Saint Germain, A., Rameau, C., and Beveridge, C. A. (2012). Antagonistic Action of Strigolactone and Cytokinin in Bud Outgrowth Control. *Plant Physiol.* 158, 487–498. doi: 10.1104/pp.111.186783

Dun, E. A., Ferguson, B. J., and Beveridge, C. A. (2006). Apical Dominance and Shoot Branching. Divergent Opinions or Divergent Mechanisms? *Plant Physiol.* 142, 812–819. doi: 10.1104/pp.106.086868

Fahlgren, N., Howell, M. D., Kasschau, K. D., Chapman, E. J., Sullivan, C. M., Cumbie, J. S., et al. (2007). High-Throughput Sequencing of *Arabidopsis* microRNAs: evidence for Frequent Birth and Death of MIRNA Genes. *PLoS One* 2:e219. doi: 10.1371/journal.pone.0000219

Ferguson, B. J., and Beveridge, C. A. (2009). Roles for Auxin, Cytokinin, and Strigolactone in Regulating Shoot Branching. *Plant Physiol.* 149, 1929–1944. doi: 10.1104/pp.109.135475

Finlayson, S. A., Krishnareddy, S. R., Kebrom, T. H., and Casal, J. J. (2010). Phytochrome Regulation of Branching in *Arabidopsis*. *Plant Physiol.* 152, 1914–1927. doi: 10.1104/pp.109.148833

Garbez, M., Galopin, G., Sigogne, M., Favre, P., Demotes-Mainard, S., and Symoneaux, R. (2015). Assessing the visual aspect of rotating virtual rose bushes by a labeled sorting task. *Food Qual. Prefer.* 40, 287–295. doi: 10.1016/j.foodqual.2014.06.008

Girault, T., Abidi, F., Sigogne, M., Pelleschi-Travier, S., Boumaza, R., Sakr, S., et al. (2010). Sugars are under light control during bud burst in Rosa sp.: photocontrol of sugars during bud burst. *Plant Cell Environ.* 33, 1339–1350. doi: 10.1111/j.1365-3040.2010.02152.x

Girault, T., Bergougnoux, V., Combes, D., Viemont, J.-D., and Leduc, N. (2008). Light controls shoot meristem organogenic activity and leaf primordia growth during bud burst in *Rosa* sp. *Plant Cell Environ.* 31, 1534–1544. doi: 10.1111/j.1365-3040.2008.01856.x

Gocal, G. F. W., Pharis, R. P., Yeung, E. C., and Pearce, D. (1991). Changes after Decapitation in Concentrations of Indole-3-Acetic Acid and Abscisic Acid in the Larger Axillary Bud of *Phaseolus vulgaris* L. cv Tender Green. *Plant Physiol.* 95, 344–350. doi: 10.1104/pp.95.2.344

González-Grandío, E., Poza-Carrión, C., Sorzano, C. O. S., and Cubas, P. (2013). BRANCHED1 Promotes Axillary Bud Dormancy in Response to Shade in *Arabidopsis*. *Plant Cell* 25, 834–850. doi: 10.1105/tpc.112.108480

Guo, C., Xu, Y., Shi, M., Lai, Y., Wu, X., Wang, H., et al. (2017). Repression of miR156 by miR159 Regulates the Timing of the Juvenile-to-Adult Transition in *Arabidopsis*. *Plant Cell* 29, 1293–1304. doi: 10.1105/tpc.16.00975

Guo, S., Xu, Y., Liu, H., Mao, Z., Zhang, C., Ma, Y., et al. (2013). The interaction between OsMADS57 and OsTB1 modulates rice tillering via DWARF14. *Nat. Commun.* 4:1566. doi: 10.1038/ncomms2542

Han, H., Yan, A., Li, L., Zhu, Y., Feng, B., Liu, X., et al. (2020). A signal cascade originated from epidermis defines apical-basal patterning of *Arabidopsis* shoot apical meristems. *Nat. Commun.* 11:1214. doi: 10.1038/s41467-020-14989-4

Henry, C., Rabot, A., Laloi, M., Mortreau, E., Sigogne, M., Leduc, N., et al. (2011). Regulation of RhSUC2, a sucrose transporter, is correlated with the light control of bud burst in Rosa sp.: sucrose transporter role in bud burst. *Plant Cell Environ.* 34, 1776–1789. doi: 10.1111/j.1365-3040.2011.02374.x

Hibrand Saint-Oyant, L., Ruttink, T., Hamama, L., Kirov, I., Lakhwani, D., Zhou, N. N., et al. (2018). A high-quality genome sequence of Rosa chinensis to elucidate ornamental traits. *Nat. Plants* 4, 473–484. doi: 10.1038/s41477-018-0166-1

Holalu, S. V., Reddy, S. K., Blackman, B. K., and Finlayson, S. A. (2020). Phytochrome interacting factors 4 and 5 regulate axillary branching via bud abscisic acid and stem auxin signalling. *Plant Cell Environ.* 43, 2224–2238. doi: 10.1111/pce.13824

Hu, G., Hao, M., Wang, L., Liu, J., Zhang, Z., Tang, Y., et al. (2020). The Cotton miR477- *CBP60A* Module Participates in Plant Defense Against *Verticillium dahlia*. *Mol. Plant Microbe Interact.* 33, 624–636. doi: 10.1094/MPMI-10-19-0302-R

Huang, J., Li, Z., and Zhao, D. (2016). Deregulation of the OsmiR160 Target Gene OsARF18 Causes Growth and Developmental Defects with an Alteration of Auxin Signaling in Rice. *Sci. Rep.* 6:29938. doi: 10.1038/srep29938

Huang, W., Peng, S., Xian, Z., Lin, D., Hu, G., Yang, L., et al. (2017). Overexpression of a tomato miR171 target gene *SlGRAS24* impacts multiple agronomical traits via regulating gibberellin and auxin homeostasis. *Plant Biotechnol. J.* 15, 472–488. doi: 10.1111/pbi.12646

Huché-Thélier, L., Crespel, L., Gourrierec, J. L., Morel, P., Sakr, S., and Leduc, N. (2016). Light signaling and plant responses to blue and UV radiations—Perspectives for applications in horticulture. *Environ. Exp. Bot.* 121, 22–38. doi: 10.1016/j.envexpbot.2015.06.009

Jiao, Y., Wang, Y., Xue, D., Wang, J., Yan, M., Liu, G., et al. (2010). Regulation of OsSPL14 by OsmiR156 defines ideal plant architecture in rice. *Nat. Genet.* 42, 541–544. doi: 10.1038/ng.591

Kamthan, A., Chaudhuri, A., Kamthan, M., and Datta, A. (2015). Small RNAs in plants: recent development and application for crop improvement. *Front. Plant Sci.* 06:208. doi: 10.3389/fpls.2015.00208

Kebrom, T. H., and Mullet, J. E. (2016). Transcriptome Profiling of Tiller Buds Provides New Insights into PhyB Regulation of Tillering and Indeterminate Growth in Sorghum. *Plant Physiol.* 170, 2232–2250. doi: 10.1104/pp.16.00014

Kebrom, T. H., Chandler, P. M., Swain, S. M., King, R. W., Richards, R. A., and Spielmeyer, W. (2012). Inhibition of Tiller Bud Outgrowth in the *tin* Mutant of Wheat Is Associated with Precocious Internode Development. *Plant Physiol.* 160, 308–318. doi: 10.1104/pp.112.197954

Knox, J. P., and Wareing, P. F. (1984). Apical Dominance in *Phaseolus vulgaris* L.: the Possible Roles of Abscisic and Indole-3-Acetic Acid. *J. Exp. Bot.* 35, 239–244.

Koornneef, M., and van der Veen, J. H. (1980). Induction and Analysis of gibberellin Sensitive Mutants in *Arabidopsis thaliana* (L.) Heynh. *Theor. Appl. Genet.* 58, 257–263.

Kotov, A. A., Kotova, L. M., and Romanov, G. A. (2021). Signaling network regulating plant branching: recent advances and new challenges. *Plant Sci.* 307:110880. doi: 10.1016/j.plantsci.2021.110880

Kozomara, A., Birgaoanu, M., and Griffiths-Jones, S. (2019). miRBase: from microRNA sequences to function. *Nucleic Acids Res.* 47, D155–D162. doi: 10.1093/nar/gky1141

Kravchik, M., Stav, R., Belausov, E., and Arazi, T. (2019). Functional Characterization of microRNA171 Family in Tomato. *Plants* 8:10. doi: 10.3390/plants8010010

Lang, G., Early, J., Martin, G., and Darnell, R. (1987). Endo-, para-, and ecodormancy: physiological terminology and classification for dormancy research. *HortScience* 22, 371–377.

Laufs, P., Peaucelle, A., Morin, H., and Traas, J. (2004). MicroRNA regulation of the CUC genes is required for boundary size control in *Arabidopsis* meristems. *Development* 131, 4311–4322. doi: 10.1242/dev.01320

Lauressergues, D., Couzigou, J.-M., Clemente, H. S., Martinez, Y., Dunand, C., Bécard, G., et al. (2015). Primary transcripts of microRNAs encode regulatory peptides. *Nature* 520, 90–93. doi: 10.1038/nature14346

Le Bris, M., Michaux-Ferrière, N., Jacob, Y., Poupet, A., Barthe, P., Guigonis, J.-M., et al. (1999). Regulation of bud dormancy by manipulation of ABA in isolated buds of *Rosa hybrida* cultured in vitro. *Funct. Plant Biol.* 26, 273–281. doi: 10.1071/PP98133

Le Hir, R., Leduc, N., Jeannette, E., Viemont, J.-D., and Pelleschi-Travier, S. (2006). Variations in sucrose and ABA concentrations are concomitant with heteroblastic leaf shape changes in a rhythmically growing species (*Quercus robur*). *Tree Physiol.* 26, 229–238. doi: 10.1093/treephys/26.2.229

Le Moigne, M.-A., Guérin, V., Furet, P.-M., Billard, V., Lebrec, A., Spíchal, L., et al. (2018). Asparagine and sugars are both required to sustain secondary axis elongation after bud outgrowth in *Rosa hybrida*. *J. Plant Physiol.* 222, 17–27. doi: 10.1016/j.jplph.2017.12.013

Leduc, N., Roman, H., Barbier, F., Péron, T., Huché-Thélier, L., Lothier, J., et al. (2014). Light Signaling in Bud Outgrowth and Branching in Plants. *Plants* 3, 223–250. doi: 10.3390/plants3020223

Li, C., and Zhang, B. (2016). MicroRNAs in Control of Plant Development. *J. Cell. Physiol.* 231, 303–313. doi: 10.1002/jcp.25125

Li, G., Tan, M., Cheng, F., Liu, X., Qi, S., Chen, H., et al. (2018). Molecular role of cytokinin in bud activation and outgrowth in apple branching based on transcriptomic analysis. *Plant Mol. Biol.* 98, 261–274. doi: 10.1007/s11103-018-0781-2

Li, X., Xia, K., Liang, Z., Chen, K., Gao, C., and Zhang, M. (2016). MicroRNA393 is involved in nitrogen-promoted rice tillering through regulation of auxin signal transduction in axillary buds. *Sci. Rep.* 6:32158. doi: 10.1038/srep32158

Lian, H., Wang, L., Ma, N., Zhou, C.-M., Han, L., Zhang, T.-Q., et al. (2021). Redundant and specific roles of individual MIR172 genes in plant development. *PLoS Biol.* 19:e3001044. doi: 10.1371/journal.pbio.3001044

Li-Marchetti, C., Le Bras, C., Relion, D., Citerne, S., Huché-Thélier, L., Sakr, S., et al. (2015). Genotypic differences in architectural and physiological responses to water restriction in rose bush. *Front. Plant Sci.* 06:355. doi: 10.3389/fpls.2015.00355

Liu, H., Yu, H., Tang, G., and Huang, T. (2018). Small but powerful: function of microRNAs in plant development. *Plant Cell Rep.* 37, 515–528. doi: 10.1007/s00299-017-2246-5

Liu, S., Mi, X., Zhang, R., An, Y., Zhou, Q., Yang, T., et al. (2019). Integrated analysis of miRNAs and their targets reveals that miR319c/TCP2 regulates apical bud burst in tea plant (*Camellia sinensis*). *Planta* 250, 1111–1129. doi: 10.1007/s00425-019-03207-1

Lu, Z., Yu, H., Xiong, G., Wang, J., Jiao, Y., Liu, G., et al. (2013). Genome-Wide Binding Analysis of the Transcription Activator IDEAL PLANT ARCHITECTURE1 Reveals a Complex Network Regulating Rice Plant Architecture. *Plant Cell* 25, 3743–3759. doi: 10.1105/tpc.113.113639

Marquat, C., Vandamme, M., Gendraud, M., and Pétel, G. (1999). Dormancy in vegetative buds of peach: relation between carbohydrate absorption potentials and carbohydrate concentration in the bud during dormancy and its release. *Sci. Hortic.* 79, 151–162. doi: 10.1016/S0304-4238(98)00203-9

Mason, M. G., Ross, J. J., Babst, B. A., Wienclaw, B. N., and Beveridge, C. A. (2014). Sugar demand, not auxin, is the initial regulator of apical dominance. *Proc. Natl. Acad. Sci. U. S. A.* 111, 6092–6097. doi: 10.1073/pnas.1322045111

Maugarny-Calès, A., and Laufs, P. (2018). Getting leaves into shape: a molecular, cellular, environmental and evolutionary view. *Development* 145:dev161646. doi: 10.1242/dev.161646

Meitha, K., Agudelo-Romero, P., Signorelli, S., Gibbs, D. J., Considine, J. A., Foyer, C. H., et al. (2018). Developmental control of hypoxia during bud burst in grapevine: developmental hypoxia in grapevine buds. *Plant Cell Environ.* 41, 1154–1170. doi: 10.1111/pce.13141

Miura, K., Ikeda, M., Matsubara, A., Song, X.-J., Ito, M., Asano, K., et al. (2010). OsSPL14 promotes panicle branching and higher grain productivity in rice. *Nat. Genet.* 42, 545–549. doi: 10.1038/ng.592

Morea, E. G. O., da Silva, E. M., e Silva, G. F. F., Valente, G. T., Barrera Rojas, C. H., Vincentz, M., et al. (2016). Functional and evolutionary analyses of the miR156 and miR529 families in land plants. *BMC Plant Biol.* 16:40. doi: 10.1186/s12870-016-0716-5

Ophir, R., Pang, X., Halaly, T., Venkateswari, J., Lavee, S., Galbraith, D., et al. (2009). Gene-expression profiling of grape bud response to two alternative dormancy-release stimuli expose possible links between impaired mitochondrial activity, hypoxia, ethylene-ABA interplay and cell enlargement. *Plant Mol. Biol.* 71, 403–423. doi: 10.1007/s11103-009-9531-9

Or, E., Vilozny, I., Fennell, A., Eyal, Y., and Ogrodovitch, A. (2002). Dormancy in grape buds: isolation and characterization of catalase cDNA and analysis of its expression following chemical induction of bud dormancy release. *Plant Sci.* 162, 121–130. doi: 10.1016/S0168-9452(01)00542-8

Ortiz-Morea, F. A., Vicentini, R., Silva, G. F. F., Silva, E. M., Carrer, H., Rodrigues, A. P., et al. (2013). Global analysis of the sugarcane microtranscriptome reveals a unique composition of small RNAs associated with axillary bud outgrowth. *J. Exp. Bot.* 64, 2307–2320. doi: 10.1093/jxb/ert089

Palatnik, J. F., Allen, E., Wu, X., Schommer, C., Schwab, R., Carrington, J. C., et al. (2003). Control of leaf morphogenesis by microRNAs. *Nature* 425, 257–263. doi: 10.1038/nature01958

Park, S. J., Choi, S. W., Kim, G. M., Møller, C., Pai, H.-S., and Yang, S. W. (2021). Light-stabilized FHA2 suppresses miRNA biogenesis through interactions with DCL1 and HYL1. *Mol. Plant* 14, 647–663. doi: 10.1016/j.molp.2021.01.020

Pashkovskiy, P. P., Kartashov, A. V., Zlobin, I. E., Pogosyan, S. I., and Kuznetsov, V. V. (2016). Blue light alters miR167 expression and microRNA-targeted auxin response factor genes in *Arabidopsis thaliana* plants. *Plant Physiol. Biochem.* 104, 146–154. doi: 10.1016/j.plaphy.2016.03.018

Pashkovskiy, P., Ryazansky, S., Kartashov, A., Voloshin, R., Khudyakova, A., Kosobryukhov, A. A., et al. (2021). Effect of red light on photosynthetic acclimation and the gene expression of certain light signalling components involved in the microRNA biogenesis in the extremophile Eutrema salsugineum. *J. Biotechnol.* 325, 35–42. doi: 10.1016/j.jbiotec.2020.11.018

Pérez, V. I., Van Remmen, H., Bokov, A., Epstein, C. J., Vijg, J., and Richardson, A. (2009). The overexpression of major antioxidant enzymes does not extend the lifespan of mice. *Aging Cell* 8, 73–75. doi: 10.1111/j.1474-9726.2008.00449.x

Porcher, A., Guérin, V., Leduc, N., Lebrec, A., Lothier, J., and Vian, A. (2021). Ascorbate–glutathione pathways mediated by cytokinin regulate H2O2 levels in light-controlled rose bud burst. *Plant Physiol.* 186, 910–928. doi: 10.1093/plphys/kiab123

Porcher, A., Guérin, V., Montrichard, F., Lebrec, A., Lothier, J., and Vian, A. (2020). Ascorbate glutathione-dependent H2O2 scavenging is an important process in axillary bud outgrowth in rosebush. *Ann. Bot.* 126, 1049–1062. doi: 10.1093/aob/mcaa130

Preston, J. C., and Hileman, L. C. (2013). Functional Evolution in the Plant SQUAMOSA-PROMOTER BINDING PROTEIN-LIKE (SPL) Gene Family. *Front. Plant Sci.* 4:80. doi: 10.3389/fpls.2013.00080

Prusinkiewicz, P., Crawford, S., Smith, R. S., Ljung, K., Bennett, T., Ongaro, V., et al. (2009). Control of bud activation by an auxin transport switch. *Proc. Natl. Acad. Sci. U. S. A.* 106, 17431–17436. doi: 10.1073/pnas.0906696106

Pulido, A., and Laufs, P. (2010). Co-ordination of developmental processes by small RNAs during leaf development. *J. Exp. Bot.* 61, 1277–1291. doi: 10.1093/jxb/erp397

Qiao, Y., Zhang, J., Zhang, J., Wang, Z., Ran, A., Guo, H., et al. (2017). Integrated RNA-seq and sRNA-seq analysis reveals miRNA effects on secondary metabolism in *Solanum tuberosum* L. *Mol. Genet. Genomics* 292, 37–52. doi: 10.1007/s00438-016-1253-5

Rabot, A., Henry, C., Ben Baaziz, K., Mortreau, E., Azri, W., Lothier, J., et al. (2012). Insight into the Role of Sugars in Bud Burst Under Light in the Rose. *Plant Cell Physiol.* 53, 1068–1082. doi: 10.1093/pcp/pcs051

Rabot, A., Portemer, V., Péron, T., Mortreau, E., Leduc, N., Hamama, L., et al. (2014). Interplay of Sugar, Light and Gibberellins in Expression of *Rosa hybrida* Vacuolar Invertase 1 Regulation. *Plant Cell Physiol.* 55, 1734–1748. doi: 10.1093/pcp/pcu106

Rajagopalan, R., Vaucheret, H., Trejo, J., and Bartel, D. P. (2006). A diverse and evolutionarily fluid set of microRNAs in *Arabidopsis thaliana*. *Genes Dev.* 20, 3407–3425. doi: 10.1101/gad.1476406

Rameau, C., Bertheloot, J., Leduc, N., Andrieu, B., Foucher, F., and Sakr, S. (2015). Multiple pathways regulate shoot branching. *Front. Plant Sci.* 5:741. doi: 10.3389/fpls.2014.00741

Raymond, O., Gouzy, J., Just, J., Badouin, H., Verdenaud, M., Lemainque, A., et al. (2018). The Rosa genome provides new insights into the domestication of modern roses. *Nat. Genet.* 50, 772–777. doi: 10.1038/s41588-018-0110-3

Reyes, J. L., and Chua, N.-H. (2007). ABA induction of miR159 controls transcript levels of two MYB factors during *Arabidopsis* seed germination: miR159 regulation of ABA responses during germination. *Plant J.* 49, 592–606. doi: 10.1111/j.1365-313X.2006.02980.x

Roman, H., Girault, T., Barbier, F., Péron, T., Brouard, N., Pìnčík, A., et al. (2016). Cytokinins Are Initial Targets of Light in the Control of Bud Outgrowth. *Plant Physiol.* 172, 489–509. doi: 10.1104/pp.16.00530

Roman, H., Girault, T., Le Gourrierec, J., and Leduc, N. (2017). *In silico* analysis of 3 expansin gene promoters reveals 2 hubs controlling light and cytokinins response during bud outgrowth. *Plant Signal. Behav.* 12:e1284725. doi: 10.1080/15592324.2017.1284725

Romanowski, A., Furniss, J. J., Hussain, E., and Halliday, K. J. (2021). Phytochrome regulates cellular response plasticity and the basic molecular machinery of leaf development. *Plant Physiol.* 186, 1220–1239. doi: 10.1093/plphys/kiab112

Sagi, M., Davydov, O., Orazova, S., Yesbergenova, Z., Ophir, R., Stratmann, J. W., et al. (2004). Plant Respiratory Burst Oxidase Homologs Impinge on Wound Responsiveness and Development in *Lycopersicon esculentum* [W]. *Plant Cell* 16, 616–628. doi: 10.1105/tpc.019398

Sánchez-Retuerta, C., Suaréz-López, P., and Henriques, R. (2018). Under a New Light: regulation of Light-Dependent Pathways by Non-coding RNAs. *Front. Plant Sci.* 9:962. doi: 10.3389/fpls.2018.00962

Schneider, A., Godin, C., Boudon, F., Demotes-Mainard, S., Sakr, S., and Bertheloot, J. (2019). Light Regulation of Axillary Bud Outgrowth Along Plant Axes: an Overview of the Roles of Sugars and Hormones. *Front. Plant Sci.* 10:1296. doi: 10.3389/fpls.2019.01296

Schulze, S., Schäfer, B. N., Parizotto, E. A., Voinnet, O., and Theres, K. (2010). LOST MERISTEMS genes regulate cell differentiation of central zone

descendants in *Arabidopsis* shoot meristems: LOM genes control meristem maintenance. *Plant J.* 64, 668–678. doi: 10.1111/j.1365-313X.2010.04359.x

Shimizu, S., and Mori, H. (1998). Analysis of Cycles of Dormancy and Growth in Pea Axillary Buds Based on mRNA Accumulation Patterns of Cell Cycle-Related Genes. *Plant Cell Physiol.* 39, 255–262. doi: 10.1093/oxfordjournals.pcp.a029365

Singh, A., Singh, S., Panigrahi, K. C. S., Reski, R., and Sarkar, A. K. (2014). Balanced activity of microRNA166/165 and its target transcripts from the class III homeodomain-leucine zipper family regulates root growth in *Arabidopsis thaliana*. *Plant Cell Rep.* 33, 945–953. doi: 10.1007/s00299-014-1573-z

Sudawan, B., Chang, C.-S., Chao, H., Ku, M. S. B., and Yen, Y. (2016). Hydrogen cyanamide breaks grapevine bud dormancy in the summer through transient activation of gene expression and accumulation of reactive oxygen and nitrogen species. *BMC Plant Biol.* 16:202. doi: 10.1186/s12870-016-0889-y

Sun, W., Xu, X. H., Wu, X., Wang, Y., Lu, X., Sun, H., et al. (2015). Genome-wide identification of microRNAs and their targets in wild type and phyB mutant provides a key link between microRNAs and the phyB-mediated light signaling pathway in rice. *Front. Plant Sci.* 6:372. doi: 10.3389/fpls.2015.00372

Sun, Z., Li, M., Zhou, Y., Guo, T., Liu, Y., Zhang, H., et al. (2018). Coordinated regulation of *Arabidopsis* microRNA biogenesis and red light signaling through Dicer-like 1 and phytochrome-interacting factor 4. *PLoS Genet.* 14:e1007247. doi: 10.1371/journal.pgen.1007247

Sun, Z., Su, C., Yun, J., Jiang, Q., Wang, L., Wang, Y., et al. (2019). Genetic improvement of the shoot architecture and yield in soya bean plants via the manipulation of *GmmiR156b*. *Plant Biotechnol. J.* 17, 50–62. doi: 10.1111/pbi.12946

Sunkar, R., Girke, T., Jain, P. K., and Zhu, J.-K. (2005). Cloning and Characterization of MicroRNAs from Rice. *Plant Cell* 17, 1397–1411. doi: 10.1105/tpc.105.031682

Sussex, I. M., and Kerk, N. M. (2001). The evolution of plant architecture. *Curr. Opin. Plant Biol.* 4, 33–37. doi: 10.1016/S1369-5266(00)00132-1

Suttle, J. C. (2009). Ethylene Is Not Involved in Hormone- and Bromoethane-Induced Dormancy Break in Russet Burbank Minitubers. *Am. J. Potato Res.* 86, 278–285. doi: 10.1007/s12230-009-9081-3

Tang, X., Bian, S., Tang, M., Lu, Q., Li, S., Liu, X., et al. (2012). MicroRNA–Mediated Repression of the Seed Maturation Program during Vegetative Development in *Arabidopsis*. *PLoS Genet.* 8:e1003091. doi: 10.1371/journal.pgen.1003091

Tian, C., Zhang, X., He, J., Yu, H., Wang, Y., Shi, B., et al. (2014). An organ boundary-enriched gene regulatory network uncovers regulatory hierarchies underlying axillary meristem initiation. *Mol. Syst. Biol.* 10:755. doi: 10.15252/msb.20145470

Tian, L., Liu, H., Ren, L., Ku, L., Wu, L., Li, M., et al. (2018). MicroRNA 399 as a potential integrator of photo-response, phosphate homeostasis, and sucrose signaling under long day condition. *BMC Plant Biol* 18:290. doi: 10.1186/s12870-018-1460-9

Tucker, D. J. (1976). ENDOGENOUS GROWTH REGULATORS IN RELATION TO SIDE SHOOT DEVELOPMENT IN THE TOMATO. *New Phytol.* 77, 561–568. doi: 10.1111/j.1469-8137.1976.tb04647.x

Vanneste, S., and Friml, J. (2009). Auxin: a Trigger for Change in Plant Development. *Cell* 136, 1005–1016. doi: 10.1016/j.cell.2009.03.001

Vergara, R., Parada, F., Rubio, S., and Pérez, F. J. (2012). Hypoxia induces H2O2 production and activates antioxidant defence system in grapevine buds through mediation of H2O2 and ethylene. *J. Exp. Bot.* 63, 4123–4131.

Voinnet, O. (2009). Origin, Biogenesis, and Activity of Plant MicroRNAs. *Cell* 136, 669–687. doi: 10.1016/j.cell.2009.01.046

Walton, E. F., Wu, R.-M., Richardson, A. C., Davy, M., Hellens, R. P., Thodey, K., et al. (2009). A rapid transcriptional activation is induced by the dormancy-breaking chemical hydrogen cyanamide in kiwifruit (*Actinidia deliciosa*) buds. *J. Exp. Bot.* 60, 3835–3848. doi: 10.1093/jxb/erp231

Wang, C.-Y., Chen, Y.-Q., and Liu, Q. (2011). Sculpting the meristem: the roles of miRNAs in plant stem cells. *Biochem. Biophys. Res. Commun.* 409, 363–366. doi: 10.1016/j.bbrc.2011.04.123

Wang, H., and Wang, H. (2015). The miR156/SPL Module, a Regulatory Hub and Versatile Toolbox, Gears up Crops for Enhanced Agronomic Traits. *Mol. Plant* 8, 677–688. doi: 10.1016/j.molp.2015.01.008

Wang, J.-W., Czech, B., and Weigel, D. (2009). miR156-Regulated SPL Transcription Factors Define an Endogenous Flowering Pathway in *Arabidopsis thaliana*. *Cell* 138, 738–749. doi: 10.1016/j.cell.2009.06.014

Wang, L., Mai, Y.-X., Zhang, Y.-C., Luo, Q., and Yang, H.-Q. (2010). MicroRNA171c-Targeted SCL6-II, SCL6-III, and SCL6-IV Genes Regulate Shoot Branching in *Arabidopsis*. *Mol. Plant* 3, 794–806. doi: 10.1093/mp/ssq042

Wang, L., Sun, S., Jin, J., Fu, D., Yang, X., Weng, X., et al. (2015). Coordinated regulation of vegetative and reproductive branching in rice. *Proc. Natl. Acad. Sci. U. S. A.* 112, 15504–15509. doi: 10.1073/pnas.1521949112

Wang, M., Le Moigne, M.-A., Bertheloot, J., Crespel, L., Perez-Garcia, M.-D., Ogé, L., et al. (2019a). BRANCHED1: a Key Hub of Shoot Branching. *Front. Plant Sci.* 10:76. doi: 10.3389/fpls.2019.00076

Wang, M., Ogé, L., Voisine, L., Perez-Garcia, M.-D., Jeauffre, J., Hibrand Saint-Oyant, L., et al. (2019b). Posttranscriptional Regulation of RhBRC1 (*Rosa hybrida* BRANCHED1) in Response to Sugars is Mediated via its Own 3′ Untranslated Region, with a Potential Role of RhPUF4 (Pumilio RNA-Binding Protein Family). *Int. J. Mol. Sci.* 20:3808. doi: 10.3390/ijms20153808

Wang, M., Pérez-Garcia, M.-D., Davière, J.-M., Barbier, F., Ogé, L., Gentilhomme, J., et al. (2021). Outgrowth of the axillary bud in rose is controlled by sugar metabolism and signalling. *J. Exp. Bot.* 72, 3044–3060. doi: 10.1093/jxb/erab046

Wang, M., Zang, L., Jiao, F., Perez-Garcia, M.-D., Ogé, L., Hamama, L., et al. (2020). Sugar Signaling and Post-transcriptional Regulation in Plants: an Overlooked or an Emerging Topic? *Front. Plant Sci.* 11:578096. doi: 10.3389/fpls.2020.578096

Wang, R., Yang, X., Guo, S., Wang, Z., Zhang, Z., and Fang, Z. (2021). MiR319-targeted *OsTCP21* and *OsGAmyb* regulate tillering and grain yield in rice. *J. Integr. Plant Biol.* 63, 1260–1272. doi: 10.1111/jipb.13097

Wang, S., Liu, S., Liu, L., Li, R., Guo, R., Xia, X., et al. (2020). miR477 targets the phenylalanine ammonia-lyase gene and enhances the susceptibility of the tea plant (*Camellia sinensis*) to disease during Pseudopestalotiopsis species infection. *Planta* 251:59. doi: 10.1007/s00425-020-03353-x

Wang, Y., Wang, Z., Amyot, L., Tian, L., Xu, Z., Gruber, M. Y., et al. (2015). Ectopic expression of miR156 represses nodulation and causes morphological and developmental changes in *Lotus japonicus*. *Mol. Genet. Genomics* 290, 471–484. doi: 10.1007/s00438-014-0931-4

Weber, M. J. (2004). New human and mouse microRNA genes found by homology search: new human and mouse microRNA gene. *FEBS J.* 272, 59–73. doi: 10.1111/j.1432-1033.2004.04389.x

Wei, S., Gruber, M. Y., Yu, B., Gao, M.-J., Khachatourians, G. G., Hegedus, D. D., et al. (2012). *Arabidopsis* mutant sk156 reveals complex regulation of SPL15 in a miR156-controlled gene network. *BMC Plant Biol.* 12:169. doi: 10.1186/1471-2229-12-169

Wei, S., Yu, B., Gruber, M. Y., Khachatourians, G. G., Hegedus, D. D., and Hannoufa, A. (2010). Enhanced Seed Carotenoid Levels and Branching in Transgenic *Brassica napus* Expressing the *Arabidopsis miR156b* Gene. *J. Agric. Food Chem.* 58, 9572–9578. doi: 10.1021/jf102635f

Wightman, B., Ha, I., and Ruvkun, G. (1993). Posttranscriptional regulation of the heterochronic gene lin-14 by lin-4 mediates temporal pattern formation in *C. elegans*. *Cell* 75, 855–862. doi: 10.1016/0092-8674(93)90530-4

Wu, G. (2013). Plant MicroRNAs and Development. *J. Genet. Genomics* 40, 217–230. doi: 10.1016/j.jgg.2013.04.002

Xia, K., Wang, R., Ou, X., Fang, Z., Tian, C., Duan, J., et al. (2012). OsTIR1 and OsAFB2 Downregulation via OsmiR393 Overexpression Leads to More Tillers, Early Flowering and Less Tolerance to Salt and Drought in Rice. *PLoS One* 7:e30039. doi: 10.1371/journal.pone.0030039

Xie, Y., Liu, Y., Wang, H., Ma, X., Wang, B., Wu, G., et al. (2017). Phytochrome-interacting factors directly suppress MIR156 expression to enhance shade-avoidance syndrome in *Arabidopsis*. *Nat. Commun.* 8:348. doi: 10.1038/s41467-017-00404-y

Xu, M., Hu, T., Zhao, J., Park, M.-Y., Earley, K. W., Wu, G., et al. (2016). Developmental Functions of miR156-Regulated SQUAMOSA PROMOTER BINDING PROTEIN-LIKE (SPL) Genes in *Arabidopsis thaliana*. *PLoS Genet.* 12:e1006263. doi: 10.1371/journal.pgen.1006263

Yan, Y., Wei, M., Li, Y., Tao, H., Wu, H., Chen, Z., et al. (2021). MiR529a controls plant height, tiller number, panicle architecture and grain size by regulating SPL target genes in rice (*Oryza sativa* L.). *Plant Sci.* 302:110728. doi: 10.1016/j.plantsci.2020.110728

Yang, T., Wang, Y., Teotia, S., Zhang, Z., and Tang, G. (2018). The Making of Leaves: how Small RNA Networks Modulate Leaf Development. *Front. Plant Sci.* 9:824. doi: 10.3389/fpls.2018.00824

Yue, E., Li, C., Li, Y., Liu, Z., and Xu, J.-H. (2017). MiR529a modulates panicle architecture through regulating SQUAMOSA PROMOTER BINDING-LIKE genes in rice (*Oryza sativa*). *Plant Mol. Biol.* 94, 469–480. doi: 10.1007/s11103-017-0618-4

Zhan, J., Chu, Y., Wang, Y., Diao, Y., Zhao, Y., Liu, L., et al. (2021). The miR164-GhCUC2-GhBRC1 module regulates plant architecture through abscisic acid in cotton. *Plant Biotechnol. J.* 19, 1839–1851. doi: 10.1111/pbi.13599

Zhang, B., Pan, X., Cobb, G. P., and Anderson, T. A. (2006). Plant microRNA: a small regulatory molecule with big impact. *Dev. Biol.* 289, 3–16. doi: 10.1016/j.ydbio.2005.10.036

Zhang, H., He, H., Wang, X., Wang, X., Yang, X., Li, L., et al. (2011). Genome-wide mapping of the HY5-mediated genenetworks in *Arabidopsis* that involve both transcriptional and post-transcriptional regulation: regulation of HY5-mediated gene networks. *Plant J.* 65, 346–358. doi: 10.1111/j.1365-313X.2010.04426.x

Zhang, Y.-C., Yu, Y., Wang, C.-Y., Li, Z.-Y., Liu, Q., Xu, J., et al. (2013). Overexpression of microRNA OsmiR397 improves rice yield by increasing grain size and promoting panicle branching. *Nat. Biotechnol.* 31, 848–852. doi: 10.1038/nbt.2646

Zhang, Z., and Zhang, X. (2012). Argonautes compete for miR165/166 to regulate shoot apical meristem development. *Curr. Opin. Plant Biol.* 15, 652–658. doi: 10.1016/j.pbi.2012.05.007

Zhao, J. P., Jiang, X. L., Zhang, B. Y., and Su, X. H. (2012). Involvement of microRNA-mediated gene expression regulation in the pathological development of stem canker disease in *Populus trichocarpa*. *PLoS One* 7:e44968. doi: 10.1371/journal.pone.0044968

Zhao, Q., Nakashima, J., Chen, F., Yin, Y., Fu, C., Yun, J., et al. (2013). LACCASE Is Necessary and Nonredundant with *Peroxidase* for Lignin Polymerization during Vascular Development in *Arabidopsis*. *Plant Cell* 25, 3976–3987. doi: 10.1105/tpc.113.117770

Zhao, Y., Wen, H., Teotia, S., Du, Y., Zhang, J., Li, J., et al. (2017). Suppression of microRNA159 impacts multiple agronomic traits in rice (*Oryza sativa* L.). *BMC Plant Biol.* 17:215. doi: 10.1186/s12870-017-1171-7

Zhou, B., Fan, P., Li, Y., Yan, H., and Xu, Q. (2016). Exploring miRNAs involved in blue/UV-A light response in Brassica rapa reveals special regulatory mode during seedling development. *BMC Plant Biol.* 16:111. doi: 10.1186/s12870-016-0799-z

Zhou, M., Li, D., Li, Z., Hu, Q., Yang, C., Zhu, L., et al. (2013). Constitutive Expression of a *miR319* Gene Alters Plant Development and Enhances Salt and Drought Tolerance in Transgenic Creeping Bentgrass. *Plant Physiol.* 161, 1375–1391. doi: 10.1104/pp.112.208702

Zhou, Y., Yan, A., Han, H., Li, T., Geng, Y., Liu, X., et al. (2018). HAIRY MERISTEM with WUSCHEL confines CLAVATA3 expression to the outer apical meristem layers. *Science* 361, 502–506. doi: 10.1126/science.aar8638

Zhu, Y., and Wagner, D. (2020). Plant Inflorescence Architecture: the Formation, Activity, and Fate of Axillary Meristems. *Cold Spring Harb. Perspect. Biol.* 12:a034652. doi: 10.1101/cshperspect.a034652

Conflict of Interest: The authors declare that the research was conducted in the absence of any commercial or financial relationships that could be construed as a potential conflict of interest.

Publisher's Note: All claims expressed in this article are solely those of the authors and do not necessarily represent those of their affiliated organizations, or those of the publisher, the editors and the reviewers. Any product that may be evaluated in this article, or claim that may be made by its manufacturer, is not guaranteed or endorsed by the publisher.

frontiers in Plant Science

MINI REVIEW
published: 22 March 2022
doi: 10.3389/fpls.2022.833322

miR160: An Indispensable Regulator in Plant

Kai Hao[1†], Yun Wang[2†], Zhanpin Zhu[1], Yu Wu[1], Ruibing Chen[1] and Lei Zhang[1,2,3,4]*

[1] Department of Pharmaceutical Botany, School of Pharmacy, Naval Medical University, Shanghai, China, [2] Biomedical Innovation R&D Center, School of Medicine, Shanghai University, Shanghai, China, [3] Institute of Interdisciplinary Integrative Medicine Research, Medical School of Nantong University, Nantong, China, [4] Shanghai Key Laboratory for Pharmaceutical Metabolite Research, Shanghai, China

MicroRNAs (miRNA), recognized as crucial regulators of gene expression at the posttranscriptional level, have been found to be involved in the biological processes of plants. Some miRNAs are up- or down-regulated during plant development, stress response, and secondary metabolism. Over the past few years, it has been proved that miR160 is directly related to the developments of different tissues and organs in multifarious species, as well as plant–environment interactions. This review highlights the recent progress on the contributions of the miR160-ARF module to important traits of plants and the role of miR160-centered gene regulatory network in coordinating growth with endogenous and environmental factors. The manipulation of miR160-guided gene regulation may provide a new method to engineer plants with improved adaptability and yield.

Keywords: miR160, *ARFs*, growth and development, stress response, secondary metabolism

OPEN ACCESS

Edited by:
Xiaozeng Yang,
Beijing Academy of Agricultural and Forestry Sciences, China

Reviewed by:
Guodong Ren,
Fudan University, China

****Correspondence:***
Lei Zhang
starzhanglei@aliyun.com

[†]These authors have contributed equally to this work

Specialty section:
This article was submitted to Plant Physiology, a section of the journal Frontiers in Plant Science

Received: *17 December 2021*
Accepted: *25 February 2022*
Published: *22 March 2022*

Citation:
Hao K, Wang Y, Zhu Z, Wu Y, Chen R and Zhang L (2022) miR160: An Indispensable Regulator in Plant. Front. Plant Sci. 13:833322. doi: 10.3389/fpls.2022.833322

INTRODUCTION

MicroRNAs (miRNA) are a class of 20–24 nt small non-coding single-stranded RNAs which are found with high conservation and are widely presented in eukaryotes (Ambros et al., 2003; Bartel, 2004). In plants, RNA polymerase II participates in miRNAs transcription to derive pri-miRNAs, which can fold to form a hairpin structure and be processed by Dicer-like RNase III endonucleases (DCLs). The pri-miRNAs are cut by DCL1/HYL1/SE to produce most of the miRNAs in the nucleus through four processing pathways (short base to loop, sequential base to loop, short loop to base, and sequential loop to base), other DCLs can also be involved in miRNA production (Bologna et al., 2013; Moro et al., 2018; Li and Ren, 2021). The nascent miRNA:miRNA* duplexes generated by DCL-mediated processing will be methylated at the 3′-ends by HUAENHANCER 1 (HEN1). Recent study shows that mature miRNA is mainly bound to the ARGONAUTE (AGO) in RNA-induced silencing complex (RISC) in the nucleus and exported to the cytosol by EXPO1. But some miRNA:miRNA* duplexes may be exported by HASTY and assembled in the cytosol (Jones-Rhoades et al., 2006; Bologna et al., 2018; Song et al., 2019; Wang et al., 2019; Brioudes et al., 2021; Cambiagno et al., 2021). Mature miRNAs recognize target messenger RNA (mRNA) sites by perfect or near perfect complementarity, then it can regulate mRNA expression negatively by cleaving it or repressing translation. The correct temporal and spatial accumulation of some highly conserved miRNAs is essential for maintaining the normal development of plants. miR160 is one of miRNAs that regulate the auxin signaling pathways and plays a critical role in various biological processes of plants. Here we reviewed the structures of miR160 family, their targets, expression patterns, and functions in plant development, abiotic/biotic responses, and secondary metabolism.

THE miR160 FAMILY AND *AUXIN RESPONSE FACTORS*

MiR160 is a conserved miRNA that is popularly confirmed in many model and non-model plants, such as *Arabidopsis*, tomato, rice, poplar, and so on. The first miR160 was identified in *Arabidopsis* and the miR160 family was encoded by three loci (Reinhart et al., 2002). *MIR160b* and *MIR160c* were very similar, but they were different from *MIR160a* (Liu et al., 2010). Recently, a large number of *MIR160* homologs have been discovered in land plants and *Brassicaceae*. *MIR160a* was considered to be the progenitor of *MIR160b* and *MIR160c* paralogs because they originated from the segmental duplication of the region encompassing the ancient prototype *MIR160a* (Singh and Singh, 2021). The miR160 family has tissue-specific expression due to various functions. In tobacco, miR160 was expressed flower buds and vascular bundles, but no expression signal could be detected in young leaves and seeds (Valoczi et al., 2006). The miR160 family in plants targets the *AUXIN RESPONSE FACTORS* (*ARFs*) transcription factors which have been found in the auxin signaling pathways (Li et al., 2016). *ARF* specifically binds to auxin-responsive elements (AuxREs) *TGTCTC* in the promoter region of auxin-responsive genes to activate or inhibit gene expression (Tiwari et al., 2003). It can also combine with Aux/indoleacetic acid (IAA) inhibitors to form dimers which are regulated by auxin.

In *Arabidopsis*, the *ARF* gene families consisting of 23 loci had been identified to date (Remington et al., 2004). It was reported that miR160 could regulate a group of *ARF* genes: *ARF10*, *ARF16*, and *ARF17* (Rhoades et al., 2002). They all had a fragment that could be recognized by miR160 in a conserved *N*-terminal DNA binding domain (DBD). But *ARF17* was different from others because of its poorly conserved *C*-terminal dimerization domain (CTD) (Tiwari et al., 2003). Recent studies demonstrated that three genes had a significant impact on the development of *Arabidopsis*. For instance, the increased levels of *ARF17* due to the missing of miR160 regulation could contribute to severe developmental abnormalities, such as defects in vegetative, adventitious root (AR), embryonic, and floral development (Sorin et al., 2005). In addition, *OsARF18* was found as the target of miR160 in rice (Huang et al., 2016). Many results show that miR160 and its target gene *ARF* family are important to plant development, anabolism, and abiotic stress.

REGULATE THE DEVELOPMENT OF PLANTS

The miR160 family targets the *ARF* gene involved in the auxin signal transduction pathway, and it is essential for the growth and development of plants (**Figure 1A**). Different *ARF* genes mediate auxin signals in different parts, thereby controlling the fate of cell differentiation. *ARF* is also of great significance for mediating the interaction between auxin and other hormones.

Seed Germination

In *Arabidopsis*, transgenic seeds overexpressing miR160 were less sensitive to abscisic acid (ABA) during germination, but miR160-resistant (*mARF10*) mutant seeds were hypersensitive to ABA and impaired seedling establishment. The negative regulation of *ARF10* by miR160 was crucial to seed germination and post-embryonic development through involving the interactions between *ARF10*-dependent auxin and ABA pathways (Liu et al., 2007). Moreover, auxin controlled the expression of ABI3 and dramatically released seed dormancy by recruiting the *ARF10* and *ARF16* during seed germination (Liu et al., 2013). By analyzing the phenotypes of the MIR160a loss-of-function mutants without a 3′ regulatory region, MIR160a and its targets *ARF10/16/17* fulfilled a key role in embryo development. Auxin took part in regulating the expression of MIR160a by its 3′ region (Liu et al., 2010). miR160-*ARF10/16/17* were also found as a modulator in the cross-talk of auxin, light, gibberellin (GA), and brassinosteroids (BR) during hypocotyl elongation of *Arabidopsis*. Among them, *ARF10* was associated with GA (Dai et al., 2021).

Root Development

The miR160-*ARF* module has been shown to affect the root development of plants (Barrera-Rojas et al., 2021). In *Arabidopsis*, *ARF17* as a regulator of auxin-inducible *GH3-like* mRNAs altered the primary root length and lateral root (LR) number (Mallory et al., 2005). *ARF10* and *ARF16* were considered as a whole controlled root cap formation, although their functions were redundant. In addition, the regulation of *ARF16* expression by miR160 was essential for maintaining the LR production (Wang et al., 2005). The same phenomenon was observed in methane-induced tomato LR formation (Zhao et al., 2019). In apple rootstock, over-expressed miR160a reduced *ARF16/17* levels and inhibited AR formation, including the number and length (Meng et al., 2020). The miR160-*ARF17* module was also an important regulator in the development of AR of poplar and lotus (Libao et al., 2020; Liu et al., 2020). It is important to control the auxin/cytokinin balance during nodule development. In soybean, miR160 negatively regulated *ARF10/16/17*, and overexpression of miR160 led to hyposensitivity to cytokinin and auxin hypersensitivity, and reduced nodule primordium initiation (Turner et al., 2013). At the later stage of nodule development, high miR160 activity favored auxin activity and promoted the nodule maturation albeit in spite of reduced nodule formation (Nizampatnam et al., 2015). The feedback regulatory loops involving miR160/*ARF* and auxin/cytokinin governed root and nodule organogenesis, which were also presented in *Medicago* (Bustos-Sanmamed et al., 2013).

Shoot and Shoot Lateral Organ Growth

Evidence shows that miR160 plays an important role in the normal growth of leaves. In *Arabidopsis*, the overexpression of *mARF* (miR160-resistant) or *eTM160* (inactivation of miR160) increased the accumulation of *ARFs* and caused severe leaf developmental defects, including leaf shape defects (serrated leaves) and leaf symmetry anomalies (Mallory et al., 2005; Wu et al., 2013). In tomatoes, miR160 was required for leaflet initiation and controlled the final leaf shape and structure. Both the miR160-targeted *ARFs* and the Aux/IAA protein SlIAA9/ENTIRE were required to locally inhibit lamellipodia growth between initiating leaflets. They reduced lamina,

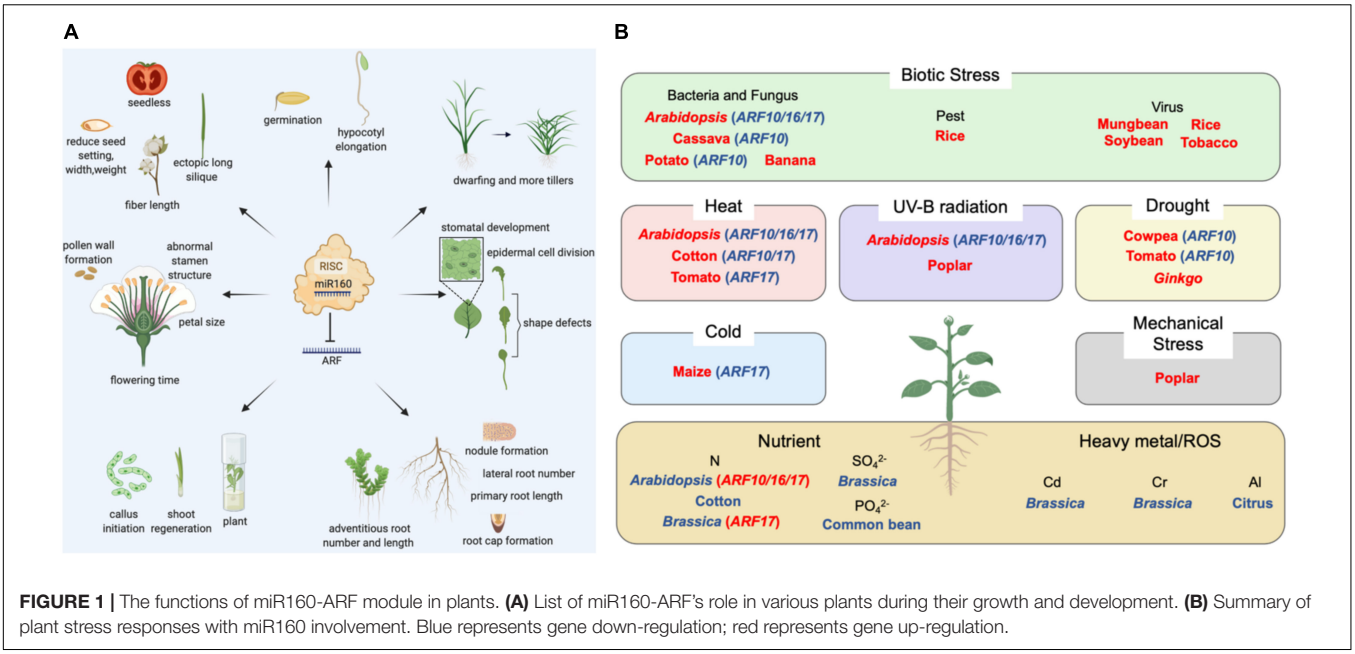

FIGURE 1 | The functions of miR160-ARF module in plants. **(A)** List of miR160-ARF's role in various plants during their growth and development. **(B)** Summary of plant stress responses with miR160 involvement. Blue represents gene down-regulation; red represents gene up-regulation.

increased leaf complexity, and decreased auxin response in young leaves (Hendelman et al., 2012; Ben-Gera et al., 2016; Damodharan et al., 2016). Among them, *ARF10A* was proved indispensable by the knockout of miR160-targeted *ARFs*, while the functions of *ARF16A* and *ARF17* were redundant (Damodharan et al., 2018). *SlARF10* also influenced stomatal development and ABA synthesis/signal response so as to close the stomata under drought. In addition, *SlARF10* enhanced hydraulic conductance by directly increasing aquaporin expression. An appropriate *ARF10* expression level controlled by miR160 was important to keep the leaf water balance between leaf development and adaptation to water stress (Liu X. et al., 2016). Moreover, miR160 controlled leaf curvature in potatoes by modulating the activity of *StTCP4* (involved in cell differentiation) and *StCYCLIND3;2* (involved in cell proliferation). The leaves of plants with overexpressed miR160 had a high positive curvature because of prolonged activation of the cell cycle in the center region of leaves. However, the leaves of miR160-knockdown plants were flattened, the *StTCP4* activity in both the central and marginal regions of leaves could be responsible for the flattened leaf phenotype (Natarajan and Banerjee, 2020). But the over-accumulation of *ARF18* showed rolled leaves in rice due to the anomaly in epidermal cell division in leaves (Huang et al., 2016).

Furthermore, miR160 decreased the accumulation of *ARFs* in the stem, reduced plant dwarfing, and formed more tillers by fine-tuning auxin signaling in rice (Huang et al., 2016).

Reproductive Development

MiR160 controlled the floral organ growth by targeting *ARFs*, especially *ARF17*, in *Arabidopsis*. The mutants expressing *mARF17* had dramatic floral developmental defects, including accelerated flowering time, reduced petal size, altered phyllotaxy along the primary and lateral stems, abnormal stamen structure, and sterility (Mallory et al., 2005). Auxin was vital in plant male reproductive development (Cecchetti et al., 2008; Cardarelli and Cecchetti, 2014). The biosynthesis and transport of auxin were related to anther and pollen formation (Bender et al., 2013). The response of *ARF17* to auxin affected both abnormal stamen structure and male sterility, the overexpression of *ARF17* led to defects in microsporocytes and tapetum (Wang et al., 2017). But rational *ARF17* was essential to pollen wall formation pollen tube growth (Yang et al., 2013). The miR160-*ARF17* module associated with anther and pollen development had been found in many other species, such as cotton, tobacco, tomato, and maize (Valoczi et al., 2006; Li et al., 2019; Chen et al., 2020; Keller et al., 2020). In tomatoes, miR160 regulated auxin-mediated floral organ patterning and abscission (Damodharan et al., 2016, 2018).

The miR160-*ARF* module has a certain regulatory influence on the fruits and seed development of plants. In *Arabidopsis*, the *mARF10* plants produced ectopic siliques with wavy silique walls (Liu et al., 2007). Furthermore, the overexpression of miR160 repressed the *ARF10/17* and increased the silique length in *Brassica napus* (Chen et al., 2018). In tomatoes, overexpressing *mARF10* changed the early development of fruits and seeds, resulting in cone-shaped and/or seedless fruit (Hendelman et al., 2012). miR160 negatively regulated *ARF17* and the related gene *GH3*, resulting in the increase of indole-3-acetic acid that is involved in fiber elongation. Finally, the fiber length of cotton was increased (Liu et al., 2019). In rice, *ARF18* decreased seed setting, seed width, and seed weight. At the same time, the starch accumulation was significantly reduced (Huang et al., 2016). miR160 inhibited *ARF10/16/17*, also contributed to the assimilation and allocation of sulfate during seed filling in *Phaseolus vulgaris* L. (Parreira et al., 2021).

While specific mechanisms are still unclear for many plants, detailed developmental research of various *mARFs* mutants in *Arabidopsis* has revealed the contribution of specific family

members to reproductive development, proving that they are indispensable for stamen development.

Regeneration Process

Auxin and cytokinin are significantly involved in the regeneration process. In *Arabidopsis*, miR160 repressed callus initiation and shoot regeneration by cutting *ARF10* which was bounded to the *ARR15* promoter, repressed *ARR15* expression, and promoted the cytokinin response (Qiao et al., 2012; Qiao and Xiang, 2013; Liu Z. et al., 2016). Being essential in LEC2-mediated somatic embryogenesis (SE), the auxin signaling pathway was controlled by miR160 and *ARF10/16/17* of *Arabidopsis*. The repression of miR160 led to the spontaneous formation of somatic embryos and the significant accumulation of auxin in the cultured explants (Wojcik et al., 2017). The similar effects of miR160-*ARF16/17* auxin signal transduction could be observed by target mimicry technology during the early stages of longan SE (Lin et al., 2015). At the late embryogenic calli callus induction stages of maize, *ARF19* was significantly increased with miR160 being heavily reduced, but their roles in regeneration remained unclear (Lopez-Ruiz et al., 2019).

ROLE OF THE miR160 IN THE INTERACTION OF PLANTS WITH THE ENVIRONMENT

Abiotic Stress

Abiotic stress is caused by the change of external natural conditions, including cold, heat, drought, high light, mechanical stress, salinity, metals (including heavy metals), nutrient deficiencies, and so on. In the wild, plants are often subjected to a combination of abiotic stresses (Mittler, 2006). It has been found that miR160 is directly associated with plant responses to several stress conditions.

In *Arabidopsis*, miR160 suppressed *ARF10/16/17* expressions to control heat shock protein (HSP) genes levels and regulate thermotolerance (Li et al., 2014; Lin et al., 2018). Accumulating evidence supports a role of the miR160-*ARF* network in male sterility caused by long-term high temperature (HT) stress. Overexpressing miR160 increased cotton sensitivity to HT stress with the decrease of *ARF10/17* mRNA levels, resulting in another indehiscence by activating the auxin response at the sporogenous cell proliferation stage (Ding et al., 2017; Chen et al., 2020). miR160 and *ARF17* also regulated the development of transition from post-meiotic to mature pollen in tomatoes under heat stress response (Keller et al., 2020). This gene pair were found to participate in the response to chilling stress in maize as well (Aydinoglu, 2020).

The expressions of several conserved miRNAs were analyzed in two cowpea genotypes during water deficit. miR160a/b has been found strongly upregulated, which inversely correlated to the expression levels of their targets *ARF10* (Barrera-Figueroa et al., 2011). In *Ginkgo biloba*, miR160a decreased *ARFs* expression and took part in the drought stress tolerance through the IAA signaling pathway (Chang et al., 2020). It is possible that the increase of miR160 and the concomitant decrease of *ARF* are part of the plant's strategy to balance water loss and growth under drought.

The exposure to ultraviolet-B (UV-B) can generally cause irreversible damage to DNA, proteins and lipids, and overwhelms antioxidant defense systems in plants because of the excessive production of reactive oxygen species (ROS). A total of 11 putative UV-B-responsive miRNAs, including miR160, were identified by UV-B radiation in *Arabidopsis* (Zhou et al., 2007). In addition, a set of miRNAs that were responsive to UV-B radiation were found by miRNA filter array assay in *P. tremula*. miR160 was one of 13 up-regulated miRNAs by UV-B radiation (Jia et al., 2009).

In poplar, miR160 belonged to a pair of mechanical stress-induced miRNAs that may function in one of the most critical defense systems for structural and mechanical fitness (Lu et al., 2005).

It is well known that metals such as Cu, Hg, Cd, Fe, and Al have the potential to induce oxidative stress with the generation of •OH in plants (Shahid et al., 2014). miR160 was transcriptionally down-regulated by metals exposure, Cd stress in *B. napus*, Cr stress in rice, Al stress in citrus plants, for example (Huang et al., 2010; Dubey et al., 2020; Zhou et al., 2020). On one hand, the low expression of miR160 causes elevated auxin which was required to combat metals stress, on the other hand, *ARFs* expression enhances adventitious and LR development, which could improve metals tolerance.

In the field, macronutrients and micronutrients are necessary for plants. As a nitrogen-starvation responsive gene, miR160 regulated the establishment of root system architecture through the auxin signaling pathway under nitrogen starvation conditions in plants (Liang et al., 2012; Hua et al., 2020; Singh and Singh, 2021). miR160 could enhance LRs or ARs developments under N-deficiency conditions to maximize the capacity of many plants, such as *Arabidopsis*, cotton, and *B. napus*, to uptake the little available nitrogen (Magwanga et al., 2019). In common beans, miR160 was found to be differentially regulated under P-deficiency in different organs. This was conducive to coping with nutrient deficiency stresses (Valdes-Lopez et al., 2010). Thus, miR160 can be used as an engineering target to improve nutrient usage efficiency and reduce fertilizer application.

Biotic Stress

Biotic stress leads to severe damage in plants. Bacterial and fungal pathogen exposure could cause induction of miR160 and downregulation of *ARFs* to generate defense responses in *Arabidopsis* (*Pst* DC3000, *Botrytis cinerea*), banana (*Fusarium oxysporum*), and cassava (*Colletotrichum gloeosporioides*) (Zhang et al., 2011; Pinweha et al., 2015; Xue and Yi, 2018; Cheng et al., 2019). miR160 downregulated *ARFs* levels and expressions of auxin-response genes (*AXR3/IAA17*, *BDL/IAA12*, and *GH3-like*), and increased callose deposition to activate basal defense PAMP-triggered immunity (Stork et al., 2010). Furthermore, it was also found that miR160 played a crucial part in local defense and systemic acquired resistance response during potato-*P. infestans* interaction by regulating antagonistic cross-talk between auxin-mediated growth and salicylic acid-mediated defense responses (Natarajan et al., 2018). Moreover, recent studies demonstrated a

TABLE 1 | List of miR160 identified in various plants during their growth and development.

Different plant groups	Species	Target genes	Functions	References
Monocots	Rice (*Oryza sativa*)	*ARF18*	Stem development (plant dwarfing); leaf development (rolled leaves); seed setting, seed width, and weight	Huang et al., 2016
	Maize (*Zea mays*)	*ARF17/19*	Embryogenic calli callus induction; anther development	Li et al., 2019; Lopez-Ruiz et al., 2019
Dicots	*Arabidopsis thaliana*	*ARF10/16/17*	Seed germination (embryo development, SE, hypocotyl elongation); root development (primary root length, lateral root number, root cap formation, AR formation); stem development (plant dwarfing); leaf development (leaf shape defects and leaf symmetry anomalies); callus formation and shoot regeneration; abnormal stamen structure (anther and pollen development) and male sterility; ectopic siliques	Mallory et al., 2005; Wang et al., 2005, 2017; Liu et al., 2007, 2010, 2013; Liang et al., 2012; Qiao et al., 2012; Qiao and Xiang, 2013; Wu et al., 2013; Yang et al., 2013; Liu Z. et al., 2016; Wojcik et al., 2017; Dai et al., 2021
	Longan (*Dimocarpus longan*)	*ARF10/16/17*	SE	Lin et al., 2015
	Soybean (*Glycine max*)	*ARF10/16/17*	Nodule development	Turner et al., 2013; Nizampatnam et al., 2015
	Tomato (*Lycopersicon esculentum*)	*ARF10A/10B/16/17*	Lateral root production; leaf shape and structure, stomatal development, and AQPs expression; pollen development, floral organ patterning, and abscission; early fruit and seed development	Hendelman et al., 2012; Ben-Gera et al., 2016; Damodharan et al., 2016, 2018; Liu X. et al., 2016; Zhao et al., 2019; Keller et al., 2020
	Brassica (*Brassica campestris*)	*ARF17*	Root development; silique length	Chen et al., 2018; Singh and Singh, 2021
	Potato (*Solanum tuberosum*)	*ARF17*	Leaf curvature	Natarajan and Banerjee, 2020
	Poplar (*Populus deltoides*)	*ARF17*	AR development	Liu et al., 2020
	Lotus (*Nelumbo nucifera*)	*ARF17*	AR development	Libao et al., 2020
	Apple (*Malus domestica*)	*ARF16/17*	AR development	Meng et al., 2020
	Medicago sativa	*ARF10/16/17*	Root development (primary root length, lateral root number); nodule development	Bustos-Sanmamed et al., 2013
	Cotton (*Gossypium hirsutum*)	*ARF10/17*	Anther development; fiber length	Liu et al., 2019; Chen et al., 2020
	Tobacco (*Nicotiana tabacum*)		Bud and vascular bundle development	Valoczi et al., 2006
	Phaseolus vulgaris	*ARF10/16/17*	Seed development	Parreira et al., 2021

critical role of miR160 in plant defense against viruses and pests, such as the mosaic virus (Bazzini et al., 2007; Yin et al., 2013; Kundu et al., 2017), rice stripe virus (Du et al., 2011), and brown planthopper (Tan et al., 2020). It may be related to the induction of RNA silencing pathway components.

PARTICIPATE IN SECONDARY METABOLISM

To our knowledge, plant secondary metabolism is an adaptation of plants to the environment, resulting from the plant interactions between biotic and abiotic factors during the long-term evolution process. There are few studies on the regulation of secondary metabolism by miR160, for example, one study showed that the overexpression of miR160a reduced the *GH3-like* level and negatively regulated the biosynthesis of tanshinones by targeting *ARF10/16/17* in *Salvia miltiorrhiza* hairy roots (Zhang et al., 2020). The miR160-*ARF10/16* pathway also regulated terpenoid indole alkaloid biosynthesis (Shen et al., 2017). Recent research suggested that miR160h-*ARF18* potentially regulated the accumulation of anthocyanins in poplar, but the exact regulation network remained unclear (Wang et al., 2020).

CONCLUSION

Plants use a complex variety of transcriptional, post-transcriptional, and translational gene expression programs to survive in the wild. miR160-guided post-transcriptional gene regulation acts a pivotal part in plants. Up to now, rapid and significant progress has been made in miR160 biogenesis, targets prediction, biological functions, and molecular mechanisms. miR160 regulates plant growth and development by interacting with target genes *ARFs*, a regulatory pathway that is closely

related to auxin signal transduction (**Table 1**). miR160, therefore, can act as a new breeding tool in plant genetic improvement to achieve better agronomic characters. Moreover, there may be feedback regulation between miRNAs and their target genes. Studies have shown that a staggering number of miRNA genes were formed under the control of their targets. Their expression level, duplication status, and miRNA–target interaction were important to the evolution of miRNAs and targets. But little research has been done on the co-evolution of miR160 and *ARF* (Carthew and Sontheimer, 2009; Huang et al., 2016; Liu T. et al., 2016).

Sessile by nature, plants have to suffer different kinds of abiotic and biotic stresses (**Figure 1B**). Limited by the resources available, plants always need to control the balance between development and stress responses (Fan et al., 2014). It has been demonstrated that transcription factors are important in the trade-off between development and stresses responses (Pajerowska-Mukhtar et al., 2012). miR160 implicates in multiple regulations of biological processes by regulating *ARFs*. For example, as the main root and floral regulator, miR160 and its *ARF* targets were proved to involve in heat stress, drought tolerance and N-deficiency stress (Magwanga et al., 2019; Chen et al., 2020; Dai et al., 2021). By controlling the establishment of the root system architecture of root, the key organ governing water and nutrients uptake, miR160 was able to regulate plants development under N-deficiency condition (Liang et al., 2012). A better understanding of miR160 in stress responses will help us design new strategies to improve the combined stress tolerance of crop plants.

In summary, the miR160-*ARF* module makes up a crucial hub coordinating developments and physiological responses with endogenous and environmental signals. Its universality among plants and diverse possibilities for modification, together make it a highly promising genetic manipulation target for crop breeding. However, overexpressing *ARFs* can cause plant dwarfing and leaf deformities, which affects the utilization of plants whose aerial part is the main source of active ingredients. Hence, there is still a lot of work to be done to exploit its biotechnological potentials, such as a new function mining of miR160, upstream regulatory mechanism, and interaction with other non-coding RNAs (long non-coding RNA, lncRNA, and siRNA). We should pay more attention to the function of miR160 in secondary metabolites, which is the key to the formation of good quality crops, especially medicinal plants.

AUTHOR CONTRIBUTIONS

KH and YWa collected the documents and wrote the manuscript. LZ conceived and developed the idea of this review and designed the overall concept. ZZ, YWu, and RC revised the manuscript. All authors contributed to the article and approved the submitted version.

FUNDING

This work was financially supported by funds from the National Natural Science Foundation of China (31970316, 32170274, and 32000231), China National Key Research and Development Program (2017ZX09101002-003-002), and Program of Shanghai Academic Research Leader (19XD1405000).

ACKNOWLEDGMENTS

We acknowledge Biorender (https://biorender.com/) since figures of the review were made by this software.

REFERENCES

Ambros, V., Bartel, B., Bartel, D. P., Burge, C. B., Carrington, J. C., Chen, X., et al. (2003). A uniform system for microRNA annotation. *RNA* 9, 277–279. doi: 10.1261/rna.2183803

Aydinoglu, F. (2020). Elucidating the regulatory roles of microRNAs in maize (*Zea mays* L.) leaf growth response to chilling stress. *Planta* 251:38. doi: 10.1007/s00425-019-03331-y

Barrera-Figueroa, B. E., Gao, L., Diop, N. N., Wu, Z., Ehlers, J. D., Roberts, P. A., et al. (2011). Identification and comparative analysis of drought-associated microRNAs in two cowpea genotypes. *BMC Plant Biol.* 11:127. doi: 10.1186/1471-2229-11-127

Barrera-Rojas, C. H., Otoni, W. C., and Nogueira, F. T. S. (2021). Shaping the root system: the interplay between miRNA regulatory hubs and phytohormones. *J. Exp. Bot.* 2, 6822–6835. doi: 10.1093/jxb/erab299

Bartel, D. P. (2004). MicroRNAs: genomics, biogenesis, mechanism, and function. *Cell* 116, 281–297. doi: 10.1016/s0092-8674(04)00045-5

Bazzini, A. A., Hopp, H. E., Beachy, R. N., and Asurmendi, S. (2007). Infection and coaccumulation of tobacco mosaic virus proteins alter microRNA levels, correlating with symptom and plant development. *Proc. Natl. Acad. Sci. U.S.A.* 104, 12157–12162. doi: 10.1073/pnas.0705114104

Bender, R. L., Fekete, M. L., Klinkenberg, P. M., Hampton, M., Bauer, B., Malecha, M., et al. (2013). PIN6 is required for nectary auxin response and short stamen development. *Plant J.* 74, 893–904. doi: 10.1111/tpj.12184

Ben-Gera, H., Dafna, A., Alvarez, J. P., Bar, M., Mauerer, M., and Ori, N. (2016). Auxin-mediated lamina growth in tomato leaves is restricted by two parallel mechanisms. *Plant J.* 86, 443–457. doi: 10.1111/tpj.13188

Bologna, N. G., Iselin, R., Abriata, L. A., Sarazin, A., Pumplin, N., Jay, F., et al. (2018). Nucleo-cytosolic shuttling of ARGONAUTE1 prompts a revised model of the plant MicroRNA pathway. *Mol. Cell.* 69, 709.e705–719.e705. doi: 10.1016/j.molcel.2018.01.007

Bologna, N. G., Schapire, A. L., Zhai, J., Chorostecki, U., Boisbouvier, J., Meyers, B. C., et al. (2013). Multiple RNA recognition patterns during microRNA biogenesis in plants. *Genome Res.* 23, 1675–1689. doi: 10.1101/gr.153387.112

Brioudes, F., Jay, F., Sarazin, A., Grentzinger, T., Devers, E. A., and Voinnet, O. (2021). HASTY, the *Arabidopsis* EXPORTIN5 ortholog, regulates cell-to-cell and vascular microRNA movement. *EMBO J.* 40:e107455. doi: 10.15252/embj.2020107455

Bustos-Sanmamed, P., Mao, G., Deng, Y., Elouet, M., Khan, G. A., Bazin, J. R. M., et al. (2013). Overexpression of miR160 affects root growth and nitrogen-fixing nodule number in Medicago truncatula. *Funct. Plant Biol.* 40, 1208–1220. doi: 10.1071/FP13123

Cambiagno, D. A., Giudicatti, A. J., Arce, A. L., Gagliardi, D., Li, L., Yuan, W., et al. (2021). HASTY modulates miRNA biogenesis by linking pri-miRNA transcription and processing. *Mol. Plant* 14, 426–439. doi: 10.1016/j.molp.2020.12.019

Cardarelli, M., and Cecchetti, V. (2014). Auxin polar transport in stamen formation and development: how many actors? *Front. Plant Sci.* 5:333. doi: 10.3389/fpls.2014.00333

Carthew, R. W., and Sontheimer, E. J. (2009). Origins and mechanisms of miRNAs and siRNAs. *Cell* 136, 642–655. doi: 10.1016/j.cell.2009.01.035

Cecchetti, V., Altamura, M. M., Falasca, G., Costantino, P., and Cardarelli, M. (2008). Auxin regulates *Arabidopsis* anther dehiscence, pollen maturation, and filament elongation. *Plant Cell* 20, 1760–1774. doi: 10.1105/tpc.107.057570

Chang, B., Ma, K., Lu, Z., Lu, J., Cui, J., Wang, L., et al. (2020). Physiological, transcriptomic, and metabolic responses of *Ginkgo biloba* L. to drought, salt, and heat stresses. *Biomolecules* 10:1635. doi: 10.3390/biom10121635

Chen, J., Pan, A., He, S., Su, P., Yuan, X., Zhu, S., et al. (2020). Different MicroRNA families involved in regulating high temperature stress response during cotton (*Gossypium hirsutum* L.) anther development. *Int. J. Mol. Sci.* 21:1280. doi: 10.3390/ijms21041280

Chen, L., Chen, L., Zhang, X., Liu, T., Niu, S., Wen, J., et al. (2018). Identification of miRNAs that regulate silique development in *Brassica napus*. *Plant Sci.* 269, 106–117. doi: 10.1016/j.plantsci.2018.01.010

Cheng, C., Liu, F., Sun, X., Tian, N., Mensah, R. A., Li, D., et al. (2019). Identification of *Fusarium oxysporum* f. sp. cubense tropical race 4 (Foc TR4) responsive miRNAs in banana root. *Sci. Rep.* 9:13682. doi: 10.1038/s41598-019-50130-2

Dai, X., Lu, Q., Wang, J., Wang, L., Xiang, F., and Liu, Z. (2021). MiR160 and its target genes ARF10, ARF16 and ARF17 modulate hypocotyl elongation in a light, BRZ, or PAC-dependent manner in *Arabidopsis*: miR160 promotes hypocotyl elongation. *Plant Sci.* 303:110686. doi: 10.1016/j.plantsci.2020.110686

Damodharan, S., Corem, S., Gupta, S. K., and Arazi, T. (2018). Tuning of SlARF10A dosage by sly-miR160a is critical for auxin-mediated compound leaf and flower development. *Plant J.* 96, 855–868. doi: 10.1111/tpj.14073

Damodharan, S., Zhao, D., and Arazi, T. (2016). A common miRNA160-based mechanism regulates ovary patterning, floral organ abscission and lamina outgrowth in tomato. *Plant J.* 86, 458–471. doi: 10.1111/tpj.13127

Ding, Y., Ma, Y., Liu, N., Xu, J., Hu, Q., Li, Y., et al. (2017). microRNAs involved in auxin signalling modulate male sterility under high-temperature stress in cotton (*Gossypium hirsutum*). *Plant J.* 91, 977–994. doi: 10.1111/tpj.13620

Du, P., Wu, J., Zhang, J., Zhao, S., Zheng, H., Gao, G., et al. (2011). Viral infection induces expression of novel phased microRNAs from conserved cellular microRNA precursors. *PLoS Pathog.* 7:e1002176. doi: 10.1371/journal.ppat.1002176

Dubey, S., Saxena, S., Chauhan, A. S., Mathur, P., Rani, V., and Chakrabaroty, D. (2020). Identification and expression analysis of conserved microRNAs during short and prolonged chromium stress in rice (*Oryza sativa*). *Environ. Sci. Pollut. Res. Int.* 27, 380–390. doi: 10.1007/s11356-019-06760-0

Fan, M., Bai, M. Y., Kim, J. G., Wang, T., Oh, E., Chen, L., et al. (2014). The bHLH transcription factor HBI1 mediates the trade-off between growth and pathogen-associated molecular pattern-triggered immunity in *Arabidopsis*. *Plant Cell* 26, 828–841. doi: 10.1105/tpc.113.121111

Hendelman, A., Buxdorf, K., Stav, R., Kravchik, M., and Arazi, T. (2012). Inhibition of lamina outgrowth following Solanum lycopersicum AUXIN RESPONSE FACTOR 10 (SlARF10) derepression. *Plant Mol. Biol.* 78, 561–576. doi: 10.1007/s11103-012-9883-4

Hua, Y. P., Zhou, T., Huang, J. Y., Yue, C. P., Song, H. X., Guan, C. Y., et al. (2020). Genome-Wide differential DNA methylation and miRNA expression profiling reveals epigenetic regulatory mechanisms underlying nitrogen-limitation-triggered adaptation and use efficiency enhancement in allotetraploid rapeseed. *Int. J. Mol. Sci.* 21:8453. doi: 10.3390/ijms21228453

Huang, J., Li, Z., and Zhao, D. (2016). Deregulation of the OsmiR160 target gene OsARF18 causes growth and developmental defects with an alteration of auxin signaling in rice. *Sci. Rep.* 6:29938. doi: 10.1038/srep29938

Huang, S. Q., Xiang, A. L., Che, L. L., Chen, S., Li, H., Song, J. B., et al. (2010). A set of miRNAs from *Brassica napus* in response to sulphate deficiency and cadmium stress. *Plant Biotechnol. J.* 8, 887–899. doi: 10.1111/j.1467-7652.2010.00517.x

Jia, X., Ren, L., Chen, Q. J., Li, R., and Tang, G. (2009). UV-B-responsive microRNAs in *Populus tremula*. *J. Plant Physiol.* 166, 2046–2057. doi: 10.1016/j.jplph.2009.06.011

Jones-Rhoades, M. W., Bartel, D. P., and Bartel, B. (2006). MicroRNAS and their regulatory roles in plants. *Annu. Rev. Plant Biol.* 57, 19–53. doi: 10.1146/annurev.arplant.57.032905.105218

Keller, M., Schleiff, E., and Simm, S. (2020). miRNAs involved in transcriptome remodeling during pollen development and heat stress response in *Solanum lycopersicum*. *Sci. Rep.* 10:10694. doi: 10.1038/s41598-020-67833-6

Kundu, A., Paul, S., Dey, A., and Pal, A. (2017). High throughput sequencing reveals modulation of microRNAs in Vigna mungo upon Mungbean Yellow Mosaic India Virus inoculation highlighting stress regulation. *Plant Sci.* 257, 96–105. doi: 10.1016/j.plantsci.2017.01.016

Li, N., and Ren, G. (2021). Systematic characterization of MicroRNA processing modes in plants with parallel amplification of RNA ends. *Front. Plant Sci.* 12:793549. doi: 10.3389/fpls.2021.793549

Li, S., Liu, J., Liu, Z., Li, X., Wu, F., and He, Y. (2014). HEAT-INDUCED TAS1 TARGET1 mediates thermotolerance *via* HEAT STRESS TRANSCRIPTION FACTOR A1a-Directed pathways in *Arabidopsis*. *Plant Cell* 26, 1764–1780. doi: 10.1105/tpc.114.124883

Li, S. B., Xie, Z. Z., Hu, C. G., and Zhang, J. Z. (2016). A review of Auxin Response Factors (ARFs) in plants. *Front. Plant Sci.* 7:47. doi: 10.3389/fpls.2016.00047

Li, Z., An, X., Zhu, T., Yan, T., Wu, S., Tian, Y., et al. (2019). Discovering and constructing ceRNA-miRNA-Target gene regulatory networks during anther development in maize. *Int. J. Mol. Sci.* 20:3480. doi: 10.3390/ijms20143480

Liang, G., He, H., and Yu, D. (2012). Identification of nitrogen starvation-responsive microRNAs in *Arabidopsis thaliana*. *PLoS One* 7:e48951. doi: 10.1371/journal.pone.0048951

Libao, C., Minrong, Z., Zhubing, H., Huiying, L., and Shuyan, L. (2020). Comparative transcriptome analysis revealed the cooperative regulation of sucrose and IAA on adventitious root formation in lotus (*Nelumbo nucifera* Gaertn). *BMC Genomics* 21:653. doi: 10.1186/s12864-020-07046-3

Lin, J. S., Kuo, C. C., Yang, I. C., Tsai, W. A., Shen, Y. H., Lin, C. C., et al. (2018). MicroRNA160 modulates plant development and heat shock protein gene expression to mediate heat tolerance in *Arabidopsis*. *Front. Plant Sci.* 9:68. doi: 10.3389/fpls.2018.00068

Lin, Y., Lai, Z., Tian, Q., Lin, L., Lai, R., Yang, M., et al. (2015). Endogenous target mimics down-regulate miR160 mediation of ARF10, -16, and -17 cleavage during somatic embryogenesis in *Dimocarpus longan* Lour. *Front. Plant Sci.* 6:956. doi: 10.3389/fpls.2015.00956

Liu, G., Liu, J., Pei, W., Li, X., Wang, N., Ma, J., et al. (2019). Analysis of the MIR160 gene family and the role of MIR160a_A05 in regulating fiber length in cotton. *Planta* 250, 2147–2158. doi: 10.1007/s00425-019-03271-7

Liu, P. P., Montgomery, T. A., Fahlgren, N., Kasschau, K. D., Nonogaki, H., and Carrington, J. C. (2007). Repression of AUXIN RESPONSE FACTOR10 by microRNA160 is critical for seed germination and post-germination stages. *Plant J.* 52, 133–146. doi: 10.1111/j.1365-313X.2007.03218.x

Liu, S., Yang, C., Wu, L., Cai, H., Li, H., and Xu, M. (2020). The peu-miR160a-PeARF17.1/PeARF17.2 module participates in the adventitious root development of poplar. *Plant Biotechnol. J.* 18, 457–469. doi: 10.1111/pbi.13211

Liu, T., Fang, C., Ma, Y., Shen, Y., Li, C., Li, Q., et al. (2016). Global investigation of the co-evolution of MIRNA genes and microRNA targets during soybean domestication. *Plant J.* 85, 396–409. doi: 10.1111/tpj.13113

Liu, X., Dong, X., Liu, Z., Shi, Z., Jiang, Y., Qi, M., et al. (2016). Repression of ARF10 by microRNA160 plays an important role in the mediation of leaf water loss. *Plant Mol. Biol.* 92, 313–336. doi: 10.1007/s11103-016-0514-3

Liu, Z., Li, J., Wang, L., Li, Q., Lu, Q., Yu, Y., et al. (2016). Repression of callus initiation by the miRNA-directed interaction of auxin-cytokinin in *Arabidopsis thaliana*. *Plant J.* 87, 391–402. doi: 10.1111/tpj.13211

Liu, X., Huang, J., Wang, Y., Khanna, K., Xie, Z., Owen, H. A., et al. (2010). The role of floral organs in carpels, an Arabidopsis loss-of-function mutation in MicroRNA160a, in organogenesis and the mechanism regulating its expression. *Plant J.* 62, 416–428. doi: 10.1111/j.1365-313X.2010.04164.x

Liu, X., Zhang, H., Zhao, Y., Feng, Z., Li, Q., Yang, H. Q., et al. (2013). Auxin controls seed dormancy through stimulation of abscisic acid signaling by inducing ARF-mediated ABI3 activation in *Arabidopsis*. *Proc. Natl. Acad. Sci. U.S.A.* 110, 15485–15490. doi: 10.1073/pnas.1304651110

Lopez-Ruiz, B. A., Juarez-Gonzalez, V. T., Sandoval-Zapotitla, E., and Dinkova, T. D. (2019). Development-related miRNA expression and target regulation during staggered *in vitro* plant regeneration of tuxpeno VS-535 maize cultivar. *Int. J. Mol. Sci.* 20:2079. doi: 10.3390/ijms20092079

Lu, S., Sun, Y. H., Shi, R., Clark, C., Li, L., and Chiang, V. L. (2005). Novel and mechanical stress-responsive MicroRNAs in Populus trichocarpa that are absent from *Arabidopsis*. *Plant Cell* 17, 2186–2203. doi: 10.1105/tpc.105.033456

Magwanga, R. O., Kirungu, J. N., Lu, P., Cai, X., Zhou, Z., Xu, Y., et al. (2019). Map-Based functional analysis of the GhNLP genes reveals their roles in enhancing tolerance to N-Deficiency in cotton. *Int. J. Mol. Sci.* 20:4953. doi: 10.3390/ijms20194953

Mallory, A. C., Bartel, D. P., and Bartel, B. (2005). MicroRNA-directed regulation of Arabidopsis AUXIN RESPONSE FACTOR17 is essential for proper development and modulates expression of early auxin response genes. *Plant Cell* 17, 1360–1375. doi: 10.1105/tpc.105.031716

Meng, Y., Mao, J., Tahir, M. M., Wang, H., Wei, Y., Zhao, C., et al. (2020). Mdm-miR160 participates in auxin-induced adventitious root formation of apple rootstock. *Sci. Hortic.* 270:109442. doi: 10.1016/j.scienta.2020.109442

Mittler, R. (2006). Abiotic stress, the field environment and stress combination. *Trends Plant Sci.* 11, 15–19. doi: 10.1016/j.tplants.2005.11.002

Moro, B., Chorostecki, U., Arikit, S., Suarez, I. P., Hobartner, C., Rasia, R. M., et al. (2018). Efficiency and precision of microRNA biogenesis modes in plants. *Nucleic Acids Res.* 46, 10709–10723. doi: 10.1093/nar/gky853

Natarajan, B., and Banerjee, A. K. (2020). MicroRNA160 regulates leaf curvature in potato (Solanum tuberosum L. cv. Desiree). *Plant Signal Behav.* 15:1744373. doi: 10.1080/15592324.2020.1744373

Natarajan, B., Kalsi, H. S., Godbole, P., Malankar, N., Thiagarayaselvam, A., Siddappa, S., et al. (2018). MiRNA160 is associated with local defense and systemic acquired resistance against Phytophthora infestans infection in potato. *J. Exp. Bot.* 69, 2023–2036. doi: 10.1093/jxb/ery025

Nizampatnam, N. R., Schreier, S. J., Damodaran, S., Adhikari, S., and Subramanian, S. (2015). microRNA160 dictates stage-specific auxin and cytokinin sensitivities and directs soybean nodule development. *Plant J.* 84, 140–153. doi: 10.1111/tpj.12965

Pajerowska-Mukhtar, K. M., Wang, W., Tada, Y., Oka, N., Tucker, C. L., Fonseca, J. P., et al. (2012). The HSF-like transcription factor TBF1 is a major molecular switch for plant growth-to-defense transition. *Curr. Biol.* 22, 103–112. doi: 10.1016/j.cub.2011.12.015

Parreira, J. R., Cappuccio, M., Balestrazzi, A., Fevereiro, P., and Araujo, S. S. (2021). MicroRNAs expression dynamics reveal post-transcriptional mechanisms regulating seed development in *Phaseolus vulgaris* L. *Hortic. Res.* 8:18. doi: 10.1038/s41438-020-00448-0

Pinweha, N., Asvarak, T., Viboonjun, U., and Narangajavana, J. (2015). Involvement of miR160/miR393 and their targets in cassava responses to anthracnose disease. *J. Plant Physiol.* 174, 26–35. doi: 10.1016/j.jplph.2014.09.006

Qiao, M., and Xiang, F. (2013). A set of Arabidopsis thaliana miRNAs involve shoot regeneration *in vitro*. *Plant Signal Behav.* 8:e23479. doi: 10.4161/psb.23479

Qiao, M., Zhao, Z., Song, Y., Liu, Z., Cao, L., Yu, Y., et al. (2012). Proper regeneration from *in vitro* cultured *Arabidopsis thaliana* requires the microRNA-directed action of an auxin response factor. *Plant J.* 71, 14–22. doi: 10.1111/j.1365-313X.2012.04944.x

Reinhart, B. J., Weinstein, E. G., Rhoades, M. W., Bartel, B., and Bartel, D. P. (2002). MicroRNAs in plants. *Genes Dev.* 16, 1616–1626. doi: 10.1101/gad.1004402

Remington, D. L., Vision, T. J., Guilfoyle, T. J., and Reed, J. W. (2004). Contrasting modes of diversification in the Aux/IAA and ARF gene families. *Plant Physiol.* 135, 1738–1752. doi: 10.1104/pp.104.039669

Rhoades, M. W., Reinhart, B. J., Lim, L. P., Burge, C. B., Bartel, B., and Bartel, D. P. (2002). Prediction of plant microRNA targets. *Cell* 110, 513–520. doi: 10.1016/s0092-8674(02)00863-2

Shahid, M., Pourrut, B., Dumat, C., Nadeem, M., Aslam, M., and Pinelli, E. (2014). Heavy-metal-induced reactive oxygen species: phytotoxicity and physicochemical changes in plants. *Rev. Environ. Contam Toxicol.* 232, 1–44. doi: 10.1007/978-3-319-06746-9_1

Shen, E. M., Singh, S. K., Ghosh, J. S., Patra, B., Paul, P., Yuan, L., et al. (2017). The miRNAome of *Catharanthus roseus*: identification, expression analysis, and potential roles of microRNAs in regulation of terpenoid indole alkaloid biosynthesis. *Sci. Rep.* 7:43027. doi: 10.1038/srep43027

Singh, S., and Singh, A. (2021). A prescient evolutionary model for genesis, duplication and differentiation of MIR160 homologs in *Brassicaceae*. *Mol. Genet. Genomics* 296, 985–1003. doi: 10.1007/s00438-021-01797-8

Song, X., Li, Y., Cao, X., and Qi, Y. (2019). MicroRNAs and their regulatory roles in plant-environment interactions. *Annu. Rev. Plant Biol.* 70, 489–525. doi: 10.1146/annurev-arplant-050718-100334

Sorin, C., Bussell, J. D., Camus, I., Ljung, K., Kowalczyk, M., Geiss, G., et al. (2005). Auxin and light control of adventitious rooting in *Arabidopsis* require ARGONAUTE1. *Plant Cell* 17, 1343–1359. doi: 10.1105/tpc.105.031625

Stork, J., Harris, D., Griffiths, J., Williams, B., Beisson, F., Li-Beisson, Y., et al. (2010). CELLULOSE SYNTHASE9 serves a nonredundant role in secondary cell wall synthesis in *Arabidopsis* epidermal testa cells. *Plant Physiol.* 153, 580–589. doi: 10.1104/pp.110.154062

Tan, J., Wu, Y., Guo, J., Li, H., Zhu, L., Chen, R., et al. (2020). A combined microRNA and transcriptome analyses illuminates the resistance response of rice against brown planthopper. *BMC Genomics* 21:144. doi: 10.1186/s12864-020-6556-6

Tiwari, S. B., Hagen, G., and Guilfoyle, T. (2003). The roles of auxin response factor domains in auxin-responsive transcription. *Plant Cell* 15, 533–543. doi: 10.1105/tpc.008417

Turner, M., Nizampatnam, N. R., Baron, M., Coppin, S., Damodaran, S., Adhikari, S., et al. (2013). Ectopic expression of miR160 results in auxin hypersensitivity, cytokinin hyposensitivity, and inhibition of symbiotic nodule development in soybean. *Plant Physiol.* 162, 2042–2055. doi: 10.1104/pp.113.220699

Valdes-Lopez, O., Yang, S. S., Aparicio-Fabre, R., Graham, P. H., Reyes, J. L., Vance, C. P., et al. (2010). MicroRNA expression profile in common bean (*Phaseolus vulgaris*) under nutrient deficiency stresses and manganese toxicity. *New Phytol.* 187, 805–818. doi: 10.1111/j.1469-8137.2010.03320.x

Valoczi, A., Varallyay, E., Kauppinen, S., Burgyan, J., and Havelda, Z. (2006). Spatio-temporal accumulation of microRNAs is highly coordinated in developing plant tissues. *Plant J.* 47, 140–151. doi: 10.1111/j.1365-313X.2006.02766.x

Wang, B., Xue, J. S., Yu, Y. H., Liu, S. Q., Zhang, J. X., Yao, X. Z., et al. (2017). Fine regulation of ARF17 for anther development and pollen formation. *BMC Plant Biol.* 17:243. doi: 10.1186/s12870-017-1185-1

Wang, J., Mei, J., and Ren, G. (2019). Plant microRNAs: biogenesis, homeostasis, and degradation. *Front. Plant Sci.* 10:360. doi: 10.3389/fpls.2019.00360

Wang, J. W., Wang, L. J., Mao, Y. B., Cai, W. J., Xue, H. W., and Chen, X. Y. (2005). Control of root cap formation by MicroRNA-targeted auxin response factors in *Arabidopsis*. *Plant Cell* 17, 2204–2216. doi: 10.1105/tpc.105.033076

Wang, Y., Liu, W., Wang, X., Yang, R., Wu, Z., Wang, H., et al. (2020). MiR156 regulates anthocyanin biosynthesis through SPL targets and other microRNAs in poplar. *Hortic. Res.* 7:118. doi: 10.1038/s41438-020-00341-w

Wojcik, A. M., Nodine, M. D., and Gaj, M. D. (2017). miR160 and miR166/165 Contribute to the LEC2-Mediated auxin response involved in the somatic embryogenesis induction in *Arabidopsis*. *Front. Plant Sci.* 8:2024. doi: 10.3389/fpls.2017.02024

Wu, H. J., Wang, Z. M., Wang, M., and Wang, X. J. (2013). Widespread long noncoding RNAs as endogenous target mimics for microRNAs in plants. *Plant Physiol.* 161, 1875–1884. doi: 10.1104/pp.113.215962

Xue, M., and Yi, H. (2018). Enhanced *Arabidopsis* disease resistance against *Botrytis cinerea* induced by sulfur dioxide. *Ecotoxicol. Environ. Saf.* 147, 523–529. doi: 10.1016/j.ecoenv.2017.09.011

Yang, J., Tian, L., Sun, M. X., Huang, X. Y., Zhu, J., Guan, Y. F., et al. (2013). AUXIN RESPONSE FACTOR17 is essential for pollen wall pattern formation in *Arabidopsis*. *Plant Physiol.* 162, 720–731. doi: 10.1104/pp.113.214940

Yin, X., Wang, J., Cheng, H., Wang, X., and Yu, D. (2013). Detection and evolutionary analysis of soybean miRNAs responsive to soybean mosaic virus. *Planta* 237, 1213–1225. doi: 10.1007/s00425-012-1835-3

Zhang, H., Chen, H., Hou, Z., Xu, L., Jin, W., and Liang, Z. (2020). Overexpression of Ath-MIR160b increased the biomass while reduced the content of tanshinones in *Salvia miltiorrhiza* hairy roots by targeting ARFs genes. *Plant Cell Tissue Organ. Culture (PCTOC)* 142, 327–338. doi: 10.1007/s11240-020-01865-8

Zhang, W., Gao, S., Zhou, X., Chellappan, P., Chen, Z., Zhou, X., et al. (2011). Bacteria-responsive microRNAs regulate plant innate immunity by modulating plant hormone networks. *Plant Mol. Biol.* 75, 93–105. doi: 10.1007/s11103-010-9710-8

Zhao, Y., Zhang, Y., Liu, F., Wang, R., Huang, L., and Shen, W. (2019). Hydrogen peroxide is involved in methane-induced tomato lateral root formation. *Plant Cell Rep.* 38, 377–389. doi: 10.1007/s00299-019-02372-7

Zhou, X., Wang, G., and Zhang, W. (2007). UV-B responsive microRNA genes in *Arabidopsis* thaliana. *Mol. Syst. Biol.* 3:103. doi: 10.1038/msb4100143

Zhou, Y. F., Wang, Y. Y., Chen, W. W., Chen, L. S., and Yang, L. T. (2020). Illumina sequencing revealed roles of microRNAs in different aluminum tolerance of two citrus species. *Physiol. Mol. Biol. Plants* 26, 2173–2187. doi: 10.1007/s12298-020-00895-y

Conflict of Interest: The authors declare that the research was conducted in the absence of any commercial or financial relationships that could be construed as a potential conflict of interest.

Publisher's Note: All claims expressed in this article are solely those of the authors and do not necessarily represent those of their affiliated organizations, or those of the publisher, the editors and the reviewers. Any product that may be evaluated in this article, or claim that may be made by its manufacturer, is not guaranteed or endorsed by the publisher.

frontiers | Frontiers in Plant Science

ORIGINAL RESEARCH
published: 18 April 2022
doi: 10.3389/fpls.2022.847086

Verticillium dahliae Secretes Small RNA to Target Host *MIR157d* and Retard Plant Floral Transition During Infection

Bo-Sen Zhang[1,2], *Ying-Chao Li*[1,3], *Hui-Shan Guo*[1,2]* *and Jian-Hua Zhao*[1,2]*

[1] State Key Laboratory of Plant Genomics, Institute of Microbiology, Chinese Academy of Sciences, Beijing, China, [2] CAS Center for Excellence in Biotic Interactions, University of Chinese Academy of Sciences, Beijing, China, [3] School of Life Sciences, Hebei University, Baoding, China

Bidirectional trans-kingdom RNA silencing [or RNA interference (RNAi)] plays a key role in plant-pathogen interactions. It has been shown that plant hosts export specific endogenous miRNAs into pathogens to inhibit their virulence, whereas pathogens deliver small RNAs (sRNAs) into plant cells to disturb host immunity. Here, we report a trans-kingdom fungal sRNA retarding host plant floral transition by targeting a miRNA precursor. From *Arabidopsis* plants infected with *Verticillium dahliae*, a soil-borne hemibiotrophic pathogenic fungus that causes wilt diseases in a wide range of plant hosts, we obtained a number of possible trans-kingdom *V. dahliae* sRNAs (VdsRNAs) by sequencing AGO1-immunoprecipitated sRNAs. Among these, a 24-nt VdsRNA derived from *V. dahliae* rRNA, VdrsR-1, was shown to be an actual trans-kingdom VdsRNA that targets the miR157d precursor *MIR157d*, resulting in increased rather than reduced miR157d accumulation in *V. dahliae*-infected plants. Consistent with the miR157 family in the regulation of vegetative and floral transitions by targeting *SPL* genes in several plant species, we detected two *SPL* genes, *SPL13A/B*, that were notably reduced in *V. dahliae*-infected and VdrsR-1-expressing plants compared with control plants. Furthermore, *V. dahliae*-infected and VdrsR-1-expressing plants also displayed delayed vegetative phase change and floral transition compared to control plants. Taken together, we disclosed a novel mode of action for a trans-kingdom fungal sRNA, VdrsR-1, which was secreted into host cells to modulate plant floral transition by employing the miR157d/*SPL13A/B* regulatory module, leading to prolonged host vegetative growth that would undoubtedly benefit fungal propagation.

Keywords: trans-kingdom RNAi, *V. dahliae*, *miR157d*, floral transition, sRNA

OPEN ACCESS

Edited by:
Xiuren Zhang,
Texas A&M University, United States

Reviewed by:
Jia-Wei Wang,
National Key Laboratory of Plant Molecular Genetics, Center for Excellence in Molecular Plant Sciences (CAS), China
Gang Wu,
Zhejiang A&F University, China

***Correspondence:**
Hui-Shan Guo
guohs@im.ac.cn
Jian-Hua Zhao
zhao_jian_hua@hotmail.com

Specialty section:
This article was submitted to Plant Physiology, a section of the journal Frontiers in Plant Science

Received: *01 January 2022*
Accepted: *15 March 2022*
Published: *18 April 2022*

Citation:
Zhang B-S, Li Y-C, Guo H-S and Zhao J-H (2022) Verticillium dahliae Secretes Small RNA to Target Host MIR157d and Retard Plant Floral Transition During Infection. Front. Plant Sci. 13:847086. doi: 10.3389/fpls.2022.847086

INTRODUCTION

In most eukaryotes, RNA silencing [or RNA interference (RNAi)] is crucial for normal development and defense against biotic and abiotic stress. Small RNAs (sRNAs), as the key mediators of RNAi, are divided into microRNAs (miRNAs) and small interfering RNAs (siRNAs) according to their origin (Treiber et al., 2019; Wang et al., 2019; Chen and Rechavi, 2021). Generally, miRNAs are derived from primary miRNA transcripts (pri-miRNAs) containing an imperfect hairpin structure (precursor, pre-miRNA) that are sequentially processed by the RNase III enzyme Dicers

(Moran et al., 2017). In *Arabidopsis thaliana*, one of the Dicer homologous proteins Dicer-like 1 (DCL1) is the primary enzyme involved in miRNA biogenesis, which processes pri-miRNAs into pre-miRNA and ∼20–24-nt miRNA/miRNA* duplexes in two steps (Song et al., 2019). Mature miRNAs load onto the AGO1 protein to form miRNA-induced silencing complexes (miRISCs). On the basis of sequence complementarity, miRISC negatively regulates gene expression by directing target mRNA degradation or translational inhibition (Yu et al., 2017; Song et al., 2019; Wang et al., 2019).

Massive evidence indicates that miRNAs are key regulators of plant development. The miR156/157 family is one of the most conserved miRNA families in all land plant lineages (Axtell and Bowman, 2008; Liu et al., 2017) and coordinates vegetative and floral transitions by targeting *SPL* genes in *Arabidopsis* (Schwab et al., 2005; Wu and Poethig, 2006; Wang et al., 2008; Xu et al., 2016; He J. et al., 2018), maize (Chuck et al., 2007), cotton (Liu et al., 2017; He X. et al., 2018), and several other species (Shikata et al., 2012; Gao et al., 2018). A series of miRNAs regulate plant development by targeting genes involved in hormone biosynthesis and signaling, such as miR164:*NAC1* (Guo et al., 2005), miR160/167:*ARF*s (Mallory et al., 2005; Wu et al., 2006; Liu et al., 2007), miR159:*MYB*s (Millar and Gubler, 2005; Reyes and Chua, 2007), and miR847:*IAA28* (Wang and Guo, 2015). In addition, miRNA-mediated regulation of gene expression plays an important role in the plant response to abiotic stresses. In rice, miR528 enhances plant resistance to viruses by increasing the production of reactive oxygen species (Wu et al., 2015, 2017). A recent study showed that *Brassica* miR1885 dynamically regulates both innate immunity and plant growth and responds to viral infection through distinct modes of action (Cui et al., 2020). The vital roles of miRNAs in the regulation of plant development, phenotypic plasticity, abiotic and biotic responses, as well as symbiotic and parasitic interactions have been summarized in several excellent reviews (Jones-Rhoades et al., 2006; Chen, 2009; D'Ario et al., 2017; Tang and Chu, 2017; Huang et al., 2019; Song et al., 2019, 2021; Wang et al., 2019; Dexheimer and Cochella, 2020; Liu et al., 2020; Chen and Rechavi, 2021; Qiao et al., 2021).

Bidirectional trans-kingdom RNAi has been demonstrated to influence plant host-pathogen interactions. An early study reported that *Botrytis cinerea* sRNAs are transmitted into hosts during infection, functioning as RNA effectors to perturb plant immune signaling pathways (Weiberg et al., 2013). In this study, Bc-siR3.2 hijacked the host RNAi machinery by loading into AGO1 to target plant mitogen-activated protein kinase transcripts, thereby suppressing host immunity to facilitate infection (Weiberg et al., 2013). More recently, a study demonstrated that *Fol-milR1*, a pathogenicity factor of *Fusarium oxysporum*, degrades the tomato *SlyFRG4* gene, which is essential for tomato wilt disease resistance by binding to the tomato SlyAGO4a protein (Ji et al., 2021). In oomycetes, the sRNAs of *Hyaloperonospora arabidopsidis* were reported to employ the host AGO for virulence (Dunker et al., 2020). On the other hand, hosts export specific endogenous miRNAs into pathogens to confer host disease resistance by targeting pathogen virulence genes (Hua et al., 2018; Zhao and Guo, 2019; Zhao et al., 2021). In our previous study, we reported that cotton plants export conserved miRNAs into the pathogenic fungus *Verticillium dahliae* (V592 strain) to inhibit fungal virulence genes. We identified 28 different cotton miRNAs from *V. dahliae* recovered from infected cotton plants. Further analysis demonstrated that miR166 and miR159 cleave the transcripts of the *Clp-1* and *HiC-15* genes, which are essential for hyphal growth and microsclerotium formation, respectively (Zhang et al., 2016). Recently, *V. dahliae* miRNA-like RNAs (VdmilRNAs) have also been identified, and VdmilR-1 represses fungal endogenous target gene expression at the transcriptional level by increasing histone H3K9 methylation (Jin et al., 2019). However, whether *V. dahliae* secretes sRNAs to regulate host genes has rarely been reported.

In the present study, aiming to identify and uncover the functions of *V. dahliae* sRNA (VdsRNA) classes associated with host AGO1 protein during fungal infection, we immunoprecipitated AGO1 using the c-myc antibody from 6myc-AGO1-overexpressing *Arabidopsis* plants (6myc-AGO1) with or without *V. dahliae* infection. Total RNA was extracted from the AGO1-IP fraction, and sRNA libraries were constructed. By analyzing sequencing data, we identified that an AGO1-associated VdsRNA derived from *V. dahliae* rRNA, named VdrsR-1, targets the precursor of host miR157d, *MIR157d*. Unexpectedly, rather than reducing miR157d accumulation, VdrsR-1 increased miR157d accumulation in the *V. dahliae*-infected plants. Consistently, the accumulation levels of two *SPL* genes, *SPL13A/B*, predicted targets of miR157d, were notably reduced in *V. dahliae*-infected plants. Phenotypic resemblance between *V. dahliae*-infected plants and VdrsR-1-overexpressing plants suggests that the trans-kingdom VdrsR-1 plays a role in delaying host floral transition by exploiting the miR157d/*SPL13A/B* module, probably beneficial to fungal development inside the infected plants.

MATERIALS AND METHODS

Plant Materials and Manipulations

6myc-AGO1 *Arabidopsis* plants (Col-0 background) were obtained by transforming 35S-6myc-AGO1 into the *ago1-27 Arabidopsis* mutant (Duan et al., 2012). *Arabidopsis* plants were grown in soil in a greenhouse at 22°C under long-day conditions (16 h/8 h day/night) with 60% humidity. For fungal infection, 10-day-old seedling mutants were uprooted, and the roots were dipped for 5 min in 1×10^7 cfu/ml spores of *V. dahliae* (V592 strain). After inoculation, the plants were transferred to soil. Control plants were treated similarly with water. Samples were collected at 2 weeks postinoculation for RNA extraction and immunoprecipitation. The pathogenic phenotype of *Arabidopsis* was recorded at 2 and 4 weeks during the experimental period. All of the infection assays were repeated three times. For transient expression, *N. benthamiana* plants were grown in soil under long-day conditions at 25°C for 4 weeks.

Vector Construction

In this article, all of the constructs were ligated by In-fusion cloning methods using the ClonExpress II One Step cloning kit (Vazyme, Nanjing, China).

For the *35S-MIR157d* and *35S-MIR159a* constructs, the 221-bp *MIR157d* and 184-bp *MIR159a* gene sequences were amplified by RT-PCR and ligated into the *Xba*I-*Sac*I-linearized pCAMBIA1300-221 binary vector. To generate artificial miRNA precursor skeletons used in infiltration assays, we synthesized all of the precursors by GenScript (Nanjing, China). We used precursor *MIR5653* to express 24-nt VdrsR-1 and amiR_{t159}, respectively. The 86-bp sequence was amplified by PCR and ligated into *Xba*I-*Sac*I-linearized pCAMBIA1300-221 binary vector. For the *35S-MIR157dm* and *35S-MIR157d*$_{asR-1}$ constructs, the 221-bp sequences were amplified by PCR and ligated into the *Xba*I-*Sac*I-linearized pCAMBIA1300-221 binary vector. For the *35S:SPL13B* construct, the 1817-bp *SPL13B* gene sequence, which is consistent with partial sequence of *SPL13A*, was amplified by RT-PCR and ligated into the *Xba*I-*Sac*I-linearized pCAMBIA1300-221 binary vector. To generate TRV-VdsrR-1, the 86-bp sequence was amplified and fused into the pTRV2 vector according to a previous report (Liu et al., 2002). All primers are listed in **Supplementary Table 1**.

RNA Isolation and RT-qPCR Analysis

Arabidopsis tissue and *N. benthamiana* leaves were collected for total RNA, using TRIzol reagent (Invitrogen, Carlsbad, CA, United States). Genomic DNA removal and reverse transcription were performed using the HiScript III RT SuperMix for qPCR kit (Vazyme, Nanjing, China). RT-qPCR was analyzed by a CFX96 real-time system (Bio-Rad, Hercules, CA, United States) using SYBR Green PCR master mix (Vazyme, Nanjing, China). The primers used in RT-qPCR were listed in **Supplementary Table 1**.

AGO Protein Immunoprecipitation

Arabidopsis protein was extracted from 8 g fresh plants collected at 2 weeks postinoculation with V592 and the control. AGO1 protein was purified with prepared c-MYC Dynabeads. For the negative control, another anti-strep II bead was incubated in a parallel process.

Small RNA Sequencing and Analysis

After total RNA was extracted from the AGO1-IP fraction, sRNA library construction and sRNA sequencing were performed with Illumina HiSeq^{TM} 2500 by Gene Denovo Biotechnology Co. (Guangzhou, China)[1]. Three repeat libraries were constructed. Clean reads were aligned to the *Arabidopsis* reference genome (TAIR10). By using read counts >10 in all three repeats as a cutoff, the unmatched reads were aligned to the *V. dahliae* genome (assembly ASM15067v2). Known *Arabidopsis* miRNAs were downloaded from miRBase release 22 (Griffiths-Jones et al., 2008). sRNAs with lengths between 18 and 30 nt were included in our analysis, and sRNA abundance was normalized into reads per million (rpm). psRNATarget (Dai et al., 2018) with a maximum expectation score of 3 was used to predict the targets of VdsRNAs. The function of VdsRNA targets was analyzed by AgriGO (Du et al., 2010), and enriched gene ontology (GO) terms were visualized by WEGO (Ye et al., 2018).

[1]https://www.omicshare.com/

Small RNA RT-PCR

RNA was extracted from *Arabidopsis* or the 6myc-AGO1 plant tissue-bound RNA fraction using TRIzol reagent (Invitrogen, Carlsbad, CA, United States). AGO1-sRNA reverse transcription was performed using the miRNA 1st Strand cDNA Synthesis Kit (Vazyme, Nanjing, China). 28 cycles were used for detecting VdrsR-1. For the positive and negative controls, 35 cycles were used to detect miR162, miR168, siRNA1003 and VdmilR-1. The primers used in sRNA RT-PCR are listed in **Supplementary Table 1**.

N. benthamiana Agrobacterium Infiltration Assays

Agrobacterium infiltration assays were performed according to a previously described method (Duan et al., 2012). With the method of electroporation, constructs were transformed into *Agrobacterium* strain EHA105 Competent individually. A single colony was cultured overnight in 5 ml LB selection medium. 1 ml of LB medium was transferred into 20 ml of LB medium and grown for 16 h. The next day, bacterial culture media were harvested and resuspended in 10 mM $MgCl_2$ buffer at an optical density before infiltration. *N. benthamiana* leaves were collected at 4 days for RNA extraction.

Arabidopsis Virus-Induced Gene Silencing Assays

Agrobacterium (EHA105) was used to transform pTRV1 or pTRV2 and its derivative constructs into *Arabidopsis.* The Agrobacterium transformation and infiltration methods were consistent with those previously described (Duan et al., 2012). 14 days, *Arabidopsis* was treated with shading overnight before and after infiltration. The plant tissues were collected at 14 days post-infiltration for RNA extraction.

Plant RNA Gel Blot Assays

Plant total RNA and sRNA gel blot methods were described in a previous report (Duan et al., 2012). For detection of *DCL1* and *SPL13A/B*, DNA probes were amplified by PCR and then labeled with [α-^{32}P]dCTP with the Rediprime II system (Amersham, Buckinghamshire, United Kingdom). For the detection of specific sRNAs, probes were labeled with T4 polynucleotide kinase (NEB, Beijing, China) with [γ-^{32}P]ATP. The primers and probes used in the RNA gel blot are listed in **Supplementary Table 1**.

RESULTS

Identification of *Arabidopsis* AGO1-Associated Trans-Kingdom *V. dahliae* sRNAs

To identify VdsRNAs that might be transferred into host plant cells and functionally, 6myc-AGO1 transgenic *Arabidopsis* plants in which the *ago1* mutation was complemented by a myc-tagged AGO1 construct (Duan et al., 2012) were used for infection with *V. dahliae*. Anti-α-myc antibody was then used to

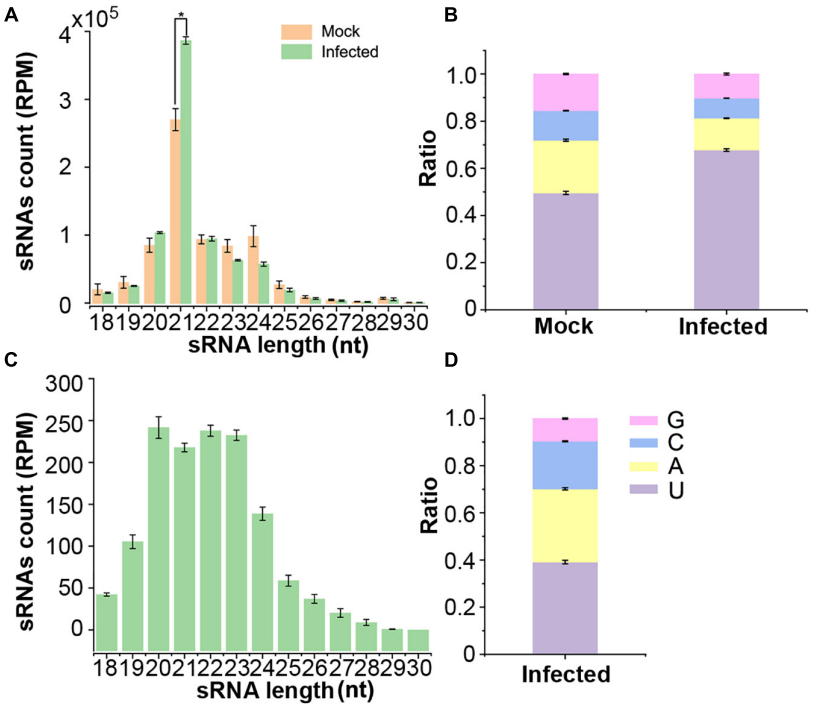

FIGURE 1 | Deep sequencing profiling of *Arabidopsis* AGO1-associated sRNAs in mock and *V. dahliae*-infected plants. **(A)** Numbers of AGO1-immunoprecipitated (AGO1-IPed) sRNAs of different lengths from plants with or without *V. dahliae* infection. **(B)** The 5′ terminal nucleotide compositions of AGO1-IPed sRNAs in different libraries. **(C)** The numbers of different lengths of AGO1-IPed sRNAs aligned to the *V. dahliae* genome. **(D)** The 5′ terminal nucleotide compositions of AGO1-IPed sRNAs aligned to the *V. dahliae* genome. Values are the means ± SD, and asterisk indicates statistically significant differences ($n = 3$; *t*-test, $P < 0.05$).

immunoprecipitate AGO1 from *V. dahliae*-infected and mock-inoculated 6myc-AGO1 plants at 2 weeks postinfection. AGO1-IP sRNAs were isolated and sequenced. Three replicates for each sample were carried out. After removing low-quality reads, we obtained approximately 20 M reads for each library. The AGO1-IP sRNAs from mock plants were dominated by 21-nt classes and 5′-terminal uracil (1U, 50%) (**Figures 1A,B**), which were consistent with previous studies (Mi et al., 2008; Wang et al., 2011). Similarly, the AGO1-IP sRNAs from *V. dahliae*-infected plants were also mainly 21 nt long with 5′-terminal uracil (**Figures 1A,B**). However, AGO1-IP 21-nt sRNAs were much more abundant, and the ratio of sRNAs with 1U (68%) was increased in *V. dahliae*-infected plants (**Figures 1A,B**). After filtering out sRNAs mapped to the *Arabidopsis* genome, the remaining reads that were mapped to the *V. dahliae* genome from AGO1-IP sRNAs in *V. dahliae*-infected plants were assumed to be "trans-kingdom" VdsRNAs. These AGO1-IP "trans-kingdom" VdsRNAs were mainly 20–24 nt in length, with high proportions of 1A (31%) and 1U (39%) (**Figures 1C,D**).

To investigate whether the "trans-kingdom" VdsRNAs possessed possible biological functions, we focused on 705 unique "trans-kingdom" VdsRNAs by using read counts >10 in all three repeats as a cutoff. Next, 1269 *Arabidopsis* mRNAs were predicted as potential targets of these "trans-kingdom" VdsRNAs. GO annotation results showed that these target genes were categorized into extensive pathways (**Figure 2**). Unsurprisingly, dozens of potential target genes were involved in immune system processes and responses to stimuli (**Figure 2**), in agreement with previous reports of trans-kingdom sRNAs acting as RNA effectors to suppress host immunity (Weiberg et al., 2013; Dunker et al., 2020; Ji et al., 2021). In addition, we noted that several target genes were annotated as developmental process, reproductive process or biological phase (**Figure 2**). Thus, our data suggest that these "trans-kingdom" VdsRNAs probably facilitate *V. dahliae* infection and regulate plant development by hijacking the host AGO1 protein.

Confirmation of a 24-nt Fungal rRNA-Derived *V. dahliae* sRNA Loaded Into Host AGO1

Among the putative "trans-kingdom" VdsRNA targets that potentially regulated plant development, we noticed that the plant miR157d transcript matched a 24-nt trans-kingdom VdsRNA derived from *V. dahliae* rRNA (**Figure 3A**). It is well known that miRNAs of the miR156/157 family coordinate vegetative and floral transitions by regulating *SPL* genes in several plant species. This prompted us to investigate whether the 24-nt VdsRNA was indeed derived into plant cells and loaded into host AGO1 as a bona fide trans-kingdom VdsRNA, and the miR157d gene was a genuine target of this trans-kingdom VdsRNA.

We first investigated whether *V. dahliae* rRNA produced sRNAs in fungal cells. Northern blot analysis was performed to detect sRNAs in *V. dahliae* cultured on PDA plates using

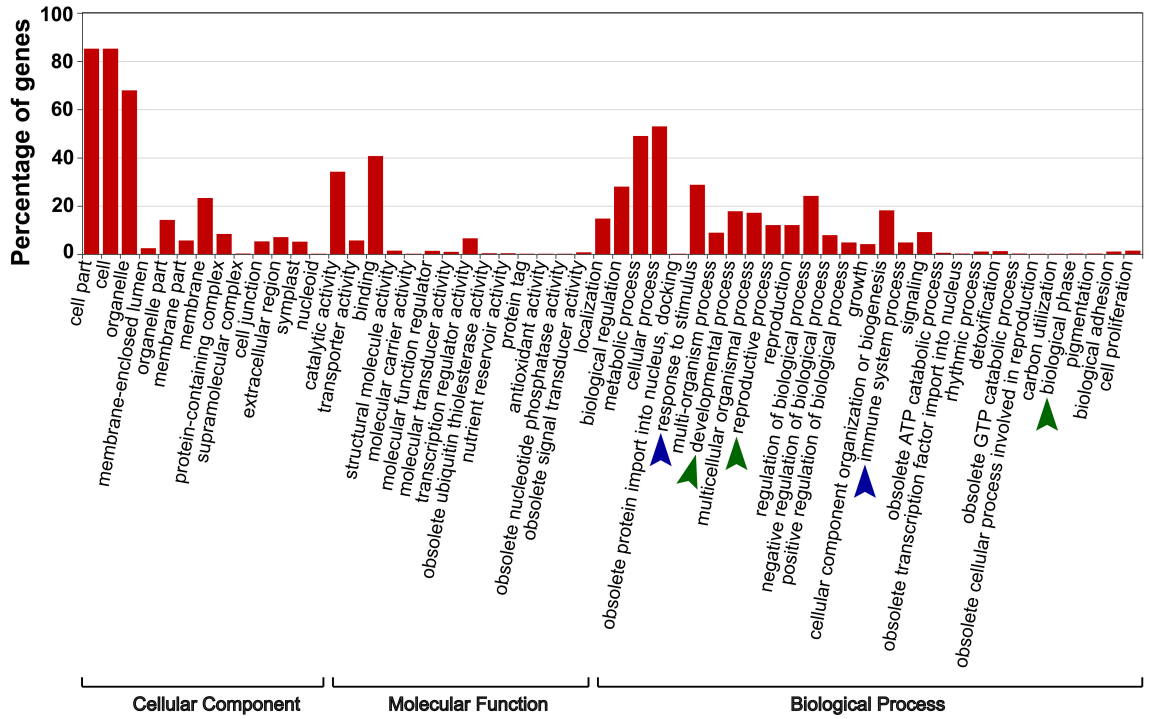

FIGURE 2 | The specific enriched GO terms of putative target genes of AGO1-IPed VdsRNAs. 1269 *Arabidopsis* mRNAs were predicted as potential targets of these VdsRNAs. Blue arrowheads mark the enriched GO terms involved in host immunity, and green arrowheads mark the enriched GO terms involved in plant development.

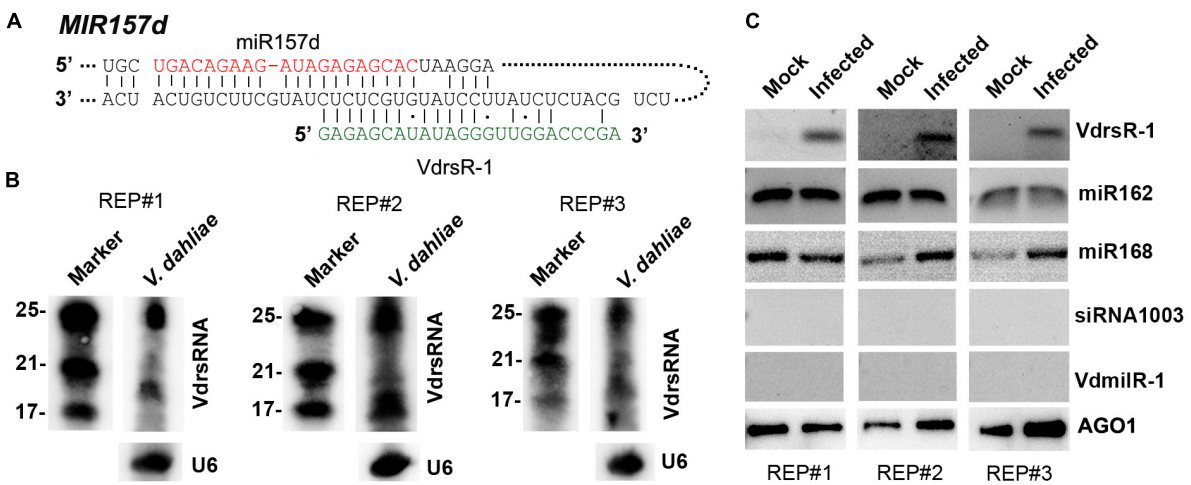

FIGURE 3 | Confirmation of the 24-nt *V. dahliae* rRNA-derived VdsRNA (VdrsR-1) loaded into host AGO1 protein. **(A)** The schematic diagram shows the complementarity between VdrsR-1 and *MIR157d*. The mature miR157d and VdrsR-1 sequences are shown in red and green letters, respectively. **(B)** Northern blotting results with three biological replicates showed that *V. dahliae* generated abundant rRNA-derived ∼24-nt and smaller sRNAs. U6 served as loading control. **(C)** VdrsR-1 was detected by RT-PCR in AGO1-IPed sRNA from *V. dahliae*-infected plants. Two known AGO1-loaded miR162 and miR168 were used as positive controls. A plant endogenous 24-nt siRNA1003 and a *V. dahliae* miRNA-like VdmilR-1 that were not present in AGO1-IPed sequencing data were also examined and not detected. Anti-α-myc antibody was used to detect the amount of AGO1-IPed from mock and infected plants. The results of three independent replicates are shown.

a 24-nt VdsRNA-specific oligo probe. The hybridization results showed that *V. dahliae* rRNA generated abundant ∼24-nt VdsRNAs. Interestingly, ∼20-nt or even smaller bands with strong hybridization signals were also detected (**Figure 3B**). However, these ∼20-nt and smaller VdsRNAs were not present in the AGO1-IP sRNA sequencing data, even though a large

number of other 20-nt and smaller VdsRNAs were in the AGO-IP samples (**Figure 1C**). These data suggest that there was possibly selectivity for either the delivery of VdsRNAs into plant cells or the loading of VdsRNAs into AGO1. Together with the *V. dahliae* miRNA-like sRNA, VdmilR-1, which has previously been reported to regulate the fungal endogenous gene at the transcriptional level (Jin et al., 2019), was not present in any AGO1-IP VdsRNA libraries. We reasoned that the AGO1-IP VdsRNAs, particularly the 24-nt tested VdsRNAs, were not due to their high accumulation in fungal cells and contamination during AGO1-IP manipulation. Hereafter, this 24-nt VdsRNA derived from *V. dahliae* rRNA was named VdrsR-1 in this study.

Next, we further confirmed the AGO1-associated VdrsR-1. RT-PCR assays were performed, and the results showed that VdrsR-1 was detected in the three replicates of AGO1-IP sRNAs from *V. dahliae*-infected plants but was absent in the samples from mock plants (**Figure 3C**). *Arabidopsis* miR162 and miR168, which have been reported to be loaded into AGO1, were also detected in AGO1-IP sRNAs from plants with or without *V. dahliae* infection (**Figure 3C**). *Arabidopsis* AGO4-associated siRNA1003 was used as a negative control and was not detected in any AGO1-IP samples (**Figure 3C**). Moreover, VdmilR-1, which was not present in the AGO1-IP VdsRNA libraries, was not detected in any samples (**Figure 3C**). Taken together, our data demonstrate that *V. dahliae* produces abundant 24-nt VdrsR-1 VdsRNAs that are secreted into plant host cells during infection and that VdrsR-1 is a bona fide trans-kingdom VdsRNA loaded into the host AGO1 protein.

V. dahliae Infection Increased the Accumulation of miR157d

Next, we examined whether there was a change in the miR157d gene, the putative target of VdrsR-1, after *V. dahliae* infection. We first performed RT-qPCR to measure the transcript of *Arabidopsis* miR157d transcript, the precursor *MIR157d*, in *V. dahliae*-infected and mock-inoculated control plants. The level of *MIR157d* was significantly reduced in *V. dahliae*-infected plants compared with that in control plants (**Figure 4A**). Subsequently, we explored whether the reduced *MIR157d* would result in reduced production of mature miR157d. Unexpectedly, AGO1-IPed miR157d was slightly increased in *V. dahliae*-infected plants compared with that in control plants (**Supplementary Figure 1A**). We then used miR157d oligo probe to detect the accumulation level of miR157d by Northern blot analysis. The hybridization signals were obviously increased in *V. dahliae*-infected plants (**Figure 4B**). In view of the members of miR156/157 family miRNAs having high similarity sequences, the enhancement of hybridization signals would be due to the increased accumulation of miR156/157 family members including miR157d. In agreement with this, we found that AGO1-IPed miR157a/b/c were also slightly increased upon *V. dahliae* infection (**Supplementary Figure 1A**).

At the top of the overexposed Northern blotting membranes, two specific hybridization bands were also detected. Decreased upper band signals and increased lower band signals were observed in *V. dahliae*-infected plants compared with control plants (**Supplementary Figure 1B**). In view of the reduced *MIR157d* in *V. dahliae*-infected plants detected by RT-qPCR (**Figure 4A**), we inferred that the upper band was the *MIR157d* precursor and that the lower band could be the DCL1-processed miR157d-containing intermediate produced as hybridized by the miR157d-specific oligo probe. The VdrsR-1 target site at the 3′-end of the *MIR157d* sequence made it difficult to use the 5′ RACE method to examine whether VdsR-1 mediates cleavage of *MIR157d.* However, the decreased accumulation of *MIR157d* but increased the intermediate product and miR157d suggested that AGO1-associated VdrsR-1 targeting presumably promotes DCL1-mediated *MIR157d* processing to produce miR157d rather than causing degradation of *MIR157d*. We then examined the expression levels of *SPL* genes, the predicted target gene family of miR157d (**Supplementary Figure 2**), and found that the expression levels of *SPL13A/B* genes with highly similar sequences (**Supplementary Figure 3**) were obviously reduced in *V. dahliae*-infected plants compared with those in control plants (**Figure 4C** and **Supplementary Figure 2**). These data demonstrate that *V. dahliae* infection reduced the expression of *SPL13A/B* resulting from the increased accumulation of miR157d, presumably due to VdrsR-1-promoted DCL1-mediated *MIR157d* processing.

We then examined the expression of *DCL1,* which is responsible for processing pre-miRNAs into mature miRNAs in *Arabidopsis* (Song et al., 2019). We found that *DCL1* was slightly induced in *V. dahliae*-infected plants (**Figure 4D**). This result was consistent with our previous finding that a class of miRNAs were increased upon *V. dahliae* infection (Jin et al., 2018). Therefore, we assumed that the slight induction of *DCL1* in *V. dahliae*-infected plants, at least partly, contributed to the increase in miR157d and other endogenous miRNAs. To test whether other increased miRNAs were also accompanied by reduced precursor levels, miR159a, which has been confirmed to be induced by *V. dahliae* infection in cotton and *Arabidopsis* plants (Zhang et al., 2016; Jin et al., 2018) was selected for examination. As expected, the accumulation of miR159a was increased upon *V. dahliae* infection (**Figure 4E**). However, unlike the reduction in *MIR157d*, *MIR159a* was induced upon *V. dahliae* infection (**Figure 4F**). These data together indicated that increased accumulation of miR157d and miR159a in response to *V. dahliae* infection was through distinct modes. Although it was not clear how *V. dahliae* infection induced the expression of *DCL1* and *MIR159a* (**Figures 4D,F**), VdrsR-1 would play a role in promoting DCL1-mediated processing of *MIR157d*. Previous studies revealed that the secondary structure of the precursors determines their processing pathway by DCL1 (Bologna et al., 2009, 2013; Liu et al., 2012; Zhu et al., 2013). Therefore, we analyzed the possible secondary structure of *MIR157d* using mfold (Zuker, 2003). In addition to a long near-perfect hairpin structure in which the mature miR157d sequence positions at the 5'-end region, the *MIR157d* precursor contains a typical terminal loop. VdrsR-1 partially paired to the 3'-end of the upper part of the stem with the 5'-terminal 8 nucleotides overlapping with the 3'-terminal 8 nucleotide of

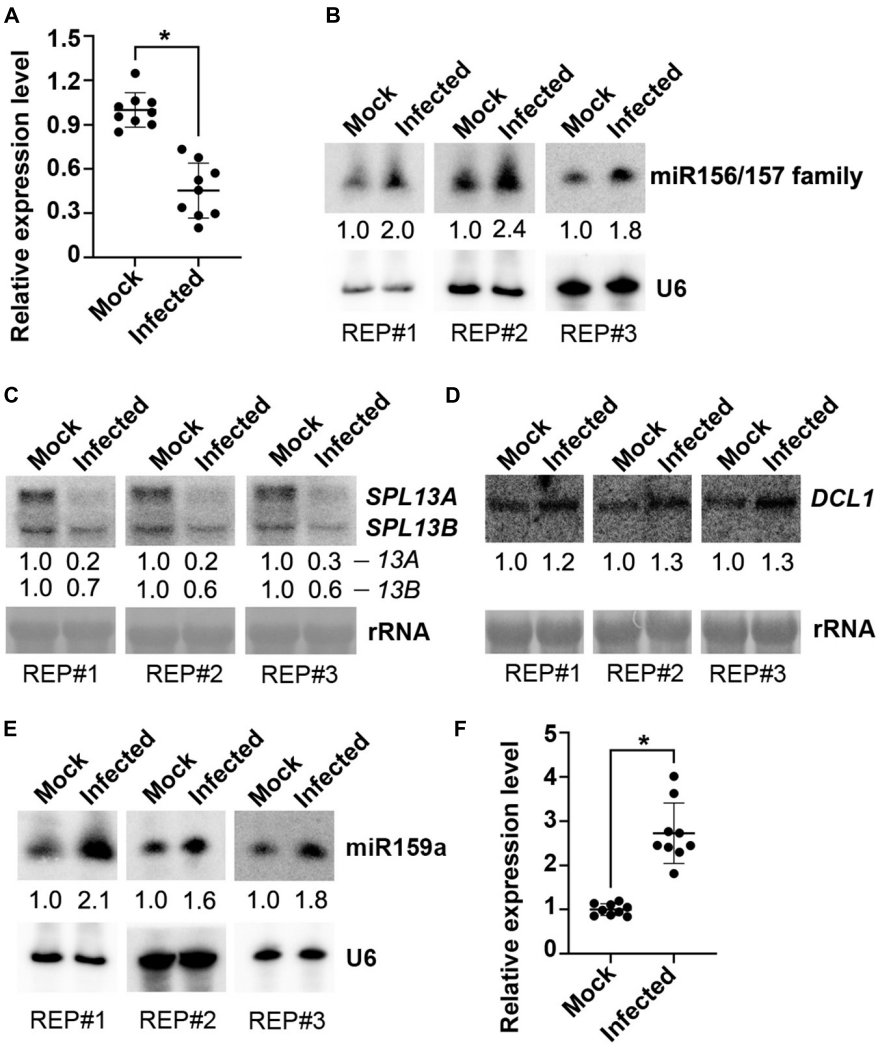

FIGURE 4 | Examination of miR157d and miR159 and related genes in response to *V. dahliae* infection. **(A,F)** Detection of the transcription of *MIR157d* **(A)** and *MIR159a* **(F)** by RT-qPCR. The asterisk indicates significantly different expression of mock plants versus infected plants ($n = 9$; *t*-test, $P < 0.05$). **(B,E)** Detection of the accumulation of miR156/157 family **(B)** and miR159 **(E)** by Northern blotting. U6 hybridization was used as a loading control. **(C,D)** Detection of the expression of *SPL13A/B* genes **(C)** and *DCL1* gene **(D)** by Northern blotting. rRNA was stained with methylene blue as a loading control. The Northern blotting signals were quantified and normalized first to those of U6 or rRNA and then to mock. The results of three biological replicates are shown.

miR157d (**Supplementary Figure 4**). We speculated that the unique stem-loop structure and the pairing between VdrsR-1 and *MIR157d* might lead to the outcome of AGO1-VdrsR-1-mediated action facilitating DCL1 process of *MIR157d* into mature miR157d.

Examination of the VdrsR-1-Facilitated Procession of *MIR157d*

To test whether VdrsR-1 facilitated the process of *MIR157d*, several *Arabidopsis* miRNA precursors were first examined for their capacity to produce specific 24-nt artificial sRNAs and found that the miRNA precursor MIR5653 could generate better 24-nt VdrsR-1 (**Supplementary Figure 5**). Therefore, MIR5653 was used to construct an artificial precursor derived by the 35S promoter, *35S-VdrsR-1*, to produce 24-nt VdrsR-1. Transient expression system in *N. benthamiana* was used to co-express *35S-MIR157d* and *35S-VdrsR-1* or a vector control together with *35S-SPL13B*, one of the miR157d target genes for indication of accurate production and function of miR157d in this transient expression system. As shown in **Figure 5**, co-expression of *35S-VdrsR-1* significantly increased miR157d accumulation and decreased *SPL13B* mRNA compared to co-expression with a vector control. To further test the requirement of pairing with VdrsR-1 for the increased accumulation of miR157d, we mutated the *MIR157d* precursor, *MIR157dm*, in which the miR157d-containing sequence and stem-loop structure were maintained; however, six nucleotides in the upper part of stem-loop were substituted not to be matched by VdrsR-1 for the 5'-end 9–14 nucleotides (**Figure 5A** and **Supplementary Figure 6**). Increased

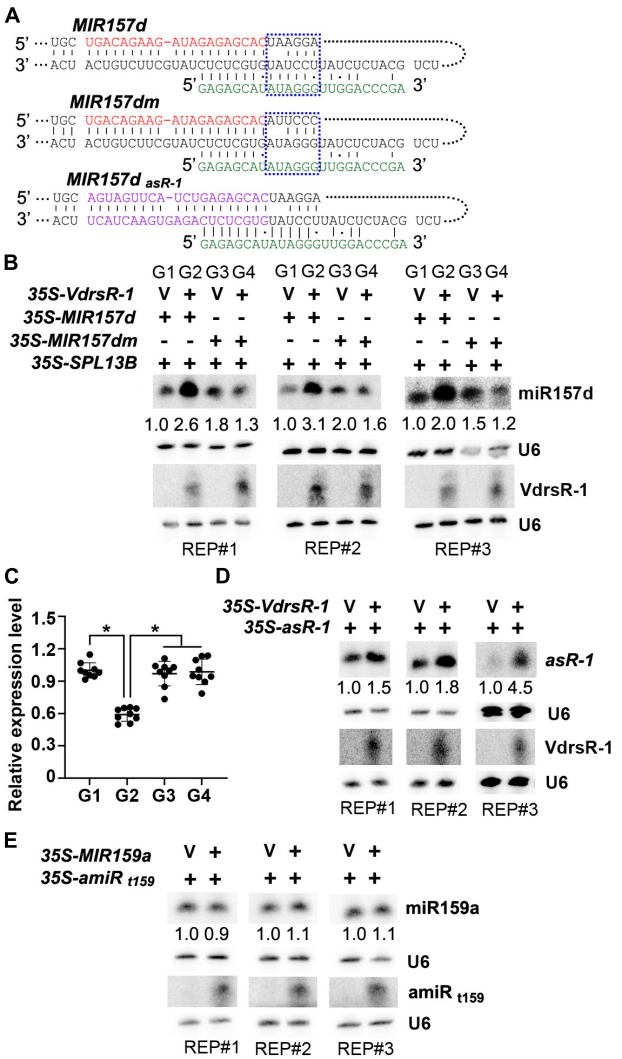

FIGURE 5 | VdrsR-1 triggered miR157d accumulation and reduced *SPL* gene expression. **(A)** The schematic diagram shows the complementarities of VdrsR-1 with wild-type *MIR157d*, with mutated *MIR157dm*, and with $MIR157d_{asR-1}$. The mature miR157d and VdrsR-1 sequences are shown in red and green letters, respectively. The blue dashed lines mark the wild-type and mutated nucleotides within the *MIR157d* and *MIR157dm* sequences. The purple letters in $MIR157d_{asR-1}$ indicate that miR157d and related complementarity nucleotides were substituted to produce art-sRNA-1. **(B)** *35S-VdrsR-1* was transiently co-expressed with *35S-MIR157d* or *35S-MIR157d* in the presence of *35S-SPL 13B* in *N. benthamiana* leaves. V indicates an empty vector. The accumulation levels of miR157d and VdrsR-1 were detected by Northern blotting. U6 hybridization served as loading control. **(C)** The relative expression level of *SPL13B*. The asterisk indicates significant difference expression of co-expression of *35S-VdrsR-1* with *35S-MIR157d* (G2) versus other co-expression combinations (G1, G3, and G4) ($n = 9$; *t*-test, $P < 0.05$). **(D)** *35S-VdrsR-1* was transiently co-expressed with *35S-* $MIR157d_{asR-1}$ in *N. benthamiana* leaves. V indicates an empty vector. The accumulation levels of asR-1 and VdrsR-1 were detected by Northern blotting. U6 hybridization served as loading controls. **(E)** Co-expression of *MIR159a* with *35S-*$amiR_{t159}$, which targets *MIR159a*. The accumulation levels of miR159a and $amiR_{t159}$ were detected by Northern blotting. U6 hybridization served as loading controls. The Northern blotting signals were quantified and normalized first to those of U6 and then to corresponding control. The experiments were repeated three times.

miR157d accumulation and decreased *SPL13B* mRNA were not detected after co-expression of *MIR157dm* with *35S-VdrsR-1* compared to the vector control (**Figures 5B,C**). These data demonstrated that the mutant *MIR157dm* was able to produce mature miR157d and that pairing of wild-type *MIR157d* with VdrsR-1 was required for the facilitation of the *MIR157d* process.

To further examine whether the precursor structure rather than the mature miR157d sequence was essential for the VdrsR-1-facilitated DCL1 process, we used the precursor *MIR157d* to express a sequence-specific artificial sRNA, asR-1. Transient expression assays showed that co-expression of VdrsR-1 clearly increased asR-1 accumulation compared to co-expression with a vector control (**Figure 5D**). Additionally, we used *MIR5653* to express a 24-nt artificial miRNA, *35S-*$amiR_{t159}$, to target the *MIR159a* precursor at a similar position of VdrsR-1 to *MIR157d* (**Supplementary Figure 7**). After co-expression of *MIR159a* with *35S-*$amiR_{t159}$ or a vector control, similar accumulation of miR159a was detected in either co-expression sample (**Figure 5E**), indicating that the *MIR159a* precursor targeted by a 24-nt $amiR_{t159}$ did not facilitate the DCL1-mediated *MIR159a* process. These data demonstrated that VdrsR-1-promoted miR157d accumulation was neither due to the miR157d nucleotide sequence nor merely due to matching to a precursor sequence.

Taken together, our data demonstrated that trans-kingdom VdrsR-1-triggered miR157d accumulation resulted from AGO1-associated VdrsR-1 targeting to *MIR157d,* which bears a typical secondary structure, facilitating DCL1-mediated processing of MIR157d and truly increasing the accumulation of miR157d.

VdrsR-1 Delayed the *Arabidopsis* Floral Transition

Previous studies reported that overexpression of miRNAs in the miR156/157 family could induce bushy architecture and delay phase transition in several plant species (Schwab et al., 2005; Chuck et al., 2007; Shikata et al., 2012; Liu et al., 2017; He X. et al., 2018). *V. dahliae* infection increased host miR157d accumulation (**Figure 4B**), prompting us to inspect the plant growing phenotypes with and without *V. dahliae* infection.

Compared to healthy growing mock-inoculated *Arabidopsis* plants, *V. dahliae*-infected plants displayed wilting and necrosis symptoms at 14 dpi (**Figure 6A**). At this time point, *V. dahliae*-infected plants showed serious stunting, while the main inflorescences of the mock plants started growing, which is associated with shoot maturation during the reproductive phase (Shikata et al., 2009). At 28 dpi, the main inflorescences were observed in a small number of *V. dahliae*-infected plants, while the mock plants all flowered (**Figure 6A**). The results showed that *V. dahliae* infection delayed the vegetative phase change and floral transition.

To determine whether VdrsR-1 contributes to morphological defects, we used a TRV vector to express VdrsR-1 in *Arabidopsis*. Expression of VdrsR-1 was detected in plants infected with TRV-VdrsR-1 at 14 dpi but not in those infected with the TRV control (**Figure 6C**). Consistent with VdrsR-1 expression, increased miR157d and decreased *SPL13A* but not other *SPL*

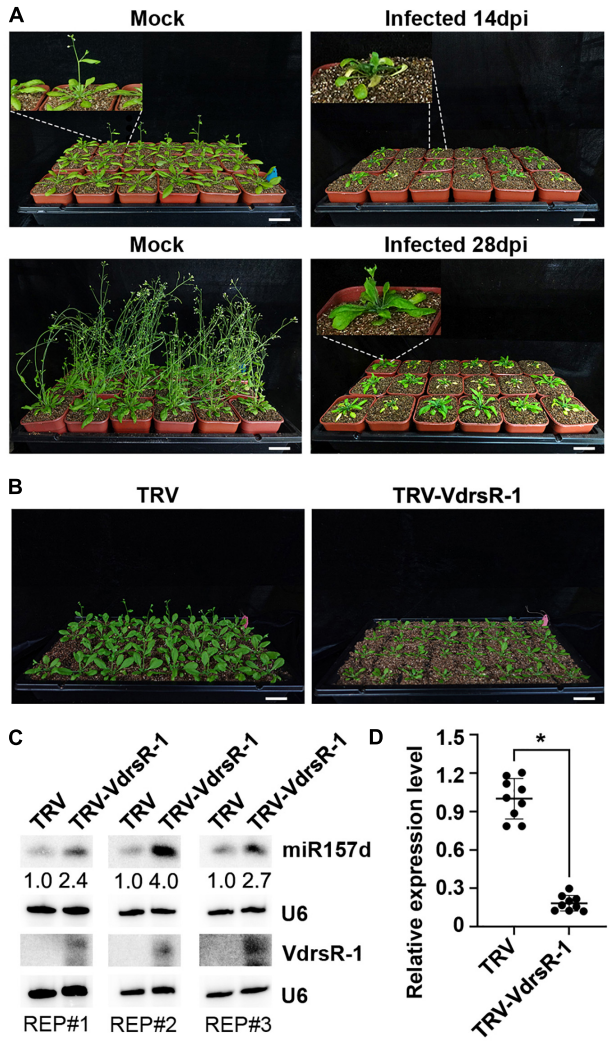

FIGURE 6 | Trans-kingdom fungal VdrsR-1-promoted plant miR157d accumulation partially contributed to *V. dahliae*-induced delayed floral transition in plants. **(A)** Phenotypic comparison of *V. dahliae*-infected plants and mock-inoculated plants at 14 and 28 dpi. In general, *V. dahliae*-infected plants displayed wilting, necrosis and serious stunting, as well as delayed floral transition. Scale bar = 5 cm. Enlarged images corresponding to each plant are linked with white dashed lines. **(B)** TRV-mediated expression of VdrsR-1 slowed plant growth and delayed floral transition. Photographs were taken at 14 dpi. Scale bar = 5 cm. **(C)** The accumulation levels of VdrsR-1 and miR157d were detected by Northern blotting. U6 hybridization served as loading control. Northern blotting signals were quantified and normalized first to those of U6 and then to TRV-infected plants. The experiments were repeated three times with similar results. **(D)** The relative expression level of endogenous *SPL13A*. The asterisk indicates significantly different expression of TRV-VdrsR-1-infected plants versus TRV-infected plants ($n = 9$; *t*-test, $P < 0.05$).

genes were detected in TRV-VdrsR-1-infected plants compared with TRV-infected plants (**Figures 6C,D** and **Supplementary Figure 8**). Evidently, TRV-VdrsR-1-infected plants exhibited stunting and delayed floral transition compared to TRV-infected plants (**Figure 6B** and **Supplementary Figure 9**). Taken together, we concluded that *V. dahliae* caused plant stunting and delayed floral transition, at least in part attributed to the fungal trans-kingdom VdrsR-1 promoting plant miR157d accumulation.

DISCUSSION

Bidirectional transmission of RNAi signals plays important roles in host-pathogen interactions. On the one hand, plant hosts export specific endogenous miRNAs into pathogens to inhibit their invasion by targeting virulence genes (Wang et al., 2016; Zhang et al., 2016). On the other hand, pathogens deliver sRNAs into host cells, which may function as RNA effectors to facilitate their colonization by interfering with host immunity (Weiberg et al., 2013; Dunker et al., 2020; Ji et al., 2021). In this study, we disclosed a new mechanism for the action of a fungal RNA effector.

By immunoprecipitation with AGO1 from *V. dahliae*-infected *Arabidopsis* plants, we obtained a number of *V. dahliae* sRNAs that were most likely associated with the host AGO1 protein and assumed to be trans-kingdom VdsRNAs (**Figures 1C,D**), which possibly matched host putative target genes in extensive pathways, including immune system processing and developmental processes (**Figure 2**). Among these, a 24-nt sRNA derived from *V. dahliae* rRNA, VdrsR-1, was shown to be a real trans-kingdom sRNA loaded into plant AGO1 and targeted to the host *MIR157d* (**Figures 3A,C**). A large number and various lengths of rRNA-derived sRNAs were generated in *V. dahliae* (**Figure 3B**). Whether *V. dahliae* rRNA-derived sRNAs play roles in the rDNA damage response, similar to the function of rDNA locus-derived sRNAs in the classical fungus *Neurospora* (Lee et al., 2009), requires further investigation. Interestingly, despite the large number and various lengths, only the 24-nt *V. dahliae* rRNA-derived sRNA VdrsR-1 was detected in AGO1-IP samples, hinting at the existence of a selective mechanism for either the delivery of VdsRNAs into plant cells or the loading of VdsRNAs into AGO1.

Arabidopsis AGO1 is the key factor mediating target mRNA cleavage, normally at the miRNA complementary site between nucleotide positions 10 and 11 of the miRNAs. Although unable to detect cleavage by using 5' RACE, the perfect match of the first 14 nucleotides between VdrsR-1 and *MIR157d* suggests that AGO1-loaded VdrsR-1 possibly mediates cleavage of *MIR157d*. The detection of reduced *MIR157d* with increased accumulation of miR157d (**Figures 4A,B**) and a possible miR157d-containing intermediate (**Supplementary Figure 1B**) in *V. dahliae*-infected plants suggests that the AGO1-VdrsR-1-mediated action facilitated DCL1 processing on *MIR157d,* which bears a typical stem-loop structure with a large terminal loop. Indeed, complex secondary structures are the determinants for DCL1 processing (Bologna et al., 2009, 2013; Liu et al., 2012; Zhu et al., 2013). The biogenesis mechanism of miRNAs in *Arabidopsis* has been well analyzed in detail (Yu et al., 2017; Song et al., 2019). miRNA biogenesis begins with the cleavage of the terminal loop and then with additional cleavage by DCL1 until mature miRNAs are released (Bologna et al.,

2009). Generally, the DCL1-mediated process of miRNAs is completed within the nucleus, whereas AGO1-directed cleavage of miRNA target occurs within the cytoplasm (Yu et al., 2017; Song et al., 2019; Wang et al., 2019). However, AGO1 has also been found to localize and function in nucleus (Song et al., 2019). The pairing of VdrsR-1 to the junction region of the terminal loop and the upper stem of *MIR157d* (**Supplementary Figure 4**) might guide AGO1-mediated removal of the terminal loop, likelihood undertaking the first cut of DCL1 in *MIR157d*, leading to facilitation of the subsequent cuts of DCL1 on the *MIR157d* stem-loop. An alternative possible mechanism of the effect of AGO1/VdrsR-1 on increasing the accumulation of miR157d might resemble the biosynthesis process of phased secondary siRNAs (phasiRNAs), a special class of siRNAs which the production requires AGO1/7-miRNA-directed cleavage of the target mRNA, and subsequently processed into phasiRNAs by a given DCL protein (Fei et al., 2013; Liu et al., 2020). Nevertheless, the in-depth mechanism of how this 24-nt trans-kingdom VdrsR-1 increased miR157d expression requires further investigation.

Previous studies reported that the miR156/157 family regulates vegetative and floral transitions by targeting *SPL* genes in several plant species (Schwab et al., 2005; Wu and Poethig, 2006; Chuck et al., 2007; Gandikota et al., 2007; Shikata et al., 2009, 2012; Xu et al., 2016; Liu et al., 2017; Gao et al., 2018; He X. et al., 2018). Induction of miR157d and miR157a/b/c upon *V. dahliae* infection was detected by Northern blotting and in AGO1-IPed libraries. However, only the transcripts of two *SPL* genes, *SPL13A/B,* were notably reduced, suggesting that the increased miR157a/b/c upon *V. dahliae* infection had little effect on the regulation of other *SPL* genes in leaves of the adult phase. Indeed, a previous study showed that *SPL* transcripts were differentially responsive to miR156/miR157, and most family members play roles in juvenile leaves (He J. et al., 2018). Moreover, in addition to developing wilting and necrosis symptoms, *V. dahliae*-infected *Arabidopsis* plants exhibited delayed floral transition and late flowering (**Figure 6A**). These phenotypic changes were at least in part attributed to the trans-kingdom VdrsR-1, as TRV-expressed VdrsR-1 in *Arabidopsis* plants also exhibited delayed floral transition and late flowering (**Figure 6B**), accompanied by increased miR157d and decreased *SPL13A/B* (**Figures 6C,D**). The predicted target of the fungal trans-kingdom VdrsR-1 was only the precursor of miR157d, *MIR157d*, but not other family members. The results from transient expression assays also demonstrated that VdrsR-1-promoted miR157d accumulation was not due to the miR157d mature sequence but the precursor *MIR157d*, which bears a typical secondary structure (**Figure 5** and **Supplementary Figure 6**). *SPL13A/B* transcripts were very slightly increased in miR156a/c/d miR157a/c mutant plants (He J. et al., 2018), whereas, only *SPL13A/B* but not other *SPL* transcripts was significantly reduced in *V. dahliae*-infected (**Figure 4C** and **Supplementary Figure 2**) and VdrsR-1-expressing plants (**Figure 6D** and **Supplementary Figure 8**). Therefore, we reasoned that the delayed floral transition was mainly due to the increased accumulation of miR157d which targeted *SPL13A/B* transcripts.

In light of the arms race between the host plant and *V. dahliae,* which is a hemibiotrophic pathogenic fungus, extending the vegetative growth stage of host plants would benefit fungal propagation during the biotrophic life cycle. Therefore, in addition to delivery sRNAs functioning as RNA effectors to facilitate fungal colonization by interfering with host immunity (Axtell and Bowman, 2008; Weiberg et al., 2013; Dunker et al., 2020; Ji et al., 2021), we disclosed a novel strategy for a trans-kingdom sRNA of *V. dahliae* by secreting VdrsR-1 into plant cells to employ the host miR157d/*SPL13A/B*, a phase transition regulatory module, to prolong vegetative growth for better feeding on living plant tissues.

DATA AVAILABILITY STATEMENT

The data presented in the study are available in the National Center for Biotechnology Information (NCBI) repository under accession number PRJNA794992.

AUTHOR CONTRIBUTIONS

H-SG and J-HZ conceived the study, designed the research, wrote the manuscript, and discussed the results. J-HZ analyzed the sequencing data. B-SZ and Y-CL performed the sampling and molecular work. All authors commented on the manuscript.

FUNDING

This study was supported by the National Natural Science Foundation of China (Grant Nos. 32020103003, 31730078, and 31770155), and Strategic Priority Research Program of Chinese Academy of Sciences (Grant No. XDPB16).

SUPPLEMENTARY MATERIAL

The Supplementary Material for this article can be found online at: https://www.frontiersin.org/articles/10.3389/fpls.2022.847086/full#supplementary-material

Supplementary Figure 1 | The accumulation of miR157d in Mock and *V. dahliae*-infected plants. **(A)** Heatmap showing the log2 transformations of the fold-change (Infected vs. Mock) of the miR156/157 family members. The values are labeled on the squares and the clustering results are based on the mean values of three biological replicates. **(B)** An overexposed Northern blotting membrane of detection for the accumulation of miR157d. Loading slots are indicated. Arrows show the possible *MIR157d* precursor (upper band) and miR157d-containing intermediate (lower band).

Supplementary Figure 2 | The relative expression level of endogenous *SPL* genes. The asterisk indicates significantly different expression of infected plants versus mock plants ($n = 9$; t-test, $P < 0.05$).

Supplementary Figure 3 | Alignment of *SPL13A* and *SPL13B* sequences. The miR157d targeted region is marked by a red line, and the probes used for Northern blotting are marked by black lines.

Supplementary Figure 4 | The predicted secondary structure of *MIR157d*. The mature miR157d and VdrsR-1 sequences are presented in red and blue letters, respectively.

Supplementary Figure 5 | Various miRNA precursors were used to test for the production of 24-nt VdrsR-1.

Supplementary Figure 6 | The predicted secondary structure of *MIR157dm*. The mature miR157d and VdrsR-1 sequences are presented in red and blue letters, respectively. The green dashed lines mark the mutated nucleotides within the *MIR157d* and *MIR157dm* sequences.

Supplementary Figure 7 | The predicted secondary structure of *MIR159a*. The artificial miRNA sequences targeting *MIR159a* are presented in blue letters. The mature miR159a sequence are presented in red letters.

Supplementary Figure 8 | The relative expression level of endogenous *SPL* genes in TRV-, and TRV-VdrsR-1-infected plants. The asterisks indicate significantly different expression ($n = 9$; t-test, $P < 0.05$).

Supplementary Figure 9 | The numbers of flowering plants after TRV and TRV-VdrsR-1 infection, respectively. The number of total plant was shown above the column. The asterisk indicates that the two groups have significantly different (Chi-square test, $P < 0.05$).

REFERENCES

Axtell, M. J., and Bowman, J. L. (2008). Evolution of plant microRNAs and their targets. *Trends Plant Sci.* 13, 343–349. doi: 10.1016/j.tplants.2008.03.009

Bologna, N. G., Mateos, J. L., Bresso, E. G., and Palatnik, J. F. (2009). A loop-to-base processing mechanism underlies the biogenesis of plant microRNAs miR319 and miR159. *EMBO J.* 28, 3646–3656. doi: 10.1038/emboj.2009.292

Bologna, N. G., Schapire, A. L., Zhai, J., Chorostecki, U., Boisbouvier, J., Meyers, B. C., et al. (2013). Multiple RNA recognition patterns during microRNA biogenesis in plants. *Genome Res.* 23, 1675–1689. doi: 10.1101/gr.153387.112

Chen, X. (2009). Small RNAs and their roles in plant development. *Annu. Rev. Cell Dev. Biol.* 25, 21–44. doi: 10.1146/annurev.cellbio.042308.113417

Chen, X., and Rechavi, O. (2021). Plant and animal small RNA communications between cells and organisms. *Nat. Rev. Mol. Cell Biol.* 23, 185–203. doi: 10.1038/s41580-021-00425-y

Chuck, G., Cigan, A. M., Saeteurn, K., and Hake, S. (2007). The heterochronic maize mutant corngrass1 results from overexpression of a tandem microRNA. *Nat. Genet.* 39, 544–549. doi: 10.1038/ng2001

Cui, C., Wang, J. J., Zhao, J. H., Fang, Y. Y., He, X. F., Guo, H. S., et al. (2020). A Brassica miRNA Regulates plant growth and immunity through distinct modes of action. *Mol. Plant* 13, 231–245. doi: 10.1016/j.molp.2019.11.010

Dai, X., Zhuang, Z., and Zhao, P. X. (2018). psRNATarget: a plant small RNA target analysis server (2017 release). *Nucleic Acids Res.* 46, W49–W54. doi: 10.1093/nar/gky316

D'Ario, M., Griffiths-Jones, S., and Kim, M. (2017). Small RNAs: big impact on plant development. *Trends Plant Sci.* 22, 1056–1068. doi: 10.1016/j.tplants.2017.09.009

Dexheimer, P. J., and Cochella, L. (2020). MicroRNAs: from mechanism to organism. *Front. Cell Dev. Biol.* 8:409. doi: 10.3389/fcell.2020.00409

Du, Z., Zhou, X., Ling, Y., Zhang, Z., and Su, Z. (2010). agriGO: a GO analysis toolkit for the agricultural community. *Nucleic Acids Res.* 38, W64–W70.

Duan, C. G., Fang, Y. Y., Zhou, B. J., Zhao, J. H., Hou, W. N., Zhu, H., et al. (2012). Suppression of *Arabidopsis* ARGONAUTE1-mediated slicing, transgene-induced RNA silencing, and DNA methylation by distinct domains of the *Cucumber mosaic virus* 2b protein. *Plant Cell* 24, 259–274. doi: 10.1105/tpc.111.092718

Dunker, F., Trutzenberg, A., Rothenpieler, J. S., Kuhn, S., Prols, R., Schreiber, T., et al. (2020). Oomycete small RNAs bind to the plant RNA-induced silencing complex for virulence. *Elife* 9:e56096. doi: 10.7554/eLife.56096

Fei, Q., Xia, R., and Meyers, B. C. (2013). Phased, secondary, small interfering RNAs in posttranscriptional regulatory networks. *Plant Cell* 25, 2400–2415. doi: 10.1105/tpc.113.114652

Gandikota, M., Birkenbihl, R. P., Hohmann, S., Cardon, G. H., Saedler, H., and Huijser, P. (2007). The miRNA156/157 recognition element in the 3' UTR of the *Arabidopsis* SBP box gene SPL3 prevents early flowering by translational inhibition in seedlings. *Plant J.* 49, 683–693. doi: 10.1111/j.1365-313X.2006.02983.x

Gao, R., Gruber, M. Y., Amyot, L., and Hannoufa, A. (2018). SPL13 regulates shoot branching and flowering time in *Medicago sativa*. *Plant Mol. Biol.* 96, 119–133. doi: 10.1007/s11103-017-0683-8

Griffiths-Jones, S., Saini, H. K., Van Dongen, S., and Enright, A. J. (2008). miRBase: tools for microRNA genomics. *Nucleic Acids Res.* 36, D154–D158. doi: 10.1093/nar/gkm952

Guo, H. S., Xie, Q., Fei, J. F., and Chua, N. H. (2005). MicroRNA directs mRNA cleavage of the transcription factor NAC1 to downregulate auxin signals for *Arabidopsis* lateral root development. *Plant Cell* 17, 1376–1386. doi: 10.1105/tpc.105.030841

He, J., Xu, M., Willmann, M. R., Mccormick, K., Hu, T., Yang, L., et al. (2018). Threshold-dependent repression of SPL gene expression by miR156/miR157 controls vegetative phase change in *Arabidopsis thaliana*. *PLoS Genet.* 14:e1007337. doi: 10.1371/journal.pgen.1007337

He, X., Wang, T., Xu, Z., Liu, N., Wang, L., Hu, Q., et al. (2018). The cotton HD-Zip transcription factor GhHB12 regulates flowering time and plant architecture via the GhmiR157-GhSPL pathway. *Commun. Biol.* 1:229. doi: 10.1038/s42003-018-0234-0

Hua, C., Zhao, J. H., and Guo, H. S. (2018). Trans-kingdom RNA silencing in plant-fungal pathogen interactions. *Mol. Plant* 11, 235–244. doi: 10.1016/j.molp.2017.12.001

Huang, C. Y., Wang, H., Hu, P., Hamby, R., and Jin, H. (2019). Small RNAs – big players in plant-microbe interactions. *Cell Host Microbe* 26, 173–182. doi: 10.1016/j.chom.2019.07.021

Ji, H. M., Mao, H. Y., Li, S. J., Feng, T., Zhang, Z. Y., Cheng, L., et al. (2021). Fol-milR1, a pathogenicity factor of *Fusarium oxysporum*, confers tomato wilt disease resistance by impairing host immune responses. *New Phytol.* 232, 705–718. doi: 10.1111/nph.17436

Jin, Y., Zhao, J. H., Zhao, P., Zhang, T., Wang, S., and Guo, H. S. (2019). A fungal milRNA mediates epigenetic repression of a virulence gene in *Verticillium dahliae*. *Philos. Trans. R. Soc. Lond. B Biol. Sci.* 374:20180309. doi: 10.1098/rstb.2018.0309

Jin, Y., Zhao, P., Fang, Y. Y., Gao, F., Guo, H. S., and Zhao, J. H. (2018). Genome-wide profiling of sRNAs in the *Verticillium dahliae*-infected *Arabidopsis* roots. *Mycology* 9, 155–165. doi: 10.1080/21501203.2018.1426062

Jones-Rhoades, M. W., Bartel, D. P., and Bartel, B. (2006). MicroRNAS and their regulatory roles in plants. *Annu. Rev. Plant Biol.* 57, 19–53. doi: 10.1146/annurev.arplant.57.032905.105218

Lee, H. C., Chang, S. S., Choudhary, S., Aalto, A. P., Maiti, M., Bamford, D. H., et al. (2009). qiRNA is a new type of small interfering RNA induced by DNA damage. *Nature* 459, 274–277. doi: 10.1038/nature08041

Liu, C., Axtell, M. J., and Fedoroff, N. V. (2012). The helicase and RNaseIIIa domains of Arabidopsis Dicer-Like1 modulate catalytic parameters during microRNA biogenesis. *Plant Physiol.* 159, 748–758. doi: 10.1104/pp.112.193508

Liu, N., Tu, L., Wang, L., Hu, H., Xu, J., and Zhang, X. (2017). MicroRNA 157-targeted SPL genes regulate floral organ size and ovule production in cotton. *BMC Plant Biol.* 17:7. doi: 10.1186/s12870-016-0969-z

Liu, P. P., Montgomery, T. A., Fahlgren, N., Kasschau, K. D., Nonogaki, H., and Carrington, J. C. (2007). Repression of AUXIN RESPONSE FACTOR10 by microRNA160 is critical for seed germination and post-germination stages. *Plant J.* 52, 133–146. doi: 10.1111/j.1365-313X.2007.03218.x

Liu, Y., Schiff, M., and Dinesh-Kumar, S. P. (2002). Virus-induced gene silencing in tomato. *Plant J.* 31, 777–786. doi: 10.1046/j.1365-313x.2002.01394.x

Liu, Y., Teng, C., Xia, R., and Meyers, B. C. (2020). PhasiRNAs in plants: their biogenesis, genic sources, and roles in stress responses, development, and reproduction. *Plant Cell* 32, 3059–3080. doi: 10.1105/tpc.20.00335

Mallory, A. C., Bartel, D. P., and Bartel, B. (2005). MicroRNA-directed regulation of *Arabidopsis* AUXIN RESPONSE FACTOR17 is essential for proper development and modulates expression of early auxin response genes. *Plant Cell* 17, 1360–1375. doi: 10.1105/tpc.105.031716

Mi, S., Cai, T., Hu, Y., Chen, Y., Hodges, E., Ni, F., et al. (2008). Sorting of small RNAs into *Arabidopsis* argonaute complexes is directed by the 5' terminal nucleotide. *Cell* 133, 116–127. doi: 10.1016/j.cell.2008.02.034

Millar, A. A., and Gubler, F. (2005). The *Arabidopsis* GAMYB-like genes, MYB33 and MYB65, are microRNA-regulated genes that redundantly facilitate anther development. *Plant Cell* 17, 705–721. doi: 10.1105/tpc.104.027920

Moran, Y., Agron, M., Praher, D., and Technau, U. (2017). The evolutionary origin of plant and animal microRNAs. *Nat. Ecol. Evol.* 1:27.

Qiao, Y., Xia, R., Zhai, J., Hou, Y., Feng, L., Zhai, Y., et al. (2021). Small RNAs in plant immunity and virulence of filamentous pathogens. *Annu. Rev. Phytopathol.* 59, 265–288. doi: 10.1146/annurev-phyto-121520-023514

Reyes, J. L., and Chua, N. H. (2007). ABA induction of miR159 controls transcript levels of two MYB factors during *Arabidopsis* seed germination. *Plant J.* 49, 592–606. doi: 10.1111/j.1365-313X.2006.02980.x

Schwab, R., Palatnik, J. F., Riester, M., Schommer, C., Schmid, M., and Weigel, D. (2005). Specific effects of microRNAs on the plant transcriptome. *Dev. Cell* 8, 517–527. doi: 10.1016/j.devcel.2005.01.018

Shikata, M., Koyama, T., Mitsuda, N., and Ohme-Takagi, M. (2009). *Arabidopsis* SBP-box genes SPL10, SPL11 and SPL2 control morphological change in association with shoot maturation in the reproductive phase. *Plant Cell Physiol.* 50, 2133–2145. doi: 10.1093/pcp/pcp148

Shikata, M., Yamaguchi, H., Sasaki, K., and Ohtsubo, N. (2012). Overexpression of *Arabidopsis* miR157b induces bushy architecture and delayed phase transition in *Torenia fournieri*. *Planta* 236, 1027–1035. doi: 10.1007/s00425-012-1649-3

Song, L., Fang, Y., Chen, L., Wang, J., and Chen, X. (2021). Role of non-coding RNAs in plant immunity. *Plant Commun.* 2:100180. doi: 10.1016/j.xplc.2021.100180

Song, X., Li, Y., Cao, X., and Qi, Y. (2019). MicroRNAs and their regulatory roles in plant-environment interactions. *Annu. Rev. Plant Biol.* 70, 489–525. doi: 10.1146/annurev-arplant-050718-100334

Tang, J., and Chu, C. (2017). MicroRNAs in crop improvement: fine-tuners for complex traits. *Nat. Plants* 3:17077. doi: 10.1038/nplants.2017.77

Treiber, T., Treiber, N., and Meister, G. (2019). Regulation of microRNA biogenesis and its crosstalk with other cellular pathways. *Nat. Rev. Mol. Cell Biol.* 20, 5–20. doi: 10.1038/s41580-018-0059-1

Wang, H., Zhang, X., Liu, J., Kiba, T., Woo, J., Ojo, T., et al. (2011). Deep sequencing of small RNAs specifically associated with *Arabidopsis* AGO1 and AGO4 uncovers new AGO functions. *Plant J.* 67, 292–304. doi: 10.1111/j.1365-313X.2011.04594.x

Wang, J., Mei, J., and Ren, G. (2019). Plant microRNAs: biogenesis, homeostasis, and degradation. *Front. Plant Sci.* 10:360. doi: 10.3389/fpls.2019.00360

Wang, J. J., and Guo, H. S. (2015). Cleavage of INDOLE-3-ACETIC ACID INDUCIBLE28 mRNA by microRNA847 upregulates auxin signaling to modulate cell proliferation and lateral organ growth in *Arabidopsis*. *Plant Cell* 27, 574–590. doi: 10.1105/tpc.15.00101

Wang, J. W., Schwab, R., Czech, B., Mica, E., and Weigel, D. (2008). Dual effects of miR156-targeted SPL genes and CYP78A5/KLUH on plastochron length and organ size in *Arabidopsis thaliana*. *Plant Cell* 20, 1231–1243. doi: 10.1105/tpc.108.058180

Wang, M., Weiberg, A., Lin, F. M., Thomma, B. P., Huang, H. D., and Jin, H. (2016). Bidirectional cross-kingdom RNAi and fungal uptake of external RNAs confer plant protection. *Nat. Plants* 2:16151. doi: 10.1038/nplants.2016.151

Weiberg, A., Wang, M., Lin, F. M., Zhao, H., Zhang, Z., Kaloshian, I., et al. (2013). Fungal small RNAs suppress plant immunity by hijacking host RNA interference pathways. *Science* 342, 118–123. doi: 10.1126/science.1239705

Wu, G., and Poethig, R. S. (2006). Temporal regulation of shoot development in *Arabidopsis thaliana* by miR156 and its target SPL3. *Development* 133, 3539–3547. doi: 10.1242/dev.02521

Wu, J., Yang, R., Yang, Z., Yao, S., Zhao, S., Wang, Y., et al. (2017). ROS accumulation and antiviral defence control by microRNA528 in rice. *Nat. Plants* 3:16203. doi: 10.1038/nplants.2016.203

Wu, J., Yang, Z., Wang, Y., Zheng, L., Ye, R., Ji, Y., et al. (2015). Viral-inducible Argonaute18 confers broad-spectrum virus resistance in rice by sequestering a host microRNA. *Elife* 4:e05733. doi: 10.7554/eLife.05733

Wu, M. F., Tian, Q., and Reed, J. W. (2006). Arabidopsis microRNA167 controls patterns of ARF6 and ARF8 expression, and regulates both female and male reproduction. *Development* 133, 4211–4218. doi: 10.1242/dev.02602

Xu, M., Hu, T., Zhao, J., Park, M. Y., Earley, K. W., Wu, G., et al. (2016). Developmental functions of miR156-regulated SQUAMOSA PROMOTER BINDING PROTEIN-LIKE (SPL) genes in *Arabidopsis thaliana*. *PLoS Genet.* 12:e1006263. doi: 10.1371/journal.pgen.1006263

Ye, J., Zhang, Y., Cui, H., Liu, J., Wu, Y., Cheng, Y., et al. (2018). WEGO 2.0: a web tool for analyzing and plotting GO annotations, 2018 update. *Nucleic Acids Res.* 46, W71–W75. doi: 10.1093/nar/gky400

Yu, Y., Jia, T., and Chen, X. (2017). The 'how' and 'where' of plant microRNAs. *New Phytol.* 216, 1002–1017. doi: 10.1111/nph.14834

Zhang, T., Zhao, Y. L., Zhao, J. H., Wang, S., Jin, Y., Chen, Z. Q., et al. (2016). Cotton plants export microRNAs to inhibit virulence gene expression in a fungal pathogen. *Nat. Plants* 2:16153. doi: 10.1038/nplants.2016.153

Zhao, J. H., and Guo, H. S. (2019). Trans-kingdom RNA interactions drive the evolutionary arms race between hosts and pathogens. *Curr. Opin. Genet. Dev.* 58–59, 62–69. doi: 10.1016/j.gde.2019.07.019

Zhao, J. H., Zhang, T., Liu, Q. Y., and Guo, H. S. (2021). Trans-kingdom RNAs and their fates in recipient cells: advances, utilization, and perspectives. *Plant Commun.* 2:100167. doi: 10.1016/j.xplc.2021.100167

Zhu, H., Zhou, Y., Castillo-Gonzalez, C., Lu, A., Ge, C., Zhao, Y. T., et al. (2013). Bidirectional processing of pri-miRNAs with branched terminal loops by *Arabidopsis* Dicer-like1. *Nat. Struct. Mol. Biol.* 20, 1106–1115. doi: 10.1038/nsmb.2646

Zuker, M. (2003). Mfold web server for nucleic acid folding and hybridization prediction. *Nucleic Acids Res.* 31, 3406–3415. doi: 10.1093/nar/gkg595

Conflict of Interest: The authors declare that the research was conducted in the absence of any commercial or financial relationships that could be construed as a potential conflict of interest.

frontiers | Frontiers in Plant Science

ORIGINAL RESEARCH
published: 06 May 2022
doi: 10.3389/fpls.2022.848474

The Construction and Exploration of a Comprehensive MicroRNA Centered Regulatory Network in Foxtail Millet (*Setaria italica* L.)

Yang Deng[1,2†], Haolin Zhang[1,3†], Hailong Wang[1,2], Guofang Xing[4,5], Biao Lei[4,5], Zheng Kuang[1,2], Yongxin Zhao[1,2], Congcong Li[1,2], Shaojun Dai[3], Xiaozeng Yang[1,2], Jianhua Wei[1,2*] and Jiewei Zhang[1,2*]*

[1] Beijing Academy of Agriculture and Forestry Sciences, Beijing, China, [2] Beijing Key Laboratory of Agricultural Genetic Resources and Biotechnology, Institute of Biotechnology, Beijing, China, [3] College of Life Science, Shanghai Normal University, Shanghai, China, [4] College of Agricultural, Shanxi Agricultural University, Jinzhong, China, [5] Shanxi Key Laboratory of Minor Crop Germplasm Innovation and Molecular Breeding, College of Agriculture, Shanxi Agricultural University, Jinzhong, China

OPEN ACCESS

Edited by:
Mehanathan Muthamilarasan, University of Hyderabad, India

Reviewed by:
Roshan Singh, National Institute of Plant Genome Research (NIPGR), India
Sha Tang, Chinese Academy of Agricultural Sciences (CAAS), China

***Correspondence:**
Xiaozeng Yang
yangxiaozeng@baafs.net.cn
Jianhua Wei
weijianhua@baafs.net.cn
Jiewei Zhang
zhangjiewei@baafs.net.cn;
jwzhang919@163.com

† These authors have contributed equally to this work and share first authorship

Specialty section:
This article was submitted to Plant Physiology, a section of the journal Frontiers in Plant Science

Received: 04 January 2022
Accepted: 14 April 2022
Published: 06 May 2022

Citation:
Deng Y, Zhang H, Wang H, Xing G, Lei B, Kuang Z, Zhao Y, Li C, Dai S, Yang X, Wei J and Zhang J (2022) The Construction and Exploration of a Comprehensive MicroRNA Centered Regulatory Network in Foxtail Millet (Setaria italica L.). Front. Plant Sci. 13:848474. doi: 10.3389/fpls.2022.848474

MicroRNA (miRNA) is an essential endogenous post-transcriptional regulatory factor, and foxtail millet (*Setaria italica* L.) is an ideal C4 model cereal that is a highly valuable crop in semiarid and arid areas. The Research on comprehensive and high confidence identification and annotation of foxtail millet miRNAs needs to be strengthened, and to our knowledge, there is no information on the regulatory network of foxtail millet miRNA. In this study, 136 high confidence miRNAs were identified through high-throughput sequencing of the small RNAs in seven tissues at the shooting and grain filling stages of foxtail millet. A total of 2,417 target genes were obtained by combining computational biology software and degradome sequencing methods. Furthermore, an analysis using transcriptome sequencing revealed the relationships between miRNAs and their target genes and simultaneously explored key regulatory modules in panicles during the grain filling stage. An miRNA regulatory network was constructed to explore the functions of miRNA in more detail. This network, centered on miRNAs and combining upstream transcriptional factors and downstream target genes, is primarily composed of feed forward loop motifs, which greatly enhances our knowledge of the potential functions of miRNAs and uncovers numerous previously unknown regulatory links. This study provides a solid foundation for research on the function and regulatory network of miRNAs in foxtail millet.

Keywords: foxtail millet, expression correlation, regulatory network, microRNA, PARE-seq, sRNA-seq

INTRODUCTION

Foxtail millet (*Setaria italica*) is well known as an important C4 cereal crop that was domesticated from its wild ancestor green foxtail (*S. viridis*). *S. italica* is evolutionarily close to pearl millet (*Pennisetum glaucum*) and broomcorn millet (*Panicum miliaceum*) among others (Yang et al., 2020). The global production of foxtail millet combined with other millet crops was estimated

to be 28.37 million tons in 2019 according to the FAO (Food and Agriculture Organization).[1] As a cereal crop that is highly drought tolerant and efficient at using water, *S. italica* is still widely cultivated in the semiarid and arid regions in the world, particularly in China and India (Jia et al., 2013). Originating from northern China, it is also one of the earliest domesticated crops. It was estimated to have been domesticated nearly 11,500 years ago (Yang et al., 2012). Foxtail millet has been chosen as the main cereal crop for arid and semiarid regions and emphasized as a strategic reserve crop to manage the increasingly severe drought. EMS-mutagenized mutant '*xiaomi*' was selected from an M2 population of the cultivated foxtail millet species 'Jingu21', which is widely cultivated in northern China for its good grain quality. '*xiaomi*' has the potential to serve as an ideal model plant like *Arabidopsis* and enable basic and applied research to be conducted on a C4 plant (Yang et al., 2020).

MicroRNAs (miRNAs) are non-coding RNAs with 20–24 nucleotide (nt) that perform important regulatory functions in eukaryotes (Fromm et al., 2020). In plants, primary miRNAs are transcribed by RNA polymerase II and then processed by Dicer-like (DCL) into precursors (pre-miRNA) with stem-loop structures (Lee et al., 2004; Carthew and Sontheimer, 2009). The HASTY protein or other mechanisms cleave these pre-miRNAs into mature miRNA:miRNA star (miRNA*) duplexes, which are then transported to the cytoplasm. To target particular mRNAs and down-regulate the production of target mRNAs, mature miRNAs are integrated into the RNA-induced silencing complex (RISC) (Park et al., 2005; Bartel, 2009). Growing evidence suggests that miRNAs have a role in a variety of plant functions, including growth, development, abiotic stress tolerance, and metabolism (Chandra et al., 2017).

With the revolution of high-throughput sequencing technologies and the development of collaborative analytical software during the last decade, the identification of miRNAs and research on their functions ushered in a breakthrough and explosive era of new data (Zhao et al., 2021). These vast and complex data increase the ratio of false-positive miRNA identification in plants and challenge the corresponding research. This problem was partially effectively solved after the release of the newest annotation criteria of plant miRNAs (Axtell and Meyers, 2018), and the annotation software was developed based on this standard (Kuang et al., 2019; Guo et al., 2021). Furthermore, when paired with RNA-seq data, the correlation of expression patterns between miRNAs and prospective targets offers not only a reference for target gene prediction but also the possibility for the identification of novel regulatory miRNA-target pairings. Motif scanning, in combination with methods, such as Chromatin Immunoprecipitation Sequencing (ChIP-Seq) (Johnson et al., 2007) or DNA Affinity Purification Sequencing (DAP-Seq) (Bartlett et al., 2017), has been widely used as high-throughput techniques to detect the regulation between transcriptional factors (TFs) and their targets, which could be used to discover the upstream regulation from TFs to miRNAs. With all these technical advantages, a whole-genome scaled image of the miRNA-based network in Arabidopsis (Gao et al., 2021) and lettuce (*Lactuca sativa*) (Deng et al., 2021) has been constructed. Despite its importance as a crop, there are few case studies of miRNAs in foxtail millet, and no comprehensive identification and annotation of miRNAs and their regulatory networks have been conducted to our knowledge.

In this study, by sequencing 14 small RNA (sRNA) libraries from four tissues under different developmental stages and analyzing them with a pipeline centered by miRDeep-P2 (Kuang et al., 2019), 136 high confidence miRNAs were identified in foxtail millet. The detailed characteristics of these miRNAs were annotated, including their sequences, structure, conservation, clusters, selection after duplication, and patterns of expression in different tissues. A total of 2,417 targets of the 136 miRNAs were identified by five different means, and Gene Ontology (GO) (Mi et al., 2019) and Kyoto Encyclopedia of Genes and Genomes (KEGG) (Ogata et al., 1999) enrichment analyses indicated that these targets primarily function in the lignin catabolic process, regulation of transcription process, and plant hormone signal transduction, protein metabolism, and sphingolipid metabolism pathways. Furthermore, an analysis of transcriptome sequencing revealed the negative correlation of expression between miRNAs and their target genes and simultaneously explored key regulatory modules in panicles during the grain filling stage. The binding of upstream transcriptional factors (TFs) enables the prediction of miRNAs and their targets. This facilitated the construction of an miRNA central regulatory network, where the connection between different feed-forward loops (FFLs) helped to define several new regulatory links. All the findings were double-checked by selecting candidates at random and examining them through real-time quantitative reverse transcription PCR (qRT-PCR) tests. Compared with previous studies (Yi et al., 2013; Han et al., 2014; Khan et al., 2014; Wang et al., 2016), this work established a strong platform for future research on foxtail millet miRNAs by methodically identifying and annotating high confidence miRNAs in foxtail millet and conducting exploratory analyses of their functions using target genes, an expression correlation, and regulatory networks.

MATERIALS AND METHODS

Plant Materials

Yugu1, as the reference genome, is an inbred line that was used in this study. The seeds were deposited in the Beijing Crop Germplasm Resources Infrastructure, part of the Biotechnology Institute of Beijing Academy of Agriculture and Forestry Sciences (BAAFS), Beijing, China. Seeds of Yugu1 were first sown in plastic pots (21 cm/21 cm diameter/height) with a 3 kg mixture of nutrient soil (Pindstrup seedling, pH 5.5, 0–10 mm) from a commercial source (Pindstrup Mosebrug, Denmark). and cultured in a greenhouse [30°/25°C (day/night), 16-h photoperiod] at 50% humidity. The roots, stems, and leaves were collected from the shooting stage (40 days after germination). The roots, stems, flag leaves and panicles were collected from the grain-filling stage (80 days after germination). After collection, the samples of each tissue were quickly frozen

[1] http://www.fao.org/

in liquid nitrogen and stored at −80°C for the extraction of total RNA and then for the construction of small RNA (sRNA), mRNA, and PARE Libraries.

Construction and Sequencing of Small RNA, mRNA, and PARE Libraries

Following the manufacturer's instructions, RNA was extracted from the seven tissues specified using an OminiPlant RNA Kit (Cwbio, China), and its integrity and quality were verified by an Agilent 2100 Bioanalyzer (Agilent Technologies, United States). cDNA libraries of sRNA and mRNA were prepared by a Small RNA Sample Prep Kit (Illumina, United States) and a TruSeq Stranded RNA LT Kit (Illumina, United States) following the manufacturer's instructions, respectively. Briefly, sRNAs were extracted from 20 μg of total RNA using 15% polyacrylamide gel electrophoresis (PAGE) and the ligation of 5′-RNA and 3′-RNA adaptors. RT-PCR was used to convert and amplify the samples to cDNA. PARE libraries were prepared as previously described (German et al., 2009) but with some modifications. Finally, Illumina HiSeq2500 was used to sequence the verified cDNA libraries. There were two, three, and one biological replicates in each of the sRNA, mRNA and PARE libraries, for a total of 42 libraries.

Identification of Conserved, Poaceae-Specific, and Foxtail Millet-Specific miRNAs

Clean reads were acquired after sRNA library sequencing by filtering low-quality sequences, such as junk reads, adaptor sequences, polyA tags, and reads lengths, that were less than 18 bp or exceeded 30 bp. For miRNA prediction, the retained clean reads (19–25 nt in length) were utilized. Reads that matched plant non-coding RNAs in the Rfam database (version 13.0) (Kalvari et al., 2018), including tRNA, rRNA small nuclear RNA (snRNA), and small nucleolar RNA (snoRNA) sequences, with no more than one mismatch, were further filtered. The remaining sequences were then mapped to the foxtail millet reference genome (Bennetzen et al., 2012), and potential miRNAs were found using miRDeep-P2 software (version 1.1.4) (Kuang et al., 2019). As specified in the miRDeep-P2 handbook, the neighboring sequences of mapped sRNAs were retrieved as putative miRNA precursor sequences. RNAfold (version 2.1.2) (Tav et al., 2016) was used to estimate the secondary structures of all the candidates. All the identification processes were based on the newly defined plant miRNA annotation criteria (Axtell and Meyers, 2018).

All the predicted mature miRNA sequences with 2 nt contiguous nucleotides were matched with the miRNA dataset in PmiREN2.0 (Guo et al., 2021), with no more than two mismatches, using Bowtie (version 1.2.2) (Langmead, 2010) software to annotate the conservation of miRNAs in foxtail millet. Those that did not match any miRNAs in PmiREN2.0 were classified as foxtail millet-specific miRNAs, while those that only matched miRNAs from other Poaceae species were annotated as Poaceae-specific miRNAs, and the rest were considered as conserved.

Validation of Reported miRNAs for Unbiased Comparisons

The genomic location and sequence information of candidate miRNAs were collected from former studies. Those candidates without miRNA star sequences were filtered based on the newest plant annotation criteria. The retained miRNAs were aligned into the PmiREN2.0 database for reclassification and reannotation. After the comparison, the miRNA sequences that were not annotated in this study were searched against the 14 sRNA libraries constructed in our research to confirm whether this study was omitted owing to deficiency in the identification process.

Identification of the Genome-Wide Synteny Analysis of miRNAs

JCVI (MCscanX python version 1.1.18) (Wang et al., 2012) was used to conduct a synteny analysis of miRNAs. The converted Browser Extensible Data (BED) file was modified following the JCVI manuscript, and protein sequences were first used as input files with default settings to produce collinearity blocks over the whole genome. Following that, BEDTools (version 2.26.0; subfunction: intersect) (Quinlan and Hall, 2010) was used to anchor the overlap region between all the miRNA genomic sites and collinearity blocks. Syntenic miRNAs were defined as members of the same miRNA family that followed comparable gene ordering in collinearity blocks. The subfunction "Advanced Circos" of TBtools (version 1.6) (Chen et al., 2020) was used to create the outcome plot.

Target Gene Prediction and Function Enrichment Analysis

The miRNA targets were predicted using four plant miRNA target prediction toolkits: psRNATarget (Dai et al., 2018), psRobot (version 1.2) (Wu et al., 2012), TargetFinder (version 1.0), and RNAhybrid (version 2.1.2) (Kruger and Rehmsmeier, 2006). The miRNA and mRNA transcript sequences were submitted to the psRNATarget webserver[2] and utilized with the current default settings (2017 version). Targets with an *E* value less than 3.0 were retained as potential miRNA targets. Under default settings, PsRobot and TargetFinder both utilized the miRNAs and mRNA transcript sequences as input data. Furthermore, considering plant-specific limitations, RNAhybrid was utilized to forecast energetically feasible miRNA-mRNA duplexes. A strict cut-off value of 0.75 was applied for minimum free energy (MFE)/minimum duplex energy (MDE) (Alves et al., 2009).

Under default settings, the CleaveLand4.0 (Addo-Quaye et al., 2009) program was used to identify probable miRNA cleavage sites using clean Degradome-seq (PARE-seq) data. To create density files, the reads were aligned to foxtail millet transcript sequences. To find possible miRNA target sites, the predicted miRNA mature sequences were matched to transcript sequences. To categorize the miRNA target candidates, the density distribution of reads and miRNA-mRNA alignment were

[2]https://www.zhaolab.org/psRNATarget/

combined. To eliminate false positives, all putative miRNA targets were divided into one of five groups, with only data from categories 0 and 1 being kept.

The Gene Ontology (GO) and Kyoto Encyclopedia of Genes and Genomes (KEGG) annotation of all protein sequences were performed using InterProScan (version 5.0) (Jones et al., 2014) and the KEGG webserver,[3] respectively. A hypergeometric analysis and Fisher test were used for the enrichment analysis of GO and KEGG by the R package "topGO" and in-house R script, respectively. The results plot was generated with the R package "ggplot2."

Quantification of the Expression of miRNAs and mRNAs

The expression of mature miRNA was standardized by reads per million to assess the miRNA expression (RPM). The reads that matched to primary miRNAs (pri-miRNAs) and anchored in the genomic locations of mature miRNAs (less than 2-nt shift) were deemed matching mature miRNAs for each sRNA-seq dataset. To compute the RPM for mature miRNAs, the total number of reads was tallied.

FastQC (version 0.11.9) (Brown et al., 2017) was used to test the quality of all raw mRNA reads, and Cutadapt (version 3.2) (Kechin et al., 2017) software was used to cut out the low-quality reads and adapters. HISTAT2 (version 2.1.0) (Kim et al., 2019) was used to align clean reads to the foxtail millet genome. To assemble the transcript and quantify each mRNA-seq dataset, StringTie (version 2.1.5) (Pertea et al., 2015) was utilized. The levels of transcript expression were derived from the StringTie data and standardized by fragments per kilobase of transcript per million mapped reads (FPKM).

Correlation Analysis Between the Expression of miRNAs and Predicted Targets

Using the R function "cor.test ()," the Pearson correlation coefficient between the expression matrix of miRNAs and their targets was obtained. The raw expression matrix of miRNAs and

[3]https://www.kegg.jp/ghostkoala/

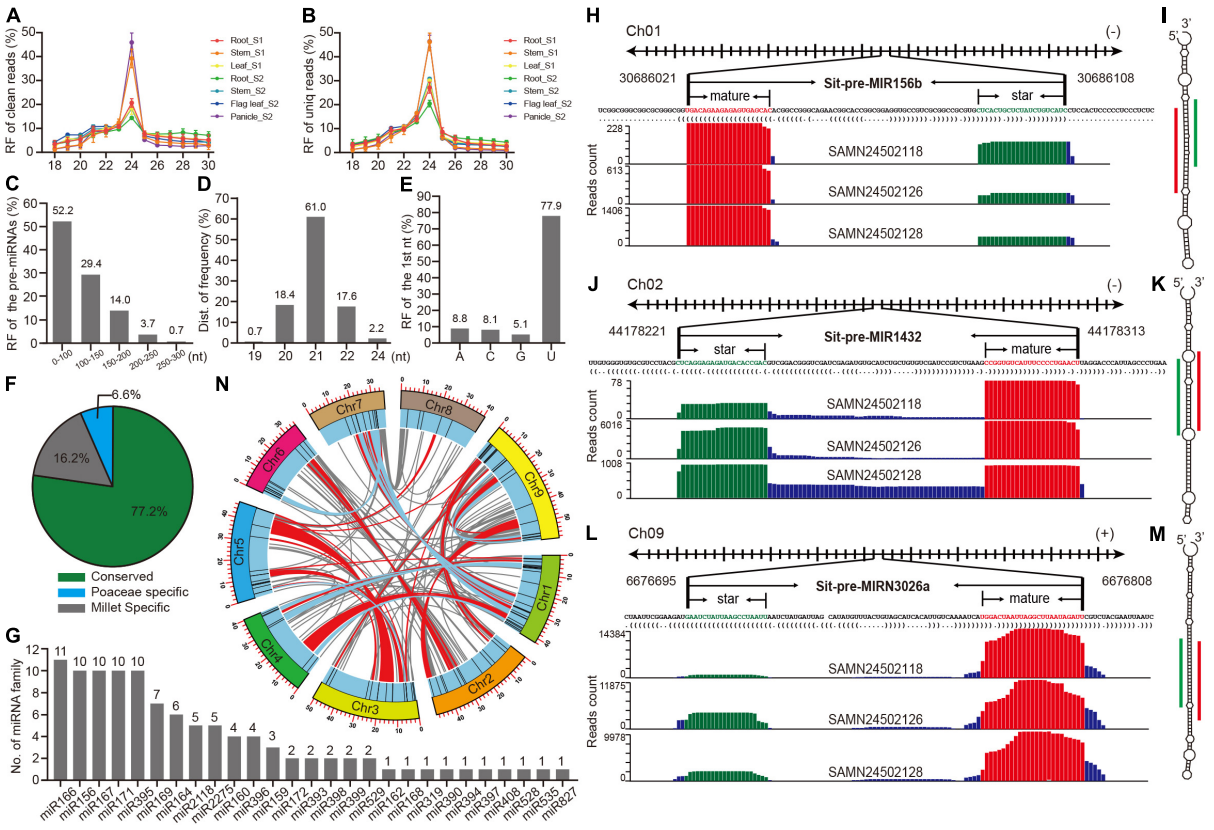

FIGURE 1 | Preliminary analysis of high confidence identified and annotated miRNAs in foxtail millet. **(A,B)** Length distribution of clean and unique reads from sRNA libraries in multiple tissues. **(C)** Length distribution of pre-miRNAs. **(D)** Length distribution of mature miRNAs. **(E)** The proportion of the first nucleotide from mature miRNAs. **(F)** The proportion of three types of miRNAs. **(G)** Member distributions of conserved miRNA families. **(H)** The detailed information and reads mapping to the genome loci of pri-miR156b and pre-miR156b sequences, where mature and star Sit-miR156b are colored with red and green, respectively. **(I)** The secondary structure of pre-miR156b by RNAfold. Mature and star Sti-miR156b are labeled with red and green lines. **(J–M)** The information of Sit-miR1432 and Sit-miRN3026N represented examples of Poaceae-specific and foxtail millet-specific miRNAs, respectively. **(N)** Anchored information of the foxtail millet miRNAs in synteny blocks, while red and blue lines manifest single miRNA and paired miRNAs located in the synteny blocks, respectively.

targets was averaged and transposed using the R function "*t* ()" to generate a matrix with miRNAs and targets as factors, based on biological replicates of seven tissues. The correlation coefficient between each miRNA and target was then calculated using "for loop" of the R language, and significance was determined using a Student's *t*-test. The R package "Pheatmap" was used to visualize the results.

Co-expression Network and Trait Association Analyses of the Predicted Targets

A weighted gene co-expression network analysis (WGCNA) was performed using the R package "WGCNA" following the "WGCNA" handbook. After filtering target genes with a variance of 0 and with >10% missing samples, the soft power estimate value was set to eight, and 12 gene modules were produced. The correlation between the module eigengenes and sample tissues was used to estimate module-trait relationships. The modules with an absolute $r > 0.75$ and $P < 0.01$ were retained. The regulatory miRNAs of these genes in the selected modules that integrated the target genes were traced to construct trait highly correlated regulatory networks. Cytoscape (version 3.7.1) (Shannon et al., 2003) software was utilized to visualize the network.

Network Construction

TF annotations were searched against the TF datasets from PlantTFDB[4] (Jin et al., 2017) in all the mRNA transcripts, and the default filtered result was maintained. To find the potential binding sites for TFs, the upstream 2,000 nucleotide sequences of all the pre-miRNAs and target transcripts were extracted as candidate promoter sequences and then submitted to the PlantRegMap webserver under default parameters[5] (Tian et al., 2020). Based on the interactions between the TFs-miRNAs, miRNAs-targets, and the TFs-miRNA targets, an in-house Perl script was used to detect FFL motifs. After that, a genome-wide miRNA network was constructed using all the FFL motifs, and the network topology was visualized by Cytoscape (version 3.7.1).

Quantitative RT-PCR of miRNAs and Targets

The total RNA of foxtail millet was extracted from separate tissues using the TRIzol reagent (Invitrogen, United States), and the RNA was purified using the RQ1 RNase-free DNase reagent (Promega, United States). It was then reverse transcribed with the Maxima First Strand cDNA Synthesis Kit 222 (Thermo Fisher, United States). Real-time PCR was performed using SYBR Premix Ex Taq^{TM} (TaKaRa, Japan) on a CFX96 Touch System (Bio-Rad, United States). The cycling parameters were as follows: 95°C for 30 s, 40 cycles of 95°C for 1 min, and 60°C for 10 s. The ubiquitin-conjugating enzyme E2 A was used as the endogenous reference. Following the manufacturer's instructions, total small RNA was isolated using a miRcute miRNA Isolation Kit (TianGen, China). The miRcute Plus miRNA First-Strand cDNA Synthesis Kit was used for reverse miRNA transcription (TianGen). The miRcute miRNA qPCR Detection Kit, SYBR Green (TianGen), and a CFX96 Touch System were used to examine the resulting cDNA (Bio-Rad). U6 snRNA was used as the reference gene. The results of relative levels of gene expression were calculated using the $2^{-\Delta\Delta Ct}$ method. Each qRT-PCR experiment was performed on three biological replicates. **Supplementary Table 19** lists all the primers for qRT-PCR experiments.

[4]http://planttfdb.gao-lab.org/prediction.php

[5]http://plantregmap.gao-lab.org/

RESULTS

Comprehensive Identification and Annotation of High Confidence miRNAs

To comprehensively identify the miRNAs in foxtail millet, 14 small RNA libraries from different tissues at different growth stages (**Supplementary Figure 1**) were constructed and produced 508.8 million raw reads and 420.2 million clean reads (**Supplementary Table 1**). Clean and unique sRNA read length distributions both peaked at 24 nt, perhaps indicating the prevalence of short interference RNAs (siRNAs) (**Figures 1A,B** and **Supplementary Tables 2, 3**). The results were similar to those of former studies in foxtail millet (Yi et al., 2013). In particular, the 24 nt small RNA from the shooting stem stage and the grain filling stage were more abundant than those of other tissues, suggesting that the activities of siRNAs were potentially higher during stem development and grain filling.

To identify high confidence miRNAs, miRDeep-P2 (Kuang et al., 2019), software that was developed based on the newest strict plant miRNA criteria was utilized (Axtell and Meyers, 2018), and only 19∼25 nt reads were selected as input datasets. A total of 136 miRNA loci that belong to 36 families were annotated in the foxtail millet genome (**Supplementary Table 4**). A statistical analysis of several basic features of these miRNA loci found that precursor sequences <150 nucleotides comprised > 80% (**Figure 1C**), and 21 nt mature miRNA was the most prevalent, reaching 61% (**Figure 1D**), and U was typically the initial nucleic acid of mature miRNAs (**Figure 1E**). These results were consistent with those of other plant research (Deng et al., 2021; Gao et al., 2021), suggesting that the identification and annotation of these 136 miRNAs were highly confident. The conservation classification of all the miRNAs was searched against the PmiREN2.0 database (Guo et al., 2021). A total of 105, including 27 families, were found to be conserved since their counterparts could be found in other non-Poaceae species, while only nine were considered specific to the Poaceae because their counterparts were only detected in Poaceae species. A total of 22 miRNAs were annotated as specific for foxtail millet since no items could be found in species other than millet (**Supplementary Table 4** and **Figure 1F**). MIR166 had the most members among the conserved families, whereas the other 17 families contained multiple members (**Figure 1G**). Three examples that are conserved and specific to the Poaceae and foxtail millet were randomly selected to illustrate the detailed information (**Figures 1H–M**). Standard stem-loop structure and

reads signature strongly supported them as high confidence candidates. Furthermore, a comprehensive comparison between this study and previous studies (Yi et al., 2013; Han et al., 2014; Khan et al., 2014; Wang et al., 2016) indicated that most of the conserved families were retrieved by this research, and we also identified 18 high-confident new miRNA families (**Supplementary Figure 2** and **Supplementary Tables 5, 6**).

A cluster analysis of the genomic loci of 136 miRNAs was further searched to preliminarily trace back the origin of these miRNAs in foxtail millet, and 11 clusters were obtained when a cluster region length < 10 kb was defined (**Supplementary Table 7**). There were two miR395 clusters that only contained members from foxtail millet, indicating that the abundance of miR395 family was owing to segmental duplication after a tandem duplication (**Supplementary Table 7** and **Figure 1G**). In addition, the genome anchored condition of the miR2275 clusters was the same as those of miR395 (**Supplementary Table 7** and **Figure 1G**), which could similarly explain the miR2275 expansion in the foxtail millet genome. Since the foxtail millet genome had experienced multiple whole-genome duplication (WGD) events (Bennetzen et al., 2012), a synteny analysis was performed to identify whether these miRNAs also expanded owing to the WGD events. Many miRNAs were anchored in the synteny block with no member expansion (**Supplementary Table 8** and **Figure 1N**), while members of miR156, miR166, miR167, miR169, miR171, and miR396 were anchored in pairs in the synteny blocks (**Supplementary Table 9** and **Figure 1N**). This demonstrated that the expansion of partial miRNAs could be owing to the WGD events, but only some were retained.

Exploration of Expression Patterns of miRNAs

The expression of plant miRNAs was dynamic and spatiotemporally specific. To analyze the expression pattern of miRNAs in foxtail millet, clean reads of 14 libraries were mapped to 136 miRNA sequences, normalized to the RPM value, and averaged for tissues (**Figure 2A**). An analysis of the expression of three classified miRNAs found that the conserved miRNAs were expressed at much higher levels than those that were specific to the Poaceae and foxtail millet (**Figure 2B**). Examining the expression profile at the level of tissue found that the expression of conserved miRNAs was higher in the roots and stems at the shooting stage, while relatively few of them were expressed in the leaves. However, the trend was opposite at the grain filling stage. The level of expression of conserved miRNAs in the flag leaves and panicles was higher than those in the roots and stems. This could be owing to the early involvement of the conserved miRNA in the development of roots and stems at the seedling stage. For example, the accumulation of conserved miRNAs in rice (*Oryza sativa* L.) directly regulated the development of rice crowns and roots (Zhu et al., 2019), and Osa-miR396d affected signaling by gibberellin and brassinosteroid to regulate the architecture of rice (Tang et al., 2018). During the latter stage, conserved miRNAs primarily regulated the processes of photosynthesis and grain filling, which are critical for the construction of source-sink system.

To analyze the profile of expression in more detail, two cutoff values of 100 and 10 were established to dissect the matrix into four patterns of expression (**Figure 2C** and **Supplementary Table 10**). The miRNAs represented by the miR166 family comprised 14.71%, demonstrating the global highly expressive pattern in the whole tissues with RPM $\geq$ 100 (**Figure 2D** and **Supplementary Table 10**). Most of these housekeeping miRNAs were primarily conserved miRNAs and contained only the two miRNAs Sit-miRN3026a and Sit-miRN3026b that are specific to foxtail millet. In addition, 29 miRNAs were highly expressed in only one specific tissue (**Figure 2E** and **Supplementary Table 10**). Except for Sit-miR156d, the members of miR156 were specifically highly expressed in roots at the shooting stage. Sit-miR2275c and Sit-miR2275e, two conserved miRNAs, were expressed at high levels in panicles, which could trigger the production and accumulation of 24 nt phased small interfering RNAs (phasiRNA) and further regulate the development of anther in grass plants (Xia et al., 2019). Compared with their levels of expression in other tissues, Sit-miR159a and Sit-miR319, members of the miR159/319 superfamily, were both poorly expressed in the leaves at the two stages, while the other two members of miR159 were housekeeping miRNAs (**Figure 2D** and **Supplementary Table 10**). Consistent with previous studies, Sit-miR408 was only poorly expressed in panicles, which had been proven to reduce crop production by regulating the expression of uclacyanin (*UCL*) in panicles during the grain filling stage in rice (Zhang et al., 2017). All these miRNAs could be candidate targets for genetic breeding improvement in foxtail millet. Finally, eight miRNAs were randomly selected and examined using qRT-PCR experiments (**Figures 2F–H** and **Supplementary Figure 3**), and the results were consistent with the profile of expression (**Figure 2A** and **Supplementary Table 10**), which further demonstrated the high confidence of the identification and annotation of miRNAs.

Functional Analysis of Predicted Targets of miRNAs

The major function of miRNAs is to dampen the expression of their targets to regulate various biological processes. Four types of computational software, psRNATarget, TargetFinder, psRobot, and RNAhybrid, were used to predict the targets of 136 miRNAs using whole-genome transcripts as input data. Combined with the results of degradome (PARE-seq) data, 2,417 targets inside 5,033 miRNA-targeted regulatory pairs were obtained as an overall dataset (**Figure 3A** and **Supplementary Table 11**). All the results of PARE-seq and the overlap results predicted by at least two types of computational software were stablished as an overlap dataset for subsequent analysis. Almost all the conserved regulatory links that had been researched or published in model plants such as Arabidopsis, rice, and maize (*Zea mays* L.) were discovered among the regulatory pairings between these miRNAs and the target genes (**Supplementary Table 11**), showing that the predictions were valid. For example, miR156 regulates the SPL genes; miR159 regulates the MYB genes, and miR160 regulates the ARF genes. There were also many new regulatory pairs uncovered. The conserved miR159a and miR171

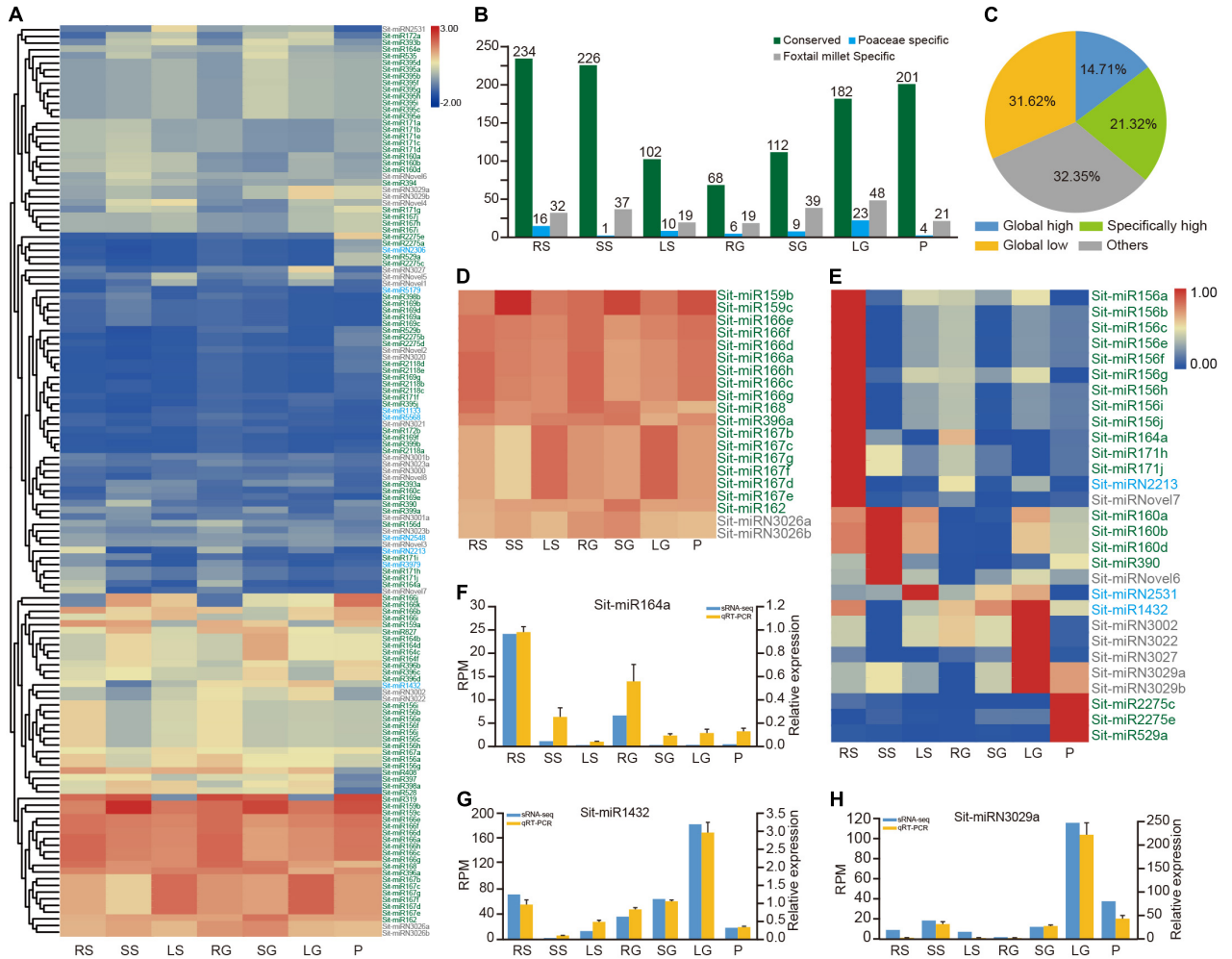

FIGURE 2 | Dynamic expression profiles of miRNAs in foxtail millet. **(A)** The average expression profile of 136 miRNAs in seven tissues. Green, blue, and gray coloring miRNA IDs represent conserved, Poaceae-specific, and foxtail millet-specific miRNAs, respectively. RS, SS, and LS indicate root, stem and leaf tissues at the shooting stage, respectively. RG, SG, LG, and P indicate root, stem, flag leaf, and panicle tissues at the grain filling stage, respectively. **(B)** Average expression values of conserved, Poaceae-specific and foxtail millet-specific types of miRNAs in all samples. **(C)** The pie chart shows the proportion of four expression patterns of miRNAs. **(D)** Global highly expressed (housekeeping) miRNAs in seven tissues. **(E)** Highly expressed miRNAs in only one specific tissue. **(F–H)** qRT-PCR results of Sit-miR164a, Sit-miR1432 and Sit-miRN3029a compared with the sRNA-seq result, respectively. RPM, reads per million; qRT-PCR, real-time quantitative reverse transcription PCR; sRNA, small RNA.

target genes, for example, may be TCP, and ARF, respectively, and these predictions were convincingly verified by the PARE-seq data (**Supplementary Data 1**). Furthermore, the regulatory pairs between Poaceae or foxtail millet-specific miRNAs and their target genes were discovered. For example, Sit-miR5179 and Sit-miRNovel8 could possibly depress TFs, such as MIKC and C2H2, according to the PARE-seq data (**Supplementary Table 11** and **Supplementary Data 1**). Six examples are shown in **Figure 3B**: Sit-miR156b and Sit-miR167h represented conserved miRNAs; Sit-miR1432 and Sit-miR5179 were specific to the Poaceae, while Sit-miRN3001b and Sit-miRN3020 were specific to foxtail millet. All these regulatory pairs were clearly supported by the PARE-seq results.

GO and KEGG enrichment analyses were performed on all miRNA target genes to have a better understanding of their general status at the genome-wide level. In GO, a biological process (BP) analysis indicated significant enrichment in the regulation of transcription, phosphate ion transport, DNA methylation, superoxide metabolic process and protein deacetylation terms (**Figure 3C** and **Supplementary Table 12**), which directly or indirectly affects the ion balance, gene transcription and the response to biological and abiotic stresses. The KEGG enrichment analysis was primarily focused on plant hormone signal transduction and the cysteine and methionine metabolism pathways (**Figure 3D** and **Supplementary Table 13**). Moreover, the results of GO and KEGG enrichment in the overlap dataset were similar to the overall condition (**Supplementary Figure 4**). These were closely related to the miRNAs as regulatory factors, which could regulate the TFs, its large class of target genes. The TFs that can be regulated by miRNAs were studied in

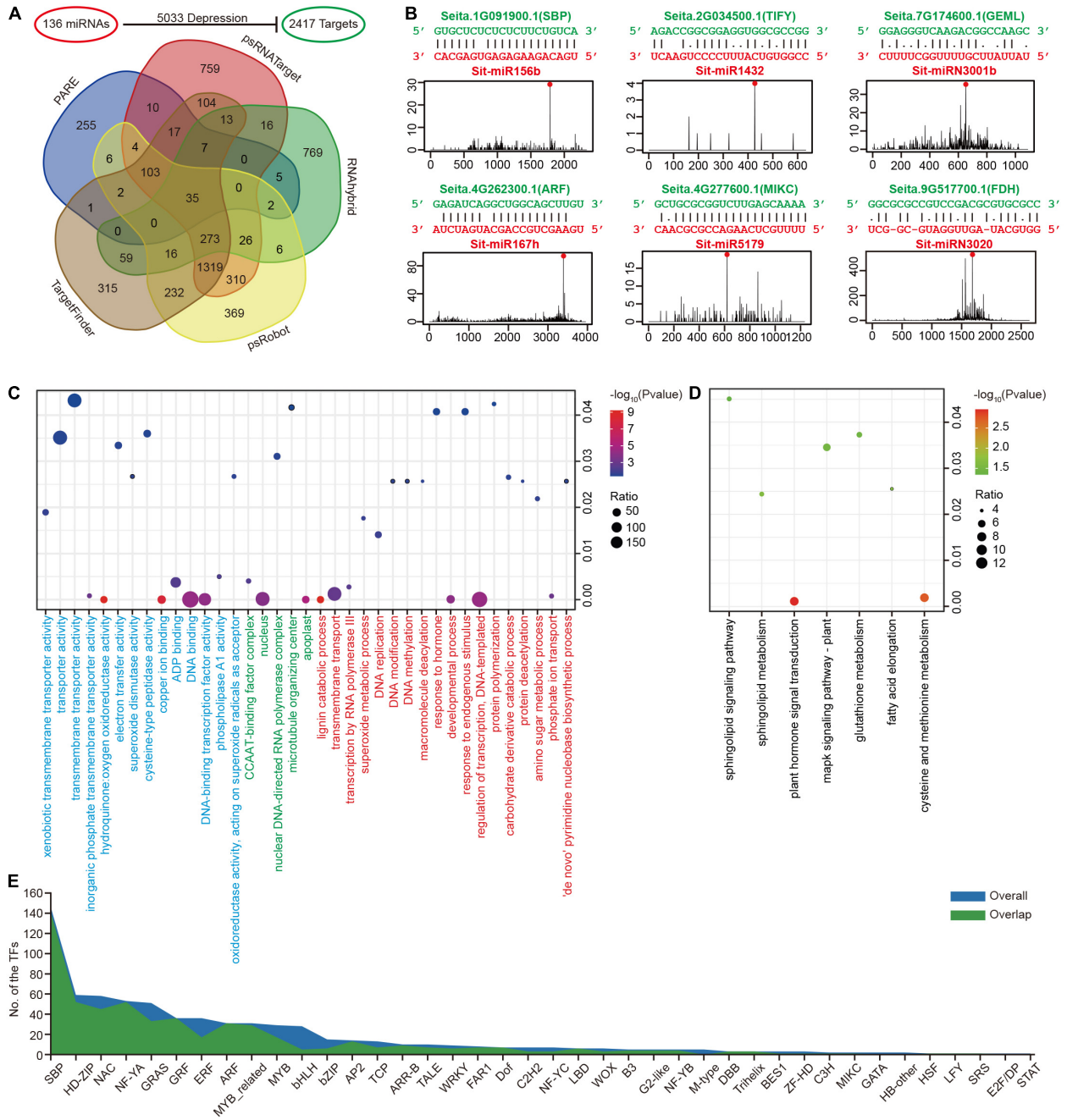

FIGURE 3 | Prediction of miRNA target genes in foxtail millet. **(A)** Candidate miRNA target genes predicted through five methods. **(B)** Six miRNA-target examples represented conserved (Sit-miR156b, Sit-miR167h, and their targets), Poaceae-specific (Sit-miR1432, Sit-miR5179, and their targets), and foxtail millet-specific (Sit-miRN3001b, SitmiRN3020, and their targets) examples. **(C)** Bubble chart of the GO enrichment analysis for miRNA targets. Terms of BP, CC, and MF are labeled red, green, and blue, respectively. **(D)** Bubble chart of the KEGG enrichment analysis for miRNA targets. **(E)** The numbers of transcriptional factor families accounted in the miRNA targets. The "overall" and "overlap" are the overall target genes dataset and overlap target genes dataset, respectively.

more detail, and 40/35 families with different constrictions were identified (**Figure 3E**). Interestingly, in this study, sphingolipid metabolism and sphingolipid signaling pathways were both detected in the GO enrichment (**Supplementary Table 12**). In addition, the gene *Seita.5G438700.1* (SPT) in these two pathways was regulated by the only global highly expressed foxtail millet-specific miRNA family miR3026 (**Figure 2D**). Simultaneously, *Seita.5G438700.1* was globally expressed at lower levels in seven tissues (**Supplementary Table 10**).

The functions of tissue-specific highly expressed miRNAs were explored in more details. In addition to the 29 miRNAs that were highly expressed in one specific tissue (**Figure 2E**), candidates

that were larger than 100 RPM in specific tissues after filtering out house-keeping miRNAs were also considered as tissue-specific highly expressed miRNAs. Their targets were then extracted and GO enrichment analyses were followed, which resulted in many new discoveries. For example, in roots, miRNA-target pairs that regulate nitrogen biosynthesis process and potassium ion transport process were enriched, suggesting their crucial roles in root structure construction, and the transportation of nutrients from soil to root. We also found that stem-specific miRNAs are involved in shoot development and the transition between different developmental stages. Moreover, panicle-specific highly expressed miRNAs were found to be able to regulate seed development and further impact the final grain yield (**Supplementary Table 14**). In general, miRNAs regulate important physiological processes, such as plant growth and development, nutritional metabolism, biotic and abiotic stresses, by regulating many functional genes in plants.

Correlation of the Expression Between miRNAs and Their Targets

The regulatory relationship between miRNAs and targets will cause a negative correlation between their levels of expression. Therefore, identifying the expression patterns of the miRNAs and their target genes in different tissues was a powerful method to corroborate their regulatory patterns. Transcripts in seven tissues were examined by high-throughput sequencing. A correlation analysis and principal component analysis showed that expression levels of the transcripts were consistent between the same samples, indicating the reliability of these data (**Supplementary Figure 5**). A correlation matrix analysis of the dynamic expression patterns of all miRNAs and their target genes in seven tissues was preliminarily conducted to explore these miRNA-target regulatory pairings (**Figure 4A** and **Supplementary Table 15**). A statistical analysis revealed that negative regulatory relationships existed in more than 46% of the miRNA-target combinations ($R < 0$, **Figure 4B**). Despite the fact that these miRNAs may depress their target genes only in a single tissue, the comprehensive matrix validly supported negative regulation of miRNA and their target genes (**Figures 4A,B**). Furthermore, nine transcripts were randomly selected for qRT-PCR experiments, and the results were highly consistent with the results of RNA-Seq (**Figures 4C–E** and **Supplementary Figure 6**).

Among the predicted regulatory pairs, many pairs exhibited a strict negative correlation. For example, the expression patterns of miR156 and miR172 and their target genes in specific tissues had been genetically verified for their function in developmental transition (Wu et al., 2009). MiR167b was a good example. Sti-MiR167b and its target *Seita.3G066900.1* (APUM1) had reverse patterns of expression in seven tissues (**Figure 4F**). Sti-miR394 is another representative conserved miRNA. Its target *Seita.9G088300.1* (Slc25a44) also had an opposite pattern of expression (**Figure 4G**). It also revealed many new regulatory relationships among the Poaceae-specific and foxtail millet-specific miRNAs with their target genes (**Supplementary Table 15**). **Figure 4H** lists a representative example of foxtail millet-specific miRNA, Sit-miRN3027 and its target gene *Seita.3G128500.1*, and presented a strong negative correlation between them. Simultaneously, six comparative miRNA-mRNA regulatory pairings were randomly selected for qRT-PCR experiments, and the results exhibited their negative regulatory relationship (**Supplementary Figure 7**).

Specific Target Genes and miRNA-Target Regulatory Modules at the Grain Filling Stage

In most cases, cluster genes exhibit a co-expression pattern when performing different biological functions, which could be related to their response to common environmental factors or their own cascade control. For this reason, after filtering 67 genes with 0 expression variance in seven tissues, 2,350 targets were retained and iterated through the R package "WGCNA" for clustering analysis (**Supplementary Figure 8**). This constructed a gene co-expression matrix that contained 12 modules. After associating the tissue phenotype, nine modules were highly correlated with the tissues ($R \geq 0.75$, $P < 0.01$) (**Figure 5A**). Transcription factors comprised a large proportion in each module (**Figure 5B**). Among them, the yellow module was the only module that was related to panicle at grain filling stage (**Figures 5A,C**). Further analysis found that this module contained 34 transcription factors in 18 TF families, including SBP, AP2, and NAC (**Figure 5D**). A GO enrichment analysis of genes in the yellow module (**Supplementary Table 16**) found that glucosamine-containing compound metabolic process, aminoglycan metabolic process and amino sugar metabolic process were enriched, and all these terms were related to sugar accumulation in the source-sink system during the grain filling process.

Hub genes normally play an important role in the co-expression network. Based on the evaluation value KME (eigengene connectivity), the top nine hub genes and the genes associated with them in the yellow module were extracted to construct the regulatory network (**Supplementary Figure 9**). The level of regulation of the miRNA was traced back to further analyze the regulatory relationship of these nine genes (**Figure 5E**), and these nine genes were only regulated by a few specific miRNAs. For example, *Seita.3G084900* (Laccase25) was only regulated by Sit-miR397, but the relationship of expression between these two nodes does not show a high negative correlation (**Supplementary Table 15**), which could be owing to the importance of these hub genes and additional simultaneous regulation by multiple TFs. To co-locate the miRNAs that were closely related to the yellow module, an analysis of the expression level between the miRNAs and targets identified the target gene, which was relatively highly expressed in panicles, while the miRNA was expressed in an opposite manner (**Supplementary Tables 11, 15**). Based on this, a new regulatory network was constructed (**Figure 5F**). Among them, miR408 occupied the most regulatory relationship pairs, indicating that miR408 may play an important regulatory role during grain filling stage, which was consistent with the previously reported miR408 regulation of seed size and other traits. This part of the regulatory relationship laid a solid foundation for subsequent genetic experiments.

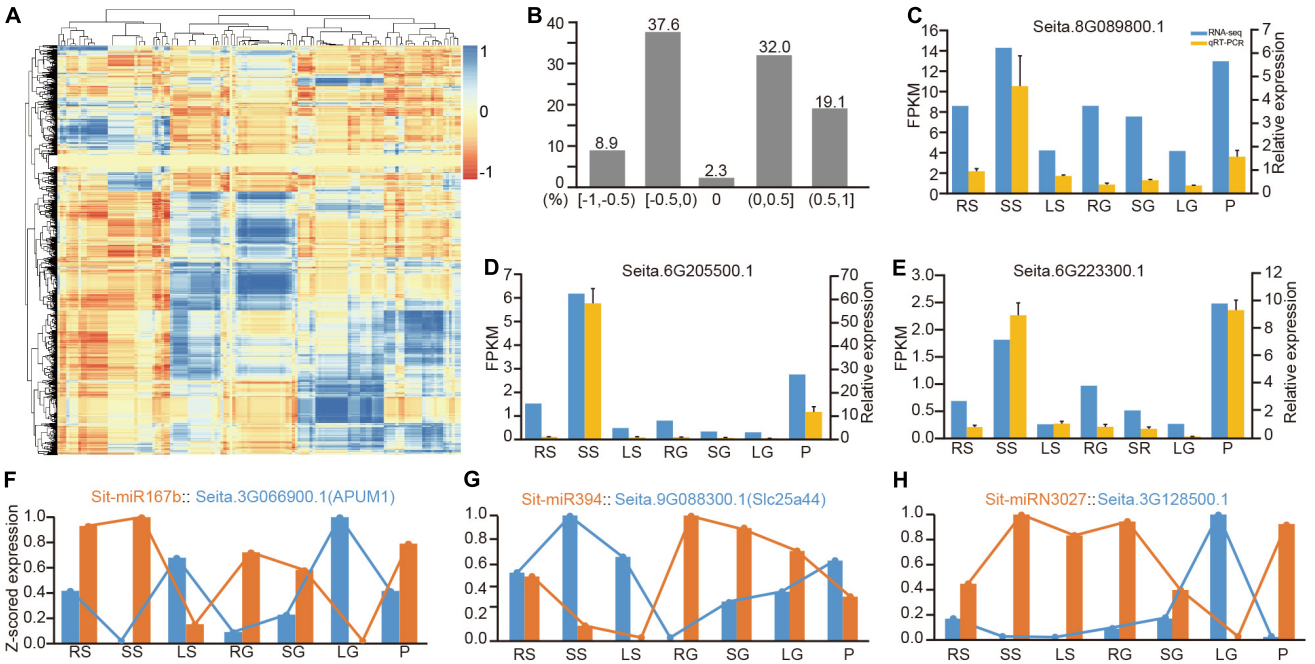

FIGURE 4 | Correlation analysis of the expression between miRNAs and their target genes. **(A)** Correlation matrix of expression between all miRNAs and their targets. **(B)** Distribution of the correlation of miRNA-target expression in divided sections of *r* (correlation value). **(C–E)** The comparison between quantitative results from RNA-Seq and their relative expression from qRT-PCR. **(F–H)** Three representative examples of the negative correlation of conserved miRNA, Poaceae-specific miRNA and foxtail millet-specific miRNA with their target transcripts, respectively. qRT-PCR, real-time quantitative reverse transcription PCR.

Exploration of the Regulatory Network of Foxtail Millet miRNAs

As important transcriptional regulatory factors, miRNAs and TFs cooperate to change the gene expression for multiple biological processes. To construct a comprehensive whole genome-wide regulatory network monitored by TFs and miRNAs, the upstream 2,000 nucleotides of the miRNAs and their target genes were extracted to predict the binding site of TFs, and 35 TF families were retained under the default parameter, including WRKY, ERF, and MYB. Every two nodes from the TFs, miRNAs and target genes formed direct regulatory relationships. The TFs regulated miRNAs and formed 3,449 TF and miRNA interactions (TMIs). The genes targeted by the miRNAs formed 5,033 miRNAs and Target interactions (MTIs), and the target genes regulated by the TFs formed 76,871 TFs and Targets interactions (TTIs) (**Figure 6A**). As for the three nodes together, TFs to miRNAs and then to target genes formed directed acyclic 127,645 cascade motifs, and 110,922 FFL motifs were extracted (**Figure 6A** and **Supplementary Table 17**). A comprehensive regulatory network, including TFs, miRNAs, and targets, was constructed based on these FFLs interactions (**Figure 6B**). To the overlap dataset, 62,328 FFLs were extracted from 71,548 cascades motifs to construct the FFLs network (**Supplementary Figures 10A,B** and **Supplementary Table 18**).

The construction of network further unveiled the regulatory relationships between the miRNAs, TFs and their target genes. In this network, any specific miRNA that occupies a central position linked by other elements can present an independent module core. As a conserved miRNA, Sit-miR827 integrated multiple TF families that regulated the expression of seven downstream target genes, including flowering-promoting factor *Seita.5G441900.1* and SPX domain-containing membrane protein encoding gene *Seita.7G205800.1* (**Figure 6C**). Sit-miR1432, a Poaceae-specific miRNA that highly expressed in flag leaves (**Figure 2E**), was triggered by various TF families and modulated four target genes expression (**Figure 6D**). In these four genes, *Seita.8G026700.1* encodes the BTB/POZ domain contained protein that includes an ankyrin repeat, which is a key positive factor for disease resistance, and the encoding protein TIFY5 of *Seita.2G034500.1* had been reported as an endogenous repressor of the salicylic acid signal. **Figure 6E** showed a foxtail millet-specific miRNA, Sit-miRNovel1, which had a similar regulatory module with the former two examples. Based on the detection of these specific modules, except for those conserved regulatory modules, increasing numbers of novel regulatory relationships were explored and could be chosen as high confidence candidates for further genetic studies and potential breeding targets.

DISCUSSION

The precise systematic identification and annotation of miRNAs is the premise for exploring their functions in a specific species. There have been several studies on the identification of miRNAs in foxtail millet (Yi et al., 2013; Han et al., 2014;

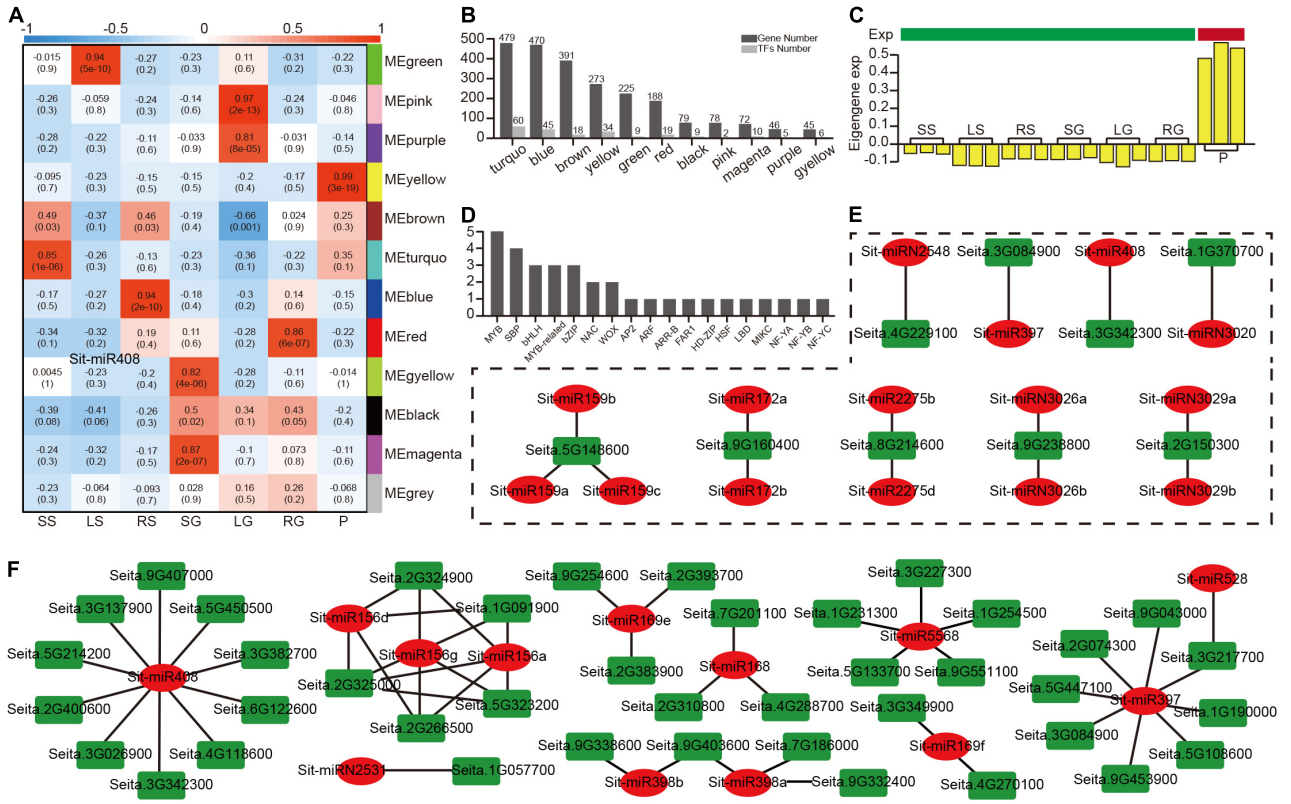

FIGURE 5 | A miRNA modules analysis based on a WGCNA analysis of 2,350 target genes. **(A)** A heatmap of 12 modules correlated with seven tissues. **(B)** The number of target genes and transcription factors in 11 modules (except for the non-sense gray module). **(C)** The bar plot of eigengene expression from the panicle-related yellow module. **(D)** The number of detailed transcription factors in the yellow module. **(E)** The regulatory modules between the nine highest-connectivity target genes in the yellow module and their relevant miRNAs. **(F)** The regulatory modules between the target genes and their relevant miRNAs with opposite patterns of expression.

Khan et al., 2014; Wang et al., 2016) with or without sRNA-seq datasets based on the 2008 criteria for plant miRNA annotations (Meyers et al., 2008). It has become clear that many miRNA annotations are questionable following the study of extensive data sets of plant small RNAs by NGS. In this study, the identification and annotation of all the miRNAs were analyzed by updating the criteria for plant miRNAs that were delineated in 2018. To acquire more precise information at the shooting and grain filling stages, we collected the different tissues of these stages. Moreover, the functions of many miRNAs have been elucidated in plants over the past several years. For example, the overexpression of *Ath-miR408* enhances photosynthesis, growth, and seed yield in Arabidopsis, rice, and tobacco (*Nicotiana tabacum*) (Pan et al., 2018), while miR858 controls flavonoid biosynthesis and development in Arabidopsis (Sharma et al., 2016). The combination of these methods and research results provides a strong foundation to precisely identify and mine the functions of miRNA in foxtail millet. Finally, 136 high confidence miRNAs were identified, annotated and classified.

It is well known that the function of miRNAs is primarily to repress the expression of their target genes. It is critical to accurately predict miRNA targets to mine miRNA functions. Four computational prediction software packages, including psRNATarget, TargetFinder, psRobot and RNAhybrid, extra with PARE data, were used to obtain 5,033 potential miRNA-targets regulatory pairs as an overall dataset. GO and KEGG pathway analyses demonstrated that these miRNA target genes were enriched in plant growth, development, nutritional metabolism, and biotic and abiotic stresses. In general, these results suggest that these miRNAs are involved in almost all biological activities (Mi et al., 2019). According to the analysis of TFs, many conservative types of regulation were also found in foxtail millet, such as miR156-SPL and miR159-MYB, which coincided with previous data (Jia et al., 2013; Yi et al., 2015). Simultaneously, a functional analysis of these tissue-specific highly expressed miRNAs revealed their regulatory roles in nutrient absorption, ion transport, carbohydrate metabolism, flower development, reproductive regulation, and seed development, further demonstrating their regulatory function in growth and development. Interestingly, *Seita.5G438700* was regulated by the only global highly expressed foxtail millet-specific miRNA family *Sit-miR3026*, and its expression pattern was globally low. In addition, expression patterns between the miRNAs and their target genes in different tissues and developmental stages were correlated. Despite the high degree of complication among them, many negative correlations were observed between miRNAs and their target genes in general.

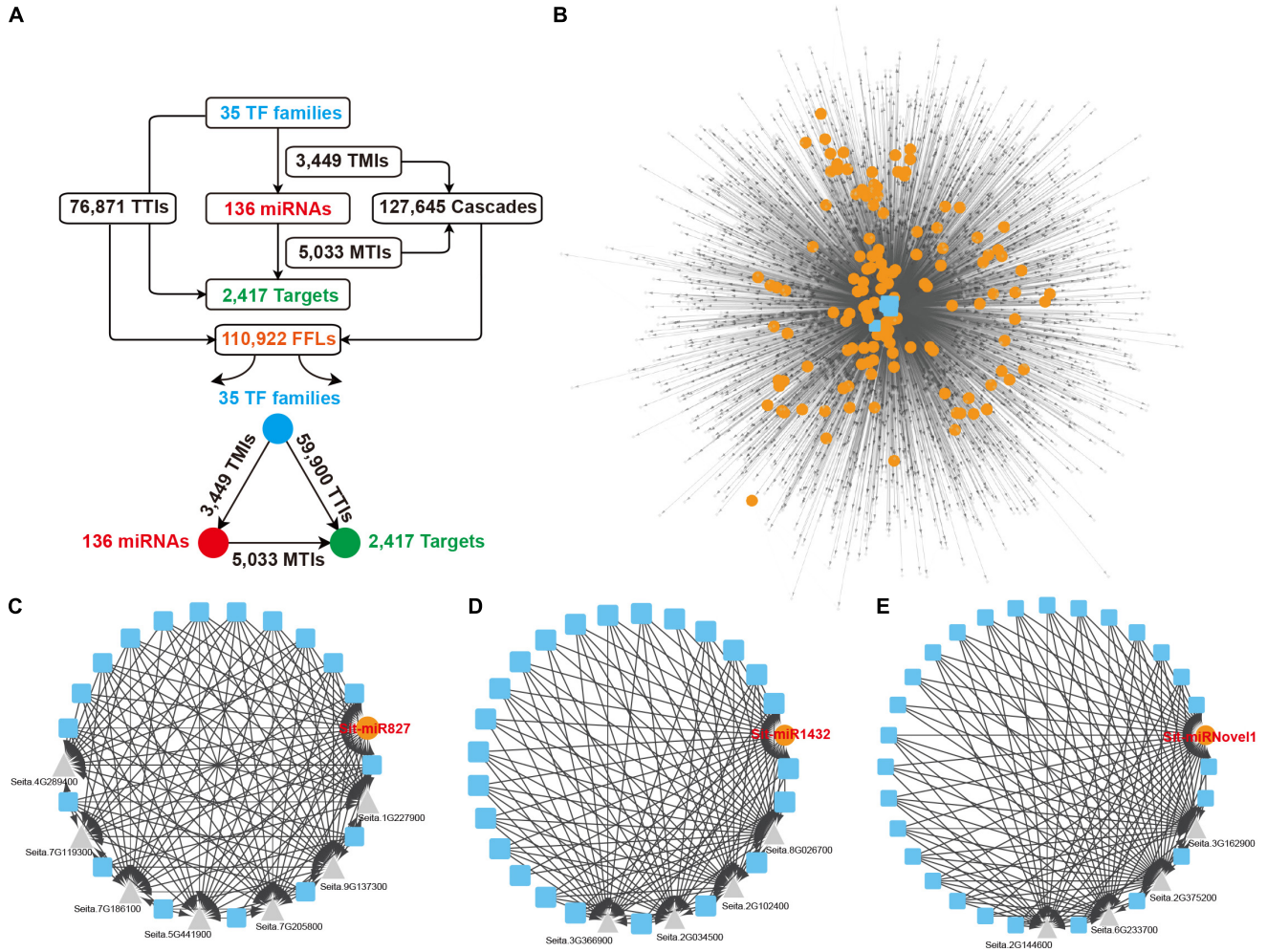

FIGURE 6 | FFLs regulatory network centered by miRNAs. **(A)** Detailed information of all interactions and miRNA-centered FFLs regulatory network from the overall dataset. **(B)** miRNA-centered FFLs regulatory network. Blue squares, orange dots, and gray triangles represent TFs, miRNAs, and targets, respectively. **(C–E)** Three examples of local FFL networks centered by Sit-miR827, Sit-miR1432, and Sit-miRNovel1. Blue squares, orange dots, and gray triangles represent TFs, miRNAs, and target genes, respectively. FFLs, feed forward loops; TFs, transcriptional factors.

Grain filling is a highly complex physiological process. During this stage, numerous storage compounds are synthesized and transported into the endosperm, which primarily determine the yield and grain quality (Wang et al., 2020). The panicle structure is an important agronomic trait that helps to determine crop yield (Xing and Zhang, 2010). The molecular mechanisms of panicle development have been the focus of intensive study (Huang et al., 2017). TFs have extensive and conserved functions in the regulation of panicle development. In this trial, the results of a WGCNA analysis showed that nine modules were highly correlated with different tissues, and only one module was related to the grain filling stage. It contained 34 transcription factors in 18 TF families, including MYB, SBP, AP2 and bZIP. A GO analysis showed that these genes focused on metabolic processes, such as glucosamine-containing, aminoglycan, and amino sugar metabolites. A new miRNA and target gene regulatory network in panicles was constructed and miR408 occupies the largest number of regulatory relationship pairs, indicating that miR408 may play an important regulatory role during the grain filling stage. It has been reported that this miRNA positively regulates the yield of grain and photosynthesis via a cytoplasm-localized phytocyanin protein, OsUCL8 (Zhang et al., 2017). In a recent study, genetic experiments indicated that *Lsa-MIR408* served as a hub gene to increase the fresh weight and achene size of lettuce (Deng et al., 2021).

The construction of a gene regulatory network that integrates multiple regulatory relationships within the appropriate biological process is a desired approach to promote plant biology (Gaudinier and Brady, 2016). The regulatory networks in plants that have been reported to date are primarily focused on transcriptional regulation. MiRNAs are known to have a higher propensity to interact with TFs in plants (Gao et al., 2021). The FFL is a prominent and versatile network motif (Gaudinier and Brady, 2016). In plants, many FFLs have been identified

in gene regulatory networks, which involve developmental processes and stress responses (Taylor-Teeples et al., 2015; Gao et al., 2021). In this study, a complex regulatory network centered on miRNAs and the combination of upstream TFs and downstream target genes was constructed in foxtail millet. Based on the reconstructed hub miRNA in an integrated gene regulatory network of Arabidopsis, the *HY5-MIR858A-MYBL2* FFL module was identified and confirmed to play an important role in the regulation of accumulation of anthocyanins in seedlings in response to light (Gao et al., 2021). The rice miR1432-OsACOT module was found to regulate grain size by controlling rice grain filling. The suppressed expression of rice miR1432 significantly increased grain weight and led to an increase of up to 17.14% in grain yield in a field trial (Zhao et al., 2019). Interestingly, Sit-miR1432 was identified as a classic miRNA specific to the Poaceae in our study, and it was highly expressed in the flag leaves and poorly expressed in the panicle. Simultaneously, Sit-miR1432 is triggered by various TF families and modulates the expression of the four target genes *Seita.8G026700.1*, *Seita.3G366900.1*, *Seita.2G102400.1,* and *Seita.2G034500.1*, excluding the homologous genes of *OsACOT*. This raises the possibility that there is a novel module in foxtail millet that regulates grain filling. Based on the regulatory network centered on miRNAs, increasing numbers of novel regulatory relationships were explored and validated by experiments, which could be exploited in crop breeding.

CONCLUSION

In conclusion, as a C4 model crop and an important economic crop, research on the variation in morphology, nitrogen and water utilization, and nutritional balance of foxtail millet is still limited. In this study, a comprehensive miRNA centered regulatory network was constructed after high confident identification and annotation of the miRNAs in foxtail millet. This study sets the groundwork and offers tools to explore the roles of miRNAs in foxtail millet, as well as providing innovative crop breeding tactics.

DATA AVAILABILITY STATEMENT

The sequencing data for this study can be found in the NCBI Sequence Read Archive (SRA) under accession number PRJNA793125. All annotated miRNA loci were deposited into PmiREN2.0 database (https://www.pmiren.com/).

AUTHOR CONTRIBUTIONS

JZ, JW, and XY initiated, designed the research, and revised the manuscript. YD, GX, CL, ZK, and SD analyzed the data. HZ, HW, YZ, BL, and GX performed the experiments. JZ, YD, and HZ wrote the manuscript. All authors contributed to the article and approved the submitted version.

FUNDING

This research was funded by the National Key R&D Program of China (Grant Nos. 2019YFD1000700 and 2019YFD1000703), the Science Foundation of the Beijing Academy of Agriculture and Forestry Sciences (Grant Nos. KJCX20200205, KJCX20210101, and KJCX20220105), and the Science Foundation of State Key Laboratory of Sustainable Dryland Agriculture (Grant No. YJHZKF2106).

SUPPLEMENTARY MATERIAL

The Supplementary Material for this article can be found online at: https://www.frontiersin.org/articles/10.3389/fpls.2022.848474/full#supplementary-material

REFERENCES

Addo-Quaye, C., Miller, W., and Axtell, M. J. (2009). CleaveLand: a pipeline for using degradome data to find cleaved small RNA targets. *Bioinform.* 25, 130–131. doi: 10.1093/bioinformatics/btn604

Alves, L. Jr., Niemeier, S., Hauenschild, A., Rehmsmeier, M., and Merkle, T. (2009). Comprehensive prediction of novel microRNA targets in Arabidopsis thaliana. *Nucleic. Acids. Res.* 37, 4010–4021. doi: 10.1093/nar/gkp272

Axtell, M. J., and Meyers, B. C. (2018). Revisiting Criteria for Plant MicroRNA Annotation in the Era of Big Data. *Plant Cell.* 30, 272–284. doi: 10.1105/tpc.17.00851

Bartel, D. P. (2009). MicroRNAs: target recognition and regulatory functions. *Cell* 136, 215–233. doi: 10.1016/j.cell.2009.01.002

Bartlett, A., O'Malley, R. C., Huang, S. C., Galli, M., Nery, J. R., Gallavotti, A., et al. (2017). Mapping genome-wide transcription-factor binding sites using DAP-seq. *Nat. Protoc.* 12, 1659–1672. doi: 10.1038/nprot.2017.055

Bennetzen, J. L., Schmutz, J., Wang, H., Percifield, R., Hawkins, J., Pontaroli, A. C., et al. (2012). Reference genome sequence of the model plant Setaria. *Nat. Biotechnol.* 30, 555–561. doi: 10.1038/nbt.2196

Brown, J., Pirrung, M., and McCue, L. A. (2017). FQC Dashboard: integrates FastQC results into a web-based, interactive, and extensible FASTQ quality control tool. *Bioinform.* 33, 3137–3139. doi: 10.1093/bioinformatics/btx373

Carthew, R. W., and Sontheimer, E. J. (2009). Origins and Mechanisms of miRNAs and siRNAs. *Cell* 136, 642–655. doi: 10.1016/j.cell.2009.01.035

Chandra, S., Vimal, D., Sharma, D., Rai, V., Gupta, S. C., and Chowdhuri, D. K. (2017). Role of miRNAs in development and disease: Lessons learnt from small organisms. *Life Sci.* 185, 8–14. doi: 10.1016/j.lfs.2017.07.017

Chen, C., Chen, H., Zhang, Y., Thomas, H. R., Frank, M. H., He, Y., et al. (2020). TBtools: An Integrative Toolkit Developed for Interactive Analyses of Big Biological Data. *Mol. Plant.* 13, 1194–1202. doi: 10.1016/j.molp.2020.06.009

Dai, X., Zhuang, Z., and Zhao, P. X. (2018). psRNATarget: a plant small RNA target analysis server. *Nucleic. Acids. Res.* 46, W49–W54. doi: 10.1093/nar/gky316

Deng, Y., Qin, Y., Yang, P., Du, J., Kuang, Z., Zhao, Y., et al. (2021). Comprehensive Annotation and Functional Exploration of MicroRNAs in Lettuce. *Front. Plant. Sci.* 12:781836. doi: 10.3389/fpls.2021.781836

Yi, F., Xie, S., Liu, Y., Qi, X., and Yu, J. (2013). Genome-wide characterization of microRNA in foxtail millet (Setaria italica). *BMC. Plant Biol.* 13:212. doi: 10.1186/1471-2229-13-212

Fromm, B., Keller, A., Yang, X., Friedlander, M. R., Peterson, K. J., and Griffiths-Jones, S. (2020). Quo vadis microRNAs? *Trends Genet* 36, 461–463. doi: 10.1016/j.tig.2020.03.007

Gao, Z., Li, J., Li, L., Yang, Y., Li, J., Fu, C., et al. (2021). Structural and Functional Analyses of Hub MicroRNAs in an Integrated Gene Regulatory Network of

Arabidopsis. *Genomics Proteomics Bioinform.* doi: 10.1016/j.gpb.2020.02.004 [Epub ahead of print].

Gaudinier, A., and Brady, S. M. (2016). Mapping Transcriptional Networks in Plants: Data-Driven Discovery of Novel Biological Mechanisms. *Annu. Rev. Plant Biol.* 67, 575–594. doi: 10.1146/annurev-arplant-043015-112205

German, M. A., Luo, S., Schroth, G., Meyers, B. C., and Green, P. J. (2009). Construction of Parallel Analysis of RNA Ends (PARE) libraries for the study of cleaved miRNA targets and the RNA degradome. *Nat. Protoc.* 4, 356–362. doi: 10.1038/nprot.2009.8

Guo, Z., Kuang, Z., Zhao, Y., Deng, Y., He, H., Wan, M., et al. (2021). PmiREN2.0: from data annotation to functional exploration of plant microRNAs. *Nucleic. Acids. Res.* 50, D1475–D1482. doi: 10.1093/nar/gkab811

Han, J., Xie, H., Sun, Q., Wang, J., Lu, M., Wang, W., et al. (2014). Bioinformatic identification and experimental validation of miRNAs from foxtail millet (Setaria italica). *Gene.* 546, 367–377. doi: 10.1016/j.gene.2014.05.050

Huang, P., Jiang, H., Zhu, C., Barry, K., Jenkins, J., Sandor, L., et al. (2017). Sparse panicle1 is required for inflorescence development in Setaria viridis and maize. *Nat Plants.* 3, 17054. doi: 10.1038/nplants.2017.54

Jia, G., Huang, X., Zhi, H., Zhao, Y., Zhao, Q., Li, W., et al. (2013). A haplotype map of genomic variations and genome-wide association studies of agronomic traits in foxtail millet (Setaria italica). *Nat. Genet.* 45, 957–961. doi: 10.1038/ng.2673

Jin, J., Tian, F., Yang, D. C., Meng, Y. Q., Kong, L., Luo, J., et al. (2017). PlantTFDB 4.0: toward a central hub for transcription factors and regulatory interactions in plants. *Nucleic. Acids. Res.* 45, D1040–D1045. doi: 10.1093/nar/gkw982

Johnson, D. S., Mortazavi, A., Myers, R. M., and Wold, B. (2007). Genome-Wide Mapping of in Vivo Protein-DNA Interactions. *Sci.* 316, 1497–1502. doi: 10.1126/science.1141319

Jones, P., Binns, D., Chang, H. Y., Fraser, M., Li, W., McAnulla, C., et al. (2014). InterProScan 5: genome-scale protein function classification. *Bioinform.* 30, 1236–1240. doi: 10.1093/bioinformatics/btu031

Kalvari, I., Argasinska, J., Quinones-Olvera, N., Nawrocki, E. P., Rivas, E., Eddy, S. R., et al. (2018). Rfam 13.0: shifting to a genome-centric resource for non-coding RNA families. *Nucleic. Acids. Res.* 46, D335–D342. doi: 10.1093/nar/gkx1038

Kechin, A., Boyarskikh, U., Kel, A., and Filipenko, M. (2017). cutPrimers: A New Tool for Accurate Cutting of Primers from Reads of Targeted Next Generation Sequencing. *J. Comput. Biol.* 24, 1138–1143. doi: 10.1089/cmb.2017.0096

Khan, Y., Yadav, A., Bonthala, V. S., Muthamilarasan, M., Yadav, C. B., and Prasad, M. (2014). Comprehensive genome-wide identification and expression profiling of foxtail millet [Setaria italica (L.)] miRNAs in response to abiotic stress and development of miRNA database. *Plant Cell, Tissue and Organ Culture (PCTOC)* 118, 279–292. doi: 10.1007/s11240-014-0480-x

Kim, D., Paggi, J. M., Park, C., Bennett, C., and Salzberg, S. L. (2019). Graph-based genome alignment and genotyping with HISAT2 and HISAT-genotype. *Nat. Biotechnol.* 37, 907–915. doi: 10.1038/s41587-019-0201-4

Kruger, J., and Rehmsmeier, M. (2006). RNAhybrid: microRNA target prediction easy, fast and flexible. *Nucleic. Acids. Res.* 34, W451–W454. doi: 10.1093/nar/gkl243

Kuang, Z., Wang, Y., Li, L., and Yang, X. (2019). miRDeep-P2: accurate and fast analysis of the microRNA transcriptome in plants. *Bioinform.* 35, 2521–2522. doi: 10.1093/bioinformatics/bty972

Langmead, B. (2010). Aligning short sequencing reads with Bowtie. *Curr. Protoc. Bioinform. Chapter.* 11, 17. doi: 10.1002/0471250953.bi1107s32

Lee, Y., Kim, M., Han, J., Yeom, K. H., Lee, S., Baek, S. H., et al. (2004). MicroRNA genes are transcribed by RNA polymerase II. *EMBO J.* 23, 4051–4060. doi: 10.1038/sj.emboj.7600385

Park, MY, Wu, G, Gonzalez-Sulser, A, Vaucheret, H, and. Poethig, RS. (2005). Nuclear processing and export of microRNAs in Arabidopsis. *Proc. Natl. Acad. Sci. U S A.* 102, 3691–3696. doi: 10.1073/pnas.0405570102

Meyers, B. C., Axtell, M. J., Bartel, B., Bartel, D. P., Baulcombe, D., Bowman, J. L., et al. (2008). Criteria for annotation of plant MicroRNAs. *Plant Cell* 20, 3186–3190. doi: 10.1105/tpc.108.064311

Mi, H., Muruganujan, A., Ebert, D., Huang, X., and Thomas, P. D. (2019). PANTHER version 14: more genomes, a new PANTHER GO-slim and improvements in enrichment analysis tools. *Nucleic. Acids. Res.* 47, D419–D426. doi: 10.1093/nar/gky1038

Ogata, H., Goto, S., Sato, K., Fujibuchi, W., Bono, H., and Kanehisa, M. (1999). KEGG: Kyoto Encyclopedia of Genes and Genomes. *Nucleic. Acids. Res.* 27, 29–34.

Pan, J., Huang, D., Guo, Z., Kuang, Z., Zhang, H., Xie, X., et al. (2018). Overexpression of microRNA408 enhances photosynthesis, growth, and seed yield in diverse plants. *J. Integr. Plant. Biol.* 60, 323–340. doi: 10.1111/jipb.12634

Pertea, M., Pertea, G. M., Antonescu, C. M., Chang, T. C., Mendell, J. T., and Salzberg, S. L. (2015). StringTie enables improved reconstruction of a transcriptome from RNA-seq reads. *Nat. Biotechnol.* 33, 290–295. doi: 10.1038/nbt.3122

Quinlan, A. R., and Hall, I. M. (2010). BEDTools: a flexible suite of utilities for comparing genomic features. *Bioinform.* 26, 841–842. doi: 10.1093/bioinformatics/btq033

Shannon, P., Markiel, A., Ozier, O., Baliga, N. S., Wang, J. T., Ramage, D., et al. (2003). Cytoscape: a software environment for integrated models of biomolecular interaction networks. *Genome. Res.* 13, 2498–2504. doi: 10.1101/gr.1239303

Sharma, D., Tiwari, M., Pandey, A., Bhatia, C., Sharma, A., and Trivedi, P. K. (2016). MicroRNA858 Is a Potential Regulator of Phenylpropanoid Pathway and Plant Development. *Plant Physiol.* 171, 944–959. doi: 10.1104/pp.15.01831

Tang, Y., Liu, H., Guo, S., Wang, B., Li, Z., Chong, K., et al. (2018). OsmiR396d Affects Gibberellin and Brassinosteroid Signaling to Regulate Plant Architecture in Rice. *Plant Physiol.* 176, 946–959. doi: 10.1104/pp.17.00964

Tav, C., Tempel, S., Poligny, L., and Tahi, F. (2016). miRNAFold: a web server for fast miRNA precursor prediction in genomes. *Nucleic. Acids. Res.* 44, W181–W184. doi: 10.1093/nar/gkw459

Taylor-Teeples, M., Lin, L., de Lucas, M., Turco, G., Toal, T. W., Gaudinier, A., et al. (2015). An Arabidopsis gene regulatory network for secondary cell wall synthesis. *Nat.* 517, 571–575. doi: 10.1038/nature14099

Tian, F., Yang, D. C., Meng, Y. Q., Jin, J., and Gao, G. (2020). PlantRegMap: charting functional regulatory maps in plants. *Nucleic. Acids. Res.* 48, D1104–D1113. doi: 10.1093/nar/gkz1020

Wang, G., Li, H., Wang, K., Yang, J., Duan, M., Zhang, J., et al. (2020). Regulation of gene expression involved in the remobilization of rice straw carbon reserves results from moderate soil drying during grain filling. *Plant J.* 101, 604–618. doi: 10.1111/tpj.14565

Wang, Y., Li, L., Tang, S., Liu, J., Zhang, H., Zhi, H., et al. (2016). Combined small RNA and degradome sequencing to identify miRNAs and their targets in response to drought in foxtail millet. *BMC. Genet.* 17:57. doi: 10.1186/s12863-016-0364-7

Wang, Y., Tang, H., Debarry, J. D., Tan, X., Li, J., Wang, X., et al. (2012). MCScanX: a toolkit for detection and evolutionary analysis of gene synteny and collinearity. *Nucleic. Acids. Res.* 40, e49. doi: 10.1093/nar/gkr1293

Wu, G., Park, M. Y., Conway, S. R., Wang, J. W., Weigel, D., and Poethig, R. S. (2009). The sequential action of miR156 and miR172 regulates developmental timing in Arabidopsis. *Cell* 138, 750–759. doi: 10.1016/j.cell.2009.06.031

Wu, H. J., Ma, Y. K., Chen, T., Wang, M., and Wang, X. J. (2012). PsRobot: a web-based plant small RNA meta-analysis toolbox. *Nucleic. Acids. Res.* 40, W22–W28. doi: 10.1093/nar/gks554

Xia, R., Chen, C., Pokhrel, S., Ma, W., Huang, K., Patel, P., et al. (2019). 24-nt reproductive phasiRNAs are broadly present in angiosperms. *Nat. Commun.* 10, 627. doi: 10.1038/s41467-019-08543-0

Xing, Y., and Zhang, Q. (2010). Genetic and molecular bases of rice yield. *Annu. Rev. Plant. Biol.* 61, 421–442. doi: 10.1146/annurev-arplant-042809-112209

Yang, X., Wan, Z., Perry, L., Lu, H., Wang, Q., Zhao, C., et al. (2012). Early millet use in northern China. *Proc. Natl. Acad. Sci. U S A.* 109, 3726–3730. doi: 10.1073/pnas.1115430109

Yang, Z., Zhang, H., Li, X., Shen, H., Gao, J., Hou, S., et al. (2020). A mini foxtail millet with an Arabidopsis-like life cycle as a C4 model system. *Nat. Plants.* 6, 1167–1178. doi: 10.1038/s41477-020-0747-7

Yi, F., Chen, J., and Yu, J. (2015). Global analysis of uncapped mRNA changes under drought stress and microRNA-dependent endonucleolytic cleavages in foxtail millet. *BMC. Plant. Biol.* 15:241. doi: 10.1186/s12870-015-0632-0

Zhang, J. P., Yu, Y., Feng, Y. Z., Zhou, Y. F., Zhang, F., Yang, Y. W., et al. (2017). MiR408 Regulates Grain Yield and Photosynthesis via a Phytocyanin Protein. *Plant Physiol.* 175, 1175–1185. doi: 10.1104/pp.17.01169

Zhao, Y., Kuang, Z., Wang, Y., Li, L., and Yang, X. (2021). MicroRNA annotation in plants: current status and challenges. *Brief. Bioinform.* 22, bbab075. doi: 10.1093/bib/bbab075

Zhao, Y. F., Peng, T., Sun, H. Z., Teotia, S., Wen, H. L., Du, Y. X., et al. (2019). miR1432-OsACOT (Acyl-CoA thioesterase) module determines grain yield via enhancing grain filling rate in rice. *Plant. Biotechnol. J.* 17, 712–723.

Zhu, J., Li, Y., Lin, J., Wu, Y., Guo, H., Shao, Y., et al. (2019). CRD1, an Xpo1 domain protein, regulates miRNA accumulation and crown root development in rice. *Plant J.* 100, 328–342. doi: 10.1111/tpj.14445

Conflict of Interest: The authors declare that the research was conducted in the absence of any commercial or financial relationships that could be construed as a potential conflict of interest.

Publisher's Note: All claims expressed in this article are solely those of the authors and do not necessarily represent those of their affiliated organizations, or those of the publisher, the editors and the reviewers. Any product that may be evaluated in this article, or claim that may be made by its manufacturer, is not guaranteed or endorsed by the publisher.

Advantages of publishing in Frontiers

OPEN ACCESS
Articles are free to read for greatest visibility and readership

FAST PUBLICATION
Around 90 days from submission to decision

HIGH QUALITY PEER-REVIEW
Rigorous, collaborative, and constructive peer-review

TRANSPARENT PEER-REVIEW
Editors and reviewers acknowledged by name on published articles

Frontiers
Avenue du Tribunal-Fédéral 34
1005 Lausanne | Switzerland

Visit us: www.frontiersin.org
Contact us: frontiersin.org/about/contact

REPRODUCIBILITY OF RESEARCH
Support open data and methods to enhance research reproducibility

DIGITAL PUBLISHING
Articles designed for optimal readership across devices

FOLLOW US
@frontiersin

IMPACT METRICS
Advanced article metrics track visibility across digital media

EXTENSIVE PROMOTION
Marketing and promotion of impactful research

LOOP RESEARCH NETWORK
Our network increases your article's readership